SANDIA REPORT

SAND2005-7331
Unlimited Release
Printed November 2005

Nuclear Energy Plant Optimization (NEPO) Final Report on Aging and Condition Monitoring of Low-Voltage Cable Materials

Kenneth T. Gillen, Roger A. Assink, Robert Bernstein

Prepared by
Sandia National Laboratories
Albuquerque, New Mexico 87185 and Livermore, California 94550

Sandia is a multiprogram laboratory operated by Sandia Corporation,
a Lockheed Martin Company, for the United States Department of Energy's
National Nuclear Security Administration under Contract DE-AC04-94AL85000.

Approved for public release; further dissemination unlimited.

Sandia National Laboratories

Issued by Sandia National Laboratories, operated for the United States Department of Energy by Sandia Corporation.

NOTICE: This report was prepared as an account of work sponsored by an agency of the United States Government. Neither the United States Government, nor any agency thereof, nor any of their employees, nor any of their contractors, subcontractors, or their employees, make any warranty, express or implied, or assume any legal liability or responsibility for the accuracy, completeness, or usefulness of any information, apparatus, product, or process disclosed, or represent that its use would not infringe privately owned rights. Reference herein to any specific commercial product, process, or service by trade name, trademark, manufacturer, or otherwise, does not necessarily constitute or imply its endorsement, recommendation, or favoring by the United States Government, any agency thereof, or any of their contractors or subcontractors. The views and opinions expressed herein do not necessarily state or reflect those of the United States Government, any agency thereof, or any of their contractors.

Printed in the United States of America. This report has been reproduced directly from the best available copy.

Available to DOE and DOE contractors from
U.S. Department of Energy
Office of Scientific and Technical Information
P.O. Box 62
Oak Ridge, TN 37831

Telephone: (865)576-8401
Facsimile: (865)576-5728
E-Mail: reports@adonis.osti.gov
Online ordering: http://www.osti.gov/bridge

Available to the public from
U.S. Department of Commerce
National Technical Information Service
5285 Port Royal Rd
Springfield, VA 22161

Telephone: (800)553-6847
Facsimile: (703)605-6900
E-Mail: orders@ntis.fedworld.gov
Online order: http://www.ntis.gov/help/ordermethods.asp?loc=7-4-0#online

SAND2005-7331
Unlimited Release
Printed November 2005

Nuclear Energy Plant Optimization (NEPO) Final Report on Aging and Condition Monitoring of Low-Voltage Cable Materials

Kenneth T. Gillen, Roger A. Assink and Robert Bernstein
Organic Materials

Sandia National Laboratories
P.O. Box 5800
Albuquerque, NM 87185-1411

Abstract

This report summarizes results generated on a 5-year cable-aging program that constituted part of the Nuclear Energy Plant Optimization (NEPO) program, an effort co-sponsored by the U. S. Department of Energy (DOE) and the Electric Power Research Institute (EPRI). The NEPO cable-aging effort concentrated on two important issues involving the development of better lifetime prediction methods as well as the development and testing of novel cable condition-monitoring (CM) techniques. To address improved life prediction methods, we first describe the use of time-temperature superposition principles, indicating how this approach improves the testing of the Arrhenius model by utilizing all of the experimentally generated data instead of a few selected and processed data points. Although reasonable superposition is often found, we show several cases where non-superposition is evident, a situation that violates the constant acceleration assumption normally used in accelerated aging studies. Long-term aging results over extended temperature ranges allow us to show that curvature in Arrhenius plots for elongation is a common occurrence. In all cases the curvature results in a lowering of the Arrhenius activation energy at lower temperatures implying that typical extrapolation of high temperature results over-estimates material lifetimes. The long-term results also allow us to test the significance of extrapolating through the crystalline melting point of semi-crystalline materials.

By utilizing ultrasensitive oxygen consumption (UOC) measurements, we show that it is possible to probe the low temperature extrapolation region normally inaccessible to conventional accelerated aging studies. This allows the quantitative testing of the often-used Arrhenius extrapolation assumption. Such testing indicates that many materials

again show evidence of "downward" curvature (E_a values drop as the aging temperature is lowered) consistent with the limited elongation results and many literature results. It is also shown how the UOC approach allows the probing of temperatures that cross through the crystalline melting point region of semi-crystalline materials such as XLPO and EPR cable insulations.

New results on combined environment aging of neoprene and hypalon cable jacketing materials are presented and offer additional evidence in support of our time-temperature-dose rate (*t-T-DR*) superposition approach that had been used successfully in the past for such situations.

Several promising condition-monitoring (CM) techniques are described by comparing the property values derived from each CM technique with ultimate tensile elongation results. The first CM approach covered is modulus profiling, a technique that can serve both as a CM approach and as a method for experimentally assessing the importance of diffusion-limited oxidation (DLO) effects and other heterogeneously based artifacts. The approach is found to be applicable to most materials that do not have important crystallinity including neoprene and hypalon jackets and EPR and silicone insulations. The second CM technique involves NMR T_2 relaxation time measurements, a technique that has a very significant advantage due to its capability to make measurements quickly and easily on extremely small samples (tenths of a mg). This approach is shown to be applicable to many materials including neoprene and hypalon cable jackets and some crosslinked polyolefin cable insulations, the latter group of materials representing a class of materials where viable CM approaches are scarce. A third promising CM approach involves gel and solvent uptake measurements. These parameters are sensitive to the crosslink density of the material and therefore to the competition between scission and crosslinking that occurs during the aging of a crosslinked material. Since modulus and NMR relaxation times are also dominated by changes in crosslink density, all three techniques tend to have similar applicability from a material point-of-view. Studies looking at the applicability of density as a CM technique are also described, where it is concluded that such measurements are much less useful than modulus, NMR and solubility.

The last part of the report focuses on the Wear-out approach, a new and useful method for estimating residual lifetimes of cable jacketing and insulation materials. It is shown that this method is especially useful for materials that show "induction-time" behavior since condition-monitoring techniques applied to such materials may give little warning of impending end-of-life. Through the use of the Wear-out approach, this non-predictability can be transformed into predictive results.

Table of Contents

I. Introduction 9
References 13
II. Experimental 18
Oven aging 18
Radiation aging 18
Tensile testing 18
Oxygen consumption and CO_2 production rate measurements 18
NMR measurements 19
Modulus profiling 20
Infrared measurements 20
Gel content and solvent uptake measurements 21
Density measurements 21
DSC runs 21
References 22
III. Thermal Aging- Improving Arrhenius Using Time-Temperature Superposition 23
Introduction to the Arrhenius approach 23
Time-temperature superposition analyses 24
Neoprene (Chloroprene) jacketing materials 25
Hypalon (Chlorosulfonated polyethylene) jacket materials 27
Chlorinated polyethylene cable jacketing material 28
Ethylene propylene rubber (EPR) cable insulation materials 29
Crosslinked polyolefin (XLPO) cable insulation materials 31
Conclusions 33
References 34
Figures 36
IV. Thermal Aging- Further Improving Arrhenius Using Ultrasensitive Oxygen Consumption (UOC) Measurements 66
Introduction 66
UOC and CO_2 measurements on Neo-02 cable jacket 67
UOC and CO_2 measurements on Hyp-03 cable jacket 68
UOC measurements on Hyp-08 cable jacket 69
UOC measurements on EPR-04 cable insulation 69
UOC and CO_2 measurements on XLPO-02B cable insulation 71
UOC and CO_2 measurements on green-colored XLPO-05 cable insulation 72
Conclusions 74
References 75
Figures 76
V. Radiation Aging Results- Elongation Measurements 99
Introduction 99
Time-temperature-dose rate superposition (*t-T-DR*) analyses 99
Testing for inverse temperature and Lazarus effects 101
Conclusions 101
References 103
Figures 104

VI. Condition Monitoring Techniques- Background.....112
Introduction.....112
Importance of recognizing when diffusion-limited oxidation is present.....113
References.....116
VII. Condition Monitoring Techniques- Modulus Profiling.....118
Introduction.....118
Modulus profiling of Neo-02.....118
Modulus profiling of hypalon jacketing materials.....120
Modulus profiling of chlorinated polyethylene (CPE-02) jacketing material.....125
Modulus profiling of EPR cable insulation materials.....125
Modulus profiling of miscellaneous insulation materials (XLPO and silicone)..128
Conclusions.....128
References.....130
Figures.....132
VIII. Condition Monitoring- NMR.....172
Introduction.....172
Thermal aging of Neo-02 and hypalon jacket materials.....172
Combined thermal/radiation aging of Neo-02 and hypalon jacket materials.....173
Thermal aging of XLPO materials.....174
Thermal aging of miscellaneous materials.....176
Conclusions.....177
References.....178
Figures.....179
IX. Condition Monitoring Techniques- Percentage Gel and Solvent Uptake Factor.....191
Introduction.....191
Gel and uptake factor measurements on Neo-02 cable jacket.....191
Gel and uptake factor measurements on hypalon cable jackets.....192
Gel and uptake factor measurements on XLPO cable insulation.....195
Gel and uptake factor measurements on CPE-2 cable jacket.....197
Gel and uptake factor measurements on EPR cable insulations.....197
Conclusions.....197
References.....199
Figures.....200
X. Condition Monitoring Techniques- Density Measurements.....235
Introduction.....235
Density measurements on Neo-02 cable jacket.....235
Density measurements on hypalon jacketing materials.....236
Density measurements on EPR insulation materials.....237
Density measurements for other materials.....237
Conclusions.....238
References.....239
Figures.....240
XI. The Wear-out Approach for Estimating the Remaining Lifetime of Materials.....249
Introduction.....249
Wear-out approach applied to EPR materials.....250
Wear-out approach applied to XLPO-02B.....254

Wear-out approach applied to Neo-01 254
Conclusions.....256
References.....257
Figures.....258
XII. Summary and Conclusions 274
XIII. Acknowledgements 279
XIV. Published Papers Partially or Wholly Supported By the NEPO Program.....280
Addendum (SCRAPS Excel file).....282

I. Introduction

The Nuclear Energy Plant Optimization (NEPO) program is co-sponsored by the U. S. Department of Energy (DOE) and the Electric Power Research Institute (EPRI). The overall program is focused on performance of currently operating U. S. nuclear power plants with an emphasis on plant aging and optimization of electrical production. With respect to plant aging, the goal is to ensure that current plants can continue to deliver adequate and affordable energy supplies for the term of their license, which can be 60 years, by providing strong technical basis for long-term operation. This entails resolving open issues related to aging mechanisms as well as the development of improved techniques for predicting equipment condition.

This report summarizes the results from a five-year NEPO effort, performed at Sandia National Laboratories (SNL), focused on the aging of low-voltage cable materials. Control and protection of nuclear reactors depend on the transmission of electrical signals. Cables provide the electrical path for power to motors for pumps, fans and valve operators and for control and instrumentation signals. Therefore, understanding and monitoring the degradation of cables is critical to optimizing plant performance. The NEPO cable-aging program has been concentrated on two important issues. The first focused on developing better lifetime prediction methods and involved the use of ultrasensitive oxygen consumption (UOC) measurements to better extrapolate accelerated aging data to use conditions. This effort also developed a novel Wear-out approach to predict remaining material lifetimes. The second thrust involved developing and testing novel condition-monitoring (CM) techniques to better allow the condition of plant-aged materials to be evaluated. Much of this effort was devoted to two unique methods, modulus profiling and solvent-swelled nuclear magnetic resonance (NMR) relaxation time measurements. This report covers the progress made in these areas.

Although the cable aging conducted under the NEPO program was an approximate 5-year effort starting in July, 2000, Sandia National Laboratories has been involved off and on with nuclear power plant cable aging issues since ~1977. The earliest work, covering the period from 1977 through 1986, was sponsored by the U. S. Nuclear Regulatory Commission. DOE sponsored some more limited work in the late 80s and mid 90s. Over this period, we had aged more than 15 different materials obtained from commonly used nuclear power plant safety cables. The materials were oven-aged at various temperatures for various times and radiation-aged under various combined dose-rate/temperature conditions. Overall, on the order of 1500 separate aging conditions were used with many representing long-term exposures of up to 5 years. For virtually every aged sample, tensile elongation measurements were made. In addition, for selected samples, other measurements were made. Over the years, most of the aged samples were saved in envelopes in our buildings. This irreplaceable asset which we refer to as SCRAPS (Sandia's Cable Repository for Aged Polymer Samples) allowed us to much more efficiently attack the cable aging objectives of the NEPO program. The data from the current and past research has been accumulated and placed in the Cable Polymer Aging Database (CPAD) in a separate NEPO Task. The CPAD database is available from EPRI.

The samples contained in the SCRAPS storage facility were particularly invaluable to the NEPO program for evaluating CM techniques. The optimum method of testing a CM technique involves seeing whether the CM technique parameter correlates with the degradation of the material of interest. Normally, the parameter most sensitive to cable degradation is the tensile elongation of the insulation or jacketing material. Retained elongation at break is indicative of the material's flexibility for manipulation and ability to function adequately under a loss-of-coolant accident (LOCA) environment. CM techniques will eventually be applied to cable materials aging under low environmental stress aging conditions (low radiation dose rates, low temperatures). Under these low stress conditions, the materials will typically be aged homogeneously throughout their cross-sections. Thus, any correlation of CM parameters with material aged under accelerated laboratory conditions should be done on samples that are aged at low enough temperatures and dose rates such that homogeneous oxidation occurs (absence of diffusion-limited oxidation). This usually requires longer-term exposures. In general, therefore, the rigorous testing of a CM technique normally involves five major steps:

1. Purchase or acquire the cable of interest
2. Select aging conditions such that homogeneous oxidation will occur based on estimates or measurements of both the oxygen consumption and oxygen permeability coefficients under the selected conditions.
3. Age the material under the selected conditions and, if possible, confirm the absence of diffusion-limited oxidation artifacts using experimental profiling techniques (e.g., density, modulus or infrared profiling).
4. Measure the tensile elongation versus the aging time.
5. Measure the CM parameter versus the aging time and examine its correlation with the elongation values.

The beauty of the samples and data available from the SCRAPS storage facility is that the first 4 steps were already complete for many of the materials. In order to test the potential utility of a CM technique on a nuclear power plant safety cable material, only step 5 was necessary. We were therefore able to begin immediate evaluation of various CM techniques using samples already available from SCRAPS. In addition, many new cable materials were aged as part of the NEPO program adding additional samples for CM studies as the NEPO program progressed. In addition, high rate aging data (high dose rates and elevated aging temperatures) was available for comparison to accelerated aging at lower temperatures.

The other important aspect of the NEPO program involved developing superior life prediction methods to improve on the often-used Arrhenius extrapolation approach. Activation energies derived under high temperature aging conditions have been historically used to make cable lifetime predictions under operating conditions. The assumption that the activation energy remains unchanged in the extrapolation region has been used for more than 50 years, primarily because no technique ever existed to check this important assumption. In the late-90s, we developed and verified the first experimental means of testing the Arrhenius extrapolation assumption based on

ultrasensitive oxygen consumption (UOC) measurements. We found that the extrapolation assumption is valid for certain materials, but is invalid for others. When invalid, the activation energy is typically found to decrease at lower temperatures (the extrapolation region). This is not surprising whenever multiple degradation pathways underlie the degradation of a material, given the expectation that the higher activation energy process would be expected to drop out as the temperature is lowered.

Again our earlier cable studies led to obvious shortcuts in applying UOC techniques, since conventional results from the Arrhenius approach were already available on several of the materials of interest. In addition, several long-term aging exposures on materials of interest were already underway when the NEPO work was initiated allowing us the opportunity to analyze and incorporate results normally inaccessible to accelerated aging programs. In particular, we show and discuss in this report aging data for 1) an ethylene propylene rubber (EPR) cable insulation that aged for 7 years at 99°C, 2) a crosslinked polyolefin (CLPO) insulation that has now aged for 12 years at 99°C and 3) a chloroprene cable jacket that aged for ~25 years at 24°C. Such long-term results allow conclusions to be made about such critical questions as the validity of Arrhenius extrapolations and the significance of attempting to extrapolate through the crystalline melting point regions of semi-crystalline polymeric materials (e.g., CLPO and EPR cable insulations). The samples already under long-term aging also allowed us to conveniently test our new Wear-out approach for estimating remaining life on really long-term samples.

Thus, the NEPO program dealt with samples that had been aged in the past as well as new materials whose aging was initiated during the NEPO studies. Tables I-1 and I-2 summarize the materials currently collected in the SCRAPS storage facility as well as the types of aging environments that each material had been exposed to over the more than 25-year history of cable aging at Sandia. Table I-3 gives values for the initial properties of the SCRAPS materials in instances where such measurements were made. Overall, the samples in SCRAPS have now been exposed to around 3000 separate aging conditions (thermal only and radiation combined with thermal). For each of these 3000 conditions, the aged samples were tensile tested. In addition, for many of the aging conditions, one or more additional tests have now been conducted (e.g., density, modulus, gel content, swelling uptake factor, NMR relaxation time) so that the total number of individual datum points taken on the 28 materials listed in these Tables probably exceeds 5000. As part of the NEPO program, much of these data are being put into a SCRAPS Database, a copy of which is included as an Excel file in this Final Report. This SCRAPS Database has been incorporated into the EPRI Cable Polymer Aging Database. These are both living Databases in the sense that additional data are added as collected and errors are continually being found and corrected. These NEPO-generated Databases are unique resources available to anyone who wants to use, analyze, or interpret the results. Given the huge number of individual data points incorporated in the Sandia SCRAPS Database and the observation that parts of the data have been previously analyzed and interpreted

in past Sandia publications, we are not able to discuss all of the data in the current NEPO document. Table I-2 summarizes the data discussed in the current document. This table also notes the data not discussed in the current report and gives references to previous publications that have dealt with this latter data.

References

I-1. K. T. Gillen and R. L. Clough, Inhomogeneous Radiation Degradation in Polymers Studied with a Density Gradient Column", Radiat. Phys. Chem., 22, 537 (1983).

I-2. K. T. Gillen, R. L. Clough and N. J. Dhooge, "Density Profiling of Polymers", Polymer, 27, 225 (1986).

I-3. K. T. Gillen and R. L. Clough, "Techniques for Monitoring Heterogeneous Oxidation of Polymers", in **Handbook of Polymer Science and Technology, Vol. 2,** N. P. Cheremisinoff, Ed., Marcel Dekker, New York, 1989, Ch. 6.

I-4. K. T. Gillen and R. L. Clough, "Time-Temperature- Dose Rate Superposition: A Methodology for Extrapolating Accelerated Radiation Aging Data to Low Dose Rate Conditions", Polym. Degrad. & Stabil., 24, 137 (1989).

I-5. K. T. Gillen and R. L. Clough, "Accelerated Aging Methods for Predicting Long-Term Mechanical Performance of Polymers", in **Irradiation Effects on Polymers,** D. W. Clegg and A. A. Collyer, Eds., Elsevier Applied Science, London, 1991., Ch. 4.

I-6. K. T. Gillen and R. L. Clough, "Predictive Aging Results in Radiation Environments", Rad. Phys. and Chem., 41, No. 6, 803 (1993).

I-7. K. T. Gillen and R. L. Clough, "Aging Predictions in Nuclear Power Plants-Crosslinked Polyolefin and EPR Cable Insulation Materials, Sandia National Laboratories Report SAND91-0822 (June, 1991).

I-8. M. Celina, K. T. Gillen, J. Wise and R. L. Clough, "Anomalous Aging Phenomena in a Crosslinked Polyolefin Cable Insulation", Radiat. Phys. Chem., 48, 613 (1996).

I-9. M. Celina, K. T. Gillen and R. L. Clough, "Inverse Temperature and Annealing Phenomena During Degradation of Crosslinked Polyolefins", Polym. Degrad. Stabil., 61, 231 (1998).

Table I-1. Summary of cable samples contained in SCRAPS.

Material	Cable No.	Manufacturer	Trade Name	Material- common name
CPE-01	C-2	Anaconda	Flameguard FR-EP ("Y")	Chlorinated polyethylene
CPE-02	C-20	Anaconda	Flameguard FR-EP ("Y")	Chlorinated polyethylene
EPR-01A	C-14	Anaconda	Flameguard	Ethylene propylene rubber
EPR-01B	C-15	Anaconda	Flameguard	Ethylene propylene rubber
EPR-02	C-2	Anaconda	Flameguard FR-EP ("Y")	Ethylene propylene rubber
EPR-03	C-5	Eaton	Dekoron Elastoset	Ethylene propylene rubber
EPR-04	C-12	Anaconda	Durasheath	Ethylene propylene rubber
EPR-05	C-18	Okonite	EPR	Ethylene propylene rubber
ETFE-01		Teledyne	Thermatic	Tefzel
Hyp-01A	C-14	Anaconda	Flameguard	Hypalon
Hyp-01B	C-15	Anaconda	Flameguard	Hypalon
Hyp-02	C-6	Kerite	FR	Hypalon
Hyp-03	C-9	Samuel Moore	Dekoron	Hypalon
Hyp-04	C-10	Anaconda	Flameguard	Hypalon
Hyp-05	C-11	Rockbestos	Firewall III	Hypalon
Hyp-06	C-5	Eaton	Dekoron Elastoset	Hypalon
Hyp-07	C-3	Brand-Rex		Hypalon
Hyp-08	C-19	BIW	Bostrad 7E	Hypalon
Ker-01	C-6	Kerite	FR	EPR type
Neo-01	C-17	Okonite	Okolene	Neoprene
Neo-02	C-8	Rockbestos	Firewall III	Neoprene
Sil-01	C-7	Rockbestos	Firewall II	Silicone
XLPE-01	C-1	GE	Vulkene Supreme	Crosslinked polyethylene
XLPO-02A	C-3	Brand-Rex		Crosslinked polyolefin
XLPO-02B	C-3	Brand-Rex		Crosslinked polyolefin
XLPO-03	C-4	Eaton	Dekoron Polyset	Crosslinked polyolefin
XLPO-04	C-13	ITT Surprenant	Exane II (composite)	Crosslinked polyolefin
XLPO-05	C-16	Rockbestos	Firewall III	Crosslinked polyolefin

Table I-2. Summary of aging conditions examined, data discussed in current report and references to data not discussed.

Material	Radiation Aging	Discussed in current report	References to previous irradiation discussions	Thermal (only) Aging	Discussed in current report	References to previous thermal aging discussions
CPE-01	Yes	No		No	N/A	
CPE-02	No	N/A		Yes	Yes	
EPR-01A	Yes	No	I-1	Yes	Yes	I-2,I-3
EPR-01B	Yes	No		No	N/A	
EPR-02	Yes	No	I-7	Yes	No	
EPR-03	Yes	No	I-7,I-9	Yes	Yes	
EPR-04	No	N/A		Yes	Yes	
EPR-05	Yes	Yes		Yes	Yes	
ETFE-01	Yes	No	I-6	No	N/A	
Hyp-01A	No	N/A		Yes	Yes	
Hyp-01B	Yes	No	I-6	No	N/A	
Hyp-02	Yes	No	I-4,I-6	Yes	Yes	
Hyp-03	Yes	Yes		Yes	Yes	
Hyp-04	Yes	Yes		Yes	Yes	
Hyp-05	Yes	Yes		Yes	Yes	
Hyp-06	Yes	Yes		Yes	Yes	
Hyp-07	No	N/A		Yes	Yes	
Hyp-08	No	N/A		Yes	Yes	
Ker-01	Yes	No	I-6	Yes	No	
Neo-01	Yes	No	I-4,I-5	Yes	Yes	I-4,I-5
Neo-02	Yes	Yes		Yes	Yes	
Sil-01	Yes	Yes	I-6	No	N/A	
XLPE-01	Yes	No	I-2,I-3,I-7,I-9	No	N/A	
XLPO-02A	Yes	No	I-7,I-8,I-9	Yes	No	I-7
XLPO-02B	No	N/A		Yes	Yes	
XLPO-03	Yes	No	I-7	No	N/A	
XLPO-04	Yes	No	I-7	Yes	Yes	I-7
XLPO-05	Yes	No	I-9	Yes	Yes	

Table I-3. Summary of initial properties of cable samples contained in SCRAPS.

Material	Nom Thick (mm)	Initial Elongation e_0 (%)	Initial TS, MPa	Initial Density (g/cc)	Initial Modulus (MPa)	Initial Uptake factor	Initial % gel	Initial NMR T2, msec	Notes
CPE-01	~1.9	240		1.376	90.0				
CPE-02	~1.8	310	14		90.0	N/A	0.0		
EPR-01A	0.9	336		1.325					
EPR-01B	1.1	346		1.325					
EPR-02	0.9	240		1.341					
EPR-03	0.8	400	11.5	1.288	62.0	4.4	72.0		
EPR-04	1.0	300	6.6	1.308	4.5	3.5	81.0		
EPR-05	0.9	345	9	1.230	12.0				
ETFE-01	0.3	173							
Hyp-01A	0.4	393	15	1.642	5.3				
Hyp-01B	0.4	340		1.607	5.0	4.9	54.0	10.9	
Hyp-02	~1.5	300	22	1.570	9.0				
Hyp-03	~1.2	381	20	1.461	14.0	3.7	78.2	13.0	
Hyp-04	~1.8	263	13	1.577	4.8	2.3	83.0	5.5	
Hyp-05	~1.3	364	16	1.595	4.1	2.3	81.0	12.9	
Hyp-06	~1.4	316	20	1.467	18.0	3.5	78.0	9.4	
Hyp-07	~1.6	380	16	1.368	5.1	2.7	72.0		
Hyp-08	~1.7	257	13	1.475	8.7	2.5	72.0		
Ker-01	1.4	274		1.270	7.0	2.2	81.0		
Neo-01	1.5	185		1.473					
Neo-02	1.5	296		1.61+-.02	6.4	2.5	91.0	6.5	
Sil-01	1.1	420		1.304	3.1	2.5	97.2		
XLPE-01	0.8	345		1.152					
XLPO-02A	0.9	310		1.293					1987-1990
XLPO-02B	0.9	347		1.293	140.0	8.0	57.0	13.5	1991 & after
XLPO-03	1.0	370		1.370					
XLPO-04	0.8	240		1.59/1.23					
XLPO-05	0.9	300	14	1.362		5.0	72.0		

II. Experimental

Oven aging

Oven aging was carried out in air-circulating ovens (average temperature controlled to better than ±1°C) equipped with thermocouples connected to continuous strip-chart recorders. Samples were protected from direct airflow by placing them in metal cans.

Radiation aging

Radiation aging was carried out in Sandia's Low Intensity Cobalt Array (LICA) facility, which has been previously described in detail [II-1]. Basically, cobalt-60 pencils contained under water in various stationary arrays irradiate the samples. The samples are held in watertight aging cans that are lowered into the water tank containing the cobalt pencils. This arrangement allows long-term aging exposures (up to 1 year or longer) to be easily conducted. The aging cans are temperature controlled (capabilities are up to 250°C) and monitored through umbilical cables that also allow for gas (air or nitrogen) circulation during the experiments.

Tensile testing

The materials for tensile testing were carefully stripped, before aging, from the low voltage electrical cables shown in Table I-1. For jacketing samples, the resulting samples were typically ~150 mm long by 6 mm wide by ~2 mm thick. After carefully removing the copper conductors the insulation samples were aged as tubes having lengths of ~150 mm. Tensile testing (5.1 cm initial jaw separation, 12.7 cm/min strain rate) was performed on an Instron 1000 tensile testing machine equipped with pneumatic grips; an extensometer clamped on the sample allowed ultimate tensile elongation values to be obtained. Although tensile strength at break values were also obtained, the main parameter of interest to the current report is the ultimate tensile elongation (elongation at break). For each aging time in a given environment, three identically aged samples were typically tensile tested with the average value reported and analyzed in the subsequent analyses. For brevity the average value of the ultimate tensile elongation results will usually be referred to as the elongation.

Oxygen consumption and CO_2 production rate measurements

A detailed description of the procedures used for these measurements has been described in an earlier publication [II-2]. Briefly, these measurements are made by initially placing a known weight of polymer with a known initial quantity of oxygen in a sealed container. After oven aging for a selected period of time, the gas in the container is analyzed for oxygen, CO_2 and CO using gas chromatography techniques. The amount of oxygen initially sealed in the container is chosen such that its initial partial pressure at the oven aging temperature is ~150 torr and the aging time chosen so that the expected final oxygen partial pressure (at elevated temperature) is ~ 120 torr. The intent of this approach is to have the average oxygen partial pressure during aging approximate the

partial pressure of oxygen in Albuquerque (132 torr) so that the oxygen consumption reflects the oxidation appropriate during air-oven aging. After aging, the gas in the aging cell is quantitatively analyzed for the oxygen consumption rate and for the production rates of CO_2 and CO. The cell is then pumped out again for several days (to remove dissolved gases in the polymer), backfilled again with the same initial partial pressure of oxygen and aged for another time interval. By repeating this procedure several times, the time dependence of the rates is obtained as well as the integrated rate versus time.

For low temperature runs where the rates are quite small, sensitivity considerations dictate that the volumes of the sealed containers are ~50% filled with polymer. Because of this high fill ratio, a correction must be made for the differing amounts of oxygen dissolved in the polymer at the beginning and end of the experiment. This correction, which is detailed in the earlier publication [II-2], reaches a maximum of ~5% for 50% fill factors. However, because the solubility coefficient for CO_2 gas is typically 10 to 20 times higher than the solubility coefficient for oxygen [II-3], this correction factor can become very large for CO_2 and must be considered for quantitative treatment of CO_2 results. This requires accurate estimates for the solubility coefficients for the material of interest. Our procedure for estimating the required CO_2 solubility coefficients has been given in detail in a previous publication [II-4].

NMR measurements

^{1}H NMR T_2 relaxation times were measured on a Bruker DRX spectrometer at 399.9 MHz using a 5-mm broadband solution probe. The relaxation times were measured using a Hahn spin-echo pulse sequence [II-5] consisting of {90°-τ-180°-τ-acquire} with a 90° pulse width of 8μs. The relaxation delay was 4 s and eight scans were accumulated for each τ value. Approximately 10 mg of polymer was placed in 90μl of solvent, typically $CDCl_3$ (deuterated chloroform), and allowed to equilibrate before measurement. The choice of solvent and time for equilibration depended on the polymer and will be reported separately for each material.

Since the signal initially decays rapidly for short spin-echo times and much more slowly for the longer spin-echo times, the delay times [τ] were selected accordingly. The following delay time list was used:

0.020 ms	1.0 ms	10. ms
0.050	1.5	12.
0.100	2.0	14.
0.200	3.0	16.
0.300	4.0	18.
0.500	6.0	20.
0.700	8.0	

The spin-echo maximum appears at twice the delay time value so relaxation times up to 40 ms can be measured with this list. Each spin-echo was Fourier transformed and an automated baseline correction applied to the spectrum. The area of the signal was plotted

vs. twice the delay time. Since the decay curve was non-exponential, T_2 was defined as the time required for the integrated signal to decay to 1/e of its initial value. The initial value was calculated using a linear extrapolation of the 0.020 and 0.050 ms spectra intensities.

Note that each Hahn spin-echo sequence consists of a single 180° pulse and a single echo. The Carr-Purcell sequence [II-5] that employs a train of echoes was also investigated but provided quite different results. Since the signal decays rapidly at first, we employed a Carr-Purcell sequence with short τ spacing. This pulse sequence pumps considerable transverse radio frequency (RF) power into the sample. As a result the experiment more closely resembles a $T_{1\rho}$ experiment and the relaxation times are much longer. The $T_{1\rho}$ for a polymer goes through several minima and maxima for the glass transition and lower temperature sub-transitions. As a result, we found that $T_{1\rho}$ can both decrease and increase as a function of crosslink density and presumable show very little response if the $T_{1\rho}$ of the unaged sample is near one of the minima or maxima. A further complication is that the result of the Carr-Purcell measurement is very much dependent on the choice of τ spacing and on the power level of the particular instrument employed and would not serve as an absolute reference.

Modulus Profiling

Modulus profiles were obtained on sample cross-sections using a computer-controlled, automated version of our modulus profiling apparatus, which has been described in detail previously [II-6, II-7]. The basic procedure typically involves mounting three small pieces of the aged material side by side in a vise-like device. This holder is then metallographically polished yielding smooth polished cross-sections of the three samples. The holder is placed in the apparatus such that a loaded probe with a paraboloidally shaped tip can be used to indent the central sample perpendicular to the cross-sectional surface of this sample. Through the use of a two-step loading procedure, the amount of indentation into the sample can be used (together with the known loading on the probe and the probe tip geometry) to calculate the inverse tensile compliance, a quantity closely related to the tensile modulus of the material. The apparatus allows measurements to be made with a resolution of ~50 μm. By scanning across the sample cross-section, a detailed map of modulus versus probe location is obtained.

Infrared measurements

Aged samples of Hyp-04 (738 days at 90°C) were analyzed using the microscope on the Nicolet 800 Sx Infrared Spectrometer. Small slices approximately 50 to 100 microns wide were obtained from the cross-section of the sample after aging and placed between two NaCl windows in a compression cell. Spectra were taken of the flattened pieces. The spectra had the water vapor subtracted, were 7-point smoothed and were baseline leveled. The carbonyl peak height at 1710 cm^{-1} was normalized to the 1458.6 cm^{-1} peak in order to estimate the changes in carbonyl occurring across the sample cross-section.

Gel content and solvent uptake measurements

Solvent uptake measurements were carried out by first exposing a known weight of sample (w_0) to refluxing p-xylene for a minimum of 24 hours. The sample was recovered from the hot solvent and then quickly placed and sealed in a small container of known weight so that solvent evaporating from the sample was trapped in the sealed container. The weight of the swollen rubber (w_s) was then determined from the weight gain of the sealed container. The final weight w_f of the remaining gel was determined after drying the swollen sample under vacuum. The solvent uptake factor is defined as the ratio of w_s to w_f. The percent gel is given by the ratio of w_f to w_0. Typical initial sample weights for these experiments were ~50 mg.

Density measurements

Macroscopic density measurements were made using the Archimedes approach [II-8], where the sample (typically 50 mg) is weighed in air and then in isopropanol on a balance with a reproducibility of better than 10 micrograms. Density profiling measurements were made in a density gradient column using calcium nitrate-water solutions. The columns were calibrated using glass calibration balls of known density. Typical column resolution is 0.002 g/cc per cm of column height. Details are provided in a previous publication [II-9].

DSC runs

Differential scanning calorimetry under argon gas flow at a scan rate of 5°C/min was carried out on ~5 mg samples of each material using a Perkin Elmer DSC 6 calibrated with indium and zinc standards.

References

II-1. Gillen KT, Clough RL, Jones LH. Investigation of cable deterioration in the containment building of the Savannah River reactor. Sandia Labs Report SAND81-2613, August, 1982.

II-2. J. Wise, K. T. Gillen and R. L. Clough, "An Ultrasensitive Technique for Testing the Arrhenius Extrapolation Assumption for Thermally-Aged Elastomers", Polym. Degrad. & Stabil., 49, 403 (1995).

II-3. Pauly S. Permeability and diffusion data. In Brandrup J, Immergut EH, Grulke EA, editors. Polymer Handbook-4th edition. New York: John Wiley and Sons, 1999, p. VI/543.

II-4. K. T. Gillen, R. Bernstein and D. K. Derzon, "Evidence of non-Arrhenius Behavior from Laboratory Aging and 24-year Field Aging of Chloroprene Rubber Materials, Polymer Degradation and Stability, 87, 57 (2005).

II-5. Farrar TC, Becker ED. Pulse and Fourier Transform NMR. New York: Academic Press, 1971.

II-6. K. T. Gillen, R. L. Clough and C. A. Quintana, "Modulus Profiling of Polymers", Polym. Degrad. & Stabil., 17, 31 (1987).

II-7. K. T. Gillen, E. R. Terrill and R. W. Winter, "Modulus Mapping of Rubbers Using Micro- and Nano-Indentation Techniques", Rubber Chemistry and Technology-**Rubber Reviews**. Invited Review, 74, 428 (2001).

II-8. Gillen KT, Celina M, Clough RL. Density measurements as a condition monitoring approach for following the aging of nuclear power plant cable materials. Radiat Phys Chem 1999;56:429.

II-9. K. T. Gillen, R. L. Clough and N. J. Dhooge, "Density Profiling of Polymers", Polymer, 27, 225 (1986).

III. Thermal Aging: Improving Arrhenius Using Time-Temperature Superposition

Introduction to the Arrhenius approach

For most polymer types, when oxygen (air) is present during aging, the degradation is dominated by oxidation reactions. The basic idea underlying the Arrhenius approach for accelerated aging studies is that the chemical (oxidative) degradation reactions can be increased (accelerated) by raising the temperature. Since the rate constant k of simple chemical reactions has an Arrhenius dependence on the absolute temperature T given by

$$k \propto \exp\left[\frac{-E_a}{RT}\right] \qquad \text{(III-1)}$$

where

E_a = activation energy
T = absolute temperature
R = Ideal gas constant

it implies that the degradation rate will have an Arrhenius dependence on temperature. That is a plot of log degradation rate, or log of the time to a certain amount of damage (or to failure) against inverse absolute temperature should follow straight-line behavior where the slope gives the activation energy. By assuming that the same reaction(s) dominate the degradation as the temperature is lowered, the Arrhenius dependence can then be extrapolated to lower temperatures corresponding to long-term aging conditions. Figure III-1 shows an example of elongation versus time results for an XLPO-04 cable jacketing material aged at nine different temperatures. A typical Arrhenius analysis would pick out the times corresponding to a certain amount of degradation and plot the log of these values versus inverse absolute temperature. If Arrhenius behavior holds, eq. (III-1) predicts that such a plot would give linear dependence, the slope of which leads to the Arrhenius activation energy E_a. For instance if the time required for the elongation to reach 100% was chosen as the degradation point for analyses (the dashed horizontal line in Fig. III-1), the resulting Arrhenius plot would be given by Fig. III-2. It is clear from the results shown in Fig. III-2 that the Arrhenius plot for 100% elongation of XLPO-04 is very linear with an activation energy of ~ 110 kJ/mol (1 kJ/mol = 0.239 kcal/mol = 0.0104 ev) derived from the slope of the line. If this linear behavior is extrapolated to 49°C (1000/T = 0.0031), the result predicts that the time required to reach 100% elongation at this temperature is ~ 250 years. Continuing the extrapolation to 25°C leads to a predicted time of 7500 years.

Although long life is predicted, the large extrapolation distances give little confidence in the predicted results. In fact, there are numerous phenomena that can lead to non-Arrhenius behavior [III-1]. For instance, the actual oxidation chemistry responsible for degradation usually involves a series of complex reactions that lead to a complex rate

expression involving many reaction rate constants. Analyses of the rate equations for even the simplest kinetic situations indicate that non-Arrhenius behavior might be expected [III-1]. For polymers in which data is being acquired or extrapolated through a physical transition such as a crystalline melting point region for semi-crystalline materials (relevant to many EPR/EPDM and XLPO cable insulations), deviations from the Arrhenius assumptions might often be anticipated. Whenever diffusion-limited oxidation (DLO) effects are present (common for typical accelerated aging conditions for cable insulation and jacketing materials- see Section VI below for detailed discussion), the material property of interest can vary across the cross-section of the material. This implies that macroscopic property measurements of the entire cross-section of the material will represent an average of a property that spatially varies. Such effects can lead to non-Arrhenius behavior when the temperature dependence of the property is being followed [III-2] or accidental Arrhenius behavior if the material properties at the sample surface happen to dominate degradation of the parameter of interest [III-1, III-3].

Many instances of non-Arrhenius behavior have been experimentally documented in the literature and most involve a drop in E_a as the temperature drops. Richters observed curvature to lower E_a values ("downward curvature") when monitoring the oxygen induction period for polypropylene [III-4]. Similar curvature to lower E_a values was observed for polyethylene materials by Bell Labs workers [III-5, III-6]. Bernstein and Lee presented evidence for downward curvature for oven-aged samples of HDPE insulated cables [III-7]. More recent studies by Gijsman on unstabilized polypropylene [III-8] and by Rosik on a stabilized ABS polymer [III-9] observed downward curvature effects. Gugumus recently found evidence of both downward and upward curvature for polypropylene films [III-10]. The upward curvature was tentatively attributed to titanium complexation by the phenolic antioxidant leading to possible passivation of the transition metal. Except for anomalous effects caused by diffusion-limited oxidation [III-2], upward curvature is seldom observed. The above implies that any extrapolation of higher temperature "Arrhenius" results to lower-temperature, application conditions is potentially misleading if the material's tendency to downward curvature of E_a is not understood. In addition, it should be noted that traditional Arrhenius approaches often use a single data point (e.g., time to loss of 75% of initial elongation) at each temperature, effectively discarding much of the experimentally generated data.

Time-temperature superposition analyses

The first improvement to the standard Arrhenius approach involves the use of time-temperature superposition analyses [III-1, III-3], which uses all of the experimentally generated data instead of a single processed data point at each temperature. The whole concept behind accelerated aging is the assumption that raising the temperature will raise all of the underlying degradation processes by a constant amount. This implies that the degradation curves at two different temperatures should be related by a constant multiplicative factor, further implying that they should have the same shape if plotted versus log time. Figure III-1 showed tensile elongation results versus aging time for the XLPO-04 cable jacketing material at nine different aging temperatures. As anticipated for the constant acceleration assumption underlying the Arrhenius model, the curves at the

various temperatures have similar shapes when plotted versus log of the aging time. This means that such log time plots should superpose if shifted horizontally. If the data at the lowest temperature is considered to be at the reference temperature condition, the data at each higher temperature is horizontally shifted by the constant multiplicative factor (a_T) that gives the best overall superposition with the reference curve ($a_T = 1$ at the reference temperature). Figure III-3 shows the time-temperature superposition of the data from Fig. III-1 versus aging time at the reference temperature of 91°C (bottom x-axis).

Since excellent superposition occurs, one immediately has evidence that raising the temperature did in fact lead to constant increases in the overall degradation rate, adding significant confidence to the results. Once the empirically determined shift factors are generated, they can be tested with various aging models. For instance the Arrhenius model would imply that a plot of log (a_T) versus inverse absolute temperature would yield a straight line with the Arrhenius activation energy available from the slope [III-1]. When the empirical shift factors used to create the superposed results of Fig. III-3 (noted versus temperature on the figure) are plotted on an Arrhenius plot (Fig. III-4), it is clear that Arrhenius behavior is confirmed for this material. It is important to point out that the time-temperature superposition approach uses every data point in the analyses as opposed to the typically used Arrhenius approach (Fig. III-2) that eliminates much of the experimental data from consideration.

The dashed line in Fig. III-4 shows the extrapolation to lower temperatures of the Arrhenius behavior found for the empirically derived shift factors. If we were interested in the estimated lifetime of this material at 50°C (1000/T = 0.003094), this extrapolation yields a shift factor a_T of ~0.01. This implies that the superposed results at 91°C in Fig. III-3 (lower x-axis) would have to be multiplied by $1/a_T \sim 100$ to predict the time scale at 50°C. Figure III-3 shows the extrapolated time scale at 50°C as the upper x-axis (100 times the lower x-axis). Extrapolated predictions at other temperatures could be handled in a similar fashion. The extrapolation of data to temperatures lower than the tensile elongation data range incorporates the unproven assumption that the same Arrhenius behavior remains valid at the lower temperatures. We will see below in Section IV that ultrasensitive oxygen consumption (UOC) measurements offer a means of gaining more confidence in such extrapolations.

Based on the above discussion, it is now apparent that the time-temperature superposed results shown in Fig. III-3 contain all of the information shown in Fig. III-1 (as well as the values of a_T plotted in Fig. III-4). For instance if we were interested in the results at 140°C, we could derive the data by examining the squares in Fig. III-3 coupled with a reduction in the lower x-axis time scale by a factor of 76 (the a_T appropriate to the 140°C data).

Neoprene (Chloroprene) jacketing materials

The elongation results for the two neoprene jacketing materials studied as part of the NEPO program were recently published in detail [III-11]. Initial studies on the Neo-01 material were done from 1978 to 1979 using oven aging temperatures ranging from 70°C

to 160°C. In addition a number of these specimens were kept in storage at various indoor locations (storage cabinets, drawers) as our laboratory changed location several times over the past 26 years. Based on periodic temperature monitoring, we estimate that these "unaged" specimens experienced an average temperature of ~24°C. We tensile tested six of these room temperature aged samples in March, 1998 and another ten in August, 2002. Since the average high-temperature experiment was started around the beginning of 1979, the 24°C aging times equivalent to the start date used for the accelerated exposures were 19.2 years (March, 1998 tensile testing) and 23.6 years (August, 2002 tensile testing). The average tensile results for the recent measurements (filled circles) plus the high temperature results from 70°C to 131°C reported many years ago [III-12] are shown in Fig. III-5. Since the results at 24°C show significant degradation, we can utilize this temperature as the reference temperature for time-temperature superposition. The resulting superposed plot is shown in Fig. III-6 together with the empirical shift factors used in the analysis. The superposition for eight temperatures ranging from 24°C to 131°C is remarkable. Figure III-7 shows an Arrhenius plot of the shift factors. The results show curvature in the Arrhenius plot to slightly lower activation energy at low temperatures. Although the curvature is slight, it leads to a reduction in the predicted room temperature lifetimes by a factor of ~2.5 times relative to extrapolation of the high-temperature (70°C and above) "Arrhenius" results. Since this curvature resulted from real-time room temperature elongation results, it is a remarkable demonstration that non-Arrhenius results can and do occur.

In order to quantitatively use time-temperature superposed elongation results and their extrapolations, one must come up with a definition of the end of life of a material. From a practical point-of-view, this is very difficult for many reasons. The first reason comes from the multitudes of cable insulation and jacket types and the differing formulations within the same generic type. This means that the time-dependence of elongation values can differ greatly, ranging from some materials where the elongation drops at a fairly constant rate to others where the decay slows down at later times and to still others where the drop in elongation is minimal through most of the aging followed by a rapid decrease to very low levels (so-called induction-time behavior). In addition, for safety related cables located in containment, aging environments can be followed by accident environments. In such cases, the aged cable material may subsequently be exposed to accident environments implying that the end-of-life criterion must factor in the possibility of the accident environment. Elongation values for unaged insulations and jackets tend to be in the range of 200 to 400% (see Table I-3) and conventional wisdom has concluded that 50% absolute elongation represents a conservative end of life for the aging of cable. Such a value allows adequate flexibility for manipulation of cables and leads during maintenance activities. In addition, the viability during simulated accidents of cable materials with 50% absolute elongation values preceding the accidents has been backed up by substantial experimental data combining aging and accident simulations [III-13, III-14]. Therefore for the purposes of the discussions in this report, we will choose 50% absolute elongation as the "practical end of life" for cable materials. For brevity the terms "lifetime" and "end of life" will also be used in this report as shortened versions of the term "practical end of life".

With this somewhat arbitrary definition, the results for Neo-01 would indicate a practical end of life of ~37 years at 24°C (Fig. III-6). Note that extrapolation of the higher temperature Arrhenius results (70°C and higher) would predict a 24°C practical end of life that is ~2.5 times longer (e.g., 93 years- see solid extrapolation in Fig. III-7). At 50°C, the comparable values for practical end of life would be predicted to occur after ~4 years (dashed curve extrapolation in Fig. III-7) versus ~6 years (solid line extrapolation in Fig. III-7). These results indicate some concern over the viability of this chloroprene jacket material for long-term exposures to moderate temperature aging environments. However, it should be noted that for low voltage cables, jacket materials are often used primarily as a means of more easily installing the cables.

Elongation versus aging time results at three temperatures for the Neo-02 cable jacketing material are shown in Fig. III-8. Since the results at all three temperatures have similar shapes when plotted versus log of the aging time, we would expect reasonable time-temperature superposition, consistent with the accelerated aging assumption that increasing the temperature increases all of the important degradation reactions by an equal amount. Time-temperature superposition of the results from the three temperatures is shown in Fig. III-9 and, as expected, excellent superposition occurs. An Arrhenius plot of the empirically derived shift factors is given in Fig. III-10 and indicates linear (Arrhenius) behavior with an Arrhenius activation energy of 98 kJ/mol. If this activation energy is assumed to be constant at lower aging temperatures and extrapolated to 25°C, we obtain $a_T \sim 2.1\text{x}10^{-3}$, implying that the extrapolated time scale at 25°C (upper x-axis in Fig. III-9) is ~476 times the 80°C lower x-axis. For a practical end of life criterion of 50% absolute elongation, conventional Arrhenius extrapolation for Neo-02 corresponds to a lifetime of ~530 years at 25°C and ~24 years at 50°C. These are substantially greater predicted lifetimes than those found for the Neo-01 material above, indicating that variations in chloroprene jacket lifetimes should be expected for different formulations. However, as will be shown below in the ultrasensitive oxygen consumption section, the lifetimes for Neo-02 are predicted to be slightly lower than 24 years at 50°C and much lower than 530 years at 25°C based on curvature in the Arrhenius plot found using the UOC method. In fact the curvature is similar to that found from the elongation results for Neo-01 (Figs. III-5 through III-7). Even taking this curvature into account, however, the lifetimes of Neo-02 are still found to be substantially greater than Neo-01.

Hypalon (Chlorosulfonated polyethylene) jacket materials

The elongation results for the eight hypalon jacketing materials studied as part of the NEPO program were recently published in detail [III-15]. Thermal aging studies on the Hyp-01A and Hyp-02 materials date back to the late 70s whereas the other six hypalon jackets (Hyp-03 to Hyp-08) were thermally aged for the NEPO program. In addition, long-term aging at 70°C was conducted on Hyp-03 and Hyp-05 as part of a US-French co-operative program [III-16] utilizing samples from the same cable reels used in our NEPO studies. The elongation results versus aging time and temperature for the eight hypalon jacketing materials are shown in Fig. III-11 through III-18. For most of the materials the relative shape of the elongation versus aging time curves are similar except for indications that Hyp-07 and Hyp-08 might drop off a little more abruptly. Figures III-

19 through III-26 show the time-temperature superposed results for these eight materials at the reference temperature (lower x-axis) always chosen to be the lowest aging temperature. Since the lowest aging temperature for half of the materials is ~100°C, the interpolated 100°C time-axis is shown as the upper x-axis for those materials whose lowest aging temperature was lower than 100°C (Figs. III-20, III-21, III-23, III-25 and III-26). This allows us to compare the aging results for all eight materials at 100°C, with the times required to reach 50% absolute elongation summarized in Table III-1. On an average the results indicate a typical hypalon lifetime of around 1 year at 100°C.

Table III-1. Times required for the elongation to drop to 50% absolute at 100°C.

Hyp-	01A	02	03	04	05	06	07	08
time, d	290	270	360	340	390	280	670	210

Figure III-27 plots the shift factors for all eight hypalon jacketing materials on a single Arrhenius plot normalizing each set of shift factors to 100°C. It is clear from the results that the temperature dependence for degradation of the elongation is similar for all eight materials. At temperatures above ~90°C, the results are reasonably linear yielding an average Arrhenius activation energy of ~107 kJ/mol. Below 90°C, there is evidence of a downward curvature in the Arrhenius plot, similar to that found from elongation results for the Neo-01 material (Fig. III-7). We will see below that UOC measurements on two of these hypalon materials show evidence of similar curvature and allow us to more confidently extrapolate to temperatures of interest to nuclear power plant aging situations.

Chlorinated polyethylene cable jacketing material

Elongation results for the CPE-02 cable jacketing material are shown in Fig. III-28. Although results have been obtained at five temperatures, changes in the elongation at the two lowest temperatures (95°C and 99°C) are too small for time-temperature superposition analyses. The superposition of the results for the three higher temperatures are shown in Fig. III-29 at a reference temperature of 109°C. It is clear from the actual results at 109°C (Fig. III-28) and the time-temperature superposed results at this temperature (Fig. III-29) that the CPE-02 jacket material has an approximate 800-day lifetime at 109°C. This compares to much lower lifetimes for the neoprene jackets (~2 to 4 weeks at 109°C) and the hypalon jackets (around half a year at 109°C). An Arrhenius plot using the empirically derived shift factors of Fig. III-29 is given in Fig. III-30 and indicates an Arrhenius activation energy of ~112 kJ/mol. If this activation energy remains unchanged at lower temperatures, an extrapolation to 50°C leads to a predicted elongation lifetime (50% absolute) of ~ 1300 years. Even though there is no data available to probe the extrapolation region, this "Arrhenius" extrapolated lifetime is so large that no realistic drop in activation energy below 109°C would yield 50°C lifetimes less than 100 years. In particular the 112 kJ/mol activation energy found above 109°C would have to drop to an average E_a of ~66 kJ/mol (15.8 kcal/mol) from 109°C to 50°C in order to reduce the 50°C lifetime to 100 years. Thus we conclude that the CPE-02

material should have a very long lifetime at typical aging temperatures encountered during aging of nuclear power plants.

Ethylene propylene rubber (EPR) cable insulation materials

In general, the generic term EPR can refer to one of two types of materials [III-17,III-18]. The first, often referred to as EPM, involves as the base polymer a simple copolymer of ethylene and propylene. For the second material, referred to as EPDM, the base polymer involves a terpolymer containing a third comonomer, a diene that introduces unsaturation into the molecule. The ratio of ethylene to propylene typically varies from ~75% ethylene to 45% ethylene with the higher ethylene containing polymers having some crystallinity. Given the above variability in the base polymers plus the multitude of additives used in EPR formulations, EPR insulations can vary widely in properties and aging resistance.

During the NEPO program, thermal aging experiments were conducted on three EPR cable insulation materials (EPR-03, EPR-04 and EPR-05). In addition, older data generated in the late 70s were analyzed for an additional EPR material (EPR-01A). Of the four materials, two exhibited relatively high levels of crystallinity (EPR-03 and EPR-05) whereas crystallinity was minor for the other two (EPR-01A and EPR-04) as evidenced by the DSC scans shown in Fig. III-31. We will first describe elongation results for the two EPR cable insulation materials with minor amounts of crystallinity and then describe the results for the two other more crystalline materials.

Elongation measurements were taken at eight temperatures ranging from 101°C to 170°C for EPR-01A- the results are plotted in Fig. III-32. As opposed to the earlier results for most of the cable jacketing materials, the elongation results for this and the other EPR insulation materials drops more abruptly near its practical end of life. This is often referred to as "induction-time" behavior, wherein material properties (elongation, modulus, density, etc.) change relatively slowly until just before the practical end of life at which point the changes occur quite rapidly. The point of rapid change (induction time) reflects the point at which the antioxidant is no longer effective in protecting the material from rapid oxidation. Since the shapes of the curves at differing temperatures are similar over a very large temperature range, the results (Fig. III-32) imply that the equal acceleration assumption underlying accelerated aging ideas appears to be valid for this material. Therefore, as expected, excellent superposition occurs when the results are time-temperature shifted as seen in Fig. III-33. An Arrhenius plot of the empirically derived shift factors is shown in Fig. III-34 and the results give very linear behavior with an Arrhenius activation energy of ~106 kJ/mol. If this activation energy remains unchanged at lower temperatures, an extrapolation to 50°C leads to a predicted elongation lifetime (50% absolute) of ~ 300 years. Even though there is no data available to probe the extrapolation region for this material, this "Arrhenius" extrapolated lifetime is quite large and therefore offers reasonable assurance that this material would be viable for more than 60 years at 50°C aging temperature. In particular the 106 kJ/mol activation energy found above 101°C would have to drop to an average E_a of ~35 kJ/mol (8.4 kcal/mol) from 101°C to 50°C (a 65% drop) in order to reduce the 50°C lifetime to 60

years. Since such a large drop in E_a has never been reported over such a small temperature range, we conclude that the EPR-01A material should have a very long lifetime at typical aging temperatures encountered during aging of nuclear power plants. The situation for EPR-04 is more complex as shown by its elongation results given in Fig. III-35. It is clear that the shapes of the curves versus aging temperature are different, transitioning from sharper drop-offs in elongation values at higher temperatures to gentler drop-offs at lower temperatures. This implies that raising the aging temperature does not equally accelerate all reactions underlying degradation, contradicting the fundamental assumption underlying accelerated aging. This means that time-temperature superposition will fail, as evidenced by Fig. III-36, where the results from Fig. III-35 are superposed in the rapid drop-off region (for elongation values less than ~150%). Although nice superposition results in this region, lack of superposition for elongation values greater than 150% is obvious. If, on the other hand, we focus only on the elongation results above 150%, reasonable superposition can be achieved as seen in Fig. III-37 using empirical shift factors that differ from those used in Fig. III-36. From Arrhenius plots of the two sets of shift factors shown in Fig. III-38 it can be seen that the activation energy appropriate to early degradation is ~100 kJ/mol whereas the activation energy relevant to the induction time region is ~128 kJ/mol. Given the uncertainties inherent in extrapolating nicely behaved Arrhenius results, attempting to extrapolate results for EPR-04 would be even more problematic and dangerous. However, it should be noted that our accelerated studies involved aging times up to ~ 7 years at 99°C. With "practical end of life" requiring ~ 7 years at this temperature, the activation energy from 99°C to 50°C would have to drop to an average value of ~ 44 kJ/mol (10.5 kcal/mol) in order for the extrapolated 50°C lifetime to be less than 60 years.

The elongation results at four temperatures for the EPR-03 cable insulation material are shown in Fig. III-39. For this material the elongation values barely change until they plummet at the induction time. Superposition of the results at the lowest aging temperature of 109°C is shown in Fig. III-40- the superposition is excellent. This is not surprising given the almost pure induction time behavior that guarantees essentially identical shapes for the aging curves at the various aging temperatures. An Arrhenius plot of the empirically derived shift factors, given in Fig. III-41, indicates approximately linear (Arrhenius) behavior with an Arrhenius activation energy of ~106 kJ/mol. Extrapolation of this activation energy to 50°C leads to a predicted lifetime of ~1600 years at this temperature. Again a radical drop in E_a would be necessary in order to not have a lifetime exceeding 60 years at 50°C. It is interesting to note that the aging at 124°C, 138°C and 160°C are all above the crystalline melting point region (see Fig. III-31), implying that aging occurs at these temperatures for totally melted material (no crystallinity). At 109°C, on the other hand, aging occurs for a partially crystalline material. Since there is no evidence of a change in slope in the Arrhenius plot at this lowest aging temperature, the data suggest that extrapolating across the crystalline melting point may have little effect for this material.

The elongation results for the other semi-crystalline EPR material (EPR-05) are given in Fig. III-42; these data have somewhat higher scatter than the results for the other three EPR materials. Since 99°C represents the lowest aging temperature examined for this

material, all of the aging conditions were above the crystalline melting point region (Fig. III-31). Time-temperature superposition of the elongation data is shown in Fig. III-43 and an Arrhenius plot of the shift factors is given in Fig. III-44. The Arrhenius plot gives reasonable linearity with an activation energy of ~ 88 kJ/mol. An extrapolation of this activation energy to 50°C predicts a lifetime of ~300 years. In order for the lifetime to fall below 60 years at this temperature, the average E_a from 99°C to 50°C would have to drop below ~ 56 kJ/mol (13.4 kcal/mol).

A summary of the results for our four EPR materials plus an additional EPR cable insulation material studied by Anandakumaran and Stonkus [III-19] are given in Figure III-45. This figure shows an Arrhenius plots of the times required for the elongation to reach 50% absolute for the five EPR cable insulation materials with the EPR studied by Anandakumaran and Stonkus labeled EPR-A&S. Even though the least robust material is EPR-01A, a simple extrapolation of the activation energy found at high temperatures for this material leads to long lifetimes (~300 years) at an aging temperature of 50°C. The other four EPR cable insulations appear to have high temperature lifetimes similar to each other and extrapolations indicate lifetimes equal to or greater than that of the EPR-01A material. It is interesting to note that the degradation and the practical end of life of the EPR-01A material are dominated by copper-catalyzed oxidation, a mechanism not observed for the other materials. This can be seen by examining density profiling results [III-20] as shown in Fig. III-46. This figure shows how the density of samples aged at 101°C for various times vary across the cross-section of the insulation. For the unaged material, the density is approximately constant across the cross-section (dashed line). With aging, large density increases occur in the material located near the inner surface and this phenomenon was shown to be due to the presence of copper-catalyzed oxidation [III-21]. It is likely that this degradation mechanism is the reason that EPR-01A degrades somewhat faster than the other EPR materials.

Crosslinked polyolefin (XLPO) cable insulation materials

Similar to EPR materials, crosslinked polyolefins constitute a huge diversity of semi-crystalline materials with differing base polymers, differing additives and widely varying properties and aging susceptibilities. In this section we discuss results for three XLPO materials.

The XLPO-04 material is a chemically crosslinked polyethylene material with a single crystalline melting point of ~124°C [III-22]. For this material, already discussed above (Figs. III-1 through III-4) oven aging was conducted at nine temperatures ranging from 91°C to 170°C. Since the crystalline melting point T_{mp} is ~124°C, aging was done at four temperatures below T_{mp} as well as five above T_{mp}. As is clear from the results shown in Fig. III-4, the linearity of the observed Arrhenius results was not affected by T_{mp}. This means for the XLPO-04 material, there are no concerns over the effect of the crystalline melting point region on the Arrhenius extrapolation assumption.

The second crosslinked polyolefin material studied (XLPO-02B) appeared to be a medium to high density ethylene-vinylacetate copolymer based material [III-23]. It has a

complex melting point region containing a major peak at ~119°C and a smaller peak at ~89°C as shown from the DSC results (Fig. III-47). For this material oven aging was carried out at 99°C, 109°C, 125°C and 152 °C with the resulting elongation values shown on Fig. III-48. The long-term exposures at 109°C and 99°C (the aging at 99°C is still ongoing after more than 11 years exposure) allowed us to probe the degradation occurring below the major melting peak as seen in Fig. III-47. Unfortunately, it is immediately apparent from the elongation results shown in Fig. III-48, that the shapes of the degradation curves for aging temperatures above the main melting point (119°) differ from those for temperatures below 119°C. This is in clear contrast to the results found above for the XLPO-04 material where data taken above and below the melting point had similar shapes and therefore showed excellent time-temperature superposition. The lack of superposition for XLPO-02B is clear if we try to time-temperature superpose the elongation results (Fig. III-49), using 150% elongation as the basis for the superposition. It is obvious from the non-superposition of the results that the shift factors listed on the figure for 125°C and 151.5°C are meaningless and cannot be used for further analyses. It does appear, however, that reasonable superposition occurs for the two temperatures below the main melting point as can also be seen in Fig. III-50. If we use the shift factor of 1.9 found in Fig. III-50 between 99°C and 109°C, this leads to an activation energy of 76 kJ/mol (18.1 kcal/mol) between these two temperatures. Using this E_a to extrapolate the lower x-axis time scale at 99°C to 50°C leads to the upper x-axis time scale shown in the figure. For a 50% residual elongation this extrapolation predicts a 470-year lifetime at 50°C, not really surprising given that practical end of life has not been reached after 11 years at 99°C. To have the predicted lifetime drop below 60 years at 50°C would require the E_a to drop to an average value of ~33 kJ/mol, an exceedingly low E_a.

The final XLPO material investigated (XLPO-05) had a much more complex DSC melting point region as evidenced by the results shown in Fig. III-51. It appears to be based on a block-copolymer structure with distinct low-density polyethylene and mid density polyethylene units [III-23]. Oven aging on three separate colors of this insulation (green, red and black) was carried out at 151°C, 138°C, 124°C and 109°C (the latter is ongoing with ~ 3 years exposure to date). Elongation results to date for the three different colors are shown in Figs. III-52 through III-54. Overall the data show more scatter than the other XLPO insulation materials. Even so, the results indicate that the degradation rates depend on the color of the insulation with the green material clearly degrading faster than red and red degrading slightly faster than black. Up to the present, not enough degradation has occurred at 109°C to allow these data to be used in superposition analyses. Therefore we can only superpose data at 124°C and higher so that all of our analyses reflect totally amorphous material (see Fig. III-51). The resulting superposed results for the three colors of insulation are shown in Figs. III-55 through III-57. The empirically derived shift factors from these three figures are then plotted on an Arrhenius plot and the results (Fig. III-58) indicate an Arrhenius activation energy of ~130 kJ/mol. If this very high E_a remained valid from 124°C to 50°C, the extrapolation would yield the time scales shown as the upper x-axes of Figs. III-55 through III-57. As indicated by the dashed line on Fig. III-55, this extrapolation would predict a 50°C lifetime for the green insulation of 24,000 years and even higher lifetimes for the red and

black colored insulations. Of course this extrapolation is ridiculous for many reasons. These include the fact that the extrapolation distance is quite long (four orders of magnitude) compared to the distance over which data was acquired (one order of magnitude). In addition all of the data was taken on completely amorphous material so that the extrapolation was through the entire crystalline melting point region of XLPO-05. Even with these caveats it is encouraging that the lifetime at 124°C is on the order of 2 years implying that the average E_a from 124°C to 50°C would have to drop below ~ 49 kJ/mol to have less than a 60-year lifetime at 50°C.

Conclusions

We saw in this section how the use of time-temperature superposition principles improves the testing of the Arrhenius model by utilizing all of the experimentally generated data instead of a few selected and processed data points. This allows one to quantitatively test the fundamental basis underlying accelerated aging protocols, the assumption that raising the temperature equally accelerates all of the reactions underlying degradation. Using rarely available long-term data on important nuclear power plant cable jacketing and insulation materials we showed that non-superposition will often occur (EPR-04, XLPO-02B) violating the constant acceleration assumption. In addition the long-term results allowed us to show that curvature in Arrhenius plots for elongation are commonly observed if data are taken over a large enough temperature range (Neo-01, several hypalon materials). The long-term results also allowed us to test the significance of extrapolating through the crystalline melting point region of semi-crystalline materials where we found that some materials are unaffected by such an extrapolation (XLPO-04) while others can show important effects (XLPO-02B). Based on the results given in this section, we concluded that chloroprene based cable jackets may sustain significant degradation after decades of aging at 50°C whereas hypalon and CPE jackets should sustain much less damage under these conditions. For the EPR and XLPO cable insulations, simple Arrhenius extrapolations imply exceedingly long lifetimes. Even though there is significant concern about such extrapolations due to possible crystalline melting point effects and the possibility of downward curvature in the Arrhenius plots in the extrapolation region, the long-term data generated in the current study offers much confidence in the long-term viability of such materials. In the next section of this report, we bolster such confidence by utilizing ultrasensitive oxygen consumption (UOC) measurements to probe the low temperature extrapolation region, thereby obtaining information on how the oxidation that dominates degradation depends on temperature in the low-temperature extrapolation region.

References

III-1. K. T. Gillen, M. Celina, R. L. Clough and J. Wise, "Extrapolation of Accelerated Aging Data- Arrhenius or Erroneous?", Review paper in **Trends in Polymer Science,** 5, 250 (1997).

III-2. K. T. Gillen, M. Celina and M. R. Keenan, "Methods for Predicting More Confident Lifetimes of Seals in Air Environments", Rubber Chem. Technol., 73, 265 (2000).

III-3. J. Wise, K. T. Gillen and R. L. Clough, "An Ultrasensitive Technique for Testing the Arrhenius Extrapolation Assumption for Thermally-Aged Elastomers", Polym. Degrad. & Stabil., 49, 403 (1995).

III-4. Richters P. Initiation Process in the oxidation of polypropylene. Macromolecules 1970;3:262.

III-5. Howard JB, Gilroy HM. Some observations on the long-term behavior of stabilized polyethylene. Polym Eng Sci, 1975;15:268.

III-6. Chan MG, Gilroy HM, Martin, WM. Long-term aging properties of polyolefins. Proc. Polyolefins IV, SPE Reg Tech Conf., Houston, Texas, 1984, p. 167.

III-7. Bernstein BS, Lee PN. Proc. 24th Int. Wire and Cable Symp., Nov. 1975, p. 202.

III-8. Gijsman P, Hennekens J, Vincent J. The influence of temperature and catalyst residues on the degradation of unstabilized polypropylene. Polym Degrad Stab, 1993;39:271.

III-9. Rosik L, Kovarova J, Pospisil J. Lifetime prediction of ABS polymers based on thermoanalytical data. J. Thermal Anal, 1996;46:465.

III-10. Gugumus F. Effect of temperature on the lifetime of stabilized and unstabilized PP films. Polym Degrad Stab, 1999;63:41.

III-11. K. T. Gillen, R. Bernstein and D. K. Derzon, "Evidence of non-Arrhenius Behavior from Laboratory Aging and 24-year Field Aging of Chloroprene Rubber Materials, Polymer Degradation and Stability, 87, 57 (2005).

III-12. Gillen KT, Clough RL. Accelerated aging methods for predicting long-term mechanical performance of polymers. In: Clegg DW, Collyer AA, editors. Irradiation Effects on Polymers. London: Elsevier Applied Science, 1991. Ch. 4.

III-13. K. Anandakumaran, W. Seidl and P. V. Castaldo, "Condition Monitoring of Cable Insulation Systems in Operating Nuclear Power Plants", IEEE Transactions on Dielectrics and Electrical Insulation, 6, 376 (1999).

III-14. G. Toman, EPRI Project Manager, "Initial Criteria Acceptance Concepts and Data for Assessing Longevity of Low-Voltage Cable Insulations and Jackets", EPRI Technical Report 1008211, Final Report, March, 2005.

III-15. K. T. Gillen, R. Bernstein and M. Celina, "Non-Arrhenius Behavior for Oxidative Degradation of Chlorosulfonated Polyethylene Materials", Polymer Degradation and Stability, 87, 335 (2005).

III-16. Nelson CF, Gauthier G, Carlin F, Attal M, Gaussens G, Le Tutour P, Morin C. Long-term radiation aging and loss-of-coolant accident (LOCA) testing of electrical cables, Sandia National Laboratories report SAND94-0485, October, 1996.

III-17. M. Morton, "Rubber Technology", 3rd Edition, Van Nostrad Reinhold Company, New York, 1987.

III-18. J. A. Brydson, “Rubbery Materials and their Compounds”, Elsevier Applied Science, London, 1988.
III-19. K. Anandakumaran and D. J. Stonkus, “Assessment of Oxidative Thermal Degradation of Crosslinked Polyethylene and Ethylene Propylene Rubber Cable Insulation”, Polym. Eng. Sci., 32, 1386 (1992).
III-20. K. T. Gillen, R. L. Clough and N. J. Dhooge, "Density Profiling of Polymers", Polymer, 27, 225 (1986).
III-21. K. T. Gillen and R. L. Clough, Inhomogeneous Radiation Degradation in Polymers Studied with a Density Gradient Column”, Radiat. Phys. Chem., 22, 537 (1983).
III-22. K. T. Gillen and R. L. Clough, “Aging Predictions in Nuclear Power Plants-Crosslinked Polyolefin and EPR Cable Insulation Materials”, SAND91-0822 (June, 1991).
III-23. M. Celina, K. T. Gillen and R. L. Clough, “Inverse Temperature and Annealing Phenomena During Degradation of Crosslinked Polyolefins”, Polym. Degrad. Stabil., 61, 231 (1998).

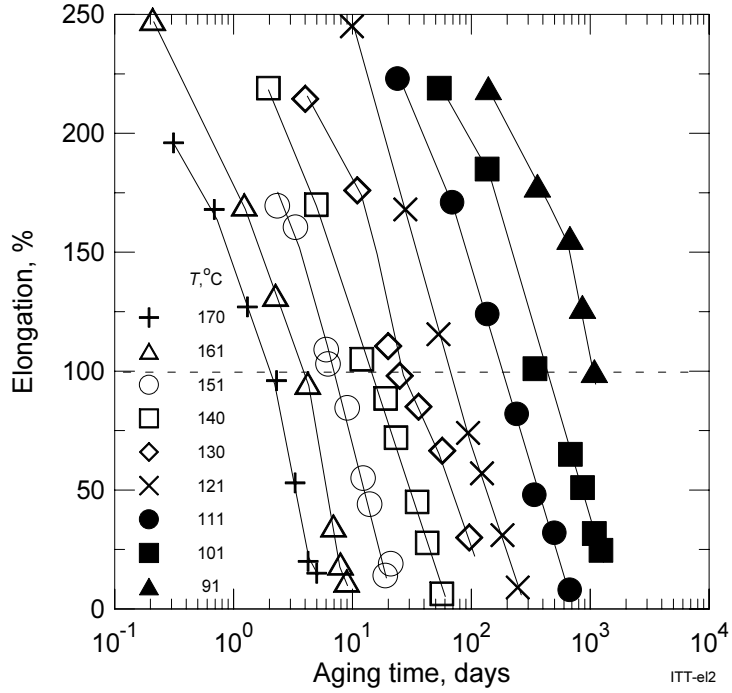

Figure III-1. Elongation versus time at the indicated temperatures for XLPO-04 cable jacketing material.

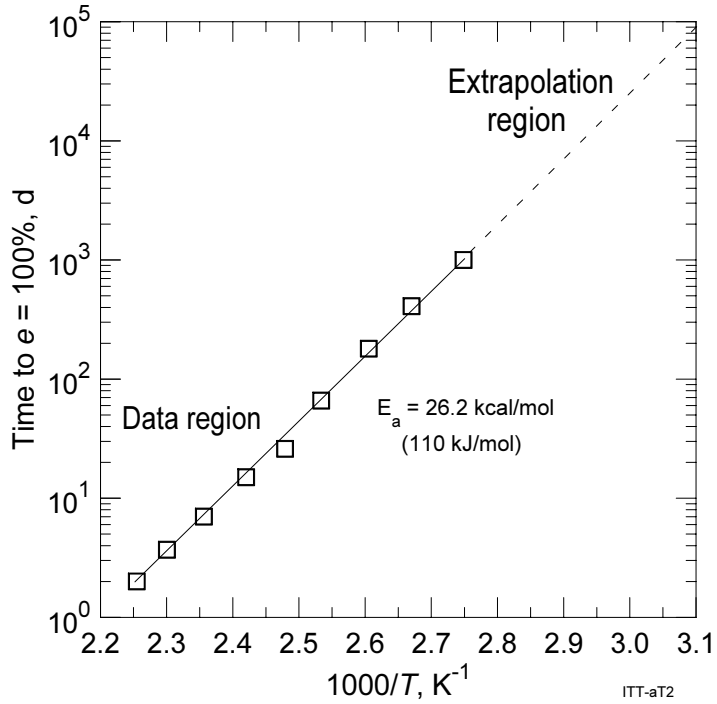

Figure III-2. Arrhenius plot of the log of the time for the elongation to reach 100% versus the inverse absolute aging temperature for XLPO-04.

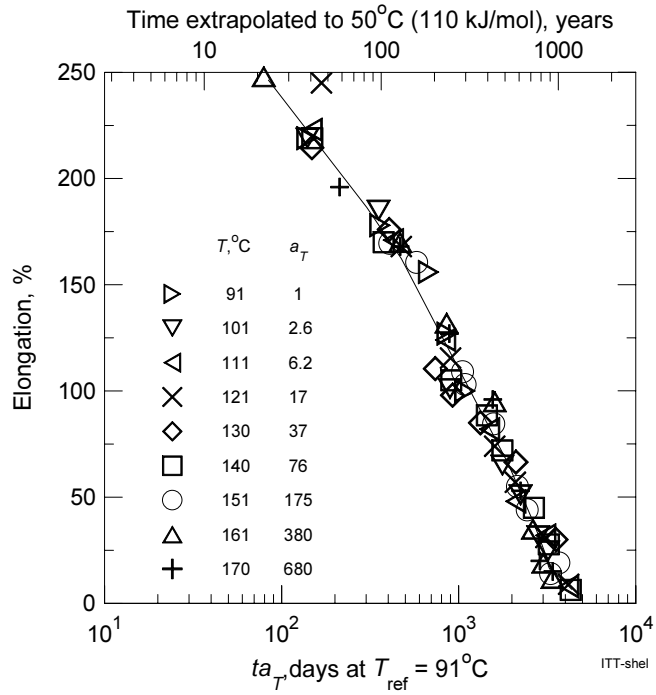

Figure III-3. Time-temperature superposed elongation results for XLPO-04 from Fig. III-1 at a reference temperature of 91°C (shift factors used are indicated on the figure).

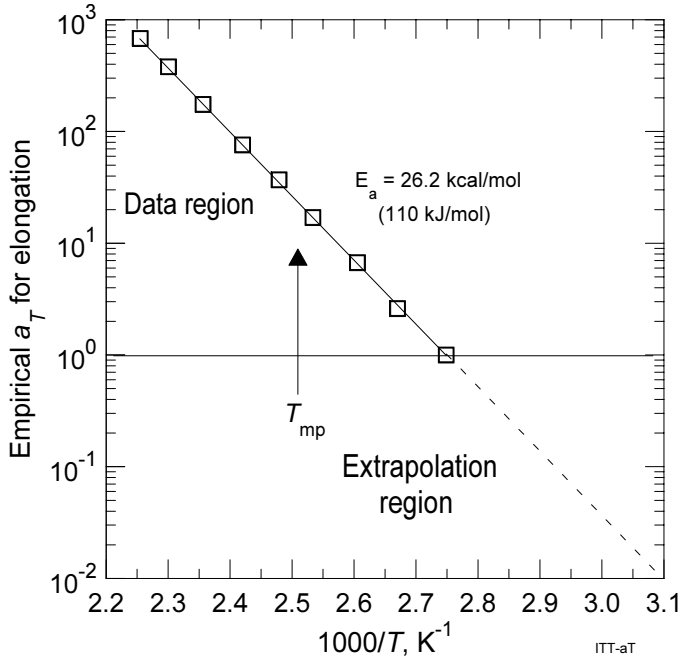

Figure III-4. Arrhenius plot for XLPO-04 of the shift factors from Fig. III-3 (T_{mp} indicates the crystalline melting point).

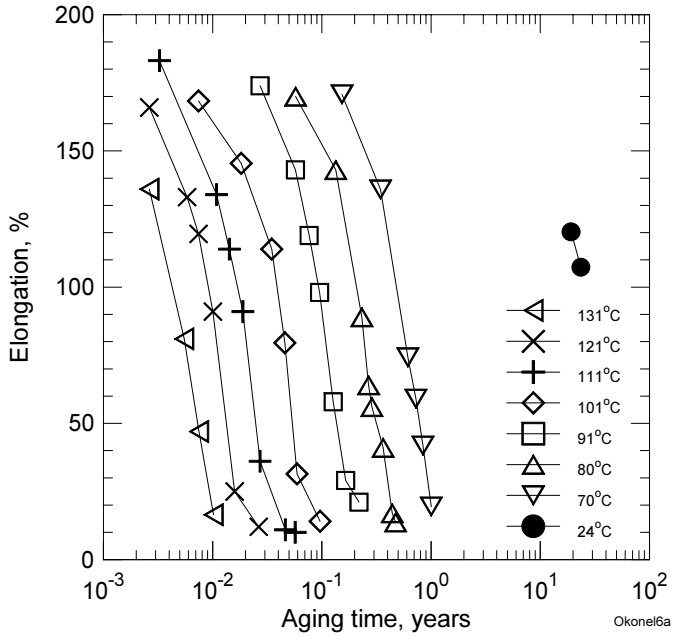

Figure III-5. Elongation versus time at the indicated temperatures for Neo-01 cable jacketing material.

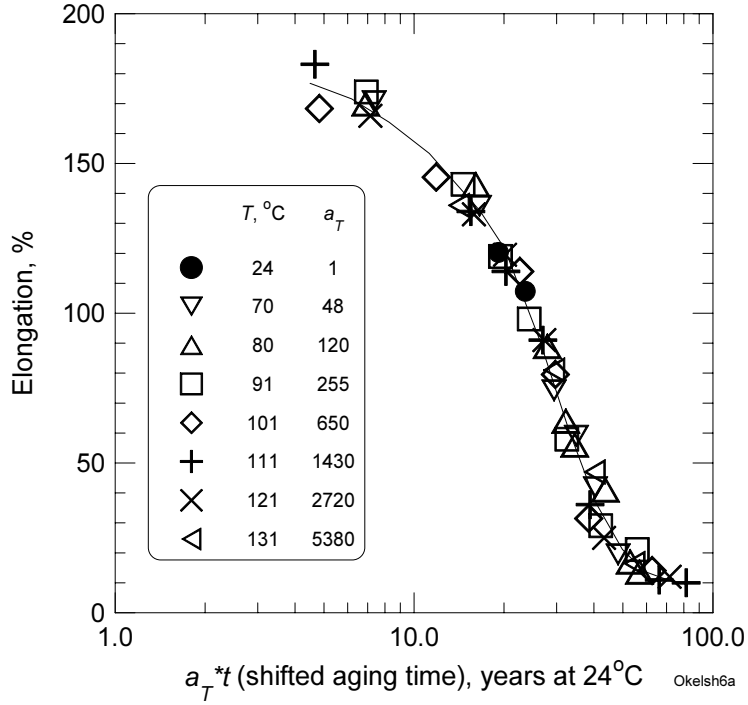

Figure III-6. Time-temperature superposed elongation results for Neo-01 from Fig. III-5 at a reference temperature of 24°C (shift factors used are indicated on the figure).

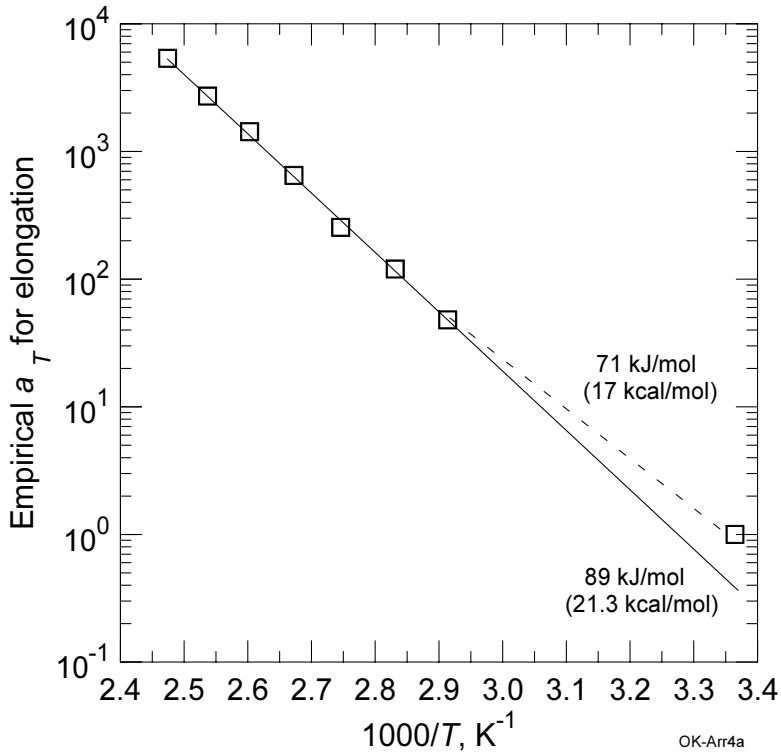

Figure III-7. Arrhenius plot for Neo-01 of the shift factors from Fig. III-6.

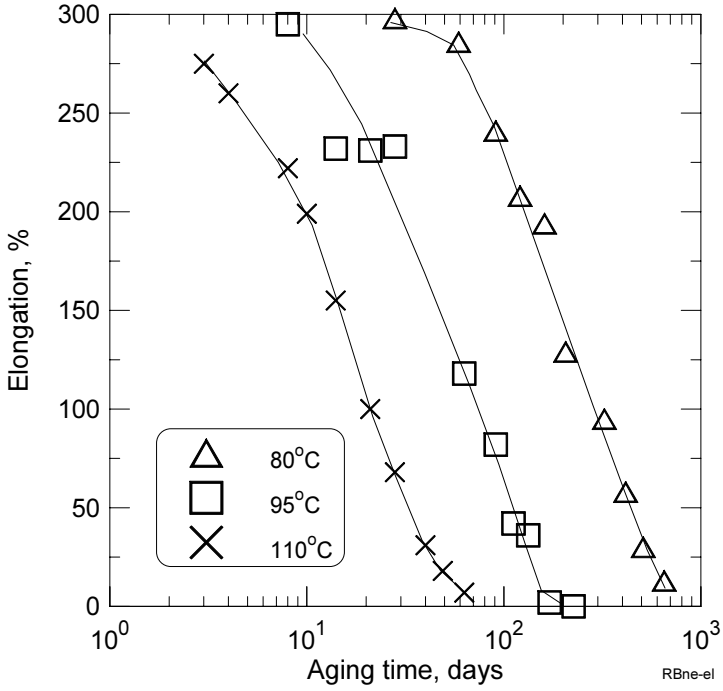

Figure III-8. Elongation versus time at the indicated temperatures for Neo-02 cable jacketing material.

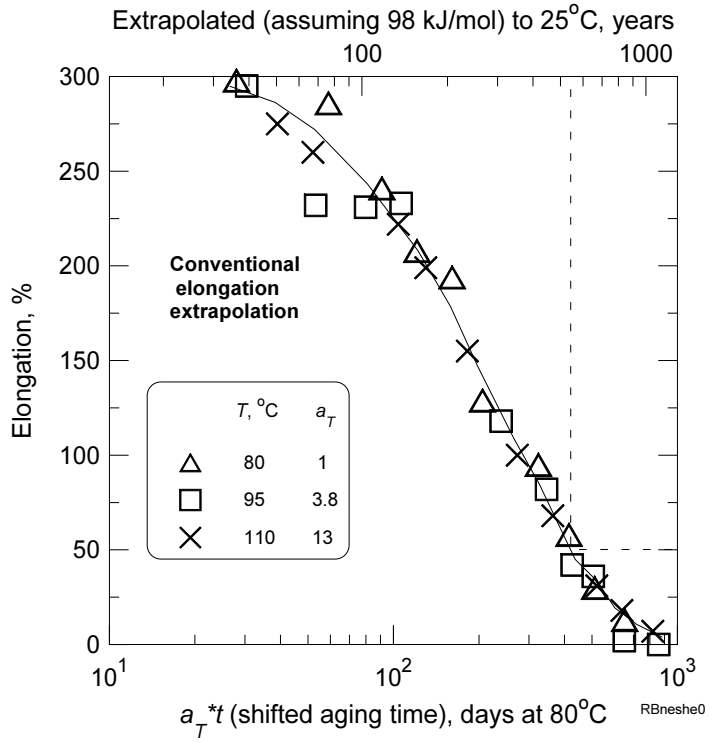

Figure III-9. Time-temperature superposed elongation results for Neo-02 from Fig. III-8 at a reference temperature of 25°C (shift factors used are indicated on the figure).

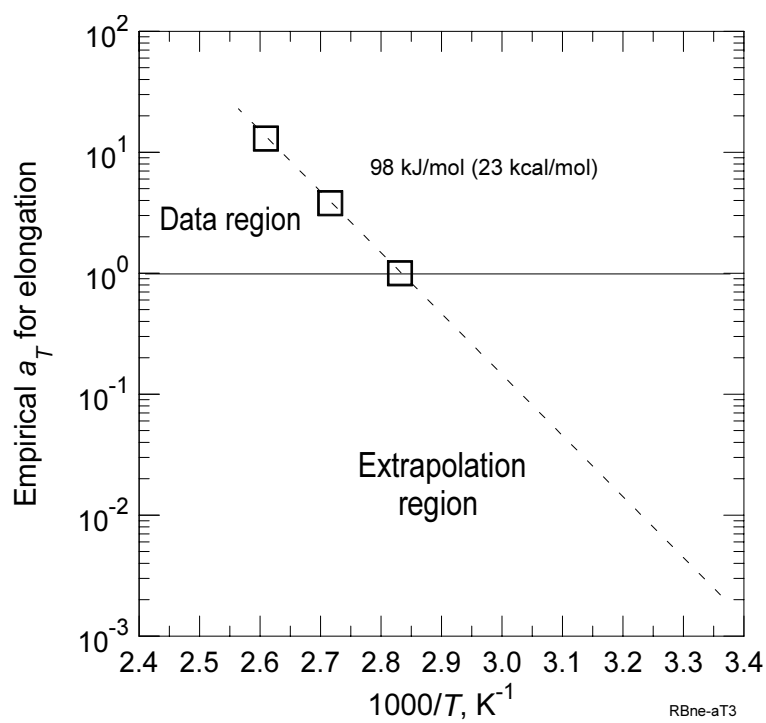

Figure III-10. Arrhenius plot for Neo-02 of the shift factors from Fig. III-9.

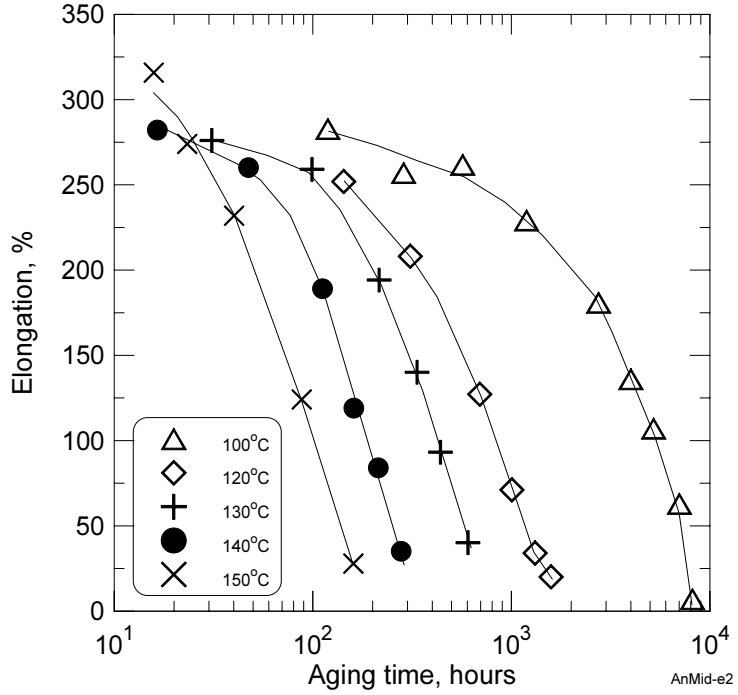

Figure III-11. Elongation versus time at the indicated temperatures for Hyp-01A cable jacketing material.

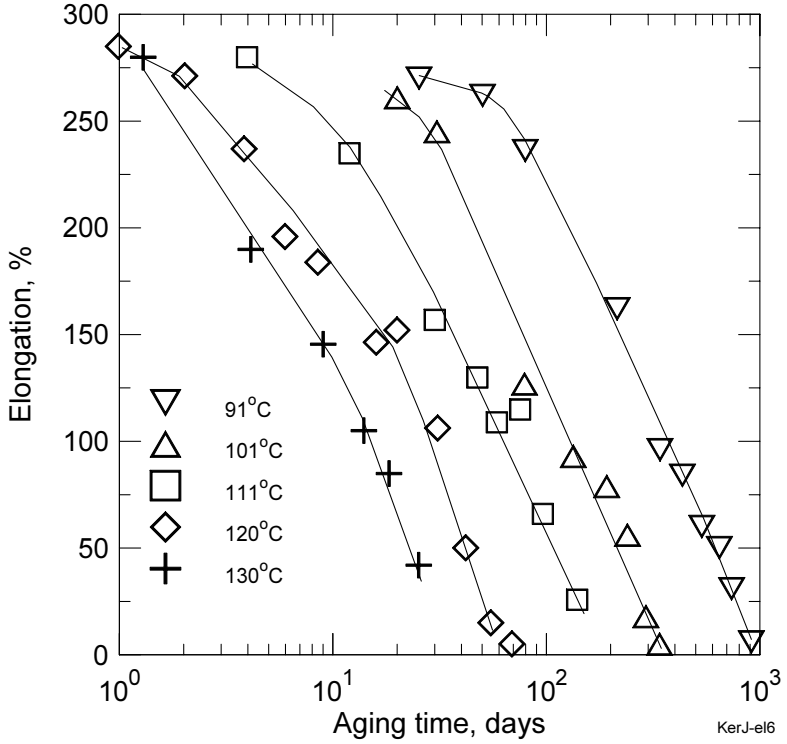

Figure III-12. Elongation versus time at the indicated temperatures for Hyp-02 cable jacketing material.

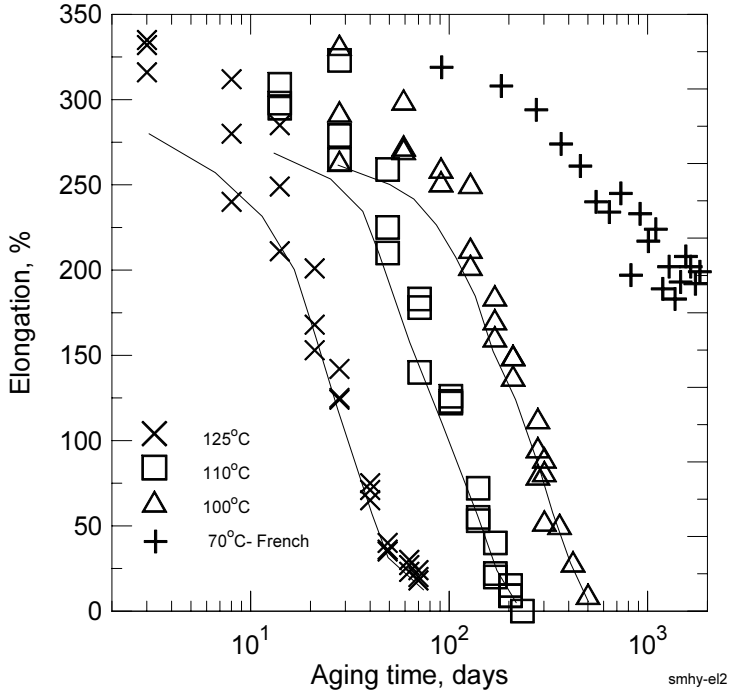

Figure III-13. Elongation versus time at the indicated temperatures for Hyp-03 cable jacketing material.

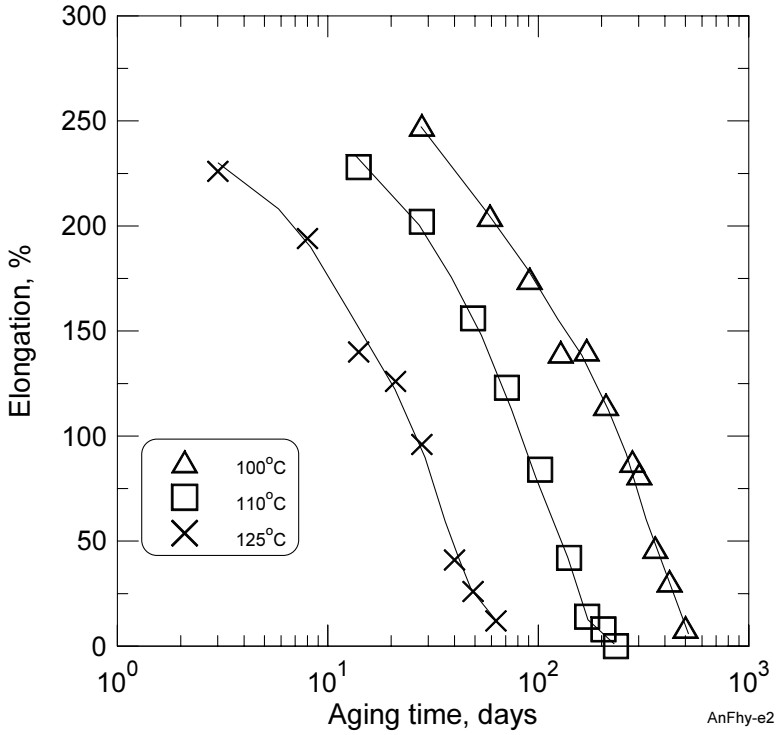

Figure III-14. Elongation versus time at the indicated temperatures for Hyp-04 cable jacketing material.

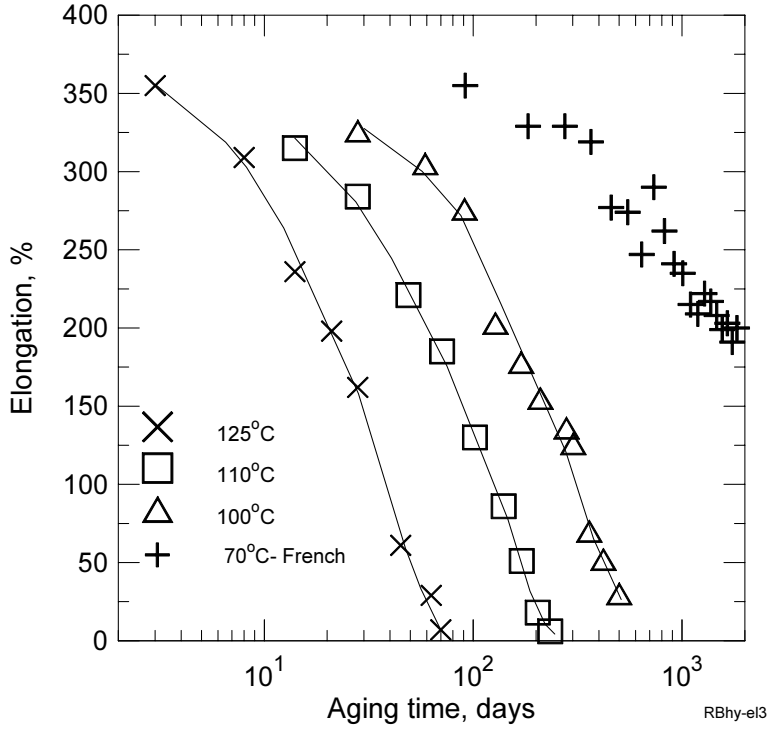

Figure III-15. Elongation versus time at the indicated temperatures for Hyp-05 cable jacketing material.

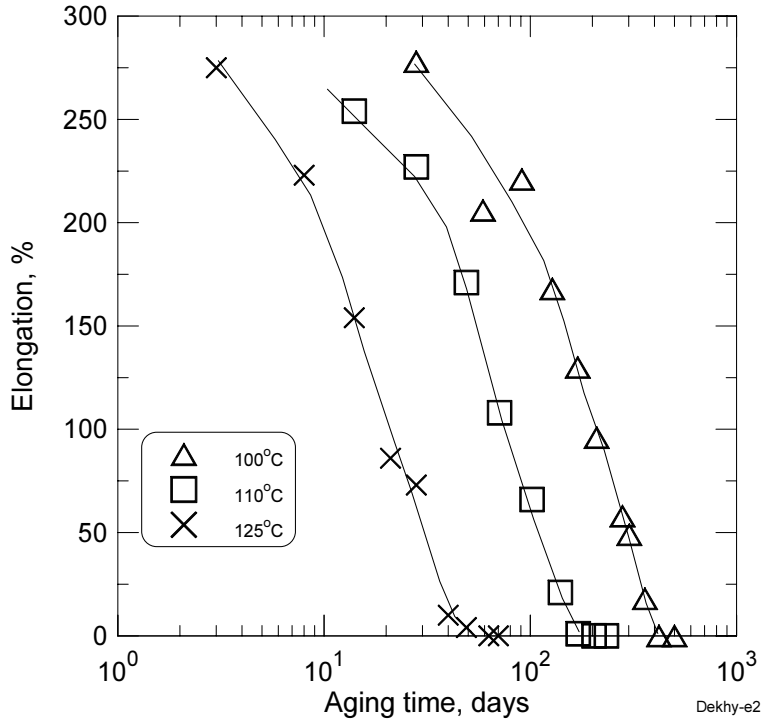

Figure III-16. Elongation versus time at the indicated temperatures for Hyp-06 cable jacketing material.

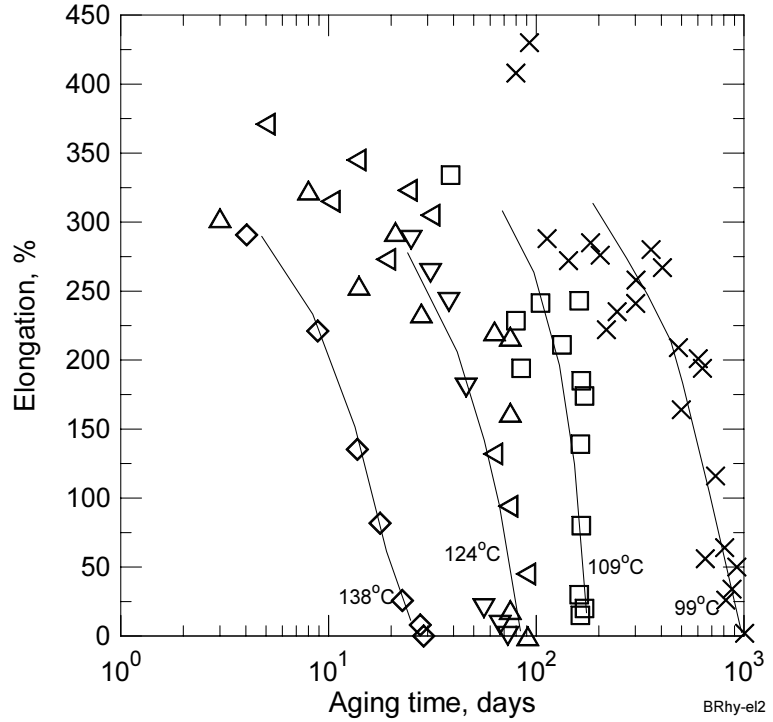

Figure III-17. Elongation versus time at the indicated temperatures for Hyp-07 cable jacketing material.

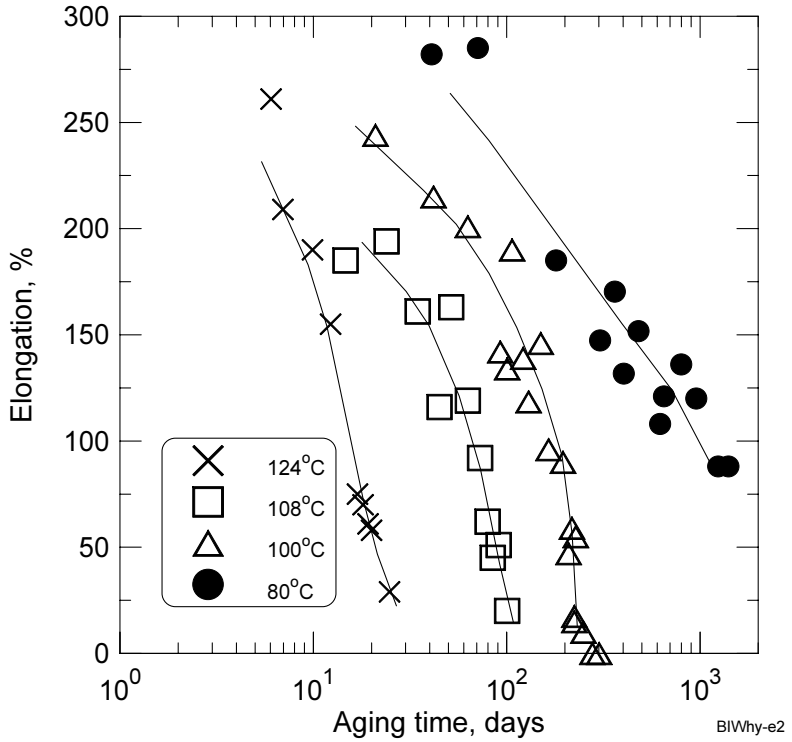

Figure III-18. Elongation versus time at the indicated temperatures for Hyp-08 cable jacketing material.

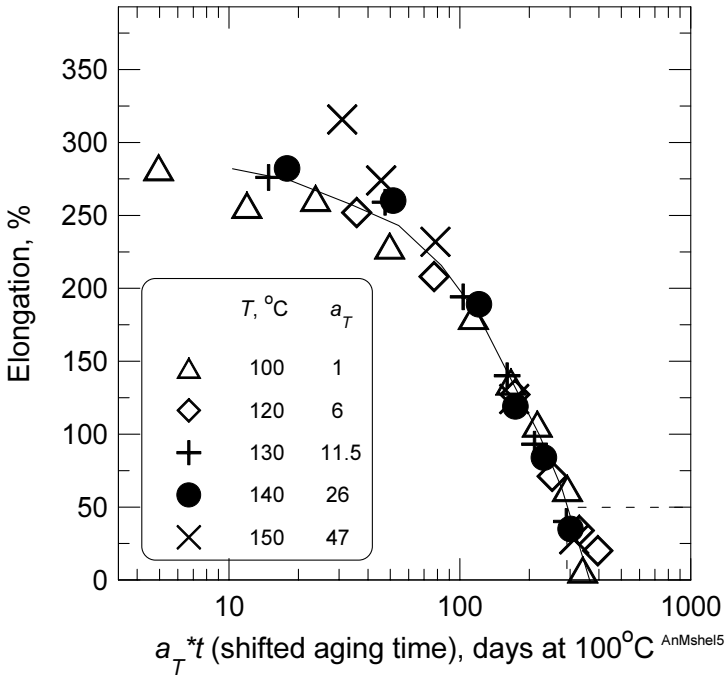

Figure III-19. Time-temperature superposed elongation results for Hyp-01A from Fig. III-11 at a reference temperature of 100°C (shift factors used are indicated on the figure).

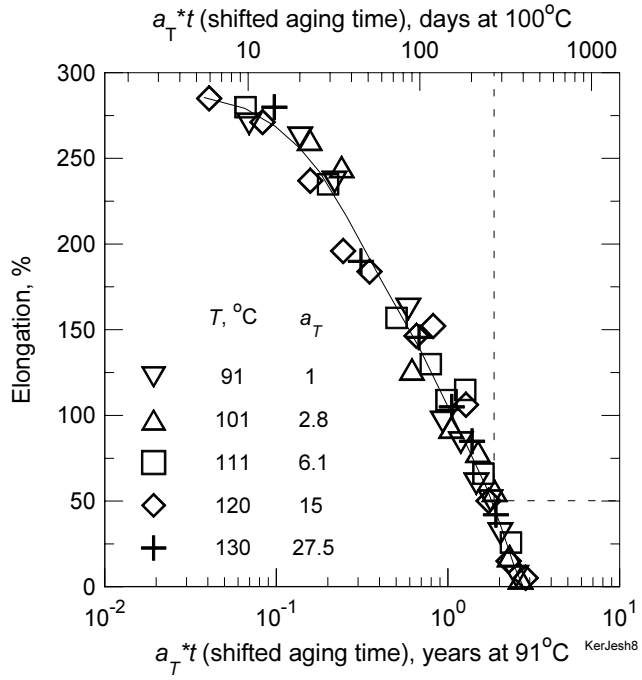

Figure III-20. Time-temperature superposed elongation results for Hyp-02 from Fig. III-12 at a reference temperature of 91°C (bottom x-axis). Top x-axis shows superposed results at 100°C.

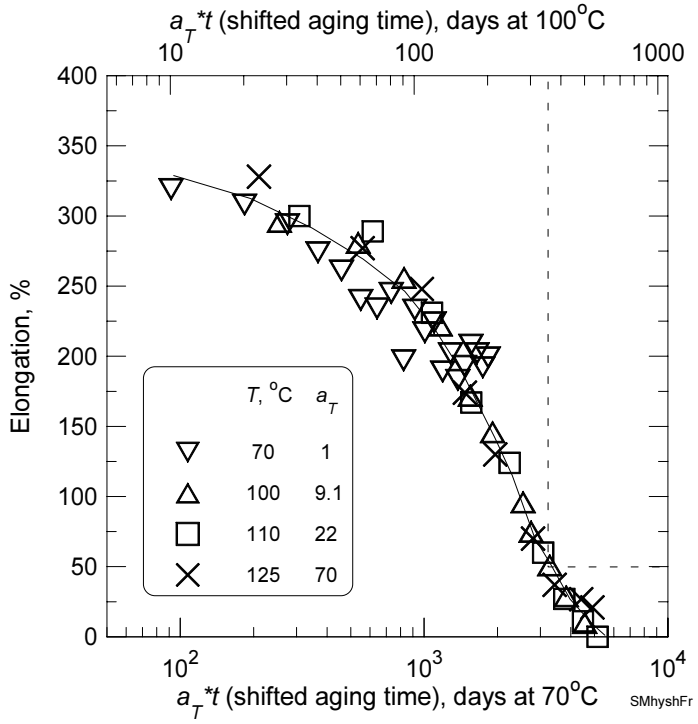

Figure III-21. Time-temperature superposed elongation results for Hyp-03 from Fig. III-13 at a reference temperature of 70°C (bottom x-axis). Top x-axis shows superposed results at 100°C.

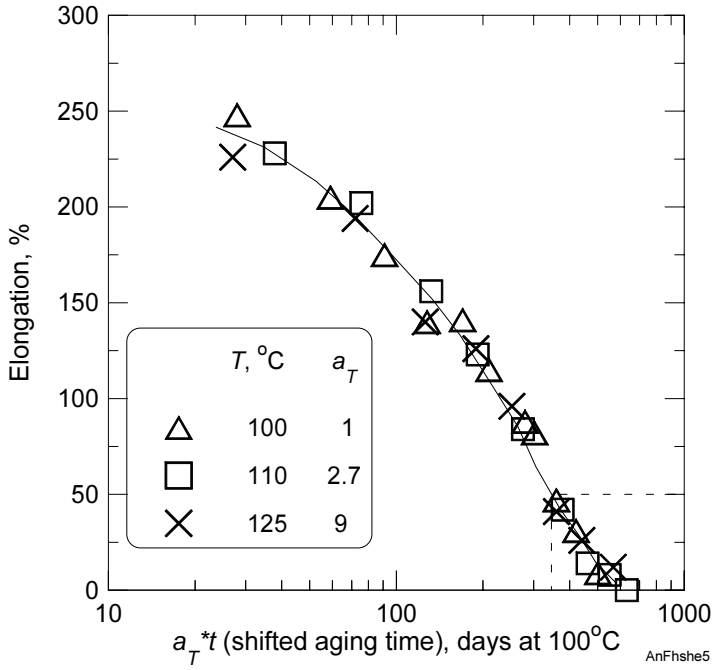

Figure III-22. Time-temperature superposed elongation results for Hyp-04 from Fig. III-13 at a reference temperature of 100°C.

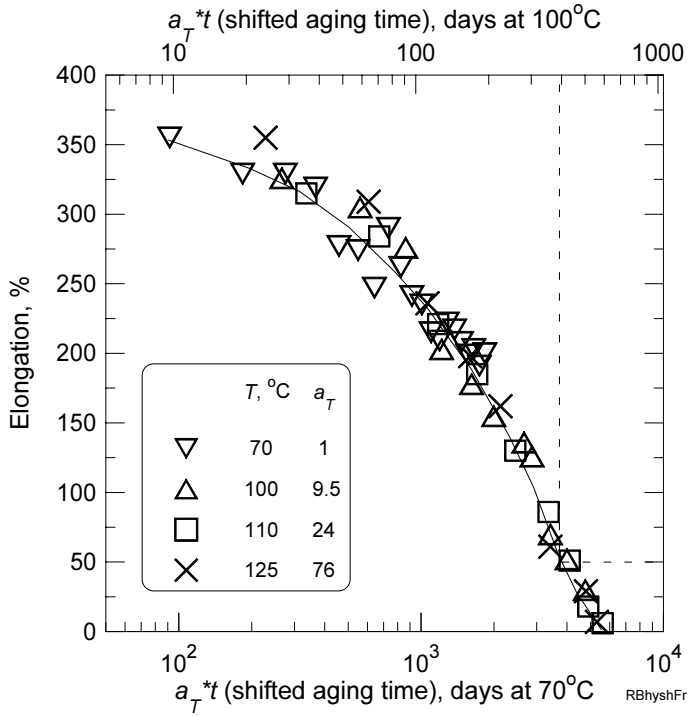

Figure III-23. Time-temperature superposed elongation results for Hyp-05 from Fig. III-15 at a reference temperature of 70°C (bottom x-axis). Top x-axis shows superposed results at 100°C.

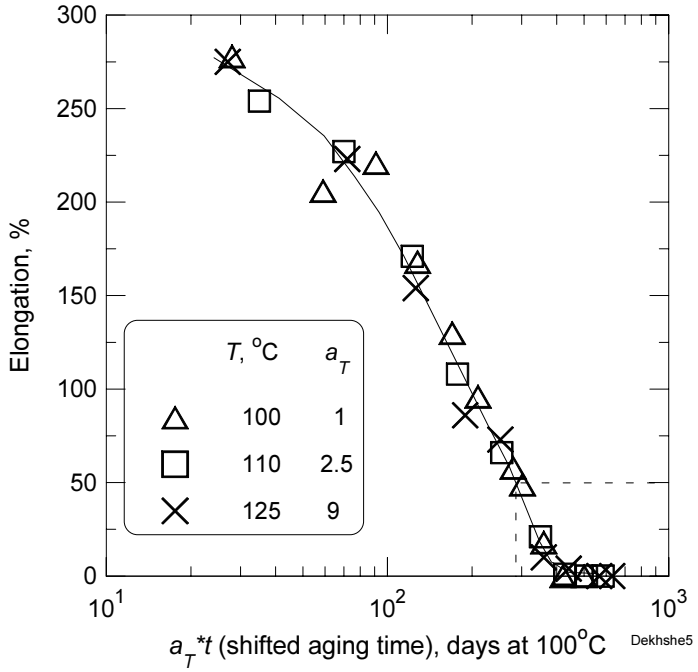

Figure III-24. Time-temperature superposed elongation results for Hyp-06 from Fig. III-16 at a reference temperature of 100°C.

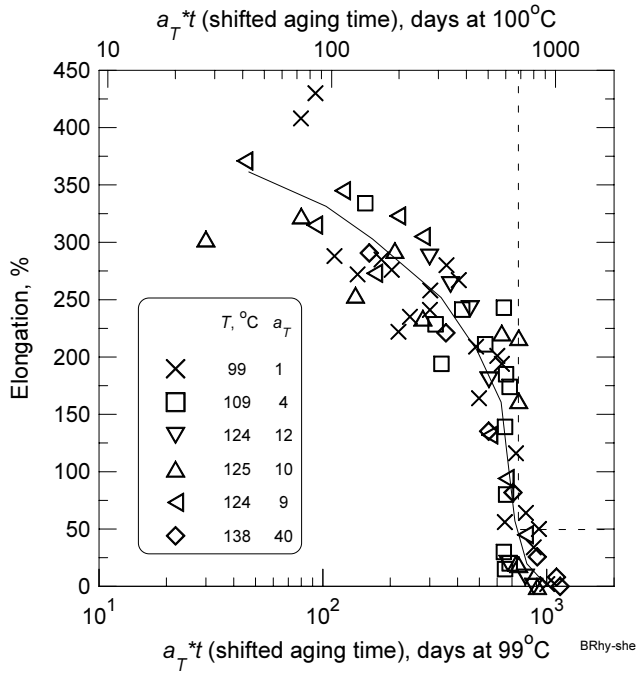

Figure III-25. Time-temperature superposed elongation results for Hyp-07 from Fig. III-17 at a reference temperature of 99°C (bottom x-axis). Top x-axis shows superposed results at 100°C.

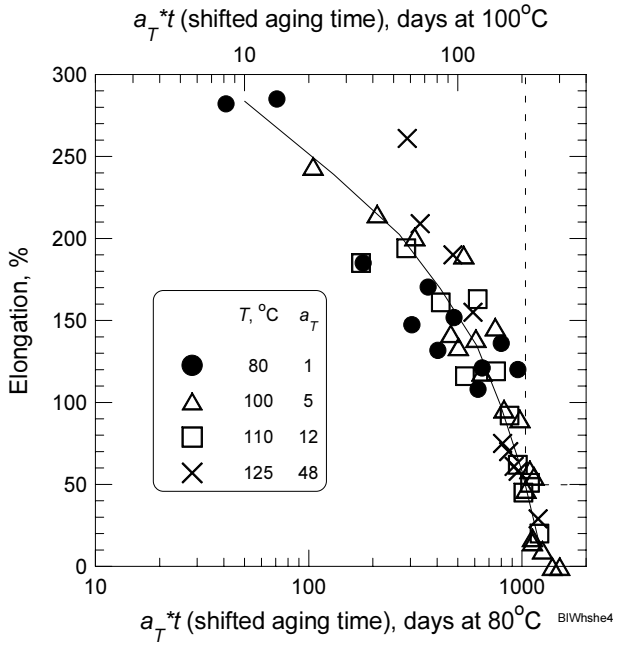

Figure III-26. Time-temperature superposed elongation results for Hyp-08 from Fig. III-18 at a reference temperature of 80°C (bottom x-axis). Top x-axis shows superposed results at 100°C.

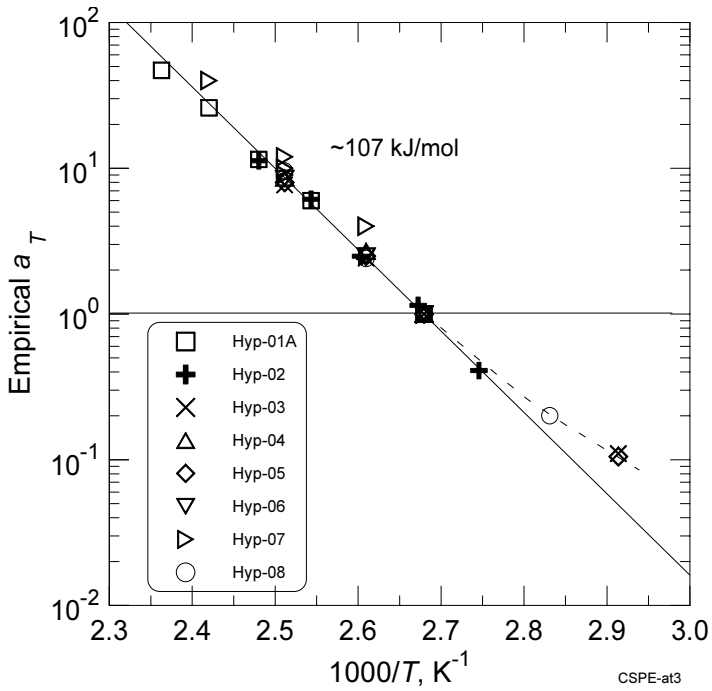

Figure III-27. Arrhenius plot of the empirically derived shift factors for elongation of the eight hypalon jacketing materials all normalized to unity at 100°C.

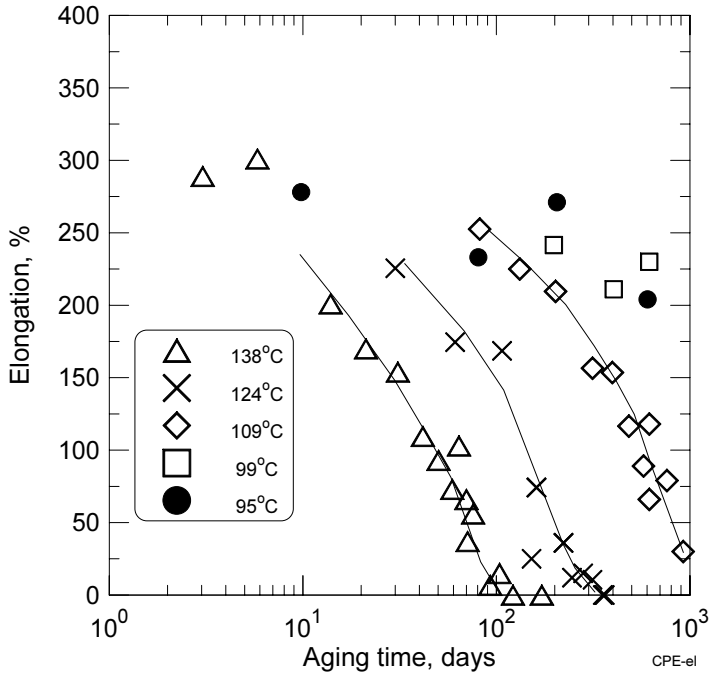

Figure III-28. Elongation versus time at the indicated temperatures for CPE-02 cable jacketing material.

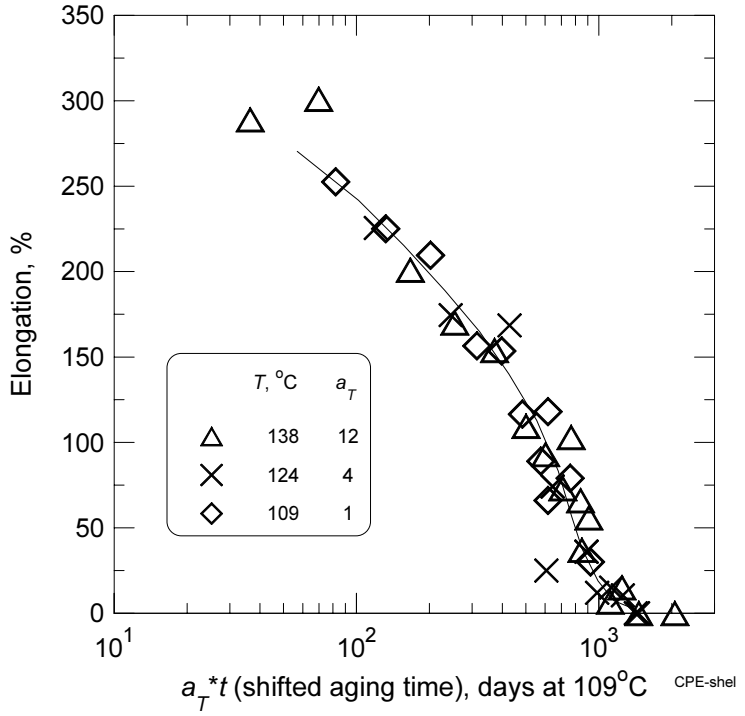

Figure III-29. Time-temperature superposed elongation results for CPE-02 from Fig. III-28 at a reference temperature of 109°C.

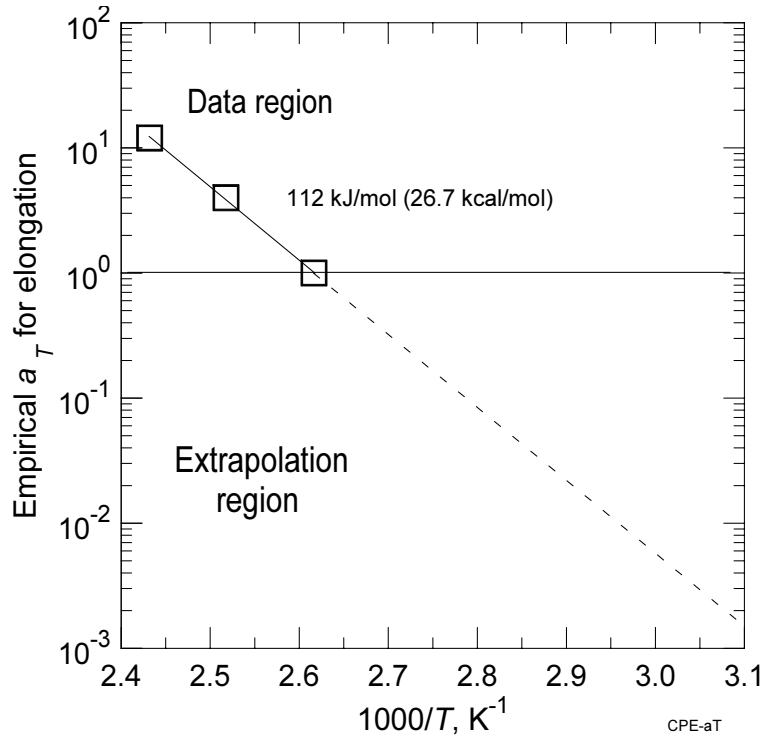

Figure III-30. Arrhenius plot for CPE-02 of the shift factors from Fig. III-29.

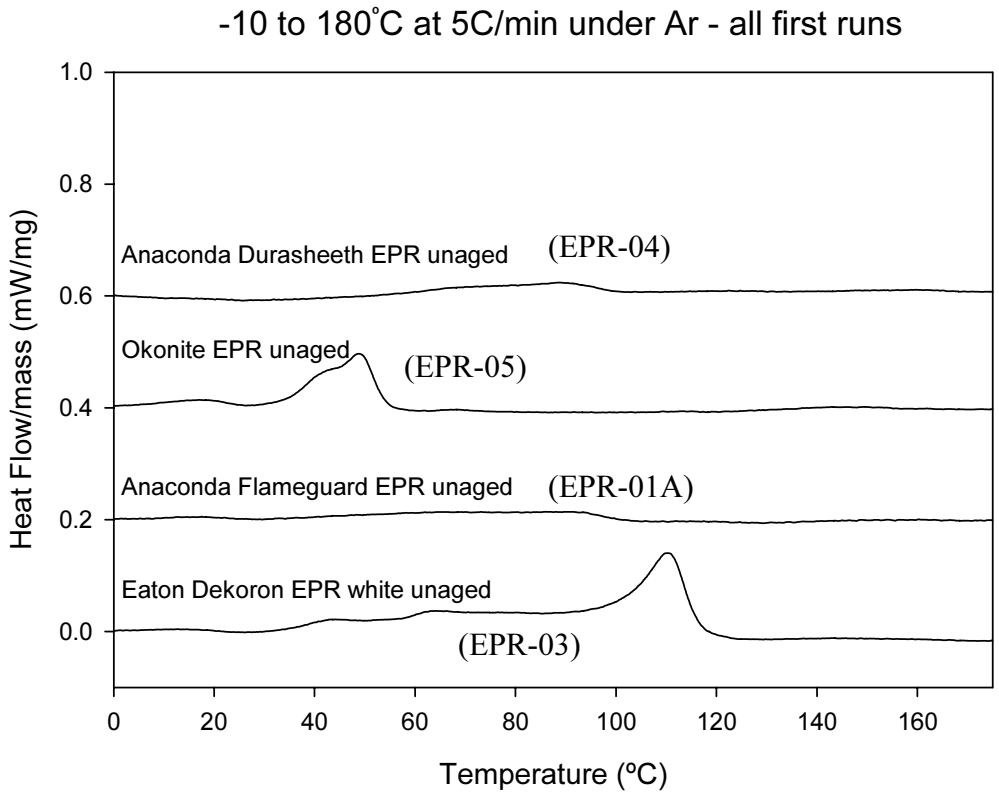

Figure III-31. DSC scans for the four EPR cable insulation materials studied.

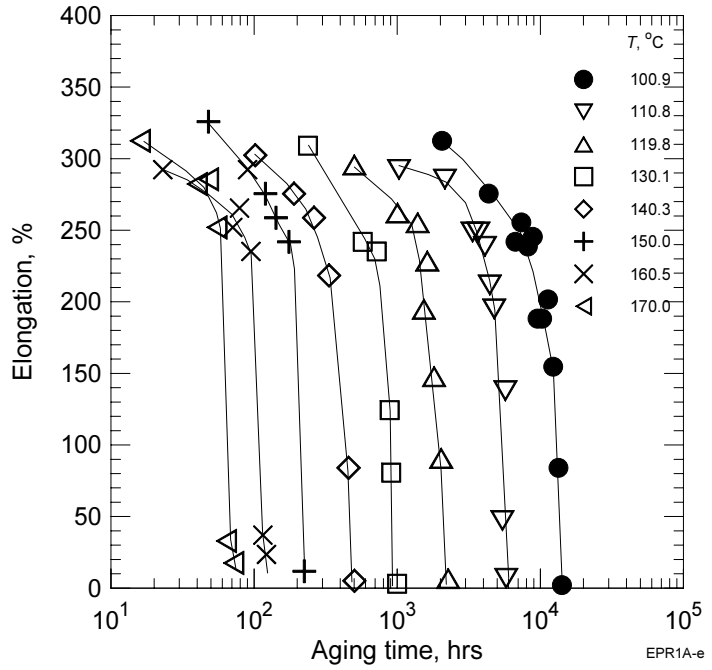

Figure III-32. Elongation versus time at the indicated temperatures for EPR-01A cable insulation material.

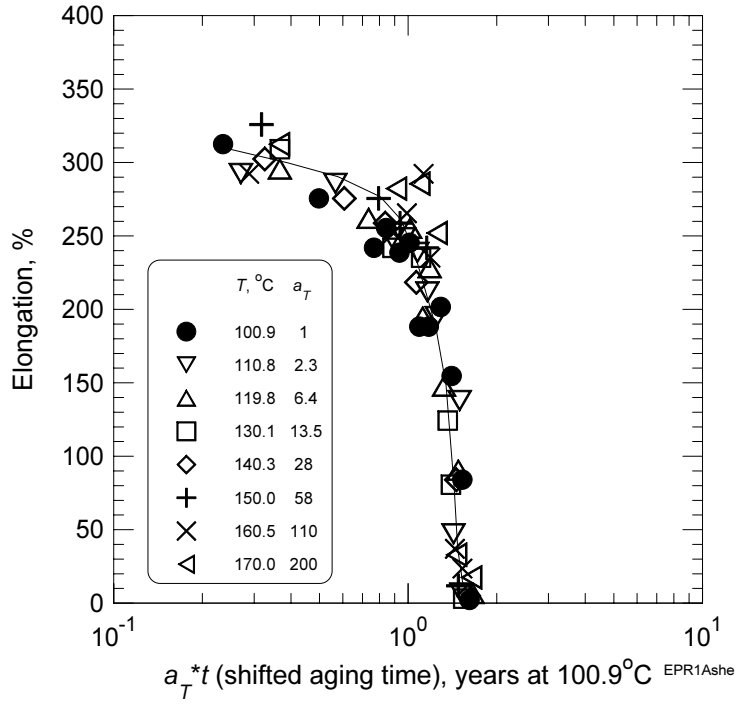

Figure III-33. Time-temperature superposed elongation results for EPR-01A from Fig. III-32 at a reference temperature of 100.9°C.

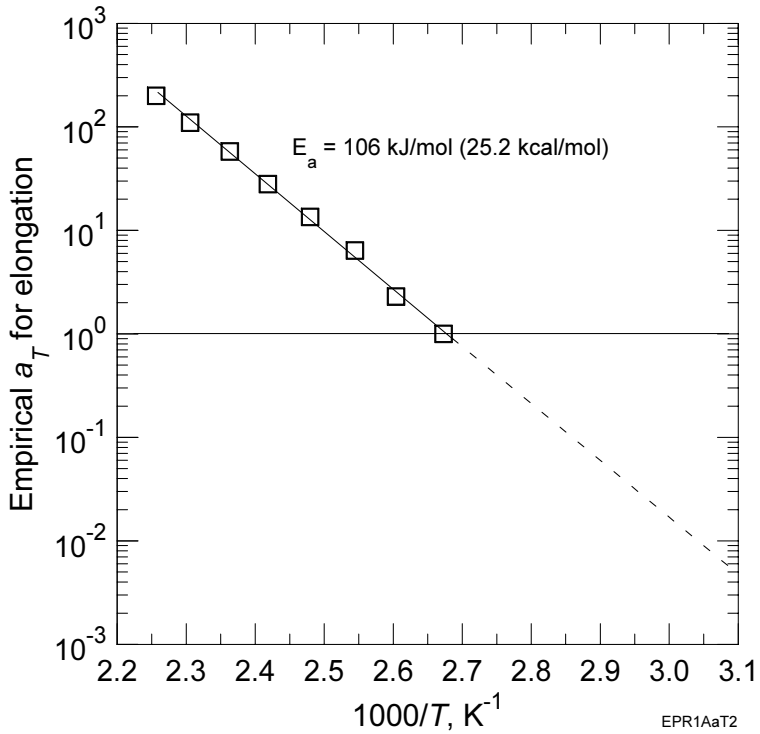

Figure III-34. Arrhenius plot for EPR-01A of the shift factors from Fig. III-33.

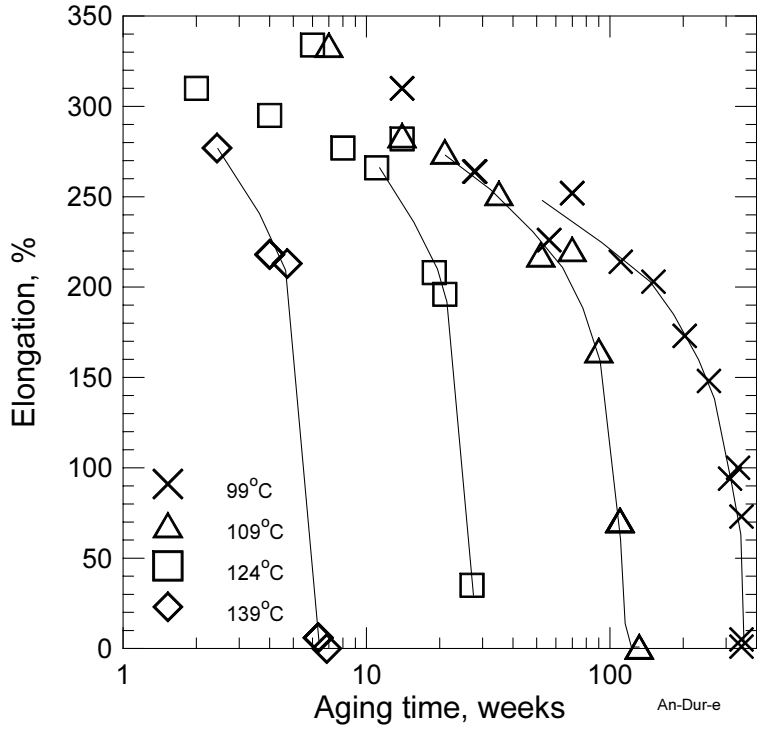

Figure III-35. Elongation versus time at the indicated temperatures for EPR-04 cable insulation material.

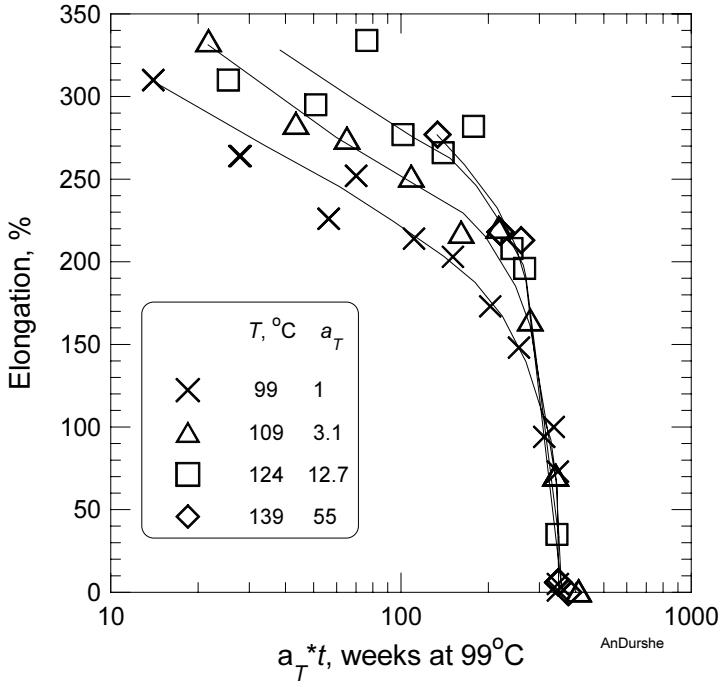

Figure III-36. Time-temperature superposed elongation results at a reference temperature of 99°C for EPR-04 from Fig. III-35 emphasizing the rapid drop-off region of the data.

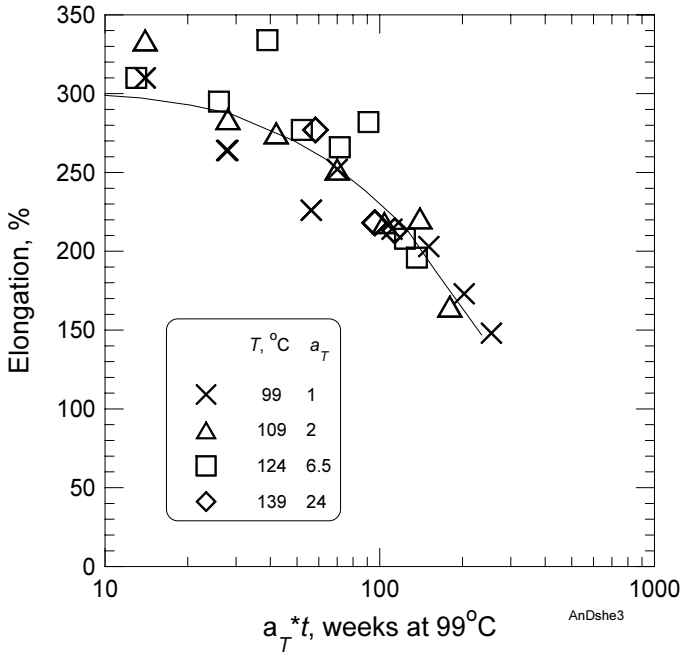

Figure III-37. Time-temperature superposed elongation results at a reference temperature of 99°C for EPR-04 from Fig. III-35 emphasizing the early degradation region of the data.

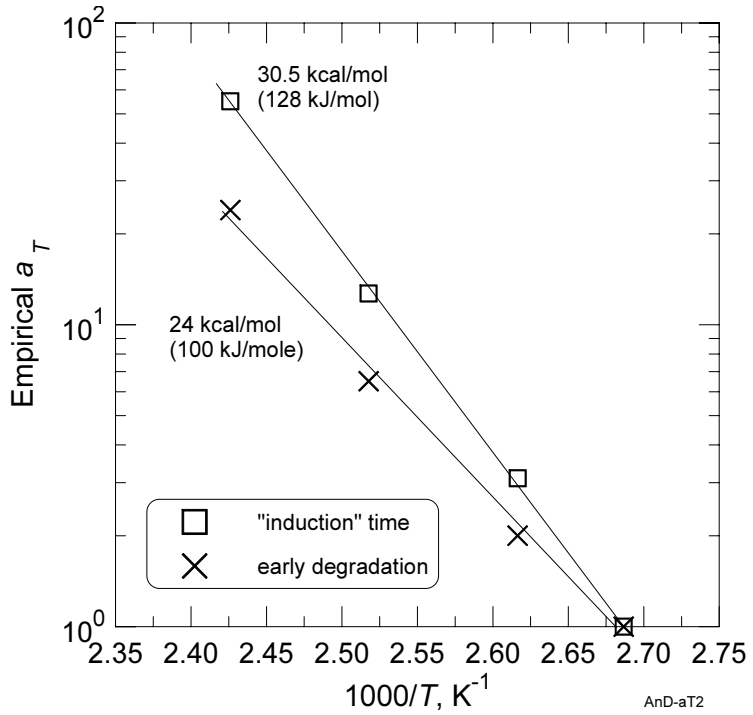

Figure III-38. Arrhenius plot for EPR-04 of the shift factors from Figs. III-36 and III-37.

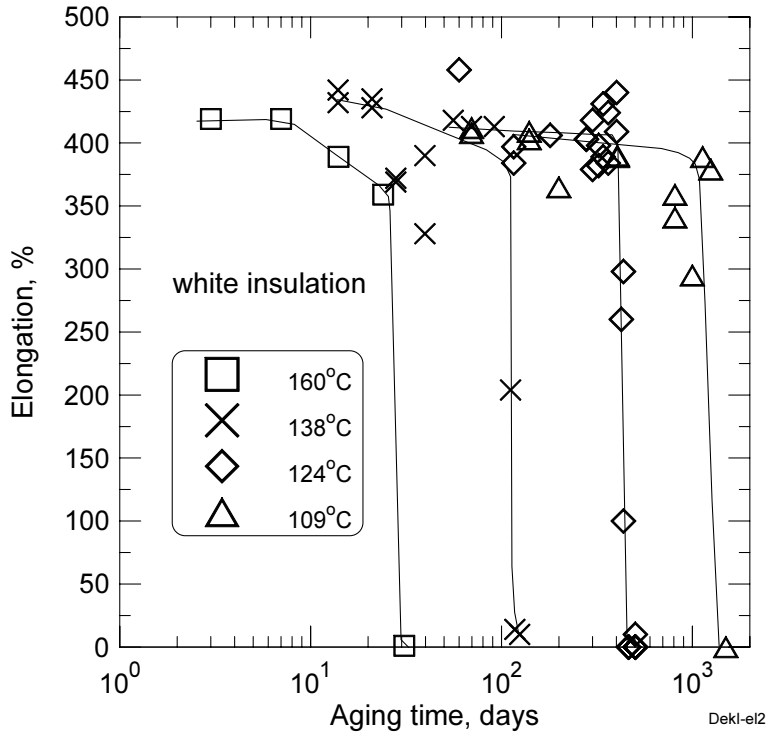

Figure III-39. Elongation versus time at the indicated temperatures for EPR-03 cable insulation material.

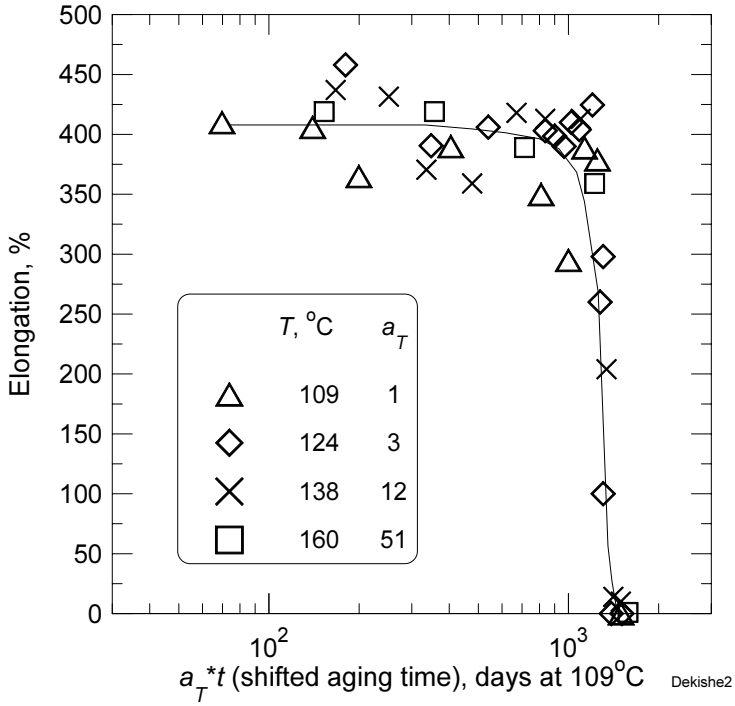

Figure III-40. Time-temperature superposed elongation results at a reference temperature of 109°C for EPR-03 from Fig. III-39.

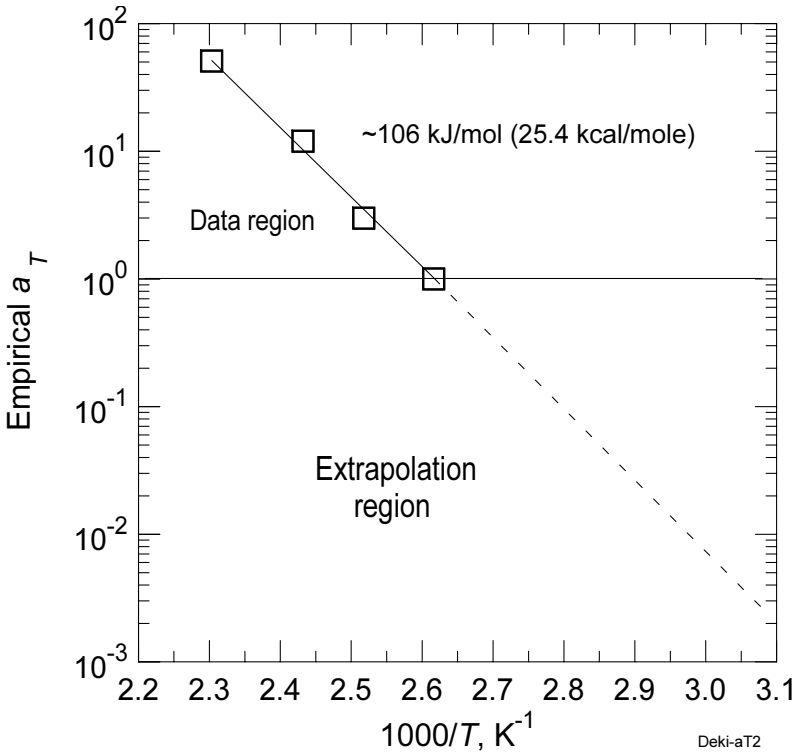

Figure III-41. Arrhenius plot for EPR-03 of the shift factors from Fig. III-40.

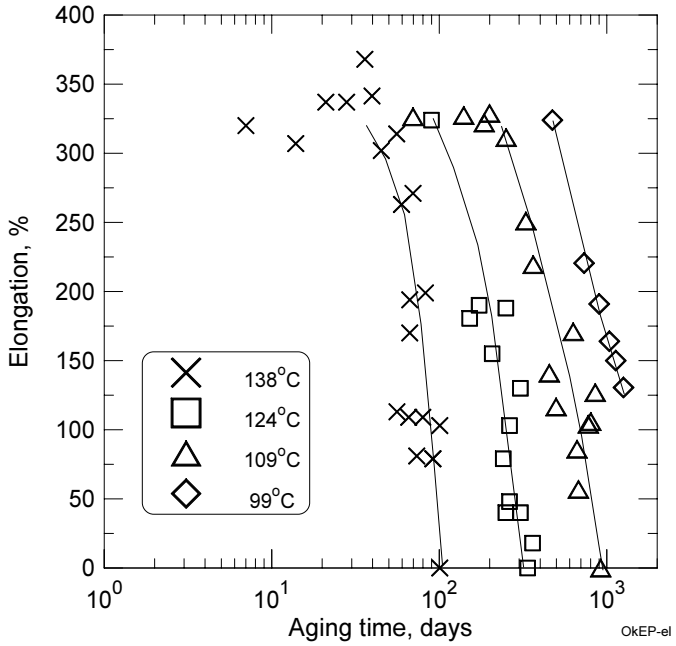

Figure III-42. Elongation versus time at the indicated temperatures for EPR-05 cable insulation material.

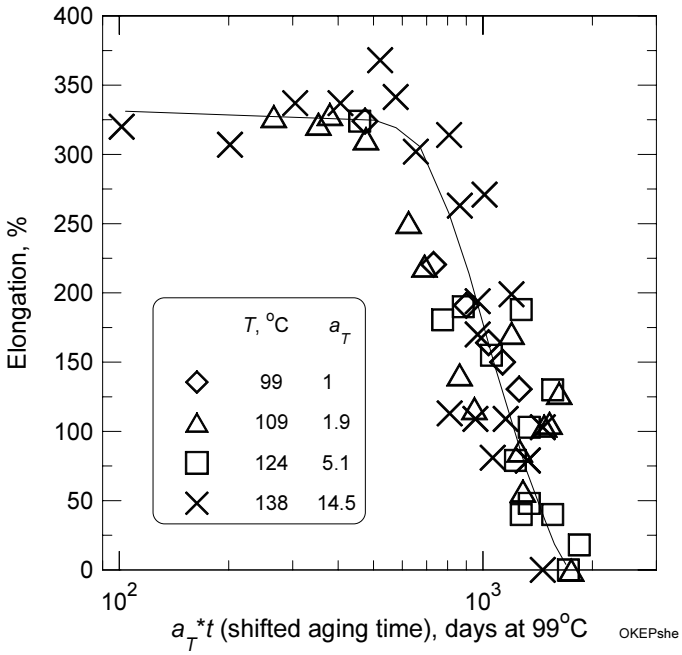

Figure III-43. Time-temperature superposed elongation results at a reference temperature of 99°C for EPR-05 from Fig. III-42.

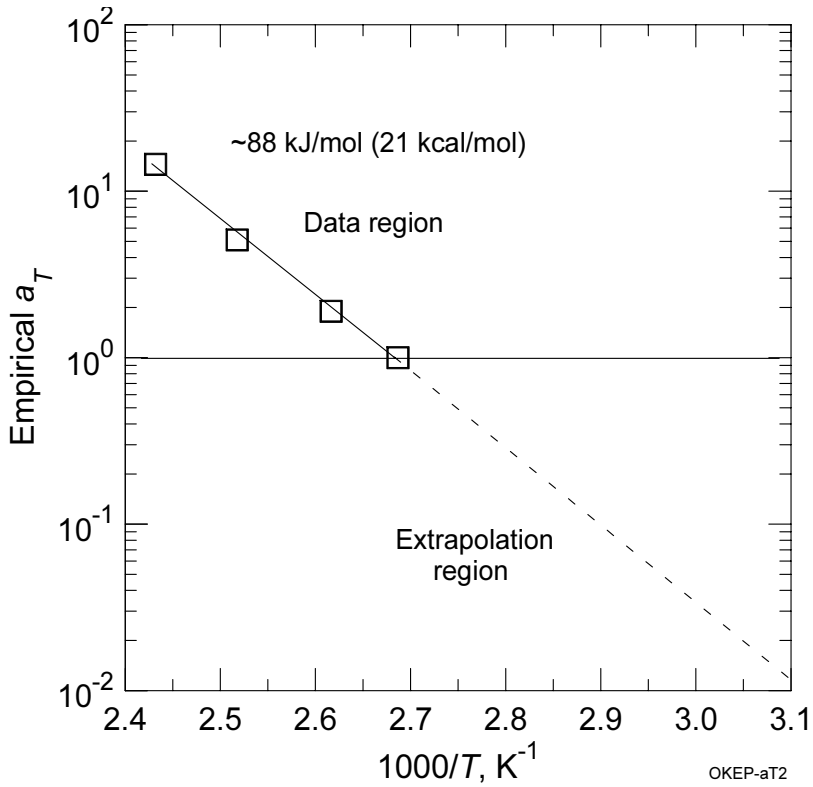

Figure III-44. Arrhenius plot for EPR-05 of the shift factors from Fig. III-43.

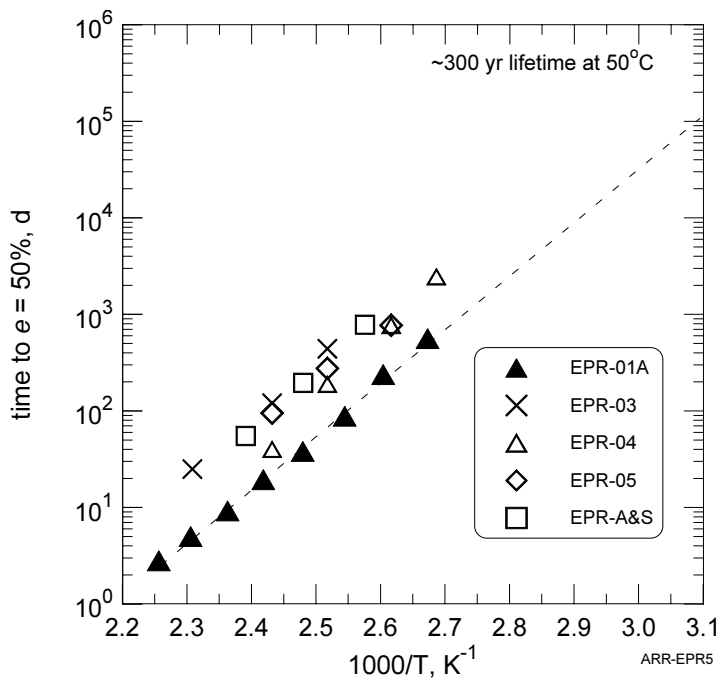

Figure III-45. Arrhenius plots of the times required for the elongation to drop to 50% absolute for five EPR cable insulation materials.

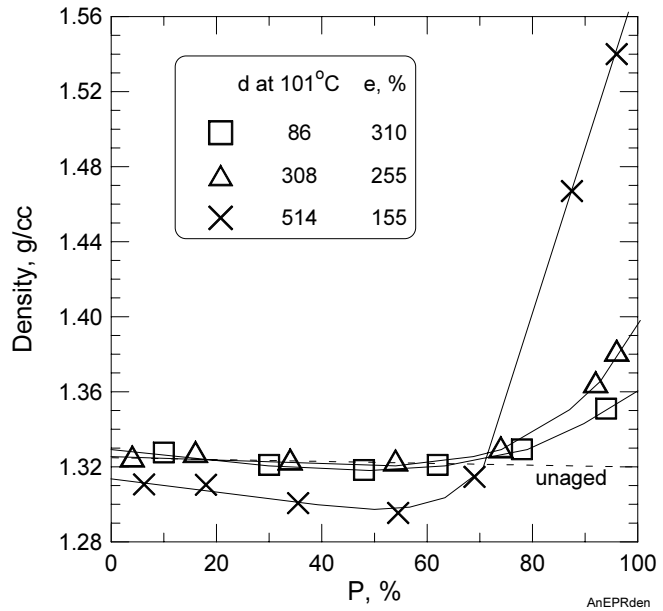

Figure III-46. Density profiling results for the EPR-01A material for aging at 101°C. *P* represents the percentage of the cross-sectional distance from the outside surface (0%) of the insulation to the inside surface (100%).

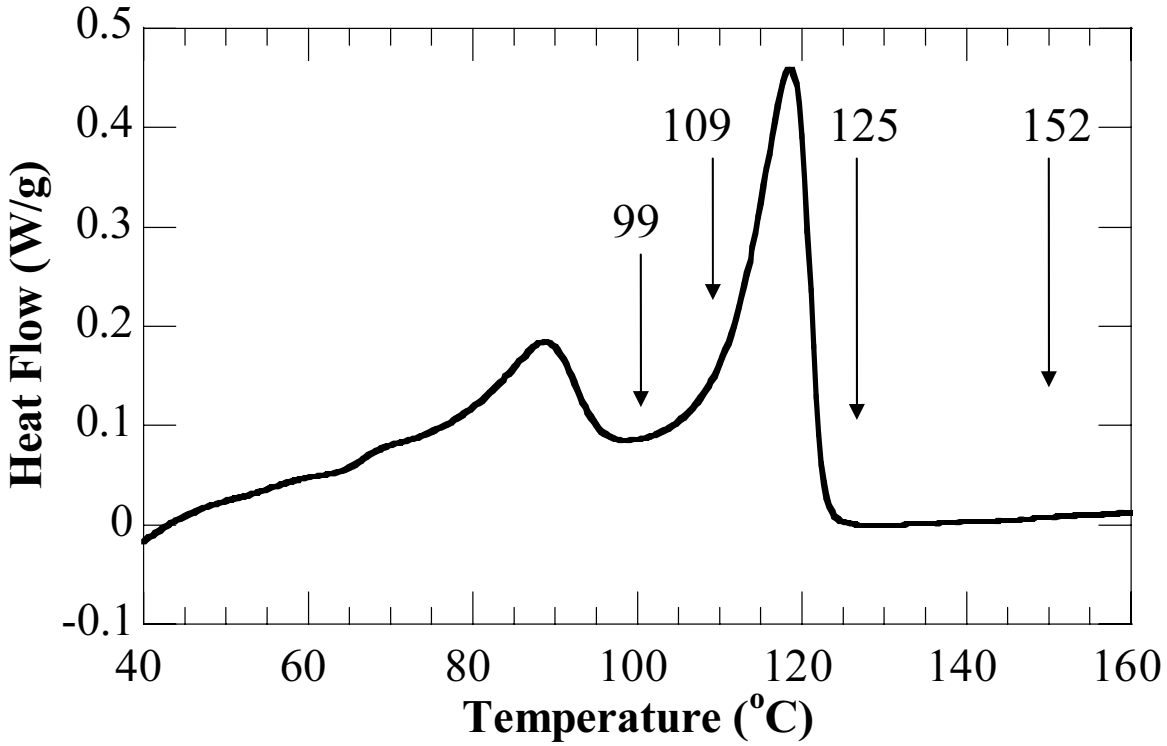

Figure III-47. DSC scan for XLPO-02B material (oven aging temperatures in °C are indicated by numbers on the figure).

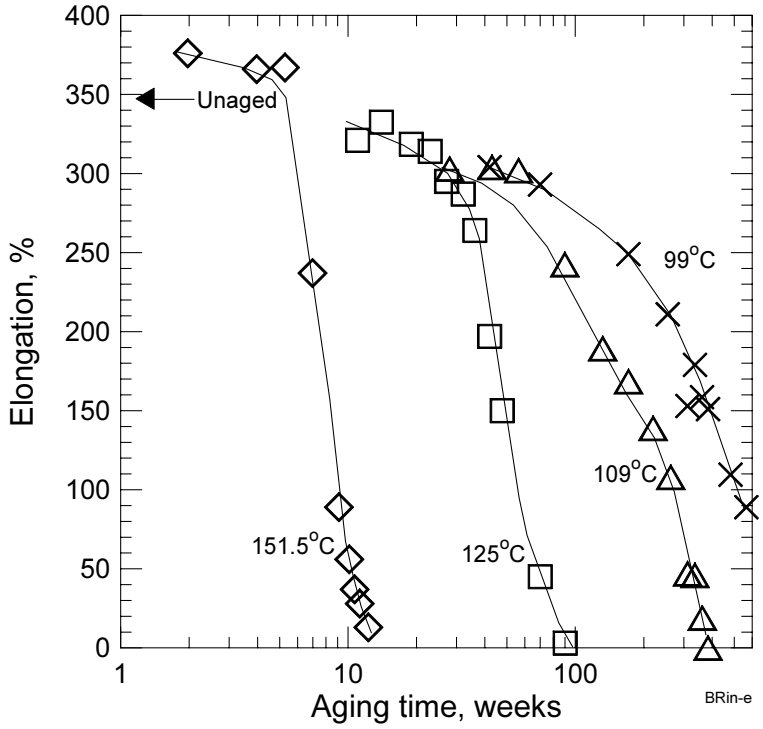

Figure III-48. Elongation versus time at the indicated temperatures for XLPO-02B cable insulation material.

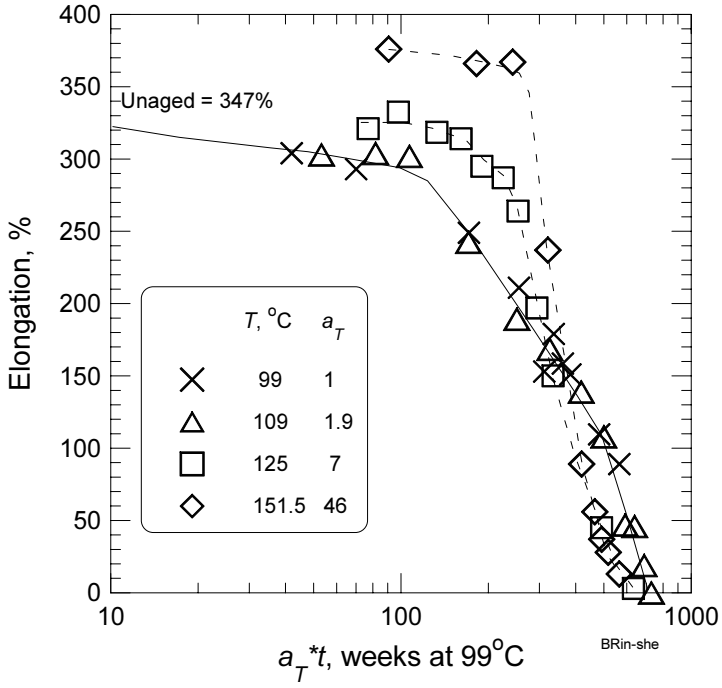

Figure III-49. Time-temperature superposed elongation results at a reference temperature of 99°C for XLPO-02B from Fig. III-48.

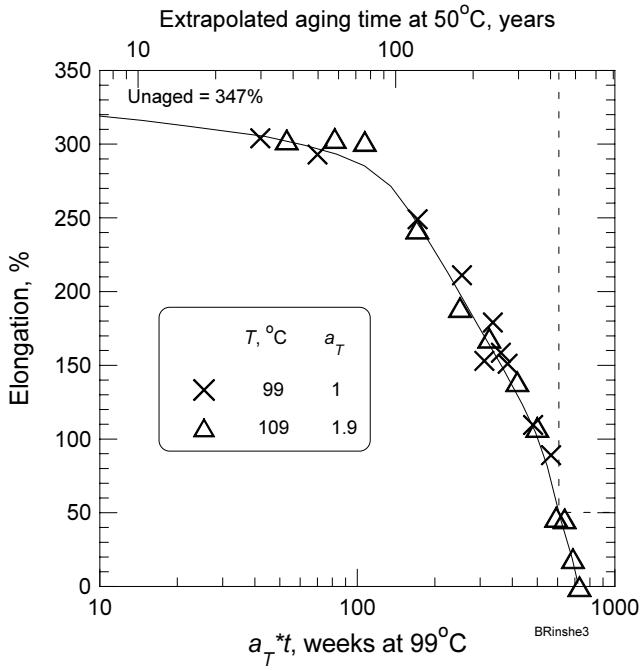

Figure III-50. Time-temperature superposed elongation results at a reference temperature of 99°C for the 99°C and 109°C data of XLPO-02B from Fig. III-48.

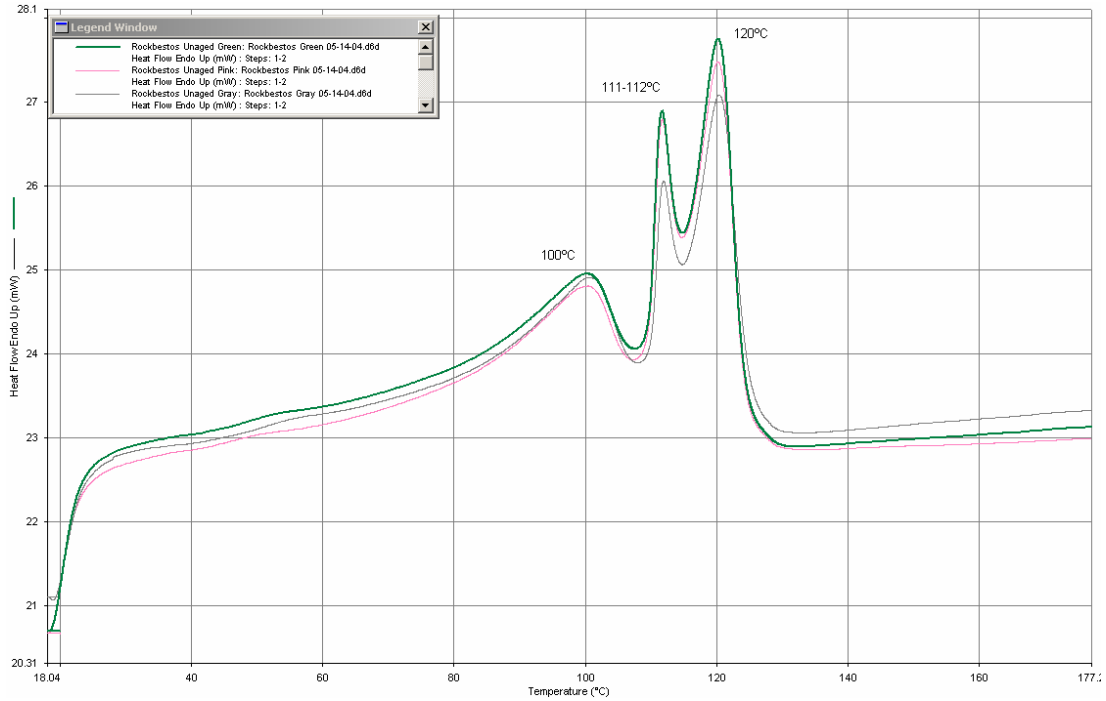

Figure III-51. DSC scan for XLPO-05 insulation material.

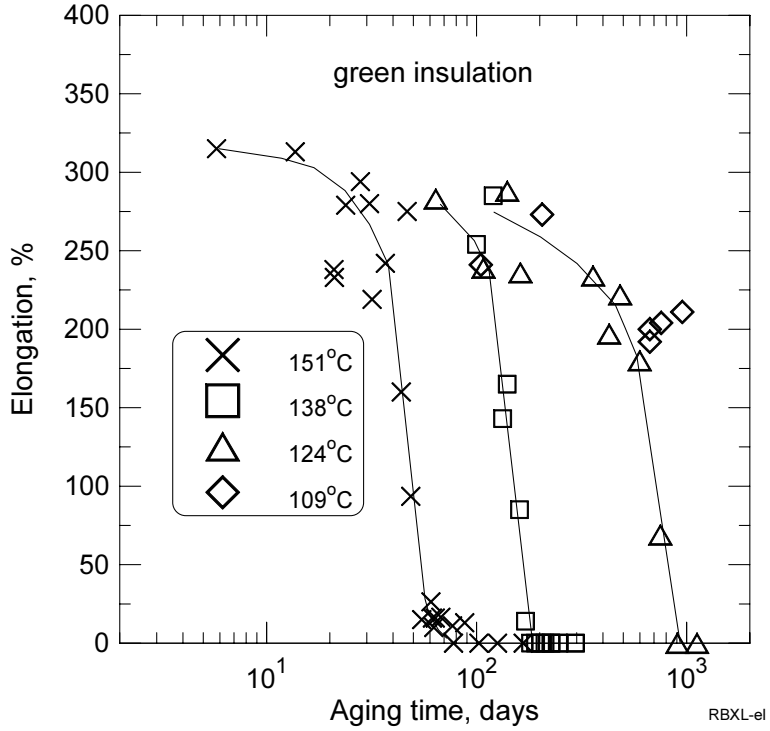

Figure III-52. Elongation versus time at the indicated temperatures for green colored XLPO-05 cable insulation.

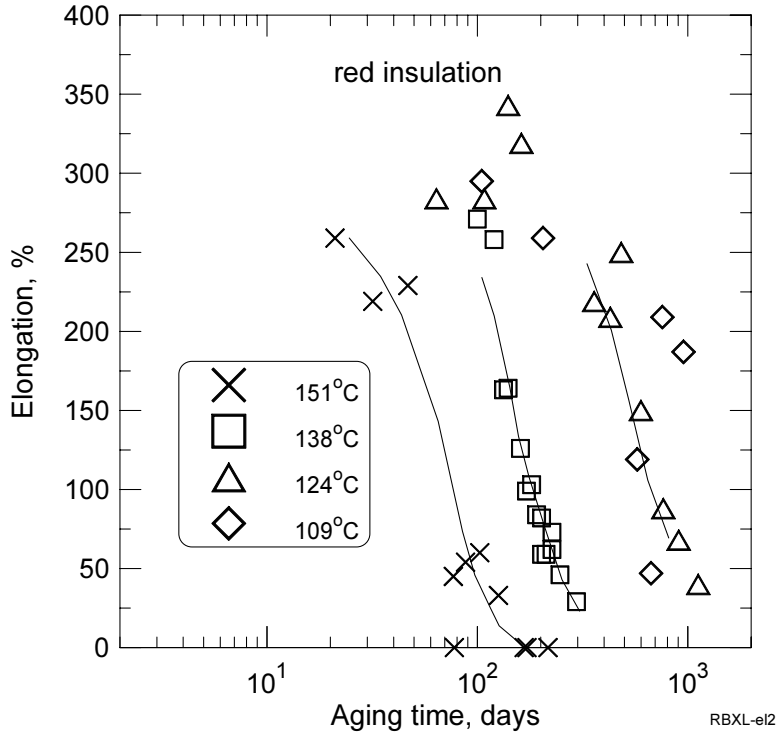

Figure III-53. Elongation versus time at the indicated temperatures for red colored XLPO-05 cable insulation.

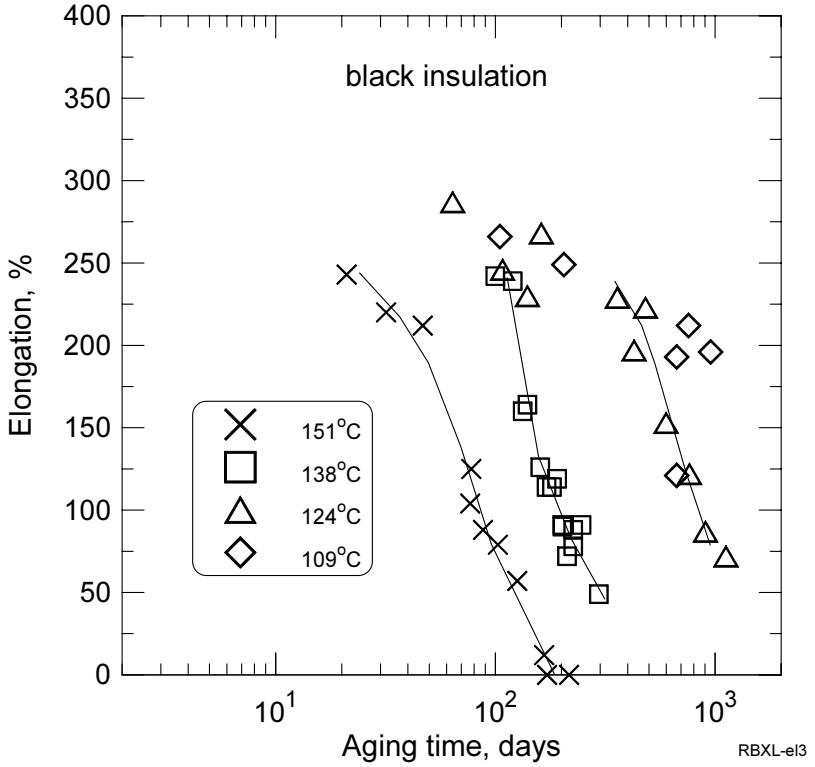

Figure III-54. Elongation versus time at the indicated temperatures for black colored XLPO-05 cable insulation.

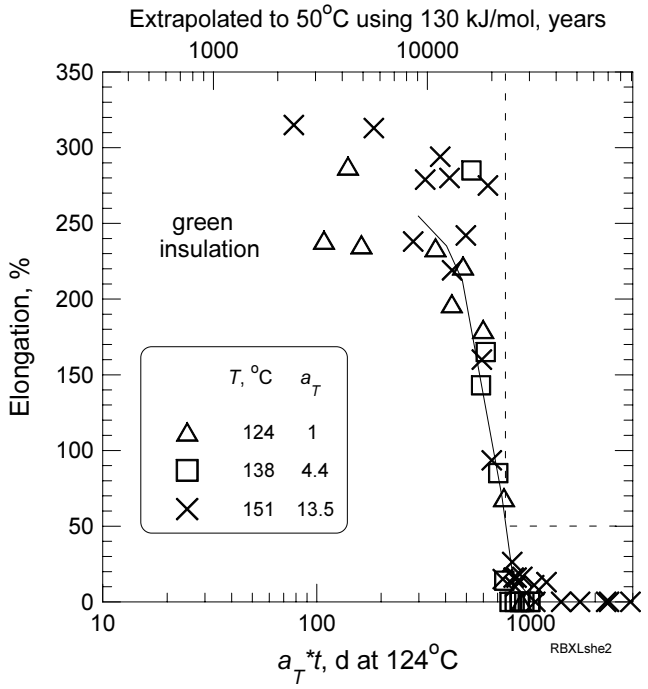

Figure III-55. Time-temperature superposed elongation results for the green insulation at a reference temperature of 124°C for XLPO-05 from Fig. III-52.

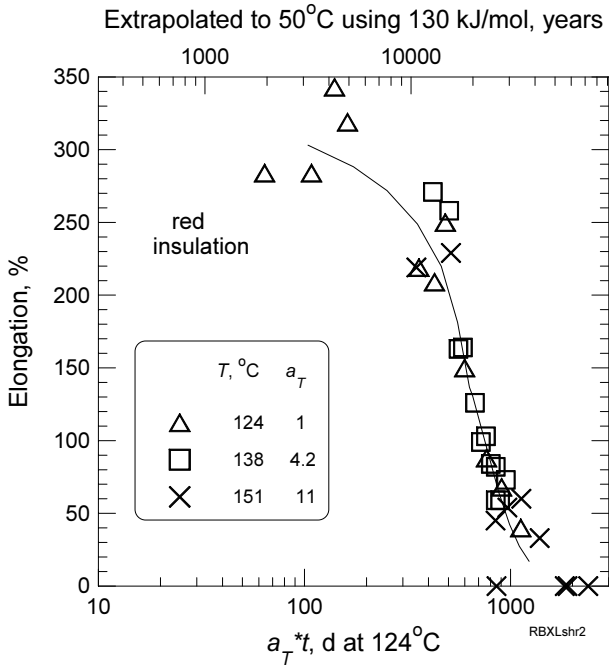

Figure III-56. Time-temperature superposed elongation results for the red insulation at a reference temperature of 124°C for XLPO-05 from Fig. III-53.

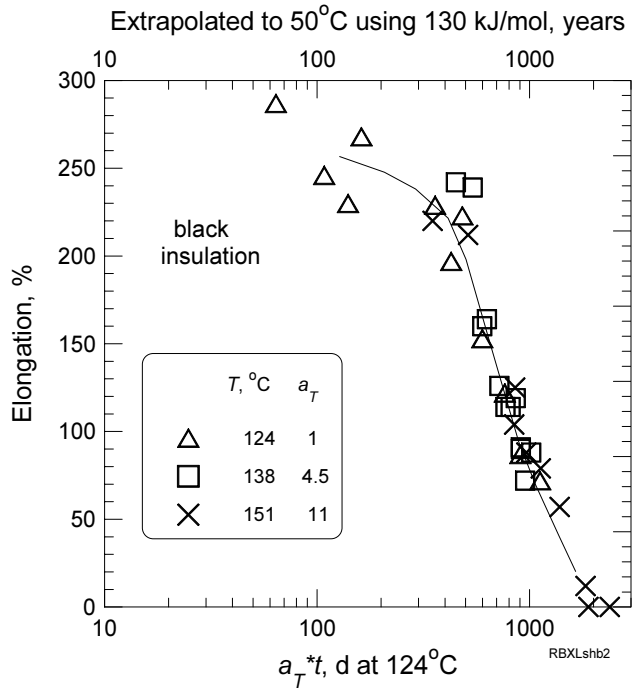

Figure III-57. Time-temperature superposed elongation results for the black insulation at a reference temperature of 124°C for XLPO-05 from Fig. III-54.

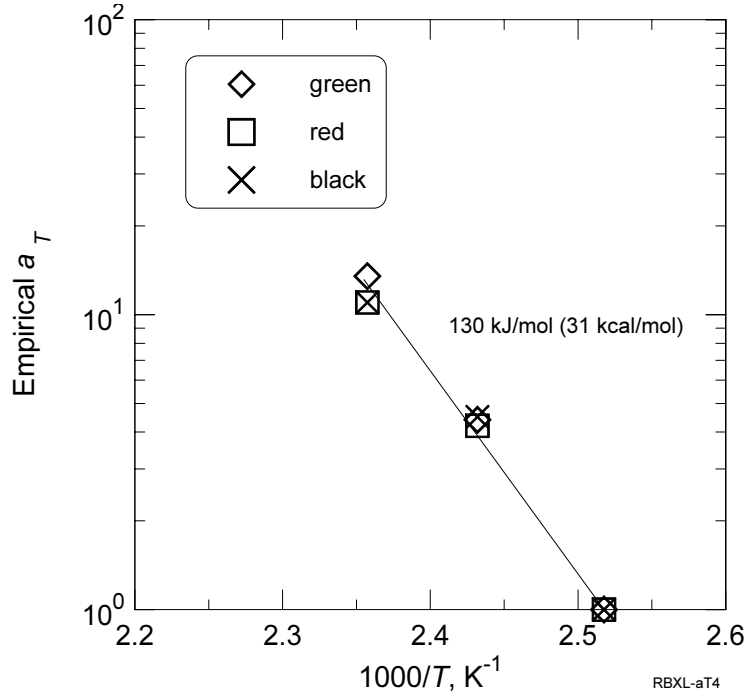

Figure III-58. Arrhenius plot of the shift factors for XLPO-05 from Figs. III-55 through III-57.

IV. Thermal Aging: Further Improving Arrhenius Using Ultrasensitive Oxygen Consumption (UOC) Measurements

Introduction

Most of the aging occurring in nuclear power plant situations involves aging in an air environment. It turns out that degradation of polymers in air environments is usually dominated by oxidation reactions involving the 20.95% oxygen contained in normal air. This can be seen by comparing the degradation rates of polymeric materials in air versus inert (e.g., nitrogen or argon) environments. Some examples are shown for nuclear power plant cable materials in Figs. IV-1 through IV-3. Results for Neo-01 at 150°C are given in Fig. IV-1. These results show that reactions with oxygen dominate the deterioration of the elongation where the time to reach 50% absolute elongation is more than an order of magnitude faster when oxygen is present. Figure IV-2 shows similar results for the Hyp-03 cable jacketing material- in this case and for other hypalon materials, the time required for the elongation to drop to 50% absolute occurs approximately 3 to 4 times faster in air versus nitrogen [IV-1]. For the EPR-01A material (Fig. IV-3) it is also clear that oxidation dominates deterioration of mechanical properties.

As noted earlier in Section III, one of the most important aspects of the normal Arrhenius method is the extrapolation of high temperature results to lower temperatures with the assumption that the activation energy found at elevated temperatures remains constant in the extrapolation region. In order to test this assumption, an extremely sensitive analytical technique that measures a parameter correlated to the degradation is required. Since oxidation typically dominates the degradation in air-containing environments, we felt that measurements of the oxygen consumed during degradation might offer a promising method of achieving this objective. We have therefore been developing the oxygen consumption approach over the past several years [IV-1 through IV-8]. This approach uses gas chromatography techniques to determine the amount of oxygen consumed after aging a closed container holding a known amount of polymeric material and a known initial quantity of oxygen. Since careful experimental technique allows us to achieve oxygen consumption sensitivities better than $1x10^{-13}$ mol/g/s, and since 10-20 cc of oxygen absorption is typically necessary to mechanically degrade polymers, the sensitivity of this technique allows measurements to be made at temperatures corresponding to hundreds of years of polymer lifetimes. This allows us to probe temperatures down to application conditions for most materials. By making measurements at higher temperatures that overlap the temperature range used for traditional mechanical property measurements, we are able to confirm/test the correlation between oxygen consumption and traditional (e.g., mechanical property) measurements. Extending the UOC measurements into the extrapolation region then allows us to determine whether the oxidation mechanism changes or remains constant in this region. This section of the report will summarize our UOC measurements made on nuclear power plant cable materials as part of the NEPO program.

UOC and CO_2 measurements on Neo-02 cable jacket

Figure IV-4 shows oxygen consumption rate results for the Neo-02 material at six temperatures ranging from 95°C to 25°C [IV-5]. Each point represents the mid-point of the time span for each measurement. For instance, the first measurement 95°C covered an exposure from time zero through 1.9 days so the first datum point gives the average oxidation rate from 0 to 1.9 days and is located at 0.95 days. The measured consumption rates at each temperature are reasonably constant indicating that the oxidative chemistry at each temperature does not change much as a function of aging time. Integration of the oxygen consumption rate results from Fig. IV-4 leads to results for the total oxygen consumption versus time (Fig. IV-5). We then use the principles underlying time-temperature superposition to time-temperature superpose the consumption results of Fig. IV-5 at 25°C (the lowest oxygen consumption temperature). Figure IV-6 shows the superposed results together with the values of the empirical shift factors a_T used for the superposition. We then normalize these shift factors to 80°C so that they can be compared to the elongation shift factors for Neo-02 previously derived above at a reference temperature of 80°C (Fig. III-9). The comparisons of the two sets of shift factors are shown in Fig. IV-7. It is clear that the slope of the oxygen consumption results (plotted as Xs on Fig. IV-7) at temperatures overlapping the elongation results is similar (E_a ~ 96 kJ/mol) to that of the elongation shift factors indicating, as anticipated, that the overall oxygen consumption is intimately related to the drop in mechanical properties. At temperatures below 80°C, however, the slope (Arrhenius E_a) of the oxygen consumption shift factors drops slowly to ~76 kJ/mol near 25°C. This implies that small changes in the oxidation chemistry are occurring below 80°C and that extrapolation of the 96 kJ/mol activation energy found for elongation above 80°C will overestimate the lifetime for temperatures lower than 80°C. It is interesting to note that the reduction in E_a values found for Neo-02 from a combination of elongation and oxygen consumption results (96 kJ/mol above 80°C dropping to ~76 kJ/mol at 25°C) is similar to the results found for elongation on the Neo-01 material (Fig. III-7).

Using the oxygen consumption results from Figs. IV-6 and IV-7 for temperatures below 80°C leads to lower predicted mechanical property lifetimes versus conventional extrapolation of the high temperature elongation results. For instance if the superposed elongation results at 80°C (lower x-axis of Fig. III-9) were extrapolated to 25°C using the oxygen consumption shift factors, the lifetime would be increased by a factor of 204 (see Fig. IV-6) leading to the upper x-axis predictions shown on Fig. IV-8. To reach 50% absolute elongation at 25°C, the oxygen consumption extrapolation predicts a lifetime of 235 years (top x-axis of Fig. IV-8) versus ~530 years for the conventional Arrhenius extrapolation (upper x-axis of Fig. III-9). At 50°C, the extrapolated results from the oxygen consumption predict a "lifetime" of ~20 years (top x-axis of Fig. IV-9). From these comparisons it is clear that fairly small changes in E_a values can lead to fairly significant reductions in extrapolated predicted lifetimes.

This observation of "downward" curvature in the Arrhenius plot for Neo-02 will be seen for several of our NEPO materials [IV-1,IV-5]. It is consistent with many of our previous oxygen consumption studies on other polymers [IV-3,IV-4,IV-6,IV-8] as well as numerous literature results that looked at other materials and properties [IV-9 through IV-14]. The downward curvature (dashed curve in Fig. IV-7) implies that certain higher activation energy oxidation processes are becoming less important at lower temperatures. We can see evidence for this statement based on the examination of CO_2 production rates that are also available from the gas analyses procedures used to monitor oxygen consumption rates [IV-5]. Figure IV-10 shows the CO_2 production rates versus time and temperature. Integration of these results leads to the CO_2 production versus time (Fig. IV-11). These latter results are then time-temperature superposed at a reference temperature of 25°C in Fig. IV-12 with the empirically derived shift factors shown on the figure. It is immediately clear that these shift factors are quite different from the shift factors used to superpose the oxygen consumption data (shown on Fig. IV-6). Figure IV-13 compares the normalized (to 80°C) shift factors for CO_2 with those for elongation and for O_2 consumption. The results indicate that the oxidative degradation chemistry leading to CO_2 has higher activation energy at low temperatures (~107 kJ/mol) than that of the overall oxygen consumption (see Fig. IV-7). Therefore the reactions resulting in CO_2 as a product gas become less important relative to the reactions consuming oxygen as the temperature is lowered.

Additional evidence that CO_2 production is less important at low temperatures can be seen by plotting the ratio of CO_2 production to O_2 consumption against the O_2 consumption shown versus temperature in Fig. IV-14. These data again indicate that the chemistry leading to CO_2 slows down relative to overall oxidation as the temperature is lowered. This is true even for the same overall amount of degradation (constant amount of oxygen consumption). For example, a dashed line is drawn at a constant oxygen consumption of $1x10^{-5}$ mol/g in Fig. IV-14. The approximate amount of CO_2 corresponding to this O_2 consumption varies from ~10% at low temperatures to ~25% at high temperatures.

When chemical degradation involves two or more processes with differing activation energies, the processes with higher activation energies will become less important as the temperature is lowered. Thus the temperature dependence of the overall degradation rate will transition to the lower activation energy process as the temperature is reduced ("downward" curvature in the Arrhenius plot). The reduction in importance of the reaction(s) leading to CO_2 is therefore consistent with the observed downward curvature in the oxygen consumption Arrhenius plot.

UOC and CO_2 measurements on Hyp-03 cable jacket

Figure IV-15 shows oxygen consumption rate results for the Hyp-03 material at six temperatures ranging from 108°C to 37°C [IV-1]. At every temperature, the results are reasonably constant with aging time indicating a reasonably constant degradation rate. The integrated O_2 consumption results are given in Fig. IV-16 and the time-temperature superposed results in Fig. IV-17. The shift factors derived from the oxygen consumption

results (Fig. IV-17) are plotted on an Arrhenius plot (Fig. IV-18) that also contains the shift factors derived from elongation measurements (Fig. III-21). For ease of comparisons, both sets of shift factors are normalized to 100°C. The results show a remarkable but anticipated correspondence between the two sets of shift factors with both sets indicating a small but measurable change in slope to lower activation energy below ~100°C. Using the shift factor results from the O_2 consumption to extrapolate the 70°C superposed elongation results (lower x-axis of Fig. III-21) to 50°C leads to the 50°C time scale shown on Fig. IV-19 (upper x-axis). This leads to a 50% absolute elongation predicted lifetime of ~80 years at 50°C for Hyp-03. The "downward" drop in slope noted from both elongation and O_2 consumption as the aging temperature is lowered is consistent with the overall results found for elongation for the hypalon materials as a group (Fig. III-27) and similar to many of the results mentioned above from the literature and from our previous studies monitoring both elongation and O_2 consumption results.

This downward curvature in the Arrhenius plot again implies that a high activation energy process is dropping out as the temperature is reduced. Similar to the results found for the Neo-02 material, evidence for this hypothesis was found from the gaseous CO_2 production results. Figure IV-20 shows the integrated CO_2 production versus time at six aging temperatures. These results are time-temperature superposed in Fig. IV-21 where it is again clear that the shift factors for CO_2 production (noted on Fig. IV-21) are very different from those obtained for O_2 consumption (shown on Fig. IV-17). A plot of the shift factors for elongation, O_2 consumption and CO_2 production is shown in Fig. IV-22; it is again apparent that a higher activation energy process leads to CO_2 production. As noted above, the CO_2 results are consistent with a changing E_a value since they point to a reaction that becomes less important (drops out) as the temperature is reduced.

UOC measurements on Hyp-08 cable jacket

The integrated oxygen consumption results versus aging time for the Hyp-08 material at five temperatures are shown in Fig. IV-23. Similar to the elongation results, the O_2 consumption results show higher scatter than usually found for polymeric materials that we have examined. Even with the higher scatter, the fairly large temperature range available to the O_2 consumption measurements allows reasonable superposition of the consumption results as shown in Fig. IV-24. Figure IV-25 plots the shift factors for O_2 consumption and for elongation on an Arrhenius plot. For this material, there is only a small indication for a drop in E_a as the temperature is reduced. By utilizing the shift factors shown on this plot, the 50°C time scale appropriate for this material is determined to be that given by the upper x-axis of Fig. IV-26. This time axis indicates that 50% absolute elongation will be reached after ~ 90 years at 50°C for Hyp-08.

UOC measurements on EPR-04 cable insulation

Oven aging studies of the mechanical properties on this EPR cable insulation material were conducted for times exceeding 7 years at the lowest aging temperature of 99°C. Although involving shorter-term exposures, extensive O_2 consumption experiments have been progressing for more than a decade with several repeat runs to determine scatter in

the results for samples obtained at differing locations along the cable reel. Figure IV-27 plots the integrated consumption results versus aging time for ten separate runs at the temperatures indicated on the figure. At four different temperatures (~65°C, 80°C, 95°C and 125°C), two repeat runs were made on samples extracted from the same cable reel but at very different locations and ~ 5 years apart. It is clear from the results shown in Fig. IV-27 that small but measurable differences were observed for the repeat runs. However, once these data were superposed (Fig. IV-28) and the empirically derived shift factors plotted on an Arrhenius plot (Fig. IV-29) it is clear that the observed scatter for repeat runs has little effect on the Arrhenius plot. This points out the strength of having a technique (UOC) that can take data over a very extended temperature range. Even though the shift factors at a given temperature can vary as seen on Fig. IV-29, having results where the shift factors vary by ~ three orders of magnitude minimizes the effect of such scatter.

The results from Fig. IV-29 indicate that the O_2 consumption has an E_a of ~100 kJ/mol. Comparison of this result to the elongation results is interesting in the present case since the EPR-04 material did not show superposition for elongation (Fig. III-36). It was found that the early degradation superposed with an E_a of ~100 kJ/mol (Figs. III-37 and III-38) whereas the induction-time (rapid fall-off) region superposed with an E_a of ~128 kJ/mol (Figs. III-36 and III-38). Thus the O_2 consumption results agree with the elongation in the earlier stages of degradation. This is not surprising, but is comforting, since the early time region is the time region accessed with the O_2 consumption measurements. Even at the highest temperature of 125°C, the consumption results go out only to ~11 weeks, a time well before much mechanical degradation occurs (Fig. III-35). Although longer times could have been probed at this highest temperature, the results would not allow one to obtain the E_a appropriate to the induction time region since the latter region could never be probed at the lower temperatures of interest (e.g., in the extrapolation region). For a material such as EPR-04 where the activation energy depends strongly on the degradation condition (time-temperature superposition is impossible), it is also impossible to probe the later stages of degradation using the UOC approach. This implies that the traditional Arrhenius extrapolation given in Fig. III-45 may be the only viable extrapolation approach. However, as we saw earlier, the EPR insulation materials are so robust (Fig. III-45) that the E_a values obtained from elongation alone would have to drop very substantially before concern over aging would occur for typical nuclear power plant aging conditions. In other words we expect very long lifetimes for EPR cable insulation materials. Further evidence for this conclusion will come later in Section XI when we discuss the Wear-out approach and its application to EPR cable insulation materials.

The elongation and UOC results for EPR-04 offer an important lesson on the applicability of UOC measurements as a means of assessing whether chemistry changes (e.g., changes in Arrhenius E_a) are likely to occur when higher temperature Arrhenius data is extrapolated to lower temperatures. For materials in which excellent time-temperature superposition occurs for accelerated aging elongation data [IV-1 through IV-3,IV-5 through IV-8], raising the temperature corresponds to equally accelerating all of the underlying degradation reactions and therefore to a single acceleration factor. In such

instances one would expect and normally finds similar acceleration factors to hold for UOC at temperatures overlapping those used for elongation measurements. On the other hand when time-temperature superposition is invalid such as the case for EPR-04 (Fig. III-36), the shift factors will depend on the amount of degradation, leading to E_a values that depend on degradation (Fig. III-38). Given that the UOC approach normally looks at the early stages of degradation (by necessity at low temperatures), one would expect the E_a values for UOC to be similar to the E_a values for elongation corresponding to the earlier stages of mechanical degradation.

In general it is much easier to see evidence for non-superposition for material properties that drop in a regular fashion than for materials that show "induction-time" behavior since the superposition of the latter will be dominated by the rapid change region. For example the time-temperature superposed density results for EPR-04 (see Fig. XI-1 below) show little indication of the non-superposition that is evident in the elongation results (Fig. III-36). This implies that one might not always be able to recognize the presence of non-superposition for some materials with "induction-time" behavior. In such instances, UOC shift factors should differ from those of mechanical properties over similar temperature ranges, implying that the UOC measurements do not reflect mechanical degradation. The results for EPR-04 show that a first guess as to the reason for such non-correspondence would be due to an E_a value that depends on degradation level.

With the above in mind, it should be noted that the UOC results for EPR-04 indicate a constant E_a value of 100 kJ/mol all the way down to 52°C, implying that the chemistry responsible for the early-time degradation remains constant down to this temperature. This offers evidence that changes in the mix of chemical reactions occurring during the induction period are unlikely between the lowest temperature mechanical property measurements (99°C) and the aging temperature of interest to nuclear power plant aging (50°C). This therefore argues against seeing large reductions in the 128 kJ/mol E_a value for the induction time at temperatures below 99°C, consistent with the earlier discussion in Section III above.

UOC and CO_2 measurements on XLPO-02B cable insulation

Oxygen consumption experiments were conducted on the XLPO-02B cable insulation material at seven aging temperatures ranging from 48°C to 138°C. This range covered from temperatures way below the crystalline melting point region to temperatures way above where the material was completely melted during aging (see Fig. III-47). The integrated O_2 consumption results at the seven aging temperatures are plotted in Fig. IV-30 and these results are time-temperature superposed at a reference temperature of 48°C in Fig. IV-31. Figure IV-32 gives an Arrhenius plot of the empirically derived O_2 consumption shift factors (normalized to 99°C) and shows that these results give nice Arrhenius behavior with an $E_a \sim 72$ kJ/mol over the entire temperature range examined. As noted above (Figs. III-49 and III-50), the elongation results could only be superposed for the two temperatures (109°C and 99°C) that were below the main melting point of this material. The shift factors appropriate to these two elongation results are also given

in Fig. IV-32. It is seen that the two sets of shift factors are consistent suggesting that the elongation results can be more confidently extrapolated to temperatures lower than 99°C using an E_a of 72 kJ/mol. Using this E_a to extrapolate the 99°C time scale of the superposed elongation results (lower x-axis of Fig. IV-33) to 50°C gives the predicted time scale shown as the upper x-axis in this figure. Based on a 50% elongation practical end of life criterion, this approach predicts a lifetime of ~430 years at 50°C. As noted in Section III, the E_a would need to drop to an average value of ~33 kJ/mol for the practical end of life to drop below 60 years at 50°C.

The CO_2 solubility in the XLPO-02B material was determined to be 0.38 ccSTP/cc/atm [IV-5]. Since this is a fairly low value for solubility, the corrections necessary for CO_2 dissolved in the material during the analyses were relatively small ranging from ~5% at 138°C to ~23% at the lowest temperatures. The resulting integrated CO_2 production values are shown in Fig. IV-34. Time-temperature superposition of these results are shown in Fig. IV-35 together with the empirically derived shift factors used for superposition. The shift factors for CO_2 (Fig. IV-35) differ somewhat from the shift factors for oxygen consumption (Fig. IV-31), as is clear when normalized results for a_T for elongation, oxygen consumption and CO_2 production are plotted together on an Arrhenius plot (Fig. IV-36). The differences found between the oxygen and CO_2 results indicate that the detailed chemical pathways must be changing over the temperature range from 138°C to 48°C. Since the E_a value for CO_2 production is lower than that of oxygen consumption below 99°C (the lowest temperature for elongation measurements), these results imply that the reactions leading to CO_2 become relatively less important in the region below 99°C. This fact and the complexity of the situation is underscored when the ratio of CO_2 produced to O_2 consumed is plotted versus the O_2 consumed (Fig. IV-37). The first obvious conclusion from this plot is the relative importance of the reaction leading to CO_2 since 30 to 50% of the oxygen consumed ends up as CO_2. It is also clear that the CO_2 reaction starts out at a high level at every temperature but quickly drops with aging time, consistent with an early reaction leading to CO_2 that becomes much less important with time. Relative to the total oxygen consumed, the CO_2 reaction becomes relatively more important (curves shift to the right) as the aging temperature increases from 48°C to around 124°C then becomes less important at 138°C. Since this progression corresponds to proceeding through the melting point region (Fig. III-47), the relative importance of the CO_2 reaction might be influenced by the partial crystallinity of this material. Given the obvious complexity of the underlying CO_2 reactions and their relative importance in terms of percentage product (Fig. IV-37), it is difficult to predict the consequences of this complication on lifetime predictions. However, given the requirement that the E_a would need to drop to the very low value of 33 kJ/mol from 99°C to 50°C for a practical lifetime less than 60 years at 50°C, we have confidence in the viability of the XLPO-02B material.

UOC and CO_2 measurements on green-colored XLPO-05 cable insulation

Oxygen consumption experiments were conducted on the green-colored XLPO-05 cable insulation material at seven aging temperatures ranging from 48°C to 138°C. This range covered from way below the crystalline melting point region to temperatures way above

where the material was completely melted during aging (see Fig. III-51). The integrated O_2 consumption results at the seven aging temperatures are plotted in Fig. IV-38 and these results are time-temperature superposed at a reference temperature of 48°C in Fig. IV-39. Figure IV-40 gives an Arrhenius plot of the empirically derived O_2 consumption shift factors (normalized to 124°C) and the shift factors derived from superposition of the elongation results for the green-colored material (Fig. III-55). Also marked on this figure are arrows at 100°C and 120°C, indicative of the lowest and highest melting peaks based on the DSC (Fig. III-51). Based on these results there is a definite change in Arrhenius slope below 124°C with a much higher E_a appropriate above the crystalline melting point. Since elongation measurements could only realistically be obtained above the melting point, this change could never be discovered from elongation results. The sensitivity of O_2 consumption allows us to probe through the melting point region and discover this change in slope. It is interesting to note that the O_2 consumption results at 138°C (well above the melting point) show a change in slope such that these results correlate with elongation results at higher temperature. This offers strong evidence that the oxidation being monitored using O_2 consumption is responsible for the degradation of the mechanical properties above the melting point and suggests that the change to a lower E_a value for UOC below the melting point probably reflects similar changes for the mechanical properties. If we now use the 98 kJ/mol E_a appropriate below 124°C to extrapolate the elongation results to 50°C we obtain the result shown in Fig. IV-41 (upper x-axis). This result allows us to estimate a 50°C lifetime of ~1800 years. Although this estimate is substantially lower than the 23,000-year estimate from conventional Arrhenius extrapolation (upper x-axis in Fig. III-55), it still underscores the robustness of XLPO materials under typical nuclear power plant aging conditions.

The CO_2 solubility in the XLPO-05 material was determined to be 0.30 ccSTP/cc/atm [IV-5]. Since this is a fairly low value for solubility, the corrections necessary for CO_2 dissolved in the material during the analyses were relatively small ranging from ~2% at 138°C to ~21% at the lowest temperatures. The resulting integrated CO_2 production values are shown in Fig. IV-42. Time-temperature superposition of these results is shown in Fig. IV-43 together with the empirically derived shift factors used for the superposition. These shift factors are slightly larger but in reasonable agreement with those for oxygen consumption, as seen when the a_T values for elongation, oxygen consumption and CO_2 production are plotted on an Arrhenius graph (Fig. IV-44). This suggests that the relative importance of CO_2 for a given amount of degradation (e.g., oxygen consumed) does not depend on temperature. Further evidence for this statement is seen when the ratio of CO_2 produced to O_2 consumed is plotted against O_2 consumed (Fig. IV-45). Except for the 138°C data point (above the crystalline melting point- see Fig. III-51), the results at all the other temperatures appear generally to fall on a single curve. Thus all evidence points to a constant mix of oxidative reactions from 124°C down to 48°C, adding more confidence to the 50°C lifetime estimate of ~1800 years (Fig. IV-41- upper x-axis).

Conclusions

The results above show that O_2 consumption measurements are usually well correlated with mechanical property (e.g., elongation) measurements as anticipated since the presence of oxygen during aging is usually found to dominate degradation. The advantage of O_2 consumption measurements is their sensitivity that allows the probing of lower temperatures. By utilizing such lower temperature data coupled with time-temperature superposition analyses, these capabilities allow us to quantitatively test the Arrhenius extrapolation assumption. Such testing indicates that many materials show evidence of "downward" curvature (E_a values drop as the aging temperature is lowered) consistent with many literature results and with the results found above for elongation measurements. The UOC approach also allows the probing of temperatures that cross through the crystalline melting point region of semi-crystalline materials such as XLPO and EPR cable insulations. Again the consumption results appear to be well-correlated with elongation results for the few cases where elongation results have been obtained below the main melting point of the material.

The evidence for correlations between elongation and UOC allows us to utilize the lower temperature E_a values obtained from O_2 consumption to more reliably extrapolate higher temperature mechanical property results. For an aging temperature of 50°C, the improved predictions allow us to conclude that the lifetime of hypalon jackets should be greater than 80 years whereas EPR and XLPO insulations have predicted lifetimes many times longer. These estimates, of course, refer only to situations where radiation doses are minor (less than 0.1 Gy/h or equivalently 10 rad/h). For higher dose rates, the importance of radiation effects must be considered (see next section of this report).

References

IV-1. K. T. Gillen, R. Bernstein and M. Celina, "Non-Arrhenius Behavior for Oxidative Degradation of Chlorosulfonated Polyethylene Materials", Polymer Degradation and Stability, 87, 335 (2005).

IV-2. J. Wise, K. T. Gillen and R. L. Clough, "An Ultrasensitive Technique for Testing the Arrhenius Extrapolation Assumption for Thermally-Aged Elastomers", Polym. Degrad. & Stabil., 49, 403 (1995).

IV-3. K. T. Gillen, M. Celina, R. L. Clough and J. Wise, "Extrapolation of Accelerated Aging Data- Arrhenius or Erroneous?", Review paper in **Trends in Polymer Science,** 5, 250 (1997).

IV-4. Gillen KT, Celina M, Bernstein, R. Validation of improved methods for predicting long-term elastomeric seal lifetimes from compression stress-relaxation and oxygen consumption techniques. Polym Degrad Stab, 2003;82:25.

IV-5. K. T. Gillen, R. Bernstein and D. K. Derzon, "Evidence of non-Arrhenius Behavior from Laboratory Aging and 24-year Field Aging of Chloroprene Rubber Materials, Polymer Degradation and Stability, 87, 57 (2005).

IV-6. Celina M, Gillen KT, Graham AC, Assink RA, Minier LM. Thermal degradation studies of a polyurethane propellant binder. Rubber Chem. Technol 2000:73:678.

IV-7. Celina M, Wise J, Ottesen DK, Gillen KT, Clough RL. Oxidation of thermally aged nitrile rubber. Polym Degrad Stab, 1998;60:493.

IV-8. Celina M, Wise J, Ottesen DK, Gillen KT, Clough RL. Oxidation profiles of thermally aged neoprene. Polym Degrad Stab, 2000;68:171.

IV-9. Richters P. Initiation Process in the oxidation of polypropylene. Macromolecules 1970;3:262.

IV-10. Gugumus, F. The use of accelerated tests in the evaluation of antioxidants and light stabilizers. In: Scott G, editor. Developments in Polymer Stabilization-8. London: Elsevier Applied Science, 1987, Ch. 6.

IV-11. Bernstein BS, Lee PN. Proc. 24th Int. Wire and Cable Symp., Nov. 1975, p. 202.

IV-12. Gijsman P, Hennekens J, Vincent J. The influence of temperature and catalyst residues on the degradation of unstabilized polypropylene. Polym Degrad Stab, 1993;39:271.

IV-13. Rosik L, Kovarova J, Pospisil J. Lifetime prediction of ABS polymers based on thermoanalytical data. J. Thermal Anal, 1996;46:465.

IV-14. Gugumus F. Effect of temperature on the lifetime of stabilized and unstabilized PP films. Polym Degrad Stab, 1999;63:41.

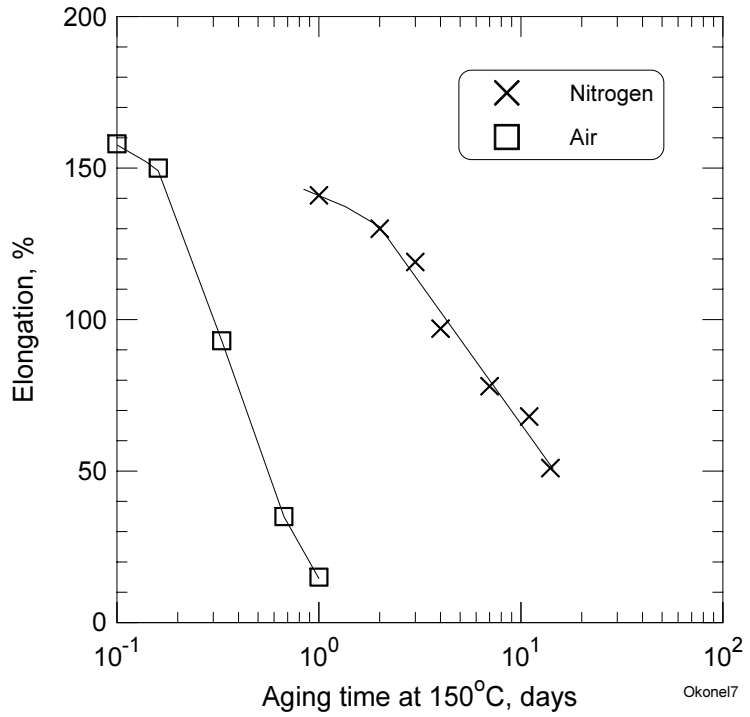

Figure IV-1. Elongation results for Neo-01 cable jacket material aged at 150°C in nitrogen and in air.

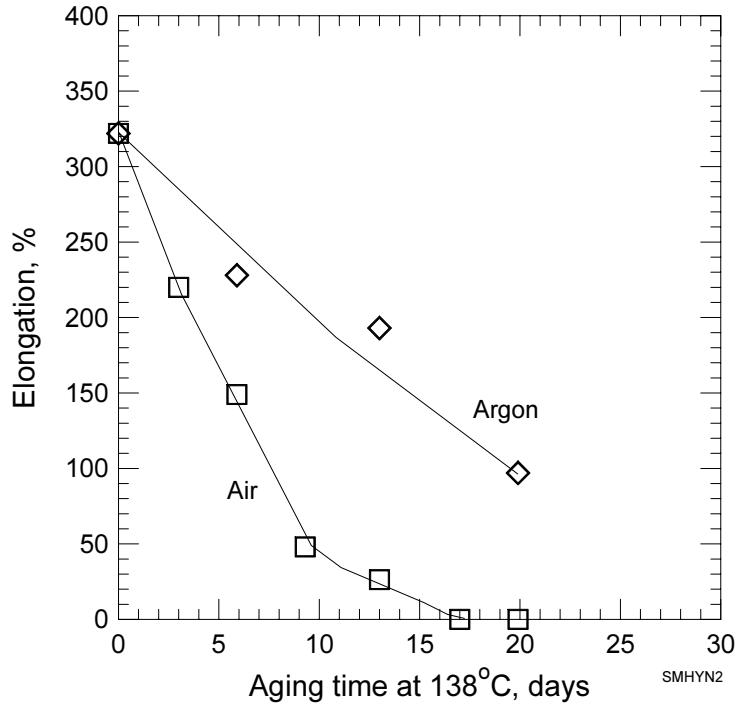

Figure IV-2. Elongation results for Hyp-03 cable jacket material aged at 138°C in argon and in air.

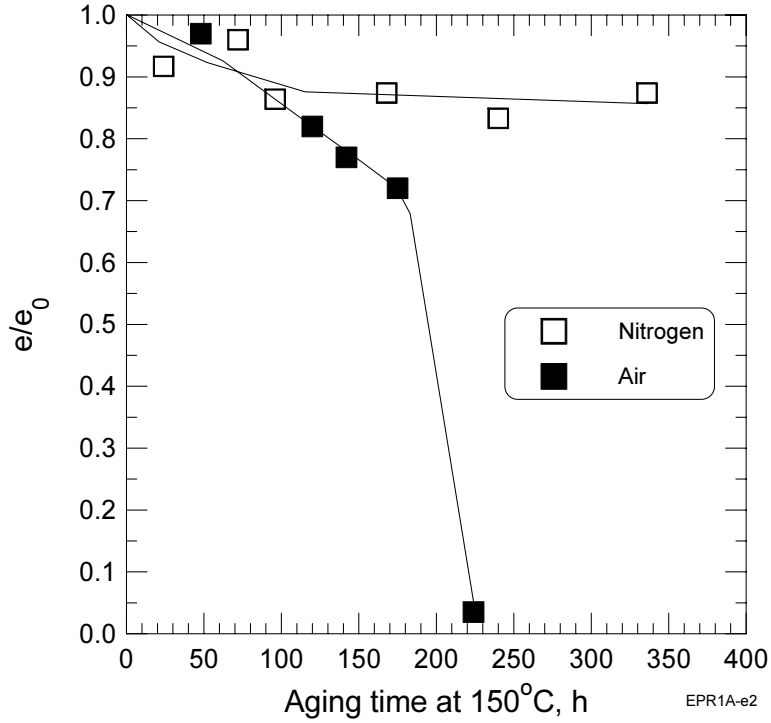

Figure IV-3. Elongation results normalized to unaged elongation value for EPR-01A cable jacket material aged at 150°C in nitrogen and in air.

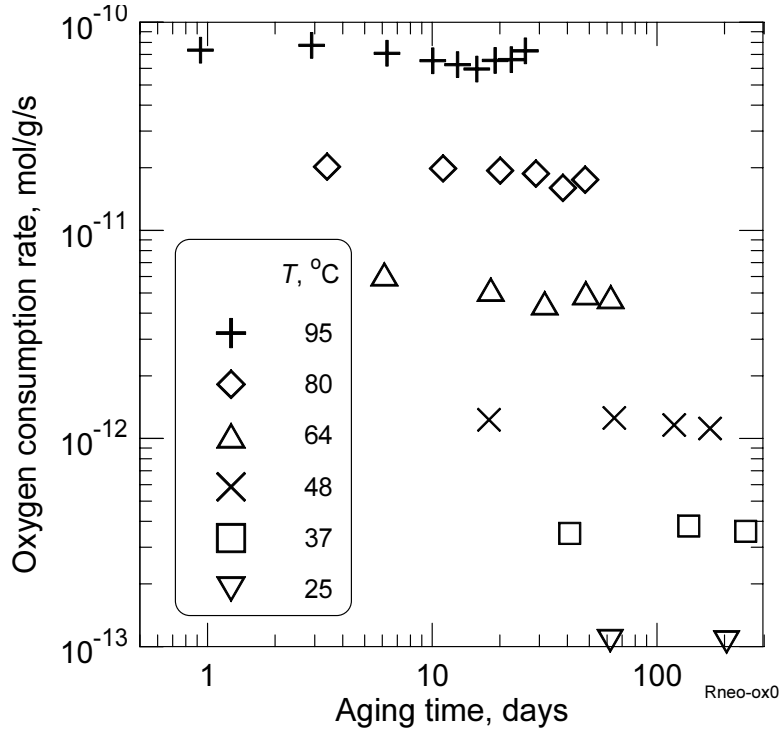

Figure IV-4. Oxygen consumption rate measurements for Neo-02 versus time at the indicated aging temperatures.

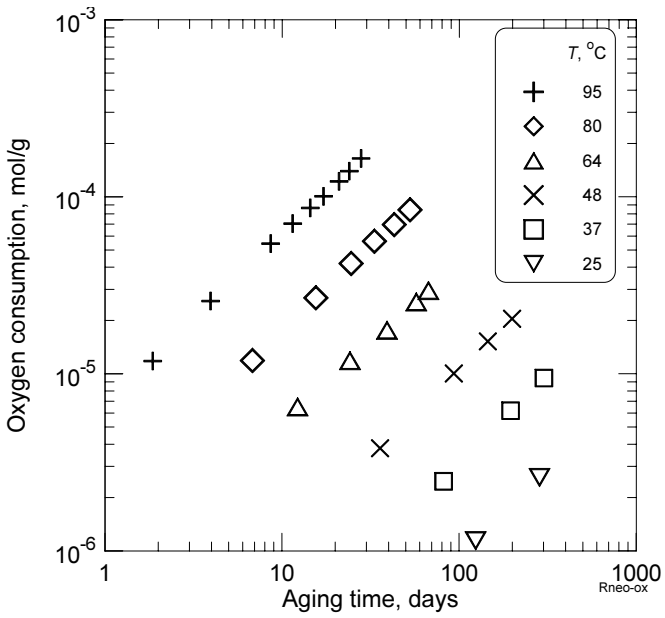

Figure IV-5. Integrated oxygen consumption results for Neo-02 from Fig. IV-4.

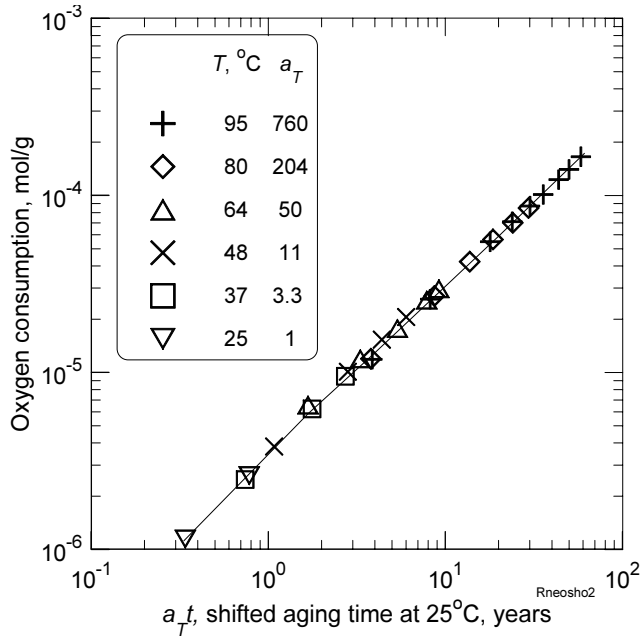

Figure IV-6. Time-temperature superposition of the oxygen consumption results for Neo-02 using the empirically derived shift factors shown on the figure.

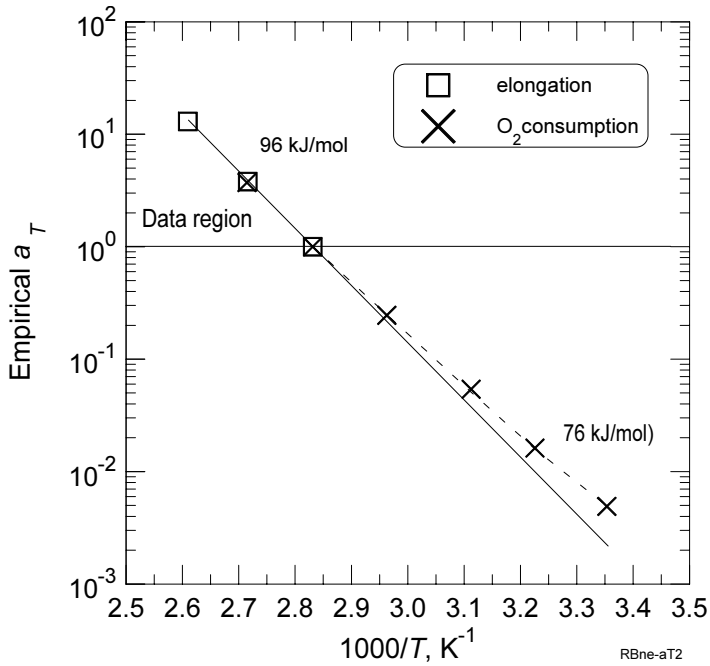

Figure IV-7. Arrhenius plot of the shift factors for Neo-02 determined for elongation and oxygen consumption (normalized at 80°C).

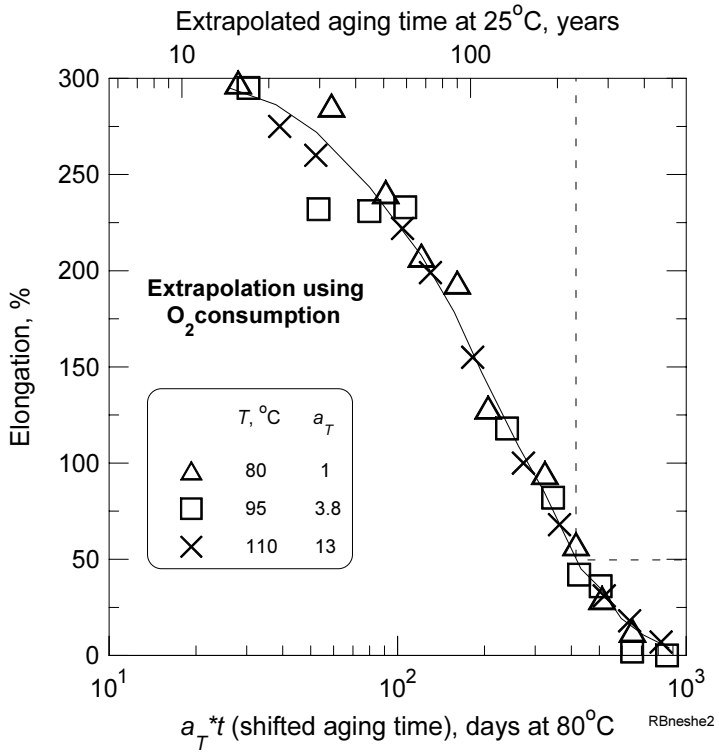

Figure IV-8. Time-temperature superposed elongation results for Neo-02 at 80°C (lower x-axis) plus the extrapolated results at 25°C from oxygen consumption (top x-axis).

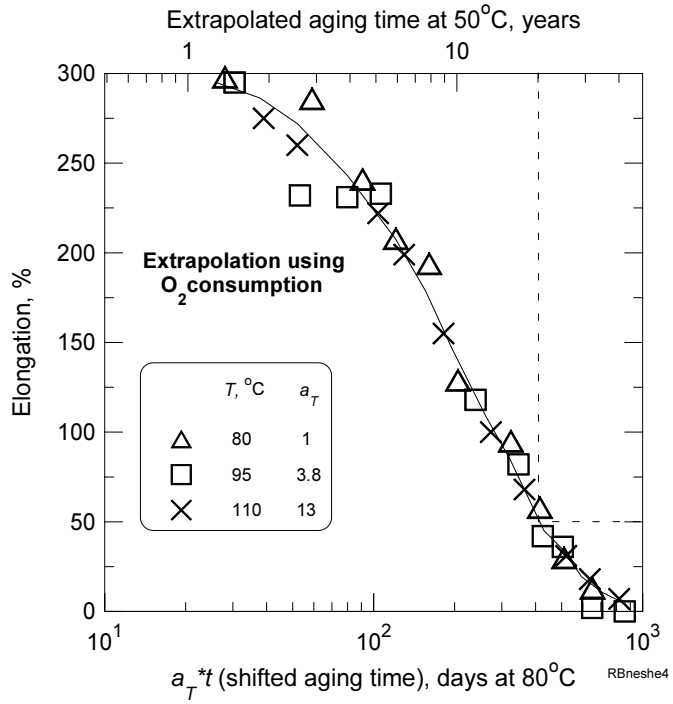

Figure IV-9. Time-temperature superposed elongation results for Neo-02 at 80°C (lower x-axis) plus the extrapolated results at 50°C from oxygen consumption (top x-axis).

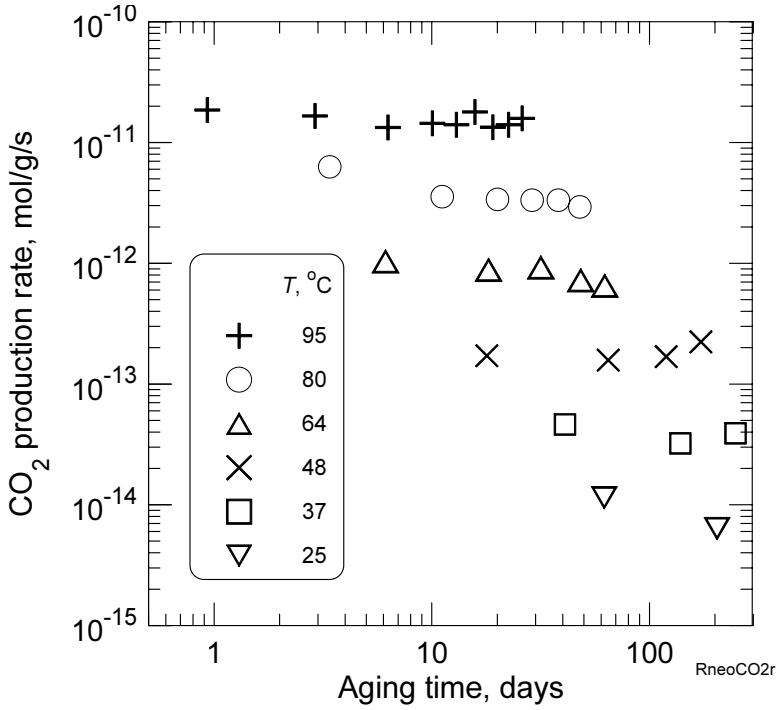

Figure IV-10. CO_2 production rate measurements for Neo-02 versus time at the indicated aging temperatures.

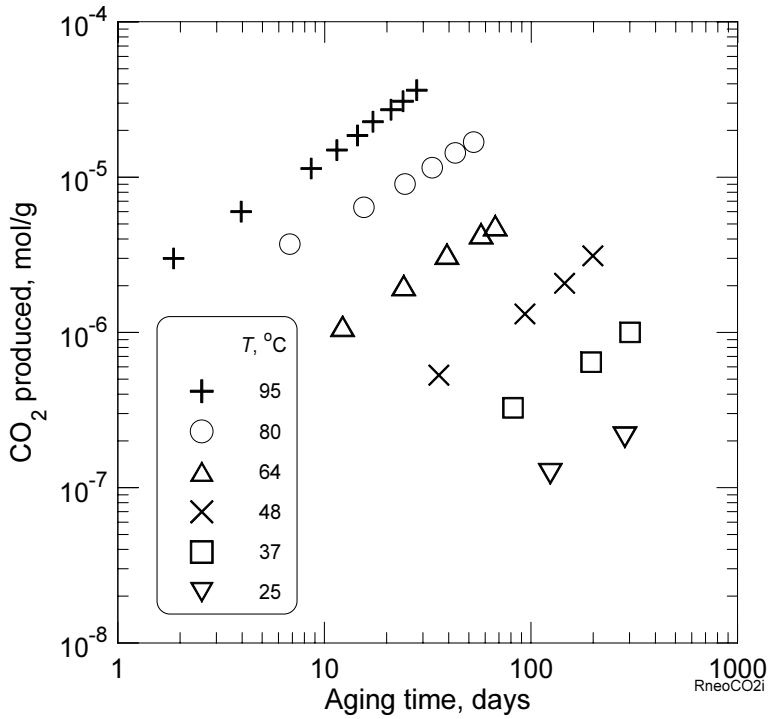

Figure IV-11. Integrated CO_2 production results for Neo-02 from Fig. IV-10.

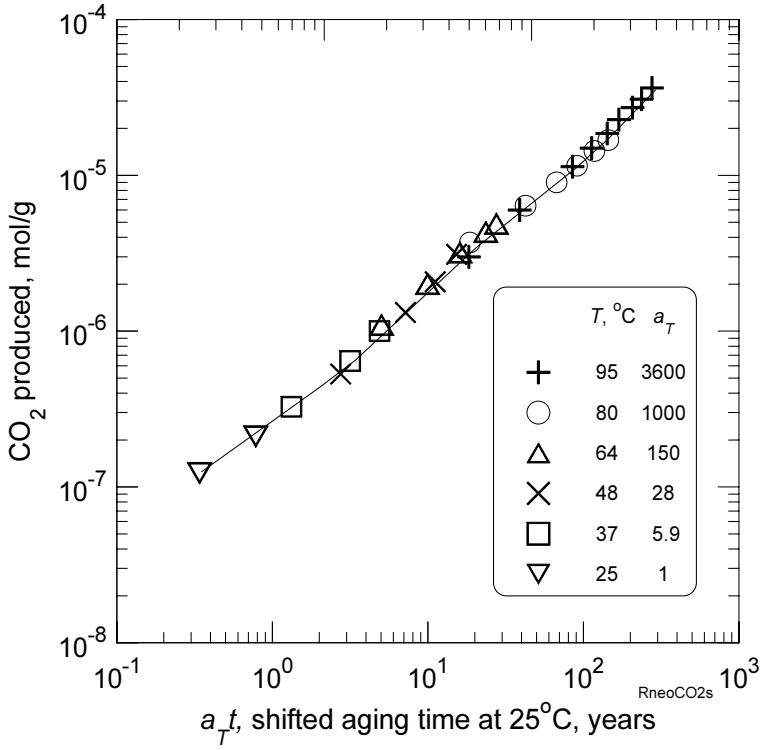

Figure IV-12. Time-temperature superposition of the CO_2 production results for Neo-02 using the empirically derived shift factors shown on the figure.

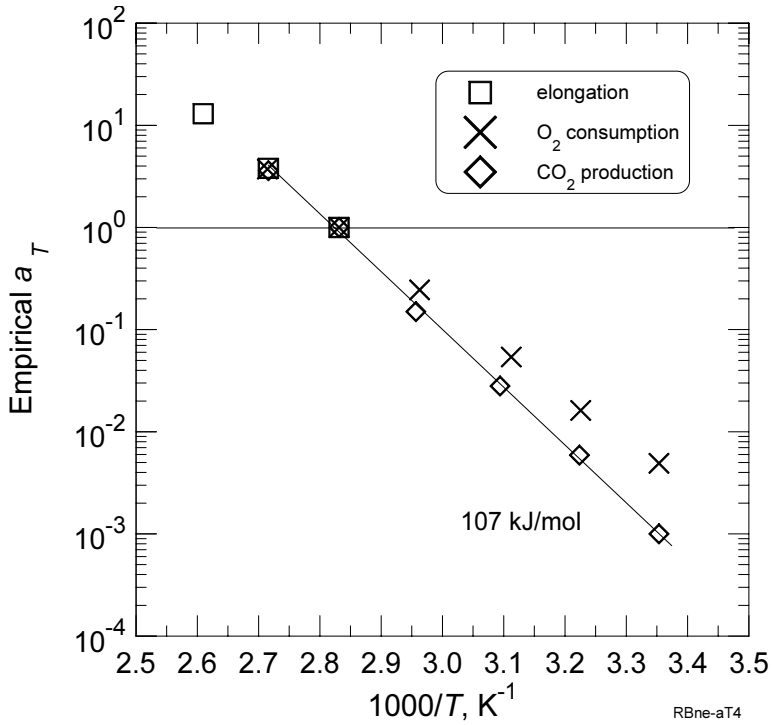

Figure IV-13. Arrhenius plot of the shift factors for elongation, oxygen consumption and CO_2 production of Neo-02 (all normalized to 80°C).

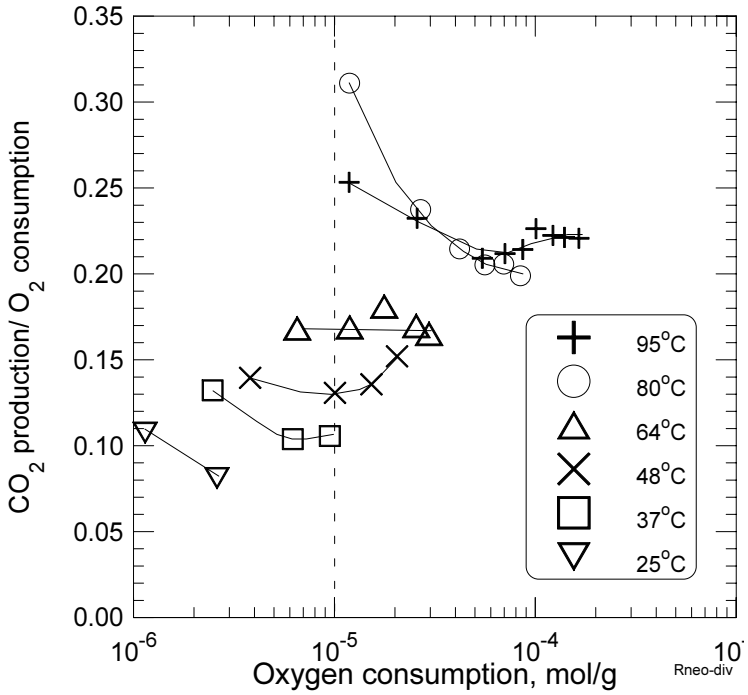

Figure IV-14. The ratio of CO_2 produced to O_2 consumed versus the O_2 consumed for Neo-02 at the indicated aging temperatures.

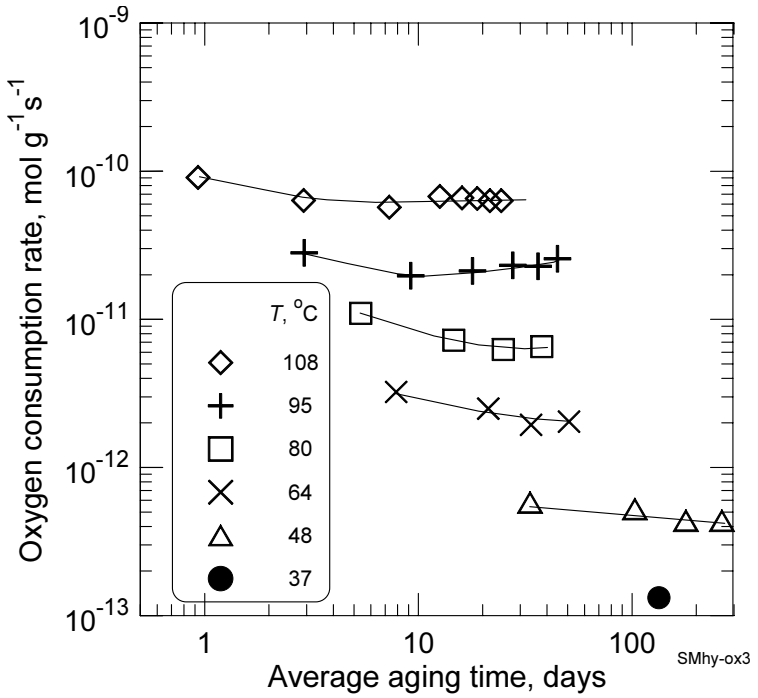

Figure IV-15. Oxygen consumption rate measurements for Hyp-03 versus time at the indicated aging temperatures.

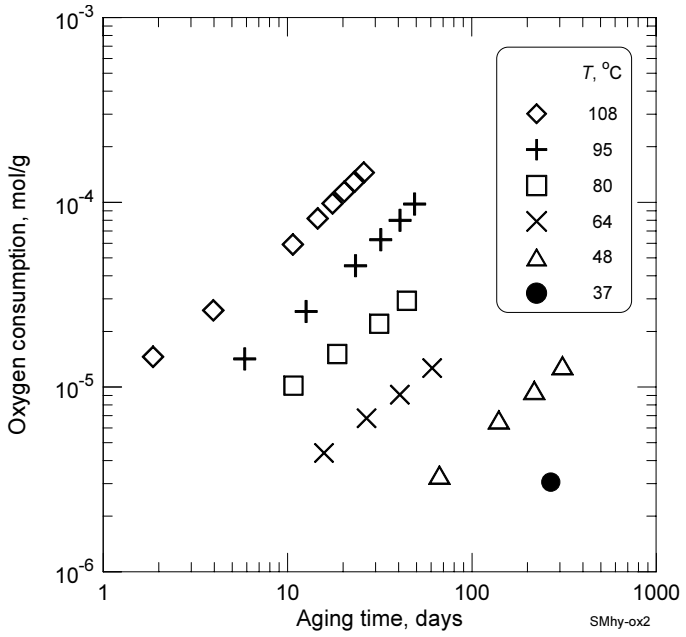

Figure IV-16. Integrated oxygen consumption results for Hyp-03 from Fig. IV-15.

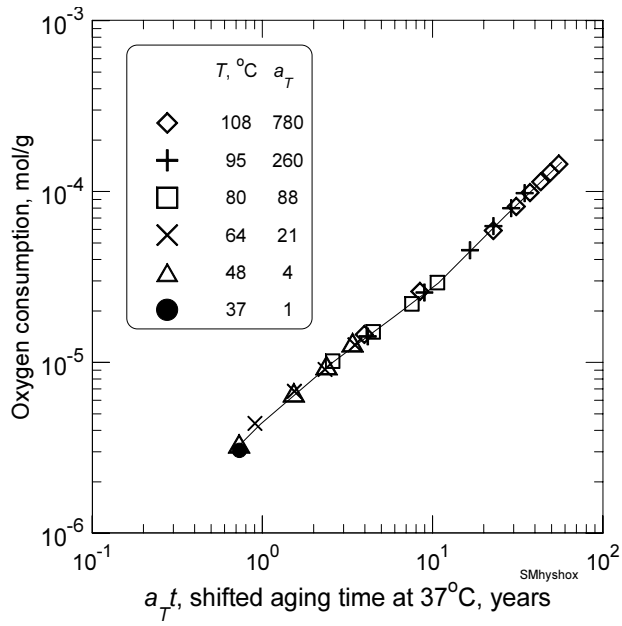

Figure IV-17. Time-temperature superposition of the oxygen consumption results for Hyp-03 using the empirically derived shift factors shown on the figure.

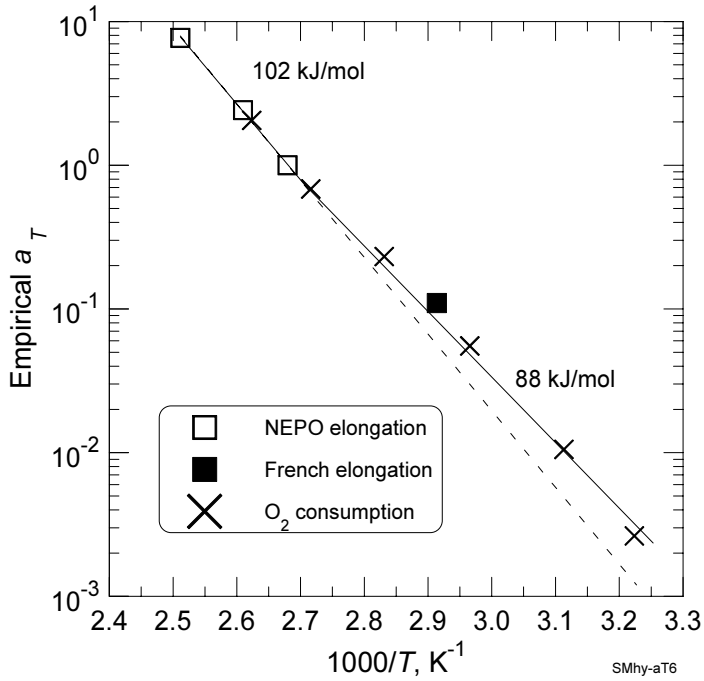

Figure IV-18. Arrhenius plot of the shift factors for Hyp-03 determined for elongation and oxygen consumption (normalized at 100°C). The dashed line is the Arrhenius line appropriate to the three high temperature NEPO elongation results.

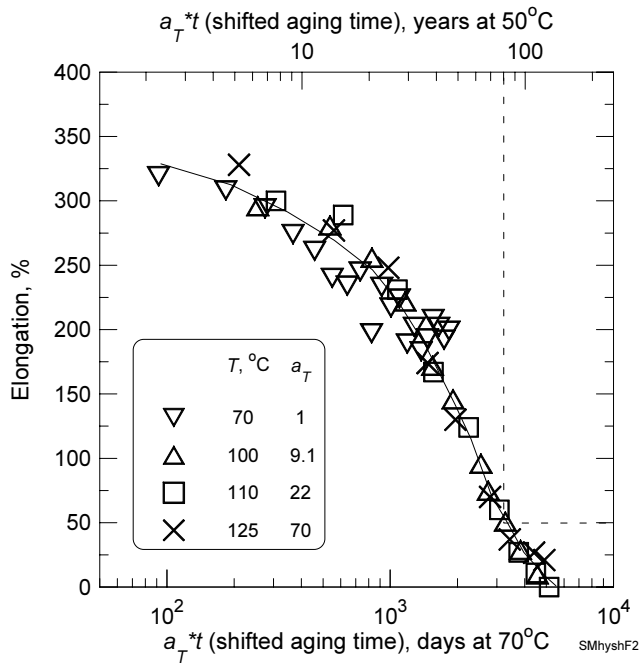

Figure IV-19. Time-temperature superposed elongation results for Hyp-03 at 70°C (lower x-axis) plus the extrapolated results at 50°C from oxygen consumption (top x-axis).

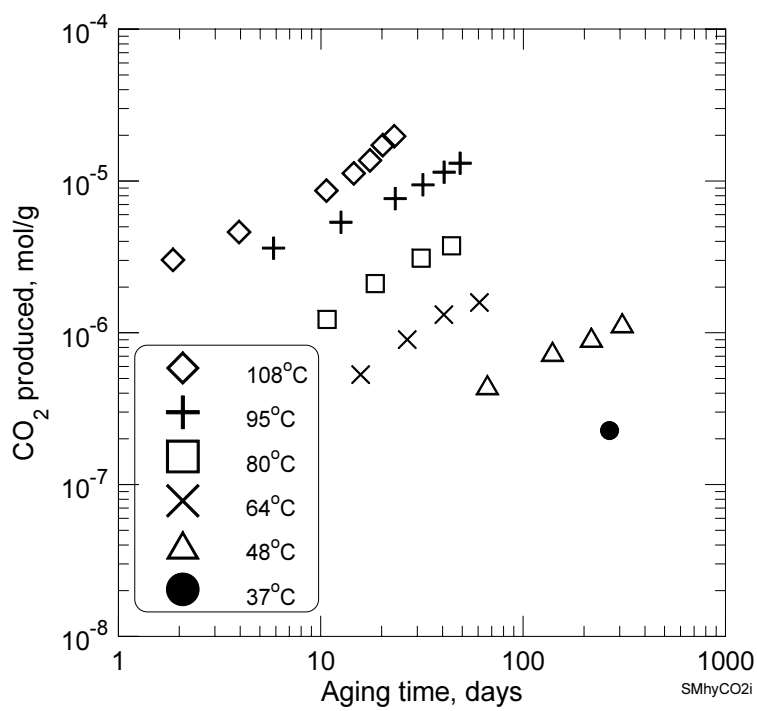

Figure IV-20. Integrated CO_2 production results versus aging time for Hyp-03 at the indicated temperatures.

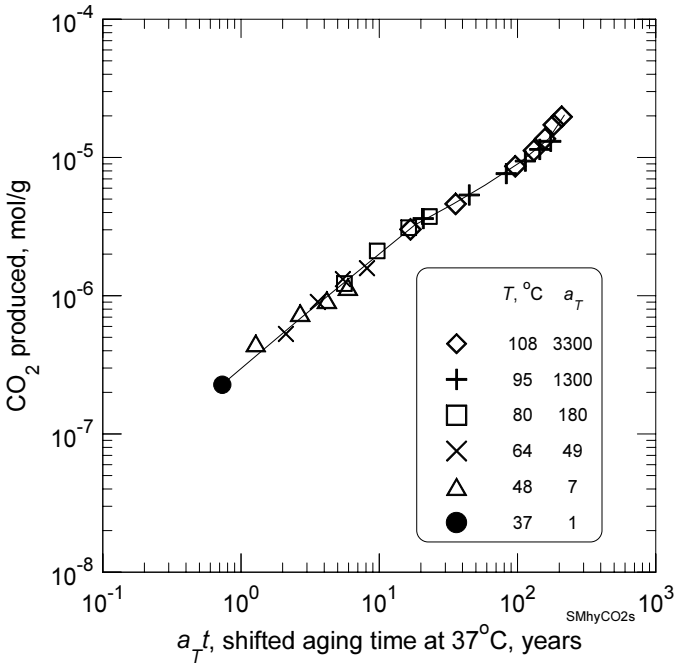

Figure IV-21. Time-temperature superposition of the CO_2 production results for Hyp-03 using the empirically derived shift factors shown on the figure.

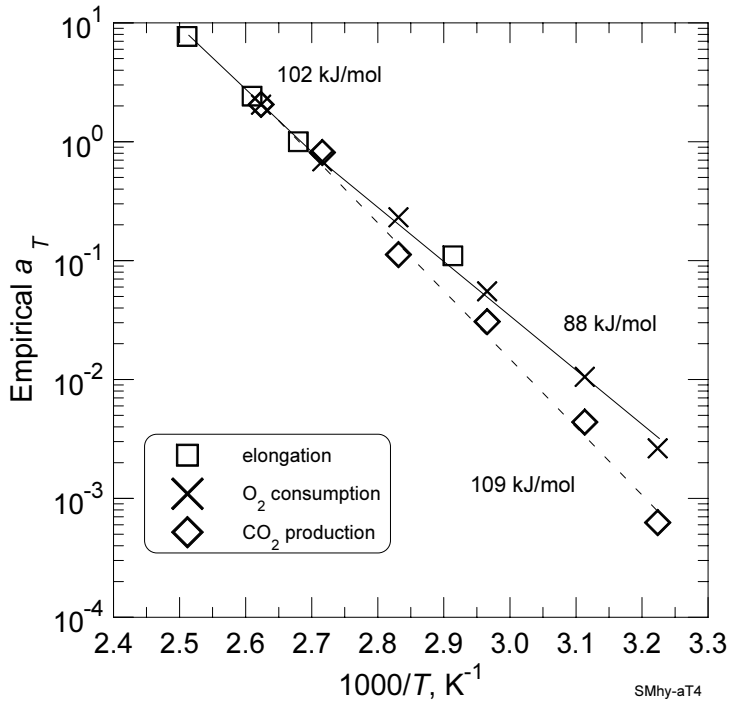

Figure IV-22. Arrhenius plot of the shift factors for elongation, oxygen consumption and CO_2 production of Hyp-03 (all normalized to 100°C).

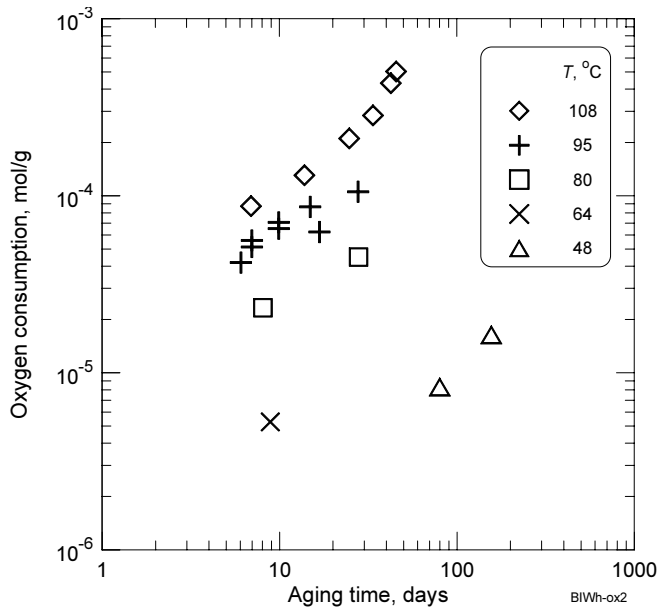

Figure IV-23. Integrated oxygen consumption results for Hyp-08 versus time at the five indicated aging temperatures.

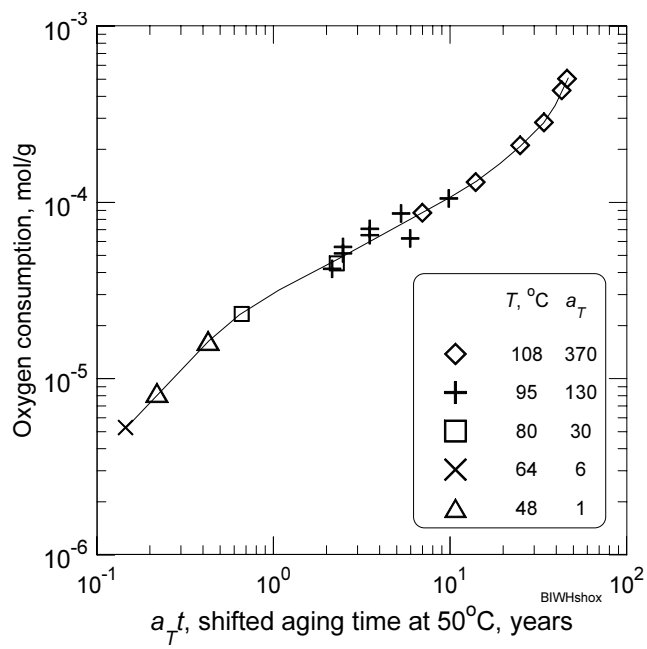

Figure IV-24. Time-temperature superposition of the oxygen consumption results for Hyp-08 using the empirically derived shift factors shown on the figure.

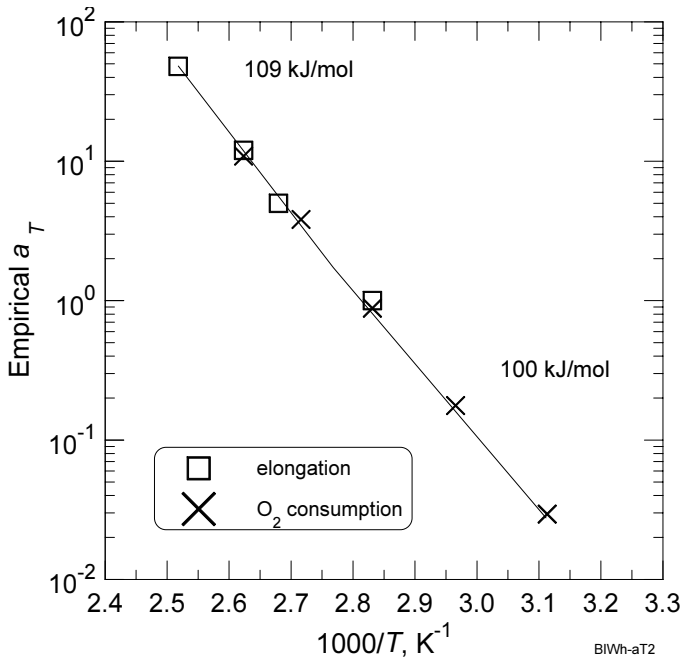

Figure IV-25. Arrhenius plot of the shift factors for Hyp-08 determined for elongation and oxygen consumption (normalized at 80°C).

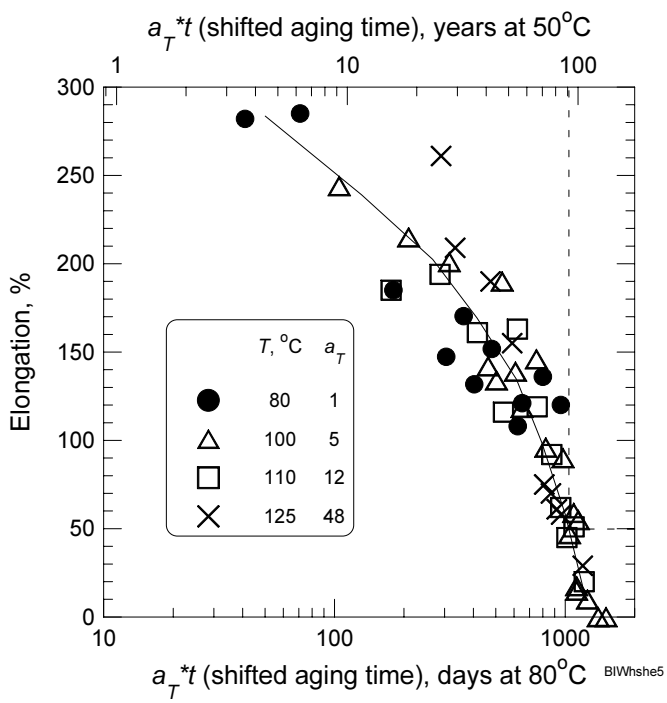

Figure IV-26. Time-temperature superposed elongation results for Hyp-08 at 80°C (lower x-axis) plus the extrapolated results at 50°C from oxygen consumption (top x-axis).

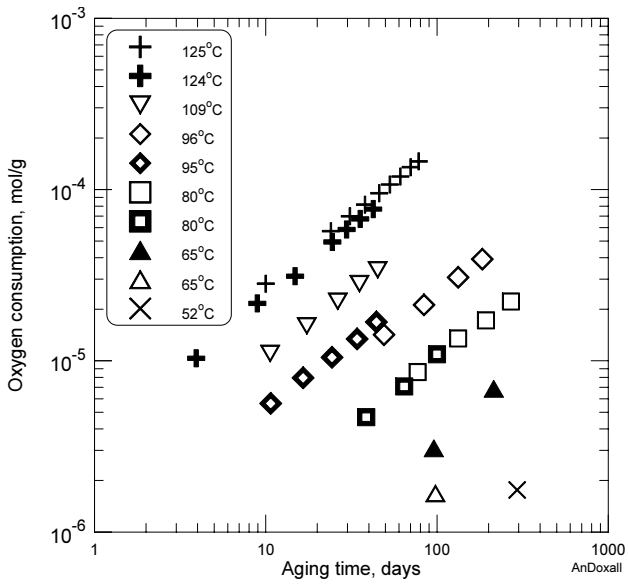

Figure IV-27. Integrated oxygen consumption results for EPR-04 versus time at the indicated aging temperatures including several repeat measurements.

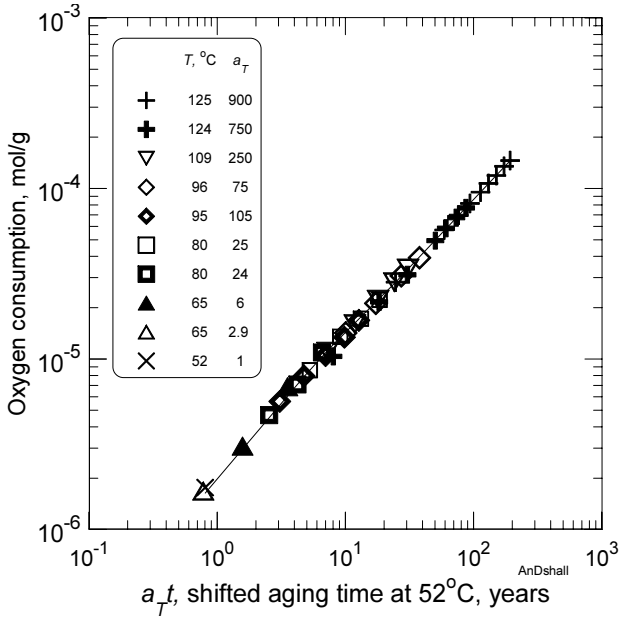

Figure IV-28. Time-temperature superposition of the oxygen consumption results for EPR-04 using the empirically derived shift factors shown on the figure.

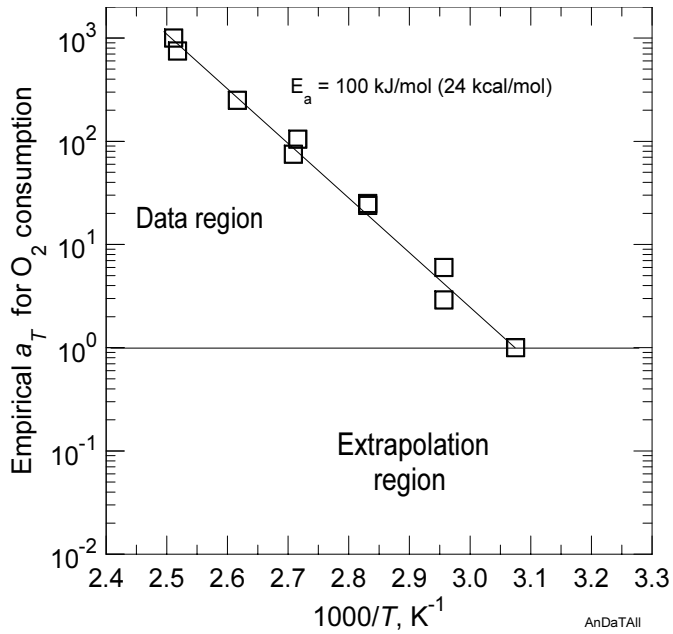

Figure IV-29. Arrhenius plot of the O_2 consumption for EPR-04 shift factors from Fig. IV-28.

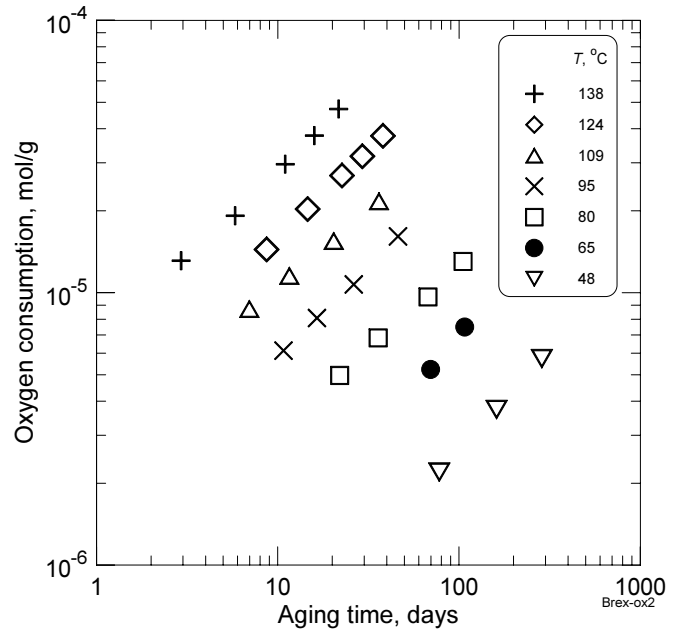

Figure IV-30. Integrated oxygen consumption results for the XLPO-02B.

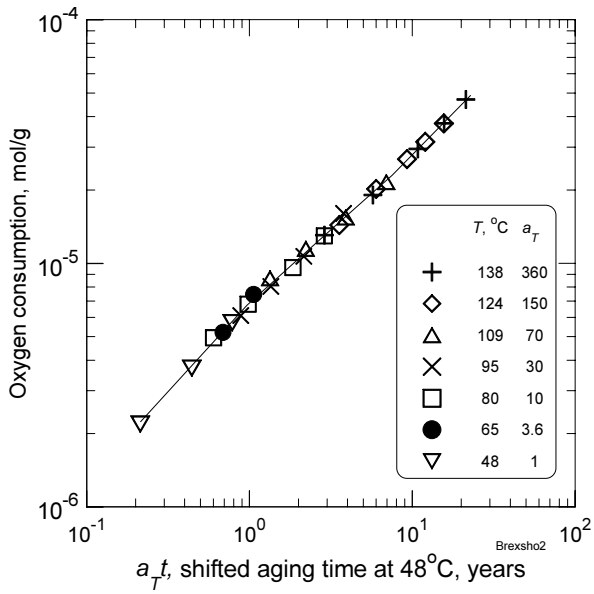

Figure IV-31. Time-temperature superposition of the oxygen consumption results for XLPO-02B using the empirically derived shift factors shown on the figure.

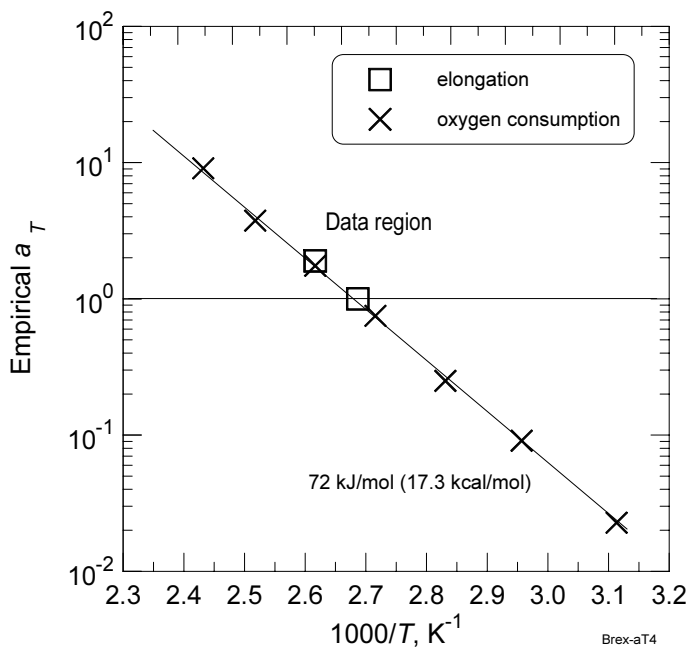

Figure IV-32. Arrhenius plot of the O_2 consumption shift factors for XLPO-02B from Fig. IV-31 plus the elongation shift factors at 99°C and 109°C.

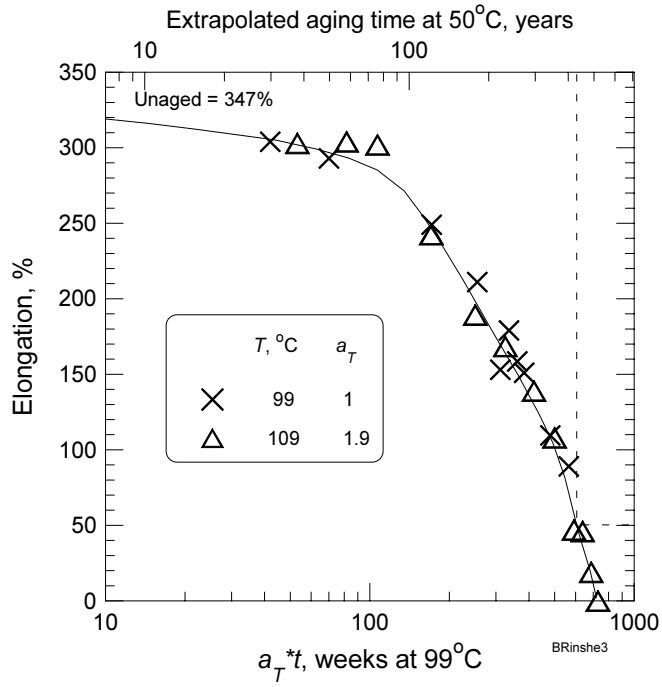

Figure IV-33. Time-temperature superposed elongation results for XLPO-02B at 99°C (lower x-axis) plus the extrapolated results at 50°C from oxygen consumption (top x-axis).

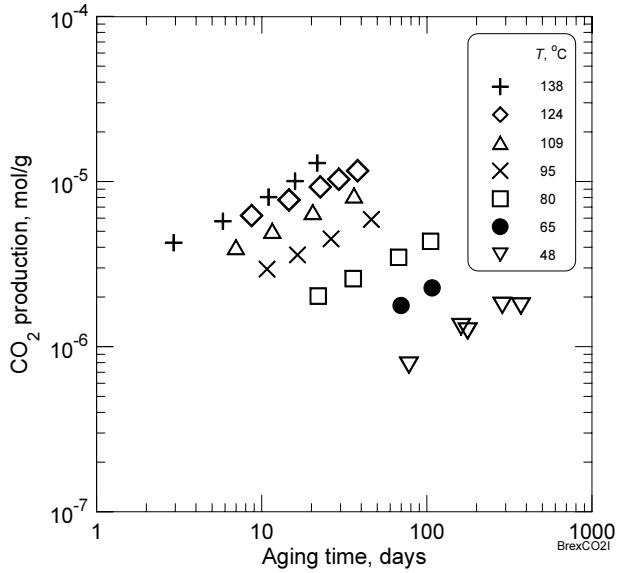

Figure IV-34. Integrated CO_2 production results versus aging time for XLPO-02B at the indicated temperatures.

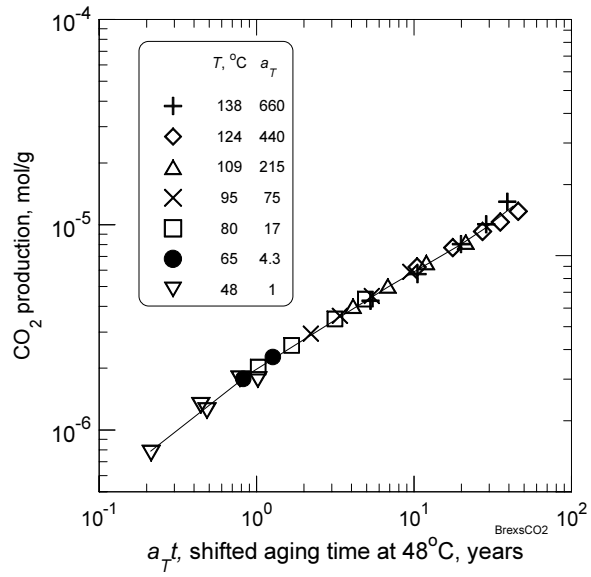

Figure IV-35. Time-temperature superposition of the CO_2 production results for XLPO-02B using the empirically derived shift factors shown on the figure.

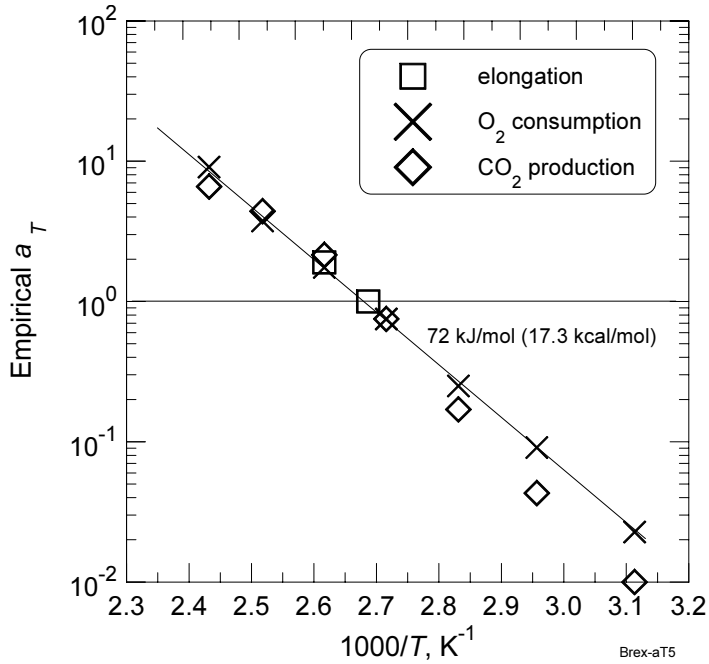

Figure IV-36. Arrhenius plot of the shift factors for elongation, oxygen consumption and CO_2 production of XLPO-02B (all normalized to 99°C).

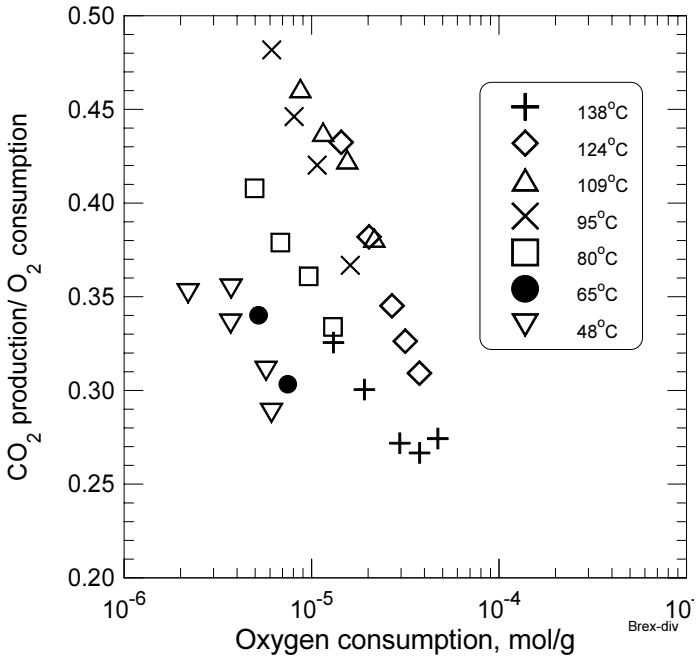

Figure IV-37. The ratio of CO_2 produced to O_2 consumed versus the O_2 consumed for XLPO-02B at the indicated aging temperatures.

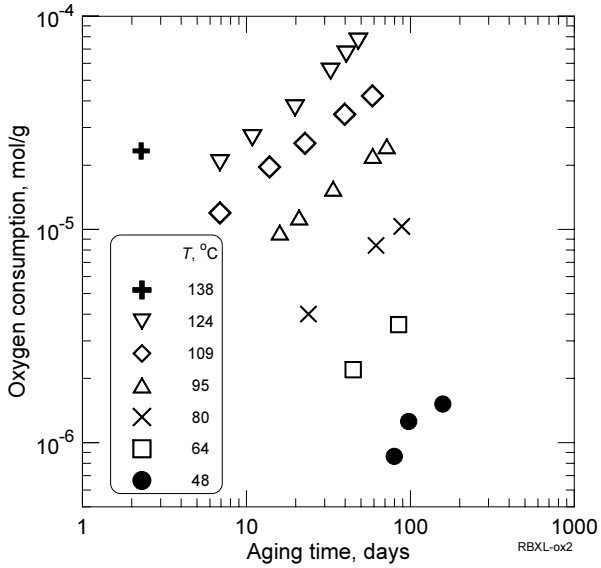

Figure IV-38. Integrated oxygen consumption results for the green XLPO-05.

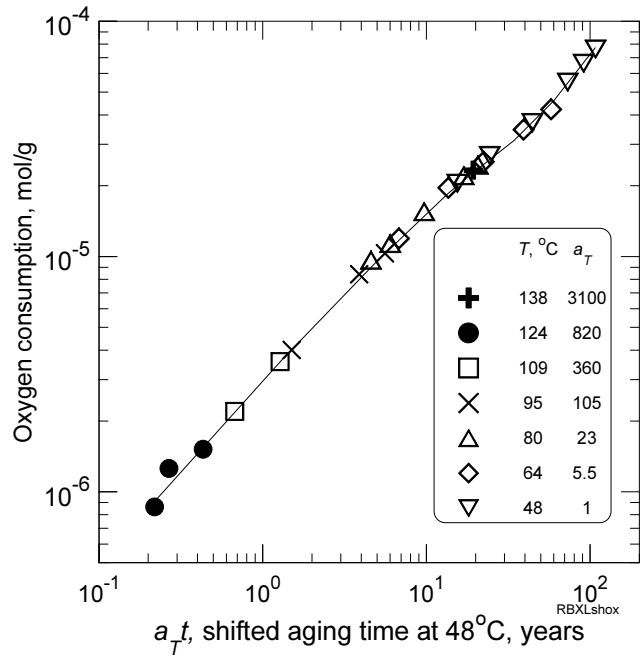

Figure IV-39. Time-temperature superposition of the oxygen consumption results for green XLPO-05 using the empirically derived shift factors shown on the figure.

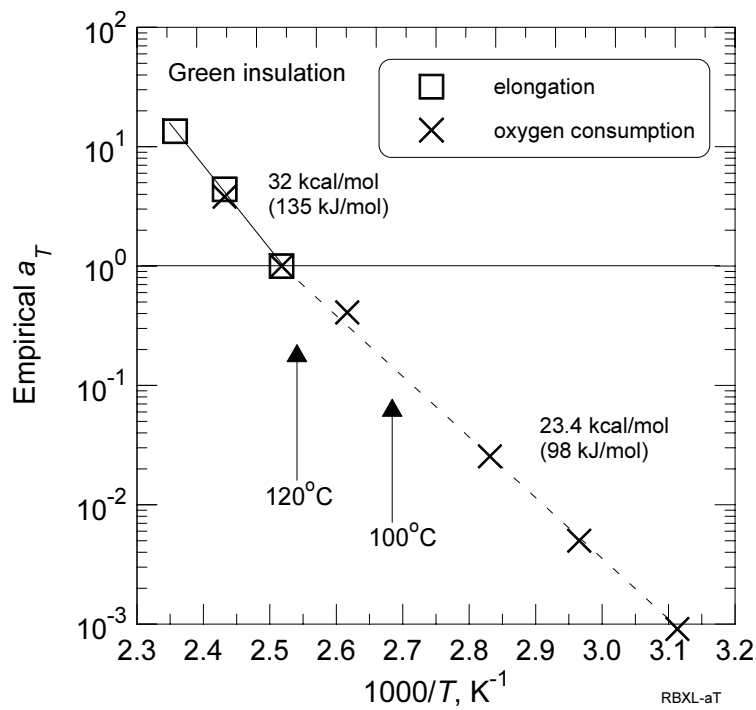

Figure IV-40. Arrhenius plot of the O_2 consumption shift factors and the elongation shift factors (both normalized at 124°C) for green XLPO-05 from Fig. IV-39.

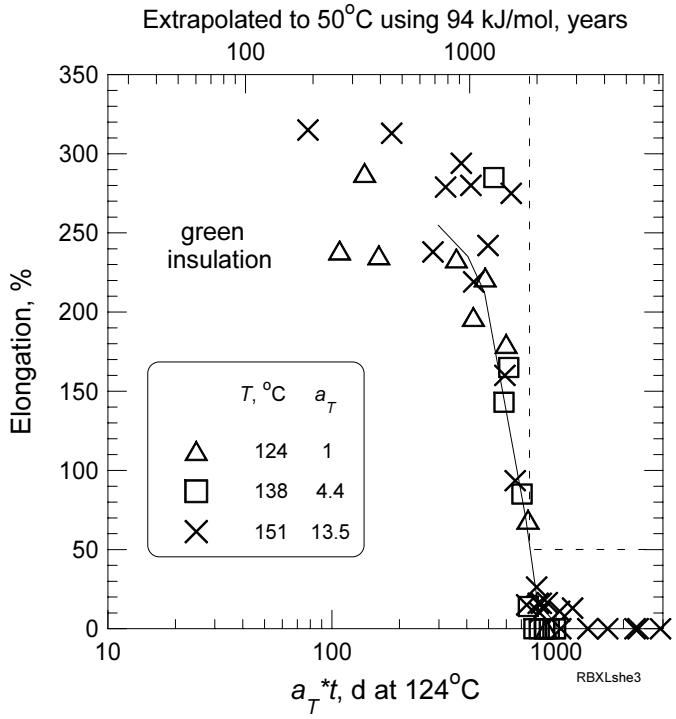

Figure IV-41. Time-temperature superposed elongation results for XLPO-05 at 124°C (lower x-axis) plus the extrapolated results at 50°C from oxygen consumption (top x-axis).

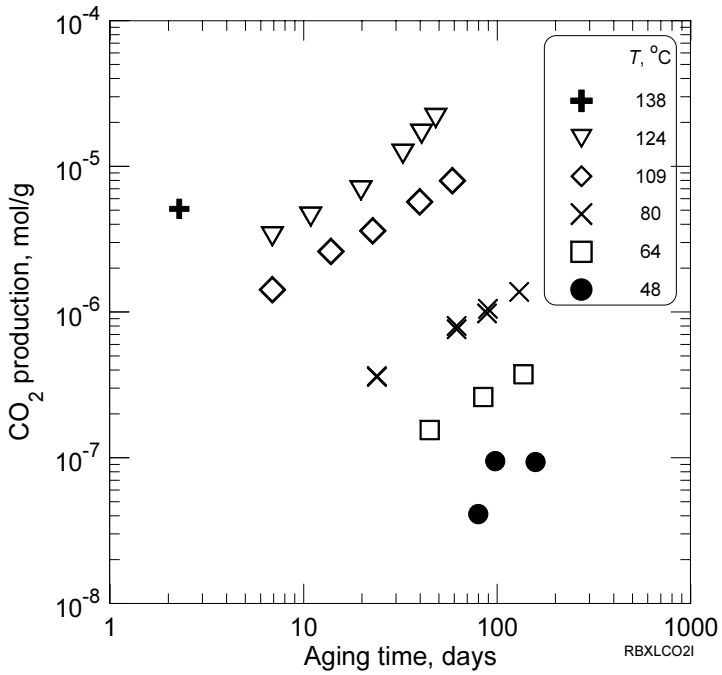

Figure IV-42. Integrated CO_2 production results for the green XLPO-05.

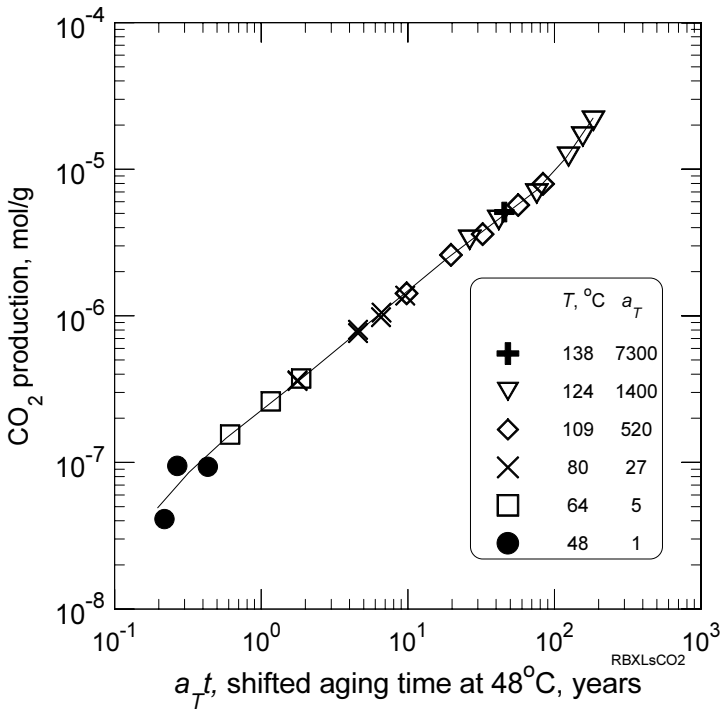

Figure IV-43. Time-temperature superposition of the CO_2 production results for green XLPO-05 using the empirically derived shift factors shown on the figure.

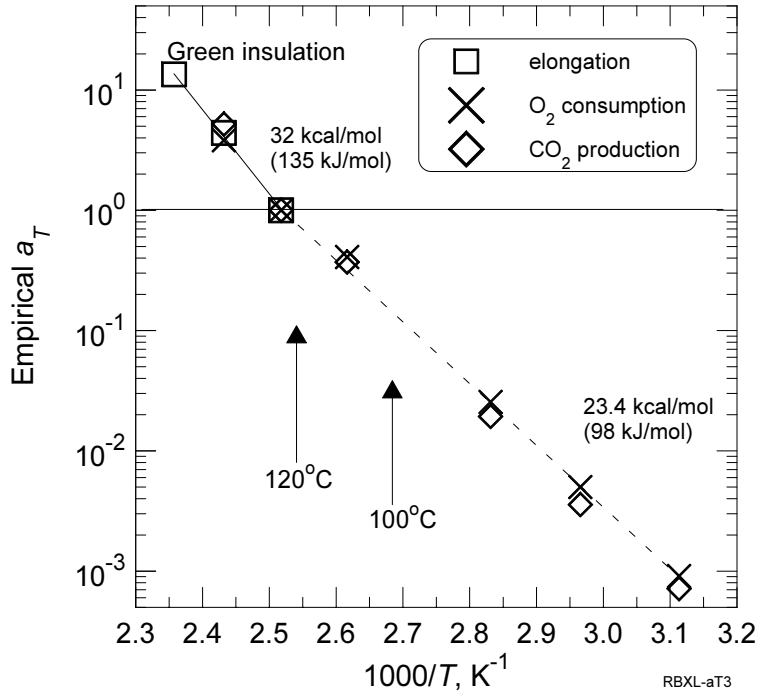

Figure IV-44. Arrhenius plot of the shift factors for elongation, oxygen consumption and CO_2 production of XLPO-05 (all normalized to 124°C).

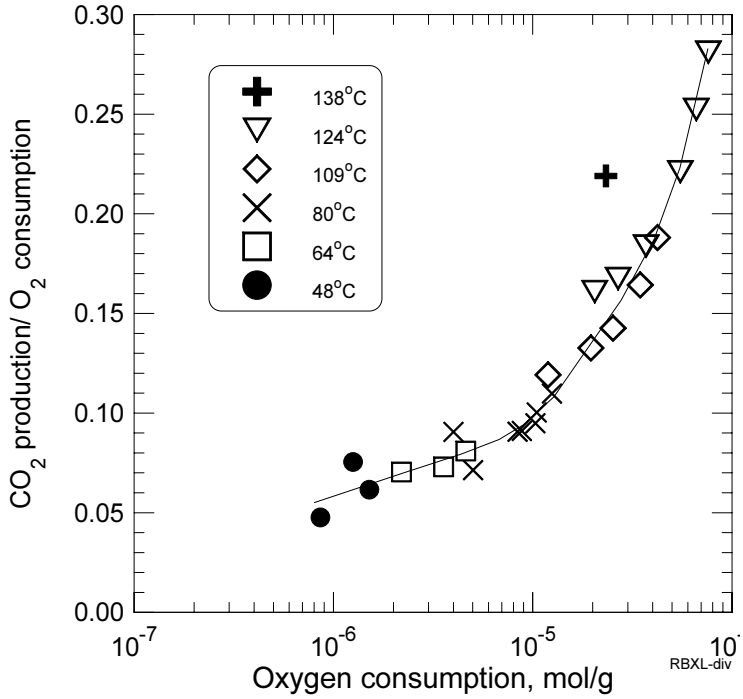

Figure IV-45. The ratio of CO_2 produced to O_2 consumed versus the O_2 consumed for XLPO-05 at the indicated aging temperatures.

V. Radiation Aging Results: Elongation Measurements

Introduction

A major thrust of our earlier studies on nuclear power plant cable materials involved elongation measurements on materials aged under combined radiation plus thermal conditions and numerous reports resulted from this work [V-1 through V-11]. The work led to a method for analyzing combined environment aging results that we referred to as time-temperature-dose rate (*t-T-DR*) superposition [V-4 through V-9]. This approach utilized concepts similar to time-temperature superposition with an added dimension (radiation) and led to predictive capabilities for combined radiation-thermal environments through a two-dimensional extrapolation procedure. The *t-T-DR* approach has been incorporated into an IEEE Standard [V-12] and into an IEC Technical Report [V-13]. The earlier studies also found some interesting anomalous effects for certain partially crystalline EPR and XLPO cable insulations aged in combined radiation-thermal environments [V-10,V-11]. One of the effects involved the observation of faster mechanical degradation occurring in radiation environments as the aging temperature was reduced (we labeled this as "inverse temperature behavior"). For certain of the materials that showed inverse temperature behavior, we found that their mechanical properties could be recovered by briefly heating the material above the crystalline melting point (we labeled this as "Lazarus behavior").

During the NEPO program and the immediately preceding DOE-funded program we carried out a limited number of combined environment exposures. There were three main reasons for these efforts. First we wanted to further test time-temperature dose rate superposition ideas on several neoprene and hypalon cable jackets to get a better feeling of their predicted lifetimes for instances where radiation dose-rates were high enough during their nuclear power plant aging exposures. In addition we wanted to obtain data on an additional important EPR cable insulation to see whether it showed evidence of inverse temperature and/or Lazarus behavior. Finally we wanted to utilize some of the newer samples to determine how condition-monitoring results were affected by radiation aging. This section briefly discusses 1) the elongation results for Neo-02, Hyp-03, Hyp-04, Hyp-05 and Hyp-06 cable jackets in terms of time-temperature dose rate analyses and 2) the possible presence of inverse temperature and Lazarus effects for EPR-05. The condition monitoring results on these radiation-aged materials will be summarized in the upcoming sections on condition monitoring techniques.

Time-temperature-dose rate superposition (*t-T-DR*) analyses

Combined radiation-thermal aging was conducted on five cable-jacketing materials (Neo-02, Hyp-03, Hyp-04, Hyp-05 and Hyp-06). For each material, four aging conditions were used. Figure V-1 shows the elongation versus dose (1 Gy = 100 rad) results for Neo-02 at the four combined environment aging conditions used for this material. Figures V-2 through V-5 show comparable plots for the four hypalon jacketing materials.

The analyses of such combined environment data in terms of the time-temperature dose rate (*t-T-DR*) superposition approach has been discussed extensively in a series of previous papers [V-4 through V-9]. Given the complex procedures involved and these previous papers, we will only briefly describe the approach and its application to the current five materials; the interested reader can consult the earlier papers for details.

The first step in the analyses is to select a degradation level for analyses. In the present case we will focus on the doses required for the elongation to reach 50% absolute (other degradation levels can be chosen and analyzed in a similar manner). Thus for the Neo-02 material (Fig. V-1), we determine the dose required to reach 50% elongation for the four aging conditions used (from the intersection of the dashed line at 50% with the elongation results). We then plot these results, referred to as the dose to equivalent damage (DED) versus the dose rate on a log-log plot as shown on Fig. V-6. The aging temperatures (°C) appropriate to each of the plotted data points are shown next to the data. We then use *t-T-DR* superposition to derive an isothermal curve for a given amount of degradation (to 50% absolute elongation in the present case) at a selected reference temperature. We do this by assuming that the Arrhenius shift factors appropriate to thermal-only aging will be valid for combined environment aging if the multiplicative change in dose rate equals the multiplicative change in shift factors for the temperature. This means that in order to shift the 70°C result (dose rate equals 940 Gy/h) on Fig. V-6 to a 50°C isothermal curve, we first need the thermal-only shift factor from 70°C to 50°C for Neo-02. This can be estimated as $a_T = 6.5$ from the UOC results for Neo-02 (Fig. IV-7). This means that the combined environment experiment at 70°C and 940 Gy/h can be extrapolated to 50°C by horizontally shifting the result in Fig. V-6 to a dose rate of 940 Gy/h divided by 6.5 or 145 Gy/h as shown by the X in Fig. V-7. In a similar fashion, the other combined environment points are horizontally shifted to 50°C (no shift is necessary for the experiment conducted at 50°C) with the results shown on Fig. V-7. The excellent agreement between the shifted 70°C point (X) and the un-shifted 50°C point (diamond) offers evidence in support of the assumptions underlying *t-T-DR* superposition. As the dose rate of combined environment experiments drops to levels such that radiation is unimportant relative to thermal aging effects, one would expect the results to asymptotically approach the 50°C thermal-only aging conditions. The dashed line with unity slope represents this limit corresponding to a 20-year predicted lifetime for 50% residual elongation (top x-axis of Fig. IV-9). The fact that the *t-T-DR* shifted results approach this limiting result at low dose rates gives further evidence in support of this methodology.

Once predicted results from *t-T-DR* analyses are generated they can be used to determine when radiation must be considered as an important aging contributor. For instance the 50°C predictions for combined environments of the Neo-02 material (the solid curve in Fig. V-7) indicate that radiation effects will become important relative to the temperature effects above ~0.5 Gy/h (50 rad/h) at 50°C. Although the above analyses were conducted for degradation to 50% elongation at an extrapolated temperature of 50°C, the same approach can be applied to a different degradation level (from Fig. V-1) and a different extrapolated aging temperature. Thus the same combined environment results (Fig. V-1)

allow lifetime predictions to be made at any conditions of interest to operating nuclear plants.

In a similar fashion the doses to 50% elongation were obtained for the four hypalon jacketing materials (Figs. V-2 through V-5) with the results shown on DED versus dose rate plots (Figs. V-8 through V-11). To carry out the *t-T-DR* analyses on these materials we note that all hypalon jackets have quite similar temperature dependence for their shift factors (Figs. III-27) so we will use the UOC shift results for the Hyp-03 material from Fig. IV-18. The resulting *t-T-DR* shifted predictions at 50°C are shown in Figs. V-12 through V-15. These results indicate that radiation effects are fairly small for hypalon materials at 50°C for dose rates below ~0.1 Gy/h, equivalent to 350 kGy (35 Mrad) over 40 years.

Testing for inverse temperature and Lazarus effects

Past studies showed that significant inverse temperature and Lazarus effects existed for the mechanical properties of several important EPR and XLPO cable insulation materials [V-10, V-11]. These included the XLPO-02A, XLPO-05 and EPR-03. Under the NEPO program another important EPR cable insulation, EPR-05 was examined to see whether such effects occurred. Combined environment aging experiments were conducted at the LICA (Low Intensity Cobalt Aging) facility under two aging conditions (430 Gy/h plus 40°C and 445 Gy/h plus 80°C). Since the dose rates were similar within experimental uncertainty, one might expect to see equal or faster degradation as the combined environment temperature was raised from 40°C to 80°C. For past materials that showed inverse temperature effects the opposite occurred with much quicker degradation occurring at the lower temperature (thus the term "inverse temperature" effects). The elongation results for the EPR-05 material are shown in Fig. V-16 plotted against time (lower x-axis) and approximate total dose (upper x-axis). Although there is substantial scatter in the measurements, no evidence of important inverse temperature effects is found for this material. Given this observation coupled with the fact that mechanical damage is moderate after a 1 MGy (100 Mrad) dose indicates that this material is very robust in terms of the aging doses expected under normal nuclear power plant aging conditions. Coupling this observation with the very long lifetimes predicted above for thermal-only aging conditions gives us more confidence in the long-term viability of EPR cable insulation materials.

Conclusions

The new results on combined environment aging of neoprene and hypalon cable jacketing materials discussed in this section offer additional evidence in support of the *t-T-DR* superposition approach. The extrapolated predictions for these materials at a 50°C aging temperature indicate that dose rates below 0.1 Gy/h (10 rad/h) and often below 0.5 Gy/h (50 rad/h) will not be important to the aging rates depending on the specific material. Since most low voltage cables are exposed to lower levels than 0.1 Gy/h under typical nuclear power plant aging conditions, radiation effects are usually of little concern. Comparison for EPR-05 of two combined-environment aging conditions at a similar dose

rate but differing temperatures (40°C versus 80°C) shows that inverse temperature effects are unimportant for this material. In addition, the robustness of this material in radiation environments underscores previous observations that nuclear power plant aging dose rates are typically too small to be of concern for EPR cable insulation materials.

References

V-1. R. L. Clough and K. T. Gillen, "Combined Environment Aging Effects: Radiation-Thermal Degradation of PVC and PE", J. Polym. Sci., PP. C. Ed., 19, 2041 (1981).

V-2. K. T. Gillen and R. L. Clough, "Occurrence and Implications of Radiation Dose-Rate Effects for Material Aging Studies", Radiat. Phys. Chem., 18, 679 (1981).

V-3. R. L. Clough and K. T. Gillen, "Radiation-Thermal Degradation of PE and PVC: Mechanism of Synergism and Dose-Rate Effects, Radiat. Phys. Chem., 18, 661 (1981).

V-4. K. T. Gillen and R. L. Clough, "A Kinetic Model for Predicting Oxidative Degradation Rates in Combined Radiation-Thermal Environments", J. Polym. Sci., Polym. Chem. Ed., 23, 2683 (1985).

V-5. K. T. Gillen and R. L. Clough, "Time-Temperature- Dose Rate Superposition: A Methodology for Extrapolating Accelerated Radiation Aging Data to Low Dose Rate Conditions", Sandia National Laboratories Report SAND88-0754 (August, 1988).

V-6. K. T. Gillen and R. L. Clough, "Time-Temperature- Dose Rate Superposition: A Methodology for Extrapolating Accelerated Radiation Aging Data to Low Dose Rate Conditions", Polym. Degrad. & Stabil., 24, 137 (1989).

V-7. K. T. Gillen and R. L. Clough, "Accelerated Aging Methods for Predicting Long-Term Mechanical Performance of Polymers", in **Irradiation Effects on Polymers,** D. W. Clegg and A. A. Collyer, Eds., Elsevier Applied Science, London, 1991., Ch. 4.

V-8. K. T. Gillen and R. L. Clough, "Aging Predictions in Nuclear Power Plants-Crosslinked Polyolefin and EPR Cable Insulation Materials, Sandia National Laboratories Report SAND91-0822 (June, 1991).

V-9. K. T. Gillen and R. L. Clough, "Predictive Aging Results in Radiation Environments", Rad. Phys. and Chem., 41, No. 6, 803 (1993).

V-10. M. Celina, K. T. Gillen, J. Wise and R. L. Clough, "Anomalous Aging Phenomena in a Crosslinked Polyolefin Cable Insulation", Radiat. Phys. Chem., 48, 613 (1996).

V-11. M. Celina, K. T. Gillen and R. L. Clough, "Inverse Temperature and Annealing Phenomena During Degradation of Crosslinked Polyolefins", Polym. Degrad. Stabil., 61, 231 (1998).

V-12. IEEE Guide for Designing Multistress Aging Tests of Electrical Insulation in a Radiation Environment, IEEE Std. 775-1993.

V-13. IEC Technical Report 1244-2, "Determination of long-term radiation ageing in polymers- Part 2. Procedures for predicting ageing at low dose rates", 1st Edition, 1996-02.

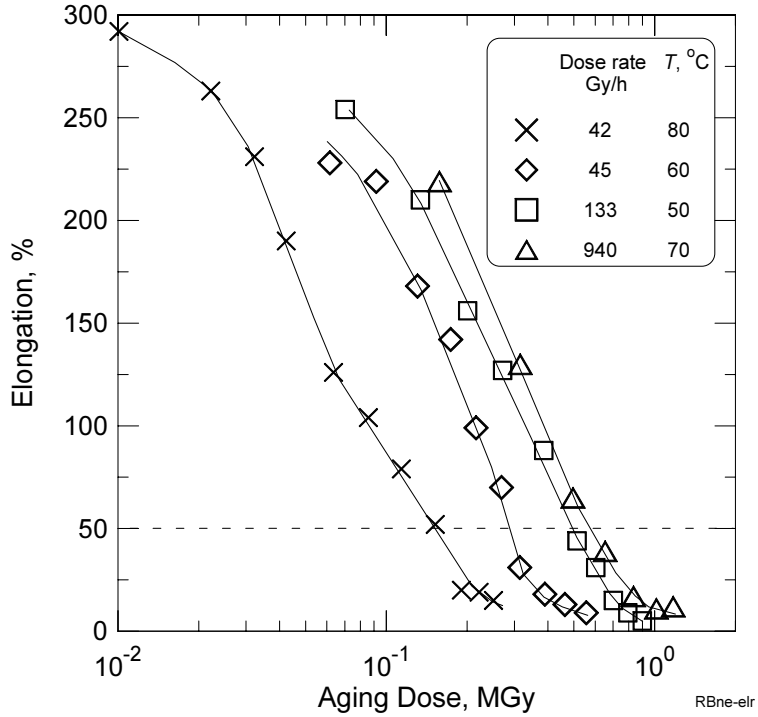

Figure V-1. Elongation versus dose for the Neo-02 cable jacket aged under the four indicated combined environment conditions.

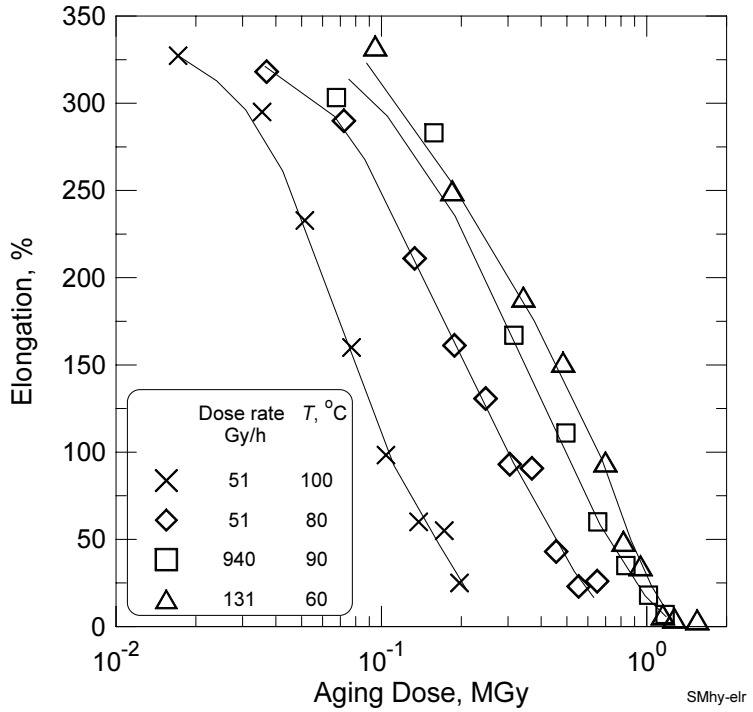

Figure V-2. Elongation versus dose for the Hyp-03 cable jacket aged under the four indicated combined environment conditions.

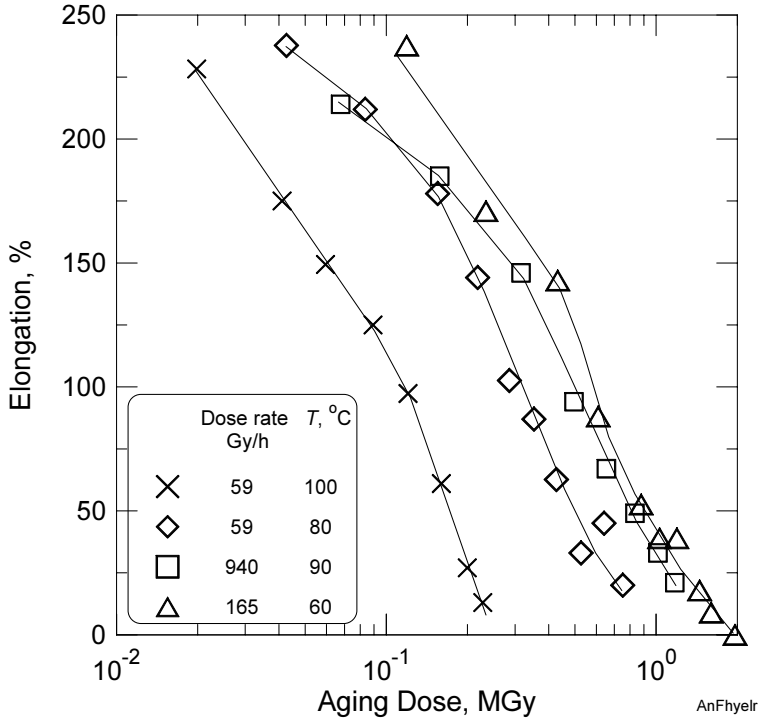

Figure V-3. Elongation versus dose for the Hyp-04 cable jacket aged under the four indicated combined environment conditions.

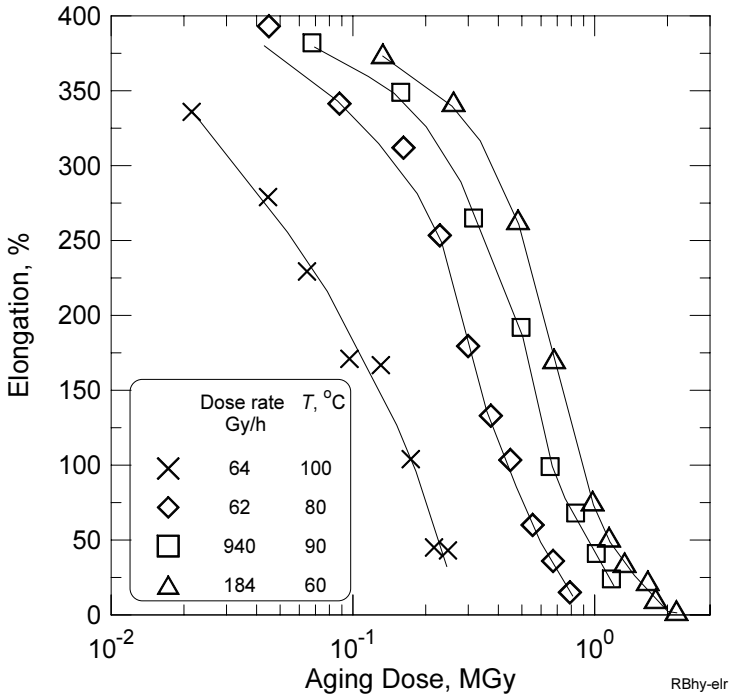

Figure V-4. Elongation versus dose for the Hyp-05 cable jacket aged under the four indicated combined environment conditions.

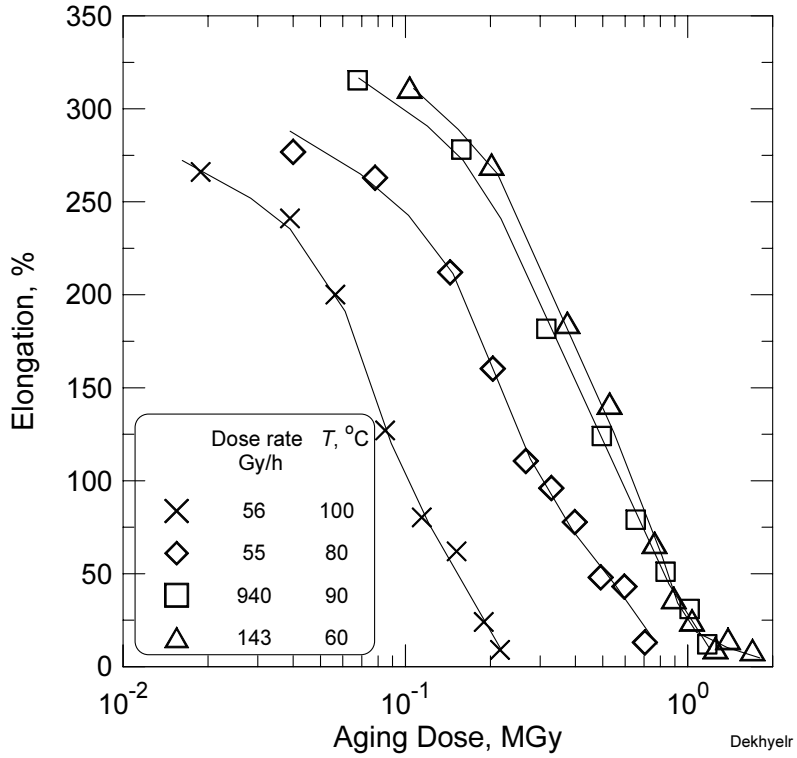

Figure V-5. Elongation versus dose for the Hyp-06 cable jacket aged under the four indicated combined environment conditions.

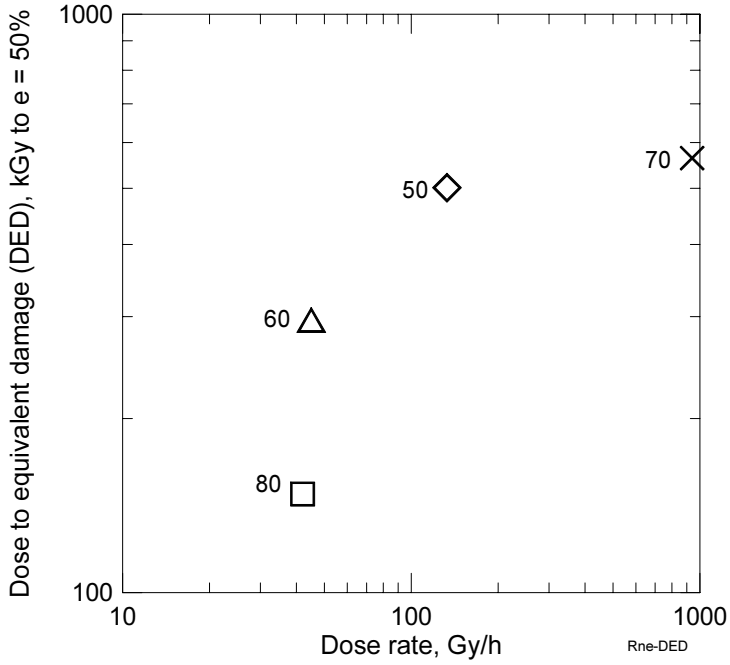

Figure V-6. Dose to reach 50% elongation versus dose rate for combined environment aging of Neo-02 material (numbers indicate aging temperature).

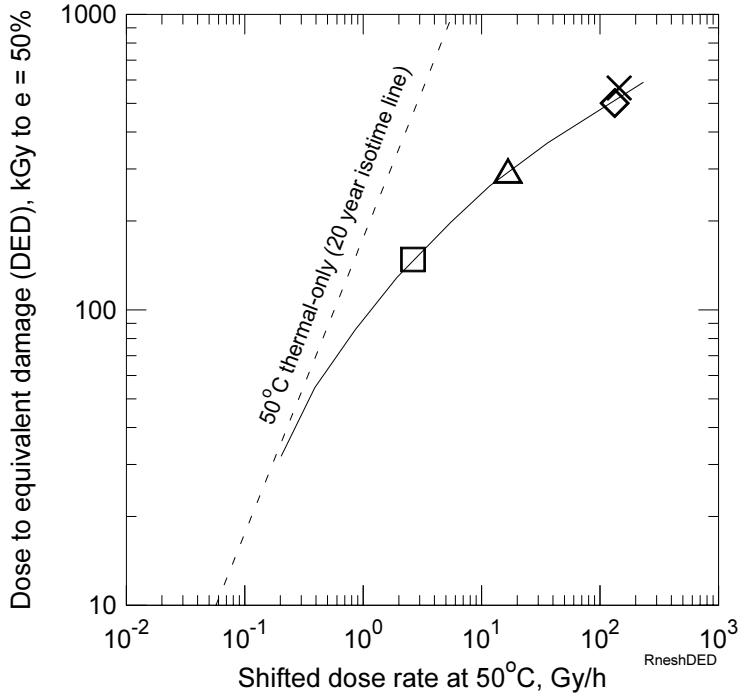

Figure V-7. Time-temperature dose rate shifted results for Neo-02 at 50°C using the combined environment aging results from Fig. V-6. The dashed line gives the thermal-only limiting line derived from the UOC extrapolated 50°C results on Fig. IV-9. Note that 1 Gy/h ~ 350 kGy (35 Mrad) over 40 years.

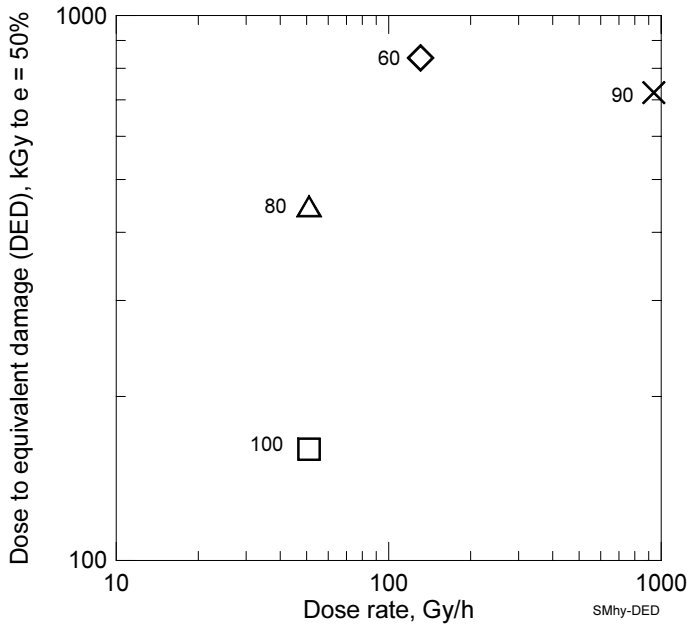

Figure V-8. Dose to reach 50% elongation versus dose rate for combined environment aging of Hyp-03 material (numbers indicate aging temperature).

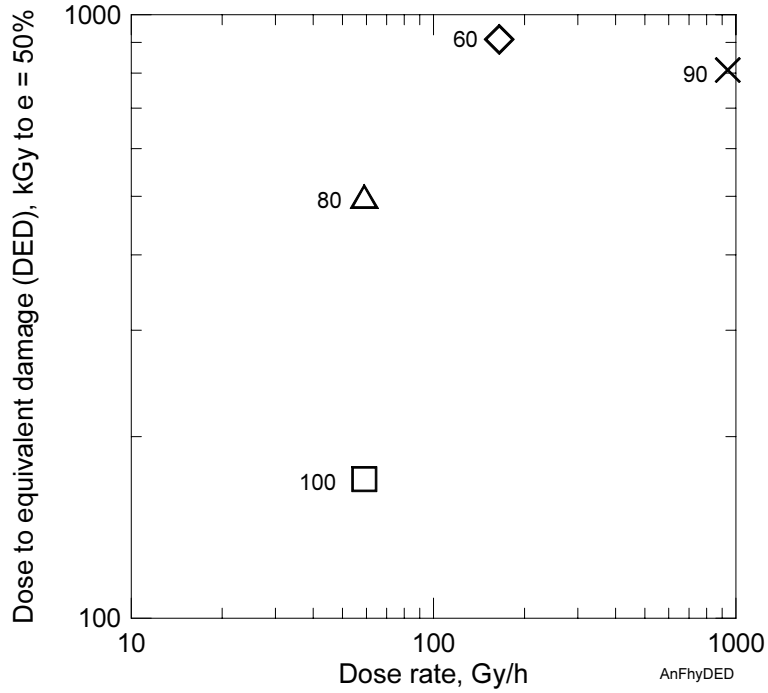

Figure V-9. Dose to reach 50% elongation versus dose rate for combined environment aging of Hyp-04 material (numbers indicate aging temperature).

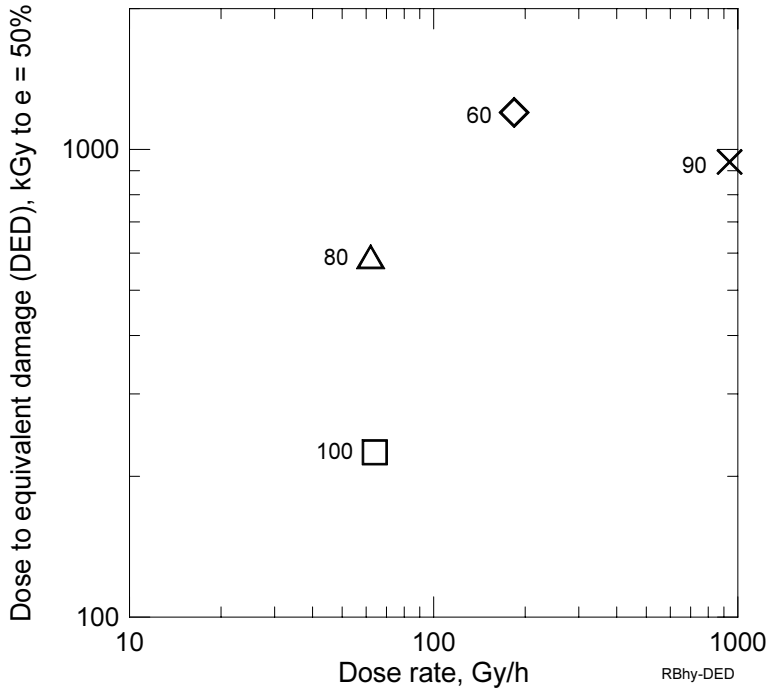

Figure V-10. Dose to reach 50% elongation versus dose rate for combined environment aging of Hyp-05 material (numbers indicate aging temperature).

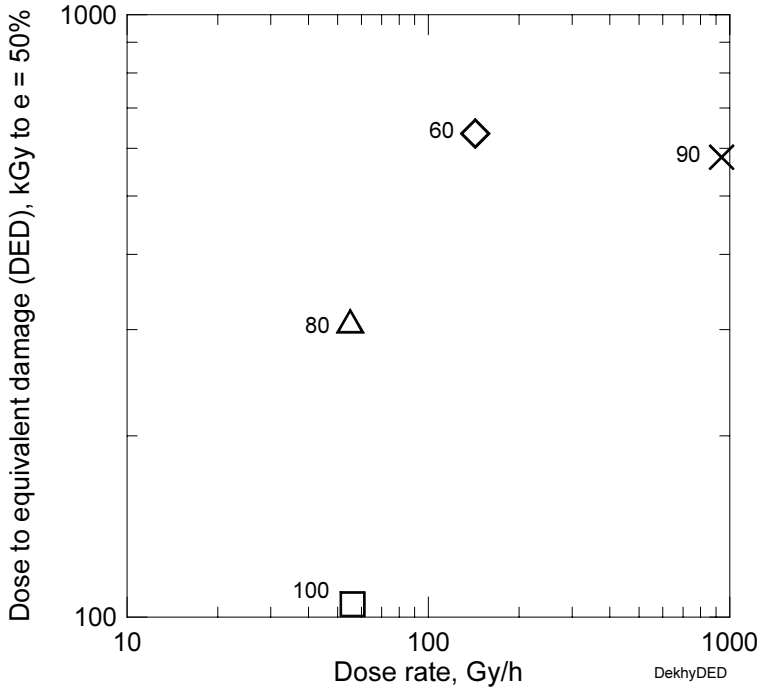

Figure V-11. Dose to reach 50% elongation versus dose rate for combined environment aging of Hyp-06 material (numbers indicate aging temperature).

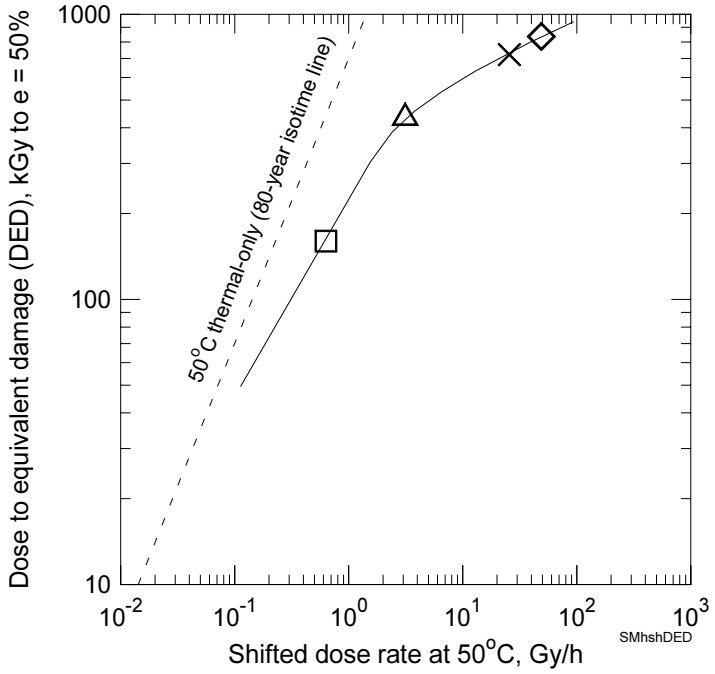

Figure V-12. Time-temperature dose rate shifted results for Hyp-03 at 50°C using the combined environment aging results from Fig. V-8. The dashed line gives the predicted thermal-only iso-time line for this material.

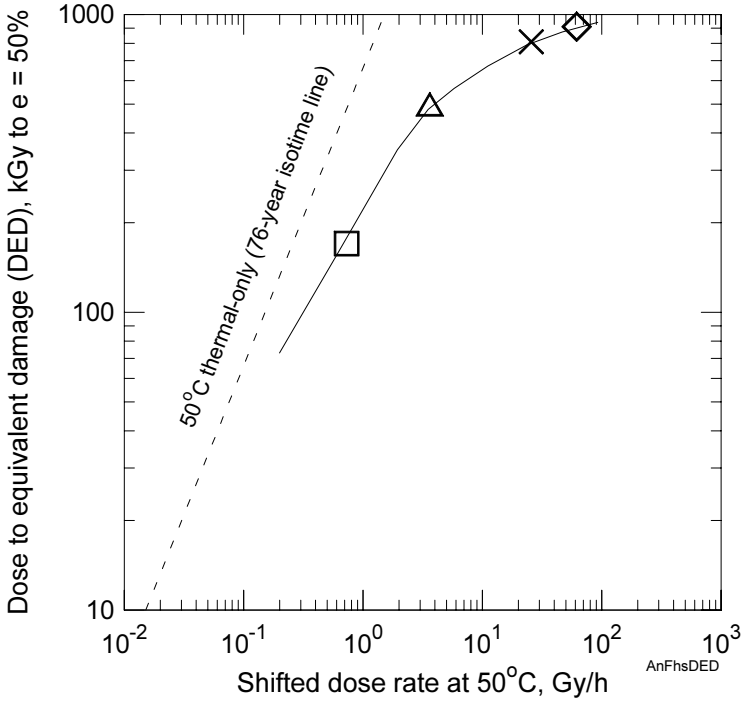

Figure V-13. Time-temperature dose rate shifted results for Hyp-04 at 50°C using the combined environment aging results from Fig. V-9. The dashed line gives the predicted thermal-only iso-time line for this material.

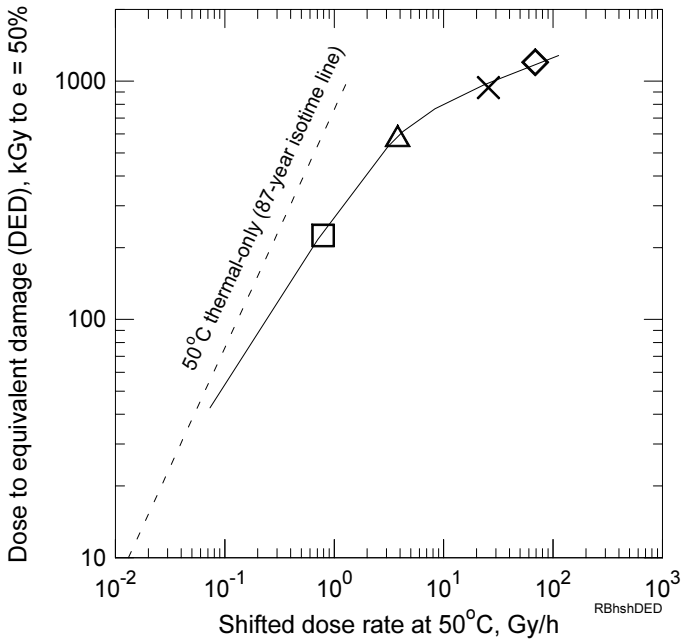

Figure V-14. Time-temperature dose rate shifted results for Hyp-05 at 50°C using the combined environment aging results from Fig. V-10. The dashed line gives the predicted thermal-only iso-time line for this material.

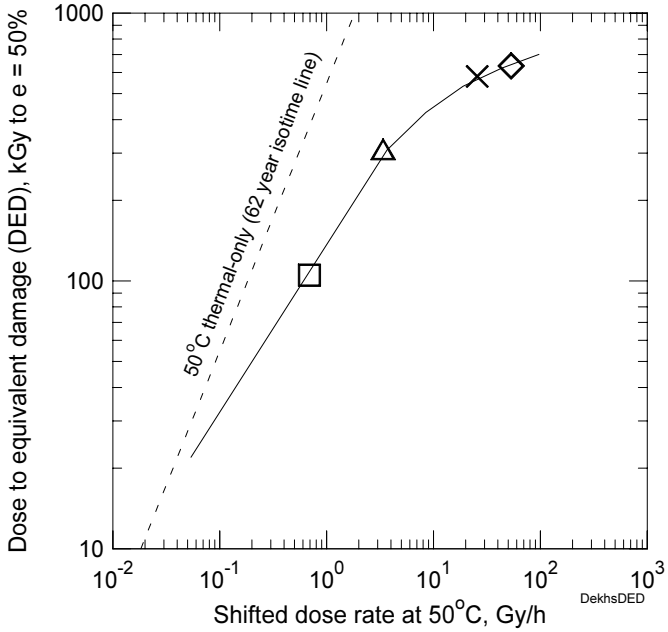

Figure V-15. Time-temperature dose rate shifted results for Hyp-06 at 50°C using the combined environment aging results from Fig. V-11. The dashed line gives the predicted thermal-only iso-time line for this material.

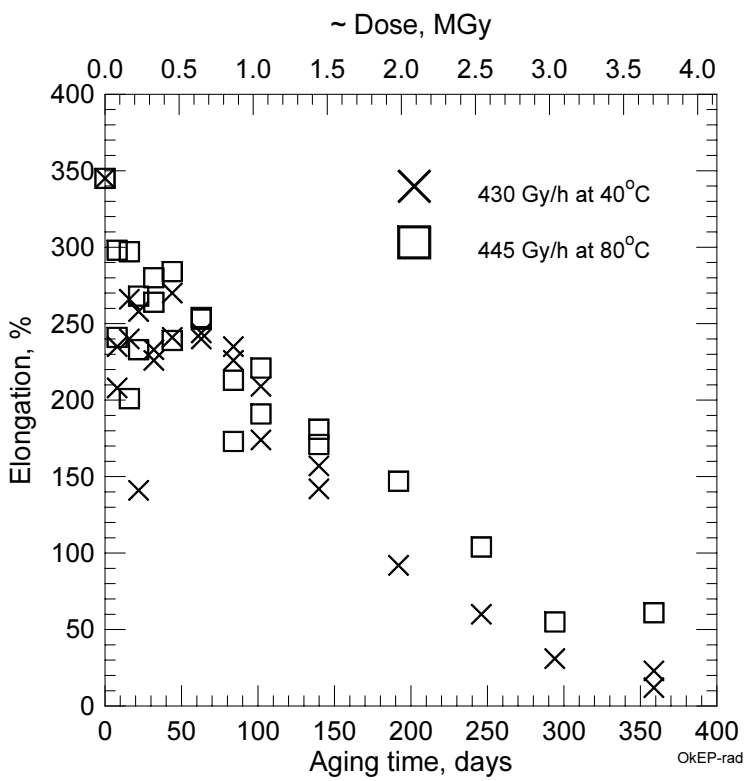

Figure V-16. Elongation versus aging time (lower x-axis) and aging dose (upper x-axis) for EPR-05 aged under the indicated combined environment conditions.

VI. Condition Monitoring Techniques: Background

Introduction

Over the years there has been a large effort focused on approaches that would allow nuclear power plants to safely operate beyond their 40-year original license period. An important aspect of this work involves the continued viability of safety-related electrical cables [VI-1 through VI-7]. Since replacement of cable is normally a complex and expensive operation, periodic determination of cable condition is of considerable interest. Historically, the monitoring method of choice for low voltage electrical cable materials involved measurements of the ultimate tensile elongation. For sufficient drops in the elongation, it is assumed that the cable may not operate in case an accident occurred. The amount of drop to end of life is somewhat arbitrary but, as described in Section III, a consensus seems to be developing that 50% absolute elongation can be used as a practical end of life criterion [VI-6].

Unfortunately elongation measurements require that fairly large samples be removed from a cable for testing so they are considered to be fairly destructive. This can create problems for nuclear plants if samples from a large number of areas in the plant need to be periodically tested. Therefore there has been considerable effort devoted to deriving less destructive condition monitoring methods [VI-2 through VI-7]. Some of these methods examined are truly non-destructive in the sense that material does not have to be removed to the lab for testing and the cable therefore sustains little or no damage during the test procedure. Probably the only test in this category that has been shown to work for many rubber materials is the cable indenter [VI-3, VI-4, VI-5, VI-7], a portable instrument that is taken into the plant to the cable of interest. It uses a probe to mechanically indent the cable jacket resulting in the "indenter modulus" that is semi-quantitatively related to the modulus of the material. This technique has been used numerous times for actual plant problems.

Another category of "essentially non-destructive" techniques involves approaches that require the removal of fairly small pieces (typically tens of milligrams) of cable jacket (e.g., thin jacket shavings or small sections at cable terminations) or insulation (e.g., at cable terminations) so damage may not be too much of a concern. Several techniques in this category have shown some potential. Two related techniques based on a differential scanning calorimetry (DSC) are oxygen induction time (OIT) and oxygen induction temperature (OITP) measurements [VI-2 through VI-7]. These techniques show some promise for certain materials especially thermally aged XLPO and EPR cable insulations. Since such measurements require ~8 to 10 mg per sample, repeat measurements required for confidence imply that 30 mg or more of material must be removed per cable location. These techniques require careful sample preparation plus an expert to run the instrument and interpret the often-complex data. In many instances, the results from OIT and OITP are insensitive to the later stages of degradation where CM techniques need to have sensitivity.

Fourier Transform Infrared Spectroscopy (FTIR), which also requires around 10 mg per sample, has been successfully used to monitor the aging of certain cable materials [VI-2 through VI-8]. A common approach monitors the carbonyl region (around 1730 cm^{-1}), which grows from the incorporation of oxidation species in the material. However FTIR is difficult to run on carbon-black filled materials and for materials with peaks present in the carbonyl region before aging. In addition, the growth in the carbonyl region is often extremely slow until just before the practical end of life when the growth rate of the carbonyl peaks greatly accelerates [VI-8]; in such instances, condition monitoring by FTIR gives little warning of imminent end of life.

Density measurements have also shown promise for monitoring aging in many cable materials [VI-2 through VI-5,VI-9]. Density measurements are easy to conduct on samples weighing tens of milligrams using the Archimedes approach. They can also be done on very small samples (fractions of a mg) using the density gradient column technique [VI-10] but such measurements are difficult to run and often adversely affected by artifacts (e.g., absorption of column liquid).

The goal of the condition monitoring portion of the NEPO cable-aging program was to test several new and several of the older CM techniques on many of the aged cable insulation and jacketing materials available from SCRAPS (Sandia's Cable Repository of Aged Polymer Samples). Because of the very large number of aged samples available from both past studies and the current NEPO aging studies (Tables I-1 through I-3), a lot of CM measurements could be conducted in a very efficient manner. This is because many of the cables had previously been acquired, aged and mechanically tested for tensile elongation so the perhaps 90% of the time and effort needed for traditional condition monitoring studies had already been completed.

Importance of recognizing when diffusion-limited oxidation is present

When air surrounds cables during aging, oxygen will be dissolved in the jacket and insulation materials. The equilibrium dissolved oxygen concentration for each material will be given by the product of its oxygen solubility coefficient S times the oxygen partial pressure p surrounding the polymer. Aging will cause the dissolved oxygen to be used up by oxidation reactions. If these reactions occur faster than diffusion processes from the surrounding air atmosphere can replenish the dissolved oxygen, the concentration of oxygen in the polymer interior will be reduced from its equilibrium value to lower or even non-existent levels. This effect can lead to diffusion-limited oxidation (DLO) effects, where the rate of oxidation is reduced or eliminated in such regions. The importance of DLO effects depends upon the material, its geometry (thickness) and its aging environment [VI-11 through VI-13.]. It is critical to note that for most cable configurations, DLO effects will likely be unimportant under the slow oxidation conditions occurring for long-term nuclear power plant ambient aging. In such instances, equilibrium oxidation should occur uniformly across the entire cross-section of the cable materials.

Unfortunately, many of the past studies examining the correlation of condition monitoring (CM) techniques with elongation results have looked at materials aged under relatively short-term laboratory conditions. For such conditions, ample evidence implicates important DLO effects [VI-9,VI-14 through VI-17]. When this occurs, CM measurements taken on whole sample cross-sections will have an anomalous dependence on sample thickness, reflecting the weighted average of the CM parameter across the heterogeneously oxidized cross-section. The magnitude of the measured CM parameter will therefore be in error by an unpredictable and thickness-dependent amount from the value that would have corresponded to the desired equilibrium oxidation conditions. Past studies invariably attempt to correlate such anomalous CM values with tensile elongation values. It turns out fortuitously, that for many elastomers, elongation is often unaffected by DLO effects because oxidation typically leads to modulus increases (hardening) of the material [VI-14,VI-15,VI-18]. When DLO effects occur, the oxidation rate at the surfaces still proceeds under equilibrium oxygen sorption conditions (reduced oxidation will occur in interior regions). This means that equilibrium hardening will still occur at the sample surfaces. When elongation measurements are carried out, cracks will invariably initiate at the hardened surfaces and, once initiated, these cracks are typically found to immediately propagate through the remainder of the sample cross-section. The hardened surface thus determines the elongation value, resulting in an insensitivity of tensile elongation to DLO effects. Therefore it is misleading and dangerous to try and correlate elongation values with bulk CM parameters when DLO effects are present. For this reason, it is important to try and select laboratory-aging conditions where oxidation will be relatively uniform across the material cross-section, thereby minimizing DLO effects. This allows quantitative correlations to be made between the elongation results and each of the bulk CM variables being screened. In cases where the importance of DLO effects is unknown or where it is impossible to eliminate DLO effects from accelerated laboratory screening studies, CM methods that are capable of mapping (profiling) across the cross-section of the aged material become invaluable for several reasons. First such profiling methods allow one to determine whether DLO effects are significant for the laboratory aging conditions being monitored. When they are significant, the CM profiling data allow one to estimate the value of the CM parameter near the sample surface that represents the desired equilibrium CM measurement.

How does one accomplish the above goals of 1) trying to choose laboratory-aging conditions such that DLO effects are unimportant and 2) having a CM profiling approach that allows the importance of DLO effects to be screened for experimentally? The first goal can be achieved through the use of theoretical models for DLO effects [VI-11,VI-12,VI-13,VI-17]. Assuming that DLO effects are unimportant when the integrated oxidation across a sample cross-section is greater than 90% of what it would be for a homogeneously oxidized material, these models lead [VI-12] to the following expression for L_{90} (defined as the maximum sample thickness that guarantees 90% oxidation).

$$L_{90} \approx 2\left[\frac{pP_{Ox}}{\phi}\right]^{0.5} \qquad \text{(VI-1)}$$

In this expression, p is the partial pressure of oxygen surrounding the sample and P_{Ox} and ϕ are the oxygen permeability coefficient and the oxygen consumption rate for the material. The oxygen consumption values are measurable (see Sections II and IV) and the partial pressure of oxygen is always known (13.2 cmHg in Albuquerque). The only other variable in the equation is the oxygen permeability coefficient, available from measurements [VI-19] or from estimates based on literature results [VI-20]. When estimates or measurements of P_{Ox} and ϕ are available, this expression allows one to estimate when DLO effects are likely to be important and hence to select aging conditions that attempt to minimize such effects. This is the approach we have used to select aging conditions for the samples being newly aged under the NEPO program. In some instances, the theoretical estimates indicate that the absence of DLO effects could not be guaranteed for realistic accelerated aging conditions, given the time constraints available for the aging. In cases where the uncertainties in the required parameters for eq. VI-1 indicate that DLO effects might enter for the aging conditions of interest, the backup approach is to have an experimental profiling technique available to experimentally determine the importance of DLO effects. In most instances the modulus profiling approach discussed in the next section of this report fulfills this latter objective.

References

VI-1. Bustard L and Holzman P. "Low-Voltage environmentally-qualified cable license renewal industry report; Revision 1", EPRI Report TR-103841, July, 1994.

VI-2. Anandakumaran K, et. al. "Improved conventional testing of power plant cables", EPRI Report TR-105581, September, 1995.

VI-3. Toman GJ, Hilditch JM, Butwin RT. "Diagnostic matrix for evaluation of low-voltage cable", EPRI Report TR-106108, November, 1997.

VI-4. Gazdzinski RF, Denny WM, Toman GJ, Butwin RT. "Aging management guideline for commercial nuclear power plants- electrical cable and terminations", Sandia Labs Report, SAND96-0344, September, 1996.

VI-5. "Assessment and management of ageing of major nuclear power plant components important to safety: in-containment instrumentation and control cables, Volumes I and II, IAEA-TECDOC-1188, December, 2000.

VI-6. G. Toman, EPRI Project Manager, "Initial Criteria Acceptance Concepts and Data for Assessing Longevity of Low-Voltage Cable Insulations and Jackets", EPRI Technical Report 1008211, Final Report, March, 2005.

VI-7. Denny WM. "Integrated cable system aging management guidance", EPRI Report 1003663, January, 2003.

VI-8. Anandakumaran K, Stonkus DJ. Assessment of oxidative thermal degradation of crosslinked polyethylene and ethylene propylene rubber cable insulation. Polym Eng Sci 1992;32:1386.

VI-9. Gillen KT, Celina M, Clough RL. Density measurements as a condition monitoring approach for following the aging of nuclear power plant cable materials. Radiat Phys Chem 1999;56:429.

VI-10. Gillen KT, Clough RL, Dhooge NJ. Density profiling of polymers Polymer 1986;27:225.

VI-11. Cunliffe AV, Davis A. Photooxidation of thick polymer samples. 2. The influence of oxygen diffusion on the natural and artificial weathering of polyolefins. Polym Degrad Stab 1982;4:17.

VI-12. Gillen KT, Clough RL. Rigorous experimental confirmation of a theoretical model for diffusion-limited oxidation, Polymer 1992;33:4358.

VI-13. Wise J, Gillen KT, Clough RL. Quantitative model for the time development of diffusion-limited oxidation profiles. Polymer 1997;38:1929.

VI-14. Gillen KT, Terrill ER, Winter RW. Modulus mapping of rubbers using micro- and nano-indentation techniques. Rubber Chem Tech Rubber Reviews 2001;74:428.

VI-15. Wise J, Gillen KT, Clough RL. An ultrasensitive technique for testing the Arrhenius extrapolation assumption for thermally-aged elastomers. Polym Degrad Stab 1995;49,403.

VI-16. Celina M, Gillen KT, Graham AC, Assink RA, Minier LM. Thermal degradation studies of a polyurethane propellant binder. Rubber Chem. Technol 2000:73:678.

VI-17. Wise J, Gillen KT, Clough RL. Time-development of diffusion-limited oxidation profiles in a radiation environment. Radiat Phys Chem 1997;49:565.

VI-18. Gillen KT, Celina M, Clough RL, Wise J. Extrapolation of accelerated aging data- Arrhenius or erroneous? Trends in Polymer Science 1997;5:250.
VI-19. M. Celina and K. T. Gillen, "Oxygen Permeability Measurements on Elastomers at Temperatures up to 225°C", Macromolecules, 2005;38:2754.
VI-20. S. Pauly, in Polymer Handbook, 4th Edition, J. Brandrup, E. H. Immergut and E. A. Grulke, Eds., John Wiley and Sons, Inc. New York, Ch. VI, p. 543 (1999).

VII. Condition Monitoring Techniques: Modulus Profiling

Introduction

The modulus profiling approach allows us to quantitatively map (profile) the modulus across the cross-section of a material with 50 μm resolution (~20 measurements per millimeter of cross-section). The instrument was developed at Sandia many years ago [VII-1] and recently modified into a computer-controlled, automated version [VII-2]. The usual procedure involves first mounting three small pieces of the polymeric material side by side in a vise-like holder. This holder is then metallographically polished exposing the cross-sections of the three samples. The holder is next placed in the apparatus such that a loaded probe with a paraboloidally shaped tip can be used to indent the central sample perpendicular to its cross-section. Utilizing a two-step loading procedure, the amount of indentation of the probe into the sample is used (together with the known loading on the probe and the probe tip geometry) to calculate the inverse tensile compliance, a quantity closely related to the tensile modulus of the material. By scanning across the sample cross-section, a detailed map of modulus versus probe location is obtained. There are currently four such instruments in existence. Three were built by Sandia with one located in Albuquerque and two transferred to Goodyear Tire and Rubber Company in Akron, Ohio as part of a Cooperative Research and Development Agreement (CRADA). Akron Rubber Development Laboratory, a commercial contractor to the rubber industry, built a fourth instrument, an instrument potentially available to the nuclear industry.

Over the years, the unique results available from modulus profiling have led to numerous publications highlighting its uses [VII-1 through VII-14]. Given the fact that modulus profiling was found to be applicable to following aging effects in most elastomeric materials and that such materials represent a substantial portion of the cable jacketing and insulation materials utilized in low voltage nuclear power plant cables, one goal of the NEPO program was assessing the applicability of modulus profiling as a cable-material CM technique. In addition the profiling ability of this technique made it ideal as a method for determining experimentally the importance of DLO effects for the various accelerated aging conditions used. It could therefore be used to eliminate from further analyses any CM measurements made on macroscopic samples influenced by important DLO effects.

Modulus profiling of Neo-02 [VII-15]

Both oven aging (see Section III) and combined radiation-thermal aging (see Section V) were done on the Neo-02 material with the elongation results shown in Figs. III-8 and V-1, respectively. Before discussing the modulus profiling results, it is useful to outline the application of eq. VI-1 for making estimates of the possible importance of DLO effects for the thermal aging conditions used for this material (80°C, 95°C and 110°C). The oxygen consumption rate for this neoprene material was measured at 95°C and found to be ~7×10^{-11} mol/g/s. Using the high-temperature activation energy (96 kJ/mol)

appropriate to this material (Fig. IV-7), we are able to estimate the consumption rates at 110°C and 125°C (Table VII-1). For estimates of P_{Ox} at these three temperatures, we use values [VII-9] derived for another polychloroprene material (shown also in Table VII-1). These results then allow estimates for L_{90} to be made at the three temperatures shown in the last row of the Table. Since the nominal sample thickness of the polychloroprene jacket is 0.15 cm, the above estimates lead us to tentatively conclude that aging at 125°C would result in important DLO effects but that aging at 110°C will probably be relatively homogeneous. We have to keep in mind that such theoretical estimates are approximate since they often involve extrapolations of data to temperatures not measured and/or the use of literature results on similar but not identical materials. This was the case for the current estimates. However if such estimates lead to results that clearly indicate the presence or absence of DLO effects, the moderate errors inherent in such estimates become unimportant.

Table VII-1. Theoretical estimates of the importance of DLO effects for Neo-02.

Aging T, °C	95	110	125
ϕ, mol/g/s	$7\text{x}10^{-11}$	$2.39\text{x}10^{-10}$	$7.43\text{x}10^{-10}$
P_{Ox}, ccSTP/cm/s/cmHg	$2.4\text{x}10^{-9}$	$3.4\text{x}10^{-9}$	$4.5\text{x}10^{-9}$
L_{90}, cm	0.223	0.144	0.092

Modulus profile results for the thermally aged samples are plotted in Figs. VII-1 through VII-3. The modulus results at each of the indicated aging times are plotted vs P, defined as the percentage of the distance across the sample cross-section from one air-exposed surface of the sample to the opposite air-exposed surface. In our modulus profile plots, P = 0% is always used to designate the outside surface of the cable jacket or insulation. Since the nominal thickness of the Neo-02 jacket material is ~0.15 cm, this is the approximate distance represented by the x-axis span. Therefore, as indicated from the figures, the typical spacing between modulus measurements is approximately 0.1 mm. The unaged sample results (open circles) indicate that the modulus is approximately homogeneous across the cross-section with an average modulus value of ~ 6.4 MPa. Aging leads to a relatively steady increase in modulus; this shows that the modulus profiling technique offers an excellent condition monitoring approach. By comparing the results of Figs VII-1 through VII-3 with the elongation results of Fig. III-8, it is clear that easily measured modulus changes are observable in the early stages of the elongation decay. The modulus increase comes from oxidation reactions and since the 80°C and 95°C modulus profiles remain relatively homogeneous as a function of aging time, important DLO effects are confirmed to be absent at these temperatures, consistent with the predictions from Table VII-1. At 110°C as shown in Figure VII-3, the modulus profiles also remain relatively homogeneous up to 49 days of aging indicating the absence of important DLO effects, again consistent with predictions (Table VII-1). At the final aging time of 63 days, there is a hint of heterogeneity in the profile, perhaps indicative of minor DLO effects beginning to enter. At this point the material is becoming quite hard (surface modulus values of several hundred MPa) and is mechanically dead (absolute elongation of ~ 10%). With substantial hardening, the

oxygen permeability coefficient will drop which from eq. (VI-1) will lead to increasing importance of DLO effects [VII-9]. Since DLO effects are predicted for unaged specimens to become important at temperatures above 110°C, any substantial decrease in P_{Ox} caused by hardening later in the aging might be expected to trigger late-stage DLO effects. It is clear from this example that a combination of theoretical modeling as a prelude to choosing aging conditions coupled with a technique capable of experimentally profiling the materials after aging leads to a viable method of monitoring the importance of DLO effects.

Figures VII-4 through VII-7 show modulus-profiling results for the four combined environments exposures used on the Neo-02 material. The conditions of 940 Gy/h at 70°C had the best chance of showing DLO effects since significant degradation took ~50 days, much shorter than the roughly 250 d to 500 d needed at the other three combined conditions. It is clear from Fig. VII-4, however, that DLO effects were unimportant at 940 Gy/h plus 70°C since the modulus profiles remained relatively homogeneous throughout the degradation. For the remaining three combined environment conditions, the modulus profiles (Figs. VII-5 through VII-7) exhibited similar behavior, with steady increases occurring as the elongation dropped and little evidence of important DLO effects except for some hints very late in the degradation.

To better assess the sensitivity of the modulus measurements to the mechanical degradation, we plot in Figure VII-8 the average modulus result versus the corresponding average elongation result as a function of aging time and temperature for the thermal-only aging conditions. It is clear that drops in elongation correspond to increases in modulus at each temperature. In addition the correlation between modulus and elongation is similar at all three aging temperatures. This is very important since it implies that a similar relationship might be expected in the lower-temperature "extrapolation region" of interest to long-term aging conditions. Assuming 50% absolute elongation represents the practical end of life [VII-16, VII-17], the results imply the practical end of life occurs when the modulus reaches around 37 MPa.

Figure VII-9 shows the correlation of modulus and elongation values for the four combined environment runs. The results give predictive correlations that are similar to those found for thermal-only aging and that are independent of the mix of dose rate and temperature used in the aging. Again, an end of life elongation criterion of 50% absolute corresponds to the modulus reaching values around 30 MPa.

Modulus profiling of hypalon jacketing materials [VII-18]

As noted in the earlier sections of this report, we have obtained elongation results for eight different commercial hypalon jacketing materials under thermal-only aging conditions ranging from 80°C to 150°C (see Figs. III-11 through III-18). In addition we reported elongation results for four of these materials aged under combined radiation-thermal environments (see Figs. V-2 through V-5). To estimate the temperatures where DLO effects might be important, we need oxygen consumption and permeability estimates for hypalon materials. As seen in Section IV, we have conducted oxygen

consumption measurements on two of the currently studied hypalon materials. At 110°C the data for Hyp-03 indicate $\phi \sim 8x10^{-11}$ mol/g/s (Fig. IV-15) whereas the results for Hyp-08 (Fig. IV-23) indicate a ϕ value at 110°C ~ $1.5x10^{-11}$ mol/g/s. To obtain an estimate for the permeability at 110°C ($P_{Ox} \sim 2.8x10^{-9}$ ccSTP/cm/s/cmHg), we extrapolated lower temperature results published by Seguchi and Yamamoto [VII-19] taken on a commercially formulated hypalon cable jacketing material. Substituting these results in eq. (VI-1) gives $L_{90} \sim 2\pm0.3$ mm at 110°C. Assuming that an E_a of ~106 kJ/mol holds for the oxygen consumption from 110°C to 150°C (see Figs. III-27, IV-18 and IV-25) and the E_a for the oxygen permeability coefficient is ~ 25 kJ/mol over this same temperature range [VII-20], the result at 150°C is $L_{90} \sim 0.6$ mm. Comparing these rough estimates to the hypalon jacket thicknesses in Table I-3 indicates that DLO effects could occur for many of the materials at temperatures as low as 110°C. However since most hypalon materials require on the order of 1 year to degrade at 100°C (see Table III-1) and accelerated aging experiments typically require a minimum of three aging temperatures, exposures of 110°C and higher are typically needed. For this reason we expected to see important DLO effects from many of the modulus profiles obtained on the aged hypalon materials.

The first material discussed is the Hyp-01A material that was aged at five temperatures ranging from 100°C to 150°C. Since this material is only ~0.4 mm thick, our estimate above that $L_{90} \sim 0.6$ mm at 150°C implies that DLO effects might not be important for this material throughout its aging temperature range. This is borne out by the results shown in Figs. VII-10 through VII-14. For the unaged material (open circles in each figure) the profile indicates approximately uniform modulus values across the sample except for a slight rise towards the outside surface- this rise is caused by a thin red "paint" covering the outside surface to distinguish the individual conductors of the three conductor cable from which this material was obtained. With aging at all five temperatures, the modulus values tend to increase similarly for all positions across the cross-section indicating homogeneous aging (no DLO effects), consistent with the theoretical predictions given above for a 0.4-mm thick material. Since cracks normally initiate at the hardest (highest modulus) part of a sample and there is a slight hardening at the outside surface of the Hyp-01A samples caused by the "red paint", we utilize the outside surface values of the modulus to compare to the ultimate tensile elongation values for the same aging condition. The resulting correlation is shown in Fig. VII-15 for all five temperatures. It is clear that, similar to the earlier results on Neo-02, excellent correlation exists between these surface modulus values and elongation independent of aging time and temperature over the entire experimentally accessed temperature range. In addition, 50% absolute elongation corresponds to the modulus reaching ~40 MPa, a value close to that found for Neo-02 above. If the average modulus value across the cross-section of the samples were used instead of the painted surface value, the 50% end of life criterion would occur at a slightly lower modulus of ~31 MPa.

The modulus profile results for Hyp-05 at 100°C, 110°C and 125°C are shown in Figs. VII-16 through VII-18. The unaged values (open circles) are homogeneous across the sample cross-section with an average value of ~4.1 MPa. For the samples aged at 100°C

and 110°C, modulus increases appear to be approximately uniform across the cross-section as aging progresses indicating DLO effects are unimportant. At 125°C, however, inhomogeneous increases occur implying that DLO effects are beginning to become important at this aging temperature. When DLO enters, the advantage of having profile results become apparent since the degradation rate at the surface (reflected in the surface modulus value) represents the oxygen-sorption equilibrium rate (not influenced by DLO) even when DLO effects enter in interior regions. The changes in modulus at the surface therefore represent the real changes expected in the absence of DLO. In addition, since the results at 125°C (Fig. VII-18) indicate the "equilibrium" hardening at the surface occurs faster than the hardening in interior regions, cracks would normally be expected to initiate at the surfaces. If these quickly propagate through the remainder of the material cross-section, the "equilibrium" hardening (modulus) at the surface will determine the tensile elongation. For this reason we plot tensile elongation results (Fig. III-15) versus the highest surface value of the modulus found for each aging condition. The results for Hyp-05 for various aging times at the three aging temperatures are shown in Fig. VII-19. For this material we again find an excellent correlation that is independent of temperature. The 50% elongation criterion corresponds to the modulus reaching ~32 MPa, a value quite similar to those found earlier for Neo-02 and Hyp-01A.

The modulus profiling results for Hyp-03, Hyp-06 and Hyp-08 at three temperatures for each material are shown in Figs. VII-20 through VII-28. Overall the behavior of these materials is similar to that found for Hyp-05 except for some slight differences in the temperatures affected by DLO for Hyp-06 and Hyp-08. For all three materials, reasonably homogeneous modulus profiles are found for the unaged material (open circles on figures) and for aging at 100°C. At an aging temperature of ~110°C the modulus profiles indicate homogeneous aging for Hyp-03 but the beginning of DLO effects for both Hyp-06 and Hyp-08. At the highest aging temperature of ~125°C all three materials show evidence of DLO effects. Therefore it is again clear that the theoretical estimates derived from eq. V-1 are consistent with the experimental modulus profile results. In fact it should be noted that the two materials (Hyp-05 and Hyp-03) that require a slightly higher temperature before DLO effects enter have slightly smaller nominal thicknesses (1.3-mm and 1.2-mm) compared to the Hyp-06 and Hyp-08 materials (1.4-mm and 1.7-mm), again consistent with theoretical expectations. This shows the power of the theoretical approach for estimating the potential importance of DLO effects before aging experiments are initiated. The correlations between tensile elongation results (Figs. III-13, III-16 and III-18) and the highest surface modulus value are shown in Figs. VII-29 through VII-31. Again the correlation is excellent for each material and the 50% absolute elongation criterion is reached when the modulus climbs to ~45 MPa (Hyp-03), ~42 MPa (Hyp-06) and ~36 MPa (Hyp-08).

The remaining three hypalon jacketing materials (Hyp-04, Hyp-07 and Hyp-02) show modulus profiling results that are somewhat different from the five hypalon materials discussed above. Modulus profiling results at three aging temperatures for Hyp-04 are given in Figs. VII-32 through VII-34. This material that has the highest nominal thickness (1.8-mm), shows DLO effects at all three aging temperatures. In addition it is clear from these figures that the unaged material (open circles) is harder (modulus of ~

7.6 MPa) at the inner surface of the jacket than in the remainder of the cross-section (modulus ~ 4.8 MPa). It is also clear that this initial inside inhomogeneity is retained during the aging as evidenced by the tendency towards slightly faster modulus increases at the inner surfaces of the aged samples. Since cracks typically initiate at the hardest portion of a sample during tensile testing and then quickly propagate to cause tensile failure, one would expect the tensile elongation results (Fig. III-14) to be dependent on the inside surface modulus values. Fig. VII-35 shows that the correlation is again quite good and indicates that tensile "end of life" occurs when the inside modulus value reaches ~ 31 MPa.

Modulus profiling results for the Hyp-07 material at four aging temperatures are shown in Figs. VII-36 through VII-39. The unaged results (open circles) indicate a homogeneous modulus across the sample. Modulus increases with aging are fairly uniform at 100°C and 109°C and during the early stages of degradation at 124°C and 138°C. Evidence of DLO effects appears later on at the two higher temperatures. This material was found to have somewhat unusual tensile behavior, with the elongation (Fig. III-17) failing in a more abrupt fashion than the other seven hypalon materials [VII-21]. As opposed to the relatively gentle drop-off in elongation with aging time found for the other hypalon materials, the drop-off for Hyp-07 becomes much more abrupt near its practical end of life with a great deal of scatter. This is illustrated in Fig. VII-40 where the individual elongation and swelling results at 109°C are plotted versus aging time. This fast drop-off type of behavior resembles the "induction-time" behavior often observed for stabilized polyolefin materials where a rapid drop-off in elongation occurs when the anti-oxidant is used up. When such behavior is operative, scatter can be quite severe near end of life since one aging specimen may use up its anti-oxidant a little earlier than a second specimen. In fact this is what is observed for aging of the Hyp-07 material at 109°C as seen for the pairs of samples that were tensile tested after 161 days, 163 days and 171 days of aging. For each of these aging conditions, one of the tensile specimens failed at high elongation values (open squares in Fig. VII-40B) and the other specimen failed at low elongation values (filled squares). The differences in each pair of samples were obvious with the high elongation (140% to 240%) samples being quite flexible, whereas the low elongation (15% to 30%) specimens had transformed into very hard and inflexible materials. These differences were also obvious from solvent uptake measurements (Fig. VII-40A) where the uptake amounts were much smaller for the harder materials. This abruptness in property change can also be seen in the 109°C modulus profiling results. With aging the modulus increases quickly to ~20 MPa and then stays reasonably constant up to the end of life region (160- 170 d). At this point the samples that are still flexible and have large elongation values are found to have modulus values around 25 MPa. On the other hand, the hard samples that give low elongation values have modulus values that are an order of magnitude higher. Although the abrupt transition near end of life makes it difficult to quantitatively determine the modulus value that corresponds to the elongation reaching 50%, it is clear that the value is similar to those found for the other six hypalon materials discussed earlier. When such scattering effects occur, one possible factor can be unevenly distributed filler material (e.g., varying antioxidant concentration) leading to the depletion of antioxidant more quickly in anti-oxidant deficient regions of the jacket.

The final material (Hyp-02) has even more unusual aging behavior, as evidenced by modulus profiling results shown in Figs. VII-41 through VII-45. Results for the unaged material (open circles) indicate a slight inhomogeneity with moderately elevated modulus values at both surfaces. Aging at all temperatures leads to much more rapid modulus increases near the inside surface of the jacket. The infrared results (carbonyl peak profile) for the sample aged to 738 d at 90°C are shown on Fig. VII-41 and give a profile of similar shape to the modulus results for this material. These results indicate that the very different rates of modulus change occurring at the inside and outside surfaces reflect very different oxidation mechanisms. We do not understand the mechanism underlying the much faster oxidation at the inner surface. At the outside surface, where slow oxidation is occurring, DLO effects do not appear to be important until around 130°C, whereas DLO effects are likely operative at all temperatures for the much faster oxidation occurring near the inner surface.

Given that modulus values increase much more rapidly near the inner surface, we expected that the inner surface modulus values would correlate with tensile failure. However this was not the case and the reason became apparent by viewing the tensile experiments. As aged samples were pulled towards failure, cracks did initiate first on the inner surface of the material. Surprisingly these cracks propagated ~40% through the cross-section and then turned upward or downward and started to run parallel to the pull direction. The sample then continued to elongate until a crack started in the remaining 60% of the cross-section that was previously intact with this latter crack leading to tensile failure. Because of this very unusual failure behavior, it would be risky to attempt a quantitative correlation between modulus and elongation for Hyp-06. However with the underlying knowledge that the failure occurs due to cracks that initiate on the outer 60% of the cross-section, we show the correlation between elongation and outside surface modulus in Fig. VII-46. Although crude given the complex failure process, the results indicate the practical end of life corresponds to the external modulus reaching ~24 MPa, a value not too different from the results for the other hypalon materials.

Figure VII-47 summarizes on one plot the correlation at all times and temperatures between the maximum surface modulus and the tensile elongation for the six "well-behaved" hypalon materials. For these materials, 50% absolute elongation corresponds to the average modulus reaching 38 MPa (dashed line on plot). This value is quite close to the value of ~37 MPa found above for the thermal aging of the polychloroprene cable jacket [VII-15]. This is not to suggest that such a value would hold for all elastomers; for example a practical end of life value of ~8 MPa was found to be appropriate to a polyurethane material whose unaged modulus was 0.6 MPa [VII-13]. However the results do suggest a "universality" criterion (~35 MPa) for the six well-behaved hypalon-based materials. For the Hyp-07 material, where practical end of life occurs more abruptly, exceeding 35 MPa would still be indicative of "end of life". Likewise, if one ignores the strange (but irrelevant to tensile failure) inside hardening occurring for Hyp-02, reaching 35 MPa on the outer surface corresponds to the elongation reaching ~25%.

The same general modulus behavior occurs when the hypalon materials are aged in combined radiation-thermal environments. Earlier we showed elongation results for materials Hyp-03, Hyp-04, Hyp-05 and Hyp-06 each aged at four different combined environment aging conditions (Figs. V-2 through V-5). Modulus profiling results for the 16 aging conditions are summarized in Figs VII-48 through VII-63. Note that the total doses used in these experiments (given in the Figure captions) are quite large compared to the much lower doses normally expected during aging. In general the radiation conditions examined lead to modulus increases with aging (material hardening) in a relatively uniform fashion with some evidence of slightly enhanced hardening near the sample surfaces. Some of the conditions show little evidence of DLO effects while other conditions indicate moderate to important DLO effects. Plots of the maximum surface modulus for each material versus the average elongation under the four combined radiation-thermal aging conditions are shown in Figs. VII-64 through VII-67. The correlations between elongation and modulus are quite similar to the results found for thermal aging of hypalon materials. At our normal "end of life" criterion of 50% absolute elongation, Fig. VII-64 indicates practical end of life occurs when the modulus reaches ~35 MPa for Hyp-03. The modulus values corresponding to 50% elongation for Hyp-05 (~38 MPa) and Hyp-06 (~40 MPa) are in the usual range. For Hyp-04, scatter in the results is quite large with end of life occurring around 58±20 MPa.

As pointed out in a journal publication on the Neo-02 material [VII-15], it might be anticipated that 50% absolute elongation would often correspond to modulus values around 30-40 MPa. This is because such modulus values correspond to Shore A hardness values of around 95 [VII-22, VII-23], the upper limit of elastomeric materials, beyond which little flexibility normally exists. Based on this observation coupled with the extensive hypalon results given above, we conclude that the use of a 35 MPa end of life criterion for modulus is a good starting point for evaluating the condition of an unknown hypalon cable jacketing material.

Modulus profiling of chlorinated polyethylene (CPE-02) jacketing material

Oven aging results for this material were reported in Section III (Fig. III-28). Modulus profiling results were obtained for samples aged at 124°C in order to determine the applicability of this CM technique to chlorinated polyethylene jackets. The results are shown in Fig. VII-68. The unaged material (open circles) has uniform modulus across the cross-section with an average value of ~90 MPa. This is a much higher modulus than typical elastomeric material and is caused by the high crystallinity of the material that in turn dominates the material hardness. As the material ages, the modulus tends to increase slowly but the changes are moderate compared to the scatter in the data, again due to the domination of the crystalline phase. Therefore we conclude that modulus profiling is not a very useful CM approach for CPE materials.

Modulus profiling of EPR cable insulation materials

As noted earlier, we have obtained elongation results for four different commercial EPR cable insulation materials under thermal-only aging conditions ranging from 99°C to

170°C (see Figs. III-32, III-35, III-39, III-42). To estimate the temperatures where DLO effects might be important, we need oxygen consumption and permeability estimates for EPR materials. As seen in Section IV, we have conducted oxygen consumption measurements on one of the currently studied EPR materials. At 125°C the average consumption result over the first 10 weeks of aging gives $\phi \sim 2\text{x}10^{-11}$ mol/g/s (Fig. IV-27). This value at 125°C can be used together with the E_a value appropriate for oxygen consumption (100 kJ/mol- see Fig. IV-29) to make estimates of ϕ at several temperatures in the temperature range of interest (Table VII-2). Estimates of the permeability coefficient at the temperatures of interest are available from actual high temperature measurements on an EPR material [VII-20]; these are also shown in Table VII-2. Assuming a typical EPR density of 1.3 g/cc (Table I-3), eq. VI-1 leads to the L_{90} values summarized in the last row of Table VII-2. Comparing these results to the typical 1-mm cross-section of EPR cable insulations makes it clear that DLO effects will be unimportant for thermal aging of these materials even at temperatures as high as 170°C.

Table VII-2. Estimates of L_{90} for EPR cable insulations.

T, °C	170	140	125	110	99
ϕ, mol/g/s	4.35e-10	6e-11	2e-11	6.1e-12	2.4e-12
P_{Ox}, ccSTP/cm/s/cmHg	5.2e-8	3.8e-8	3e-8	2.4e-8	1.9e-8
L_{90}, mm	3.3	5.7	8.8	14.3	26.8

We showed earlier in Section III that EPR materials tend to follow induction-time behavior where changes in properties are slow until just before end of life where the changes accelerate rapidly. The analyses summarized in Table VII-2 utilize ϕ values taken before the induction time region and therefore predict unimportant DLO effects only before the induction time. Once the induction time region is reached the degradation rate (oxidation rate) will greatly accelerate implying large increases in values. Therefore we would anticipate negligible DLO effects until the induction times are reached but might anticipate a possibility of DLO effects after reaching the induction time.

Evidence for induction-time behavior was presented above for the elongation results of EPR-03 (Fig. III-39), EPR-04 (Fig. III-35) and EPR-05 (Fig. III-42). We would expect the situation (slow changes until the induction time) to be similar for other properties and that turns out to be the case. For instance modulus profiling results are shown for the EPR-04 insulation at its four thermal aging temperatures in Figs. VII-69 through VII-72. In these plots the usual x-axis parameter P (percentage of distance from the outside surface to the inside surface) has been replaced by the actual distance in mm from the outside surface. This change reflects the difficulty in making modulus measurements near the inside surface especially when significant hardening occurs after the induction time. Fig. VII-69 shows the results at 139°C. The unaged sample (open circles) has a homogeneous profile with an average modulus of ~4.5 MPa. For the first 4 weeks of aging (corresponding to times just before the induction time- see Fig. III-35), the

modulus increases slowly and uniformly. The results from two separate samples are shown after 6.3 weeks and 6.9 weeks to show the late life effects of induction time behavior. After the induction time (6.3 and 6.9 week data- see Fig. III-35), the modulus increases dramatically with large sample-to-sample variation and important DLO effects. The scatter is expected near the induction time since different sections of the insulation may use up their anti-oxidant at slightly differing times due to slight spatial variations in antioxidant concentration, slight temperature differences during aging, etc. The entrance of DLO effects indicates a very large increase of oxidation must occur in the induction-time region. Looking at Table VII-1, an L_{90} of ~6 mm represents the pre-induction-time situation. If the oxygen permeability coefficient remained constant through the induction period, eq. V-1 implies that the oxygen consumption rate would have to increase by ~two orders of magnitude to cause L_{90} to drop below 1 mm. The actual situation is somewhat more complex since the hardening occurring in the induction-time region leads to drops in oxygen permeability coefficients [VII-9] thereby reducing the amount of increase necessary in ϕ to cause DLO effects.

Very similar behavior occurs at an aging temperature of 124°C as seen in Fig. VII-70. Again comparisons with the elongation results at this temperature (Fig. III-35) indicate that modulus changes are moderate and without DLO effects until the induction-time region where the changes accelerate and show both substantial scatter and DLO effects. As the aging temperature decreases to 109°C, the overall behavior is similar except for the absence of DLO effects even after the induction time (Fig. VII-71). This implies for the EPR-04 material that the increase in ϕ and the decrease in P_{Ox} in the induction-time region is insufficient to cause DLO effects at 109°C and below. At 99°C we ran modulus profiles on five sections (Fig. VII-72) taken from samples that had aged to 347 weeks (elongation was below 10% (Fig. III-35). We selected a soft piece (#1), two harder pieces (#2 and #4) and two very hard pieces (#3 and #5) and obtained the expected results.

Modulus profiling results for the white EPR-05 insulation at aging temperatures of 138°C, 124°C and 109°C are given in Figs. VII-73 through VII-75. Comparing these results to the tensile elongation data (Fig. III-42), we see behavior quite similar to that shown above by the EPR-04 material. The only major difference is the observation that DLO effects are still important after the induction time at all temperatures including 109°C. Similar results and conclusions hold for the modulus profile data of the EPR-03 material (Figs VII-76 through VII-78) except for a slight amount of initial softening observed for the early degradation at 124°C. Finally it should be noted that the unaged moduli of the three EPR materials are quite different (~62 MPa for EPR-03, ~4.5 MPa for EPR-04 and ~12 MPa for EPR-05) reflecting primarily their differences in crystallinity (see Fig. III-31).

Thus, similar to elongation results, we conclude that modulus profiling is relatively insensitive to degradation for EPR insulation materials until the induction-time region is approached. This lack of warning of end of life for CM techniques applied to materials with induction-time behavior is common, as we will see below when discussing density, gel fraction and solvent swelling results. Such behavior unfortunately argues against

attempts to utilize CM approaches to follow the aging of cable materials that have such behavior since little or no warning of impending failure will exist. Fortunately there is another approach that can be used to transform such non-predictive behavior into fairly linear predictive behavior. This approach, that we term the Wear-out method, will be discussed in Section XI of this report.

Modulus profiling of miscellaneous insulation materials (XLPO and silicone)

Because of their crystallinity that dominates the hardness and modulus of XLPO materials, we were not able to find much sensitivity of modulus to the aging of such materials either in thermal or in combined radiation-thermal aging environments. For the XLPO-02A material, for example, the unaged modulus averaged around 160 MPa. Severe aging either in radiation or thermal environments led to essentially no change in modulus value within the experimental uncertainty.

The Sil-01 cable insulation material was not aged under thermal conditions since silicone insulations are extremely robust in thermal-only environments. Aging was conducted, however, under several combined radiation-thermal environments since this insulation is less resistant in radiation environments. To see whether modulus profiling would be a useful technique for silicone insulation materials, we ran one comparison of modulus results with elongation results for samples aged at 77 Gy/h plus 120°C. The results are shown in Fig. VII-79. Under these aging conditions, the elongation (bottom of figure) drops quickly at first and then asymptotically approaches low values. The modulus measurements (top of figure) start at 3.1 MPa and linearly increase with aging dose as the elongation drops. This very linear behavior suggests that modulus profiling might be useful for silicone insulations exposed to radiation environments. Figure VII-80 shows the correlation plot for elongation and modulus.

Conclusions

Modulus profiling appears to be a very promising CM technique for nuclear power plant cable jacketing and insulation materials. It appears to be applicable to most materials that do not have important crystallinity including neoprene and hypalon jackets and EPR and silicone insulations. It shows sensitivity for these materials both in thermal-only and combined radiation plus thermal environments. In general modulus values increase with aging in both temperature-only and combined radiation-thermal environments. This implies that the overall crosslink density increases (crosslinking processes dominate scission processes) during the aging. For the neoprene and hypalon jacketing materials, the vast majority of the results both in thermal-only and combined radiation-thermal environments indicate that 50% absolute elongation is reached when modulus values get above ~35 MPa. For EPR insulations, modulus measurements are similar to other CM parameters in that they are relatively insensitive before the induction time but quite sensitive once the induction-time region is reached. Experimental modulus profiles in combination with theoretical modeling are invaluable for determining when DLO or other heterogeneously based effects are operative both for accelerated aging experiments and for heterogeneous aging mechanisms that might occur under ambient aging conditions (e.g., copper-catalyzed oxidation).

References

VII-1. K. T. Gillen, R. L. Clough and C. A. Quintana, "Modulus Profiling of Polymers", Polym. Degrad. & Stabil., 17, 31 (1987).

VII-2. Gillen KT, Terrill ER, Winter RW. Modulus mapping of rubbers using micro- and nano-indentation techniques. Rubber Chem Tech Rubber Reviews 2001;74:428.

VII-3. K. T. Gillen and R. L. Clough, "Techniques for Monitoring Heterogeneous Oxidation of Polymers", in **Handbook of Polymer Science and Technology, Vol. 2,** N. P. Cheremisinoff, Ed., Marcel Dekker, New York, 1989, Ch. 6.

VII-4. R. L. Clough and K. T. Gillen, "Polymer Degradation under Ionizing Radiation: The Role of Ozone", J. Polym. Sci., P. C. Ed., 27, 2313 (1989).

VII-5. K. T. Gillen and R. L. Clough. "Polymer Insights Available from Modulus Profiling Data.", Polym. Eng. and Sci., 29, 29 (1989).

VII-6. R. L. Clough and K. T. Gillen, "Oxygen Diffusion Effects in Thermally Aged Elastomers", Polym. Degrad. & Stabil., 38, 47 (1992).

VII-7. B. Mattson, B. Stenberg, K. T. Gillen, R. L. Clough and E. Ostman, "Novel Techniques used to Assess the Ageing of Carbon-black filled Materials", Polym. Degrad. And Stabil., 41, 211 (1993).

VII-8. J. Wise, K. T. Gillen and R. L. Clough, "An Ultrasensitive Technique for Testing the Arrhenius Extrapolation Assumption for Thermally-Aged Elastomers", Polym. Degrad. & Stabil., 49, 403 (1995).

VII-9. J. Wise, K. T. Gillen and R. L. Clough, "Quantitative Model for the Time Development of Diffusion-Limited Oxidation Profiles", Polymer, 38, 1929 (1997).

VII-10. J. Wise, K. T. Gillen and R. L. Clough, "Time-Development of Diffusion-Limited Oxidation Profiles in a Radiation Environment", Radiat. Phys. and Chem., 49, 565 (1997).

VII-11. M. Celina, J. Wise, D. K. Ottesen, K. T. Gillen and R. L. Clough, "Oxidation of Thermally Aged Nitrile Rubber", Polym. Degrad. Stabil., 60, 493 (1998).

VII-12. M. Celina, J. Wise, D. K. Ottesen, K. T. Gillen and R. L. Clough, "Oxidation Profiles of Thermally Aged Neoprene", Polym. Degrad. Stabil., 68, 171 (2000).

VII-13. M. Celina, A. C. Graham, K. T. Gillen, R. A. Assink and L. M. Minier, "Thermal Degradation Studies of a Polyurethane Propellant Binder", Rubber Chem. Technol., 73, 678 (2000).

VII-14. B. Dinzburg and K. T. Gillen, "Use of Modulus Profiling to Monitor the Carbonization (Surface Hardening) of Rubber after Aging in Oil", Lubrication Engineering., 58, No. 2, 21 (February, 2002)

VII-15. K. T. Gillen, R. A. Assink and R. Bernstein, "Condition Monitoring Approaches Applied to a Polychloroprene Cable Jacketing Material", Polym. Degrad. Stabil., 84, 419 (2004).

VII-16. Anandakumaran K, Seidl W, Castaldo PV. Condition assessment of cable insulation systems in operating nuclear power plants. IEEE Trans. Diel & Elect Ins 1999;6:376.

VII-17. G. Toman, EPRI Project Manager, "Initial Criteria Acceptance Concepts and Data for Assessing Longevity of Low-Voltage Cable Insulations and Jackets", EPRI Technical Report 1008211, Final Report, March, 2005.

VII-18. K. T. Gillen, R. A. Assink, R. Bernstein and M. Celina, "Condition Monitoring Methods Applied to Chlorosulfonated polyethylene cable jacketing materials", Polym. Degrad. Stabil., in press.
VII-19. Seguchi T, Yamamoto Y. Diffusion and solubility of oxygen in gamma-ray irradiated polymer insulation materials. Japan Atomic Energy Research Institute Report JAERI 1299, March, 1986.
VII-20. M. Celina and K. T. Gillen, "Oxygen Permeability Measurements on Elastomers at Temperatures up to 225°C", Macromolecules, 38, 2754 (2005).
VII-21. K. T. Gillen, R. Bernstein and M. Celina, "Non-Arrhenius Behavior for Oxidative Degradation of Chlorosulfonated Polyethylene Materials", Polymer Degradation and Stability, 87, 335(2005).
VII-22. Gent AN . In: Eirich FR, editor. Rubber elasticity: Basic concepts and behaviors. New York: Academic Press, 1978, p. 17.
VII-23. Briscoe BJ, Sebastian KS. An analysis of the "durometer" indentation. Rubber Chem Technol 1993;66:827.

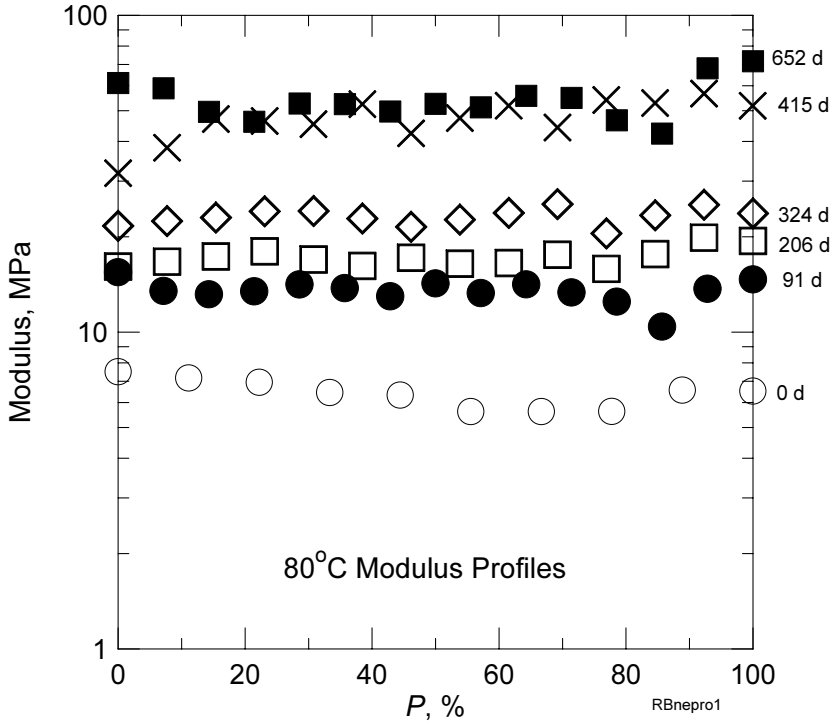

Figure VII-1. Modulus profiling results for the Neo-02 material aged at 80°C for the indicated aging times.

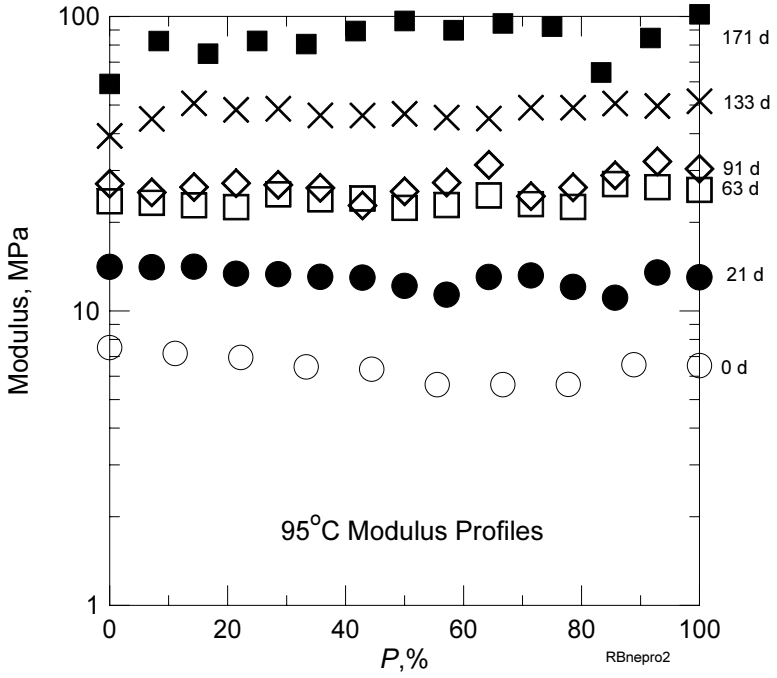

Figure VII-2. Modulus profiling results for the Neo-02 material aged at 95°C for the indicated aging times.

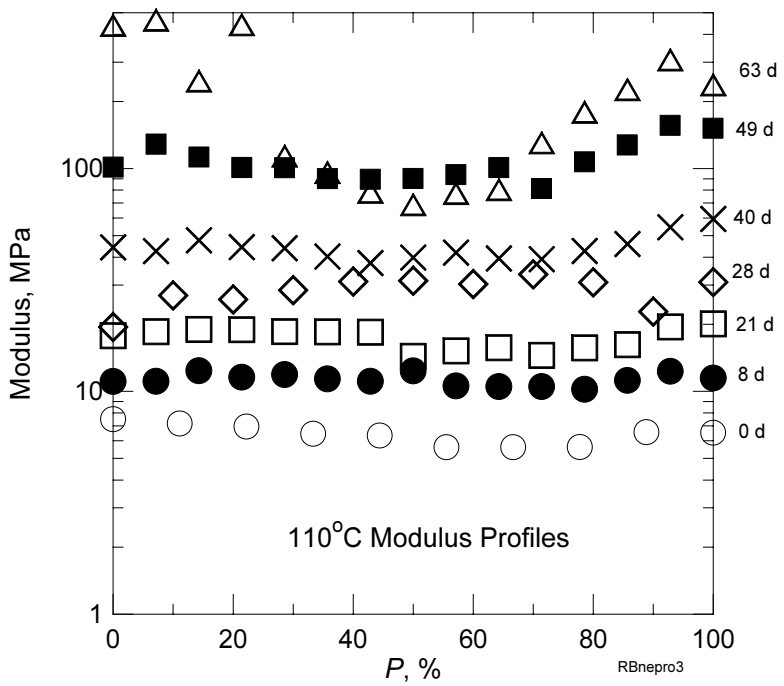

Figure VII-3. Modulus profiling results for the Neo-02 material aged at 110°C for the indicated aging times.

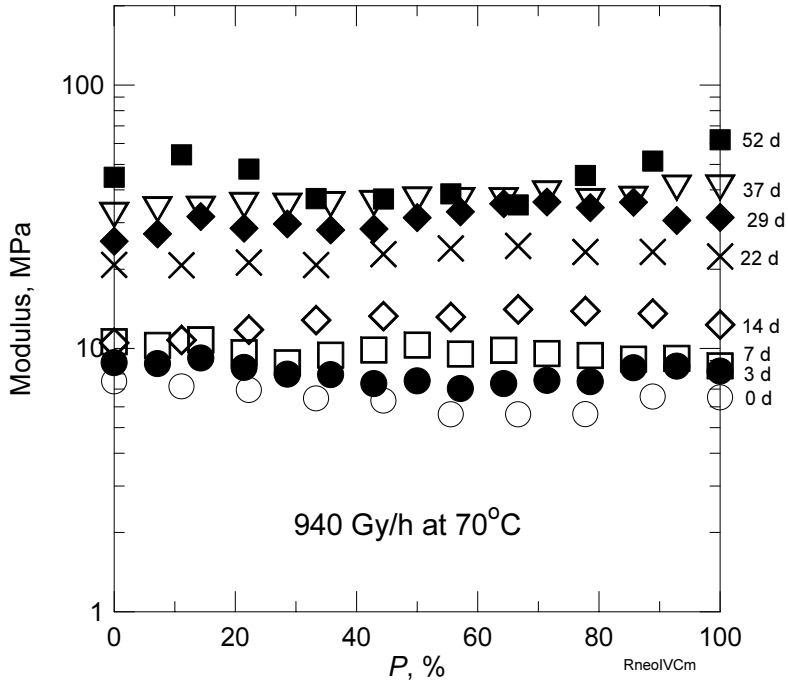

Figure VII-4. Modulus profiling results for the Neo-02 material aged at 940 Gy/h plus 70°C for the indicated aging times.

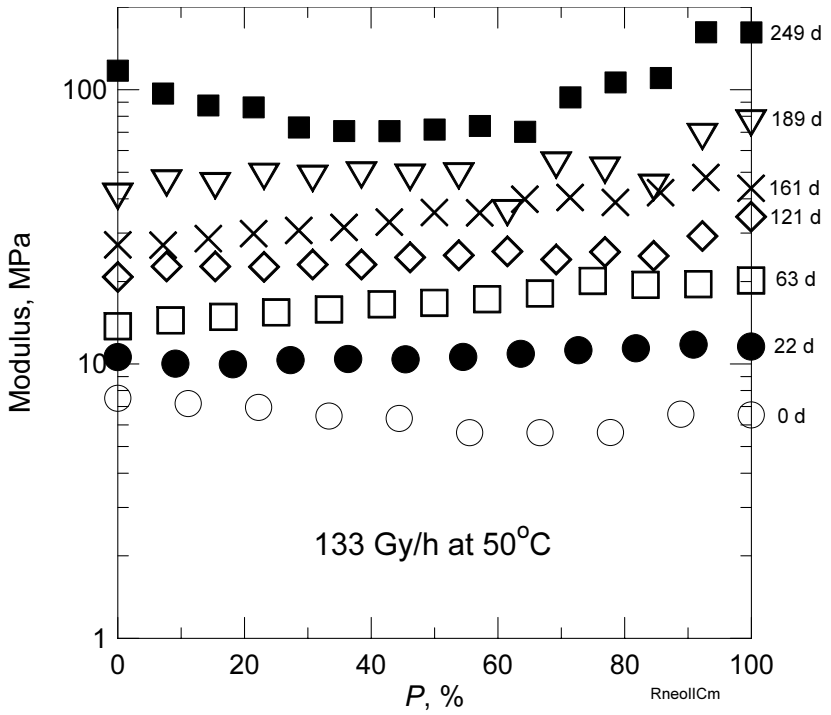

Figure VII-5. Modulus profiling results for the Neo-02 material aged at 133 Gy/h plus 50°C for the indicated aging times.

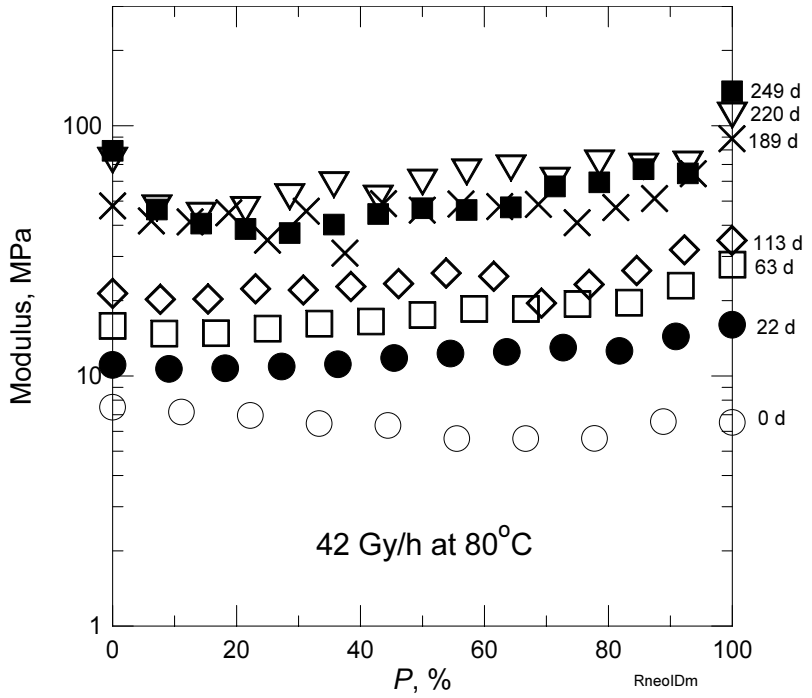

Figure VII-6. Modulus profiling results for the Neo-02 material aged at 42 Gy/h plus 80°C for the indicated aging times.

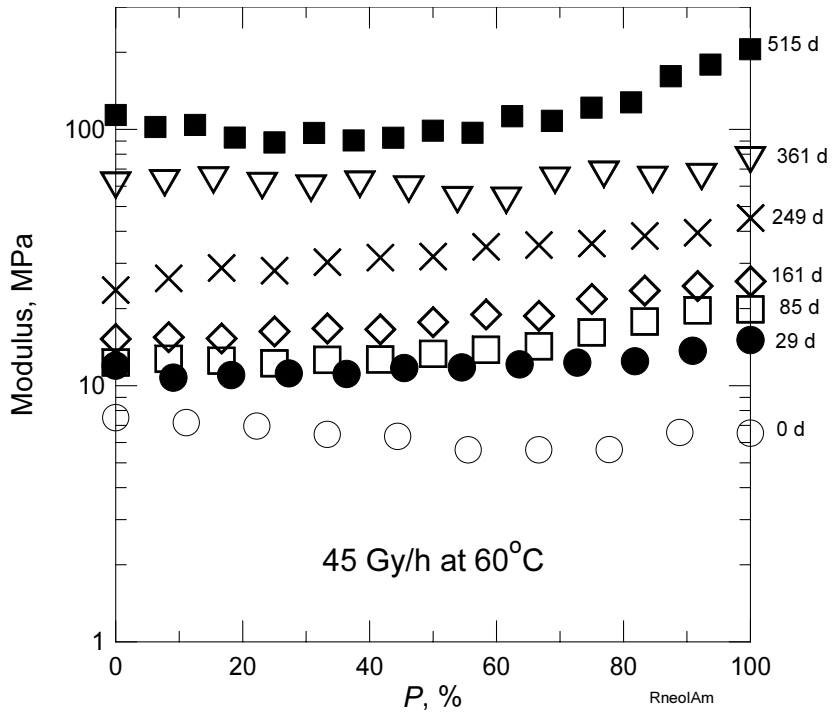

Figure VII-7. Modulus profiling results for the Neo-02 material aged at 45 Gy/h plus 60°C for the indicated aging times.

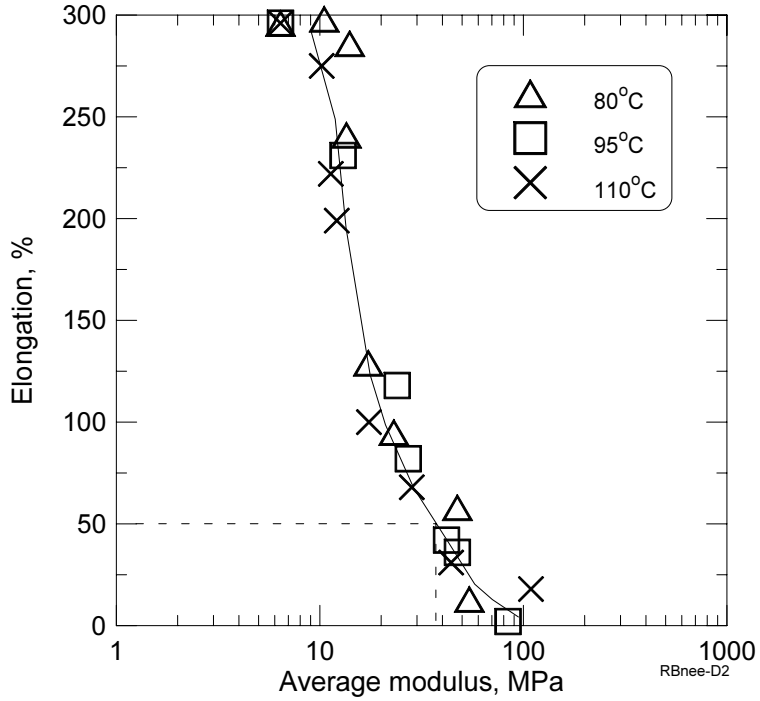

Figure VII-8. Average elongation plotted versus average modulus for Neo-02 material at the indicated aging temperatures.

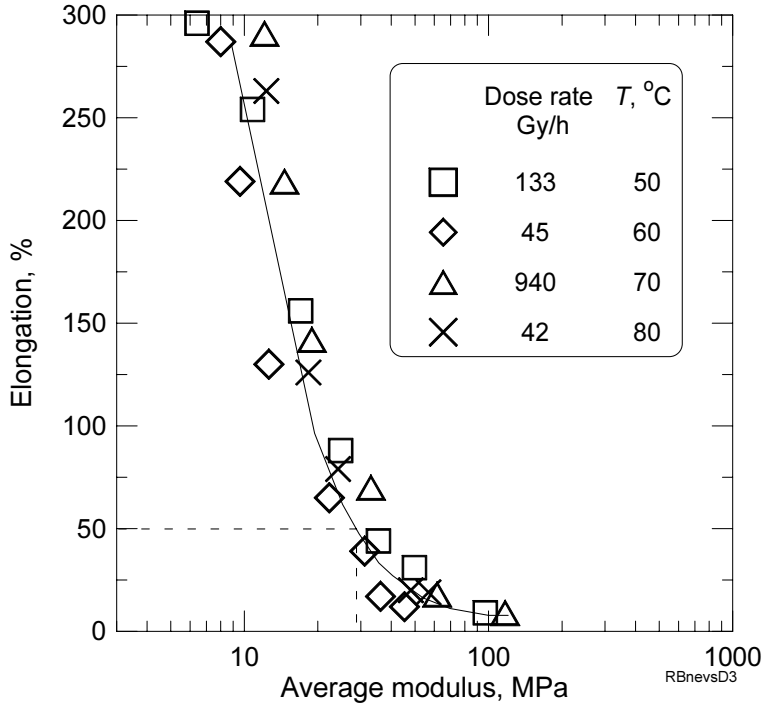

Figure VII-9. Average elongation plotted versus average modulus for Neo-02 material at the indicated combined environment aging conditions.

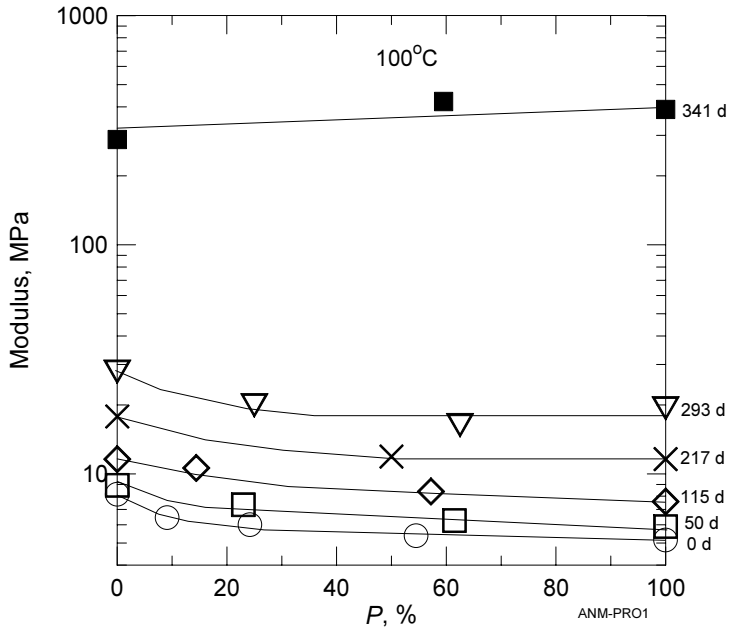

Figure VII-10. Modulus profiling results for the Hyp-01A material aged at 100°C for the indicated aging times.

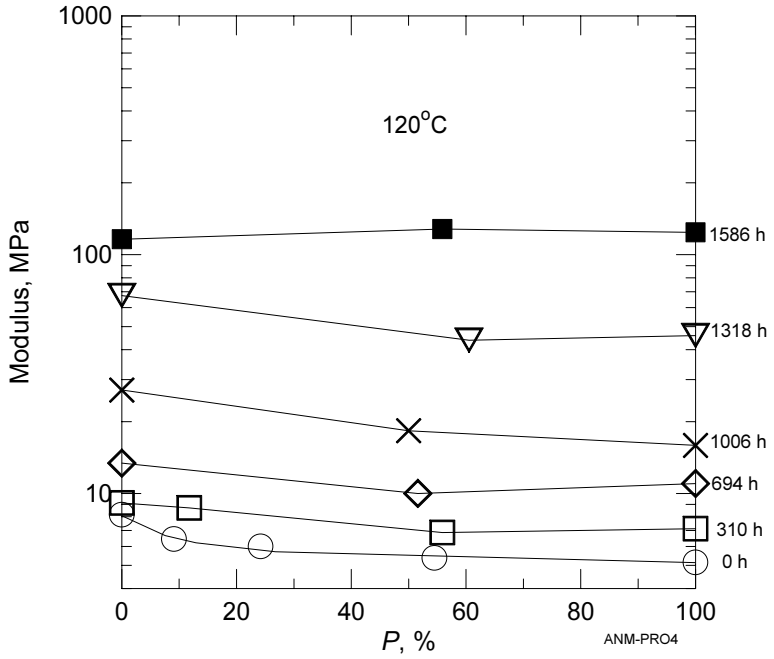

Figure VII-11. Modulus profiling results for the Hyp-01A material aged at 120°C for the indicated aging times.

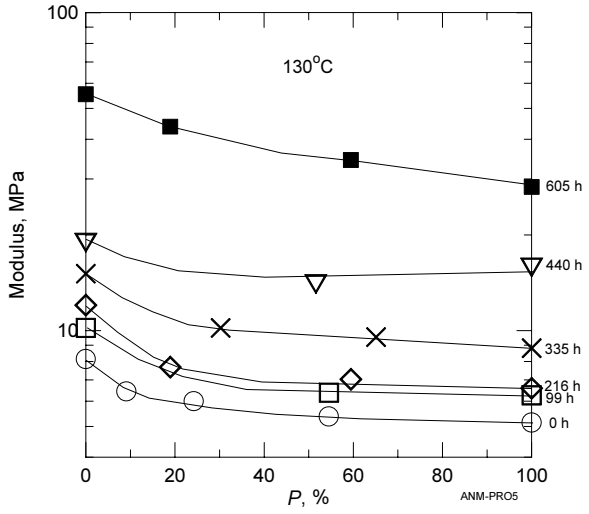

Figure VII-12. Modulus profiling results for the Hyp-01A material aged at 130°C for the indicated aging times.

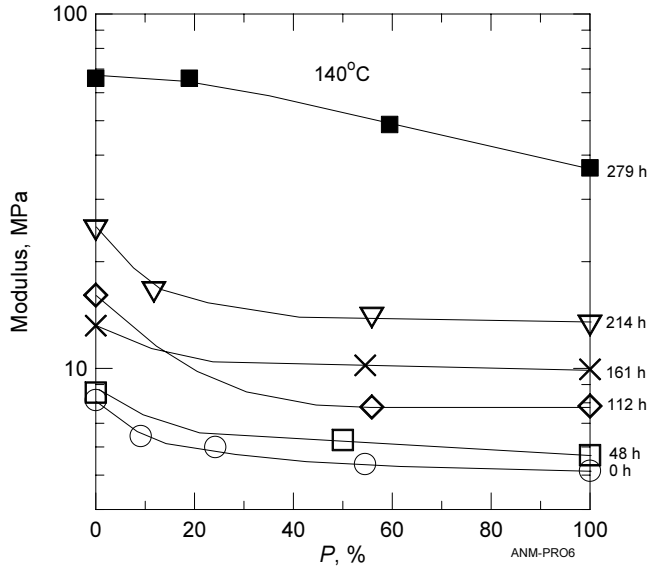

Figure VII-13. Modulus profiling results for the Hyp-01A material aged at 140°C for the indicated aging times.

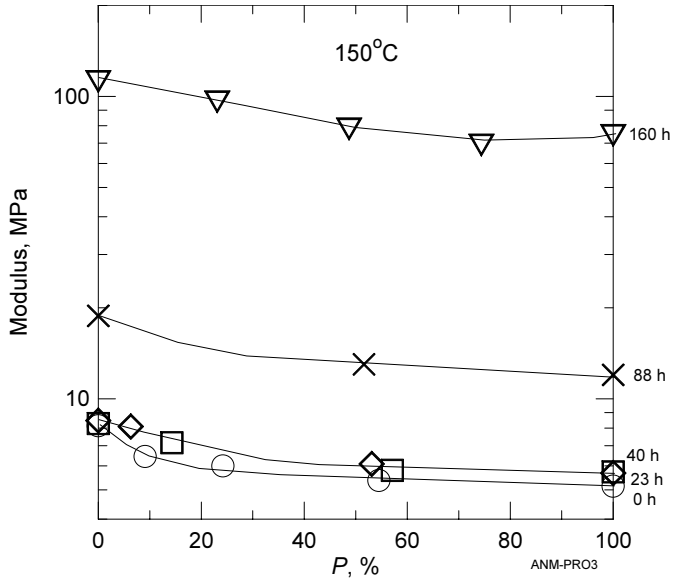

Figure VII-14. Modulus profiling results for the Hyp-01A material aged at 150°C for the indicated aging times.

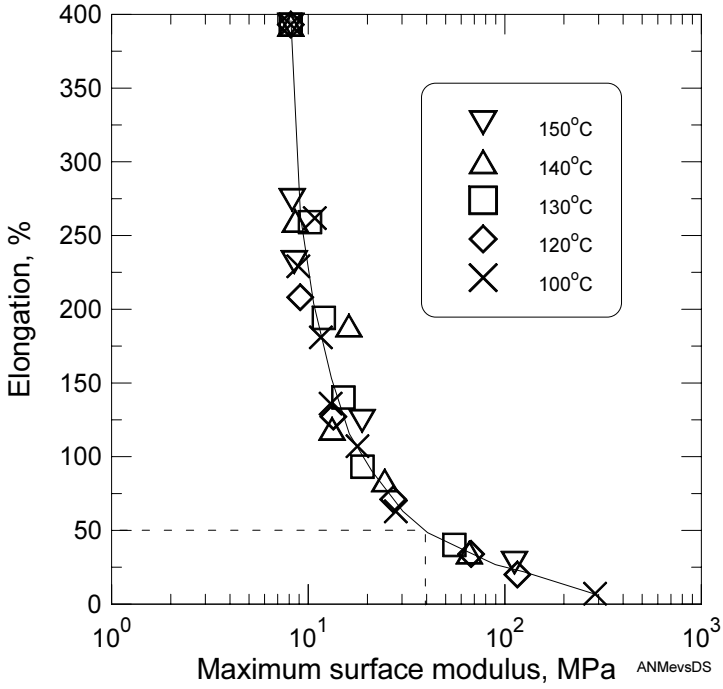

Figure VII-15. Average elongation plotted versus outside surface modulus for Hyp-01A material at the indicated aging temperatures.

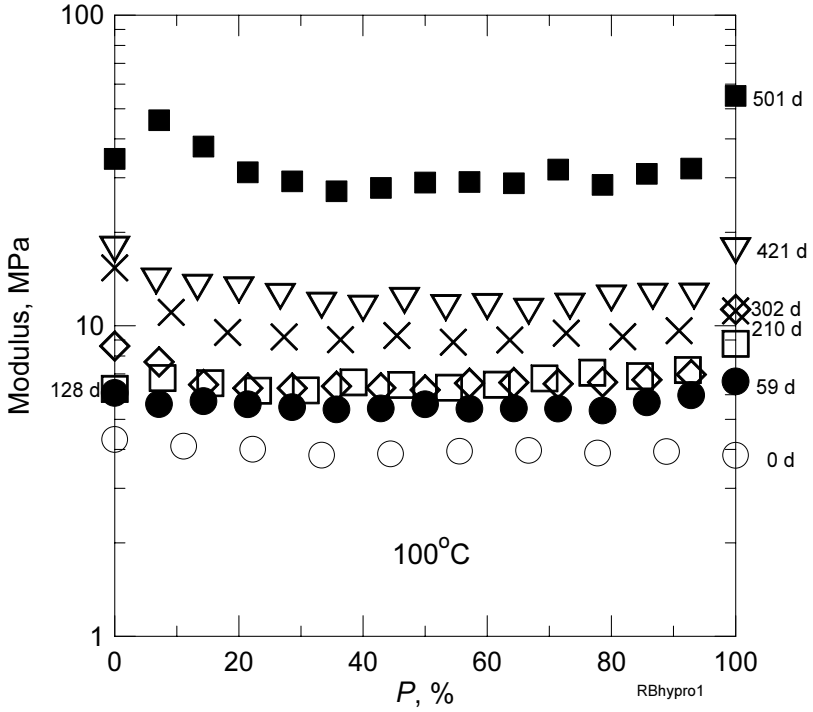

Figure VII-16. Modulus profiling results for the Hyp-05 material aged at 100°C for the indicated aging times.

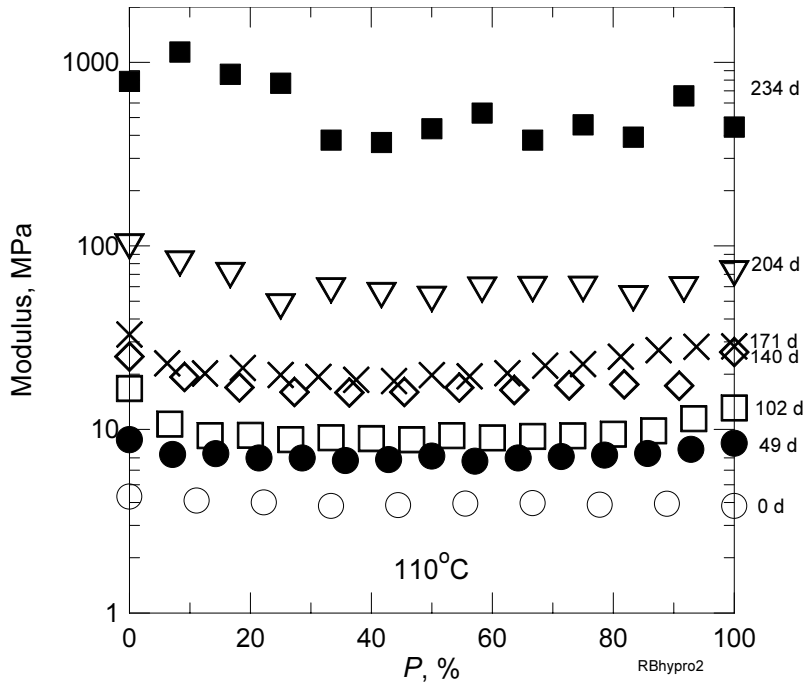

Figure VII-17. Modulus profiling results for the Hyp-05 material aged at 110°C for the indicated aging times.

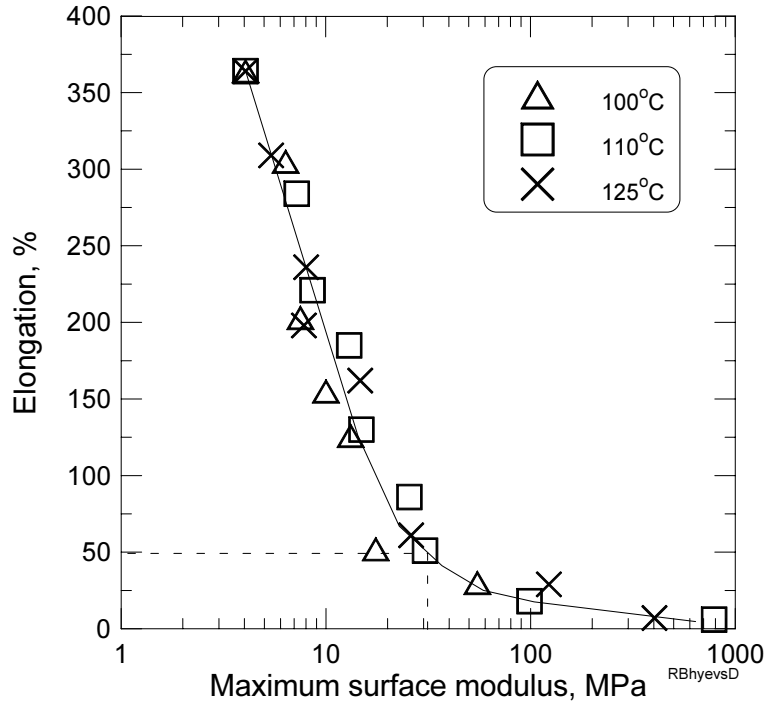

Figure VII-18. Modulus profiling results for the Hyp-05 material aged at 125°C for the indicated aging times.

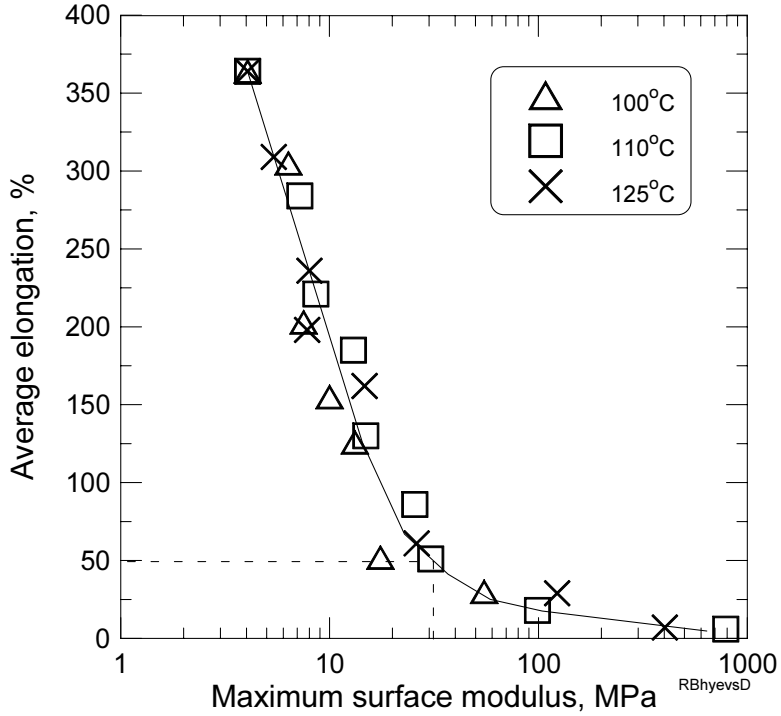

Figure VII-19. Average elongation plotted versus highest surface modulus for Hyp-05 material at the indicated aging temperatures.

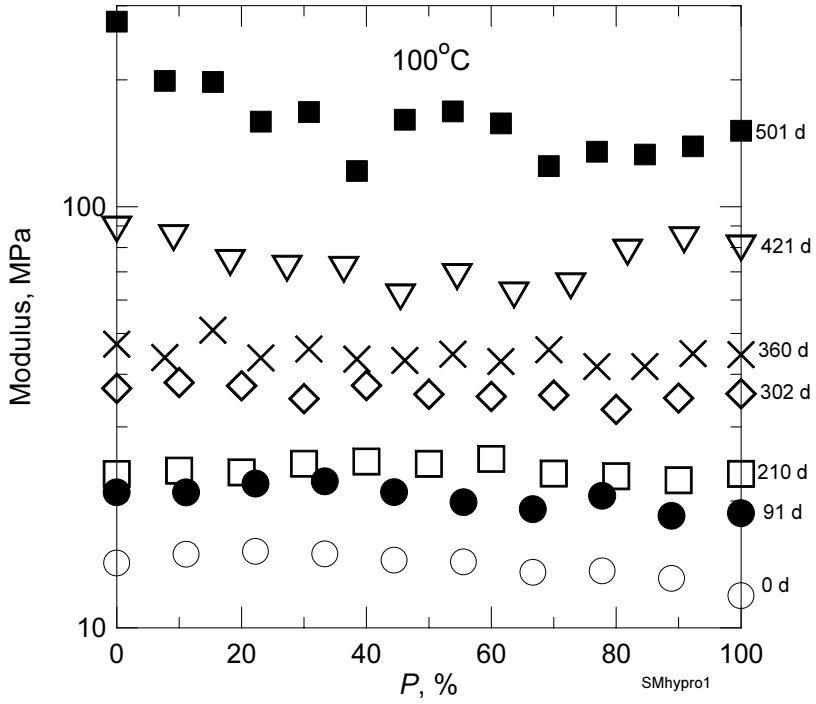

Figure VII-20. Modulus profiling results for the Hyp-03 material aged at 100°C for the indicated aging times.

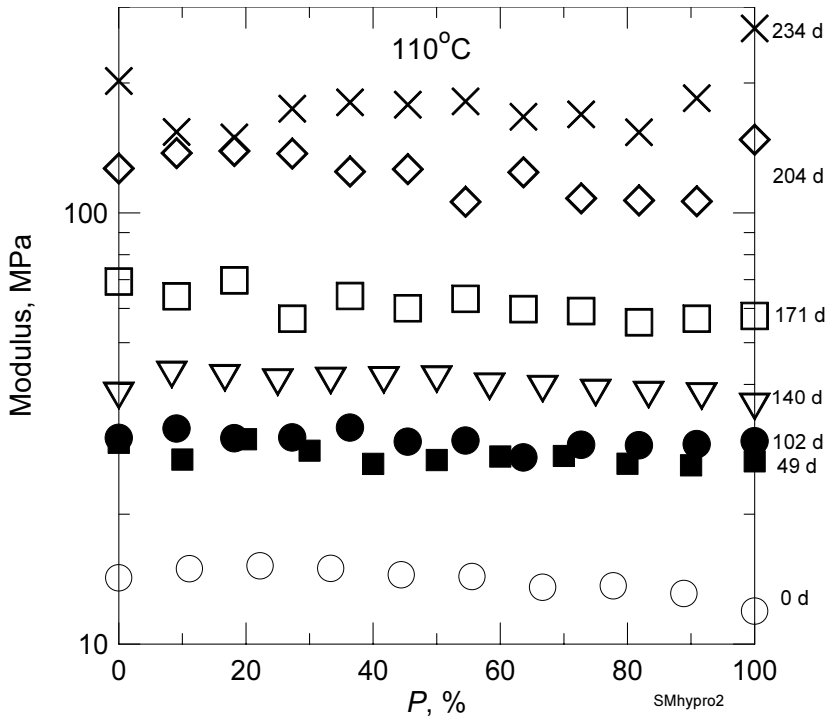

Figure VII-21. Modulus profiling results for the Hyp-03 material aged at 110°C for the indicated aging times.

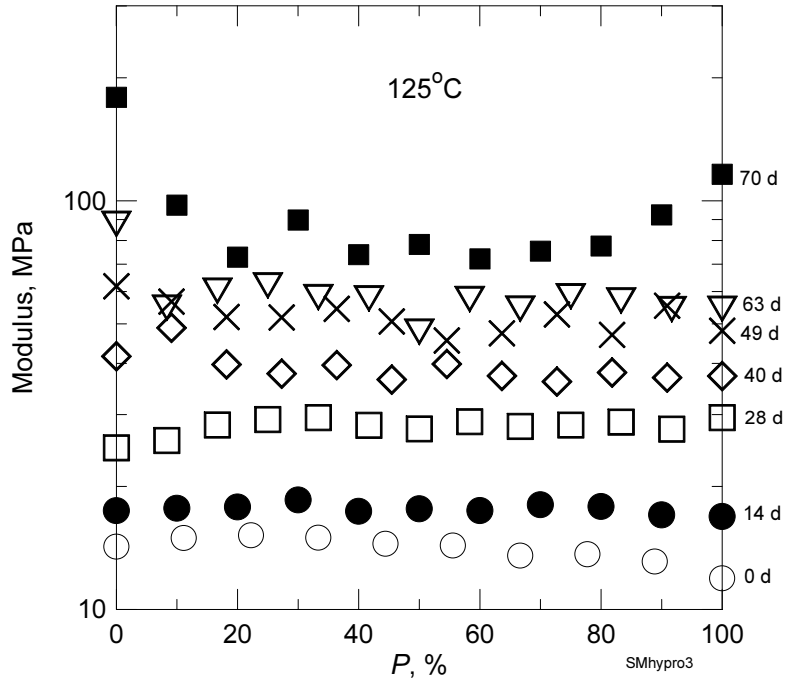

Figure VII-22. Modulus profiling results for the Hyp-03 material aged at 125°C for the indicated aging times.

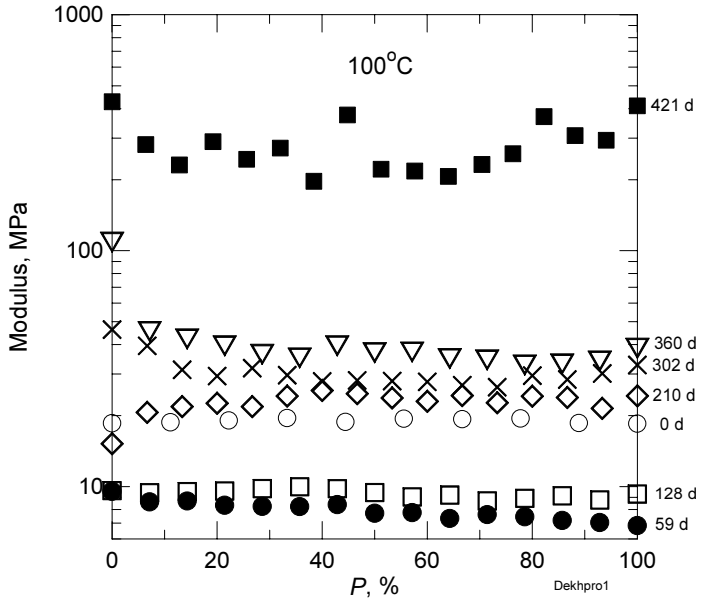

Figure VII-23. Modulus profiling results for the Hyp-06 material aged at 100°C for the indicated aging times.

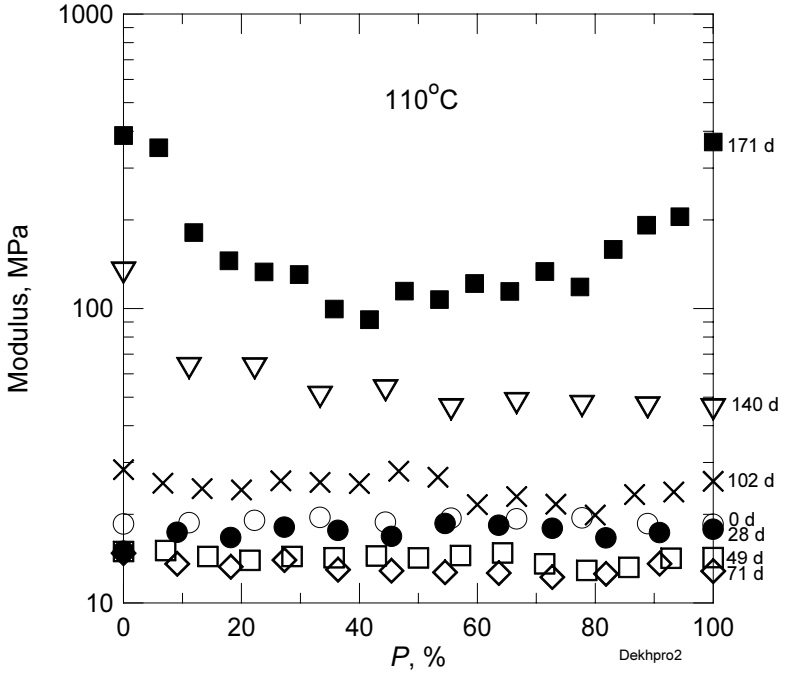

Figure VII-24. Modulus profiling results for the Hyp-06 material aged at 110°C for the indicated aging times.

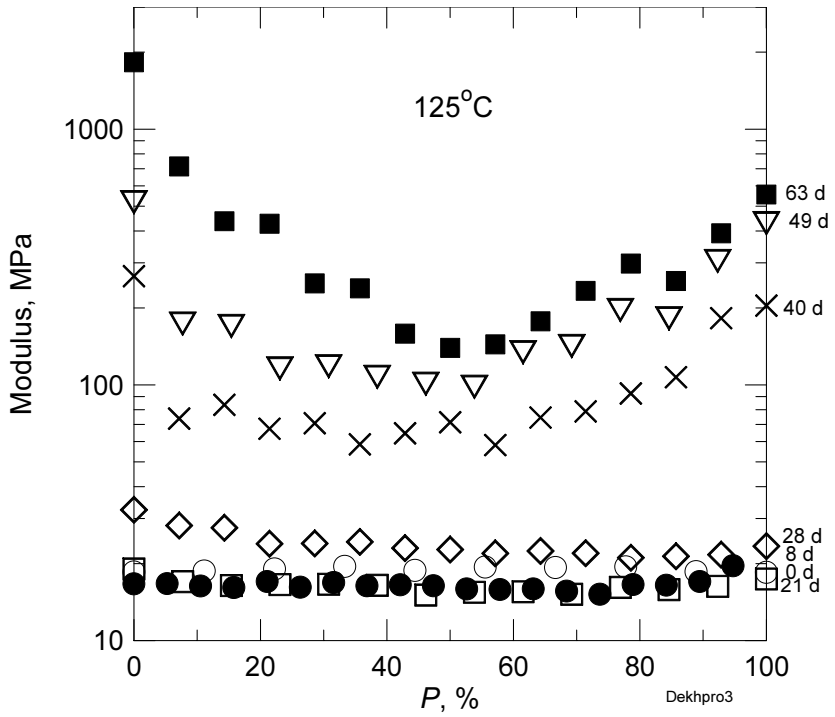

Figure VII-25. Modulus profiling results for the Hyp-06 material aged at 125°C for the indicated aging times.

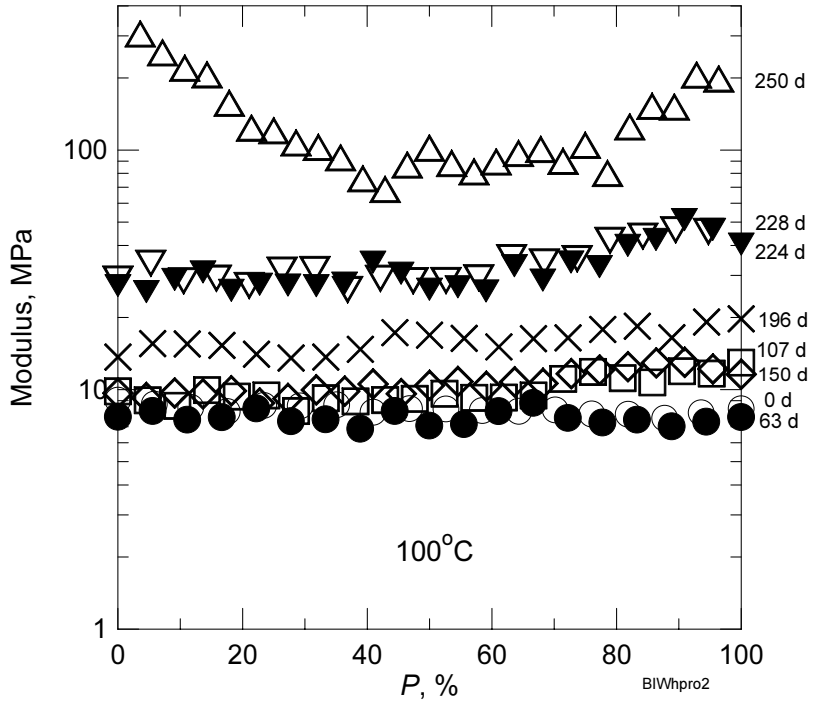

Figure VII-26. Modulus profiling results for the Hyp-08 material aged at 100°C for the indicated aging times.

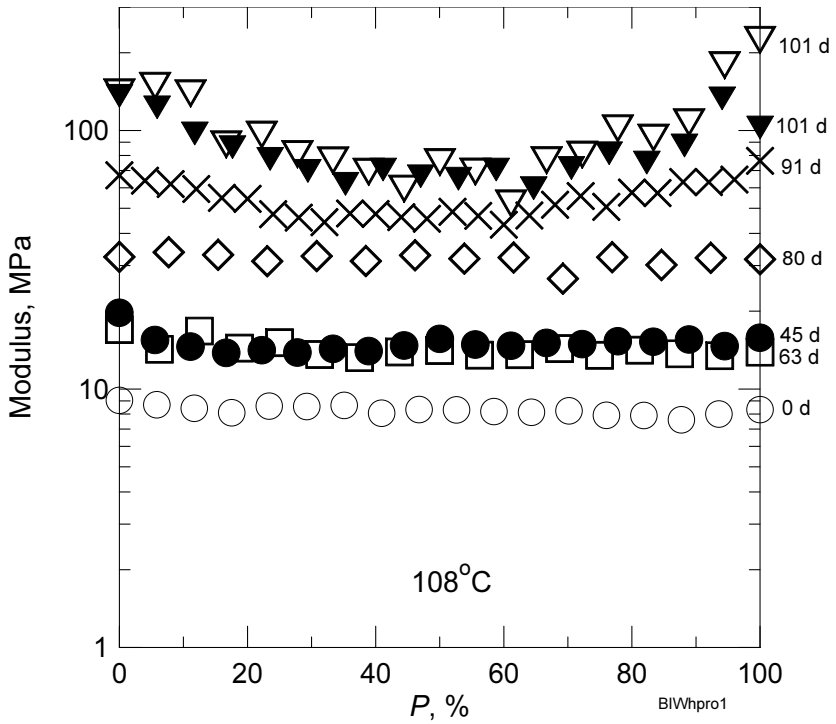

Figure VII-27. Modulus profiling results for the Hyp-08 material aged at 108°C for the indicated aging times.

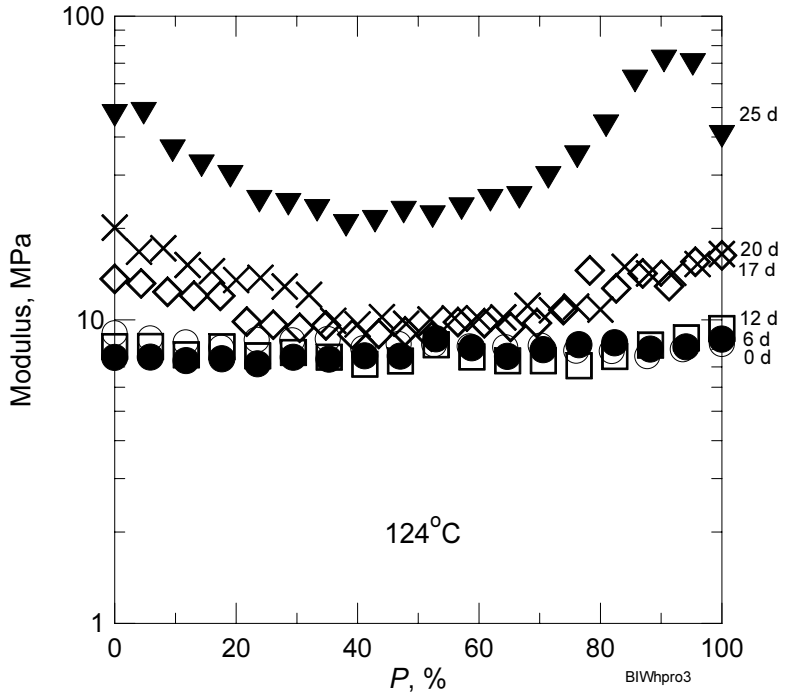

Figure VII-28. Modulus profiling results for the Hyp-08 material aged at 124°C for the indicated aging times.

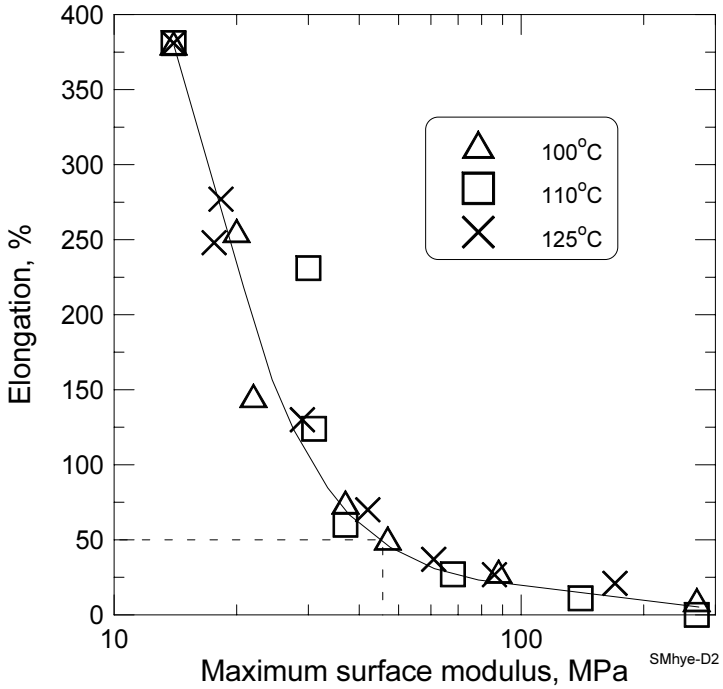

Figure VII-29. Average elongation plotted versus highest surface modulus for Hyp-03 material at the indicated aging temperatures.

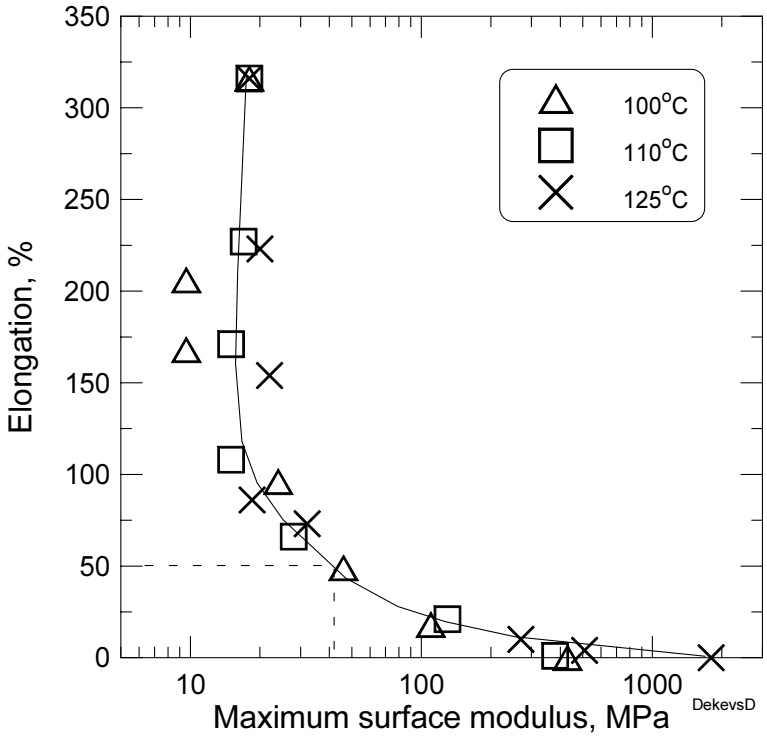

Figure VII-30. Average elongation plotted versus highest surface modulus for Hyp-06 material at the indicated aging temperatures.

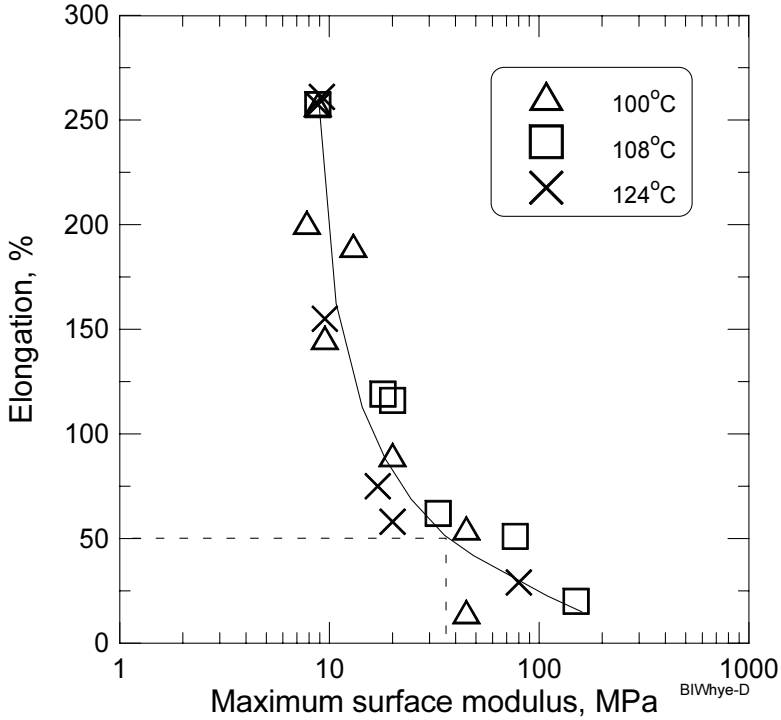

Figure VII-31. Average elongation plotted versus highest surface modulus for Hyp-08 material at the indicated aging temperatures.

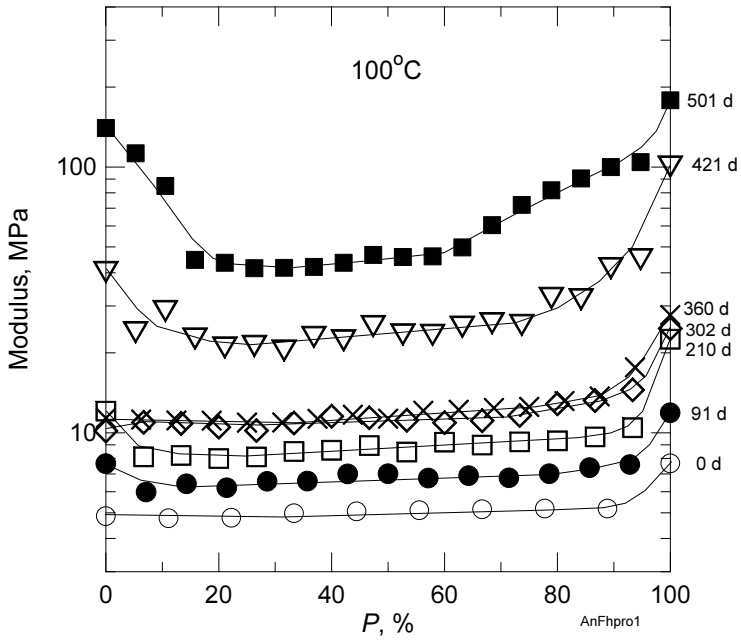

Figure VII-32. Modulus profiling results for the Hyp-04 material aged at 100°C for the indicated aging times.

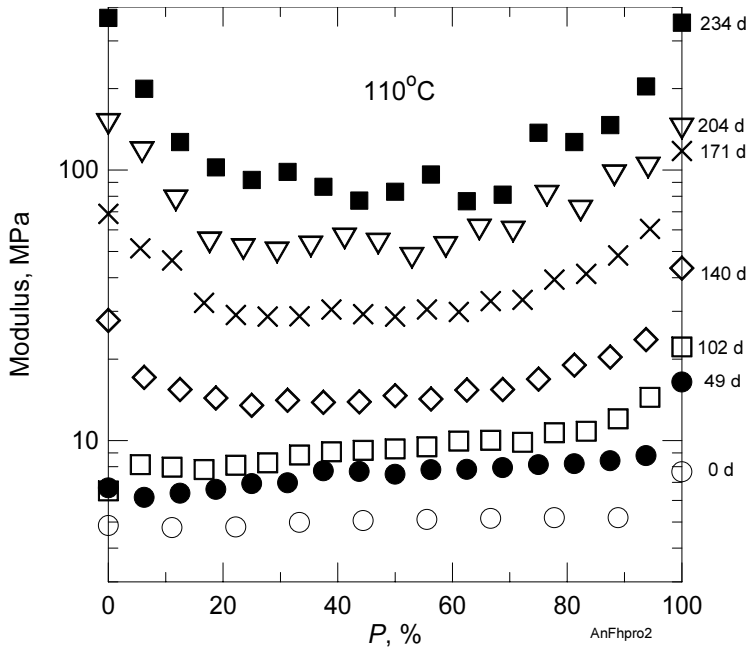

Figure VII-33. Modulus profiling results for the Hyp-04 material aged at 110°C for the indicated aging times.

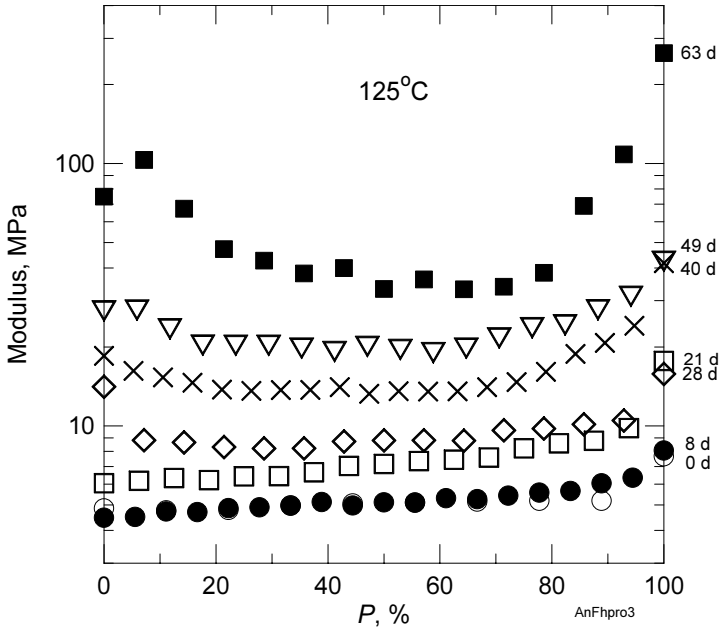

Figure VII-34. Modulus profiling results for the Hyp-04 material aged at 125°C for the indicated aging times.

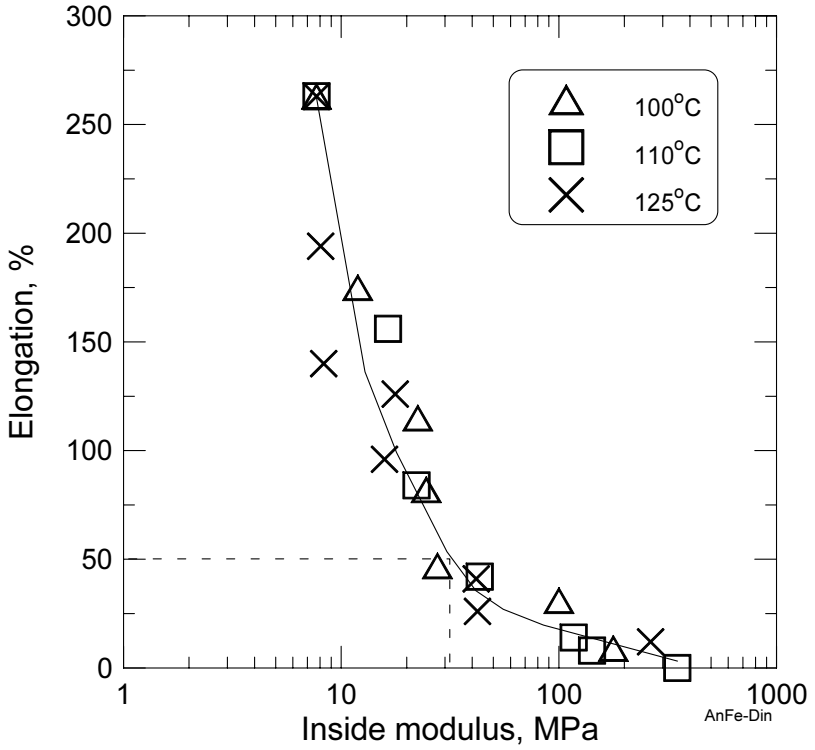

Figure VII-35. Average elongation plotted versus inside modulus for Hyp-04 material at the indicated aging temperatures.

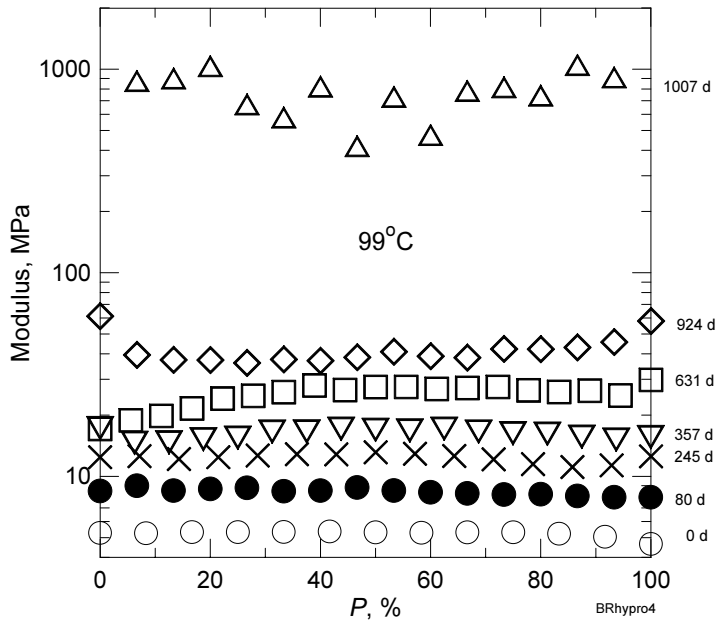

Figure VII-36. Modulus profiling results for the Hyp-07 material aged at 99°C for the indicated aging times.

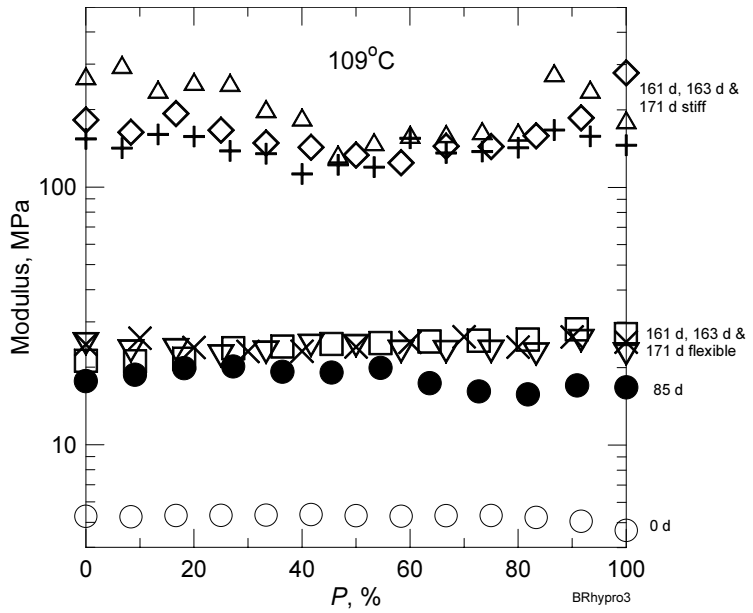

Figure VII-37. Modulus profiling results for the Hyp-07 material aged at 109°C for the indicated aging times.

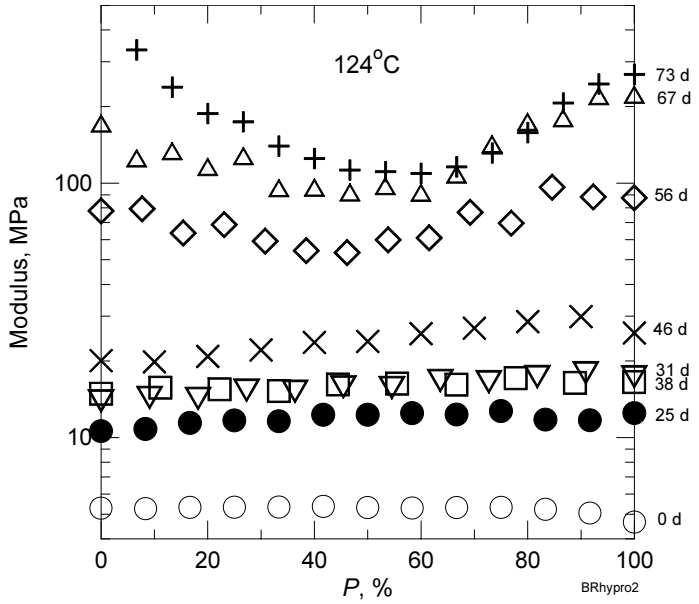

Figure VII-38. Modulus profiling results for the Hyp-07 material aged at 124°C for the indicated aging times.

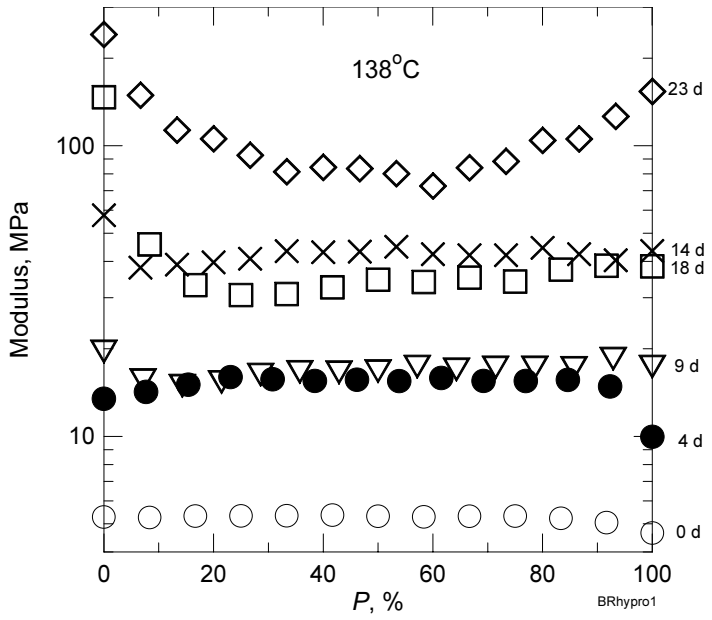

Figure VII-39. Modulus profiling results for the Hyp-07 material aged at 138°C for the indicated aging times.

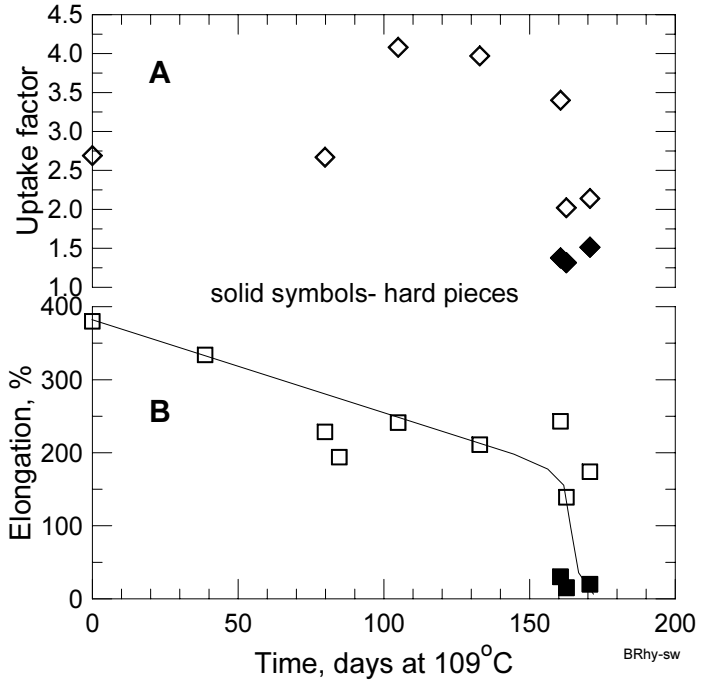

Figure VII-40. Elongation and swelling result for individual samples of Hyp-07 versus aging time at 109°C. Filled symbols denote hard samples.

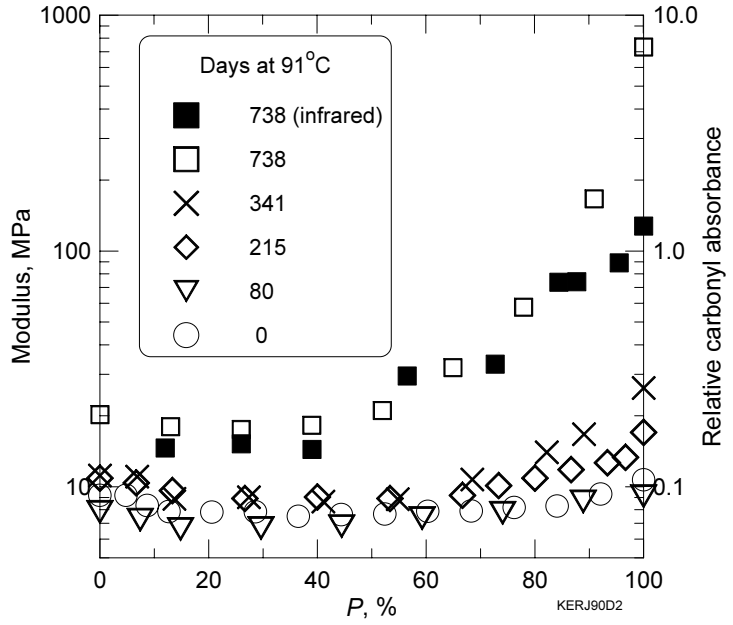

Figure VII-41. Modulus profiling results (left y-axis) for the Hyp-02 material aged at 91°C for the indicated aging times plus infrared carbonyl profile (right y-axis) for 738 d sample.

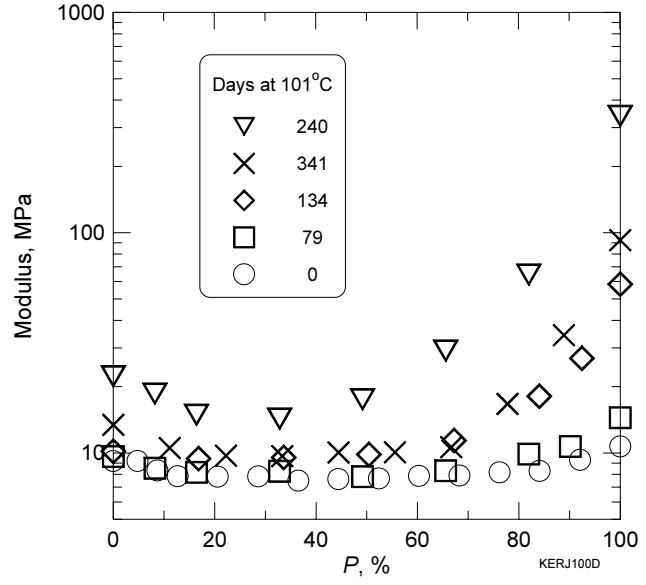

Figure VII-42. Modulus profiling results for the Hyp-02 material aged at 101°C for the indicated aging times.

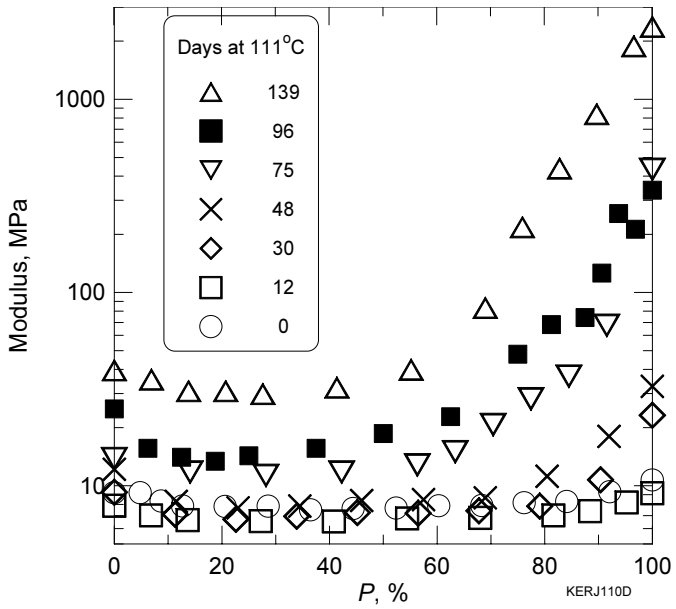

Figure VII-43. Modulus profiling results for the Hyp-02 material aged at 111°C for the indicated aging times.

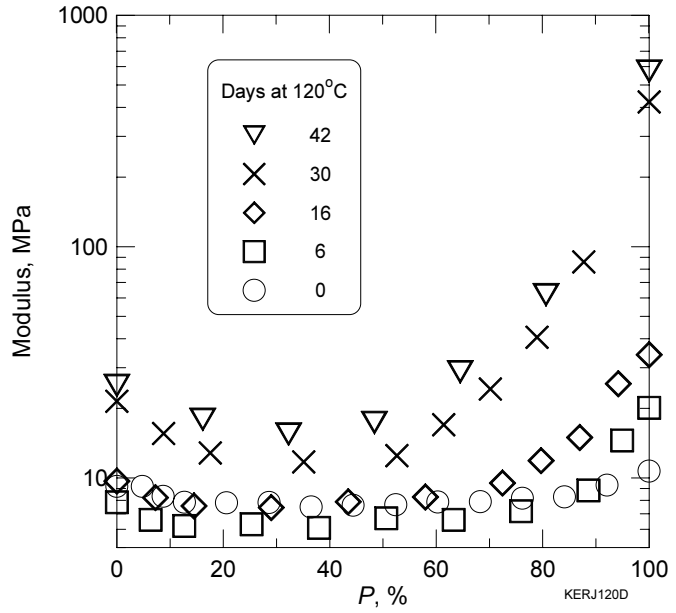

Figure VII-44. Modulus profiling results for the Hyp-02 material aged at 120°C for the indicated aging times.

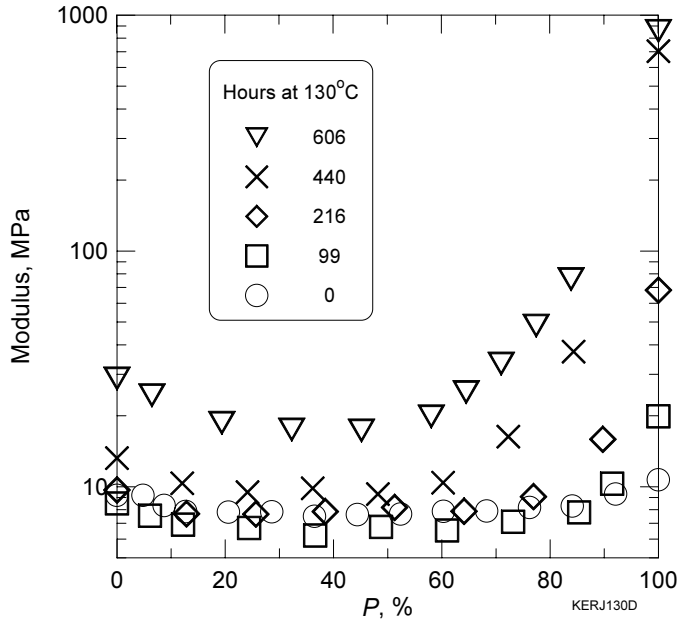

Figure VII-45. Modulus profiling results for the Hyp-02 material aged at 130°C for the indicated aging times.

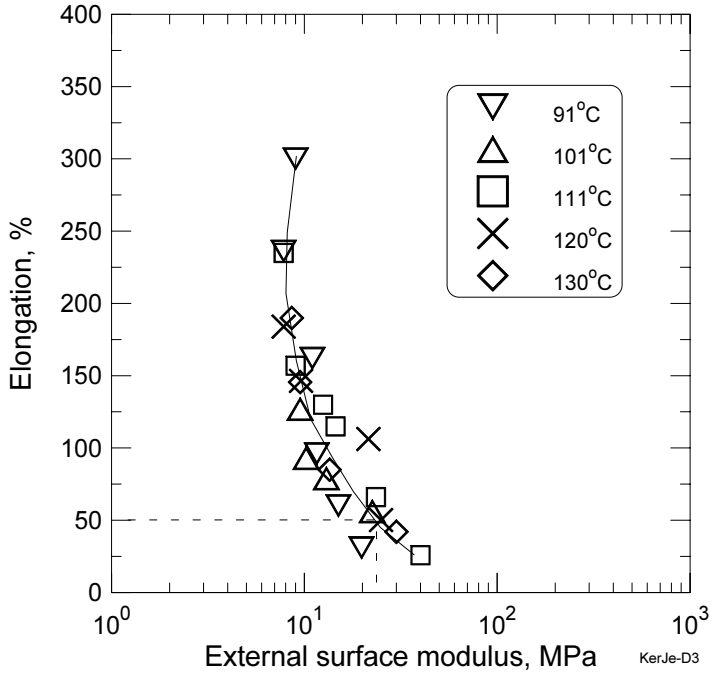

Figure VII-46. Average elongation plotted versus external surface modulus for Hyp-02 material at the indicated aging temperatures.

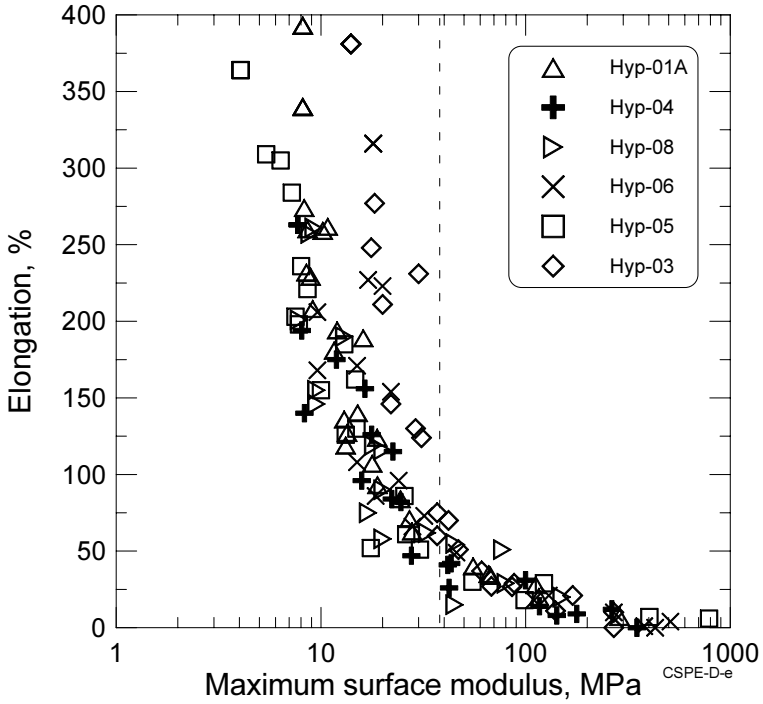

Figure VII-47. Average elongation versus maximum surface modulus for the six well-behaved hypalon materials at all of their aging temperatures.

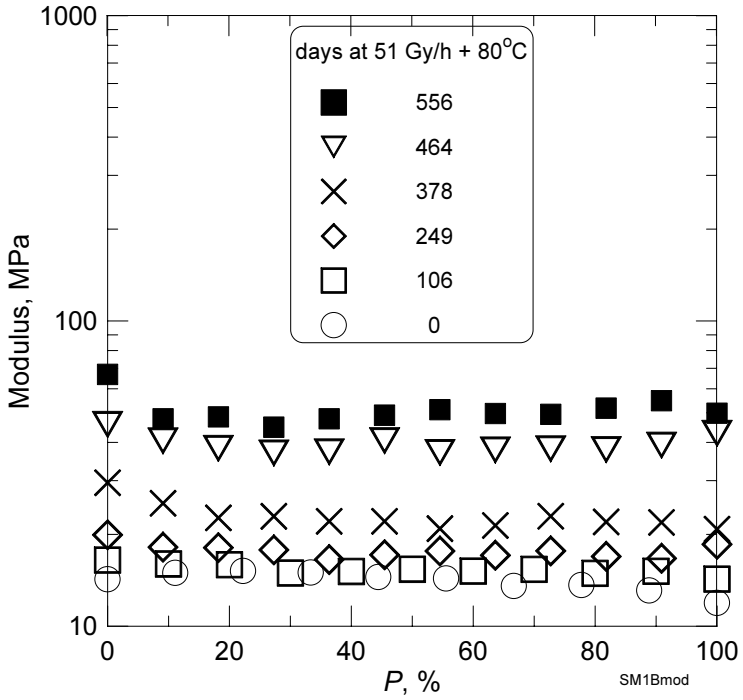

Figure VII-48. Modulus profiling results for the Hyp-03 material aged under the indicated combined environment conditions (total dose ~ 0.68 MGy after 556 days).

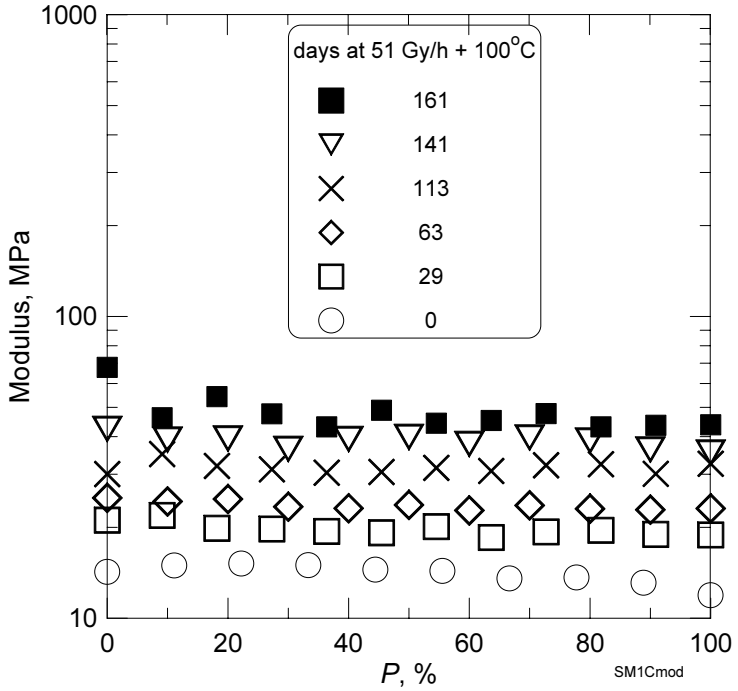

Figure VII-49. Modulus profiling results for the Hyp-03 material aged under the indicated combined environment conditions (total dose ~ 0.20 MGy after 161 days).

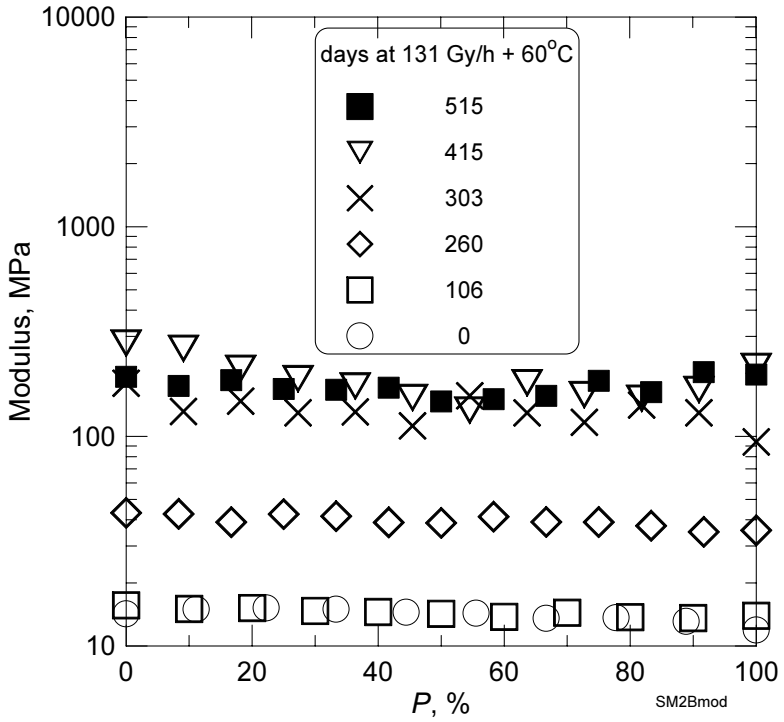

Figure VII-50. Modulus profiling results for the Hyp-03 material aged under the indicated combined environment conditions (total dose ~ 1.6 MGy after 515 days).

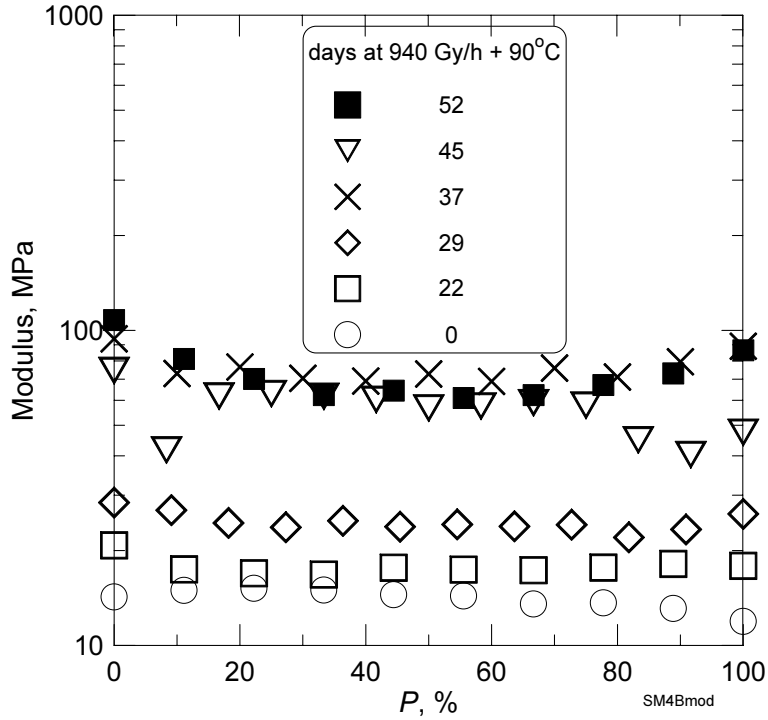

Figure VII-51. Modulus profiling results for the Hyp-03 material aged under the indicated combined environment conditions (total dose ~ 1.17 MGy after 52 days).

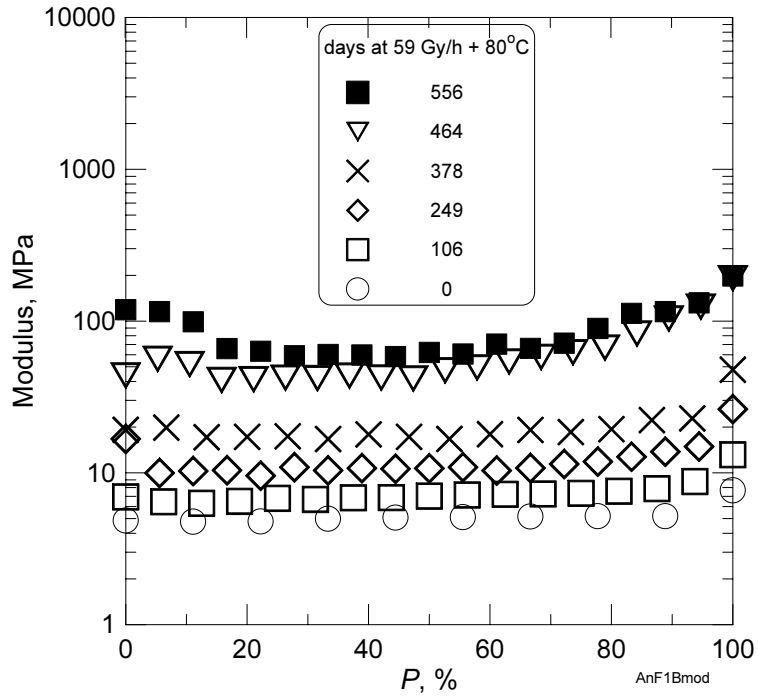

Figure VII-52. Modulus profiling results for the Hyp-04 material aged under the indicated combined environment conditions (total dose ~ 0.79 MGy after 556 days).

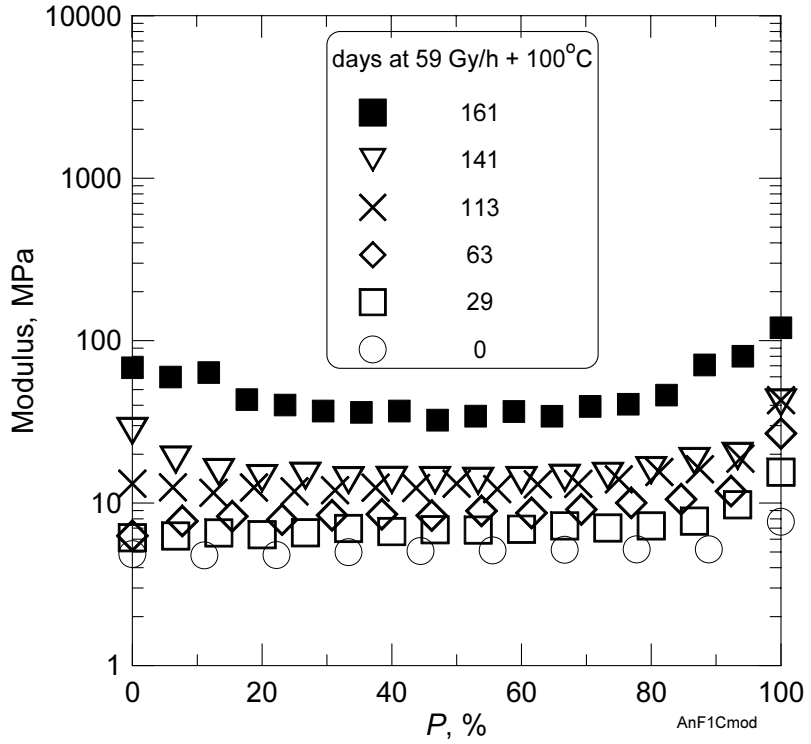

Figure VII-53. Modulus profiling results for the Hyp-04 material aged under the indicated combined environment conditions (total dose ~ 0.23 MGy after 161 days).

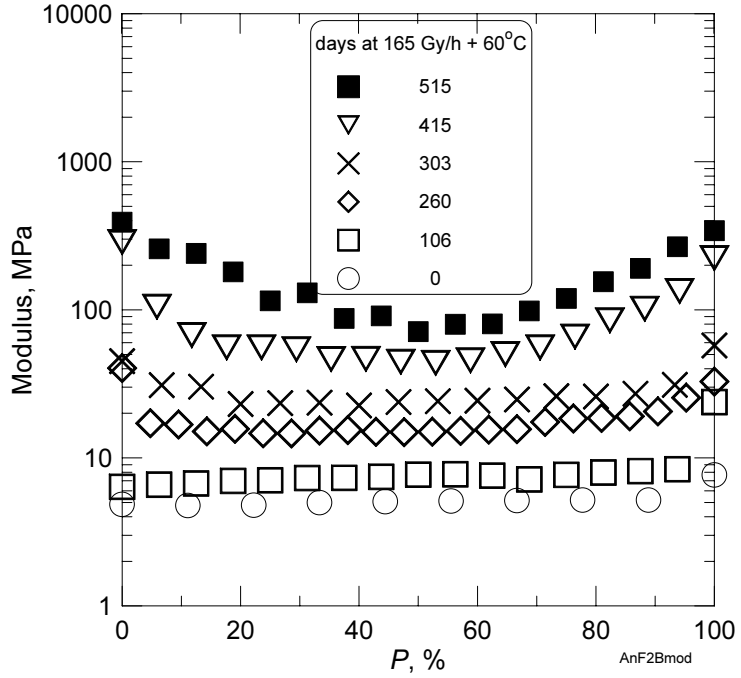

Figure VII-54. Modulus profiling results for the Hyp-04 material aged under the indicated combined environment conditions (total dose ~ 2.0 MGy after 515 days).

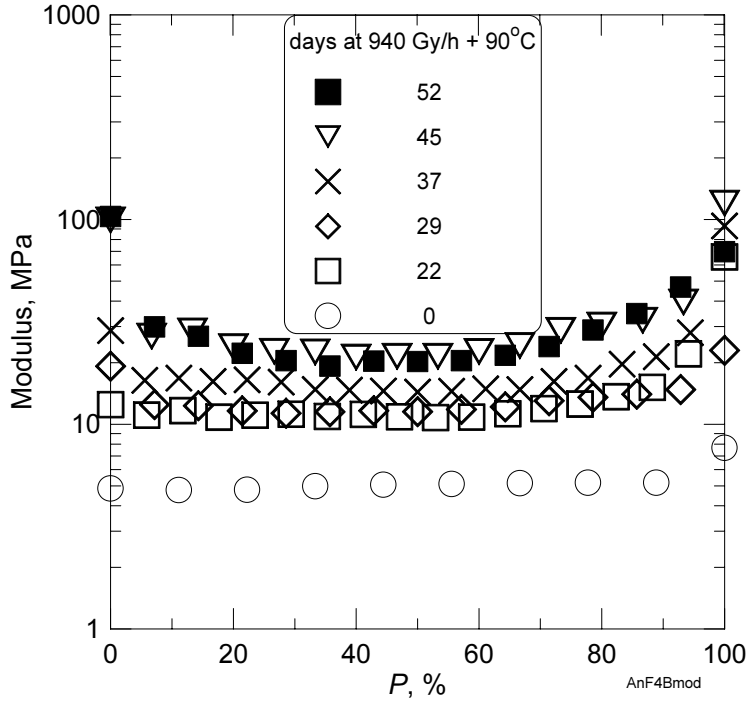

Figure VII-55. Modulus profiling results for the Hyp-04 material aged under the indicated combined environment conditions (total dose ~ 1.17 MGy after 52 days).

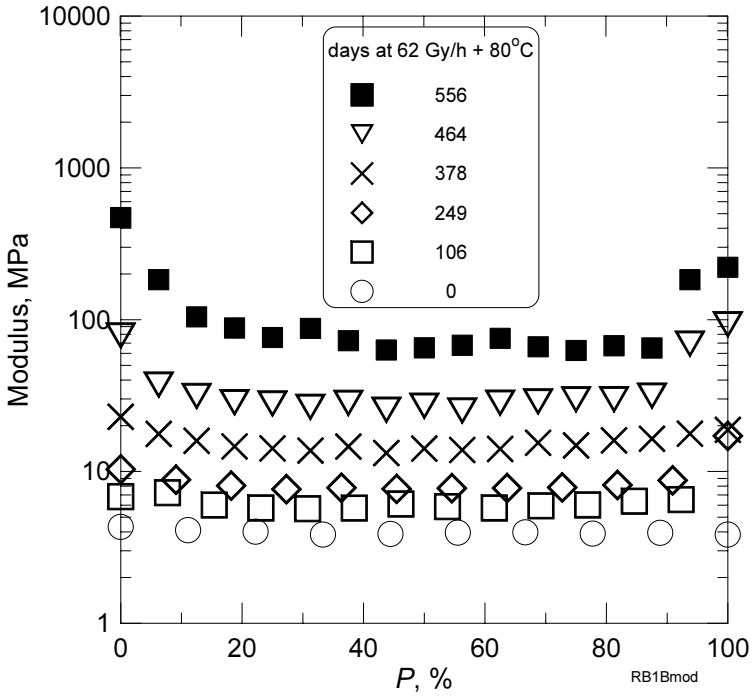

Figure VII-56. Modulus profiling results for the Hyp-05 material aged under the indicated combined environment conditions (total dose ~ 0.83 MGy after 556 days).

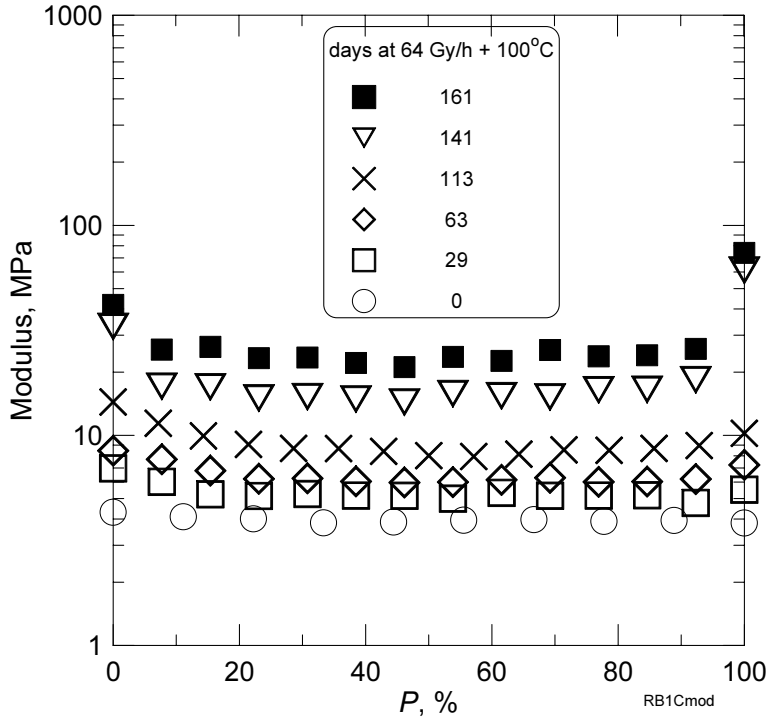

Figure VII-57. Modulus profiling results for the Hyp-05 material aged under the indicated combined environment conditions (total dose ~ 0.25 MGy after 161 days).

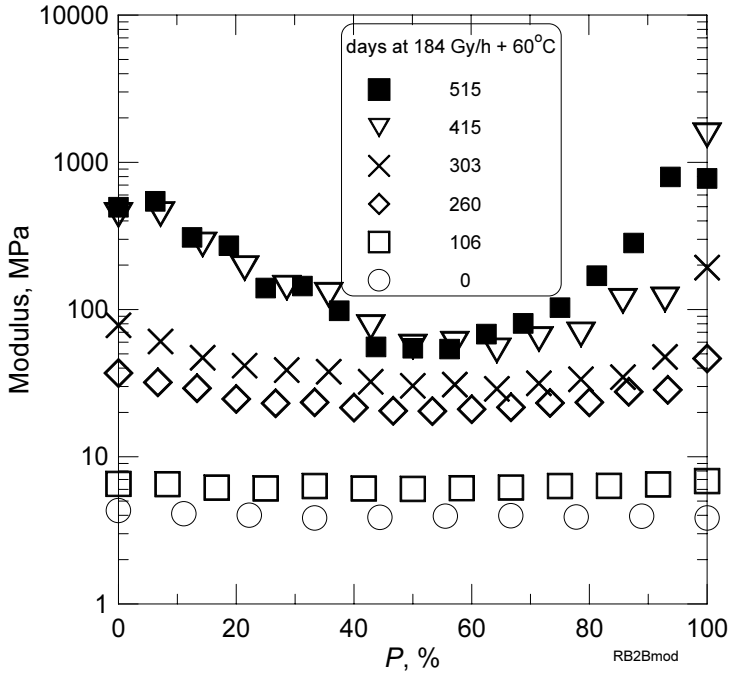

Figure VII-58. Modulus profiling results for the Hyp-05 material aged under the indicated combined environment conditions (total dose ~ 2.27 MGy after 515 days).

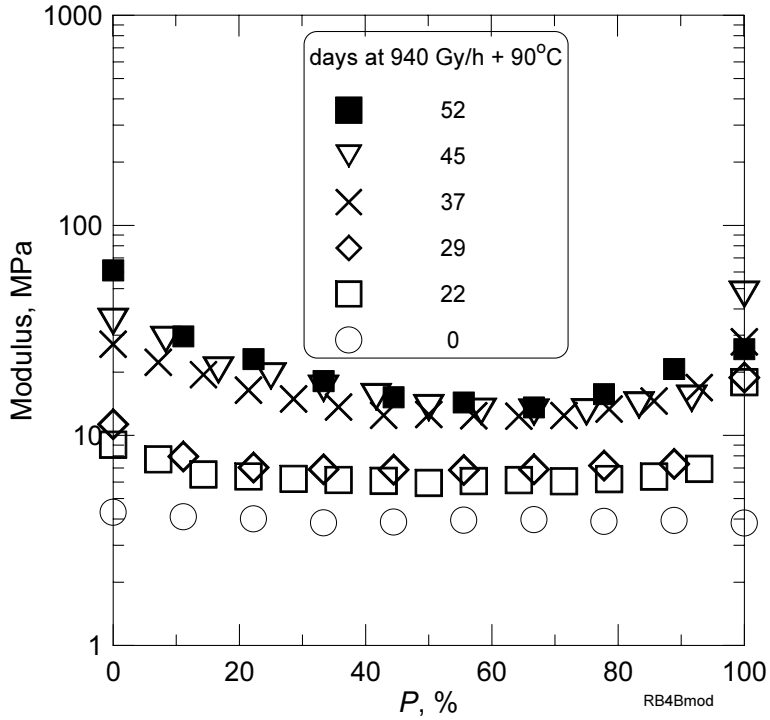

Figure VII-59. Modulus profiling results for the Hyp-05 material aged under the indicated combined environment conditions (total dose ~ 1.17 MGy after 52 days).

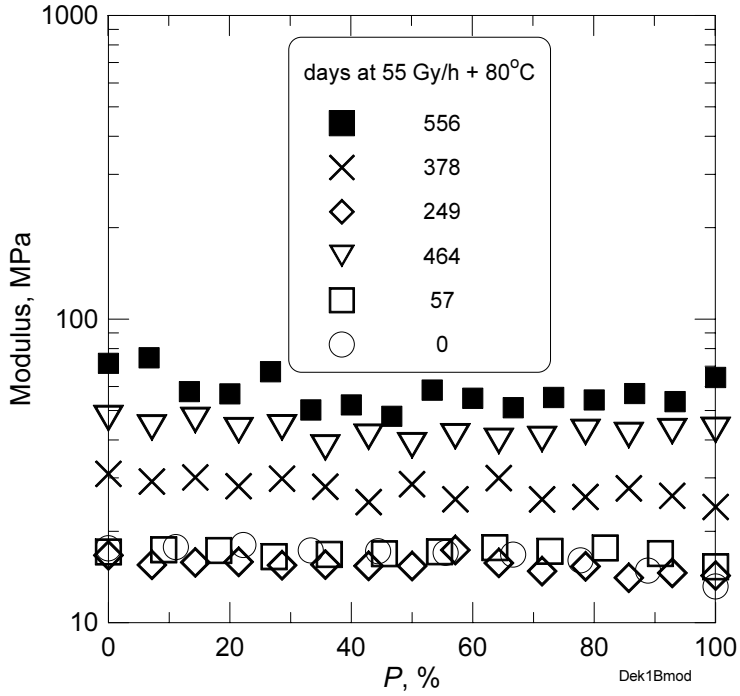

Figure VII-60. Modulus profiling results for the Hyp-06 material aged under the indicated combined environment conditions (total dose ~ 0.73 MGy after 556 days).

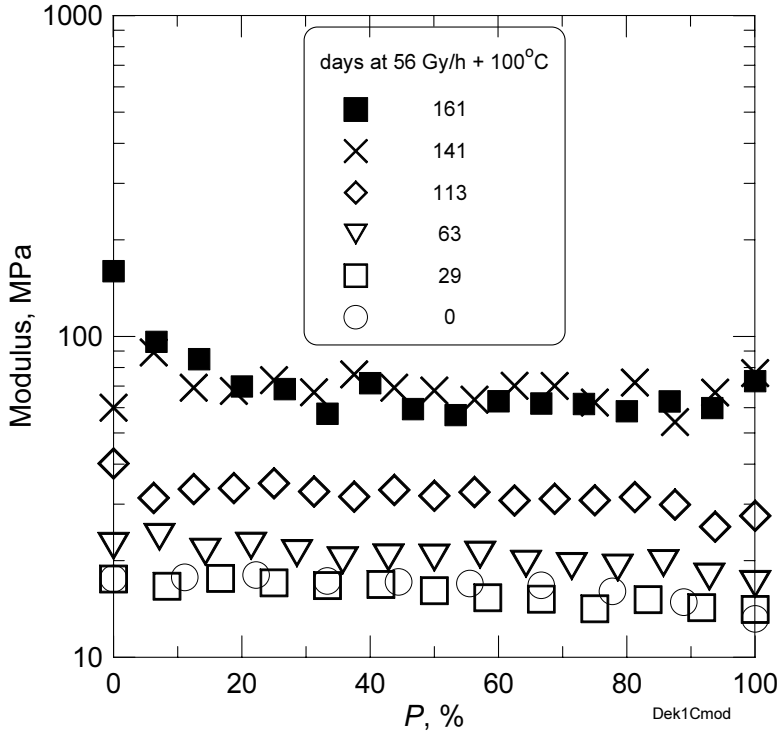

Figure VII-61. Modulus profiling results for the Hyp-06 material aged under the indicated combined environment conditions (total dose ~ 0.22 MGy after 161 days).

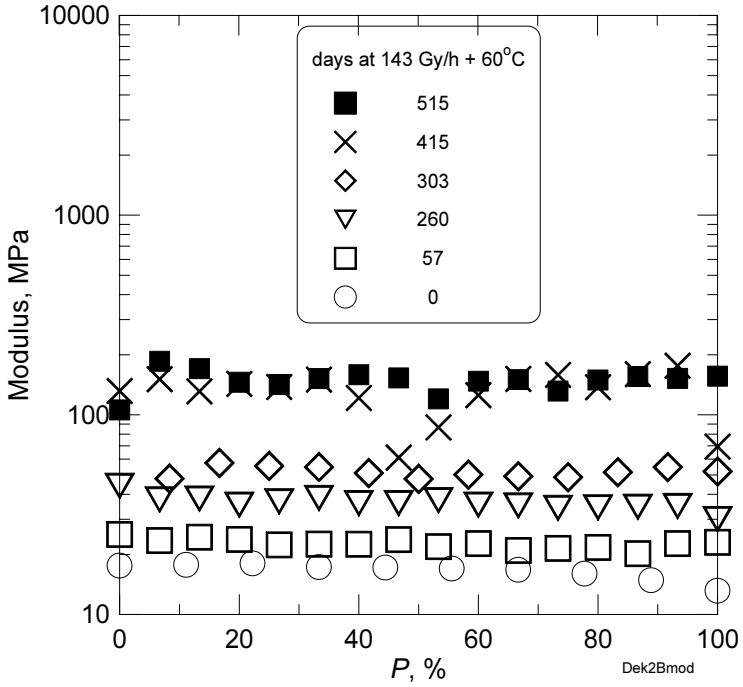

Figure VII-62. Modulus profiling results for the Hyp-06 material aged under the indicated combined environment conditions (total dose ~ 1.77 MGy after 515 days).

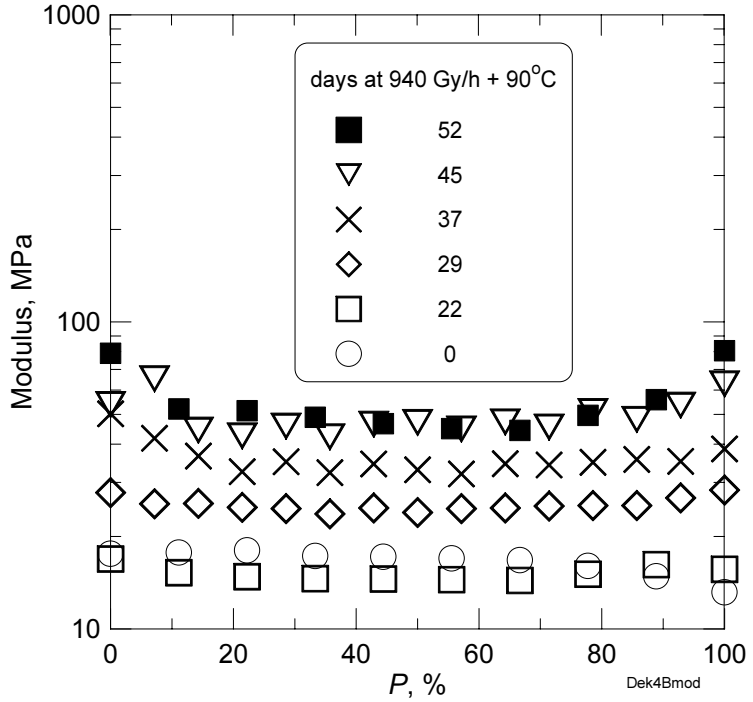

Figure VII-63. Modulus profiling results for the Hyp-06 material aged under the indicated combined environment conditions (total dose ~ 1.17 MGy after 52 days).

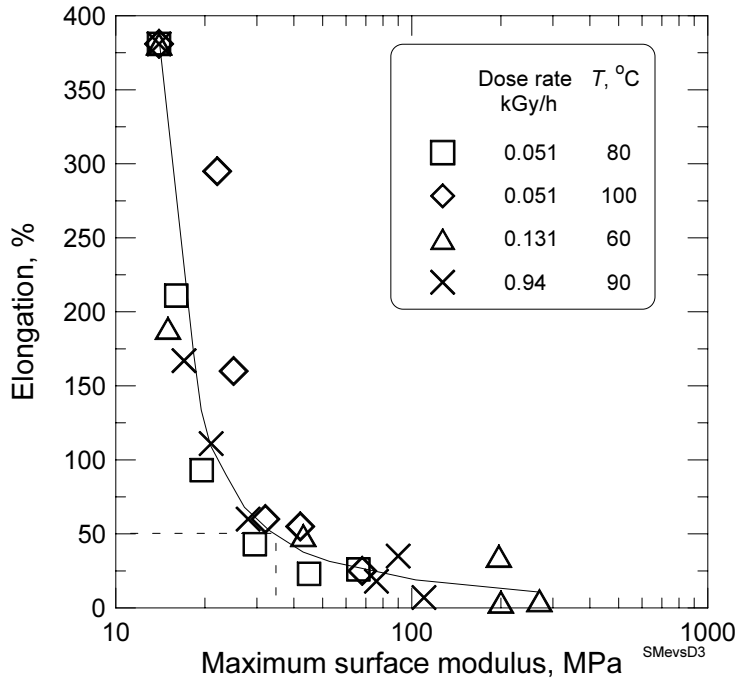

Figure VII-64. Elongation versus modulus for Hyp-03 material after aging under the indicated combined environment conditions.

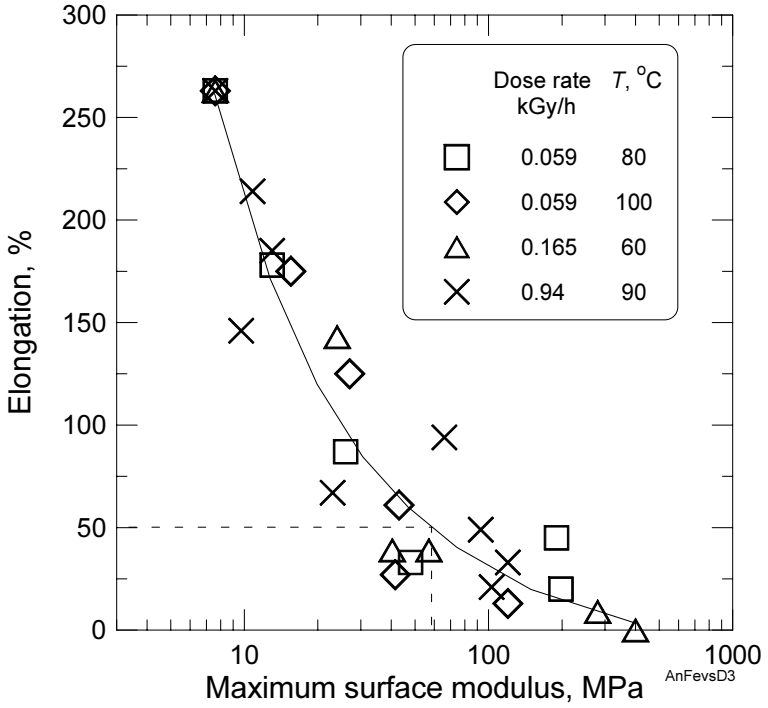

Figure VII-65. Elongation versus modulus for Hyp-04 material after aging under the indicated combined environment conditions.

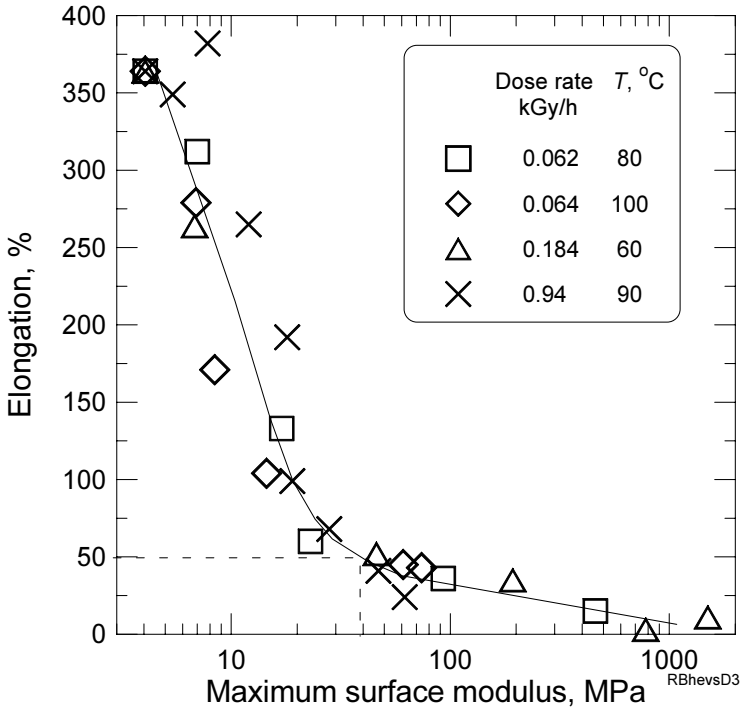

Figure VII-66. Elongation versus modulus for Hyp-05 material after aging under the indicated combined environment conditions.

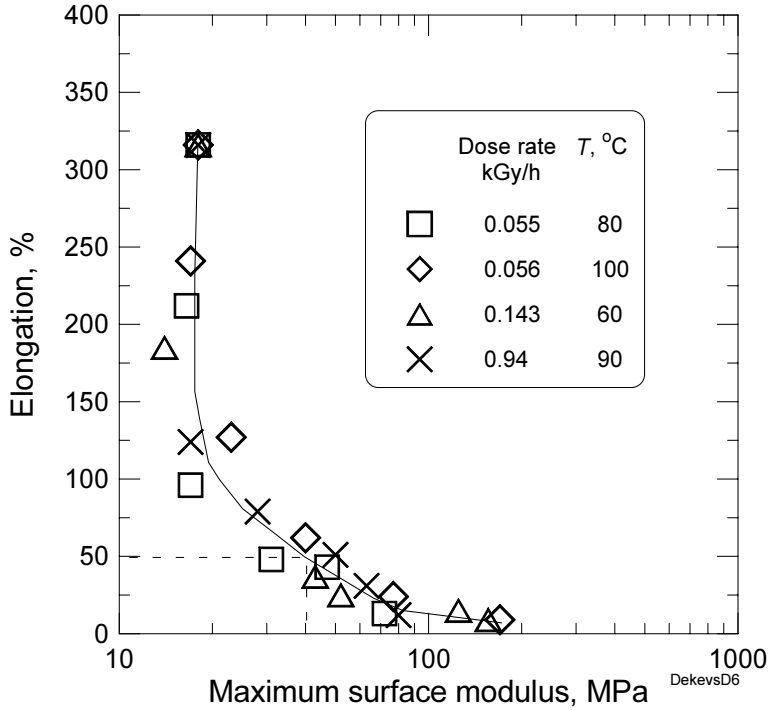

Figure VII-67. Elongation versus modulus for Hyp-06 material after aging under the indicated combined environment conditions.

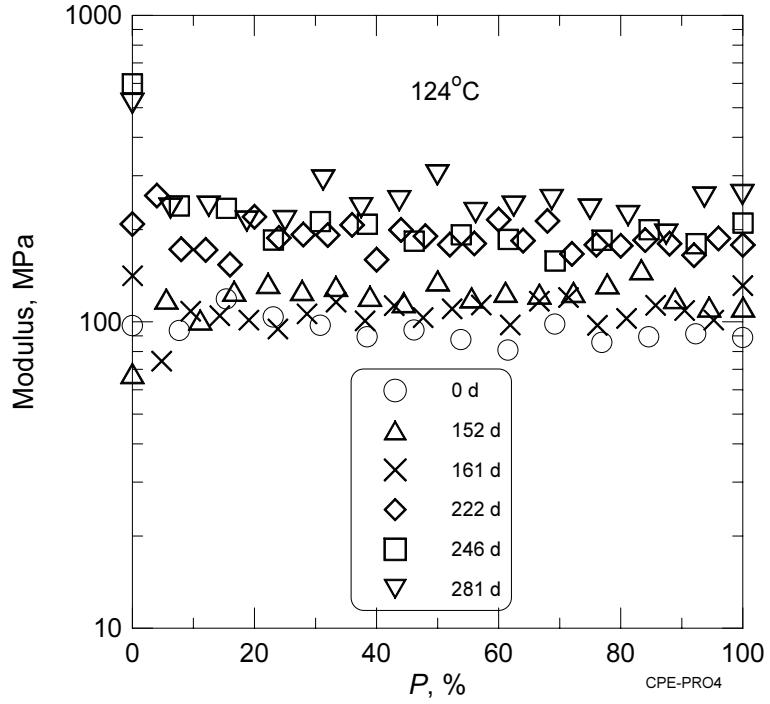

Figure VII-68. Modulus profiling results for the CPE-02 material aged at 124°C for the indicated aging times.

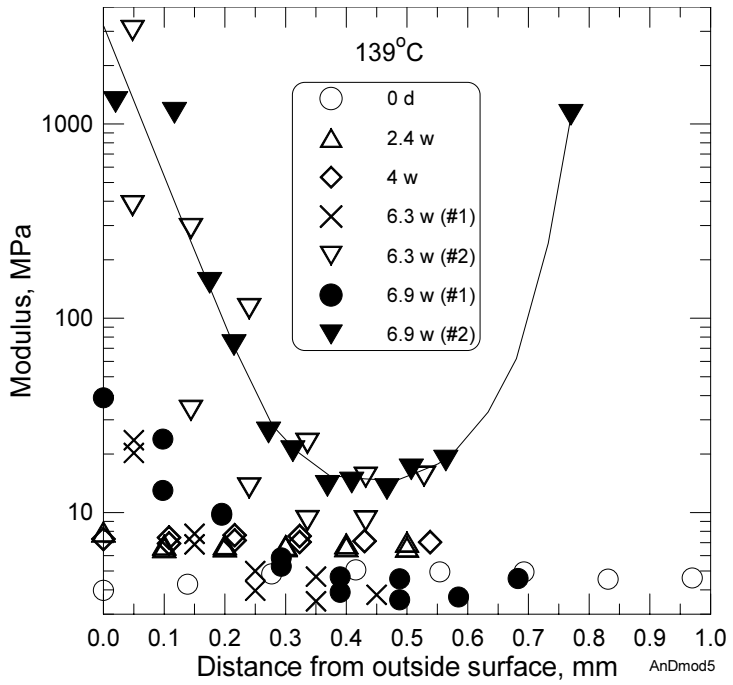

Figure VII-69. Modulus profiling results for the EPR-04 material aged at 139°C for the indicated aging times.

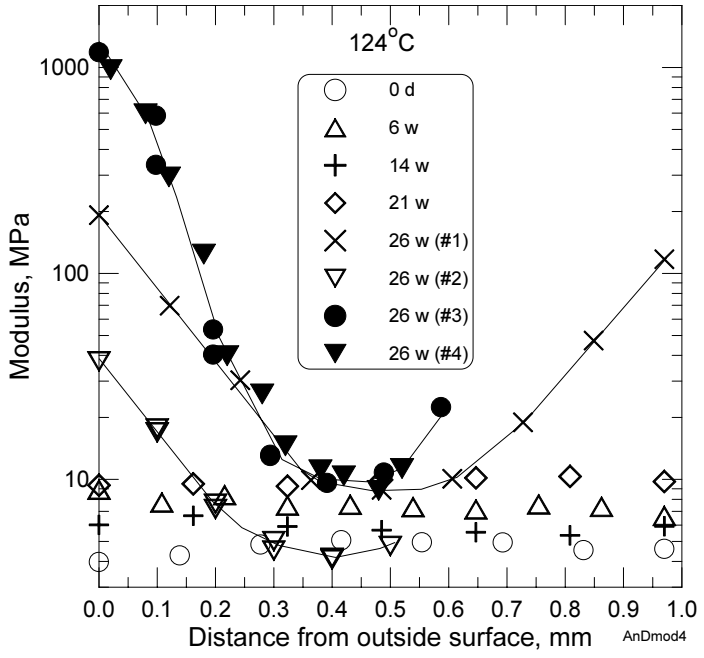

Figure VII-70. Modulus profiling results for the EPR-04 material aged at 124°C for the indicated aging times.

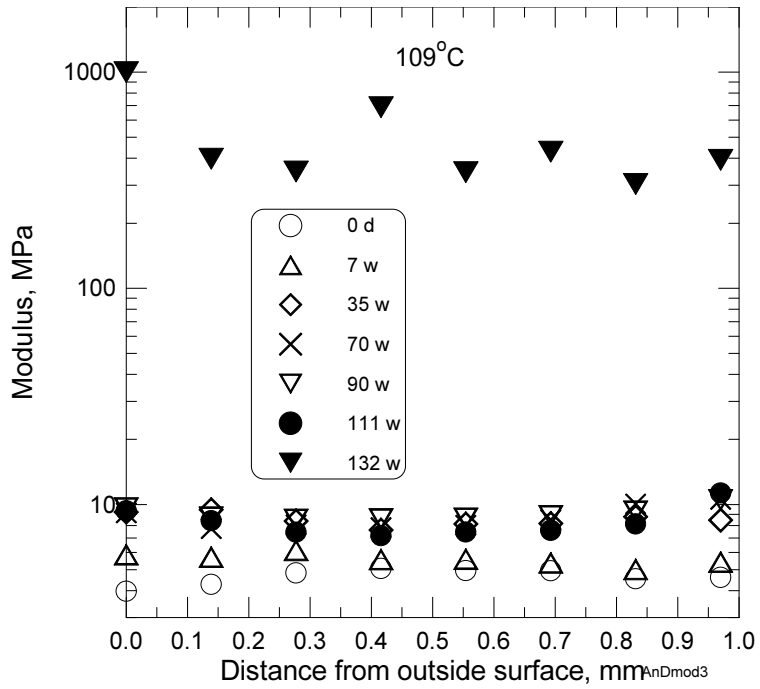

Figure VII-71. Modulus profiling results for the EPR-04 material aged at 109°C for the indicated aging times.

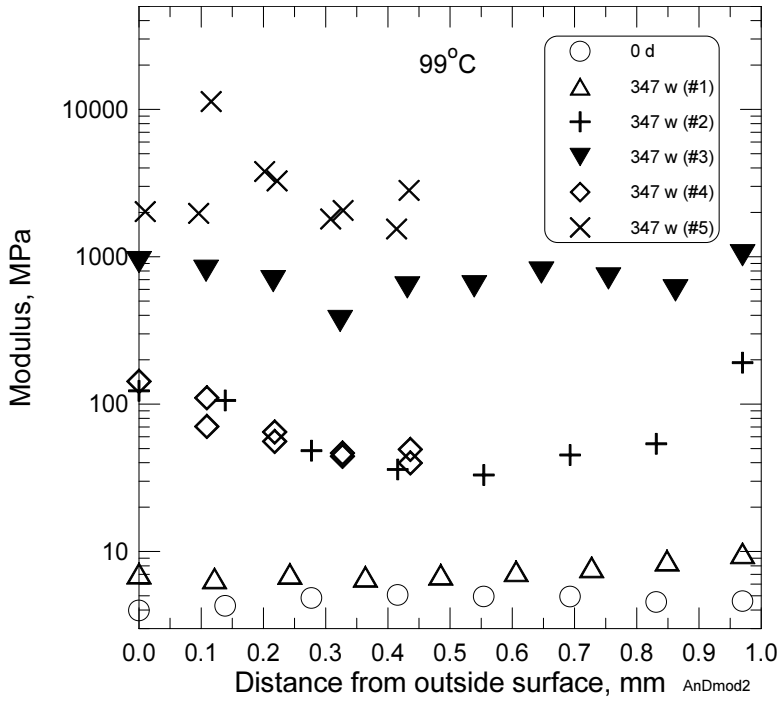

Figure VII-72. Modulus profiling results for the EPR-04 material aged at 99°C for the indicated aging times (five samples run after 347 weeks of aging).

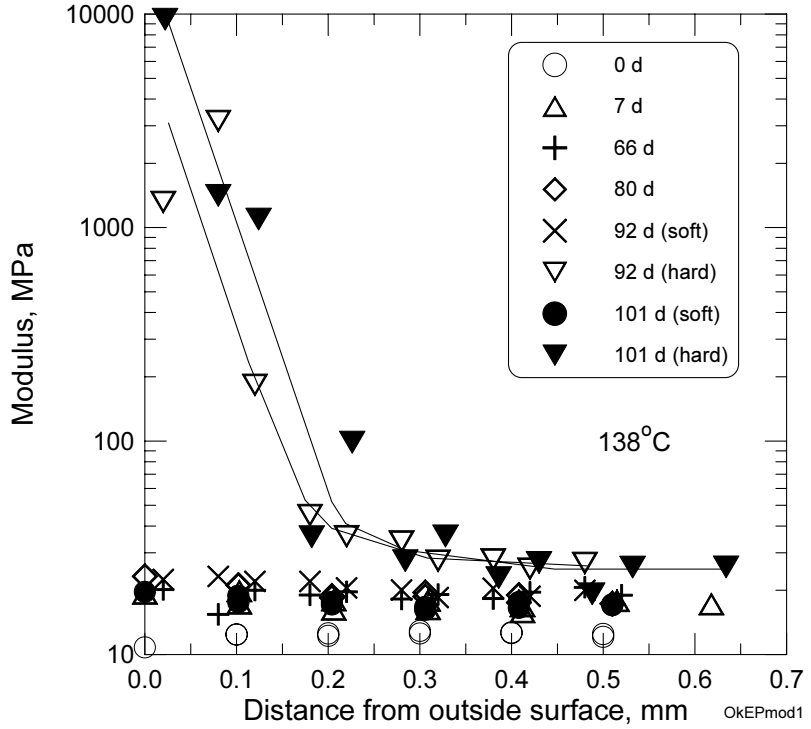

Figure VII-73. Modulus profiling results for the EPR-05 material aged at 138°C for the indicated aging times.

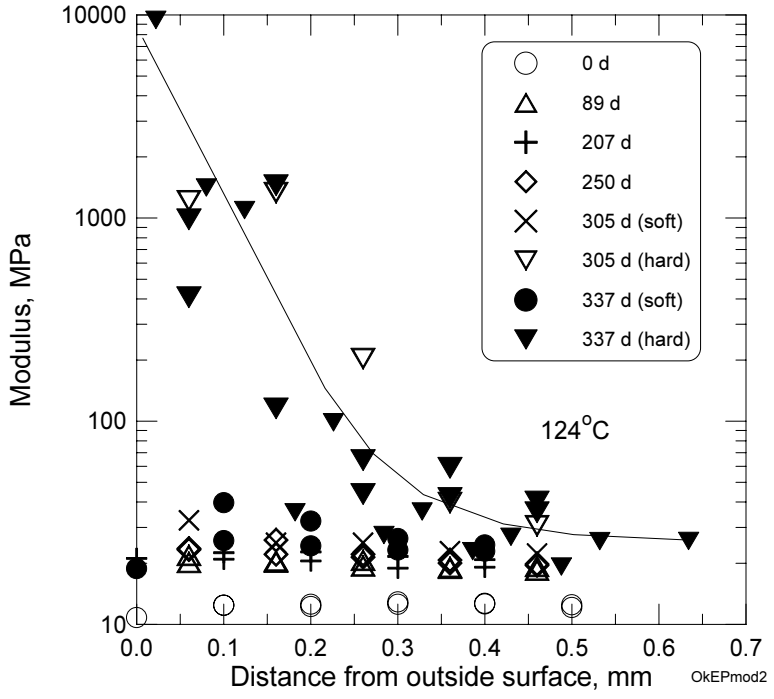

Figure VII-74. Modulus profiling results for the EPR-05 material aged at 124°C for the indicated aging times.

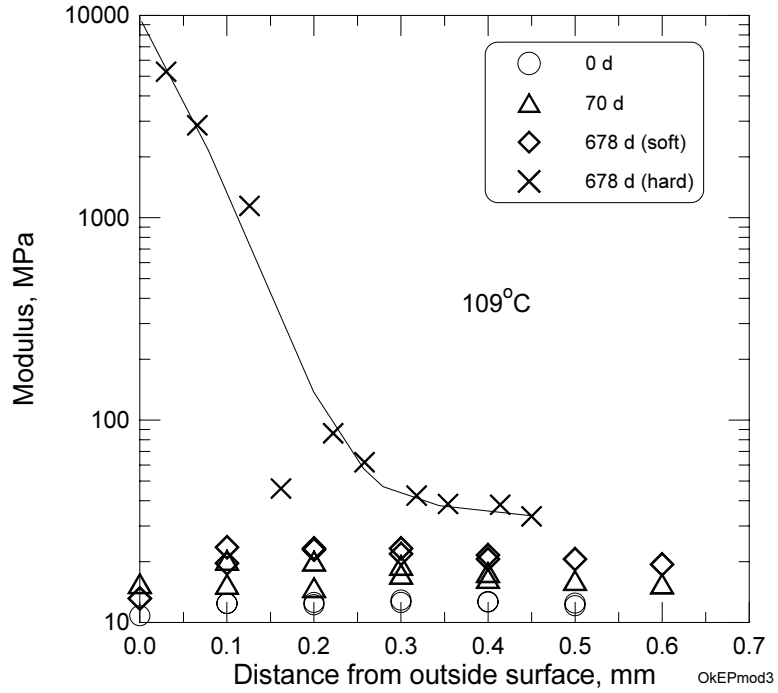

Figure VII-75. Modulus profiling results for the EPR-05 material aged at 109°C for the indicated aging times.

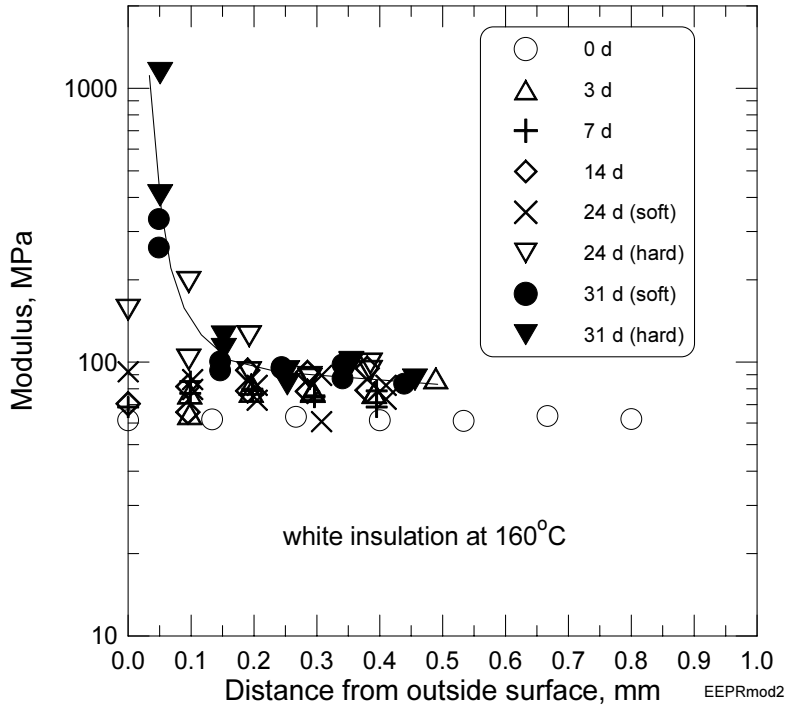

Figure VII-76. Modulus profiling results for the EPR-03 material aged at 160°C for the indicated aging times.

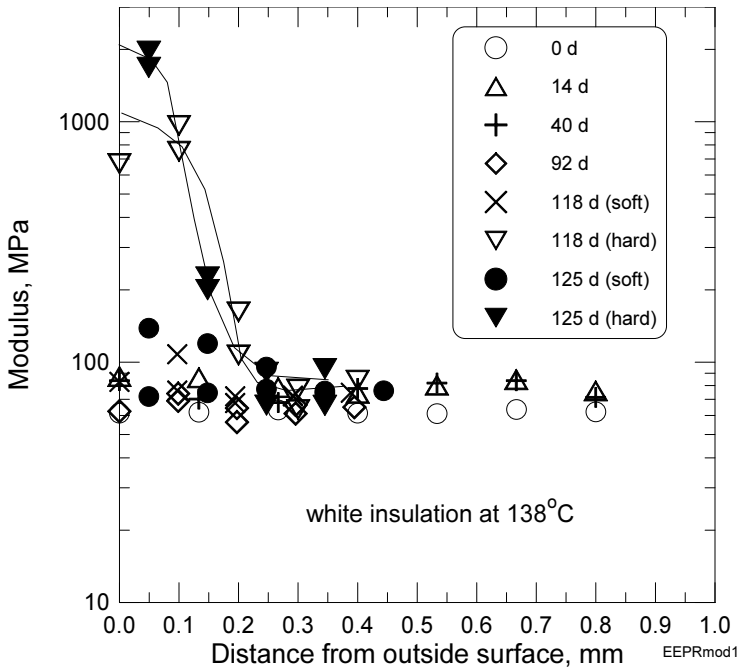

Figure VII-77. Modulus profiling results for the EPR-03 material aged at 138°C for the indicated aging times.

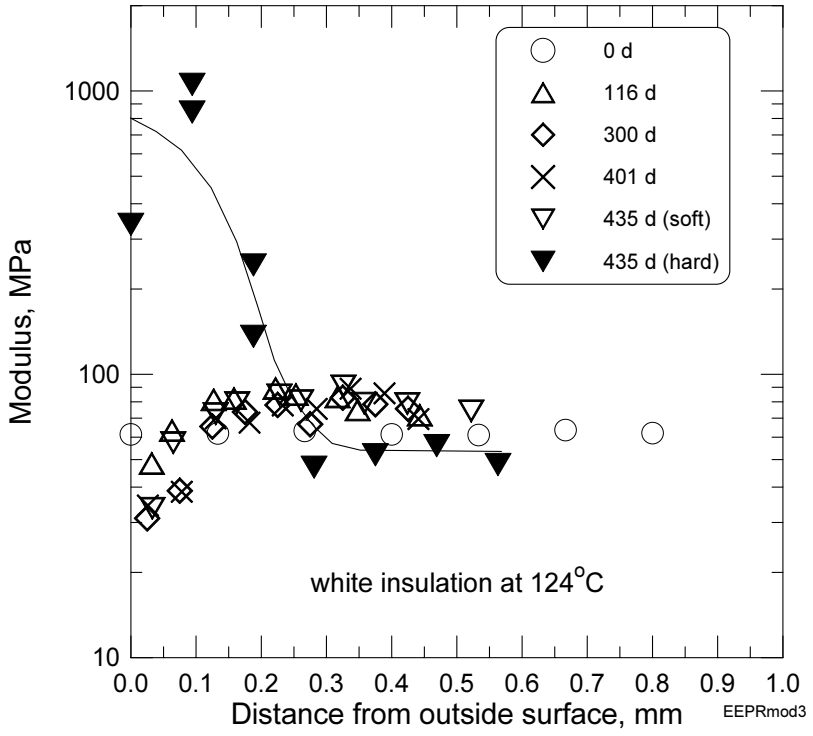

Figure VII-78. Modulus profiling results for the EPR-03 material aged at 124°C for the indicated aging times.

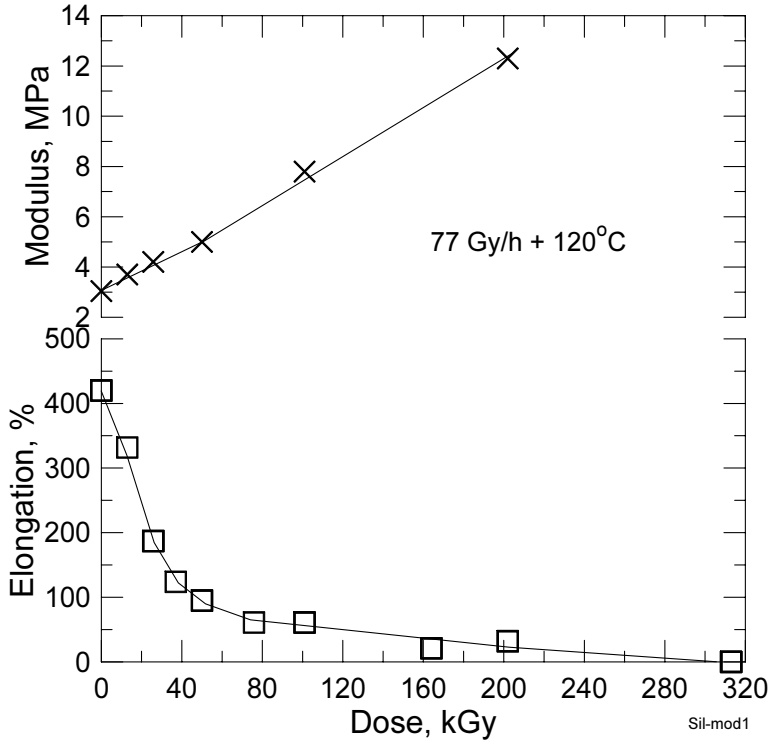

Figure VII-79. Elongation (lower plot) and modulus (upper plot) results versus radiation dose for Sil-01 insulation aged at 77 Gy/h plus 120°C.

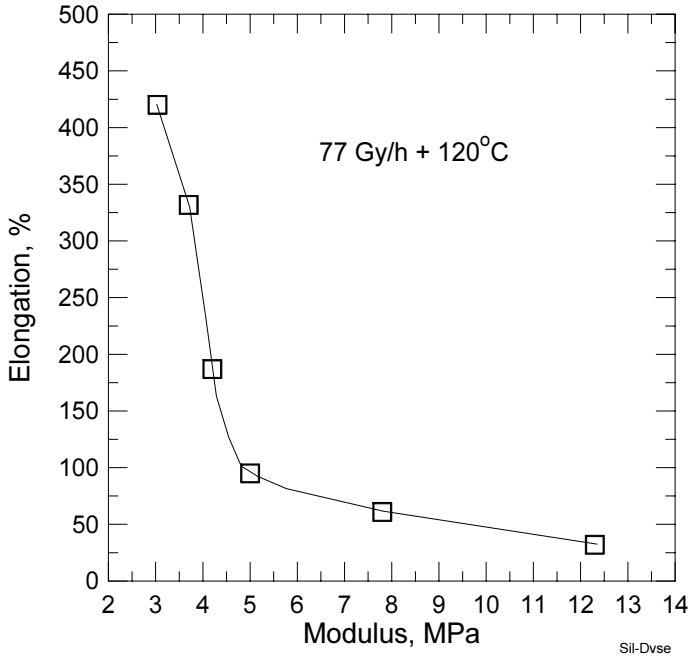

Figure VII-80. Elongation versus modulus for Sil-01 material aged at 77 Gy/h plus 120°C.

VIII. Condition Monitoring: NMR

Introduction

The NMR relaxation time T_2 is related to the mobility of polymer chains [VIII-1]. Since an increase in crosslink density reduces chain mobility, crosslinking results in decreases in T_2, but these decreases are often fairly small and show little difference between unaged and highly aged specimens. When polymers are swollen in a deuterated solvent, however, the increased mobility caused by the expanded network tends to significantly increase T_2 values for unaged specimens. Since the solvent is deuterated, swelling also decreases the density of hydrogen atoms and causes an additional increase in T_2. (The contribution to relaxation from deuterated atoms is significantly less than that from hydrogen atoms.) With aging, crosslinking leads to a reduction in solvent uptake and an increase in the concentration of protons so that the T_2 values are substantially reduced. When T_2 measurements are taken on samples swelled in a good solvent, the swelling and hydrogen density factors lead to a significant amplification effect so that the T_2 sensitivity to differing levels of crosslinking (aging) is much greater and the needed resolution between unaged and aged specimens is obtained. This method has been successfully employed for a variety of elastomeric materials [VIII-2 to VIII-6].

Thermal aging of Neo-02 and hypalon jacket materials

The Neo-2 samples were swollen in deuterated chloroform ($CDCl_3$) at room temperature for at least 1 hour after which the relaxation times were relatively constant as a function of temperature. Using the conventional linear plotting format, Fig. VIII-1 shows a comparison of the time-dependence of elongation and NMR T_2 results for Neo-02 at the 95°C aging temperature. Large, easily measured changes in T_2 occur as the material degrades. Since the T_2 values decrease fairly regularly as the elongation drops towards the practical end of life, the NMR method shows excellent potential as a CM approach. Figure VIII-2 shows the correlation of the T_2 values with the elongation results for all three aging temperatures. Although the scatter tends to be relatively high at higher elongation values, the scatter is reduced for values near our normal practical end of life criterion of 50% absolute elongation. It appears that for all three temperatures a T_2 value of approximately 2.4 msec corresponds to an elongation value of approximately 50% absolute.

The hypalon materials were somewhat more difficult to swell than the neoprene materials and their relaxation times were still increasing after 2 hours in deuterated chloroform at room temperature. Swelling the material overnight results in a 10 to 20 % increase in the relaxation time compared to the 2 hour swell time. Since we have found that the best response is provided by maximum swelling, all of the relaxation times reported for the hypalon materials were conducted on samples that had been swollen overnight. Fig. VIII-3 shows the elongation vs. NMR T_2 for Hyp-01A at aging temperatures ranging from 100 to 150°C. Figs. VIII-4 through VIII-7 show the elongation vs. NMR T_2 for Hyp-03, -04, -05 and -06 at aging temperatures of 100, 110 and 125°C. Fig. VIII-8

shows the elongation vs. NMR T_2 for Hyp-07 aged at 109°C and Fig. VIII-9 shows the elongation vs. NMR T_2 for Hyp-08 aged at 99 and 124°C.

The correlations between elongation and NMR T_2 for Hyp-01A, -03, -04, -05 and -06 show similar characteristics. All show considerable scatter for high elongation values, while the scatter is reduced when the elongation approaches its practical end of life value of 50 %. The correlation appears to be independent of aging temperature over the range of temperatures investigated. Although the general characteristics of the correlations appear similar, the value of NMR T_2 at 50 % elongation ranges from approximately 2.3 ms for Hyp-03 to 4.2 ms for Hyp-04 and -05. This variation is too great for the establishment of a useful "universal" practical end of life NMR T_2 criterion.

The scatter and apparent lack of correlation between elongation and NMR T_2 for Hyp-07 shown in Fig. VIII-8 requires an explanation. The elongation values for aged Hyp-07 exhibited considerable scatter. For example, two independent elongation measurements of a sample aged for 160.6 days at 109°C provided values of 243 and 30 %. Two independent elongation measurements of a sample aged for 170.7 days at 109°C yielded values of 174 and 20 %. Thus the aging of this material varied considerably from sample to sample. The NMR T_2 measurements were performed on a single sample that could not be traced to an elongation value. The NMR T_2 of the sample aged for 160.6 days was 0.92 msec. This result could be reasonably compared to the sample with 30 % elongation, but provides a poor comparison to the sample with 243 % elongation. Likewise the NMR T_2 of the sample aged for 170.7 days was 11.6 msec which compares well with the sample with 174 % elongation, but compares poorly with the sample with 20 % elongation. All of the data points in Fig. VIII-8 which correspond to low values of elongation or low values of NMR T_2 are generated by heavily aged samples that display spatial inhomogeneity. We believe that a reasonable correlation may be obtained if the NMR T_2 samples were associated with a specific elongation sample or a specific region of an elongation sample, but this supposition has not been tested.

The correlation of elongation values of Hyp-08 with NMR T_2 shown in Fig. VIII-9 is somewhat atypical compared to that observed for other Hypalon jacket materials. The rate of decrease of NMR T_2 with decreasing elongation values appears to be less than that of the other Hypalon materials investigated. The initial NMR T_2 is much higher than for the other hypalon materials (12 to 13 versus 5 to 6 ms). The value of NMR T_2 at 50 % elongation at break (practical end of life) is over 7 msec while the NMR T_2 values for the other Hypalons were always less than 4.2 msec. Also a "dead" material (elongation at break of 0%) had an NMR T_2 value over 7 msec, while the corresponding number for the other Hypalons were in the 1 to 2 msec range. Although the correlation may still be useful, the condition of this material could not be determined by NMR T_2 with same accuracy as that of a typical Hypalon.

Combined thermal/radiation aging of Neo-02 and hypalon jacket materials

The correlation between elongation results and NMR T_2 results for Neo-02 aged at four combined thermal/radiation conditions are shown in Fig. VIII-10. Under the combined

environment condition where thermal effects are more significant than radiation effects (42 Gy/h plus 80°C results with a solid curve drawn through the data) the correlation is reasonably similar to the correlations found under oven-aging conditions. Under the conditions where radiation becomes relatively more important than temperature (higher dose rates, lower temperatures), the data have tended to shift to the left on the plot.

The correlation between elongation results and NMR T_2 results for Hyp-05 aged at 60°C and 184kG/h is shown in Fig. VIII-11. The correlation between the two quantities is excellent. Similar to the results for the aging of Neo-02 under combined environments, the data for aging with a high dose rate and low temperature is shifted to the left compared to the thermal only aging (Fig. VIII-6).

Thermal aging of XLPO materials

The condition of crosslinked polyolefins is more difficult to analyze by both conventional mechanical tests and by NMR T_2 relaxation measurements. The partial crystallinity of these materials can mask the effect of aging on mechanical properties such as modulus while relaxation measurements are complicated by their limited swelling. To improve the response of relaxation measurements to aging we decided to swell XLPO-02B at 70°C which is the highest temperature possible for long term operation of our spectrometer. This condition eliminated the use of chloroform which has a boiling point of 62°C. A series of deuterated solvents with a range of polarities were investigated: heptane-d_{16}, $\delta = 7.4$; methyl cyclohexane-d_{14}, $\delta = 7.8$; cyclohexane-d_{12}, $\delta = 8.2$; toluene-d_8, $\delta = 8.9$; benzene-d_6, $\delta = 9.2$; chlorobenzene-d_5, $\delta = 9.5$; nitrobenzene-d_5, $\delta = 10.0$; acetic acid-d_4, $\delta = 10.1$; acetonitrile-d_3, $\delta = 11.9$; and dimethyl sulfoxide-d_6, $\delta = 12.0\ (\mathrm{cal/cm^3})^{1/2}$. A study showed that after 5 minutes at 70°C the samples had reached a state of equilibration. Fig. VIII-12 shows the response of NMR T_2 as a function of solvent polarity for unaged XLPO-02B and for XLPO-02B aged for 154 and 2353 days at 109°C. These materials had elongations of 347, 139 and 46%. Although swelling is affected by solvent polarity, the response is relatively constant over a wide range of solvents. On the basis of high degree of swelling and low cost, benzene-d_6 was selected as the standard solvent for further investigations.

Fig. VIII-13 shows the average elongation of aged XLPO-02B as a function of NMR T_2 for aging at 99 and 109°C. We see an excellent correlation between the two quantities. Note that these aging temperatures are below the main melting point of the material as shown by DSC results, Fig. III-47. The correlation between elongation and NMR T_2 for aging temperatures above the melting point, shown in Fig. VIII-14, does not follow the same relationship. This illustrates the danger of using accelerated aging results from data obtained above a phase transition. Fig. VIII-15 shows the average elongation of XLPO-02B that had been subjected to ^{60}Co radiation as a function of NMR T_2. The lack of response of NMR T_2 to aging implies that radiation damage is fundamentally different from that of thermal damage. Note that the radiation aging was performed at temperatures below the thermal aging experiments shown in Figs. VIII-13 and -14 so the relationship between phase transitions and aging may also play a role.

The XLPO-4 is a composite cable insulation composed of a black inner sleeve and a green outer sleeve. The material has a single crystalline melting point of ~ 124°C [III-22] and its elongation behavior, discussed in section III, exhibited time-temperature superposition over thermal aging temperatures ranging from 91 to 170°C. We performed NMR T_2 measurements on the inner and outer sleeves individually and correlated these results with elongation measurements which were conducted on the intact composite insulation. The samples were swollen in deuterated benzene and allowed to equilibrate at 70°C for 10 minutes before the relaxation experiments were begun.

The correlation between elongation results for XLPO-04 and NMR T_2 results for the inner and outer sleeves of XLPO-04 are shown in Fig. VIII-16 and Fig. VIII-17, respectively. The NMR T_2 of the black inner sleeve shows little dependence on the elongation, while the NMR T_2 of the green outer sleeve is reasonable well correlated with the elongation. The insensitivity of the NMR T_2 of the black inner sleeve to elongation of the composite insulator could be caused by insensitivity of the NMR T_2 to changes in mechanical properties of the black inner sleeve or by a much slower degradation process for this sleeve. We believe the latter explanation is more likely since degradation processes appear to shorten the NMR T_2 of other materials that have been thermally aged. The elongation of the composite insulation may be dominated then by a more rapid degradation of the green outer sleeve. The correlations between elongation and NMR T_2 for the green outer sleeve appear to cluster in two groups: those materials aged at 121°C and above and those aged at 111°C and below. This difference may be attributed to a change in morphology of the material due to temperature excursions near or above its crystalline melting point. Fig. VIII-18 shows the initial NMR T_2's of the black and green sleeves that have been aged at various temperatures. These initial values were obtained by plotting NMR T_2 vs. aging time for each aging temperature and extrapolating these data back to zero aging time. Note that these NMR T_2's reflect the response of a material that has been exposed or annealed at the aging temperature but has not experienced significant aging. Thus, changes in the NMR T_2 as a function of temperature correspond to morphological changes rather than chemical degradation. The lines are least squares fit of the data. We observe a definite trend, especially for the green sleeve, to higher values of NMR T_2 for what should be chemically similar material. This effect, which can be associated with an annealing process of a partially crystalline material, will be illustrated in greater detail for the XLPO-05 material discussed below.

The final XLPO that we investigated by NMR T_2 relaxation times is the green version of XLPO-05. The samples were swollen in deuterated benzene at 70°C and required 12 minutes to reach an equilibrium state. The NMR T_2 vs. aging time at 124°C is shown in Fig. VIII-19. The NMR T_2 of the unaged material does not fall on the smooth curve drawn for the aged samples. This DSC of this material, Fig. III-51, shows a complex melting pattern with melting peaks ranging from 100 to 120°C. We believe that even short aging exposures at 124°C cause a change in morphology of the material that is reflected in the relaxation data. To test this hypothesis, we annealed a sample of unaged material at 124°C for 27 hrs. This time is too short to cause significant chemical damage but should lead to similar morphological changes as those experienced by the aged samples. The NMR T_2 relaxation times of the annealed material is shown by the solid

symbols in Fig. VIII-9 and now fall on the smooth curve drawn through all of the aged samples. The elongation of XLPO-05 as a function of NMR T_2 is shown in Fig. VIII-20. The relaxation time of the annealed sample is used for the unaged data and the correlation between the two quantities is excellent. Thus, NMR T_2 relaxation times can be used to monitor the condition of the XLPO-05 cable insulation with the stipulation that the sample must first be annealed at 124°C in order to use the calibration curve that we have derived. A similar correlation between elongation and NMR T_2 may exist for samples that have never been exposed to temperatures above their melting point. We cannot establish this correlation, however, because the material degrades very slowly at these temperatures and sufficiently degraded samples are not available for evaluation.

Thermal aging of miscellaneous materials

The correlation between elongation at break and NMR T_2 for EPR-05 aged at 109°C is shown in Fig. VIII-21. The samples were swollen in deuterated benzene at 70°C for 12 minutes before measurement. The NMR T_2 with a value of 9.28 ms corresponds to unaged sample and does not appear to lie on the same line as the aged samples. We believe that this variation is due to annealing effects associated with the aging process. Fig. III-31 shows that this material has a significant amount of crystallinity that would be above its melting point at the aging temperature. The elongation of this material exhibited more scatter than normal. Hard and soft sections of the sample were apparent by simply flexing the material. The figure shows two measurements at 678 days of aging and two measurements at 921 days of aging for which we attempted to chose a soft and hard section of the sample. In each instance, the soft section has a significantly longer relaxation time. The NMR T_2 of the soft section correlated well with the larger elongation value of the 678 day sample, while the NMR T_2 of the hard section correlated well with the smaller elongation value of the 678 day sample. After 921 days of aging, much of the sample was brittle; the elongation could not be measured and was assigned a value of 0%. As discussed in the previous section, EPR-05 samples would need to be annealed at 109°C in order to use the calibration curve displayed in Fig. VIII-21.

We found that the CPE-02 was particularly difficult to swell. After 12 minutes in $CDCl_3$ at ambient temperature, the NMR T_2 for the unaged sample was only 4 ms, a very short time that usually implies very little dependence on additional crosslinking. The NMR T_2's of CPE-02 as a function of aging time at 124°C were measured in $CDCl_3$ at 50°C, in cyclohexane-d_{12} at 70°C and in toluene-d_8 at 100°C. The temperatures for each solvent are approximately 10°C below their boiling points. Although toluene-d_8 provided the longest NMR T_2 relaxation times, the data for toluene-d_8 also had more scatter than the lower temperature measurements and required the use of a special high temperature probe. For this reason, we proceeded to investigate relaxation of CPE-02 swollen in cyclohexane-d_{12} at 70°C.

The NMR T_2 of a sample aged for 30 days at 124°C is shown as a function of swelling time in Fig. VIII-22. The normal procedure (which we term "non preconditioned") is to heat the sample to 70°C while it resides in the probe. The lower set of data points in the figure shows that the relaxation time begins at 4.9 ms after 5 minutes and increases to

11.0 ms after 33 minutes. Because the relaxation time continues to increase, this procedure would require a significant amount of instrumental time. The preconditioned sample, along with the cyclohexane-d_{12} was placed in an oven at 65°C for a period of 3.5 hours. During this time the sample reached an equilibrium state. During the transfer from the oven to the spectrometer, the sample cools momentarily, but appears to again reach an equilibrium state in a much shorter period of time. We realized that the time to reach equilibrium is also affected by the size of the sample. Fig. VIII-23 shows the NMR T_2 vs. swell time for a single large cube, approximately 2 mm on each side, and the NMR T_2 vs. swell time for several small cubes approximately 0.5 mm on each side. The relaxation times of the sample with the smaller pieces obviously swelled more rapidly than the sample with a single large piece.

The measurements conducted in order to derive the relationship between elongation and NMR T_2 of CPE-02 were performed by utilizing small pieces, approximately 0.5 mm on a side, and by preconditioning the samples in cyclohexane-d_{12} for 3 to 4 hrs in an oven at 65°C. The samples were allowed to equilibrate for 19 minutes in the spectrometer before a measurement was begun. The correlation between elongation at break and NMR T_2 for CPE-02 aged at 124°C is shown in Fig. VIII-24. The correlation between the two quantities is excellent.

Conclusions

For the current NMR T_2 studies, ~10 mg samples were used. However, a very significant advantage of the NMR approach is its capability for quickly and easily making measurements on extremely small samples. The 10 mg samples, that required less than 10 min per T_2 measurement on a fully automated NMR instrument, provided very high signal to noise ratios. We have shown in previous work that samples as small as 0.1 mg can easily be run [VIII-4], with samples in the μg region possible if desired [VIII-5]. All of the "essentially non-destructive" CM techniques examined to date require on the order of 10-20 mg. Since the NMR approach can be done on fractions of a mg, this represents an important step towards developing a true "non-destructive" CM technique. In addition, it should be noted that the NMR approach is applicable to at least some crosslinked polyolefin cable insulations. Because the mechanical properties of these semi-crystalline materials are dominated by their hard crystalline components, slight hardening of the amorphous regimes caused by aging has little effect on overall hardness, negating the applicability of such CM approaches as modulus and indenter. The NMR T_2 measurement of a specimen swollen in a solvent at 70°C provides an indication of this difficult to observe aging mechanism. The correlation curves for the crosslinked polyolefin materials were derived from samples that had been aged above their crystalline melting points. This means that the materials to be investigated need to be annealed for a short period of time at equivalent temperatures before the NMR measurements are performed.

References

VIII-1. Ibbett RN, editor. NMR spectroscopy of polymers. London: Blackie; 1993.

VIII-2. Gillen KT, Assink, RA, Bernstein R. Condition monitoring approaches applied to a polychloroprene cable jacketing material. Polym Degrad Stab 2004;84:419.

VIII-3. Assink RA, Lang DP, Celina M. Condition monitoring of a thermally aged hydroxy-terminated polybutadiene (HTPB)/isophorone diisocyanate (IPDI) elastomer by nuclear magnetic resonance cross-polarization recovery times. J Appl Polym Sci 2001;81:453.

VIII-4. Assink RA, Gillen KT, Sanderson B. Monitoring the degradation of a thermally aged EPDM terpolymer by H-1 NMR relaxation measurements of solvent swelled samples. Polymer 2002;43:1349.

VIII-5. Assink RA, Celina M, Gillen KT. Monitoring the condition of thermally aged polymers by NMR relaxation measurements. Polymer News 2003;28:102.

VIII-6. Harris DJ, Assink RA, Gillen KT. 1H T_2 NMR monitoring of crosslinked polyolefin aging. J App Polym Sci 2003;90:2578.

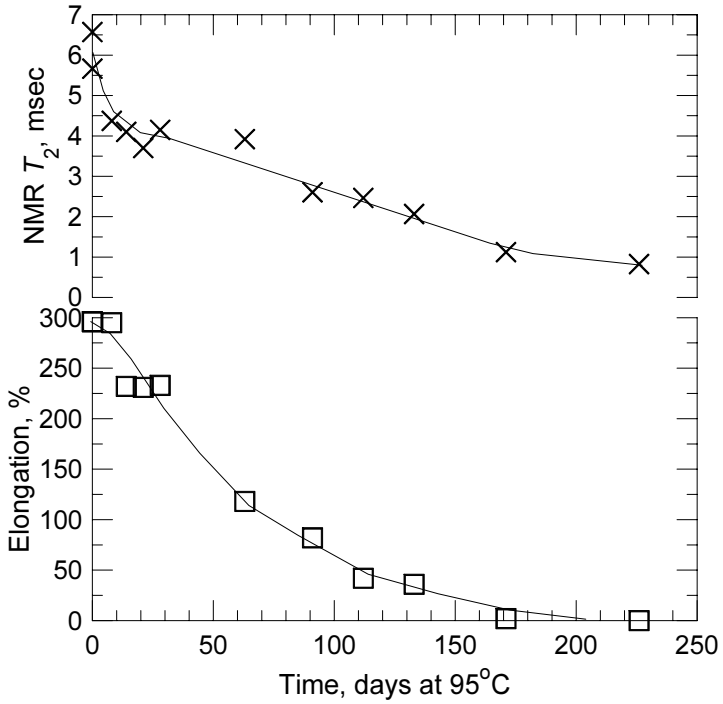

Figure VIII-1. Average elongation results and NMR T_2 results plotted versus aging time for Neo-2 at 95°C.

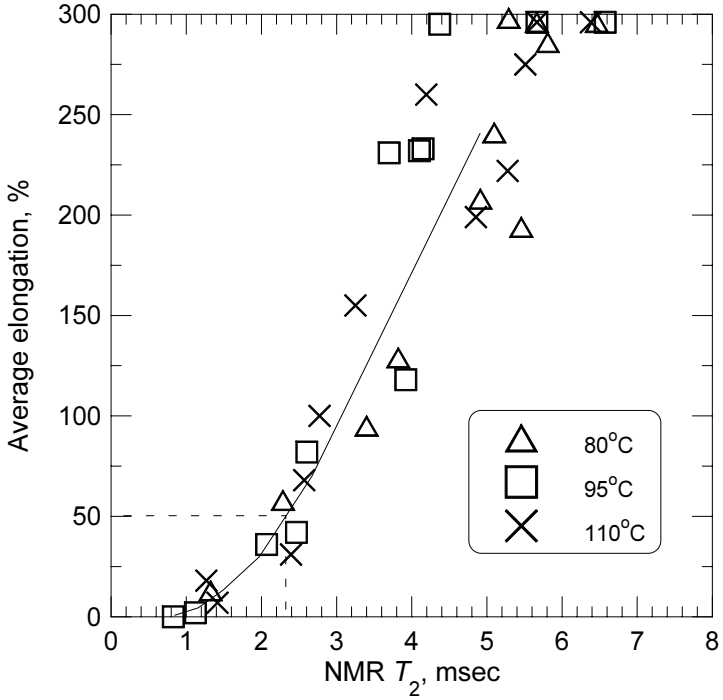

Figure VIII-2. Average elongation results plotted versus NMR T_2 results for Neo-02 at the three indicated aging temperatures.

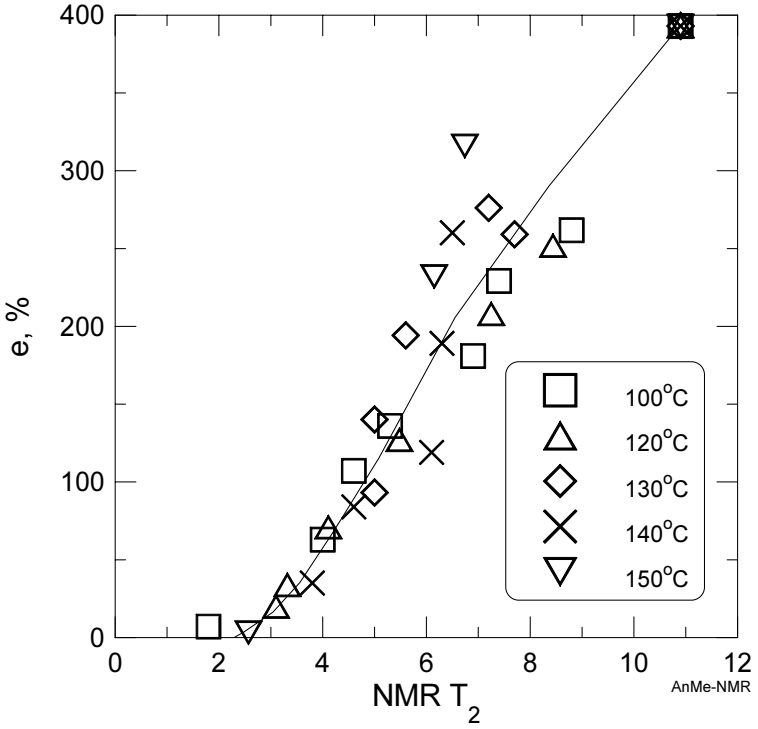

Figure VIII-3. Average elongation results plotted versus NMR T_2 results for Hyp-01A at the five indicated aging temperatures.

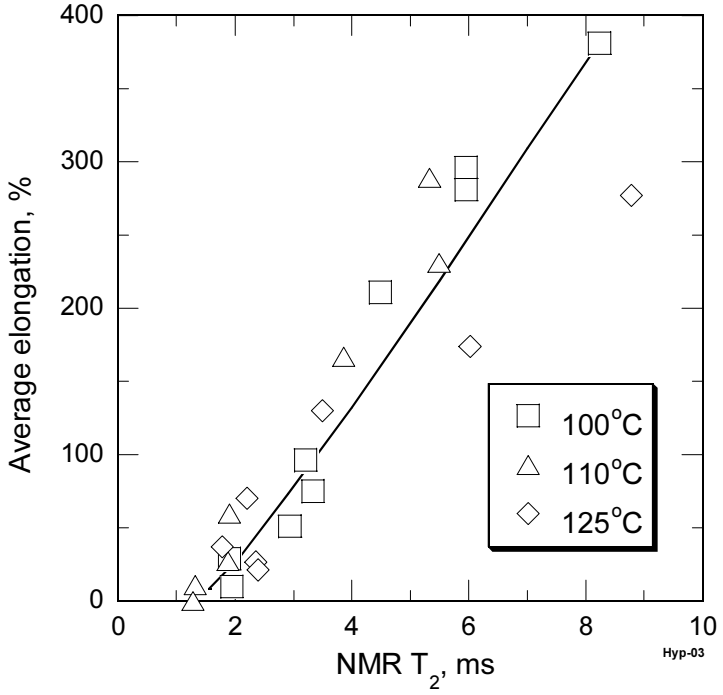

Figure VIII-4. Average elongation results plotted versus NMR T_2 results for Hyp-03 at the three indicated aging temperatures.

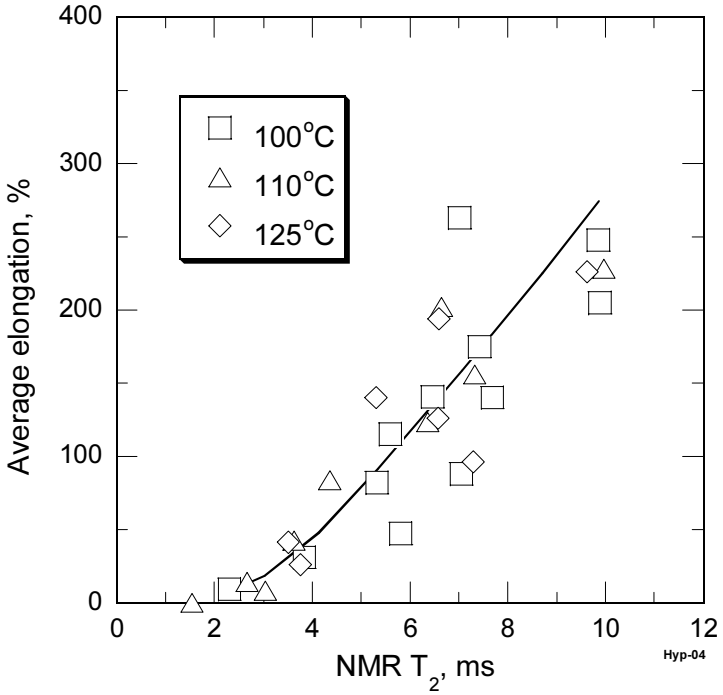

Figure VIII-5. Average elongation results plotted versus NMR T_2 results for Hyp-04 at the three indicated aging temperatures.

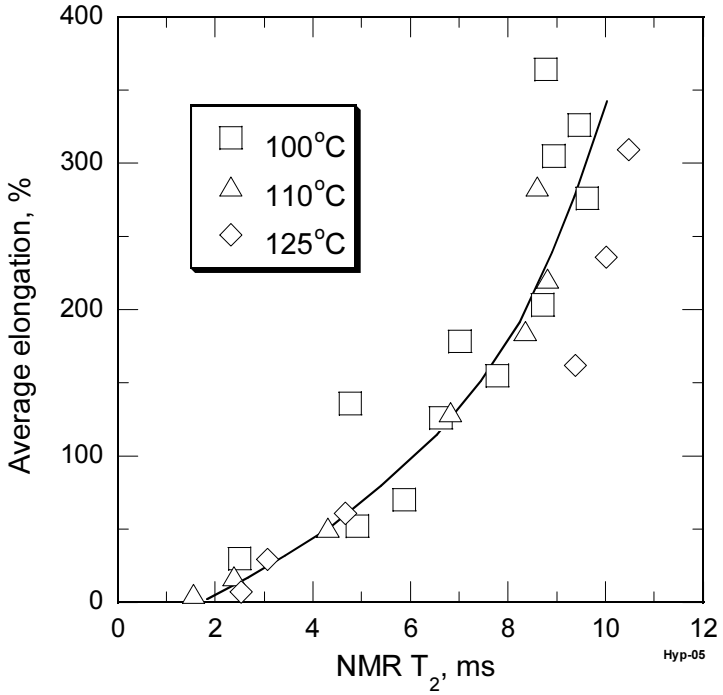

Figure VIII-6. Average elongation results plotted versus NMR T_2 results for Hyp-05 at the three indicated aging temperatures.

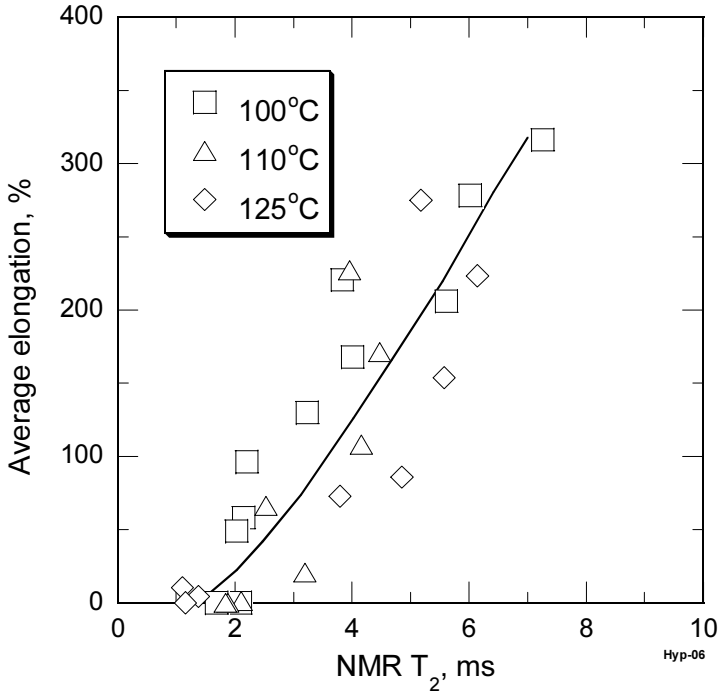

Figure VIII-7. Average elongation results plotted versus NMR T_2 results for Hyp-06 at the three indicated aging temperatures.

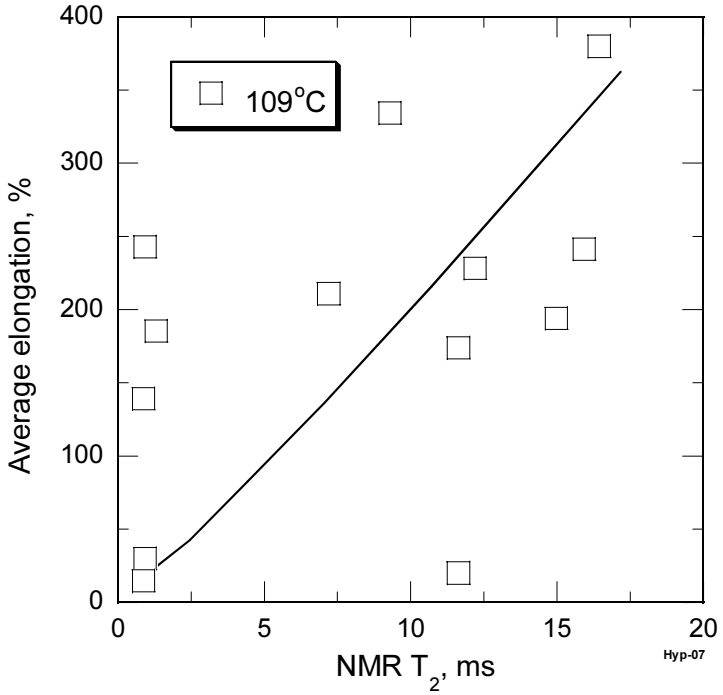

Figure VIII-8. Average elongation results plotted versus NMR T_2 results for Hyp-07 at an aging temperature of 109°C.

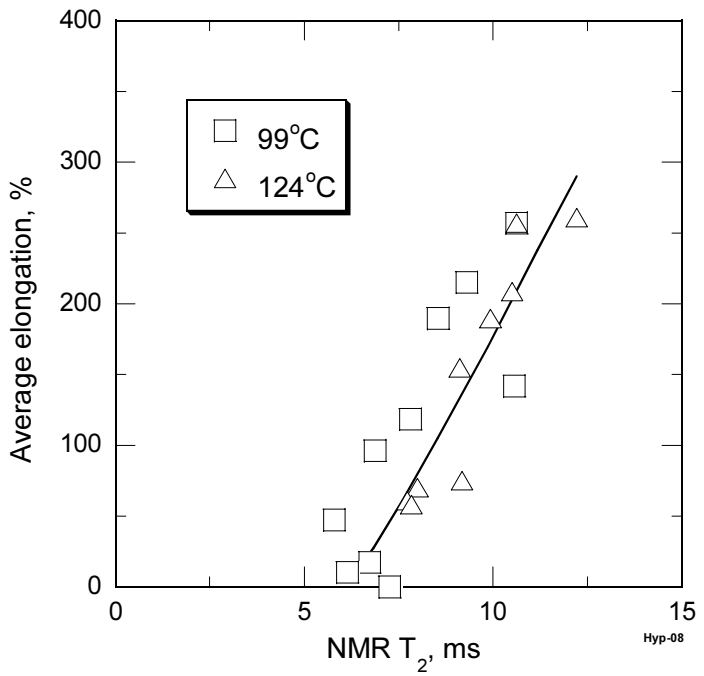

Figure VIII-9. Average elongation results plotted versus NMR T_2 results for Hyp-08 at the two indicated aging temperatures.

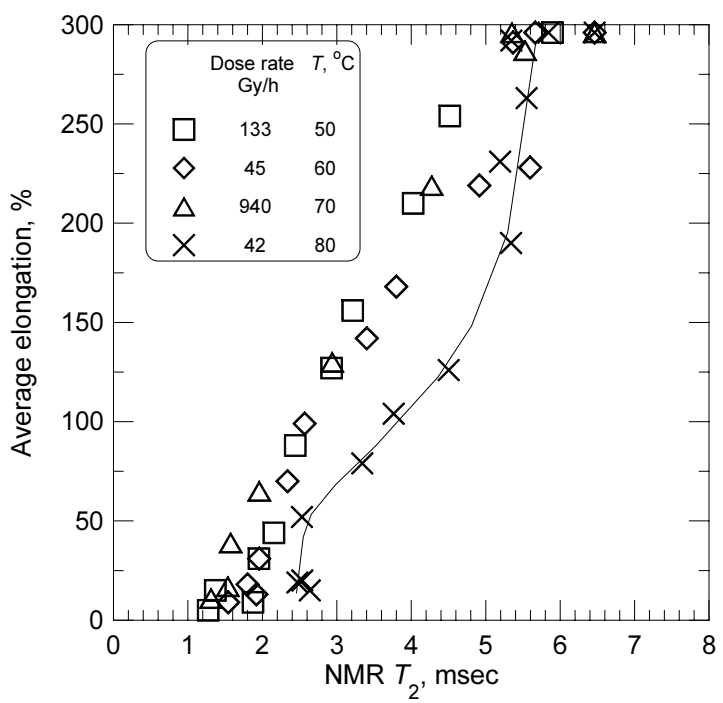

Figure VIII-10. Average elongation results plotted versus NMR T_2 results for Neo-02 at the four indicated combined-environment aging conditions.

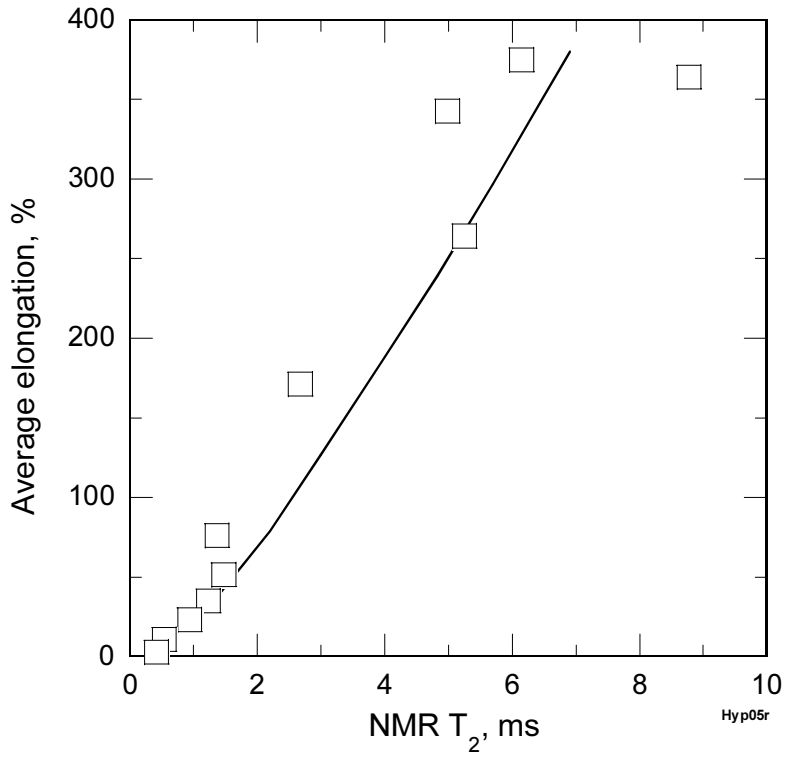

Figure VIII-11. Average elongation results plotted versus NMR T_2 results for Hyp-05 at 60°C and 184 Gy/h combined-environment aging conditions.

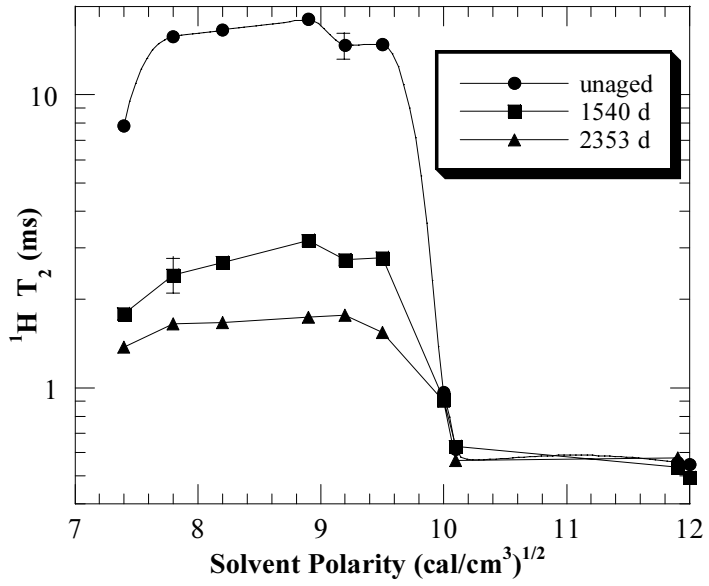

Figure VIII-12. NMR T_2 results as a function of solvent polarity for XLPO-02B aged for the times indicated at 109°C.

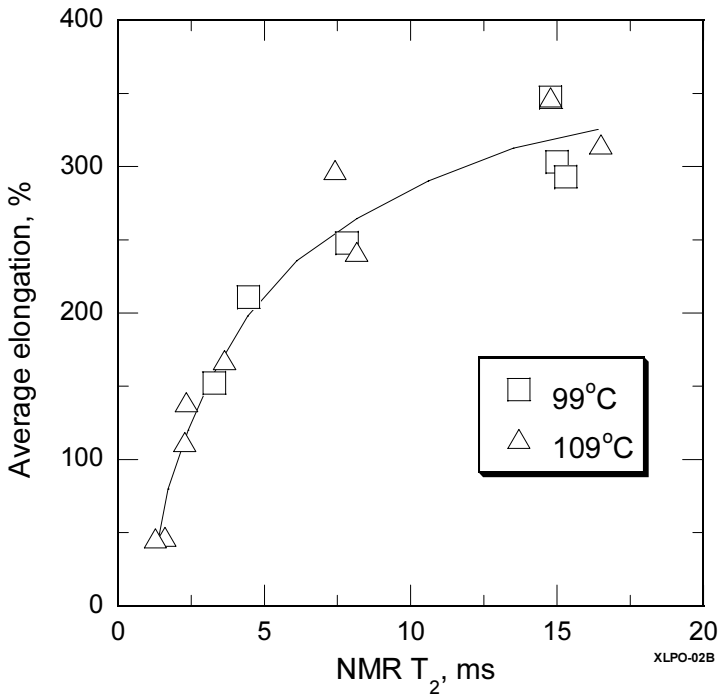

Figure VIII-13. Average elongation results plotted versus NMR T_2 results for XLPO-02B aged at 99 and 109°C.

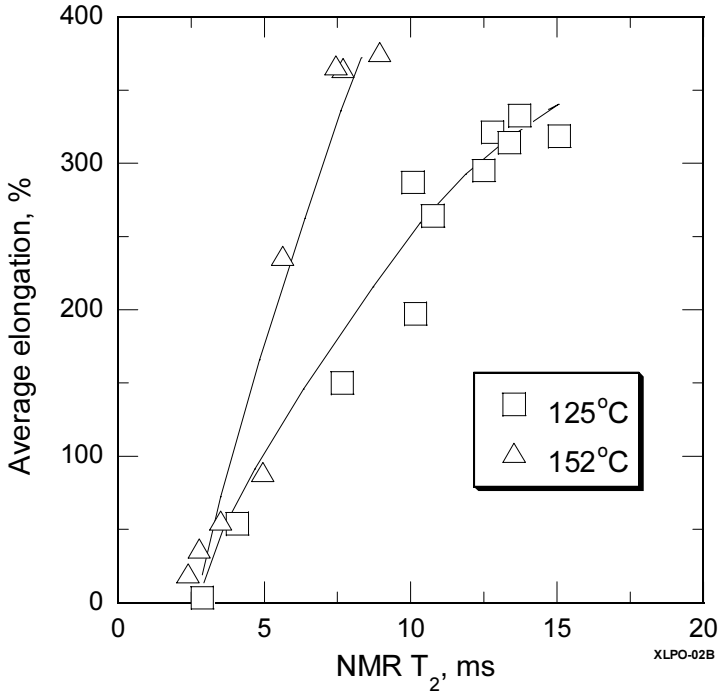

Figure VIII-14. Average elongation results plotted versus NMR T_2 results for XLPO-02B aged at 125 and 152°C.

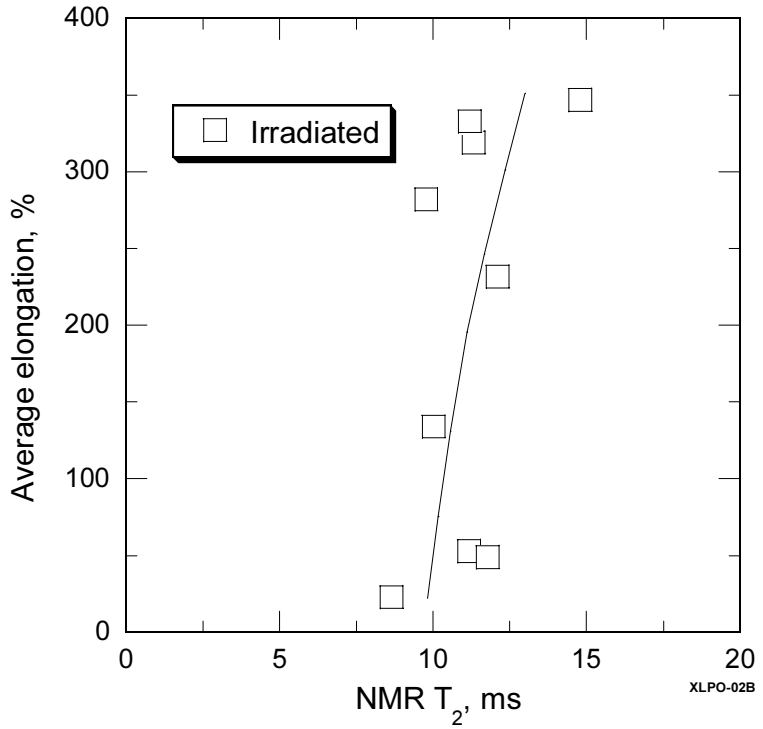

Figure VIII-15. Average elongation results plotted versus NMR T_2 results for XLPO-02A subjected to ^{60}Co radiation with a dose of 200 Gy/h at ambient temperatures.

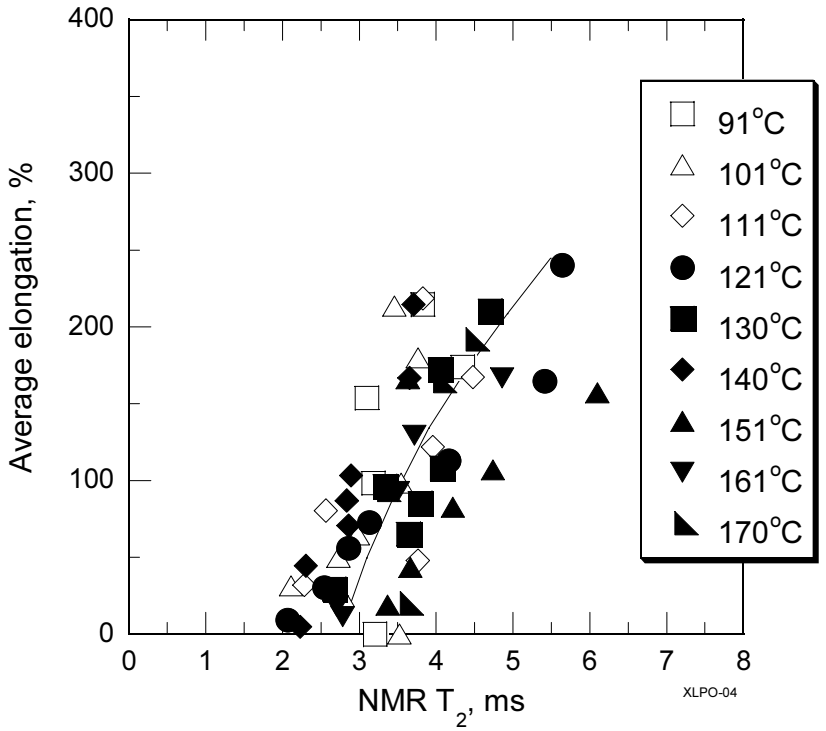

Figure VIII-16. Average elongation results plotted versus NMR T_2 results for the black portion of XLPO-04 for the aging temperatures indicated.

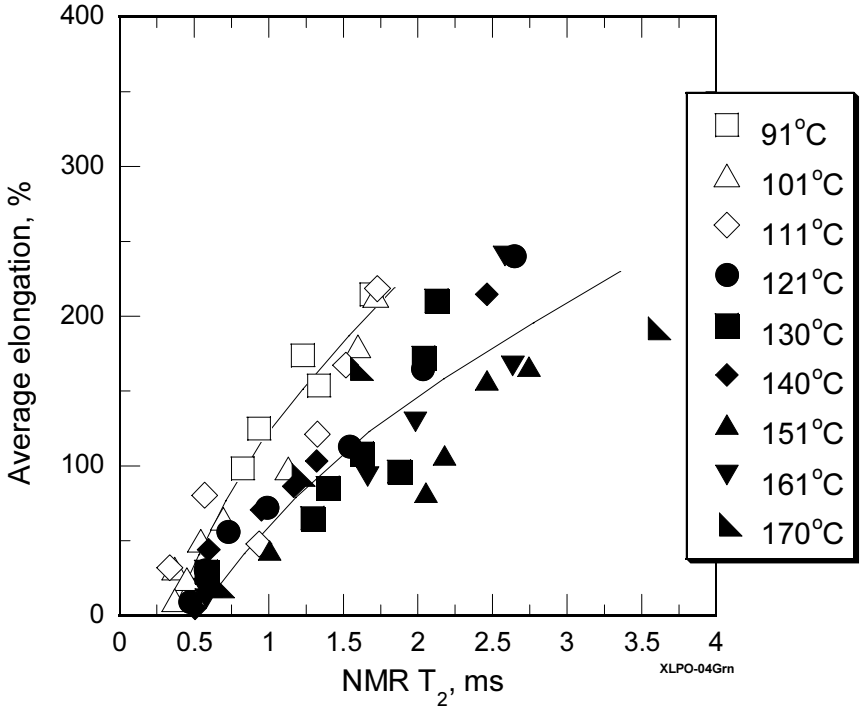

Figure VIII-17. Average elongation results plotted versus NMR T_2 results for the green portion of XLPO-04 for the aging temperatures indicated.

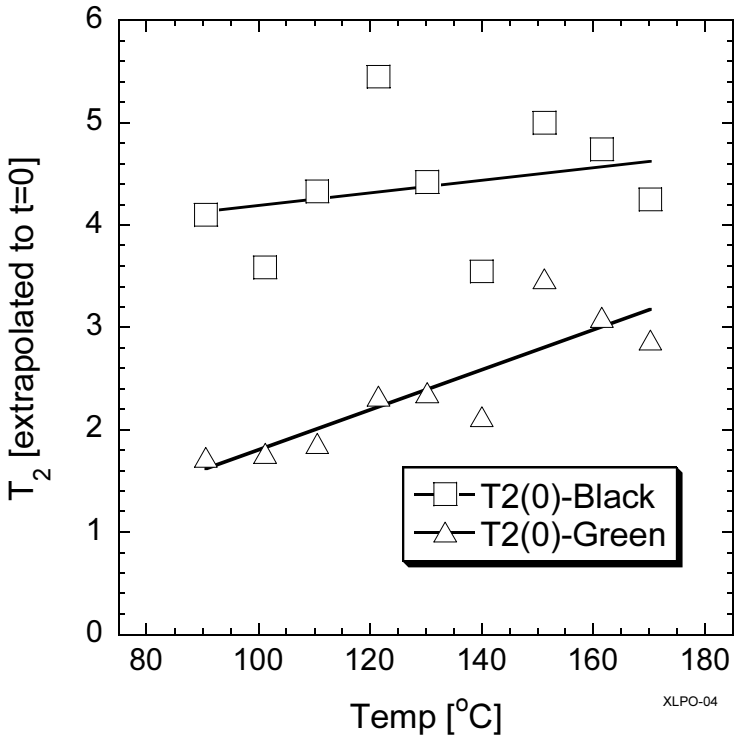

Figure VIII-18. Dependence of the initial (derived by extrapolation) NMR T_2 results for the black and green portions of XLPO-04 for the aging temperatures indicated.

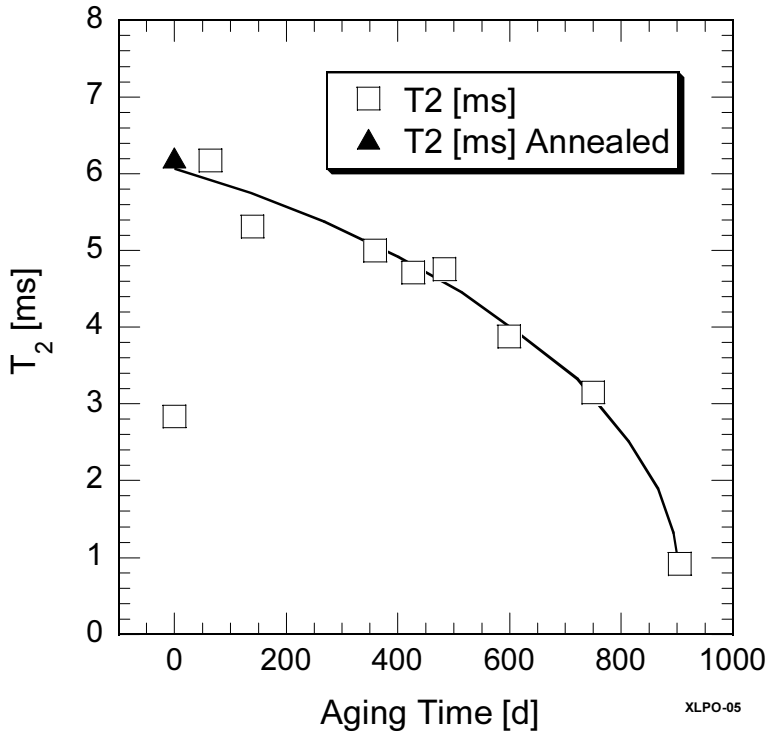

Figure VIII-19. NMR T_2 results for green XLPO-05 as a function of aging time at 124°C. The solid symbol corresponds to an unaged sample that was annealed at 124°C for 27 hrs.

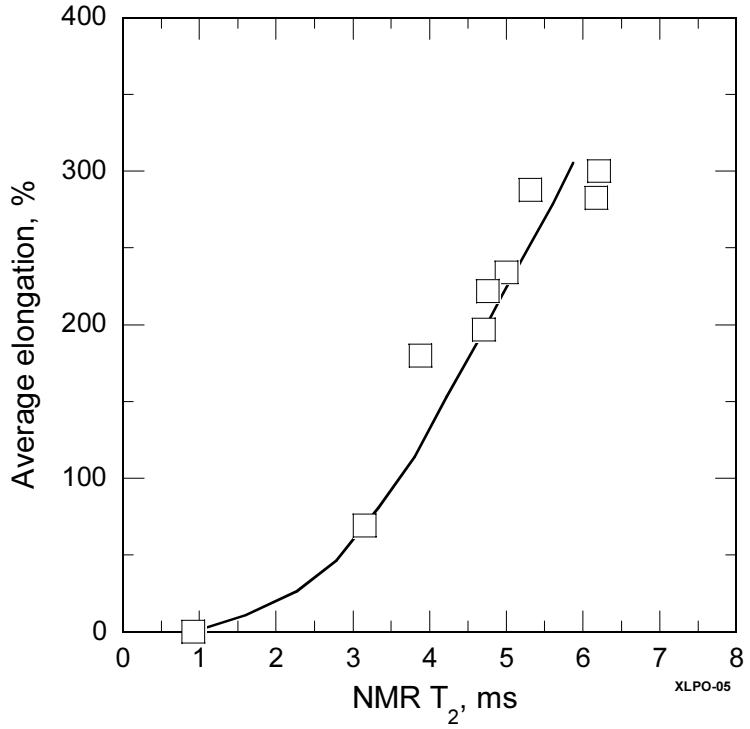

Figure VIII-20. Average elongation results plotted versus NMR T_2 results for green XLPO-05 for an aging temperature of 124°C.

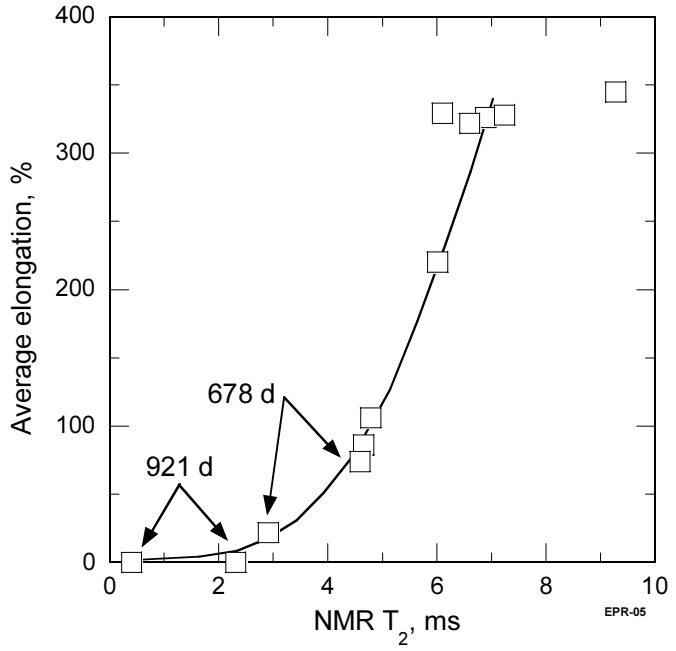

Figure VIII-21. Average elongation results plotted versus NMR T_2 results for green EPR-05 for an aging temperature of 109°C. The dual points for 678 and 921 days correspond to hard and soft portions of the sample.

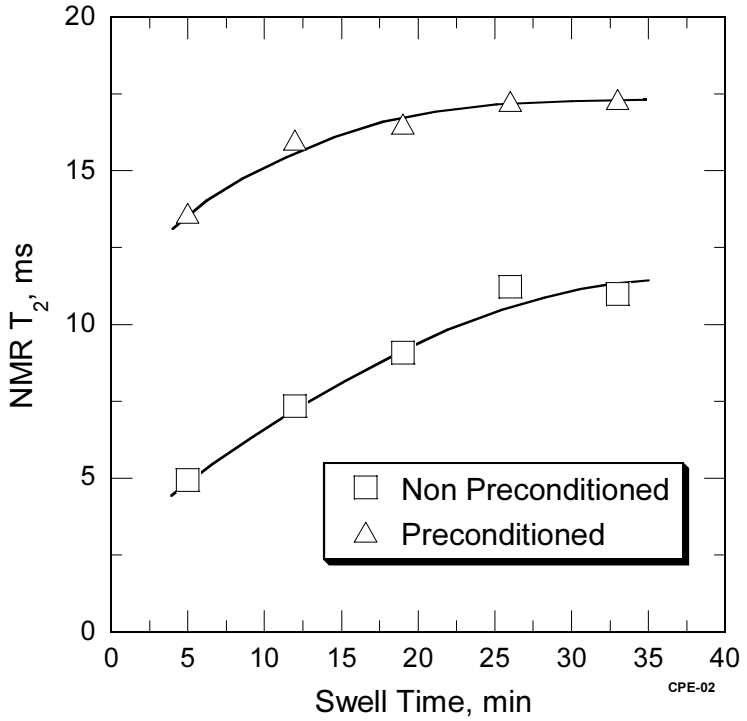

Figure VIII-22. The effect of swell time on the NMR T_2 of non-preconditioned CPE-02 and CPE-02 preconditioned for 3-4 hours at 65°C.

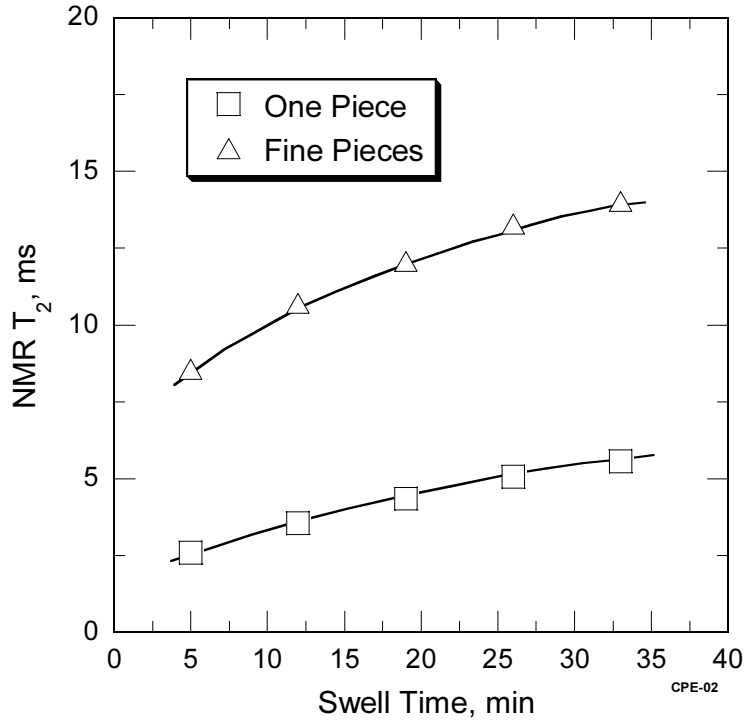

Figure VIII-23. The effect of swell time on the NMR T_2 of a single large sample of CPE-02 compared to the NMR T_2 of several small pieces of CPE-02.

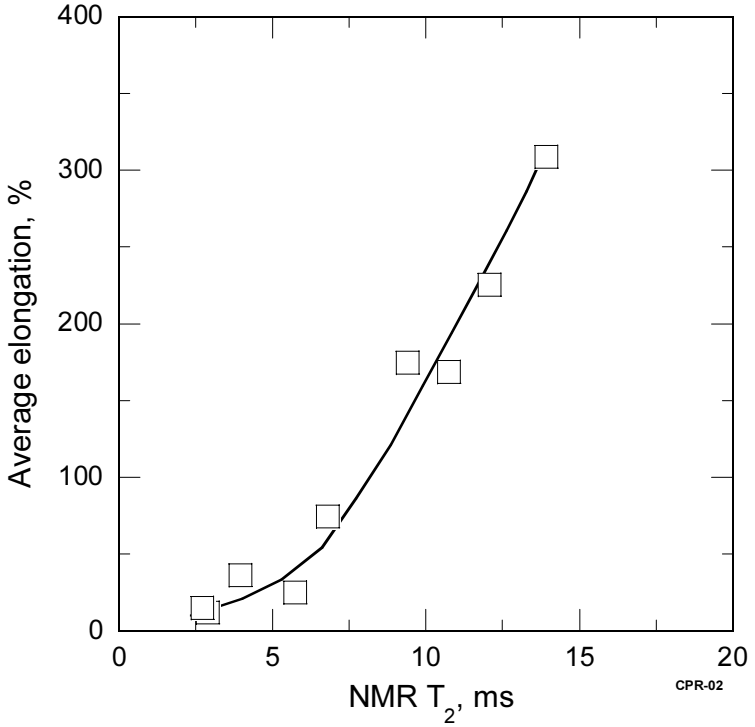

Figure VIII-24. Average elongation results plotted versus NMR T_2 results for CPE-02 for an aging temperature of 124°C.

IX. Condition Monitoring Techniques: Percentage Gel and Solvent Uptake Factor

Introduction

A very common polymer analysis method for evaluating crosslinked materials involves placing the material in refluxing solvent, weighing the sample when swollen by the solvent, then drying the sample under vacuum to drive off the solvent. The final weight of sample divided by the initial weight before swelling gives the percentage gel for the sample. The swollen weight divided by the final weight gives the solvent uptake factor. Both of these parameters are sensitive to the overall crosslink density of the material. During aging, the changes in overall crosslink density reflect the relative importance of the crosslinking and scission processes caused by the degradation reactions. In general when crosslinking dominates scission, the percentage gel goes up and the uptake factor goes down. The opposite trends tend to occur when scission dominates crosslinking. Since both modulus profiling and NMR relaxation times appear to be promising CM techniques and both of these parameters are strongly dependent on the changes in overall crosslink density occurring during aging, we felt that gel and uptake factor measurements might also prove useful as a CM technique. Some limited effort has been devoted previously to these approaches (particularly gel measurements) for nuclear power cable materials [IX-1 through IX-4] and the results from these previous studies further encouraged us to examine gel and uptake approaches.

Gel and uptake factor measurements on Neo-02 cable jacket [IX-5]

We showed earlier in Section VII that DLO effects were unimportant for the Neo-02 material under the three thermal-only and the four combined environment conditions used in the aging of this material. Therefore we have no concerns over utilizing data from a macroscopic CM technique that probes the entire cross-section of the material such as the presently considered gel and uptake measurements. Figures IX-1 through IX-6 show the gel and uptake factor results for the three thermal-only aging conditions used on the Neo-02 material. For convenience the plots show the elongation results at the bottom of each plot so one can see how well the gel and uptake factors track elongation. In general the percentage gel increases with aging time and the uptake factor decreases implying that crosslinking processes are more important relative to scission processes during the aging. This conclusion is consistent with similar conclusions derived from the observed increases in modulus and decreases in NMR relaxation times, both implying domination by crosslinking reactions. Figures IX-1 through IX-3 show that the changes in percentage gel with aging are quite small. This lack of sensitivity to crosslinking is due to the fact that the material starts out highly gelled (~91%) and further crosslinking occurs mostly in the already gelled material with little effect on the 9% of the material that is not initially tied to the network.

The uptake factor, on the other hand, tends to be more sensitive to crosslinking of materials like elastomers that start out already highly crosslinked. This is because

additional crosslinks in the already gelled material will have an effect by further tying the network together, thereby impeding the amount of swelling possible. This is clear from the results shown in Figs IX-4 through IX-6, where the uptake factor drops from ~2.5 for unaged material (e.g., 150% by weight solvent pickup) to ~1.2 for severely degraded material (e.g., 20% by weight solvent pickup). Similar to the results for modulus of this material, fairly regular changes occur in the uptake factor as the elongation drops towards end of life, implying utility as a CM approach.

The small changes in gel percent relative to scatter in this quantity are apparent when elongation is plotted versus gel percent (Fig. IX-7). A similar plot for uptake factor against elongation, shown in Fig. IX-8, again shows that uptake factor is a more promising CM parameter. Although the scatter in uptake factor is relatively large at high values of elongation, the results are much closer together as the practical end of life (50% elongation) is approached. For all three aging temperatures, elongation reaches ~50% absolute when the uptake factor drops to ~ 1.65. Uptake factor results for the four combined environment conditions are plotted versus elongation in Fig. IX-9. A curve is drawn through the data representing the experiment at 42 Gy/h plus 80°C. As can be seen from Figs. V-6 and V-7, this combined environment condition is closest to the thermal only limit (lowest dose rate combined with the highest temperature). The results for this combined environment condition are similar to the results for thermal-only conditions (Fig. IX-8), with 50% absolute elongation corresponding to the uptake factor dropping to ~1.7. As the importance of radiation increases there is a shift of the combined environment correlation data towards the left in Fig. IX-9 (uptake factor of ~1.4 corresponding to 50% elongation).

Gel and uptake factor measurements on hypalon cable jackets [IX-6]

As determined in Section VII using modulus profiles, DLO effects and other heterogeneities appear for some of the hypalon material aging conditions. Since our uptake factor measurements require reasonable size specimens (whole cross-sections were typically utilized), the results will be adversely influenced by DLO effects and other such heterogeneous effects. Given the very strange heterogeneous profiles corresponding to Hyp-02 (Figs. VII-41 through VII-45), we decided not to carry out gel and uptake measurements on this material, concentrating our efforts on the remaining seven hypalon jackets. Similar to the results found on the Neo-02 material, we determined that aging of the hypalon materials tended to lead to increases in gel percentage and decreases in uptake factor. This is consistent with the dominance of crosslinking over scission found from both modulus and NMR measurements for such materials. Overall we found that the uptake factor tended to be much more sensitive than gel percent to changes in the hypalon elongation. As such we will show below for each hypalon material the uptake factor data on plots that also show elongation for comparison and then show on a single plot the correlations between uptake and elongation at all temperatures. For the various plots we either highlight or eliminate measurements where significant DLO effects were found from the modulus profiling results (Section VII). When DLO effects enter, a condition monitoring technique that averages a property across the entire sample cross-section such as the currently described solvent uptake measurements will be anomalously

affected by sample geometry effects. In other words, the measurement will not reflect the result expected for a homogeneously oxidized sample. Since the gel measurements again turn out to be not very promising as a CM approach, we will only show single plots giving the correlation between percent gel and elongation at all temperatures.

Figures IX-10 through IX-14 show the uptake factor results (right-hand y-axis) and the corresponding elongation results (left-hand y-axis) for the Hyp-01A material. As elongation decreases, the uptake factor changes dramatically, generally dropping from 5 for unaged (400% by weight solvent pickup) to values less than 1.5 (50% by weight solvent pickup). Thus the weight pickup of solvent drops by almost an order of magnitude over the useful life of the material. Figure IX-15 shows the correlation of elongation versus uptake factor for all times and temperatures. In this instance none of the uptake factor results were eliminated from the correlation plot since DLO effects are totally absent for this thin (~0.4-mm thick) hypalon jacketing material. The uptake factor corresponding to 50% absolute elongation is ~1.5, a value similar to the 50% elongation value found above for the Neo-02 material. Although large scatter is observed at early aging times as evidenced by the early results between 6 and 7 in Figs. IX-11 and IX-14 (the outliers in Fig. IX-15), the data scatter is much less near the "end-of-life" point. The gel results for Hyp-01A are summarized on Fig. IX-16.

Figures IX-17 through IX-19 show the uptake factor results (upper plot) and the corresponding elongation results (lower plot) for the Hyp-03 material. As elongation decreases, the uptake factor drops from ~3.7 for unaged (270% by weight solvent pickup) to values less than 1.5 (50% by weight solvent pickup). Figure IX-20 shows the correlation of elongation versus uptake factor for all times and temperatures. For this plot, only one uptake factor result was eliminated due to the presence of reasonably large DLO effects (70 days at 125°C- see Fig. VII-22). In addition to the thermal results shown on Fig. IX-20, this figure also gives uptake results for the two combined environment experiments that were radiation-dominated (minor DLO effects- see Figs. VII-50 and VII-51). The results for the five aging conditions indicate that uptake factor again has an excellent correlation with elongation at high levels of mechanical degradation. The uptake factor corresponding to 50% absolute elongation is ~1.6, again similar to those found above for the Neo-02 and Hyp-01A materials. The gel results for Hyp-03 are summarized on Fig. IX-21.

Figures IX-22 through IX-24 show the uptake factor results (upper plot) and the corresponding elongation results (lower plot) for the Hyp-04 material. DLO effects are much more significant for this material (see Section VII modulus profiling results). Therefore many of the uptake factors (and corresponding gel percentages) were eliminated from the figures, as is obvious from comparing elongation and uptake results on a given figure. As elongation decreases, the uptake factor drops from ~2.3 for unaged to values around 1.7. Figure IX-25 shows the correlation of elongation versus uptake factor for all times and temperatures. In this instance, much of the later time data had to be eliminated from the correlation plot due to the reasonably large DLO effects. The results shown therefore only suggest that the uptake factor corresponding to 50% absolute

elongation is again around 1.6, similar to the results found above. The non-DLO influenced gel results for Hyp-04 are summarized on Fig. IX-26.
Figures IX-27 through IX-29 show the uptake factor results (upper plot) and the corresponding elongation results (lower plot) for the Hyp-05 material. DLO effects are significant at 125°C for this material (see Section VII modulus profiling results). Therefore the 63 d and 70 d results at 125°C were eliminated from Fig. IX-27. As elongation decreases, the uptake factor drops from ~2.3 for unaged to values below 1.5. Figure IX-30 shows the correlation of elongation versus uptake factor for all times and temperatures and includes results for the two times at 125°C influenced by DLO effects. The results for the three aging temperatures indicate that uptake factor again has an excellent correlation with elongation at high levels of mechanical degradation. The uptake factor corresponding to 50% absolute elongation is ~1.5, again similar to the earlier results. The non-DLO influenced gel results and the DLO-influenced results (filled symbols) for Hyp-05 are summarized on Fig. IX-31. One might expect the two DLO-influenced points to show a bit less degradation than if they were homogeneously oxidized (e.g., a bit higher uptake factor and a bit lower gel content) and this appears to be the case from the results shown on Figs. IX-30 and IX-31.

Figures IX-32 through IX-34 show the uptake factor results (upper plot) and the corresponding elongation results (lower plot) for the Hyp-06 material. For this material, DLO effects are significant for several of the later data at 125°C and for the last two data points at 110°C (see Section VII modulus profiling results), so these points are eliminated from analyses. As elongation decreases, the uptake factor drops quickly from ~3.5 for unaged to around 2.3 then more slowly but steadily to values below 1.5. Figure IX-35 shows the correlation of elongation versus uptake factor for all times and temperatures and includes results for radiation-dominated combined environment results that are uninfluenced by DLO (see Figs. V-11, V-15 and VII-62). The results again indicate that the uptake factor has an excellent correlation with elongation at high levels of mechanical degradation. The uptake factor corresponding to 50% absolute elongation is ~1.6, again similar to the earlier results. The non-DLO influenced gel results for the thermal-only exposures of Hyp-06 are summarized on Fig. IX-36.

Figures IX-37 through IX-39 show the uptake factor results (upper plot) and the corresponding elongation results (lower plot) for the Hyp-08 material. For this material, DLO effects are significant for several of the later data at 124°C (Fig. VII-28) and for the 101-day point at 108°C (Fig. VII-27), so these points are eliminated from the analyses. As elongation decreases, the uptake factor drops from ~2.5 for unaged to values below 1.5. Figure IX-40 shows the correlation of elongation versus uptake factor for all times and temperatures that are uninfluenced by DLO. The results indicate that the uptake factor again has an excellent correlation with elongation at high levels of mechanical degradation. The uptake factor corresponding to 50% absolute elongation is ~1.55, again similar to the earlier results. Although a drop from 2.5 to 1.5 might seem to be a relatively small change compared to the much larger drops noted for earlier materials, these changes still represent the percentage weight pickup of solvent going from 150% to 50% (see top x-axis of Fig. IX-40). Given the accuracy with which weight can be measured and the excellent reproducibility of results once "end-of-life" is approached,

the uptake measurement remains promising even for the Hyp-08 material. The non-DLO influenced gel results for the thermal-only exposures of Hyp-08 are summarized on Fig. IX-41.

The uptake factor results for the Hyp-07 material at 109°C have previously been shown in Fig. VII-40. For this material the elongation was found to drop off very quickly (induction-time behavior) implying that the uptake values will depend upon whether a sample in the induction-time region is still soft or has transitioned to a hard material. Figs. IX-42 and IX-43 show uptake results at two additional aging temperatures and Fig. IX-44 plots the elongation results versus uptake factor for samples uninfluenced by DLO effects. The uptake factor corresponding to 50% absolute elongation is ~1.65, again similar to the earlier results. The non-DLO influenced gel results for the thermal-only exposures of Hyp-08 are summarized on Fig. IX-45.

Finally all of the hypalon uptake factor results uninfluenced by DLO effects are plotted on a single graph versus elongation. The results, given in Fig. IX-46, further emphasize the fact that essentially every hypalon material reaches an uptake factor of ~1.6±0.1 when the elongation reaches 50% absolute. Thus an apparently "universal" end of life criterion appears to hold for hypalon cable jacketing materials. This "universal" value of 1.6±0.1 for hypalon is similar to the value found for the thermal-only aging of Neo-02.

Gel and uptake factor measurements on XLPO cable insulation

Before attempting to apply gel and uptake measurements to XLPO cable jacketing material, we must determine if DLO effects are important for such materials. Since modulus profiling could not be applied to these materials because of their crystallinity, we resort to the theoretical modeling given in Section VI. From eq. VI-1, we need estimates of the oxygen consumption rate ϕ and the oxygen permeability coefficient P_{Ox} at the aging temperatures of interest. As seen in Section IV, we have conducted oxygen consumption measurements on two of the currently studied XLPO materials at temperatures up to 138°C and elongation measurements at temperatures up to 151°C. We focus in on the worst-case material (XLPO-05) in terms of potential DLO effects because it has both the highest consumption values and the highest E_a value at high temperatures. For this material, the average consumption result over the first few months of aging at 124°C gives $\phi \sim 2\text{x}10^{-11}$ mol/g/s (Fig. IV-38). This value at 124°C can be used together with the E_a values appropriate for oxygen consumption (see Fig. IV-40) to make estimates of ϕ at several temperatures in the temperature range of interest (Table IX-1). Estimates of the high temperature permeability coefficients come from a combination of literature values for polyethylene materials [IX-7] and typical E_a values expected at high temperatures [IX-8]; these are also shown in Table IX-1. Assuming a typical XLPO density of 1.35 g/cc (Table I-3), eq. VI-1 leads to the L_{90} values summarized in the last row of Table IX-1. Comparing these results to the typical 1-mm cross-section of XLPO cable insulations makes it clear that DLO effects will be unimportant for thermal aging of typical XLPO materials even at temperatures as high as 151°C.

Table IX-1. Estimates of L_{90} for XLPO cable insulations.

T, °C	151	138	124	109	99
ϕ, mol/g/s	2.7e-10	8.05e-11	2e-11	6.5e-12	2.95e-12
P_{Ox}, ccSTP/cm/s/cmHg	1.7e-8	1.4e-8	1e-8	8e-9	6e-9
L_{90}, mm	2.3	3.9	6.6	10.4	13.3

Figures IX-47 through IX-50 show the uptake factor results (top plot) and the corresponding elongation results (bottom plot) for the XLPO-02B material. As elongation decreases, the uptake factor drops from 8 for unaged (700% by weight solvent pickup) to values around 2 (100% by weight solvent pickup). This very large change in solvent pickup indicates that uptake factor may be a useful CM approach for an important XLPO material. As noted in the NMR section, XLPO materials are among the most difficult materials in terms of finding viable CM techniques. The correlations between elongation results and uptake factors at all four aging temperatures and times are shown in Fig. IX-51. Although the correlation is quite reasonable, we must note that XLPO-02B was the material where the shape of the elongation curves was quite different for aging carried out above its main melting peak (125°C and 151.5°C) compared to the shape of elongation decay for aging at temperatures below this peak (99°C and 109°C). This is clear from the elongation results shown in Figs. IX-47 through IX-50. Because of this problem with data above the crystalline melting point, extrapolations of elongation results were accomplished using only the data at 99°C and 109°C (Figs. IV-32 and IV-33). We therefore eliminate the uptake factor results taken from aging temperatures above the main melting peak and replot the correlation for the two lower temperatures in Fig. IX-52. Our usual end of life criterion for elongation (50%) corresponds to the uptake factor reaching ~2.7 for XLPO-02B. This result is quite different from the values near 1.6 found for Neo-02 and the hypalon jackets. The presence of crystallinity in XLPO-02B can clearly affect both elongation and uptake measurements and this could be one reason for the difference.

The gel results for this material, given in Figs. IX-53 through IX-56, also showed reasonable sensitivity to degradation. In particular it should be noted that gel percentage measurements can be made accurately on extremely small samples (~1 mg or less). This is because modern balances makes it easy to accurately weigh small samples before they are exposed to solvent and after they have been exposed to solvent and dried out. Therefore when gel uptake represents a viable CM approach, it can be applied to extremely small samples. As an example, once we determined that gel was viable for XLPO-02B using our usual ~50 mg sample sizes (data plotted with Xs in Figs. IX-53 through IX-56), we made some additional gel measurements on several 1-mg samples of unaged and severely aged material from the 109°C exposure. The results from these experiments, plotted as diamonds on Fig. IX-55, show the power of gel measurements to examine samples of 1 mg or less. The correlation plots between elongation and gel percentage are shown in Fig. IX-57 (all four temperatures) and Fig. IX-58 (99°C and 109°C only).

Although gel and uptake look promising on the XLPO-02B insulation, the situation is less promising for XLPO-05. For this material, changes in uptake and gel percentage large enough to be significant relative to data scatter appear to occur only near the mechanical end of life of this material. This can be seen from the uptake results for the green-colored insulation aged at 138°C and 151.5°C given in Figs. IX-59 and IX-60. Gel results are similar with measurable changes observed only in the induction-time region.

Gel and uptake factor measurements on CPE-2 cable jacket

The chlorinated polyethylene cable jacket results were quite unusual in the sense that the unaged material was completely dissolved by the solvent, implying that the percentage gel for unaged was 0 and the uptake factor for unaged was undefined. Sufficient crosslinking occurred with thermal aging to create a gel so that uptake measurements became possible for aged material. The results for uptake and gel at aging temperatures of 109°C, 124°C and 138°C are shown in Figs. IX-61 through IX-66. Note that the earliest times at each aging temperature are sufficient to cause the gel percentage to quickly jump from 0% to around 40%, followed by much slower changes later in time. This suggests that the cable jacket was not properly cured during the extrusion process and did not represent a crosslinked material when shipped by the factory. With additional aging at each temperature the gel continues to slowly increase and the uptake slowly decrease. The correlation plots are given in Figs. IX-67 and IX-68. Even though we have only limited results, both percentage gel and uptake factor appear to show reasonable promise as CM techniques for the CPE-02 material. The uptake results indicate that 50% absolute elongation corresponds to uptake factors near 2.7, similar to that found for XLPO-02B.

Gel and uptake factor measurements on EPR cable insulations

Similar to the results found for elongation, modulus, NMR relaxation time (and density-see Section X below), uptake factor and gel measurements on EPR insulations remain essentially unchanged until the induction-time region is reached so these approaches offer little advanced warning of the approach to the end of life for this material. For instance uptake and gel results for the EPR-04 material for aging at 109°C are given in Figs. IX-69 and IX-70.

Conclusions

Gel and uptake measurements are sensitive to the crosslink density of the material and therefore to the competition between scission and crosslinking that occurs during the aging of a crosslinked material. Since modulus and NMR relaxation times are also sensitive to changes in crosslink density, all three techniques tend to have similar applicability from a material point-of-view. In the case of gel and uptake, it appears that these approaches show promise for neoprene, hypalon and chlorinated polyethylene cable jackets both in thermal-only and combined radiation-thermal environments. These techniques also show promise for certain XLPO insulations. For EPR insulations and

other XLPO insulations, these techniques are only sensitive near the "induction-time" region, thereby offering little or no warning of impending end of life. Of the two approaches, uptake factor measurements are more promising for several reasons. First, the changes in uptake factors tend to be greater than the changes in gel percentage mainly because additional crosslinks often have little effect on the already high initial gel percentage whereas new crosslinks can lead to substantial decreases in solvent weight pickup. In addition, it appears that a "universality" criterion may exist for hypalon cable jacketing (and perhaps neoprene cable jacketing) materials where the elongation reaches 50% absolute corresponds to the uptake factor reaching ~1.6. This "universality" criterion is similar to the 35 MPa criterion that appears to hold for the modulus of hypalon and neoprene materials. If true, such universality criteria might allow property condition estimates to be made on hypalon jacketing materials from other manufacturers in the absence of extensive laboratory testing results. It is also interesting to note that gel measurements can be easily and accurately made on very small samples (1 mg or less), implying that useful measurements could be made on very small pieces sliced from the outside of cable jackets.

References

IX-1. Anandakumaran K, et. al. "Improved conventional testing of power plant cables", EPRI Report TR-105581, September, 1995.

IX-2. Toman GJ, Hilditch JM, Butwin RT. "Diagnostic matrix for evaluation of low-voltage cable", EPRI Report TR-106108, November, 1997.

IX-3. Gazdzinski RF, Denny WM, Toman GJ, Butwin RT. "Aging management guideline for commercial nuclear power plants- electrical cable and terminations", Sandia Labs Report, SAND96-0344, September, 1996.

IX-4. Anandakumaran K, Stonkus DJ. Assessment of oxidative thermal degradation of crosslinked polyethylene and ethylene propylene rubber cable insulation. Polym Eng Sci 1992;32:1386.

IX-5. K. T. Gillen, R. A. Assink and R. Bernstein, "Condition Monitoring Approaches Applied to a Polychloroprene Cable Jacketing Material", Polym. Degrad. Stabil., 84, 419 (2004).

IX-6. K. T. Gillen, R. A. Assink, R. Bernstein and M. Celina, "Condition Monitoring Methods Applied to Chlorosulfonated polyethylene cable jacketing materials>", Polym. Degrad. Stabil., in press.

IX-7. T. Seguchi and Y. Yamamoto, "Diffusion and solubility of oxygen in gamma-ray irradiated polymer insulation materials", JAERI 1299 (March, 1986).

IX-8. M. Celina and K. T. Gillen, "Oxygen Permeability Measurements on Elastomers at Temperatures up to 225°C", Macromolecules, 38, 2754 (2005).

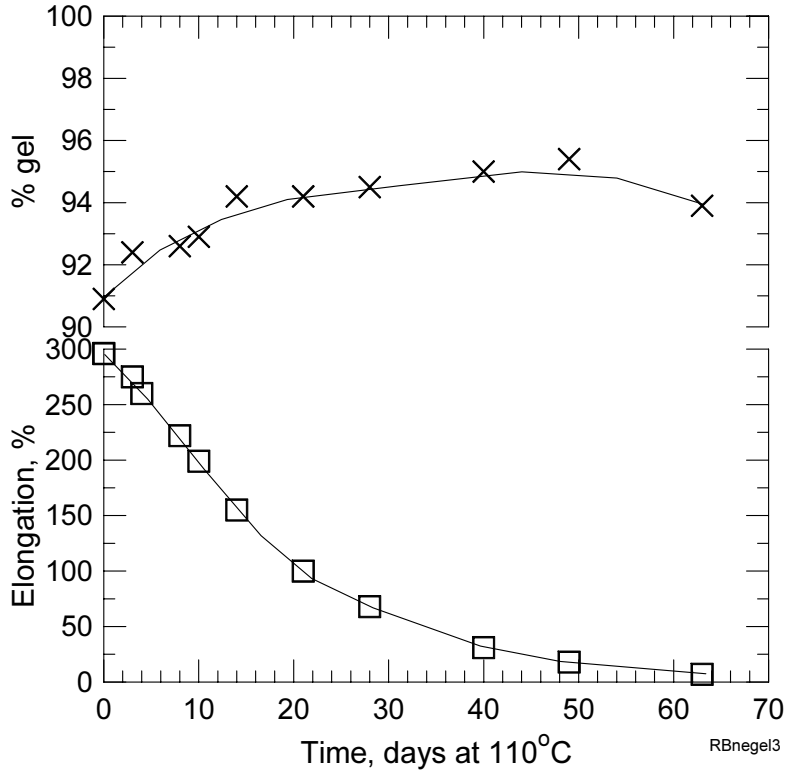

Figure IX-1. Elongation and percentage gel for Neo-02 versus aging time at 110°C.

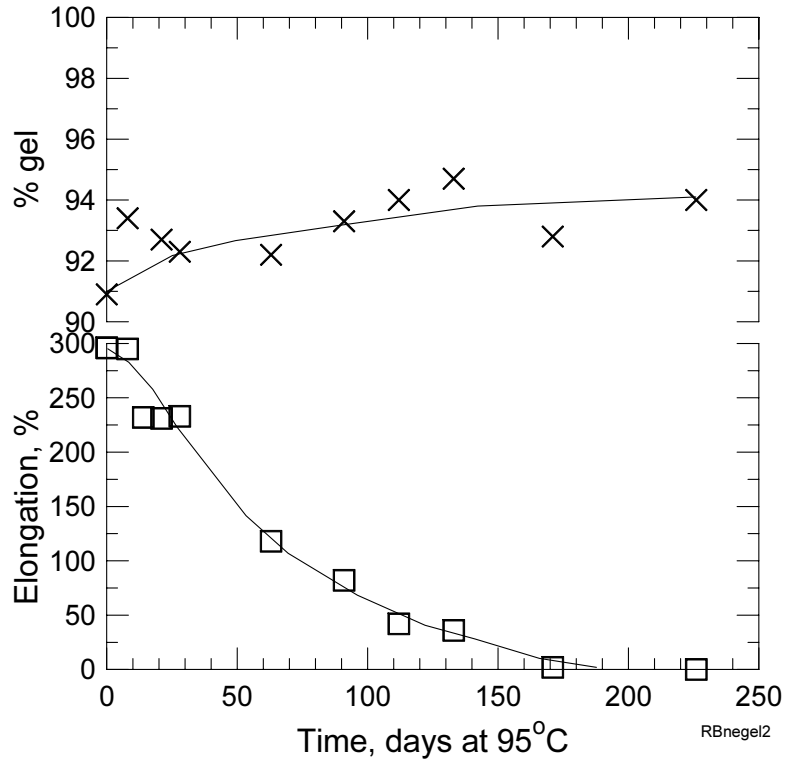

Figure IX-2. Elongation and percentage gel for Neo-02 versus aging time at 95°C.

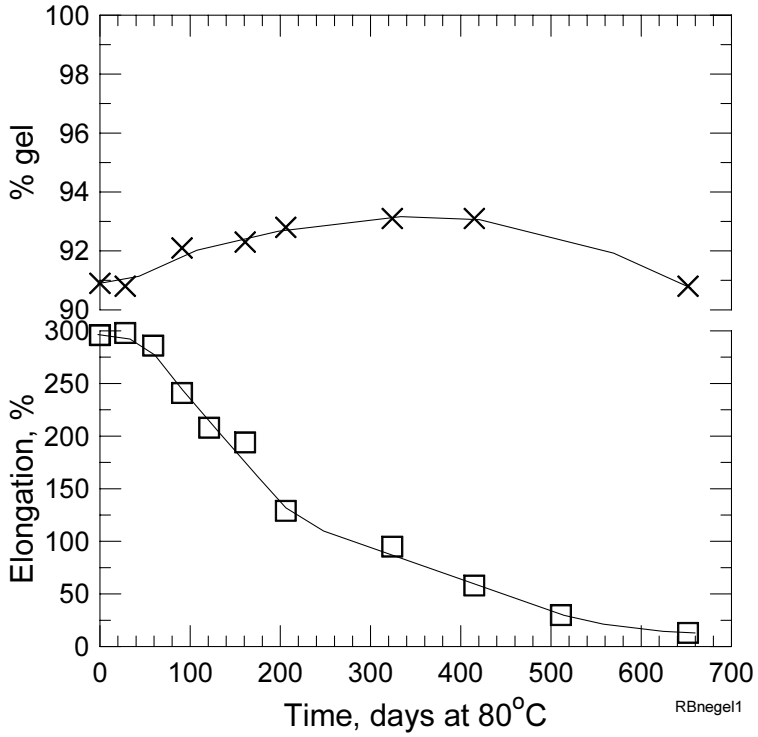

Figure IX-3. Elongation and percentage gel for Neo-02 versus aging time at 80°C.

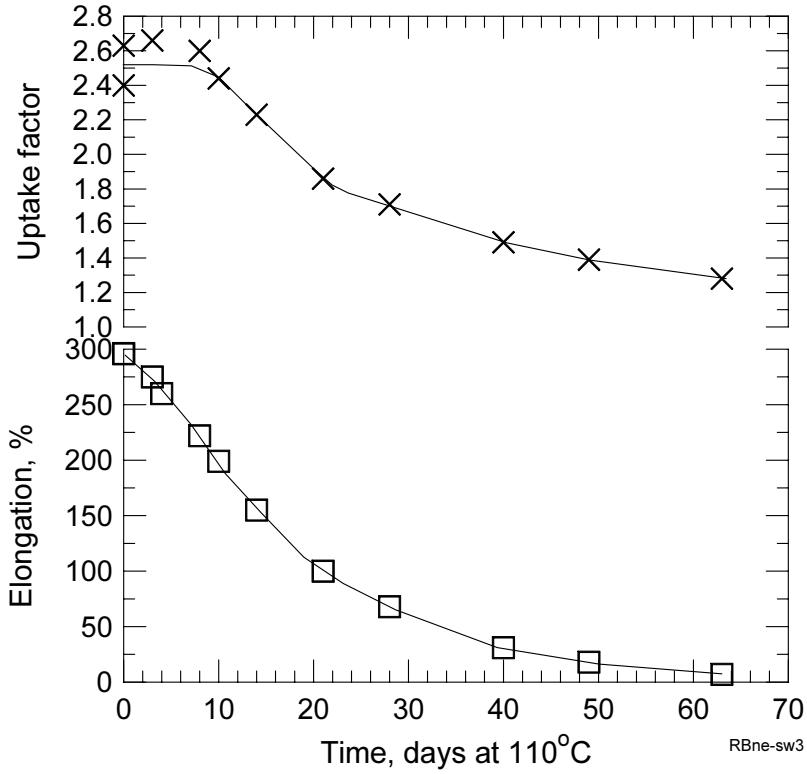

Figure IX-4. Elongation and uptake factor for Neo-02 versus aging time at 110°C.

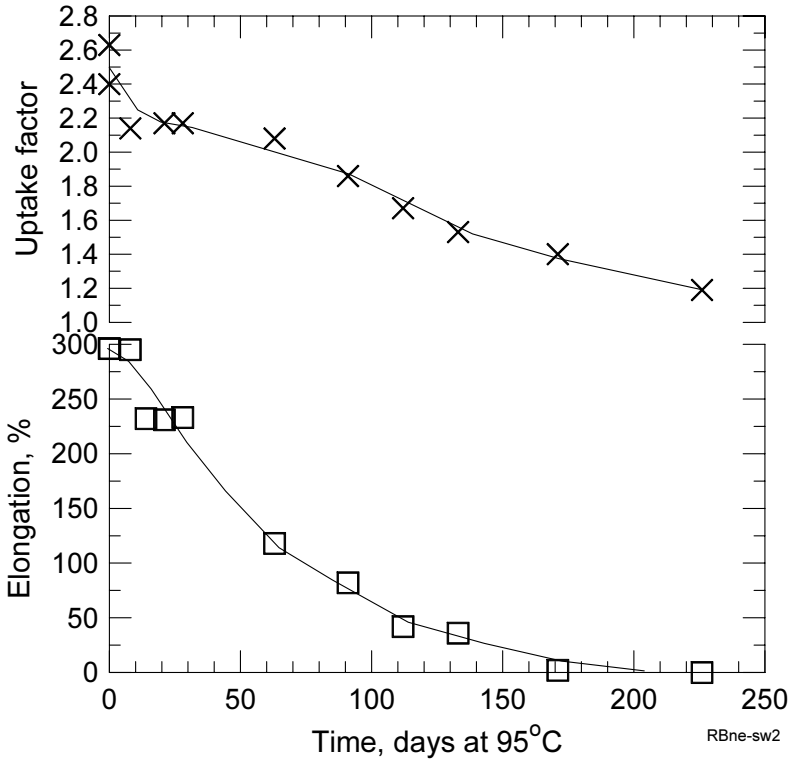

Figure IX-5. Elongation and uptake factor for Neo-02 versus aging time at 95°C.

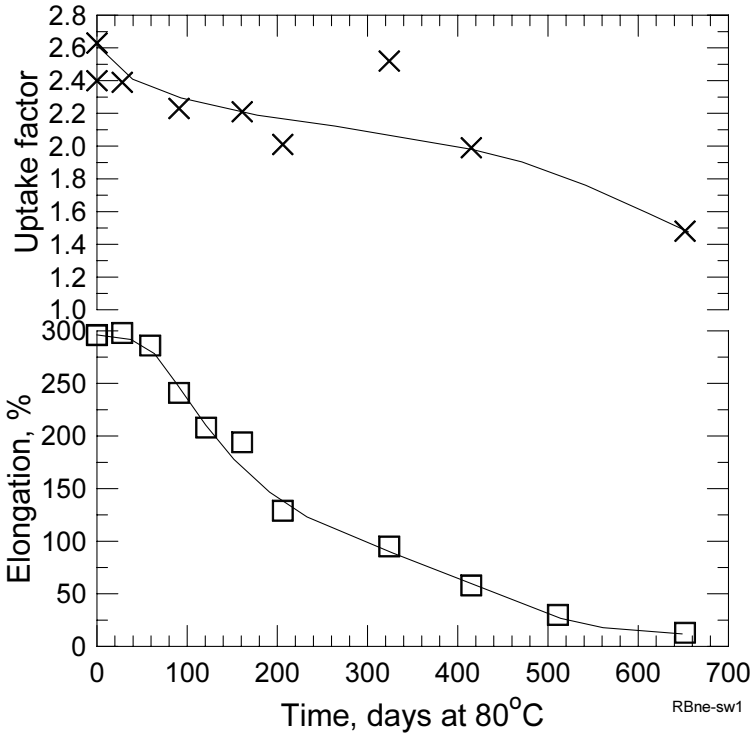

Figure IX-6. Elongation and uptake factor for Neo-02 versus aging time at 80°C.

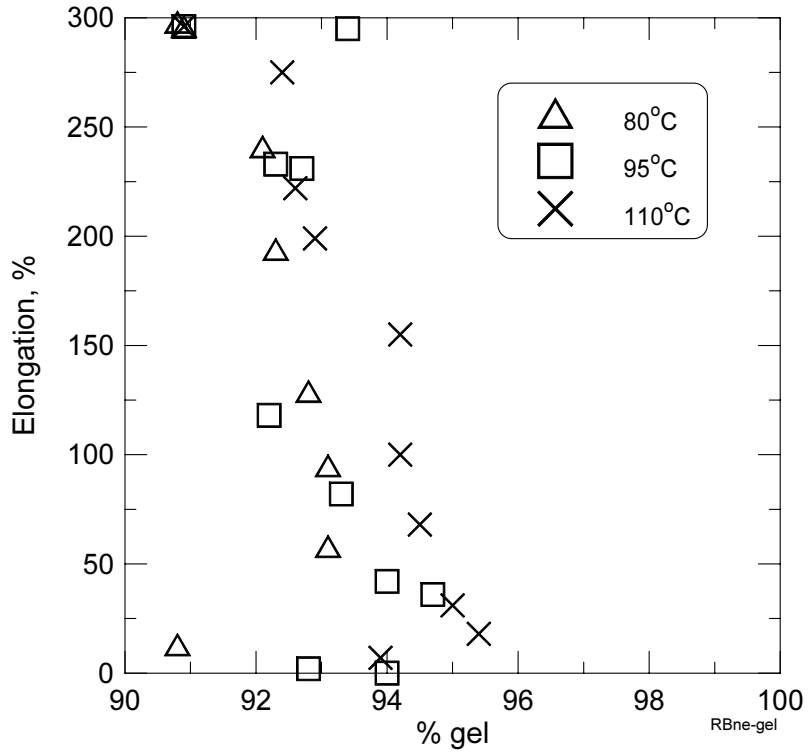

Figure IX-7. Elongation versus % gel for Neo-02 at the indicated aging temperatures.

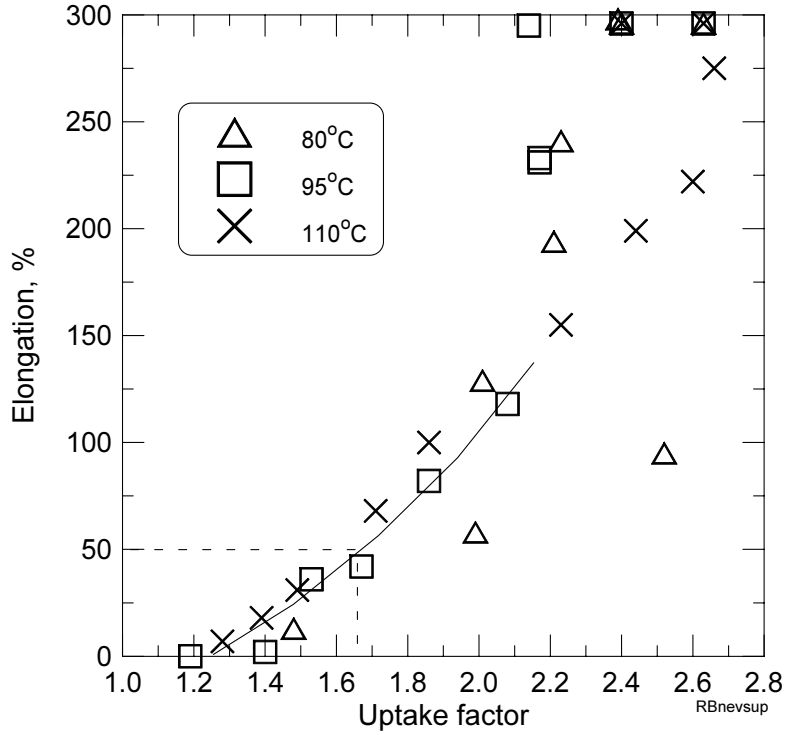

Figure IX-8. Elongation versus uptake factor for Neo-02 at the indicated aging temperatures.

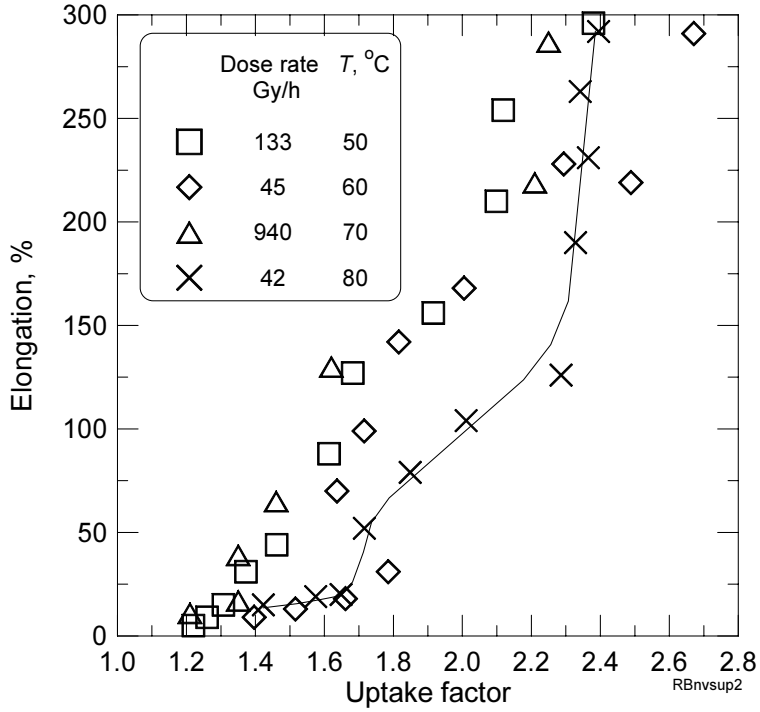

Figure IX-9. Elongation versus uptake factor for Neo-02 at the indicated combined-environment aging conditions.

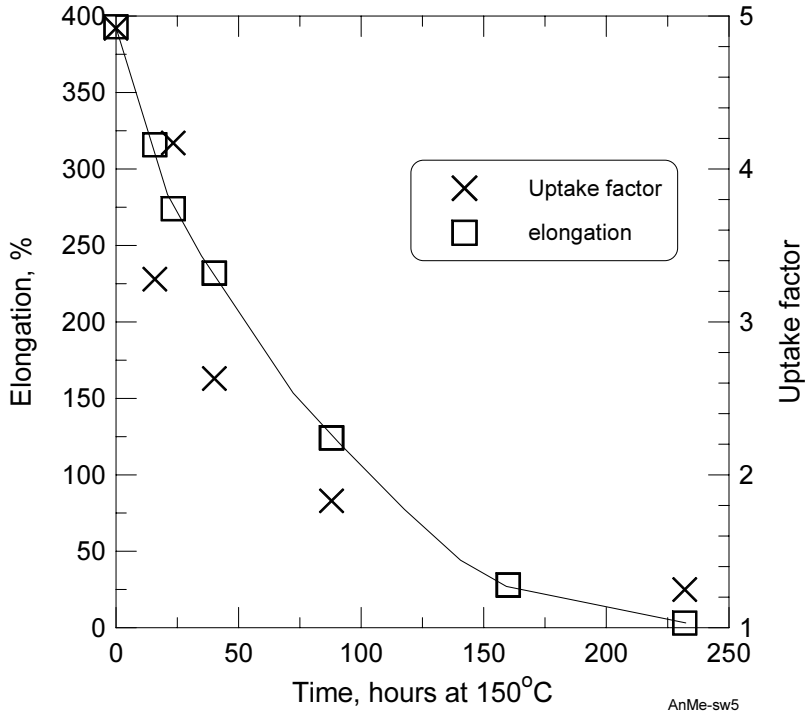

Figure IX-10. Elongation and uptake factor for Hyp-01A versus aging time at 150°C.

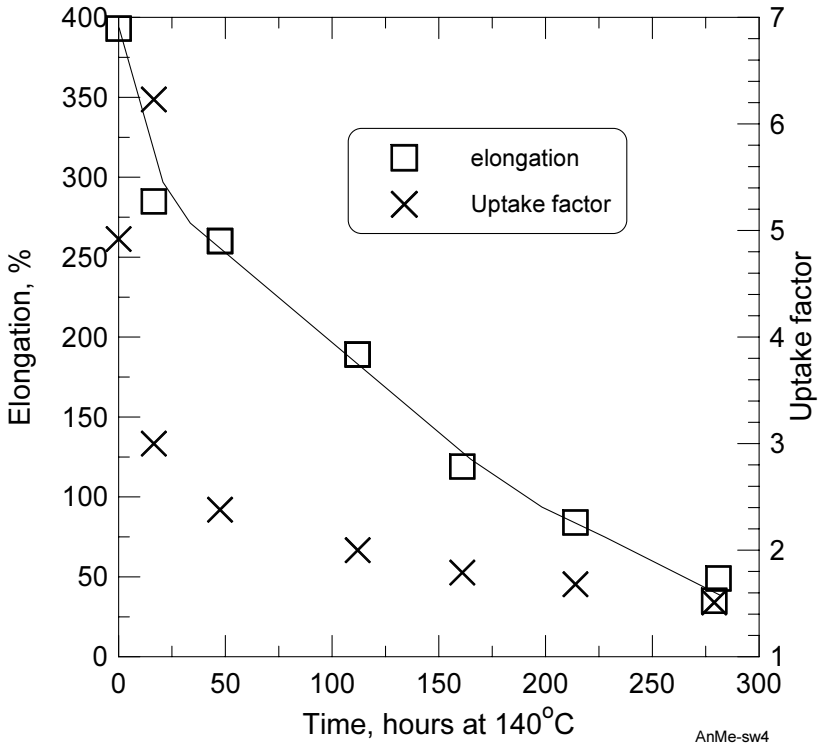

Figure IX-11. Elongation and uptake factor for Hyp-01A versus aging time at 140°C.

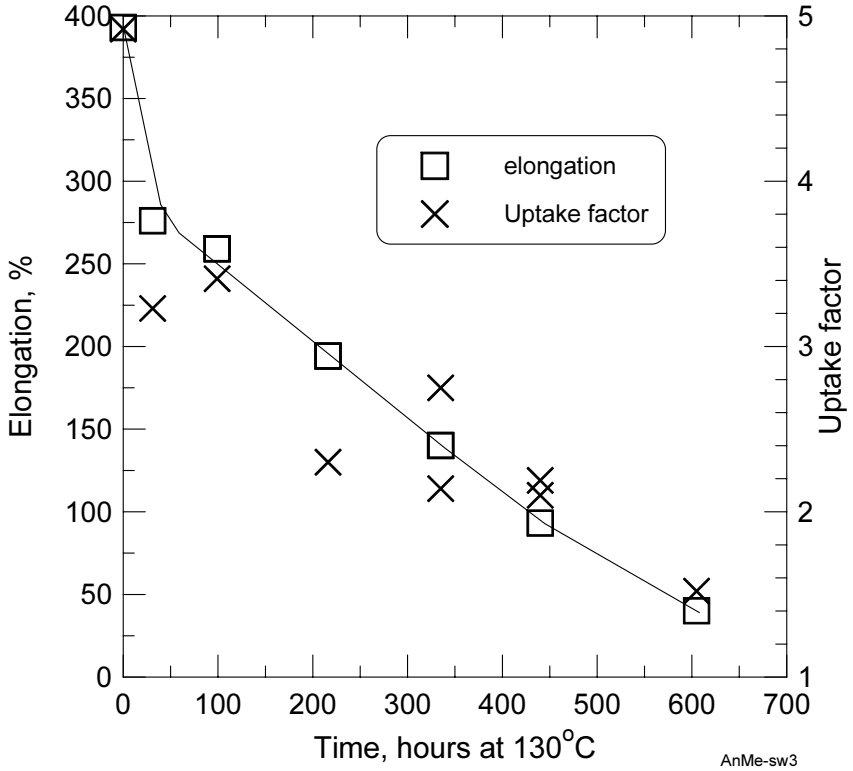

Figure IX-12. Elongation and uptake factor for Hyp-01A versus aging time at 130°C.

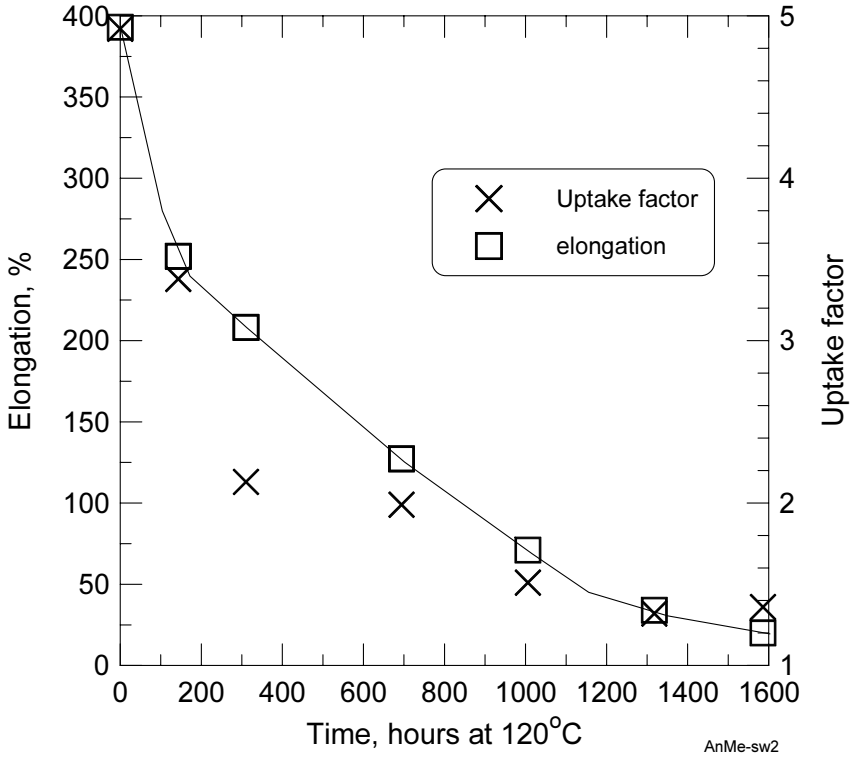

Figure IX-13. Elongation and uptake factor for Hyp-01A versus aging time at 120°C.

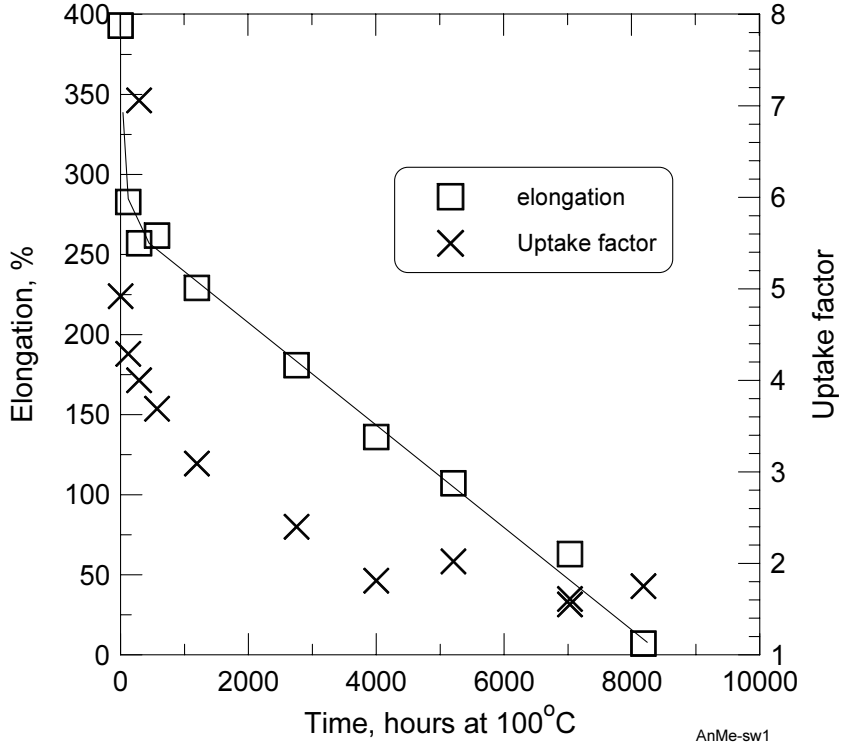

Figure IX-14. Elongation and uptake factor for Hyp-01A versus aging time at 100°C.

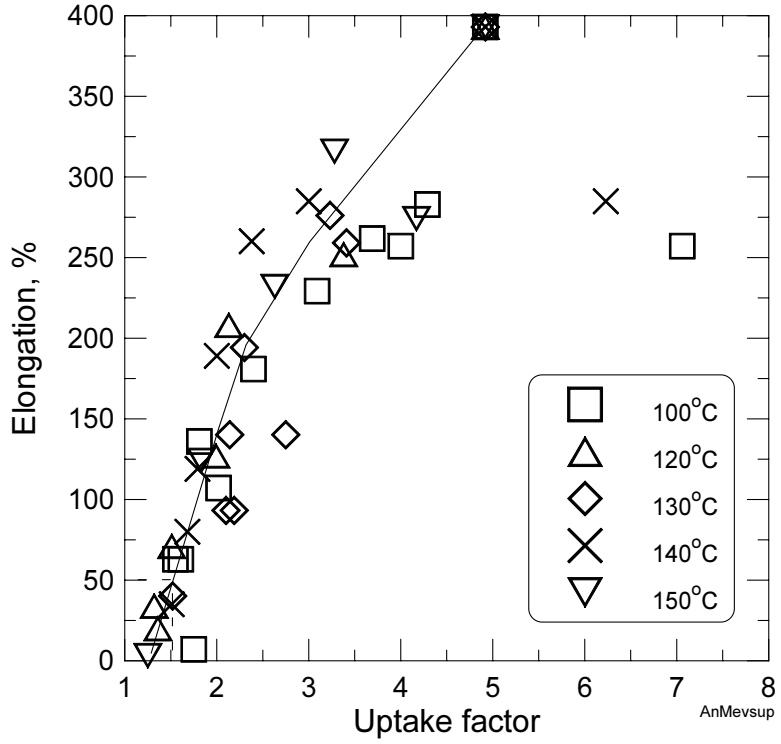

Figure IX-15. Elongation versus uptake factor for Hyp-01A at the indicated aging temperatures.

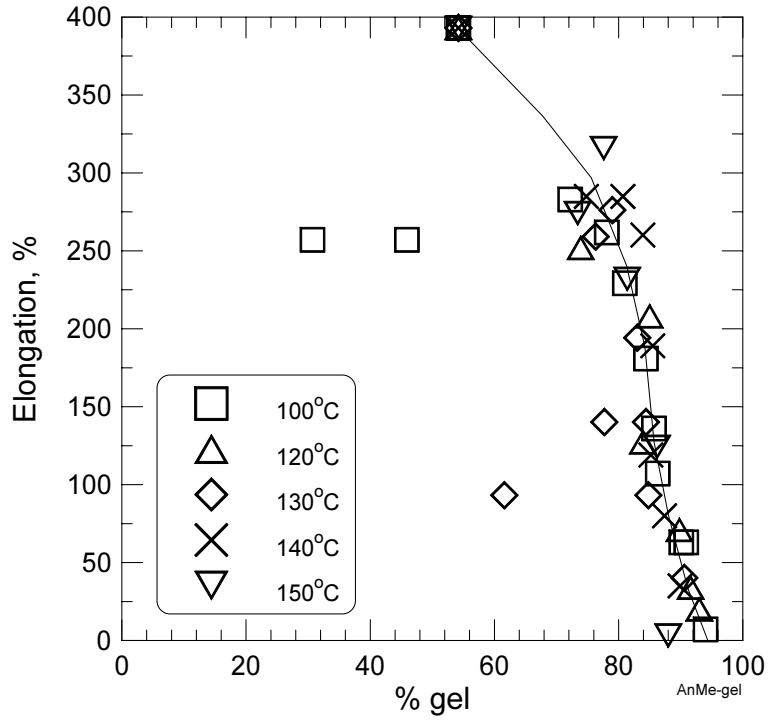

Figure IX-16. Elongation versus percentage gel for Hyp-01A at the indicated aging temperatures.

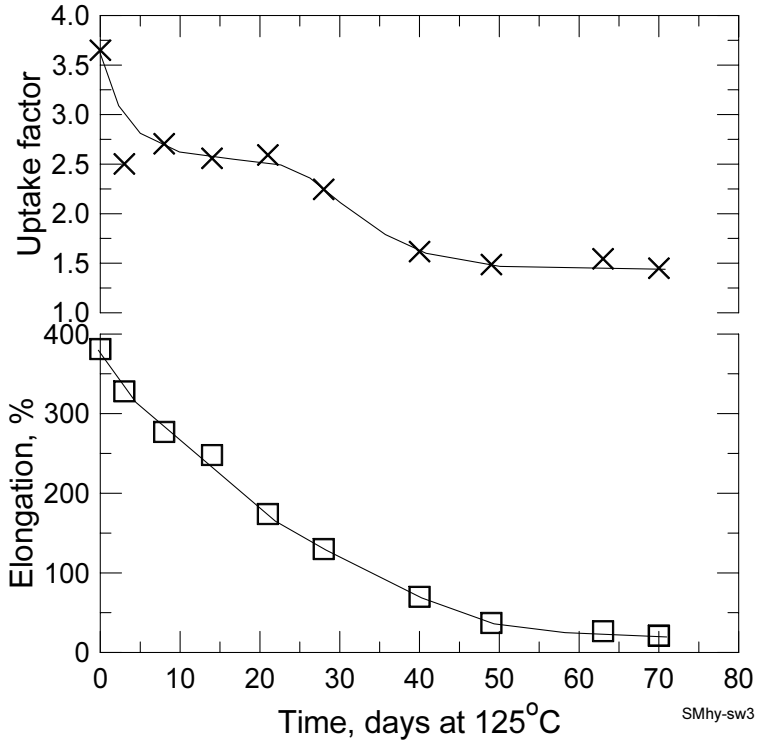

Figure IX-17. Elongation and uptake factor for Hyp-03 versus aging time at 125°C.

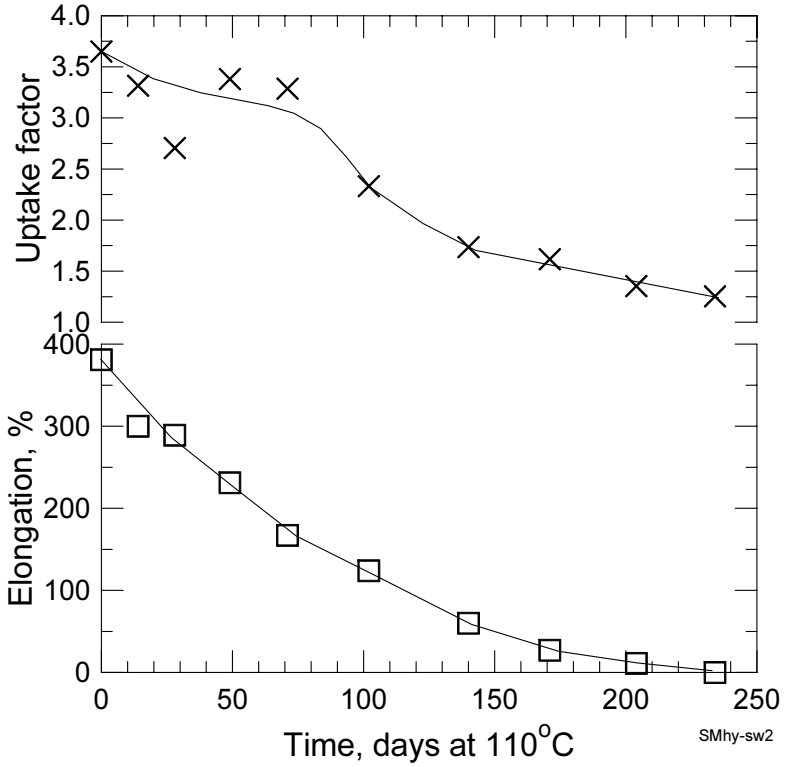

Figure IX-18. Elongation and uptake factor for Hyp-03 versus aging time at 110°C.

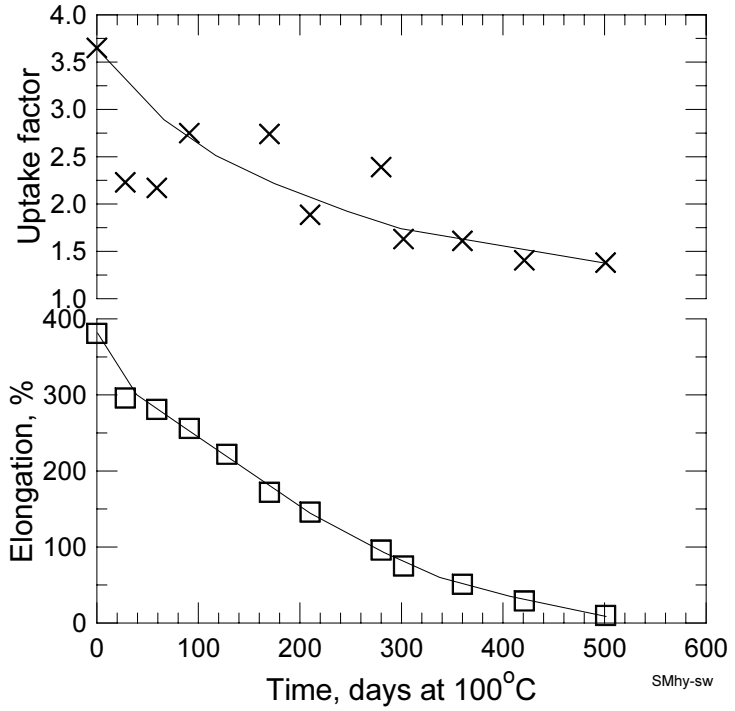

Figure IX-19. Elongation and uptake factor for Hyp-03 versus aging time at 100°C.

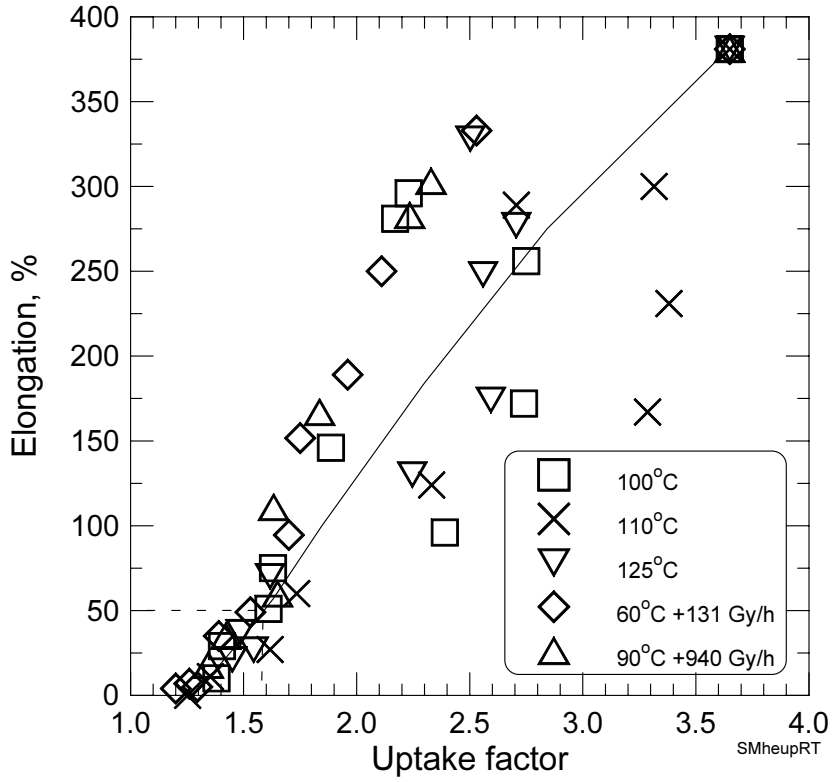

Figure IX-20. Elongation versus uptake factor for Hyp-03 at the indicated aging temperatures and combined environments.

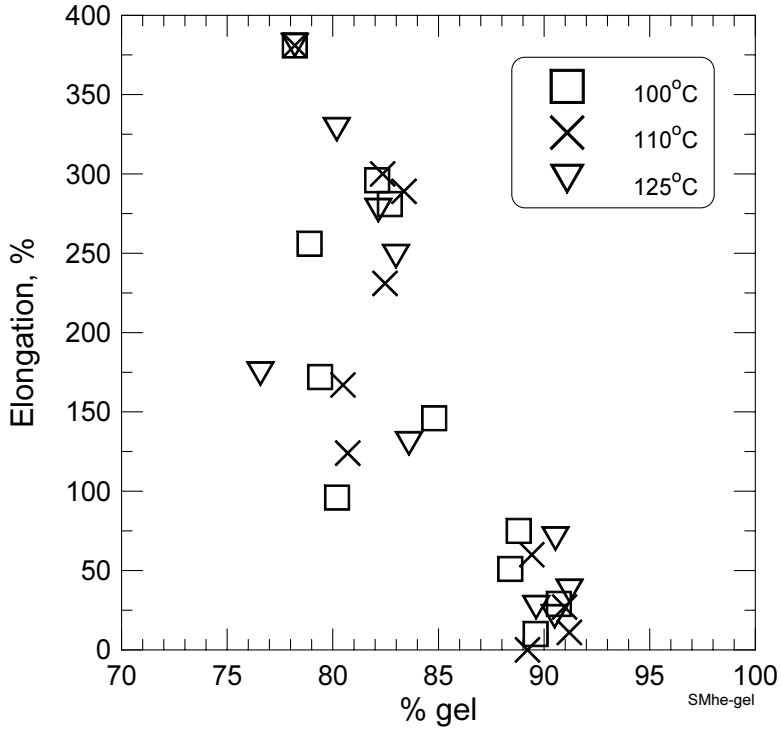

Figure IX-21. Elongation versus percentage gel for Hyp-03 at the indicated aging temperatures and combined environments.

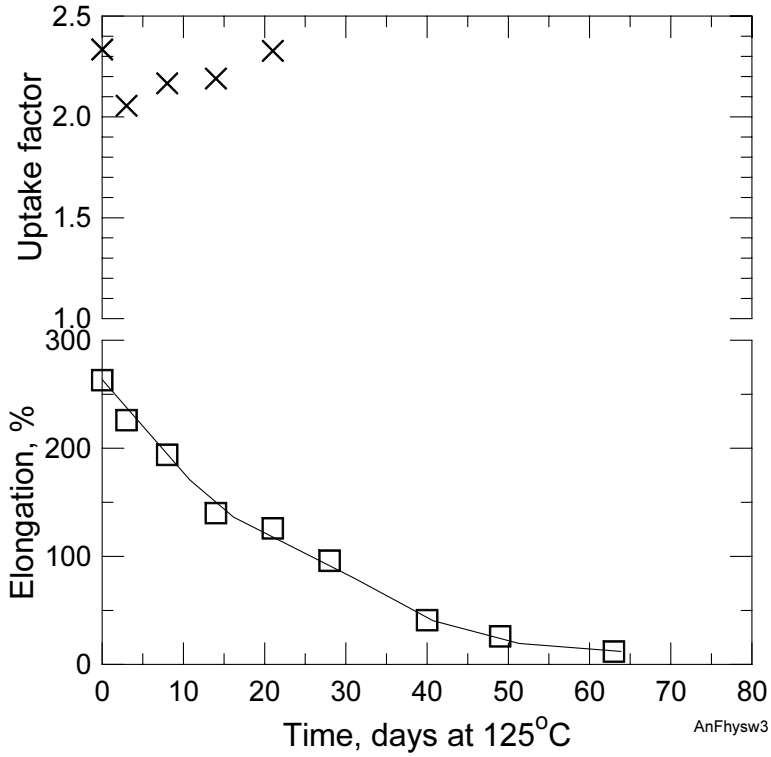

Figure IX-22. Elongation and uptake factor for Hyp-04 versus aging time at 125°C.

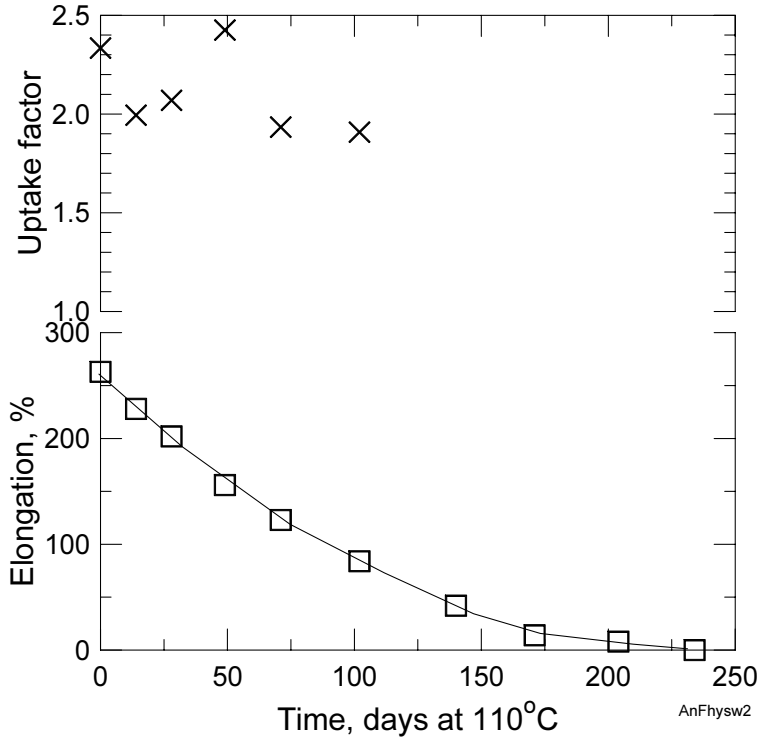

Figure IX-23. Elongation and uptake factor for Hyp-04 versus aging time at 110°C.

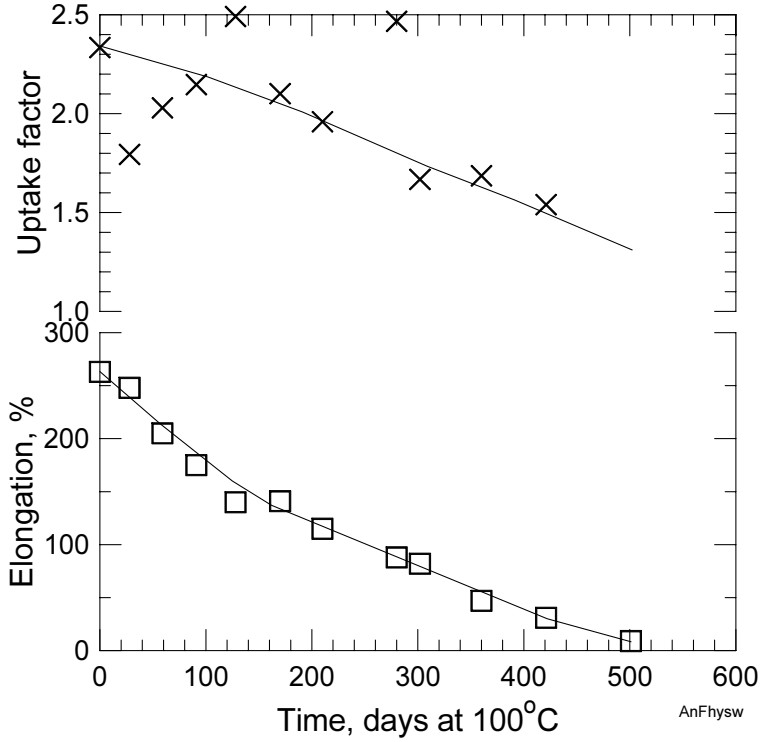

Figure IX-24. Elongation and uptake factor for Hyp-04 versus aging time at 100°C.

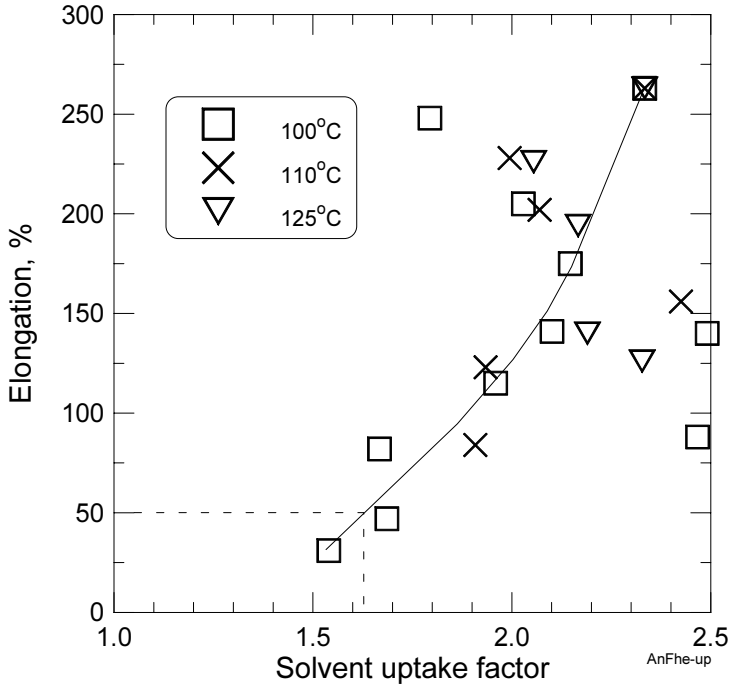

Figure IX-25. Elongation versus uptake factor for Hyp-04 at the indicated aging temperatures.

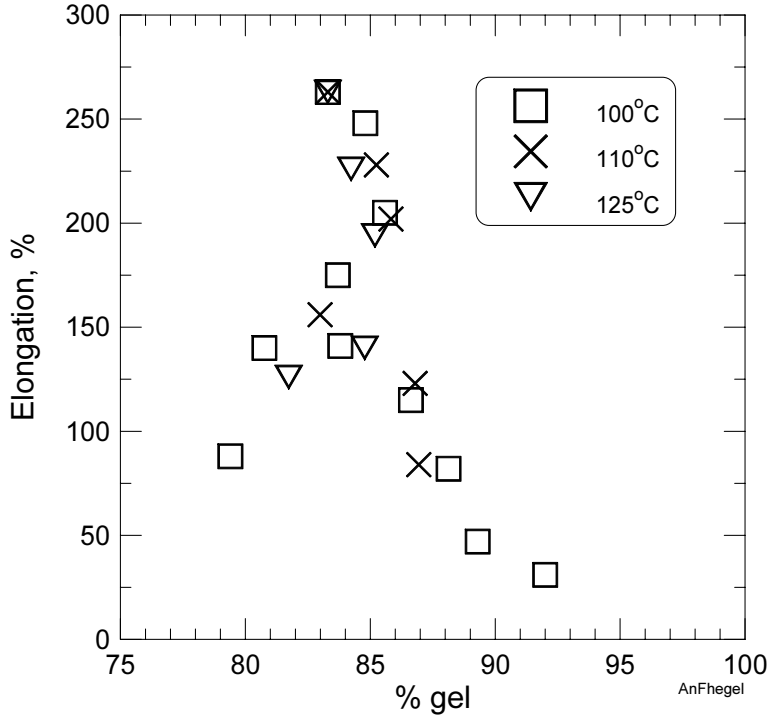

Figure IX-26. Elongation versus percentage gel for Hyp-04 at the indicated aging temperatures.

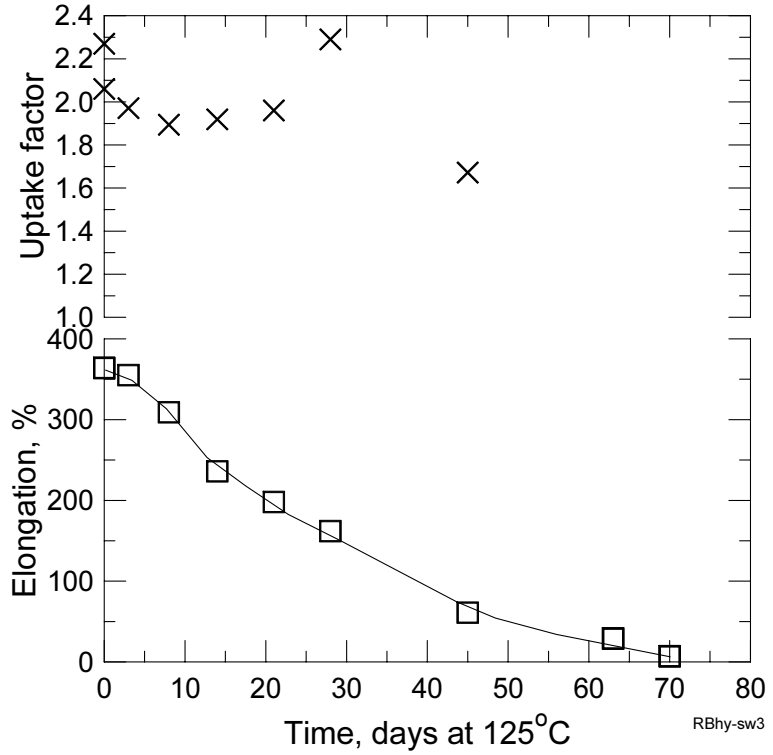

Figure IX-27. Elongation and uptake factor for Hyp-05 versus aging time at 125°C.

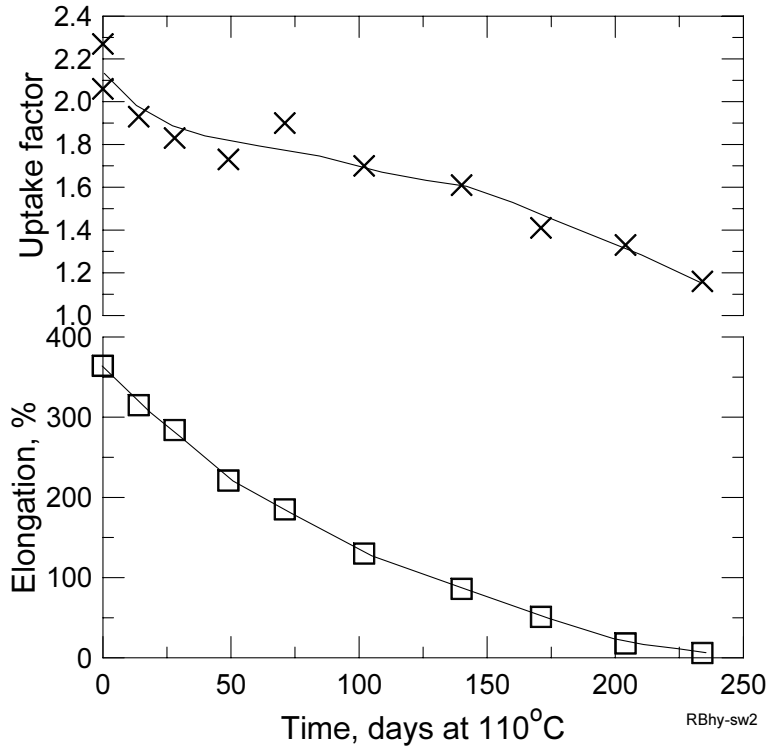

Figure IX-28. Elongation and uptake factor for Hyp-05 versus aging time at 110°C.

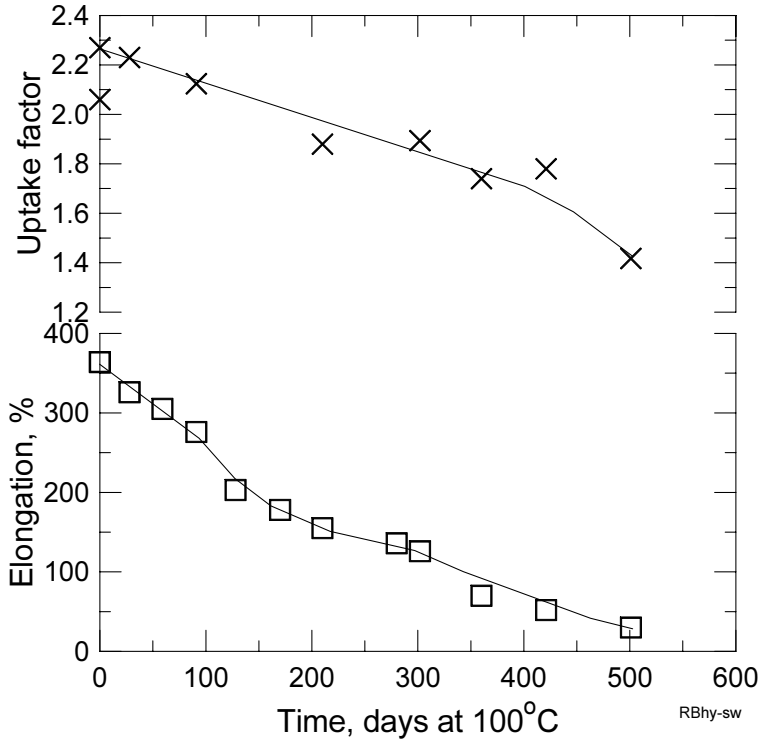

Figure IX-29. Elongation and uptake factor for Hyp-05 versus aging time at 100°C.

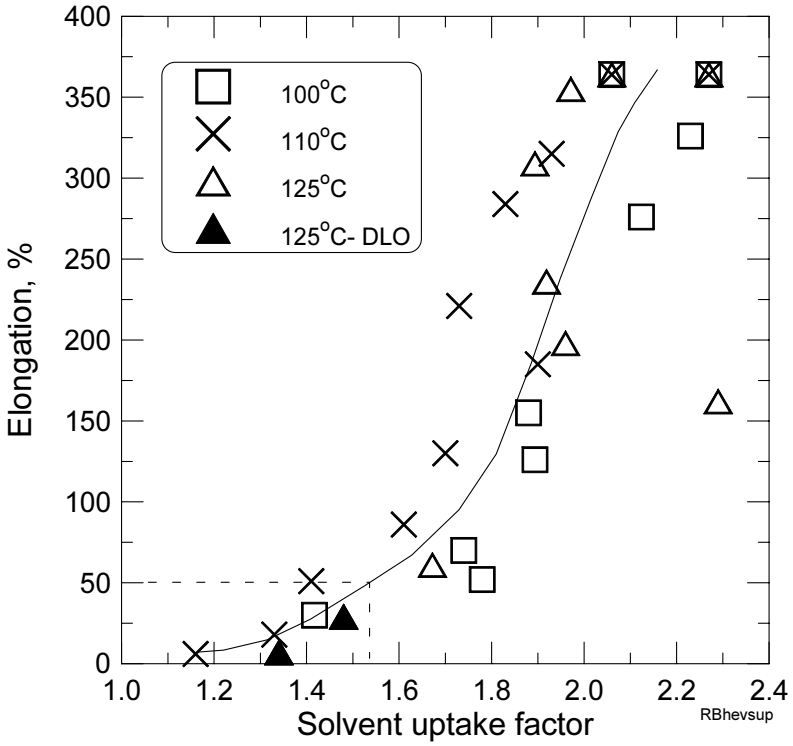

Figure IX-30. Elongation versus uptake factor for Hyp-05 at the indicated aging temperatures, including two data points influenced by DLO effects.

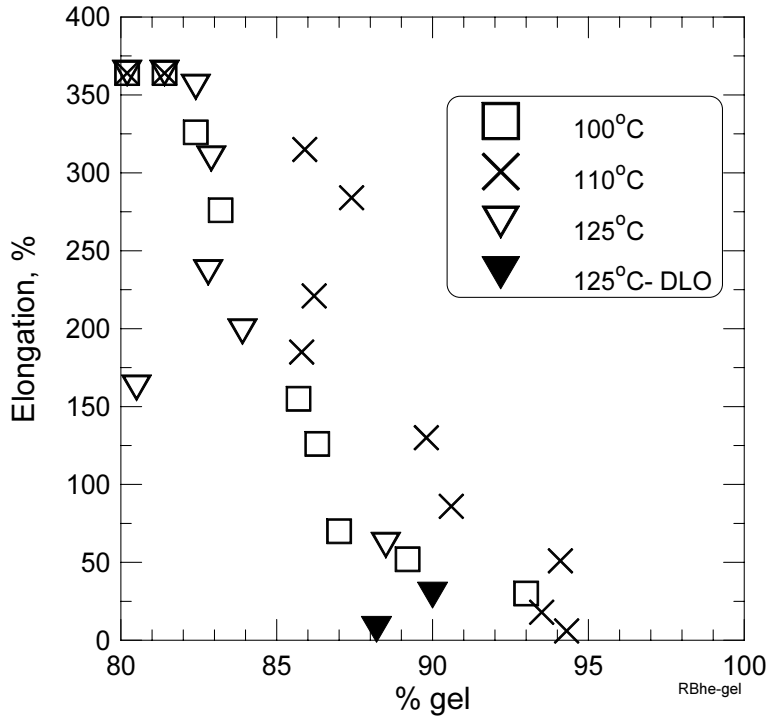

Figure IX-31. Elongation versus percentage gel for Hyp-05 at the indicated aging temperatures, including two data points influenced by DLO effects.

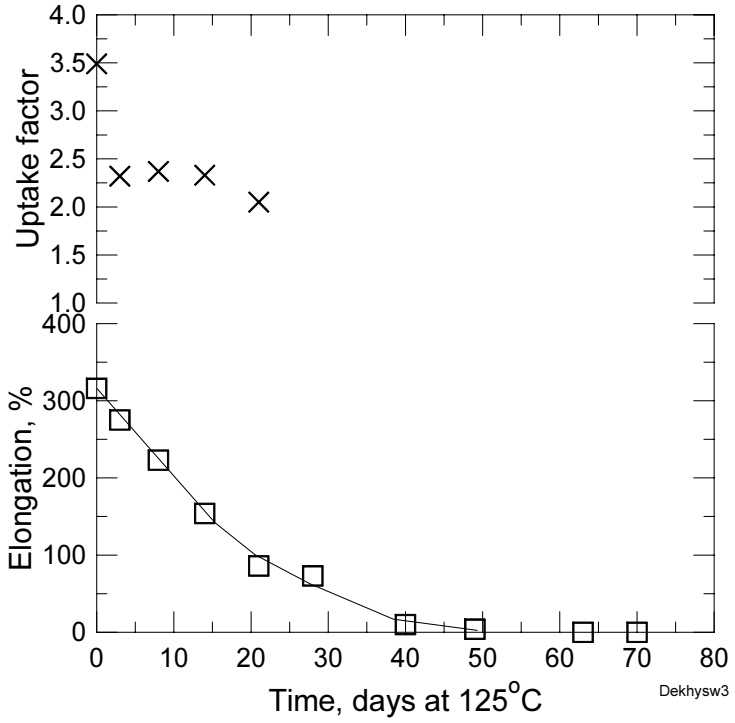

Figure IX-32. Elongation and uptake factor for Hyp-06 versus aging time at 125°C.

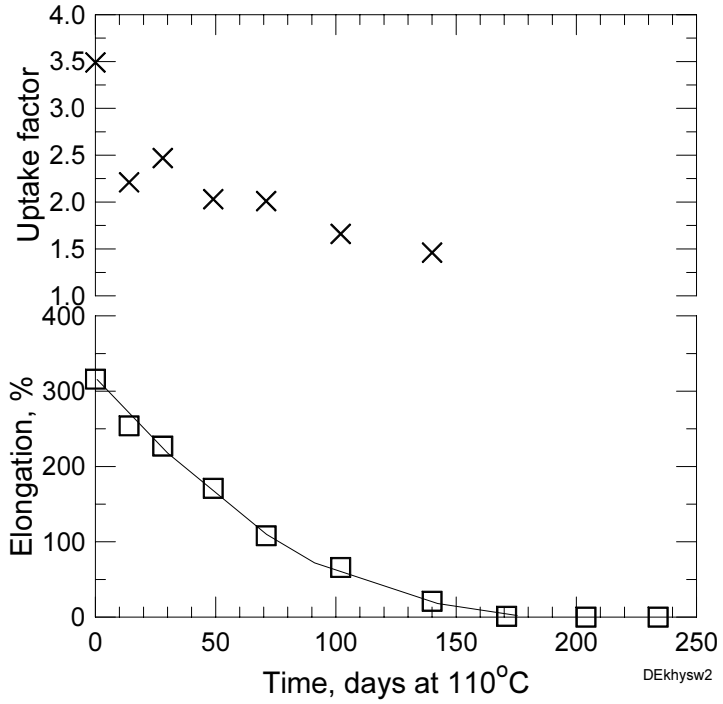

Figure IX-33. Elongation and uptake factor for Hyp-06 versus aging time at 110°C.

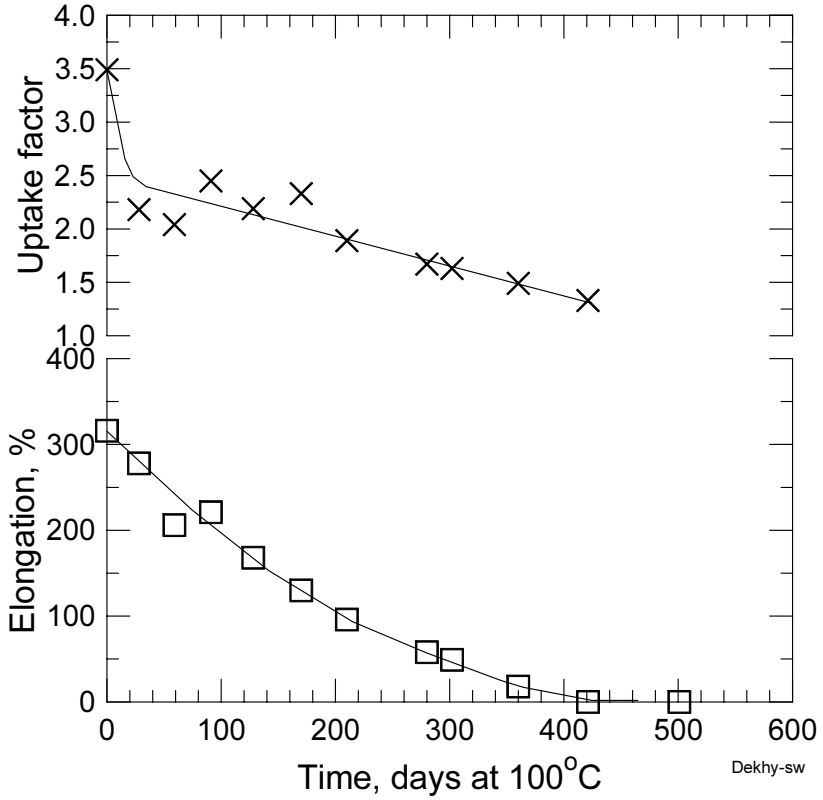

Figure IX-34. Elongation and uptake factor for Hyp-06 versus aging time at 100°C.

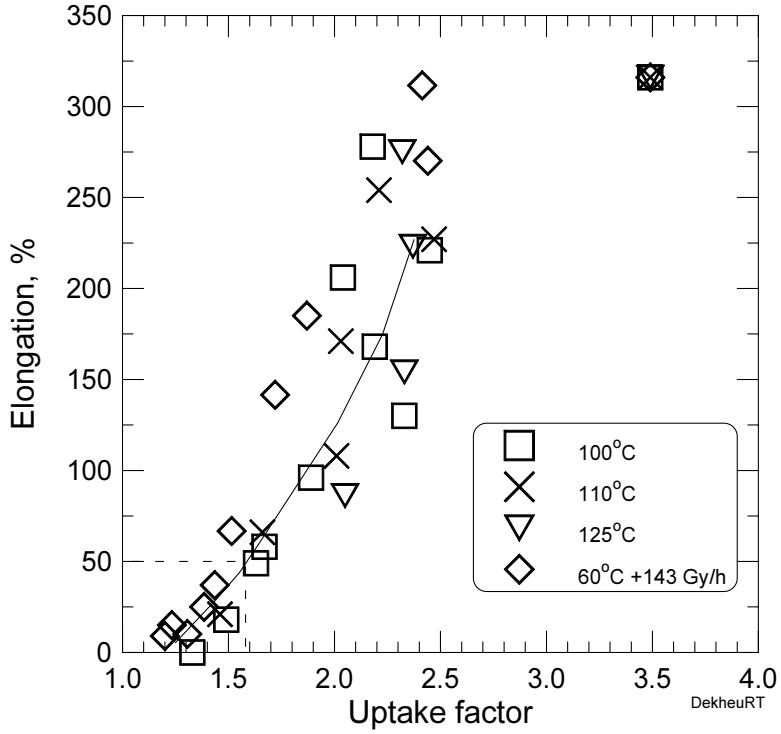

Figure IX-35. Elongation versus uptake factor for Hyp-06 at the indicated aging conditions.

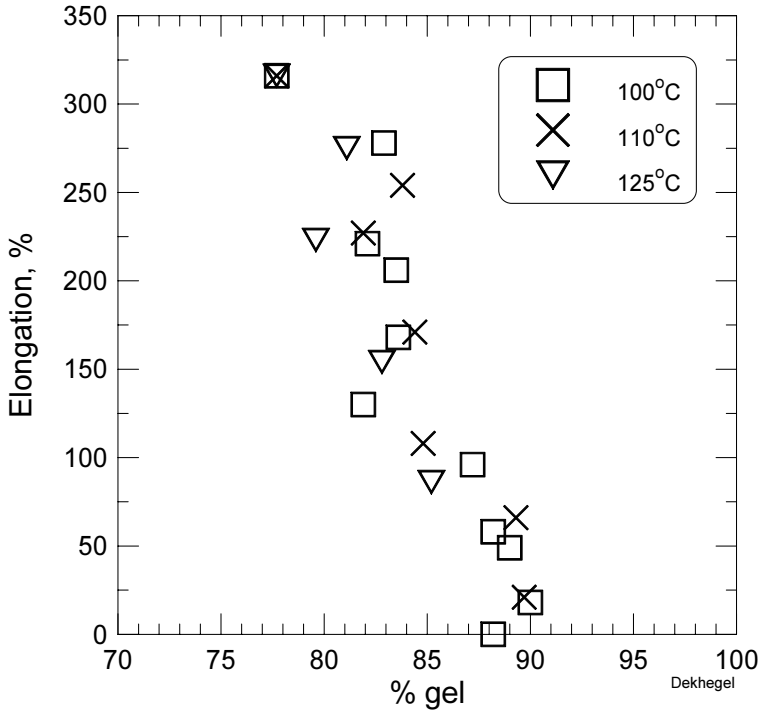

Figure IX-36. Elongation versus percentage gel for Hyp-06 at the indicated aging conditions.

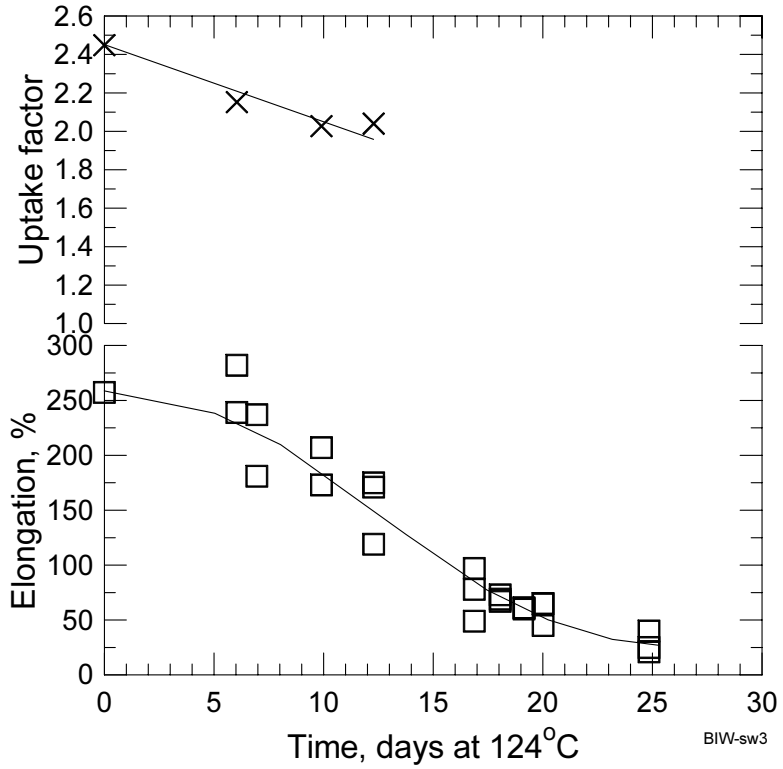

Figure IX-37. Elongation and uptake factor for Hyp-08 versus aging time at 124°C.

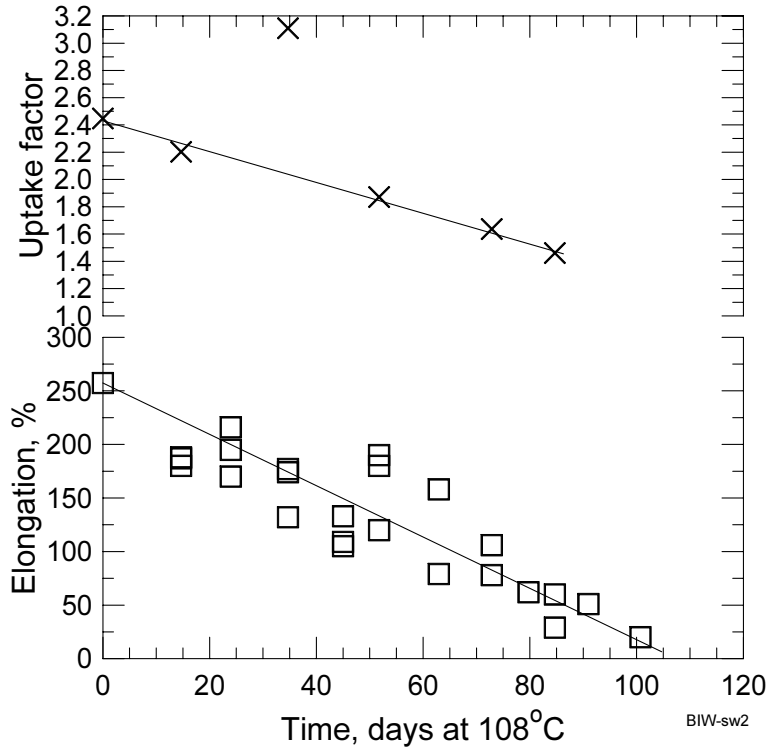

Figure IX-38. Elongation and uptake factor for Hyp-08 versus aging time at 108°C.

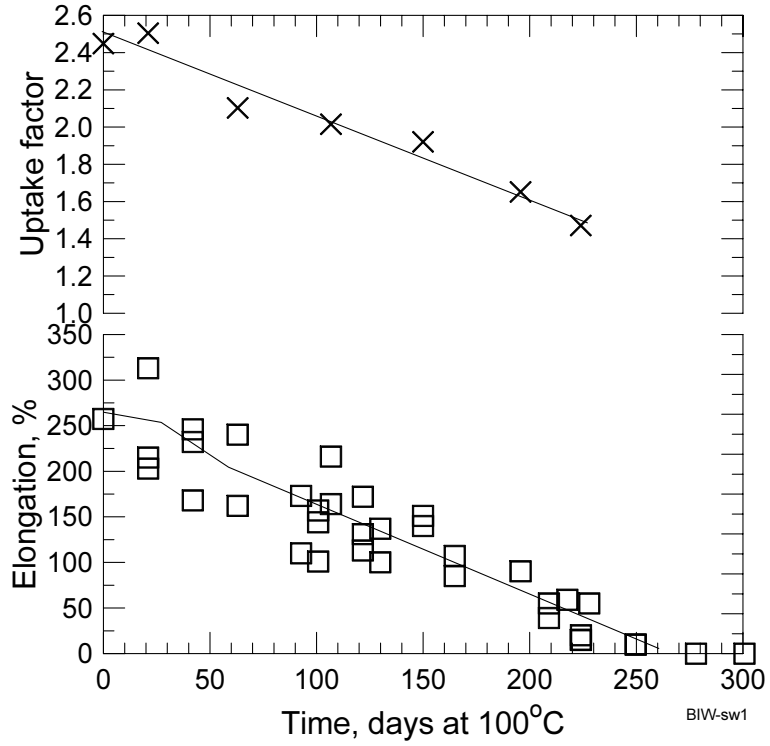

Figure IX-39. Elongation and uptake factor for Hyp-08 versus aging time at 100°C.

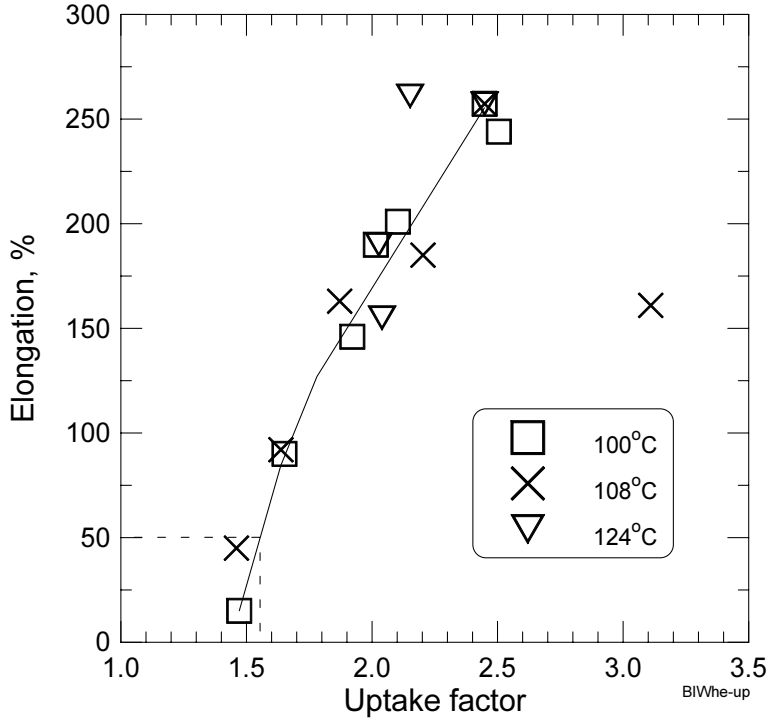

Figure IX-40. Elongation versus uptake factor for Hyp-08 at the indicated aging conditions.

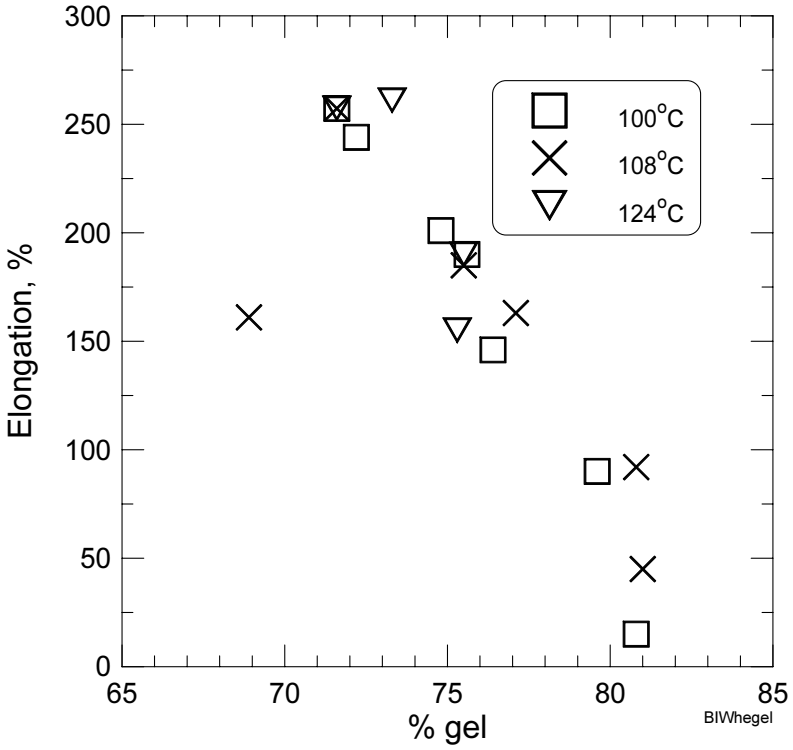

Figure IX-41. Elongation versus percentage gel for Hyp-08 at the indicated aging conditions.

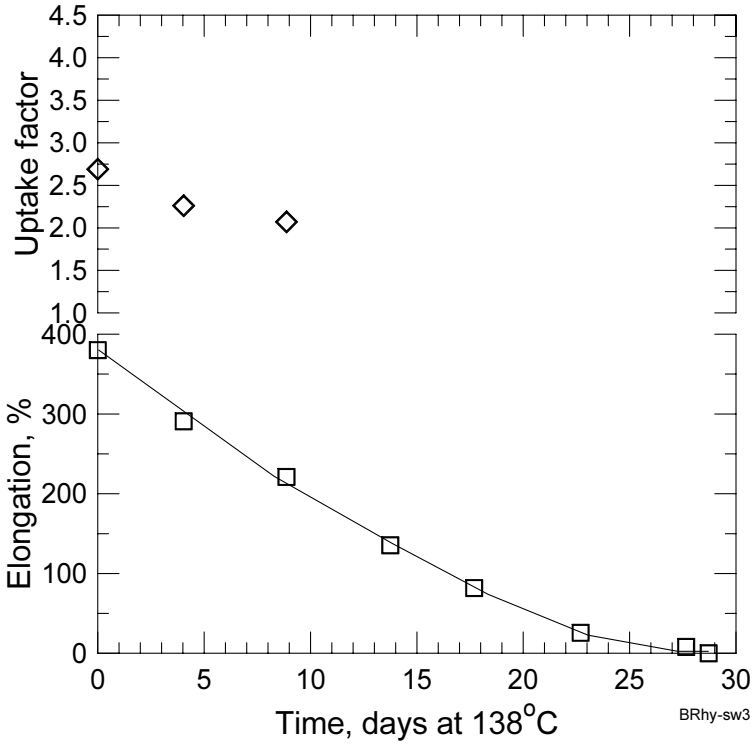

Figure IX-42. Elongation and uptake factor for Hyp-07 versus aging time at 138°C.

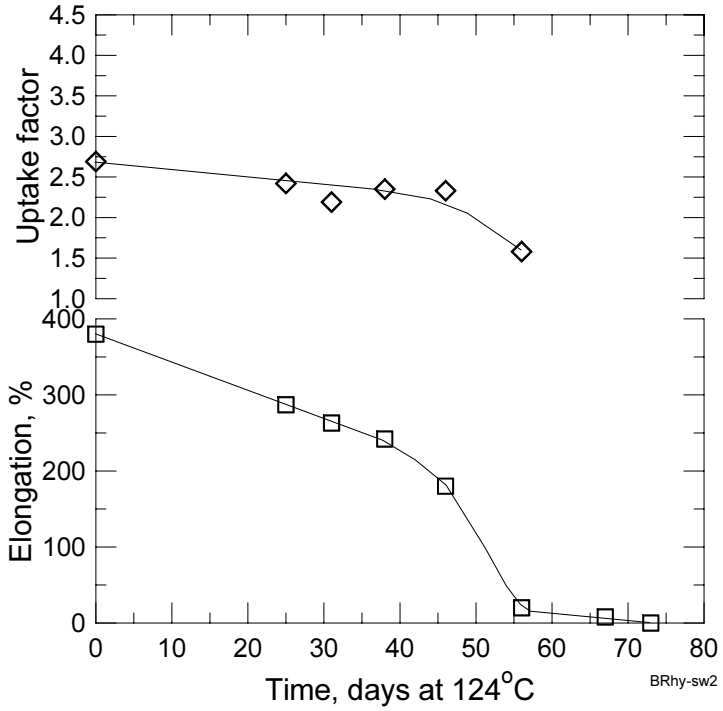

Figure IX-43. Elongation and uptake factor for Hyp-07 versus aging time at 124°C.

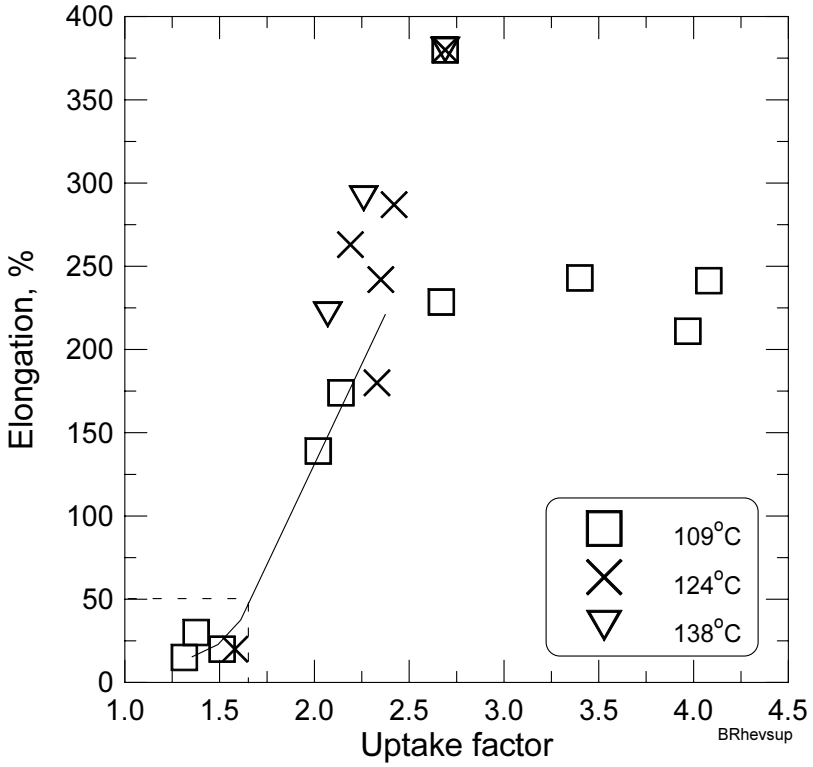

Figure IX-44. Elongation versus uptake factor for Hyp-07 at the indicated aging conditions.

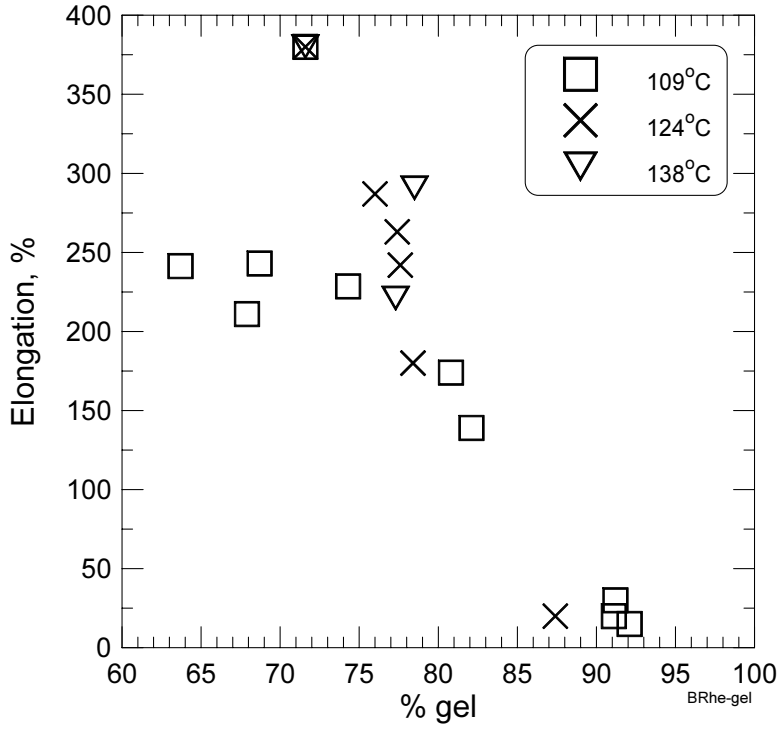

Figure IX-45. Elongation versus percentage gel for Hyp-07 at the indicated aging conditions.

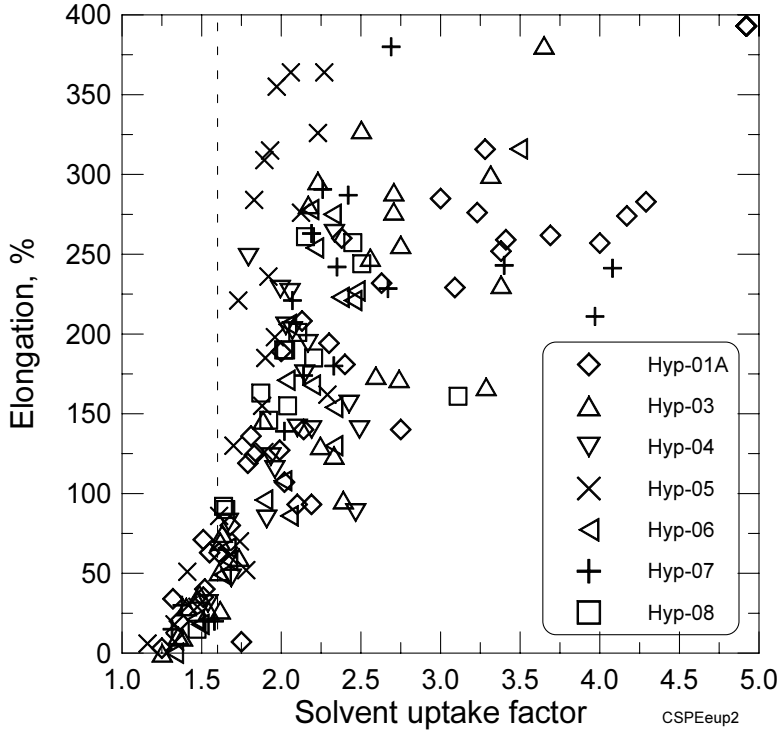

Figure IX-46. Elongation versus uptake factor (non-DLO-influenced samples) for the seven indicated hypalon materials for every thermal-only aging condition.

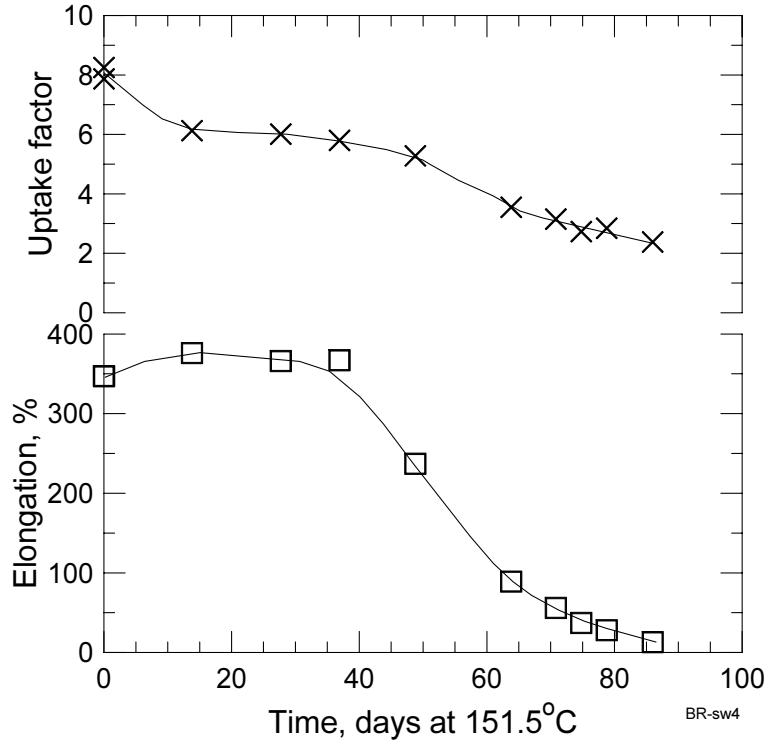

Figure IX-47. Elongation and uptake factor for XLPO-02B versus aging time at 151.5°C.

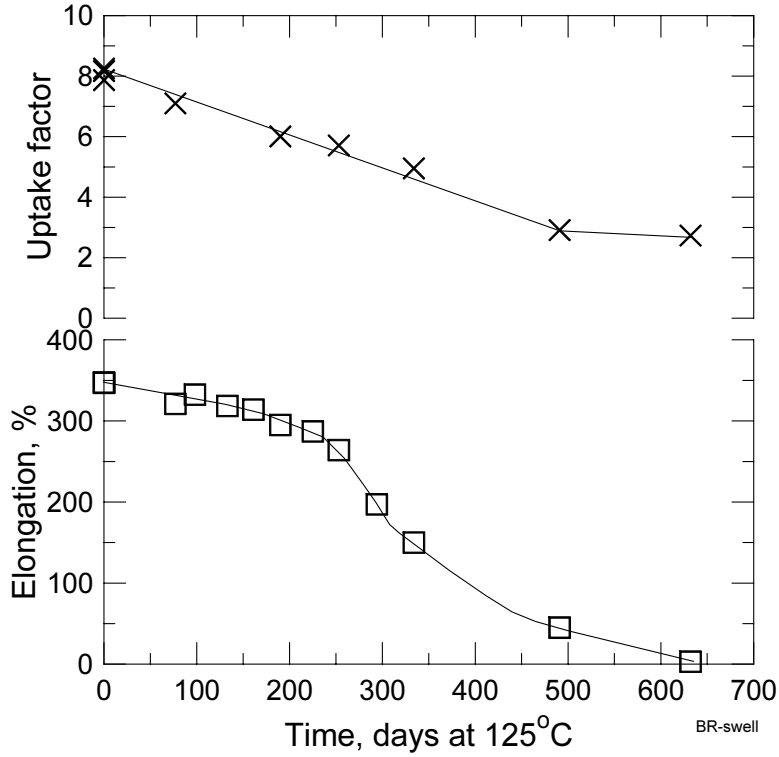

Figure IX-48. Elongation and uptake factor for XLPO-02B versus aging time at 125°C.

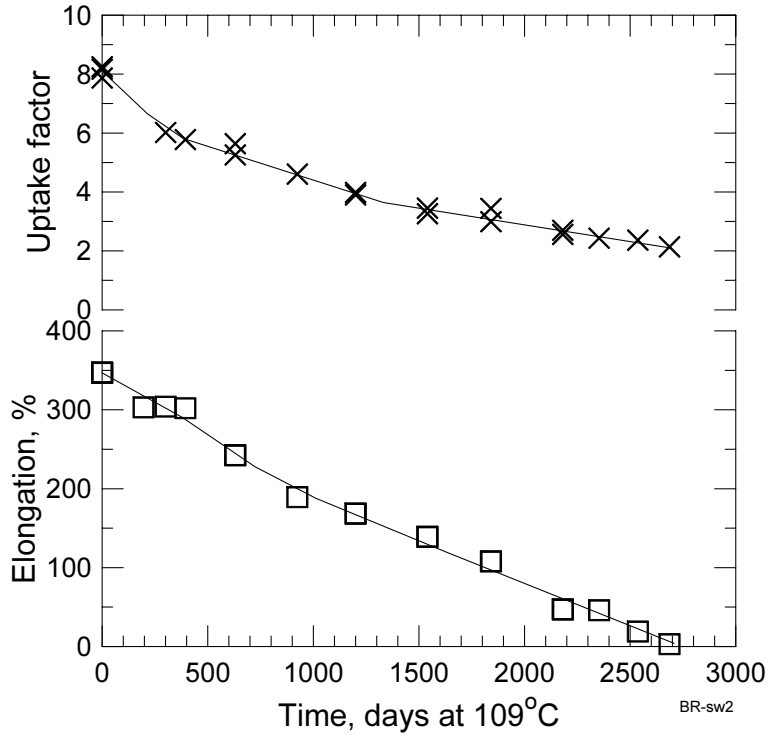

Figure IX-49. Elongation and uptake factor for XLPO-02B versus aging time at 109°C.

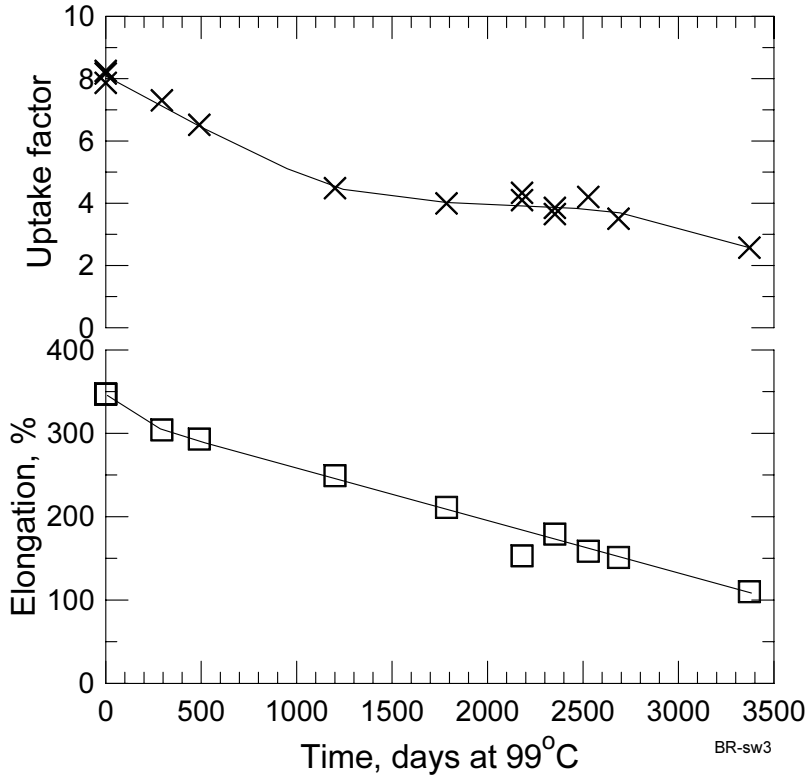

Figure IX-50. Elongation and uptake factor for XLPO-02B versus aging time at 99°C.

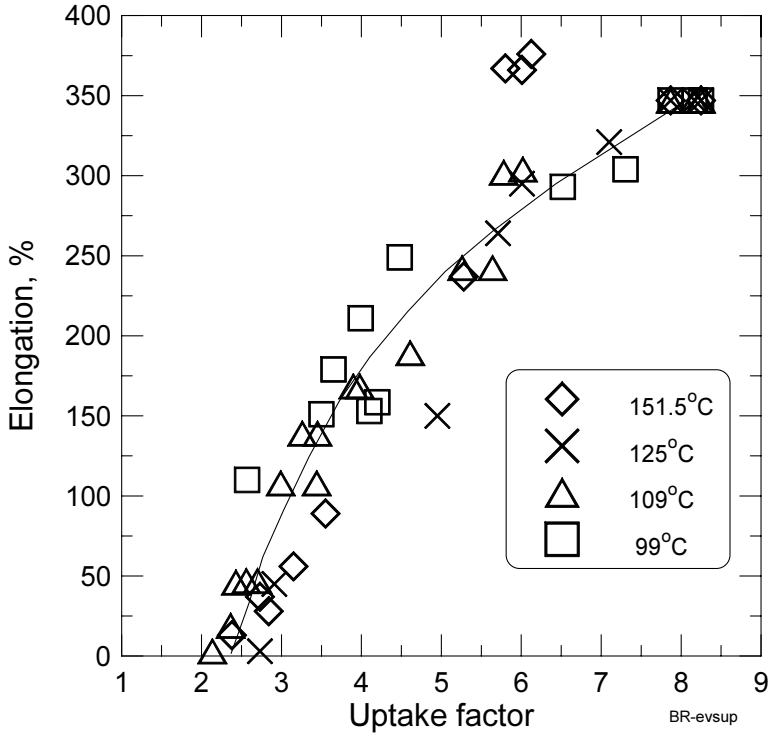

Figure IX-51. Elongation versus uptake factor for XLPO-02B for all thermal aging conditions.

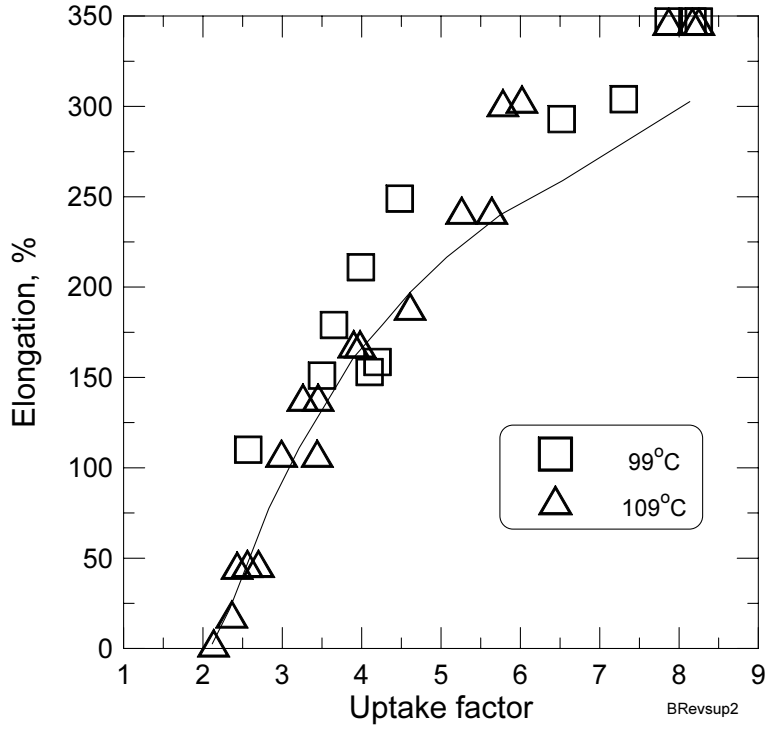

Figure IX-52. Elongation versus uptake factor for XLPO-02B for the two aging temperatures below the main melting peak.

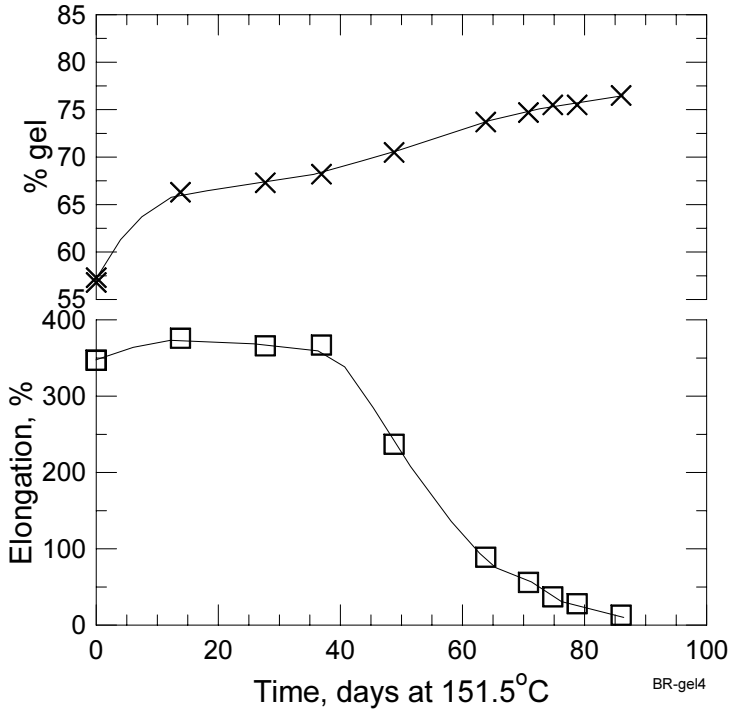

Figure IX-53. Elongation and percentage gel for XLPO-02B versus aging time at 151.5°C.

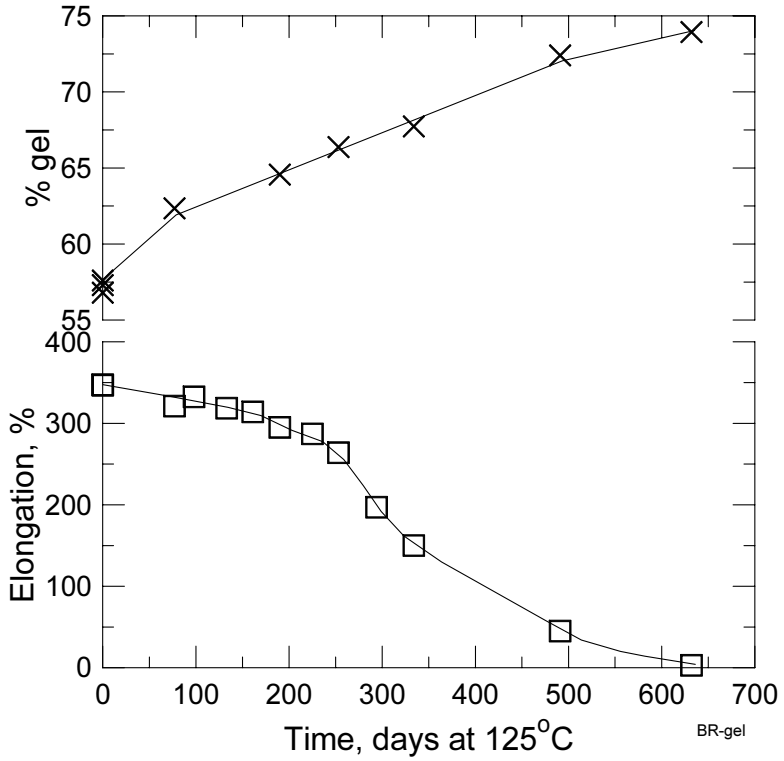

Figure IX-54. Elongation and percentage gel for XLPO-02B versus aging time at 125°C.

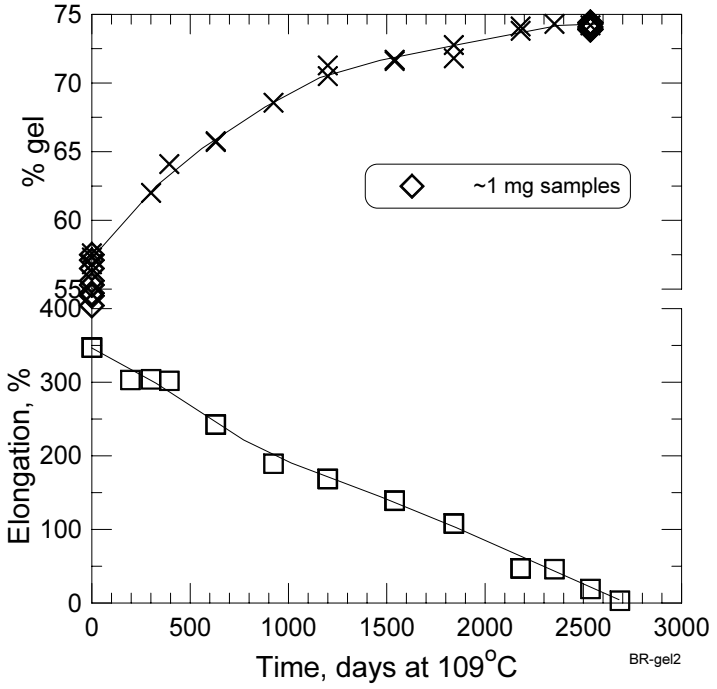

Figure IX-55. Elongation and percentage gel for XLPO-02B versus aging time at 109°C. Repeat runs (diamonds) on ~ 1 mg samples were conducted on unaged and severely aged samples to show sensitivity of gel percentage measurements.

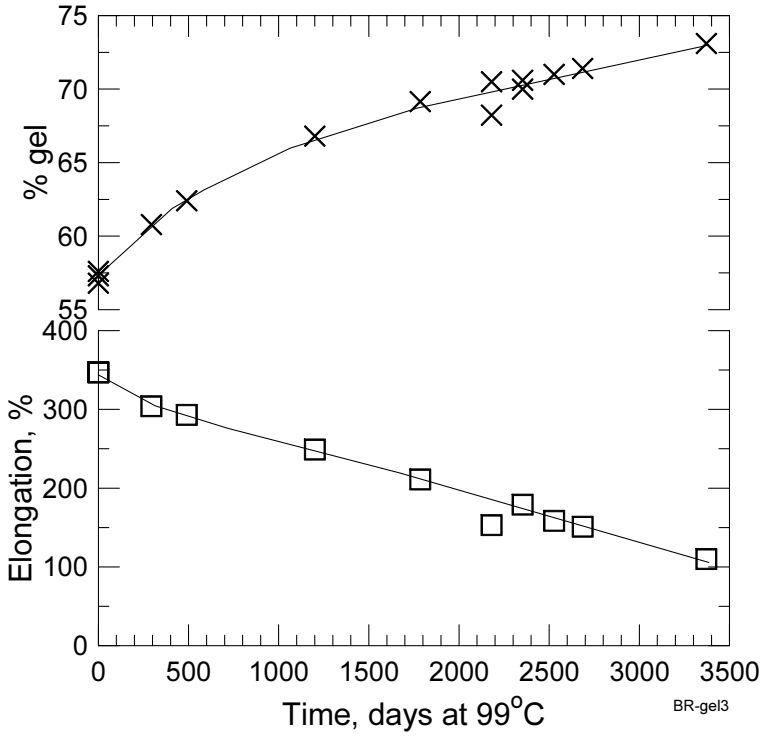

Figure IX-56. Elongation and percentage gel for XLPO-02B versus aging time at 99°C.

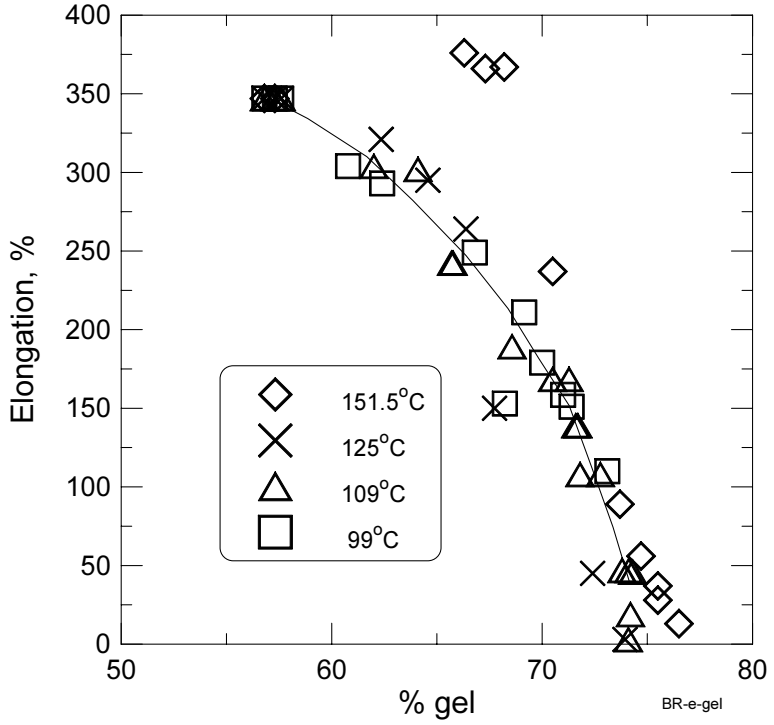

Figure IX-57. Elongation versus percentage gel for XLPO-02B for all thermal aging conditions.

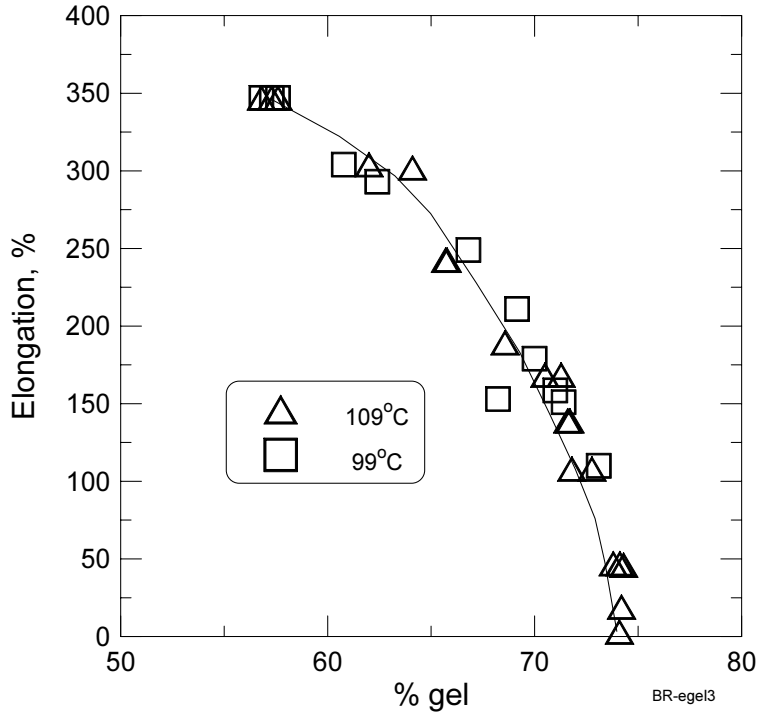

Figure IX-58. Elongation versus percentage gel for XLPO-02B for the two aging temperatures below the main melting peak.

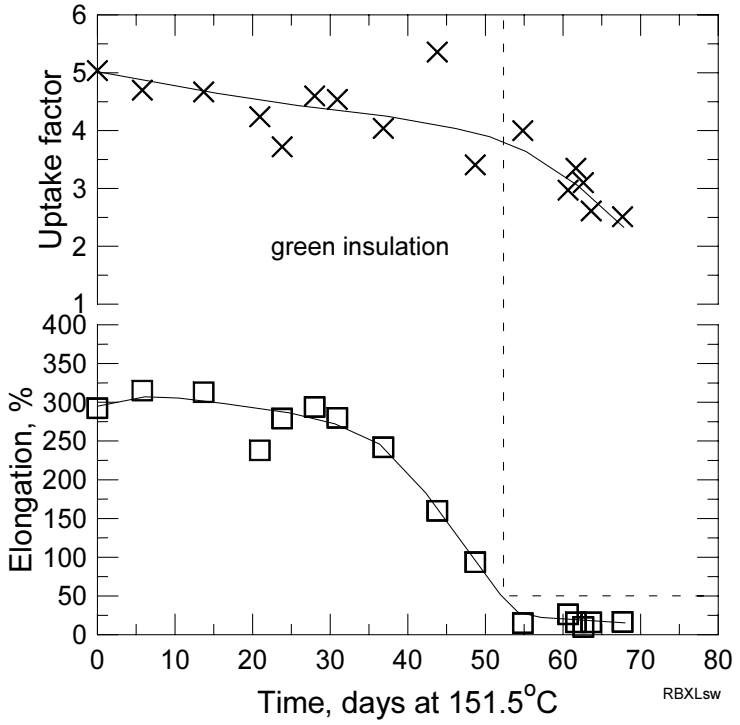

Figure IX-59. Elongation and uptake factor results for XLPO-05 versus aging time at 151.5°C.

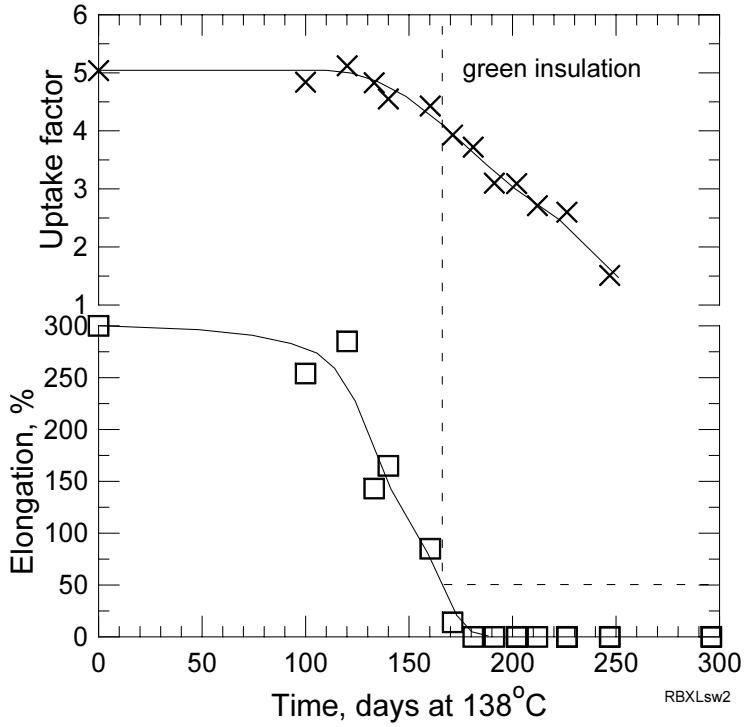

Figure IX-60. Elongation and uptake factor results for XLPO-05 versus aging time at 138°C.

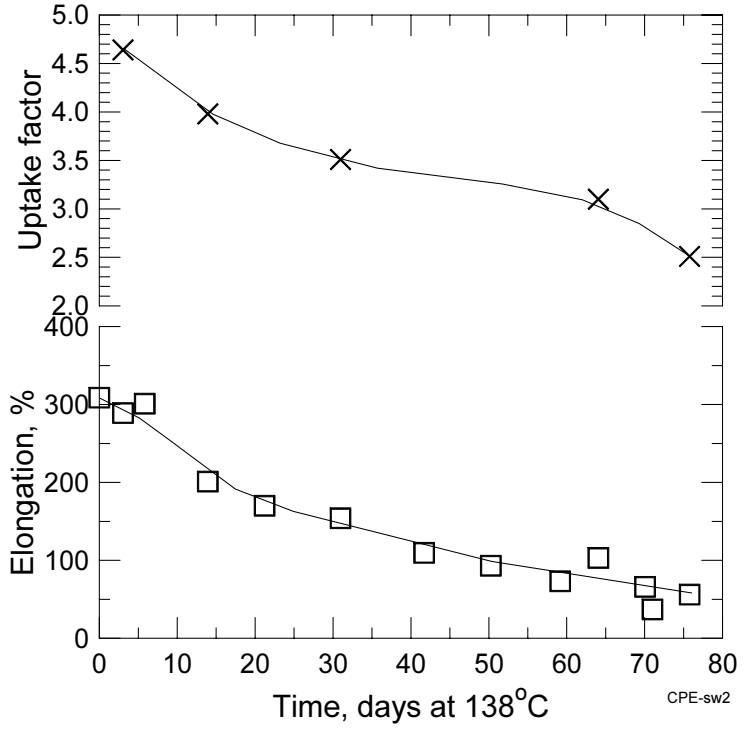

Figure IX-61. Elongation and uptake factor results for CPE-02 versus aging time at 138°C.

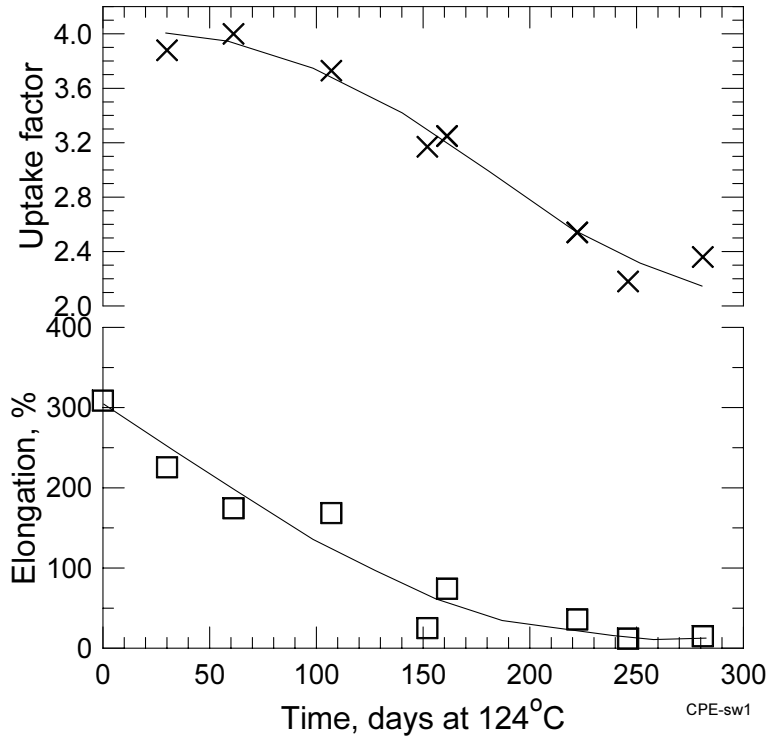

Figure IX-62. Elongation and uptake factor results for CPE-02 versus aging time at 124°C.

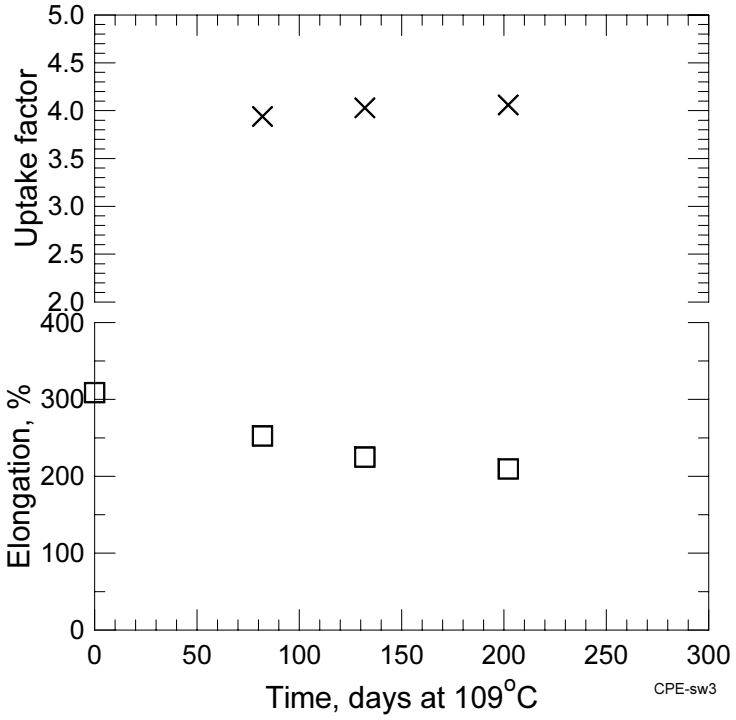

Figure IX-63. Elongation and uptake factor results for CPE-02 versus aging time at 109°C.

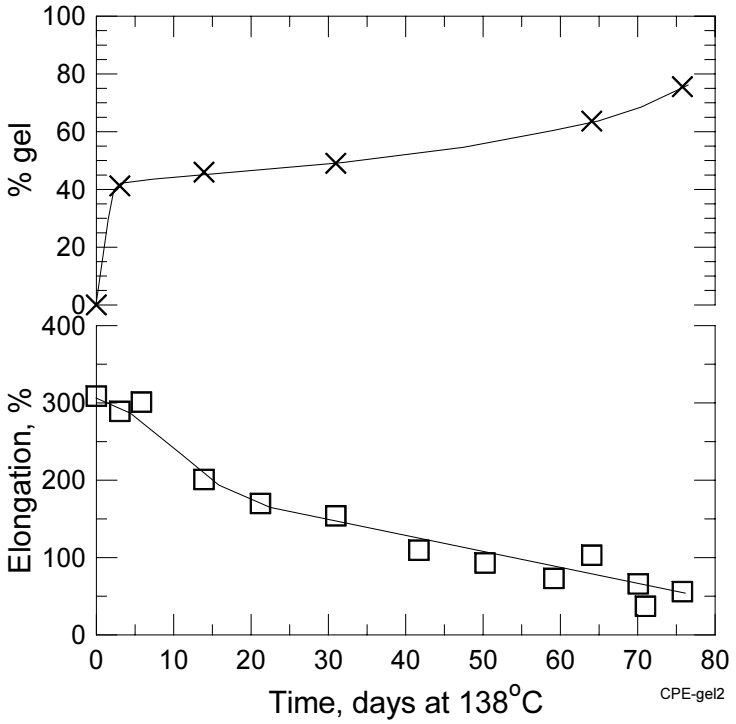

Figure IX-64. Elongation and percentage gel results for CPE-02 versus aging time at 138°C.

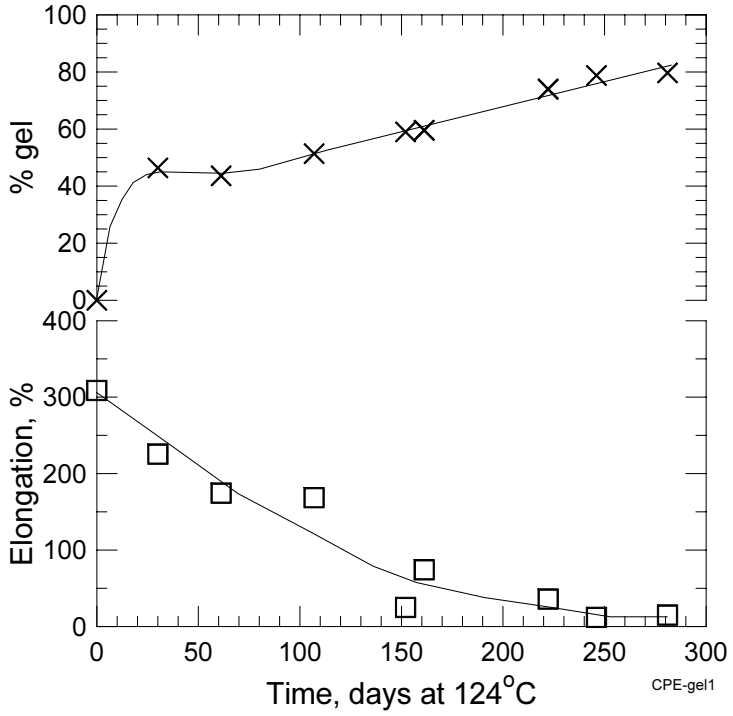

Figure IX-65. Elongation and percentage gel results for CPE-02 versus aging time at 124°C.

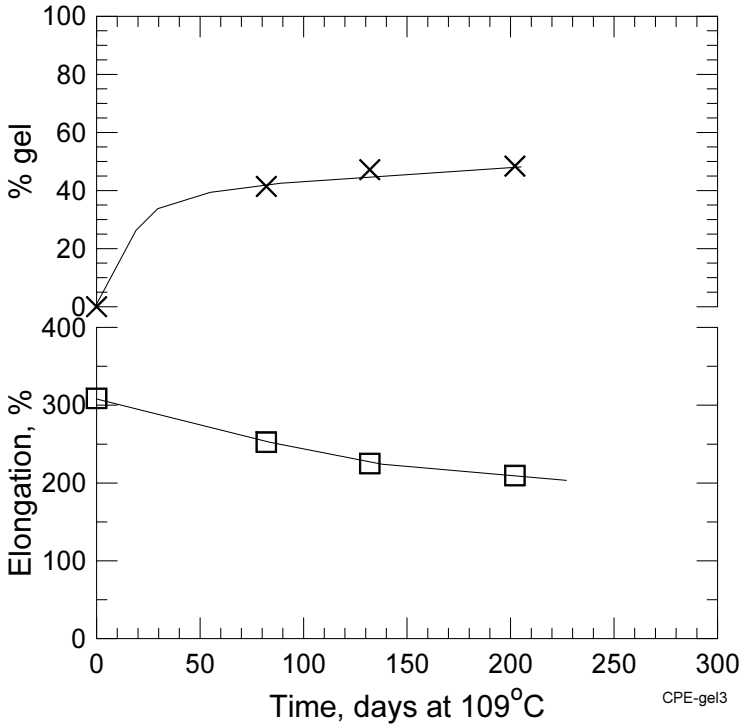

Figure IX-66. Elongation and percentage gel results for CPE-02 versus aging time at 109°C.

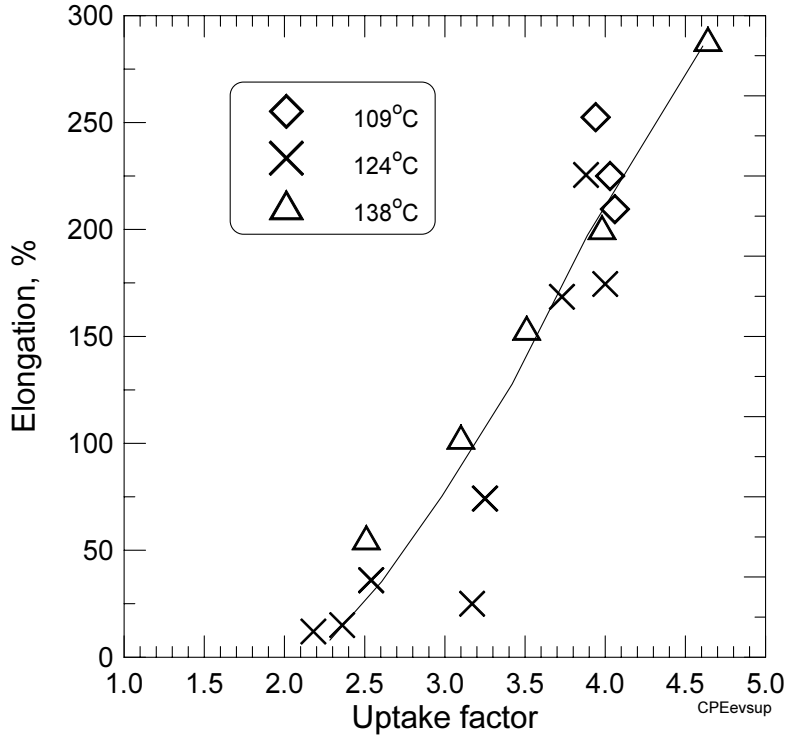

Figure IX-67. Elongation versus uptake factor for CPE-02 for all thermal aging conditions.

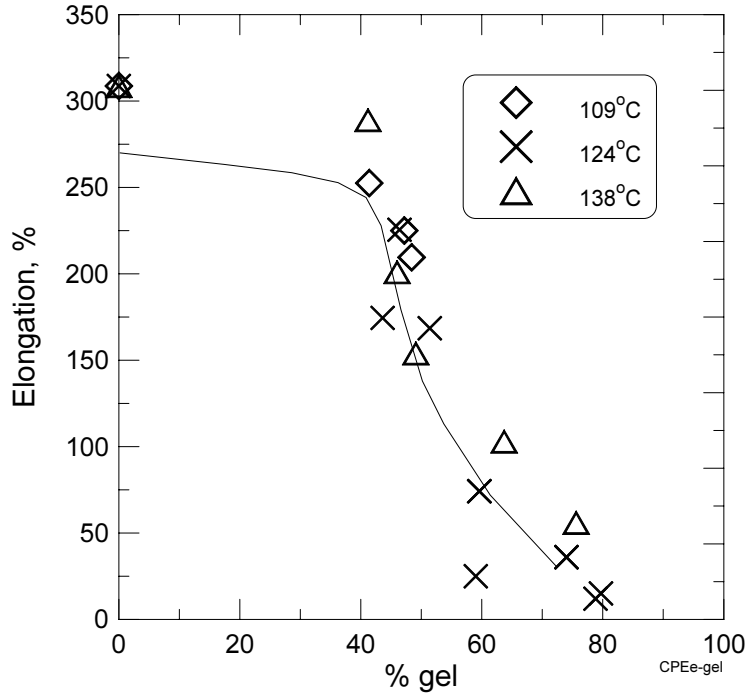

Figure IX-68. Elongation versus percentage gel for CPE-02 for all thermal aging conditions.

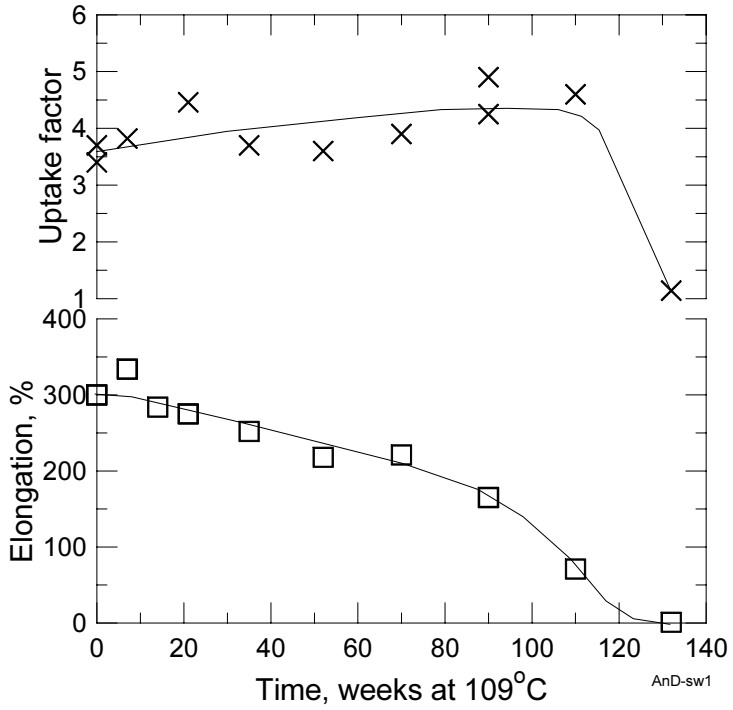

Figure IX-69. Elongation and uptake factor results for EPR-04 versus aging time at 109°C.

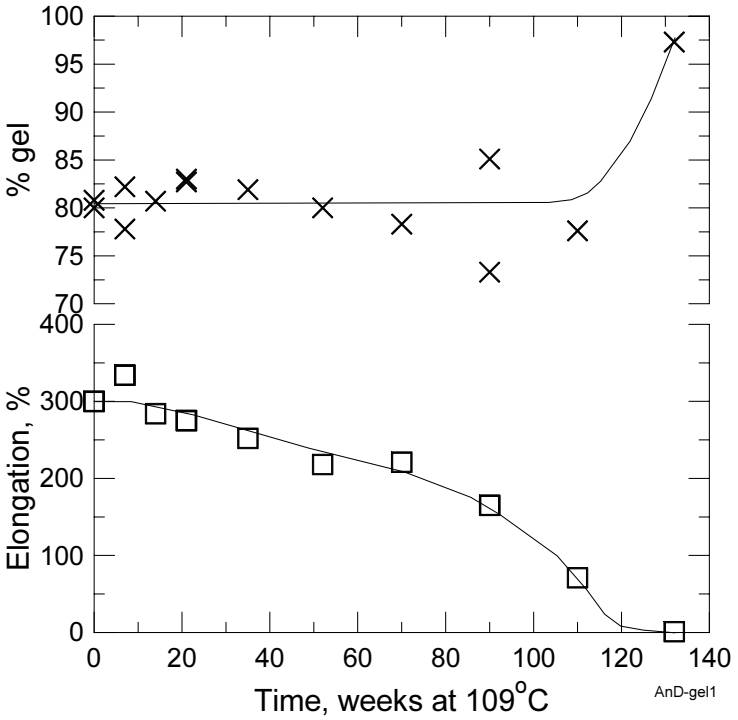

Figure IX-70. Elongation and percentage gel results for EPR-04 versus aging time at 109°C.

X. Condition Monitoring Techniques: Density Measurements

Introduction

Density measurements have been used extensively to follow aging of polymers [X-1] and have shown promise for monitoring the degradation of many cable materials [X-2 through X-6]. These measurements are easy to conduct on samples weighing tens of milligrams using the Archimedes approach [X-7]. They can also be done on very small samples (fractions of a mg) using the density gradient column technique [X-1] but such measurements are difficult to run and often adversely affected by artifacts (e.g., absorption of column liquid). Given the large number of samples available for screening, one early goal of the NEPO cable-aging program was to determine what types of samples and environments were best probed using density measurements. Since it became apparent early on that some of the other CM approaches being evaluated were often superior to the density approach, the CM part of the NEPO cable-aging program switched emphasis away from density measurements. Only in places where density offered substantial advantages did pursuit of this approach continue. One of the areas where density proved useful was as a monitoring technique for following degradation during Wear-out experiments on EPR cable insulation materials that showed "induction-time" behavior (Section XI below). This is due to the fact that samples could be periodically tested for density using the Archimedes approach by repeatedly measuring density on the same small piece of material as a function of Wear-out aging time. For use with the Wear-out method, other monitoring techniques required either new (and often large) samples for each measurement (destructive tests such as elongation, solvent uptake, gel) or required substantial sample preparation time for each measurement (e.g., modulus profiling).

Density measurements on Neo-02 cable jacket

Density measurements were made on the Neo-02 jacket samples that had been aged at 80°C. Measurements on fairly large samples (~100 mg) were made on twelve unaged specimens from somewhat separated sections of the same cable reel (meters apart) plus two measurements at each aging time. The density results and individual elongation results (ten unaged specimens and three specimens at most aging times) are plotted on Fig. X-1. It is clear that, similar to most polymers aged in thermal environments, the density tends to increase with aging, going from around 1.62 g/cc to 1.69 g/cc. However the scatter in the density results is quite large compared to the scatter in the individual elongation results. The observation that the density of unaged specimens varied from 1.595 g/cc to 1.635 g/cc for large (~100 mg) specimens located within a few meters of each other on a single cable reel implies that the distribution of fillers is not well controlled for this material. It also makes it likely that the inherent (real) scatter in density would be even greater for smaller Archimedes samples (10 mg) or the even smaller samples (1 mg or less) that would be used in a density gradient column. Although the variations in density are quite large, the filler variations have much less impact on the mechanical degradation as seen from the individual elongation results on Fig. X-1. Given that modulus, NMR and swelling results show much less scatter than density and

correlate well with the elongation results, density is clearly not a viable CM approach for this material.

Density measurements on hypalon jacketing materials

The Hyp-01A material came from a three-conductor cable and represented the thin hypalon jacket covering the EPR-insulation of the three individual conductors. To distinguish the three conductors, two of the black hypalon materials were covered with a thin "color" coat (white for one and red for the second). Therefore there were three individual materials that we label red, white and black for convenience. Elongation results were conducted on all three colors at five aging temperatures and, within the experimental scatter, the rate of degradation was identical for all three colors. Density measurements were conducted on all three colors at every thermal aging condition- again no differences in behavior as a function of the color were observed, perhaps not surprising given that all three materials were black hypalon except for thin "paint" layers on the "red" and "white" insulations. The results for aging at 140°C are shown in Fig. X-2, where two samples of each color were monitored at three of the five aging times. The results show that 1) density tends to increase with aging as anticipated, 2) scatter is relatively large and 3) no apparent dependence on color exists. The results for every aging condition (time, temperature and color of insulation) are plotted versus the average elongation in Fig. X-3. Although there is clearly an increase in density with loss of mechanical properties and a tendency towards a larger rate of change in density near end of life, scatter in the results is fairly substantial. The large scatter is even more obvious when one compares the density correlation (Fig. X-3) with the modulus correlation (Fig. VII-15). Thus, as expected, density increases with aging but appears to be a much less promising CM approach compared to other viable alternatives.

Density measurements were made on most of the other hypalon materials at all aging temperatures and aging times. In general, the situation is similar to that found for Hyp-01A where density increases with degradation, but scatter tends to be much larger relative to observed changes compared to other CM approaches such as modulus profiling results. The results for Hyp-03, Hyp-04, Hyp-05 and Hyp-06 are summarized in plots showing the correlation of elongation and density for aging at 100°C, 110°C and 125°C in Figs. X-4 through X-7. Comparing the scatter in these correlations with the scatter in correlations of modulus to elongation (Figs. VII-29, VII-35, VII-19 and VII-30, respectively) indicates that modulus represents a superior CM approach. An additional advantage of modulus (and uptake factor) is the presence of an apparent "universality" for their end of life criterion. Such a universality is impossible for density measurements owing to the differing filler contents used by different manufacturers.

Scatter in the density results for Hyp-08 are also too large relative to the density changes to consider density as a viable CM approach (Fig. X-8). For Hyp-07, the density climbs quickly at first but then levels out and shows little sensitivity to the important later stages of degradation (Fig. X-9).

Another problem that impacts the hypalon density results is the presence of DLO effects for many of the aging conditions as seen from the earlier modulus profiling results. When DLO effects are important, the reduced oxidation occurring in interior regions would lead to density values that are less than would be measured under equilibrium (homogeneous) oxidation conditions. The only method available to circumvent this problem would involve density-profiling techniques using density gradient columns [X-1]. However, density profiling is a very tedious and difficult technique. In addition it requires very small samples (less than 1 mg) so that the scatter found above with the 50 to 100 mg samples would be expected to greatly increase.

Density measurements on EPR insulation materials

As pointed out earlier, EPR insulation materials tend to follow "induction-time" behavior where property changes are minor until abrupt failure occurs in the induction-time region. We saw evidence of such behavior from elongation results (Figs. III-32, III-35, III-39 and III-42), modulus results (Figs. VII-69 through VII-78) and gel/uptake results (Figs. IX-69 and IX-70). Similar "induction-time" behavior occurs for density measurements as seen in for EPR-04 (Figs. X-10) and EPR-03 (Fig. X-11). It was pointed out in the modulus profiling section that DLO effects often enter in the induction-time region of EPR materials (Figs. VII-69 through VII-78) implying that the density results are influenced by DLO effects when they start to quickly increase. However the point of increase can be considered the practical end of life for mechanical properties and the increase is usually so rapid that the errors introduced by DLO effects will not significantly change this point. This circumstance will prove to be useful in the next section on the Wear-out approach where we use density results as a means of estimating Wear-out lifetimes.

Similar induction-time behavior is observed for density measurements of the EPR-05 material as seen from Fig. X-12 that shows elongation and density results versus aging time at 109°C. Density measurements for EPR-05 under the combined environment conditions of 430 Gy/h plus 40°C are given in Fig. X-13. Comparing these results with the elongation results (Fig. V-16) indicates that density changes are occurring in a regular fashion as radiation-degradation occurs. This implies that density may be a viable CM technique when radiation effects significantly impact an EPR insulation. One has to keep in mind, however, that significant density changes are not observed until doses greater than ~2000 kGy (200 Mrad) occur. This dose level is beyond the total accident and normal worst case dose for any US plant.

Density measurements for other materials

Density screening on several other types of materials indicated that the sensitivity of density to degradation was insufficient for the application of density as a CM approach. For XLPO-02A insulation, the changes in density were small relative to scatter in the measurements as seen in thermal aging results at 109°C (Fig. X-14). For the XLPO-05 material, density changes were found to be very small until the elongation drops to very low values as seen from results for the green-colored insulation aged at 138°C (Fig. X-15.). The thermal degradation of the CPE-02 material shows no sensitivity to density as

evidenced by the results at 124°C shown in Fig. X-16. Although density does increase slightly for radiation-aging of the Sil-01 insulation, the relatively small changes coupled with the large scatter in the results for the severely aged material indicate that density is not a recommended CM approach for this material (see- Fig. X-17).

Conclusions

Density is usually found to increase with aging in both thermal-only and combined radiation-thermal environments. For some materials the increases are fairly small so that following density is not helpful. Even when the changes are significant, it is often found that the scatter in density is large enough to make its applicability as a CM approach more difficult than other available techniques. The scatter can come from large variations in filler content along the cable as well as from variations in aging. When DLO effects are important, application of the density approach becomes very difficult. For materials with "induction-time" behavior, density tends to follow such behavior with small changes up to the induction-time region followed by large increases. Although this makes density useless as a CM technique for such materials, we will see in the next Section on the Wear-out approach that the sensitivity to the practical end of life region coupled with other advantages makes density an ideal measurement technique for determining end of life during Wear-out experiments.

References

X-1. K. T. Gillen, R. L. Clough and N. J. Dhooge, "Density Profiling of Polymers", Polymer, 27, 225 (1986).

X-2. Anandakumaran K, et. al. “Improved conventional testing of power plant cables”, EPRI Report TR-105581, September, 1995.

X-3. Toman GJ, Hilditch JM, Butwin RT. “Diagnostic matrix for evaluation of low-voltage cable”, EPRI Report TR-106108, November, 1997.

X-4. Gazdzinski RF, Denny WM, Toman GJ, Butwin RT. “Aging management guideline for commercial nuclear power plants- electrical cable and terminations”, Sandia Labs Report, SAND96-0344, September, 1996.

X-5. “Assessment and management of ageing of major nuclear power plant components important to safety: in-containment instrumentation and control cables, Volumes I and II, IAEA-TECDOC-1188, December, 2000.

X-6. Gillen KT, Celina M, Clough RL. Density measurements as a condition monitoring approach for following the aging of nuclear power plant cable materials. Radiat Phys Chem 1999;56:429.

X-7. ASTM Standard D792-91.

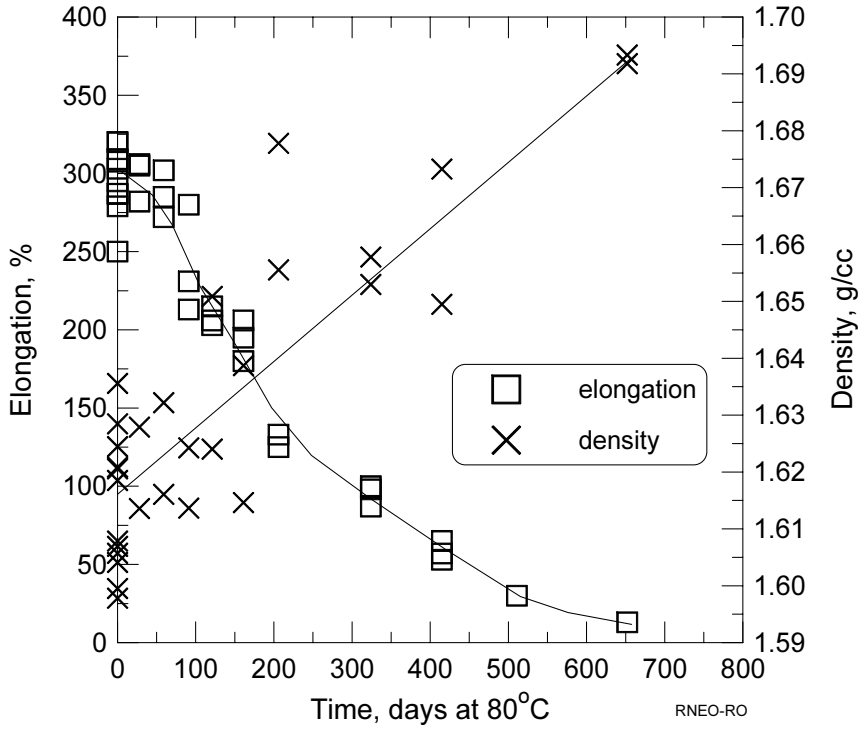

Figure X-1. Elongation and density results versus aging time at 80°C for Neo-02.

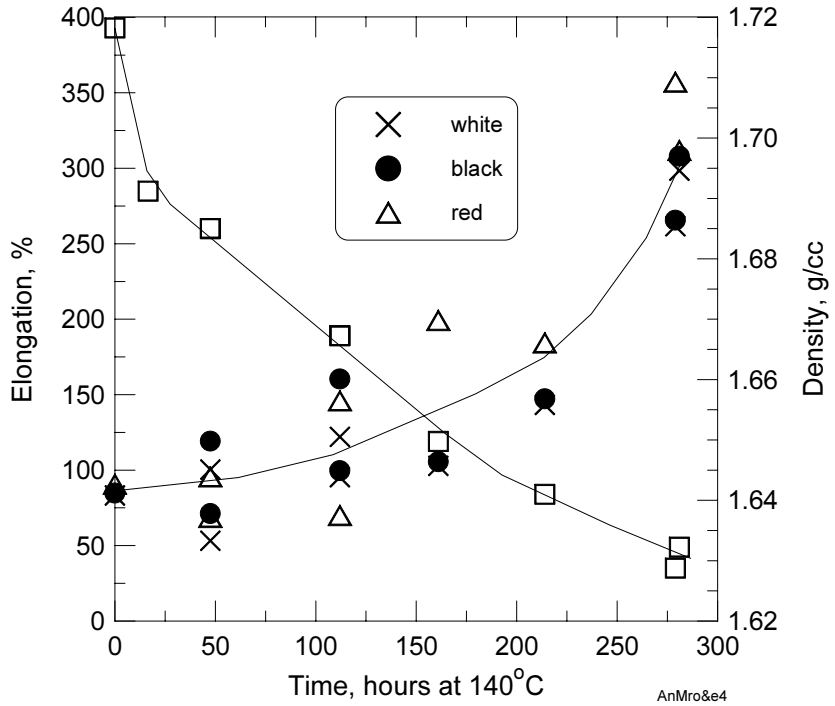

Figure X-2. Elongation and density results versus aging time at 140°C for Hyp-01A.

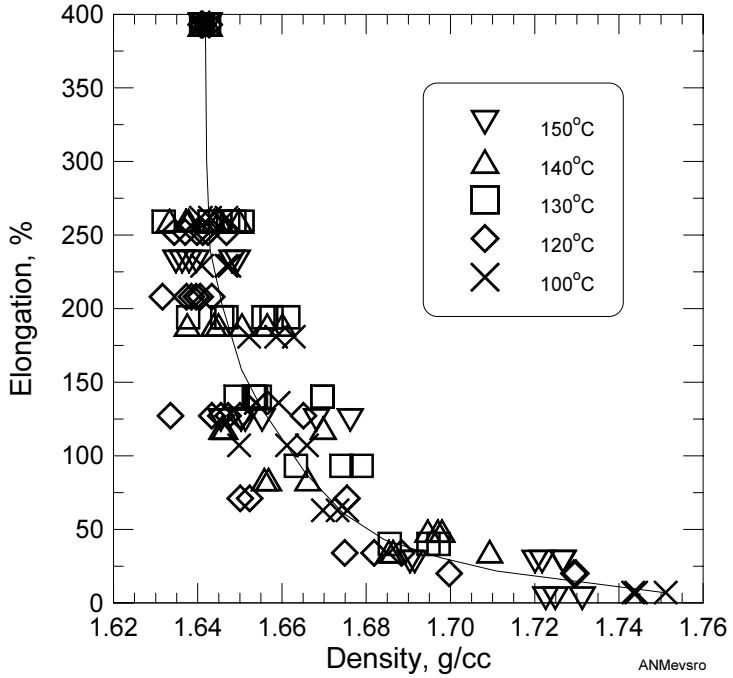

Figure X-3. Elongation versus density for all aging times, temperatures and insulation colors of Hyp-01A.

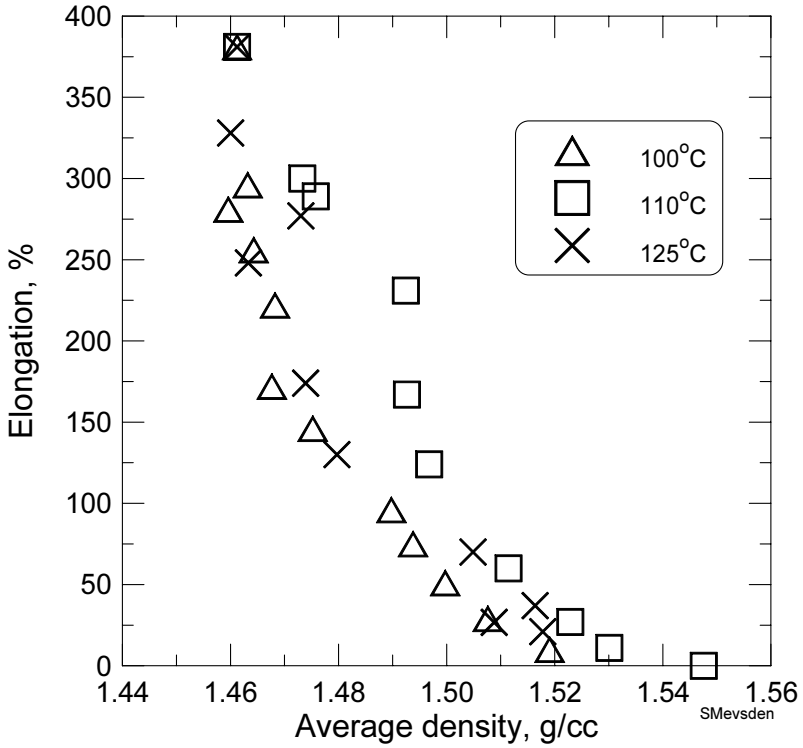

Figure X-4. Elongation versus density for all aging times, temperatures and insulation colors of Hyp-03.

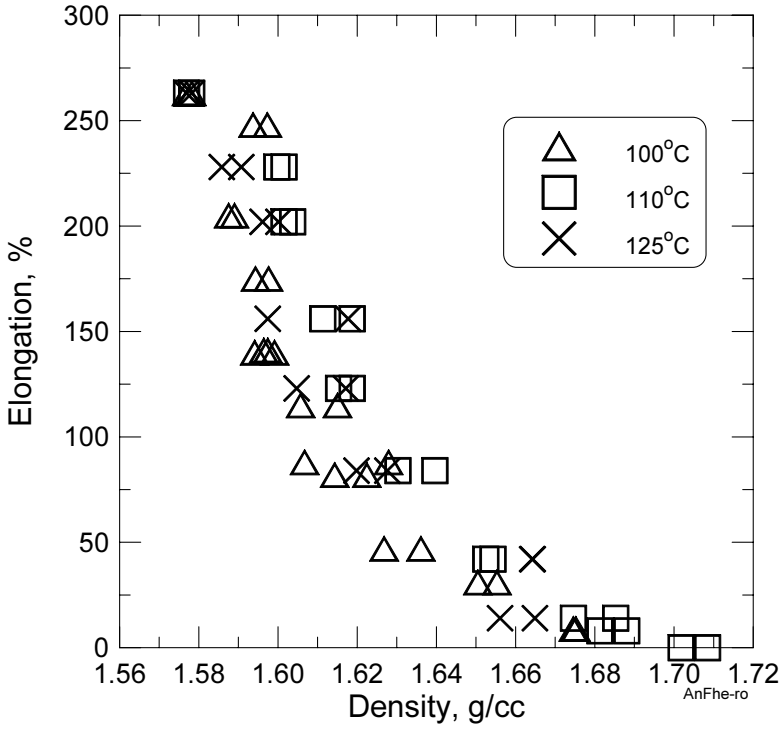

Figure X-5. Elongation versus density for all aging times, temperatures and insulation colors of Hyp-04.

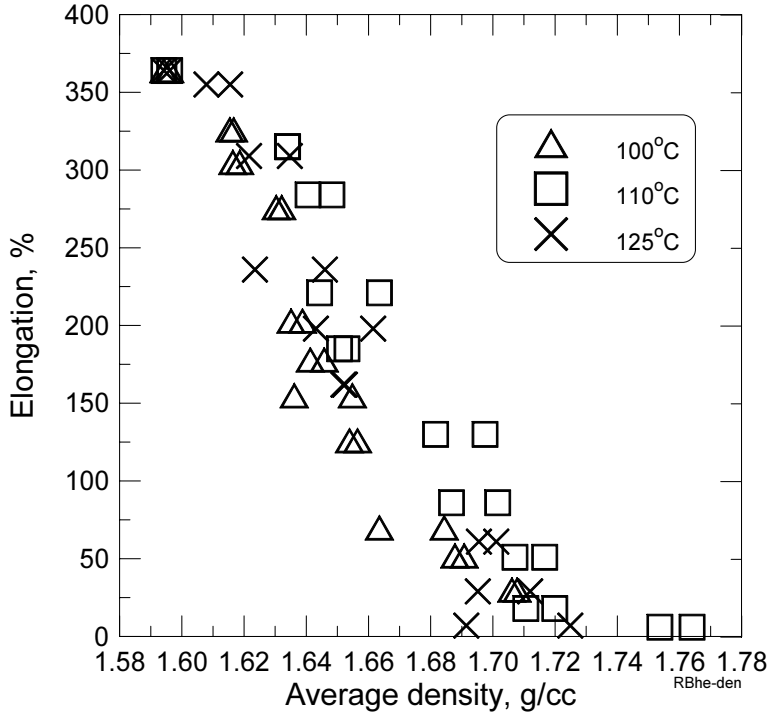

Figure X-6. Elongation versus density for all aging times, temperatures and insulation colors of Hyp-05.

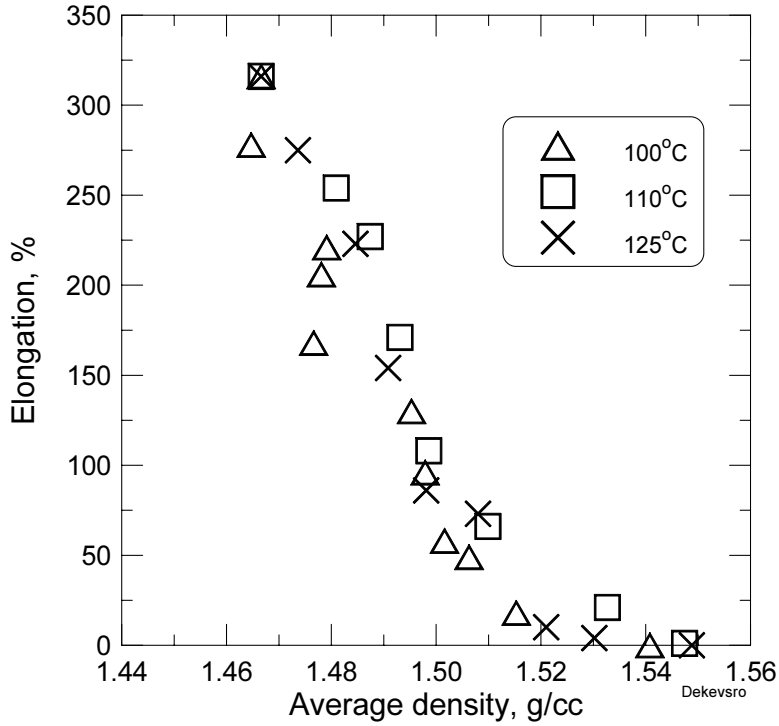

Figure X-7. Elongation versus density for all aging times, temperatures and insulation colors of Hyp-06.

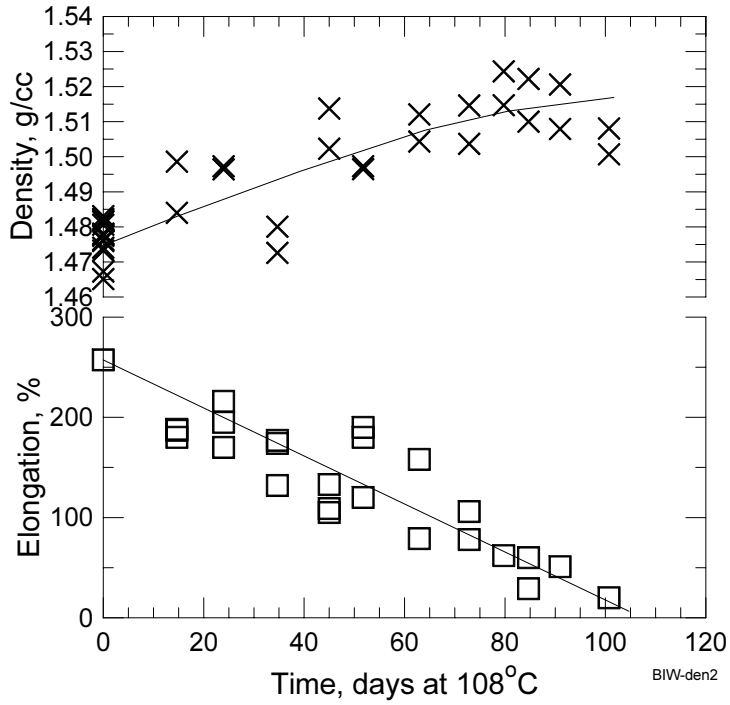

Figure X-8. Elongation (bottom) and density (top) versus aging time at 108°C for Hyp-08.

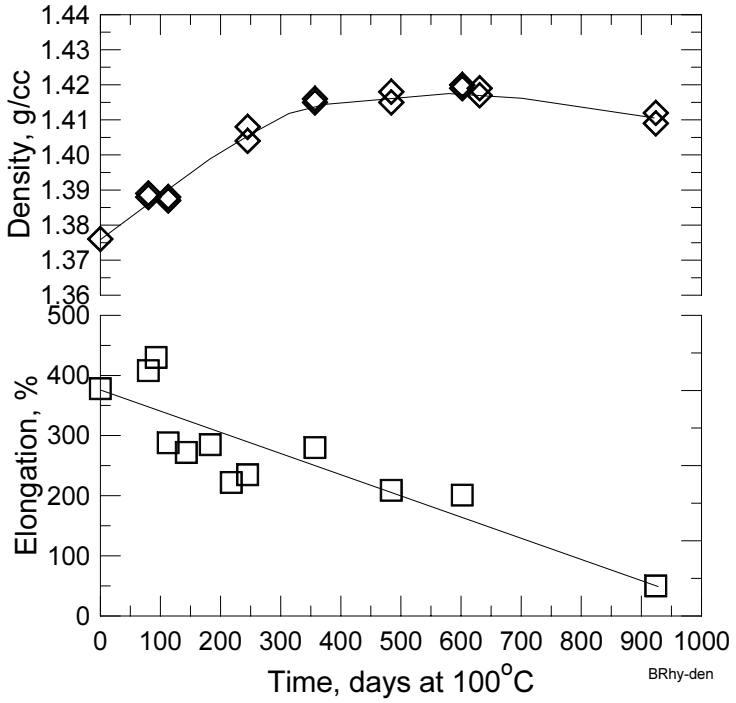

Figure X-9. Elongation (bottom) and density (top) versus aging time at 100°C for Hyp-07.

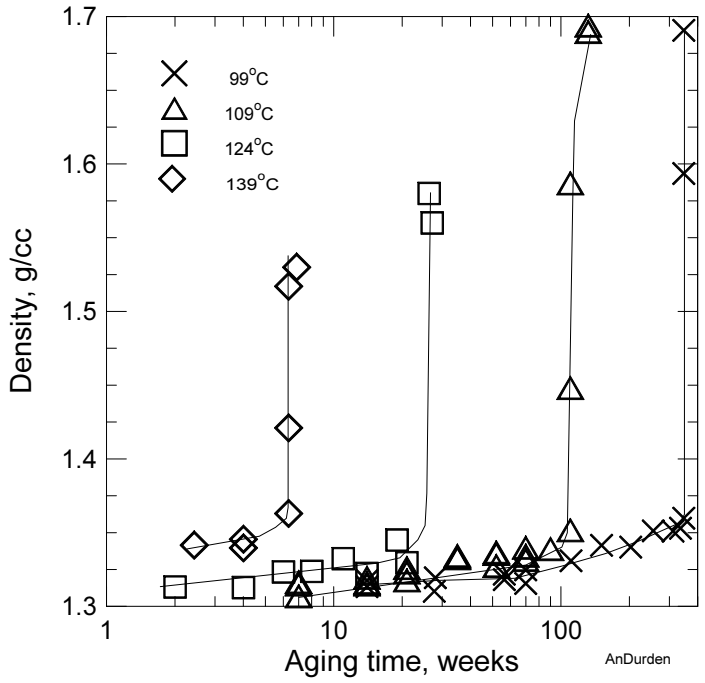

Figure X-10. Density results for EPR-04 at the indicated aging temperatures.

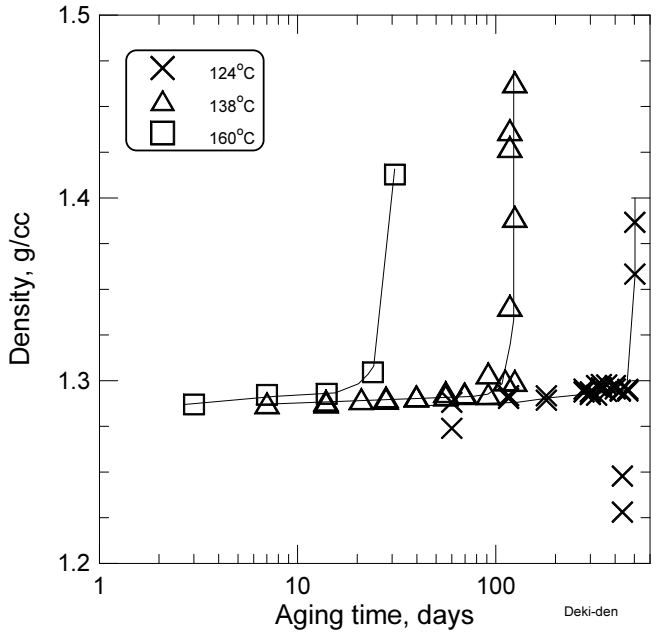

Figure X-11. Density results for EPR-03 at the indicated aging temperatures.

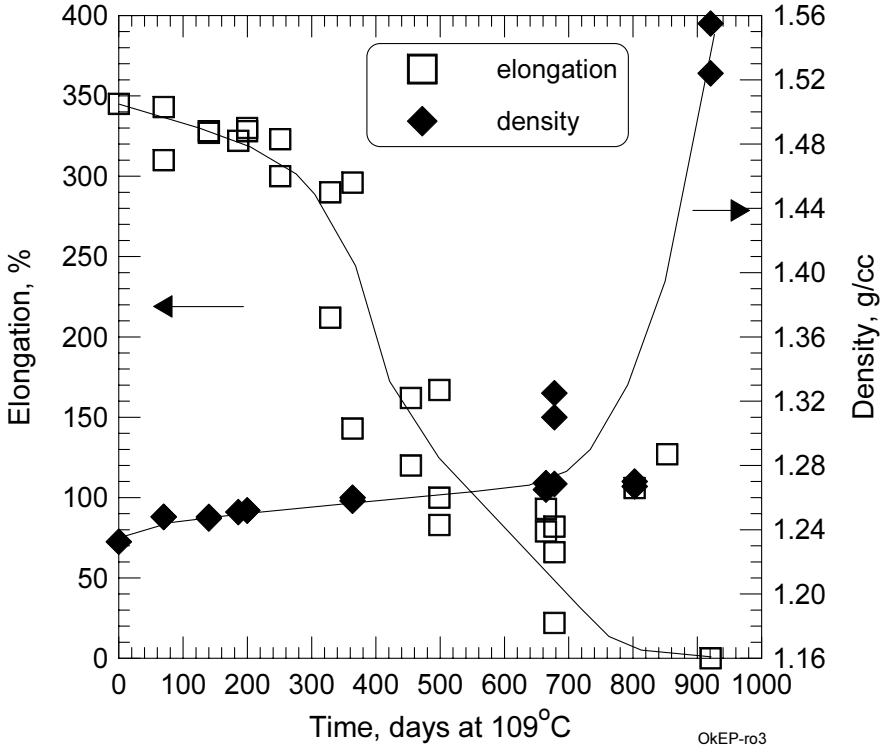

Figure X-12. Elongation and density versus aging time at 109°C for EPR-05.

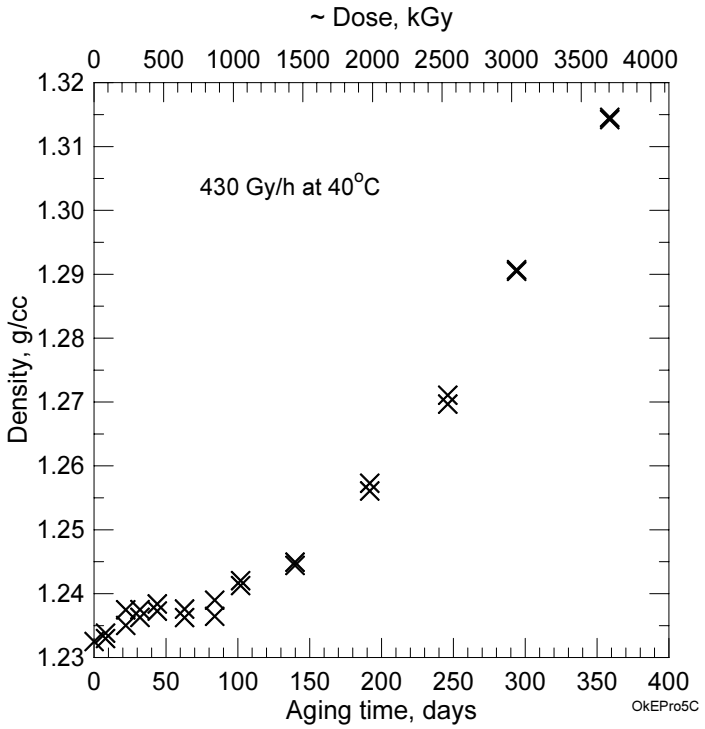

Figure X-13. Density results for EPR-05 versus aging time at 430 Gy/h plus 40°C.

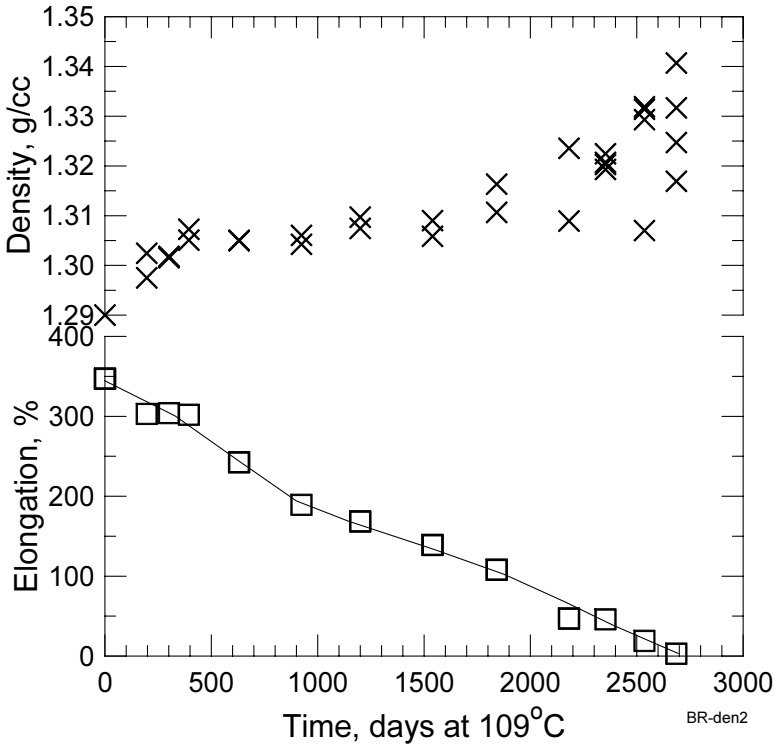

Figure X-14. Elongation (bottom) and density (top) versus aging time at 109°C for XLPO-02A.

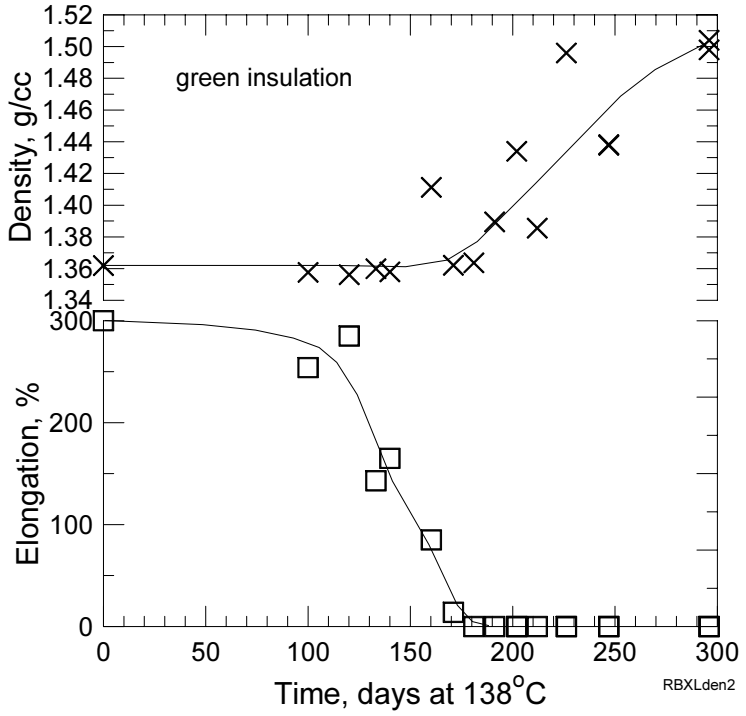

Figure X-15. Elongation (bottom) and density (top) versus aging time at 138°C for XLPO-05.

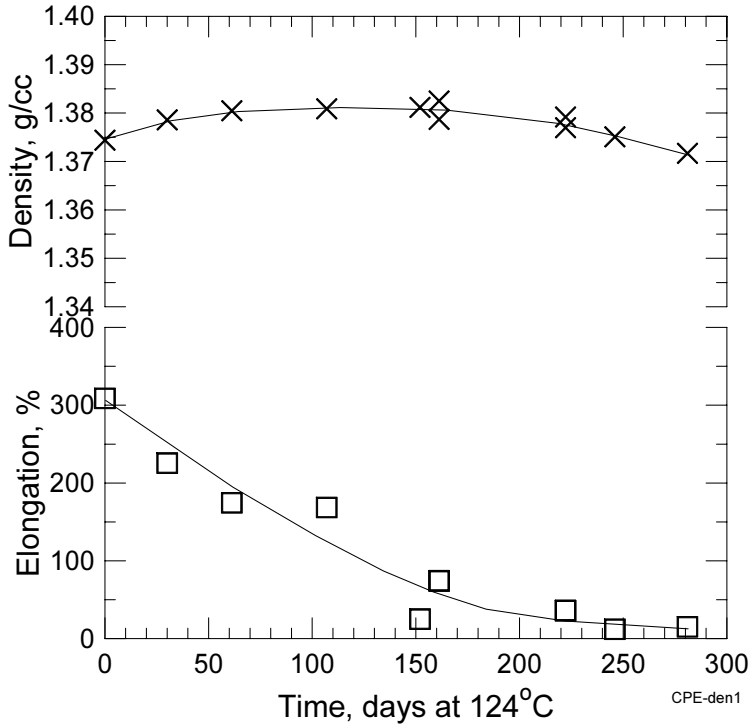

Figure X-16. Elongation (bottom) and density (top) versus aging time at 124°C for CPE-02.

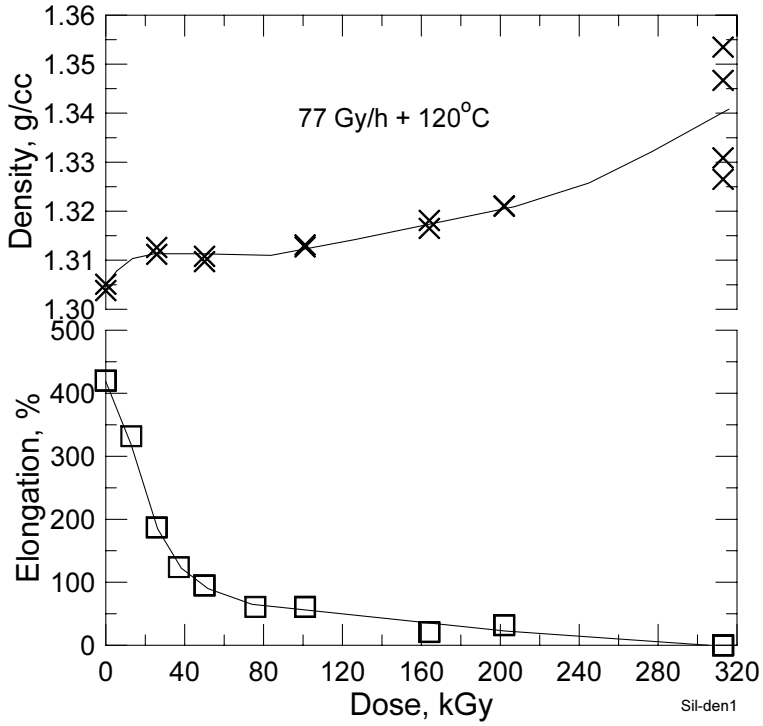

Figure X-17. Elongation (bottom) and density (top) versus aging dose for Sil-01 insulation aged under the indicated conditions.

XI. The Wear-out Approach for Estimating the Remaining Lifetime of Materials

Introduction

In earlier sections of this report we showed how to make better predictions of cable lifetimes and introduced some new CM approaches that may be useful for monitoring the condition of ambiently aged cables. In addition to predicting and monitoring the condition of ambiently aged samples, it would be advantageous to use field-aged samples for estimating the material's remaining lifetime in the ambient environment. This section summarizes a new approach for achieving this goal that we refer to as the Wear-out approach. Since very detailed descriptions [XI-1, XI-2] have been published on the theoretical bases for the Wear-out approach, we will only briefly highlight the principles underlying this method, preferring to show in detail the experimental results obtained on nuclear power plant cables. The reader interested in the theoretical background is advised to examine the relevant publications [XI-1,XI-2].

The Wear-out method is a generalization of cumulative damage failure models that have been used mainly for fatigue life predictions for metals and composite materials. The aging time to reach failure takes the place of the number of fatigue cycles to failure. For thermal aging of polymers, the usual accelerated aging assumption is that an increase in temperature will lead to a constant increase in the reaction rate underlying degradation (the basis underlying the time-temperature superposition concept described above in Section III). The Wear-out approach takes samples that have aged for a certain time at a low temperature T_1 (e.g., the ambient temperature) and completes the degradation to "end of life" at a higher temperature, T_w (the Wear-out temperature). When time-temperature superposition is valid over the temperature range from T_1 to T_w, the approach predicts that the remaining lifetime at T_w should be ***linearly*** related to the aging time prior to the temperature step. It should therefore be possible to estimate the service lifetime by completing the aging of ambiently aged samples at the Wear-out temperature.

One important advantage of this approach comes from its potential for converting totally non-predictive results to linear predictive behavior. For example, we saw above that many important cable materials exhibit so-called "induction-time" behavior, where the degradation property of interest changes very little until large changes occur at the end of life. When such behavior occurs, CM techniques will be useless since they will not give any warning before the practical end of life. An ideal CM technique would yield a degradation parameter that 1) changes approximately linearly with time and 2) reaches a known (universal) value at practical end of life. By converting non-predictive CM parameter results to linear results that extrapolate to zero at the end-of-life, the Wear-out approach achieves the two goals of an ideal CM technique. Of course the situation is more complex when time-temperature superposition is not valid as was noted for the EPR-03 material (Fig. III-36) and the XLPO-02B material (Fig. III-49). In this case there is no way to predict beforehand the relationship between the remaining lifetime at T_w and

the aging time at the lower or ambient temperature, T_1. However the modeling suggests that the relationship should involve a relatively smooth predictive curve and the Wear-out method offers a way to generate results to map out this curve to see how predictive it turns out to be [XI-1,XI-2].

Wear-out approach applied to EPR materials

Applying the Wear-out approach involves taking samples that had previously aged for a given amount of time at the pre-aging or ambient temperature and completing their degradation at a higher Wear-out temperature. The degradation during the Wear-out exposures must be monitored using a convenient and quantifiable degradation parameter. Since periodic measurements are necessary after various times at the Wear-out temperature, sufficient material from the pre-aged condition must be available for the Wear-out aging. Given that the time to failure at the Wear-out condition is unknown, a degradation parameter that involves destructive testing requires that a substantial number of samples be placed under Wear-out aging conditions so that the material is not exhausted before end of life occurs. If tensile elongation is being followed where three tensile tests are required per Wear-out aging time, this can lead to the need for a large amount of pre-aged material, an often onerous requirement. In addition, material could still run out before end of life is achieved. On the other hand if the degradation parameter involved testing that is non-destructive so that one small sample could be used repeatedly for Wear-out testing, very little material would need to be extracted from the low-temperature or ambient aging condition. For EPR materials that show induction-time behavior, following the density to failure turns out to offer a convenient "non-destructive" method that requires only small amounts of sample (10s of mg) to be taken from lower temperature or ambient aging conditions. As noted above in Section X, density rapidly increases near the practical end of life for EPR insulation materials and can therefore yield good estimates of "end of life". In addition the Archimedes density approach simply weighs the sample dry then weighs it in alcohol (chosen because it is a solvent that has a minimal swelling effect on EPR materials). After removal from the short exposure to alcohol, the alcohol quickly evaporates, and the sample can be returned to the Wear-out aging temperature for further aging. Thus one sample can be used for repeated density measurements versus Wear-out aging time until it fails. Adding this non-destructive advantage to the ease of carrying out Archimedes density measurements makes density the ideal parameter for Wear-out measurements on EPR insulation materials.

Density results versus aging time for the EPR-04 material at four aging temperatures were shown in Fig. X-10. Since very long aging times were required to reach the induction-time region at 109°C (~110 weeks) and 99°C (~310 weeks), we selected samples that had been pre-aged for various times at these two temperatures (the "lower temperature) and completed the aging of these samples at higher Wear-out temperatures. To understand the concept behind the wear-out approach it is useful to look at a time-temperature superposed density plot. Figure XI-1 represents a time-temperature superposition of the density results from Fig. X-10. The first observation to note is that the empirically derived shift factors for density shown on Fig. XI-1 are virtually identical

to the empirical shift factors found for the induction-time of elongation (Fig. III-36). This shows, not surprisingly, that the density results correlate with the elongation results in terms of monitoring the induction-time. The other thing to notice is that Fig. XI-1 has all four aging time scales indicated below the superposed data. This arrangement of the time scales makes it useful for discussing the principal behind the Wear-out approach. For instance, we can immediately see the times to "end of life" at each temperature from the intersection of the dashed line at the induction point with each time scale (~6 weeks at 139°C, ~25 weeks at 124°C, ~110 weeks at 109°C and ~310 weeks at 99°C). If we carry out a Wear-out experiment on a sample that had aged for 35 weeks at 109°C, corresponding to ~1/3 of its lifetime and then switch to a Wear-out temperature of 139°C, true time-temperature superposition implies that 1/3 of the 139°C lifetime (2 weeks) would initially be used up, leaving 2/3 of its lifetime remaining (~4 weeks). The arrows shown on Fig. XI-1 denote this situation pictorially. Thus the simplest model would predict that preaging for 1/3 of lifetime at the lower temperature T_1 would require Wear-out aging for 2/3 of lifetime at the Wear-out temperature of T_w. Similarly 2/3 of lifetime at T_1 would require an additional 1/3 of lifetime at T_w. Therefore a plot of the time or fractional lifetime spent at T_1 versus the time or fractional lifetime needed at T_w to complete the degradation to end of life would be predicted to be linear as shown in Fig. XI-2. In this plot τ_1 and τ_w refer to the times required at each temperature for end of life with the top and right axes referring to the times and the bottom and left axes referring to fractional lifetimes.

Now that the concepts underlying the Wear-out approach are clear, we can look at some actual results for the EPR-04 material. Figure XI-3 shows density results versus aging time at a Wear-out temperature of 138°C for samples of EPR-04 that had been preaged at 109°C for the times indicated on the plot. From Fig. XI-1 we arbitrarily denote practical end of life as the time required for the density to reach 1.45 g/cc. The dashed line shown on Fig. XI-3 corresponds to this criterion. It is clear from the Wear-out results that more preaging at 109°C corresponds to shorter lifetimes at the Wear-out temperature as expected. In general scatter should be expected for induction time values since different locations along an extruded cable would be expected to have small variations in anti-oxidant concentrations (see Fig. VII-72). In addition, slight differences in aging temperatures for differing samples will lead to scatter. For these reasons, we ran three unaged samples (0 weeks at 109°C) obtained several meters apart from each other on an unaged cable reel. The results for all three of these samples are shown on Fig. XI-3 and indicate the type of sample-to-sample scatter that might be expected for such materials.

The times at the Wear-out temperatures required for the density to reach 1.45 g/cc were obtained from Fig. XI-3. These Wear-out times (squares) were plotted versus the pre-aging times at 109°C on Fig. XI-4; also plotted on this figure were the density results (diamonds) versus aging time at 109°C. It is clear from the results shown on this figure that simply following density versus aging time at 109°C does not give any effective warning of impending end of life. On the other hand, the Wear-out results drop in a reasonably linear fashion so that the point of impending end of life can be reasonably predicted. Thus the Wear-out approach transformed non-predictive "induction-time"

behavior into predictive (~ linear) behavior. The linear extrapolation predicts a 109°C lifetime of 110 weeks, very close to the lifetime actually found at this temperature.

Wear-out experiments for the EPR-04 samples pre-aged for various times at 99°C were carried out both at 124°C and at 138°C. The Wear-out density results at a Wear-out temperature of 124°C are shown in Fig. XI-5 and the Wear-out times plotted against pre-aging time at 99°C are given in Fig. XI-6. Again we find reasonably linear results for the Wear-out plot with a predicted lifetime at 99°C of ~270 weeks. Comparable Wear-out results at 138°C for 99°C pre-aging are shown in Figs. XI-7 and XI-8. In this case not quite linear behavior is observed for the Wear-out plot (Fig. XI-8), perhaps not surprising given the lack of time-temperature superposition noted for the elongation results (Fig. III-36). A linear fit (solid line) to the Wear-out results predicts a 99°C lifetime of ~260 weeks whereas a curve fit (dashed curve) predicts around 300 weeks. The predictions from the Wear-out experiments therefore range from ~260 to ~300 weeks compared to the actual 99°C lifetime of around 310 weeks.

It is important to point out that the choices used for the Wear-out temperatures (124°C and 138°C) were temperatures at which the degradation took up to 25 weeks for the former and 6 weeks for the latter. These are moderate but not unrealistic aging times. We could have used much higher Wear-out aging temperatures in order to significantly shorten the experimental times but there are several reasons for avoiding higher temperatures. Perhaps the most important reason is to minimize the temperature difference between the low-temperature condition and the Wear-out temperature. The bigger this difference, the greater the chance of changes in the degradation chemistry and therefore the greater the possibility of non-predictive Wear-out plots.

Wear-out experiments were carried out on samples of EPR-03 that had pre-aged for various times at 124°C and 109°C, conditions where the degradation had been completed over a 3.7 year exposure at 109°C (Fig. III-39). In addition, Wear-out experiments were conducted on samples pre-aged for up to 1250 days at 99°C in order to estimate the approximate lifetime to be expected at this even lower temperature. The Wear-out density results for 124°C pre-aged white and black insulations at a Wear-out temperature of 148°C are shown in Figs. XI-9 and XI-10 and the Wear-out times from these figures are plotted against pre-aging time in Figs. XI-11 and XI-12. Again we find reasonably linear results for the Wear-out plot with a predicted lifetime at 124°C of ~450 days. Similar results occur for the 124°C pre-aged samples when a Wear-out temperature of 138°C is used, as shown in Figs. XI-13 through XI-16. Overall the linear plots from the four Wear-out runs on 124°C pre-aged samples imply a lifetime of ~440 to 480 days, very close to the actual result at this aging temperature (Fig. III-39). The Wear-out density results for 109°C pre-aged white insulation at a Wear-out temperature of 148°C are shown in Fig. XI-17. The Wear-out plot for these results, shown in Fig. XI-18, is reasonably linear and predicts a 1240-day lifetime at 109°C, consistent with the elongation results (Fig. III-39). The Wear-out density results for 99°C pre-aged white insulation at a Wear-out temperature of 148°C are shown in Fig. XI-19. The Wear-out plot for these results, shown in Fig. XI-20, predicts an approximate 99°C lifetime of 2570

days. This represents a true prediction since aging at this temperature currently stands at ~1300 days (February, 2005), thereby requiring another 3.3 years to reach 2570 days. It is interesting to use this prediction of 2570 days versus the 1240 days found for 109°C to extend the Arrhenius plot shown in Fig. III-41 to 99°C. The appropriate a_T for 99°C would be 1240/2570 = 0.482. This result is added to the plot, leading to perhaps a hint of downward curvature (Fig. XI-21), similar to that found above for many elongation and oxygen consumption results. Although if real, this curvature would lead to lower extrapolated lifetimes at temperatures lower than 99°C, the very robust nature of EPR insulations implies that the lifetimes will still be sufficient. Evidence for this statement will come immediately below from Wear-out studies on an actual EPR insulation material that had aged at 51°C for 23 years in a nuclear power plant.

Our final example of the use of the Wear-out approach on EPR materials involves samples of EPR cable insulation that we obtained from nuclear power plant cables. The cables were aged at an estimated aging temperature of 51°C and pieces extracted periodically for future testing. Extractions were made at times that corresponded to 6, 10, 19 and 23 years of effective exposure to the 51°C environment. Since we predict EPR lifetimes at 51°C exceeding 300 years from our elongation results (Fig. III-45), we expected negligible aging to occur for the nuclear power plant EPR insulation. Elongation and density measurements were made on the plant materials with the results shown in Fig. XI-22. Within the scatter of the results, the elongation showed no change with time. The density showed a slight drop at 23 years but this small drop was small compared to typical scatter in such measurements when considering that the sections of cable examined came from different conductors. In fact aging almost invariably increases density values. Therefore the elongation and density measurements show no indication of aging. However, due to the "induction-time" behavior of EPR materials, this lack of change in measured properties is insufficient evidence for long-life.

As we saw above, the Wear-out approach offers a way out of this dilemma. Wear-out exposures at 138°C were conducted on the 5.6-year and 23.2-year samples (shortest and longest aging exposures). The elongation and density results versus aging time at 138°C are shown in Figs. XI-23 and XI-24. Since the elongation results essentially superimpose they indicate no differences between the 5.6-year and the 23.2-year exposures in the plant. The density results show a slight difference with the 5.6-year samples "failing" (defined as the density reaching 1.39 g/cc) a little bit earlier. This is the opposite of expectations and probably reflects the slightly lower initial density values for the 23.2-year samples (See Fig. XI-22). Therefore the wear-out results show no evidence of any aging up to 23.2 years. In terms of the Wear-out plot, the results imply essentially horizontal behavior as seen from Fig. XI-25. Horizontal behavior implies very long lifetimes consistent with our expectations for EPR insulation materials. Therefore the Wear-out approach confirms the accelerated aging extrapolations. By periodically obtaining additional ambiently aged samples of increasing age, future Wear-out experiments can be used to generate more such data, thereby further enhancing confidence in long lifetimes for this material.

Wear-out approach applied to XLPO-02B

As noted earlier in this report, density measurements are not a viable CM approach for XLPO materials. Since the NMR relaxation approach is applicable to such materials we decided to use NMR measurements to test the Wear-out approach on XLPO-02B samples that had pre-aged at 109°C for times up to ~7 years. The results for NMR T_2 versus aging time at 138°C are shown on Fig. XI-26. The results for the aged materials are somewhat unusual in that they tend to increase slightly at first before decreasing later on in time. This effect is probably because the time-zero samples had been aged at 109°C (below the main melting peak of the material) causing perfection of the crystallites and a consequent lowering of the NMR T_2. Since the Wear-out aging occurs above the melting point region, this perfection is destroyed by placing the samples in the Wear-out oven leading to an increase in T_2 before subsequent aging causes it to begin decreasing. This explanation is consistent with the lack of an increase in the unaged sample that never experienced aging at 109°C. For samples aged beyond 171 days, the small changes in T_2 coupled with the maximum in the observed values makes Wear-out analysis difficult. However, it is possible to use the earlier time data with an end of life criterion of 2-msec to create the Wear-out plot shown in Fig. XI-27. The extrapolation of the early time results yields a predicted lifetime of ~270 weeks at 109°C close to the actual result of ~320 weeks (Fig. III-48).

Although this type of analysis appears to be pushing the credibility factor, it is interesting to note that our predictions from accelerated aging estimate extremely long lifetimes for the XLPO materials. Therefore similar to the situation found for the nuclear power plant EPR cable insulation above, little aging would be expected for XLPO materials obtained from natural aging conditions in a nuclear plant. Thus we can expect that such materials will be in the early stages of aging for any material extracted from plant environments. In other words, we would expect samples of this XLPO-02B material to have T_2 values close to 13-msec regardless of age, implying that Wear-out studies using NMR will give horizontal behavior similar to the EPR material (Fig. XI-25). This of course holds true for aging at 50°C. However, XLPO that is inadvertently aged at high temperatures (e.g., 80°C to 110°C), due to conditions such as being adjacent to uninsulated high-energy pipes, can experience severe aging well before 40-year ambient exposures. The Wear-out technique would be useful in evaluating the condition of cables that have been exposed to such severe conditions.

Wear-out approach applied to Neo-01

The Neo-01 is the neoprene material where we had long-term aging results at 24°C (19.2 years and 23.6 years) in addition to aging results from 70°C to 131°C (Fig. III-5). As discussed in Section III, extrapolation of time-temperature superposed results for the temperature range of 70°C to 131°C led to a practical end of life estimate of ~93 years at 24°C. By including the 19.2 year and 23.6 year results at 24°C in the analysis, the resulting curvature in the Arrhenius plot lowered this estimate to ~37 years. Because we had samples that had aged for long periods of time at 24°C, it was possible to carry out Wear-out studies on these ambiently aged samples to make Wear-out predictions for the

practical end of life at 24°C. Sufficient material was available to do Wear-out studies using elongation as the degradation parameter. In particular, when the 19.2-year samples were tensile tested in March, 1998, 16 additional 19.2 year-old tensile specimens were available and placed into an 80°C Wear-out experiment. Two tensile specimens were extracted and tested after each of eight Wear-out aging times at 80°C. Figure XI-28 shows the average elongation values versus aging time at 80°C together with a solid curve that represents the 80°C time-temperature superposed data obtained from accelerated aging studies. This latter curve was derived from Fig. III-6 by dividing the x-axis time scale by 120 (the a_T value from 24°C to 80°C as noted in the figure). From the dashed curve through the Wear-out results in Fig. XI-28, we can estimate a Wear-out time to 50% elongation of 69 days. Similar 80°C Wear-out experiments were conducted at the same time the 23.6 year-old samples were tensile tested in August, 2002. For these experiments 27 tensile specimens were placed in the 80°C oven and three samples were extracted for tensile testing at nine different aging times. Figure XI-29 shows the average elongation values versus aging time at 80°C again together with the solid curve that represents the 80°C time-temperature superposed data obtained from accelerated aging studies. The dashed curve through the Wear-out results allows us to estimate a Wear-out time to 50% elongation of 62 days.

The procedure used to derive the 69-day (19.2 years at 24°C) and 62-day (23.6 years at 24°) Wear-out time results for Neo-01 is identical to the procedure used for all of the earlier examples in this Section. However, there is another analysis approach that can be used for Wear-out results that is a superior approach when it is available. We refer to this approach as time-degradation superposition [XI-1, XI-2]. Instead of selecting the Wear-out time to 50% elongation, thereby eliminating most of the Wear-out data from the analyses, time-degradation superposition uses all of the Wear-out results by additively time shifting the Wear-out data so that it gives the best superposition with the 80°C aging curve (the solid curves in Figs. XI-28 and XI-29). When this procedure is carried out on the 19.2-year data (Fig. XI-28), we find that an additive shift a_D in time of 46 days leads to the best superposition, as shown in Fig. XI-30. Similarly a shift of 53 days leads to the best superposition for the 23.6-year results (Fig. XI-31).

The main advantage of time-degradation superposition is the use of all the data instead of a single processed data point. This advantage is similar to the advantage time-temperature superposition has over conventional Arrhenius approach as discussed in Section III of this document. It is easy to see that this approach is not applicable to materials that show "induction-time" behavior since the only time amenable to analysis is the induction time for such materials. For this reason, it would not be useful to attempt the application of time-degradation superposition to materials that show little change in properties until rapid changes occur at the induction time.

Another advantage to time-degradation superposition is that a defined "end of life" criterion (e.g., 50% elongation) is not needed. In order to use the shift factors for predicting practical end of life, however, an end of life criterion must be selected. With our usual choice of 50% elongation, the solid curves for previously unaged material at 80°C (Figs. XI-28 or XI-29) indicate that 112 days at 80°C is required. The Wear-out

time is then given by 112 days minus the time-degradation shift factor a_D. Since the a_D values are 46 days and 53 days for the 19.2 year and 23.6 year samples, respectively, the Wear-out times will equal 66 days and 59 days. Figure XI-32 plots these Wear-out times (diamonds) and the Wear-out times from the earlier conventional analyses (squares) on the final Wear-out plot for this material. Linear extrapolation of the Wear-out results indicates a 24°C lifetime of ~49 years. This compares to the 93 year prediction from a conventional Arrhenius extrapolation using the data from 70°C and above and a 37 year lifetime predicted from the analysis that includes the 24°C data out to 23.6 years (Section III). Although the Wear-out result (49 years) is somewhat higher than the 37 year prediction, it is clearly an improvement over the conventional extrapolation result (93 years). In addition, one must remember that the 37-year prediction represents an extrapolation of the 24°C data with the assumption that the results after 19.2 and 23.6 years will exactly follow the shape of the superposed degradation curve derived from the higher temperature results.

Conclusions

The Wear-out approach can be a useful method for estimating residual lifetimes of cable jacketing and insulation materials. It is especially useful for materials that show "induction-time" behavior since condition-monitoring techniques applied to such materials may give little warning of impending end of life. Through the use of the Wear-out approach, this non-predictability can be transformed into predictive results. When time-temperature superposition is valid over the temperature range from ambient to the Wear-out temperature, theory predicts a linear Wear-out plot. Wear-out experiments on two EPR insulation materials lead to fairly linear Wear-out predictive plots even though one of the materials does not show time-temperature superposition. Wear-out experiments on an EPR insulation obtained from a nuclear power plant environment estimated to be 51°C for up to 23 years indicated very long residual lifetime for this material. This prediction is consistent with the extrapolated results of accelerated aging experiments on five different EPR cable insulations.

References

XI-1. K. T. Gillen and M. Celina, "The Wear-out Approach for Predicting the Remaining Lifetime of Materials", Polym. Degrad. Stabil., 71, 15 (2001).

XI-2. K. T. Gillen and M. Celina, "New Methods for Predicting Lifetimes, Part 2: The Wear-out Approach for Predicting the Remaining Lifetimes of Materials", Sandia Report SAND2000-0715 (March, 2000).

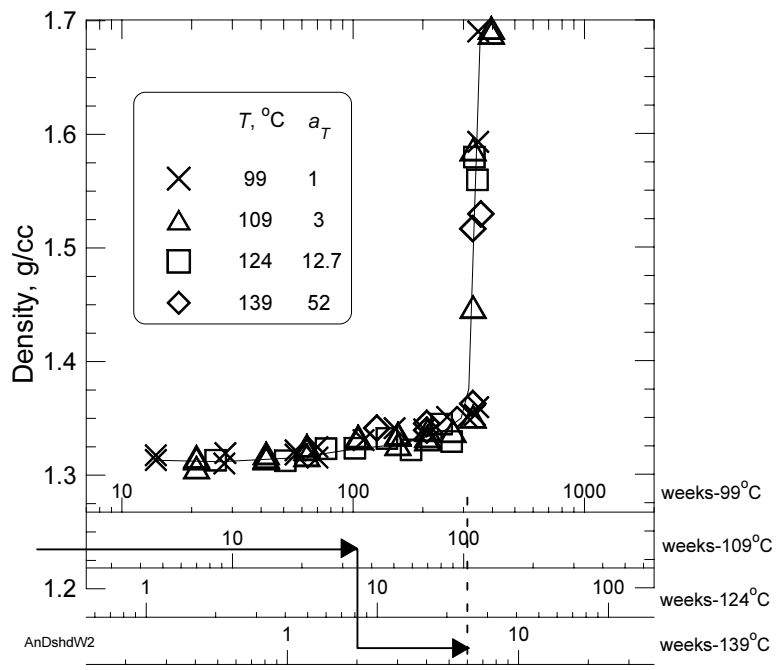

Figure XI-1. Time-temperature superposition of the density results for EPR-04 using the empirically derived shift factors shown on the figure. The time-scales appropriate to each temperature are shown below the superposed results.

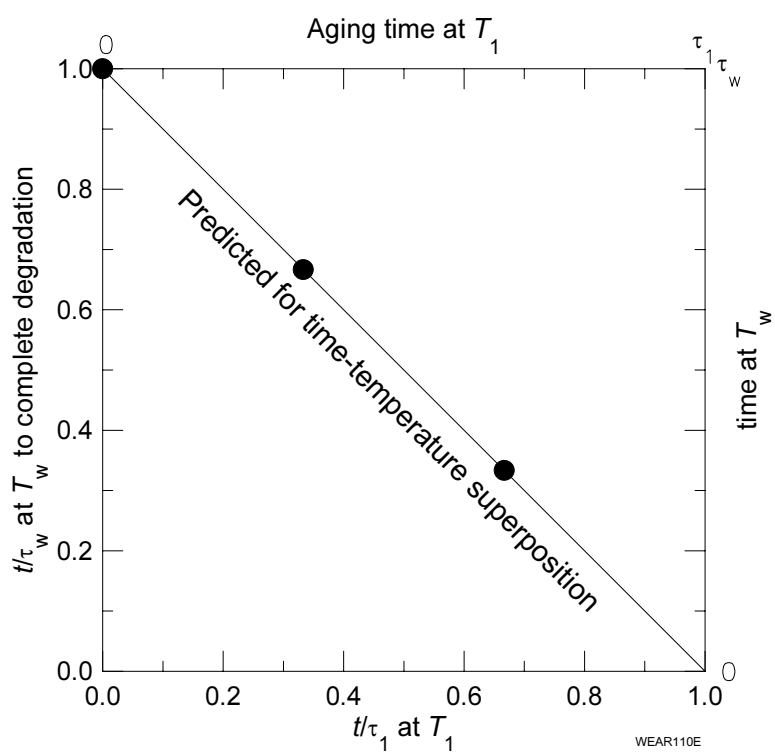

Figure XI-2. Hypothetical Wear-out plot when time-temperature superposition holds from the preaging temperature T_1 to the wear-out temperature T_w.

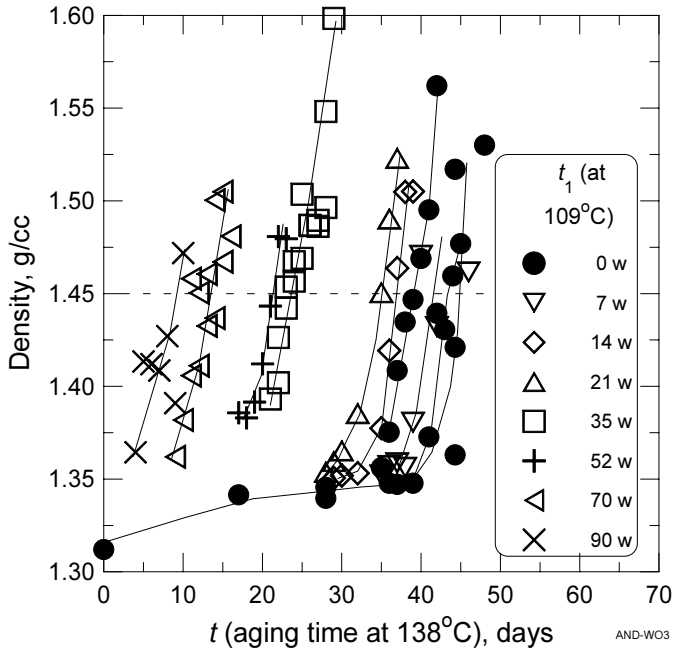

Figure XI-3. Density results versus aging time at 138°C for EPR-04 samples that were pre-aged at 109°C for the times indicated.

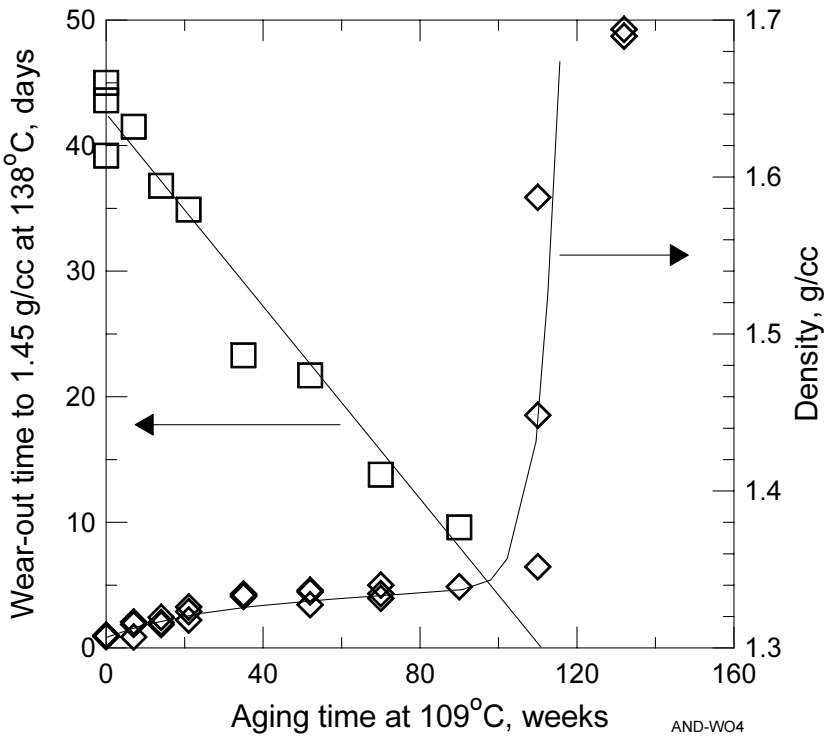

Figure XI-4. Wear-out times (squares- left y-axis) to 1.45 g/cc density obtained from Fig. XI-3 plotted versus pre-aging time at 109°C. Density results (diamonds- right y-axis) versus 109°C aging time are also shown.

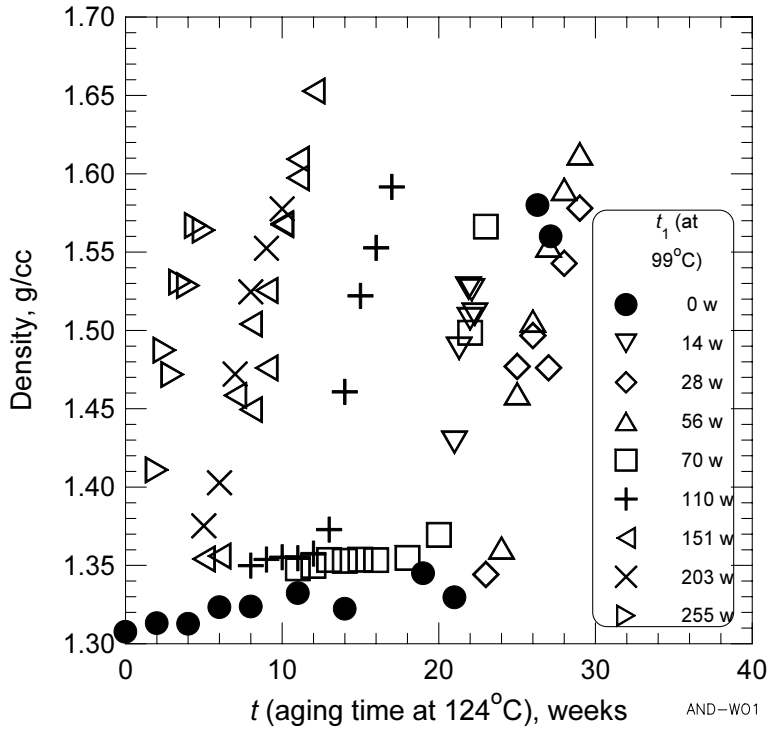

Figure XI-5. Density results versus aging time at 124°C for EPR-04 samples that were pre-aged at 99°C for the times indicated.

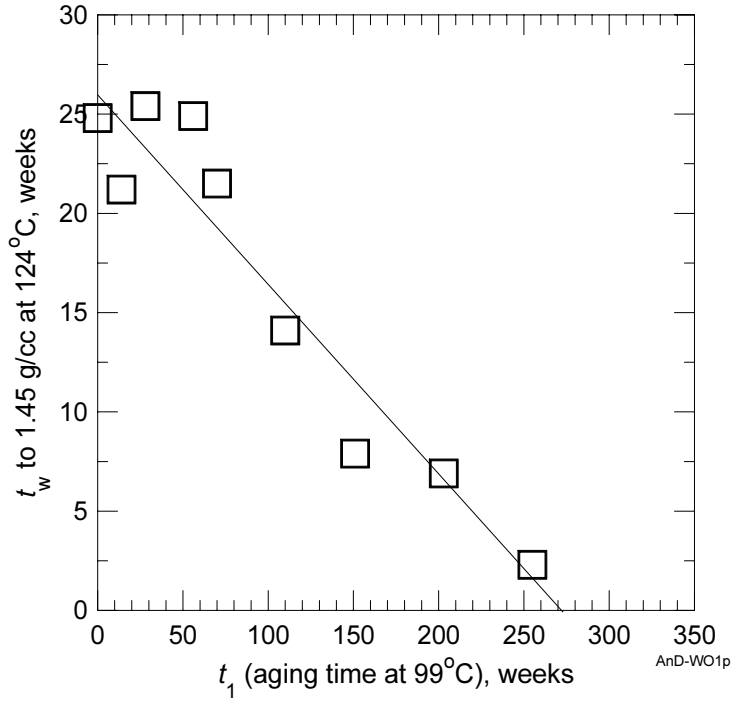

Figure XI-6. Wear-out times to 1.45 g/cc density obtained from Fig. XI-5 plotted versus pre-aging time at 99°C.

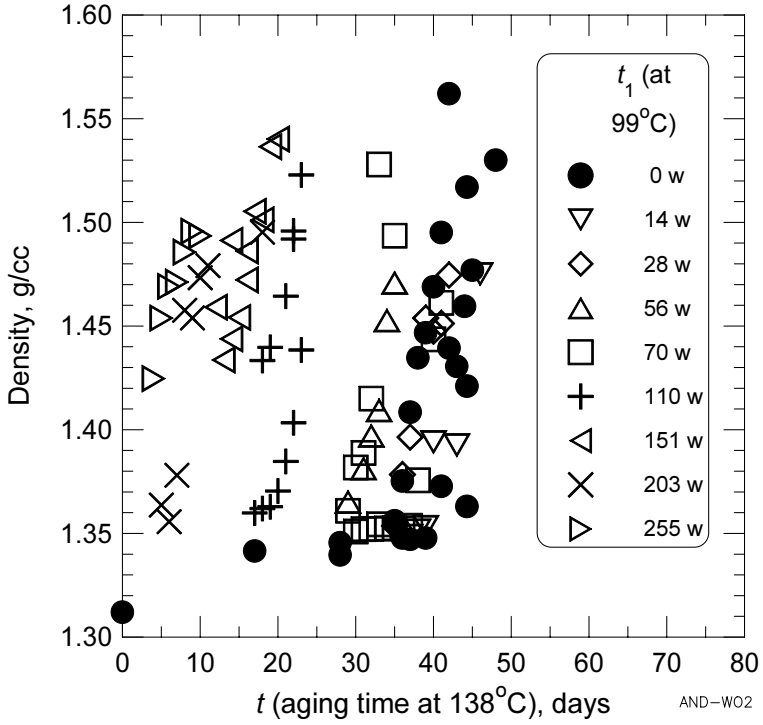

Figure XI-7. Density results versus aging time at 138°C for EPR-04 samples that were pre-aged at 99°C for the times indicated.

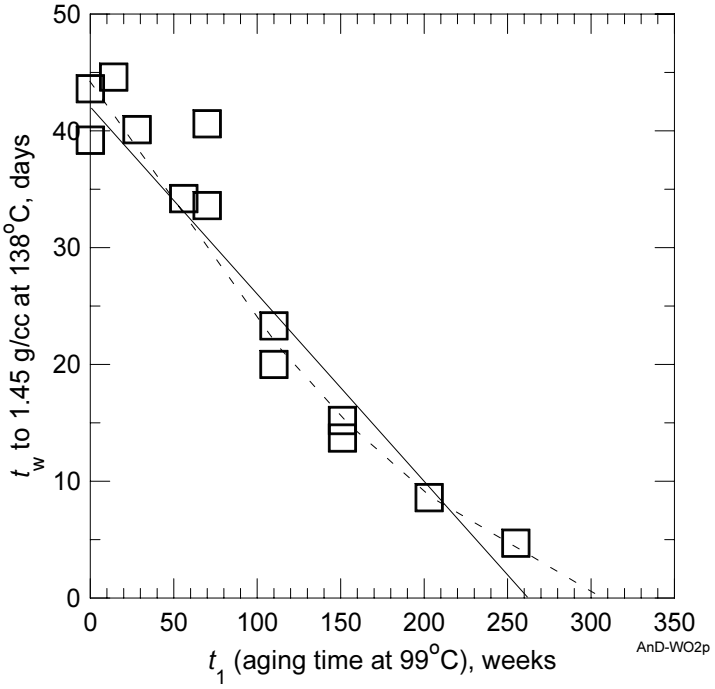

Figure XI-8. Wear-out times to 1.45 g/cc density obtained from Fig. XI-7 plotted versus pre-aging time at 99°C.

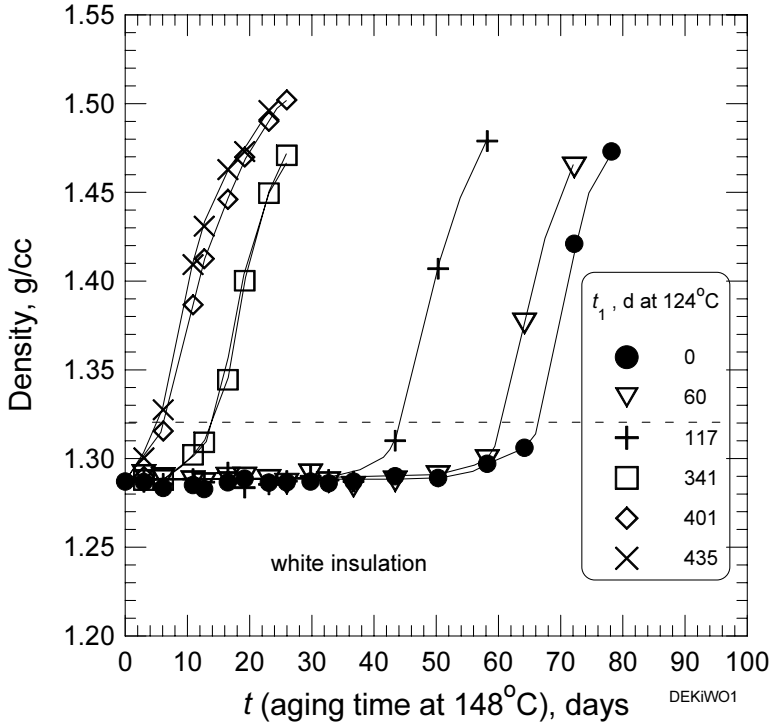

Figure XI-9. Density results versus aging time at 148°C for white EPR-03 samples that were pre-aged at 124°C for the times indicated.

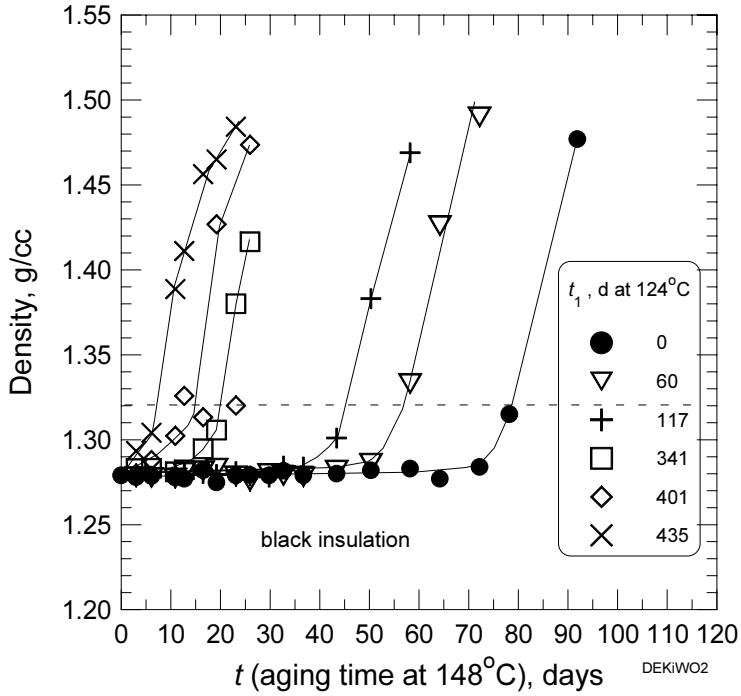

Figure XI-10. Density results versus aging time at 148°C for black EPR-03 samples that were pre-aged at 124°C for the times indicated.

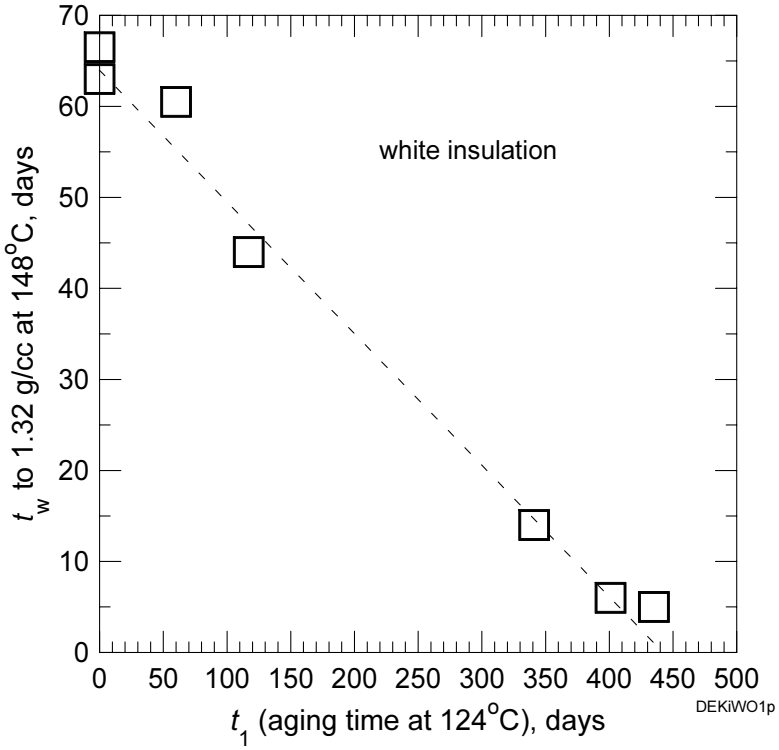

Figure XI-11. Wear-out times at 148°C to 1.32 g/cc density obtained from Fig. XI-9 plotted versus pre-aging time at 124°C.

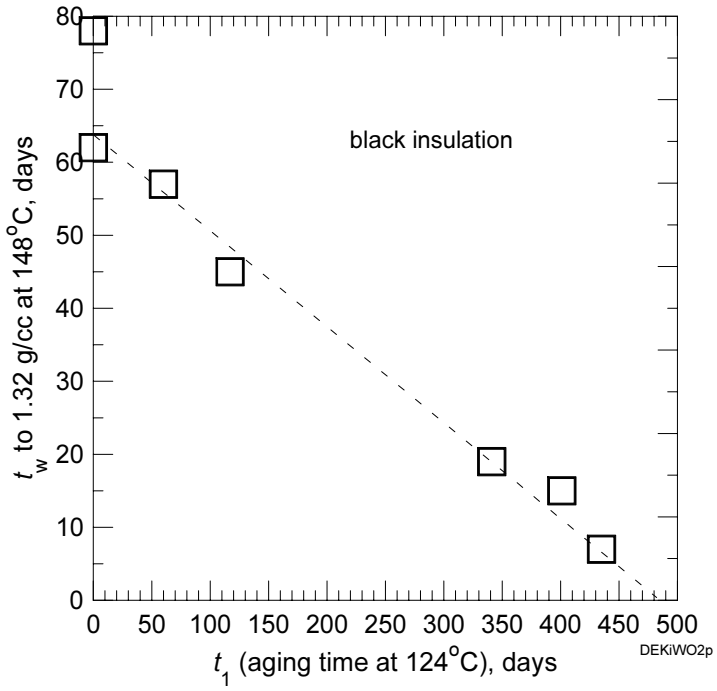

Figure XI-12. Wear-out times at 148°C to 1.32 g/cc density obtained from Fig. XI-10 plotted versus pre-aging time at 124°C.

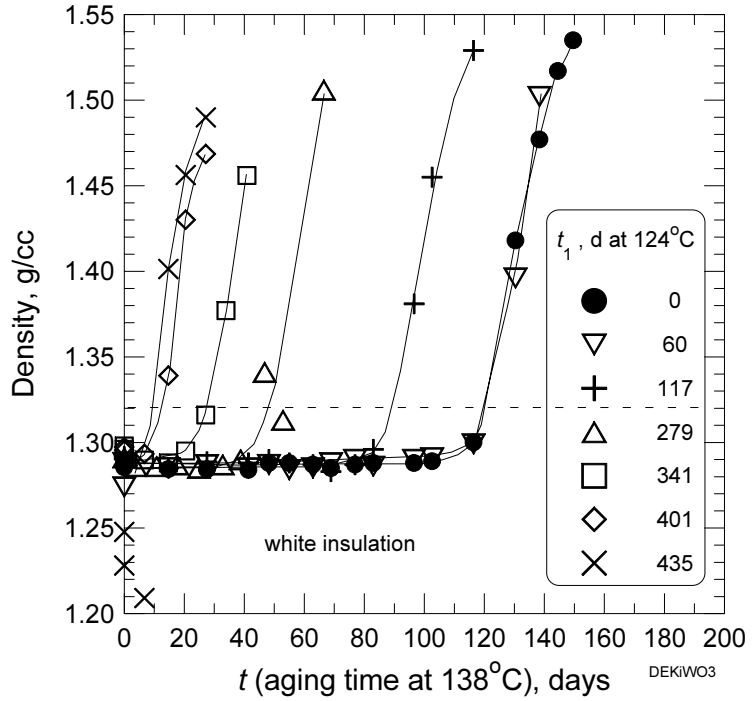

Figure XI-13. Density results versus aging time at 138°C for white EPR-03 samples that were pre-aged at 124°C for the times indicated.

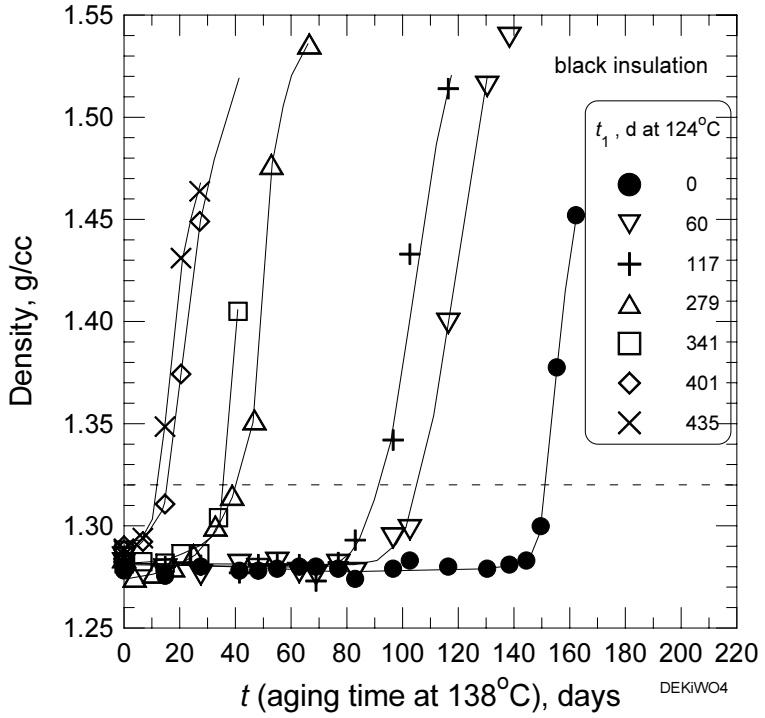

Figure XI-14. Density results versus aging time at 138°C for black EPR-03 samples that were pre-aged at 124°C for the times indicated.

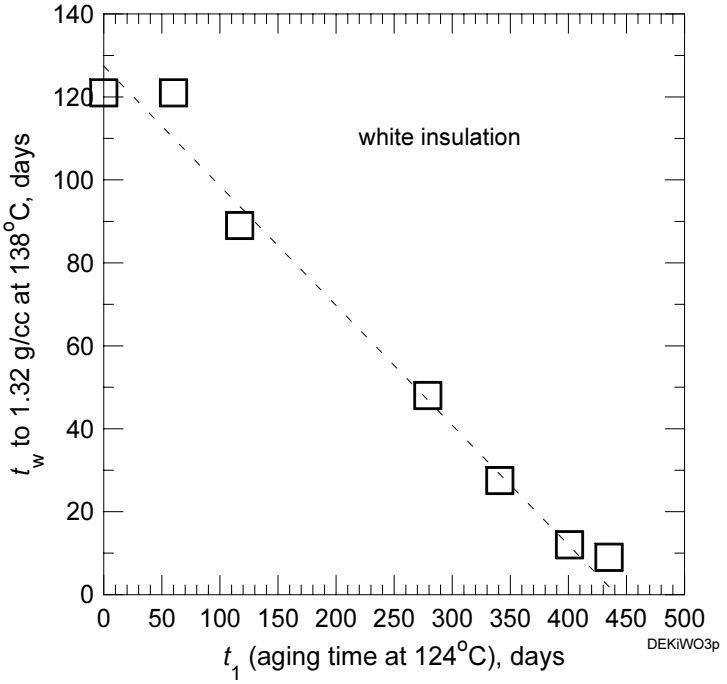

Figure XI-15. Wear-out times at 138°C to 1.32 g/cc density obtained from Fig. XI-13 plotted versus pre-aging time at 124°C.

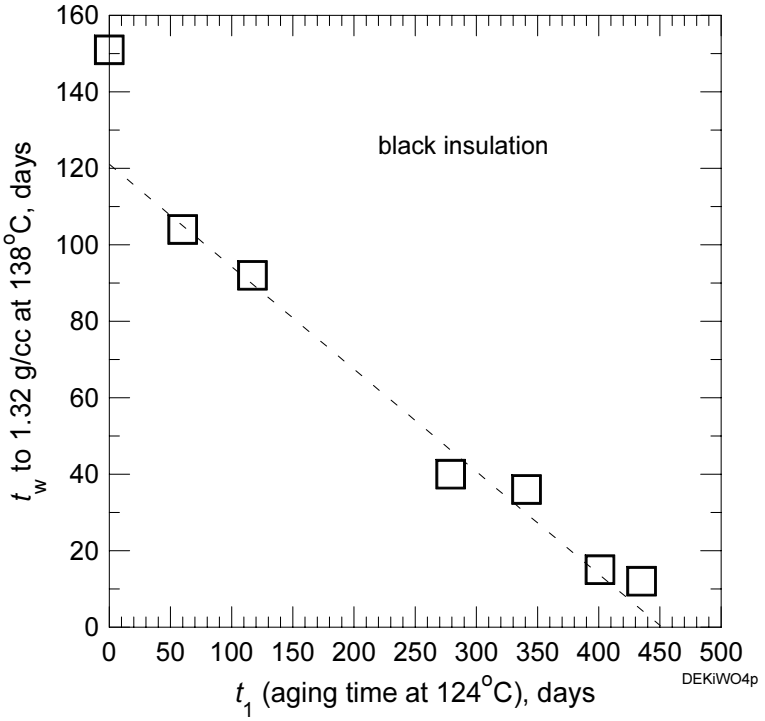

Figure XI-16. Wear-out times at 138°C to 1.32 g/cc density obtained from Fig. XI-14 plotted versus pre-aging time at 124°C.

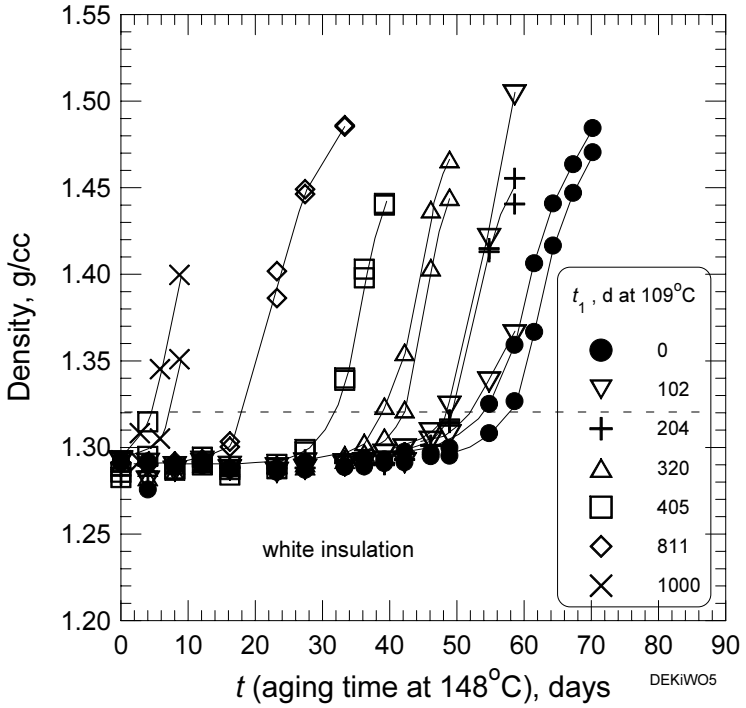

Figure XI-17. Density results versus aging time at 148°C for white EPR-03 samples that were pre-aged at 109°C for the times indicated (1133 and 1250 d samples left off plot).

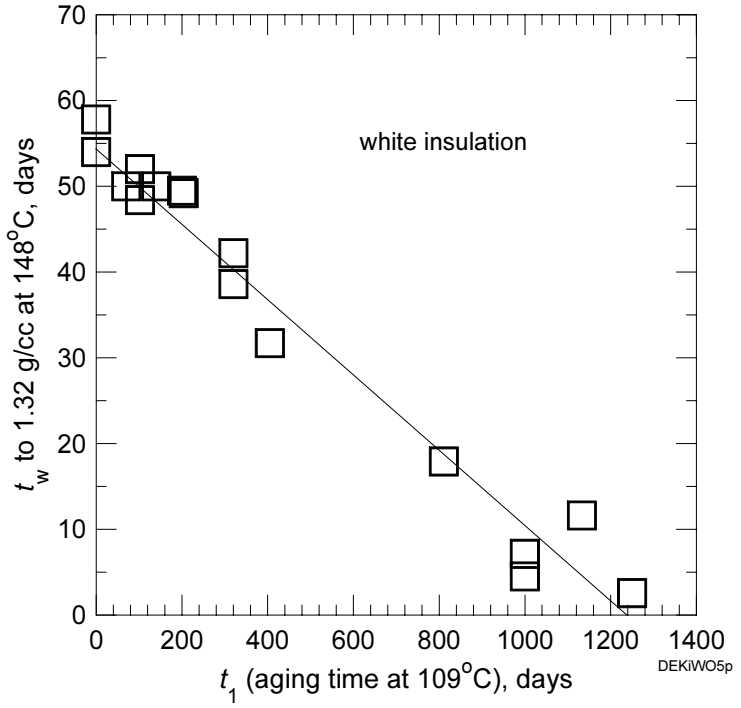

Figure XI-18. Wear-out times at 148°C to 1.32 g/cc density obtained from Fig. XI-17 plotted versus pre-aging time at 109°C.

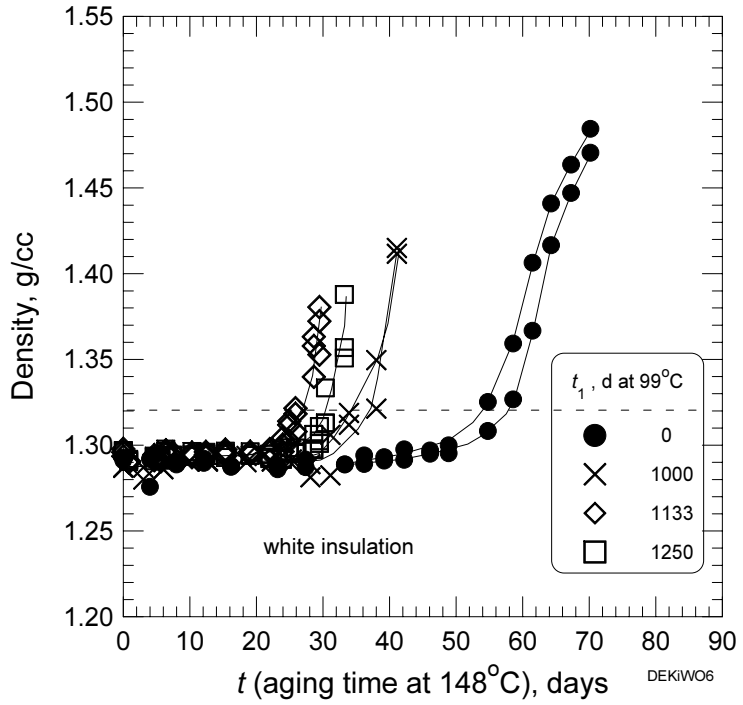

Figure XI-19. Density results versus aging time at 148°C for white EPR-03 samples that were pre-aged at 99°C for the times indicated (1133 and 1250 d samples left off plot).

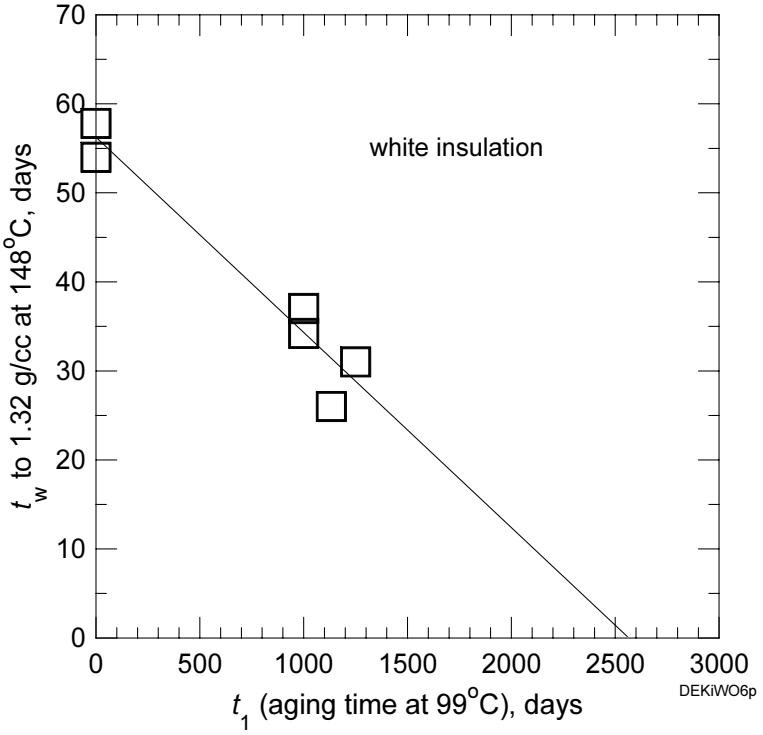

Figure XI-20. Wear-out times at 148°C to 1.32 g/cc density obtained from Fig. XI-19 plotted versus pre-aging time at 99°C.

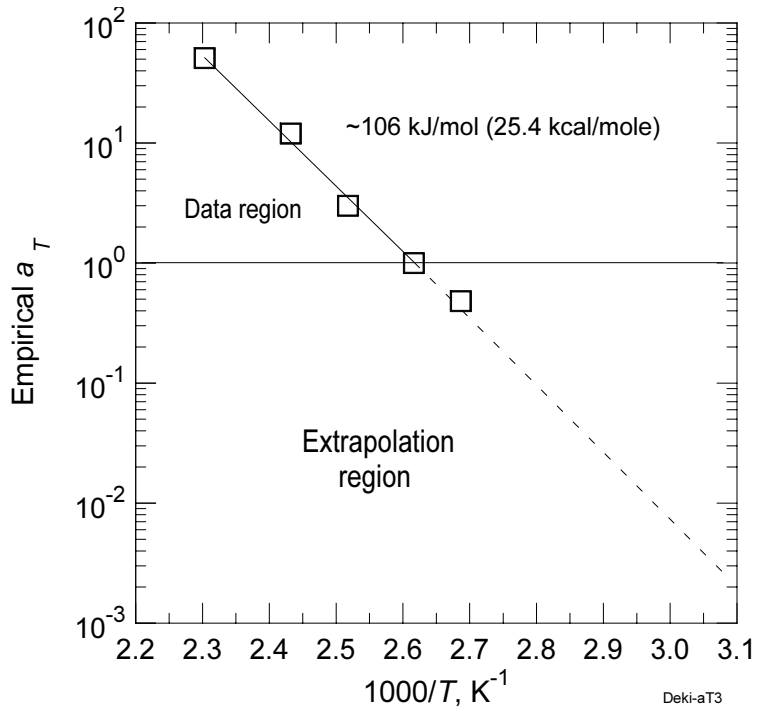

Figure XI-21. Arrhenius plot for EPR-03 including the 99°C point estimated from the Wear-out experiments on samples aged at this temperature.

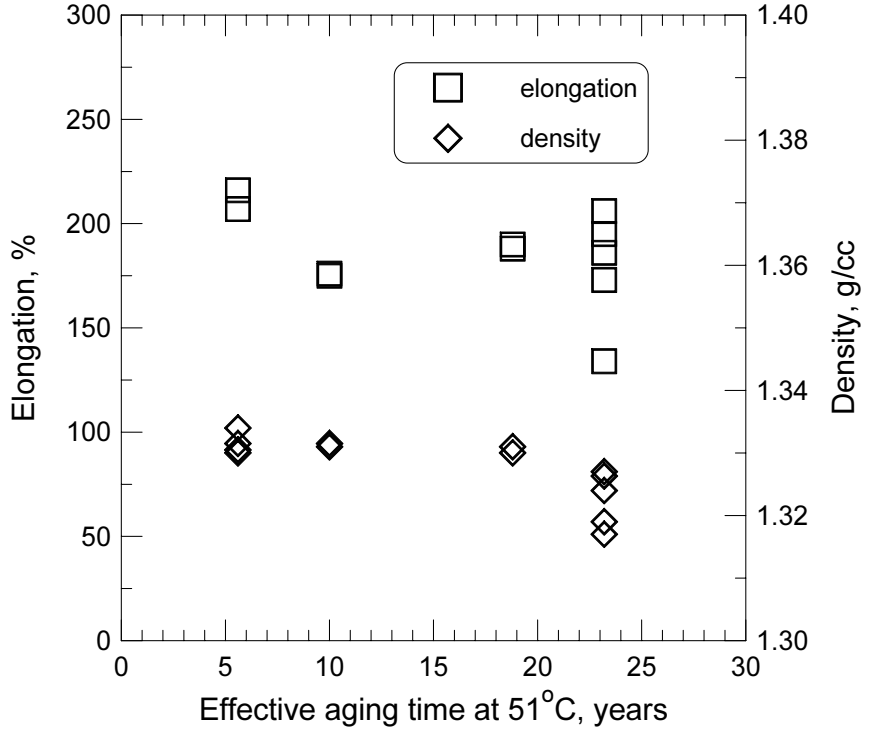

Figure XI-22. Elongation and density results for EPR materials aged at 51°C in a nuclear power plant.

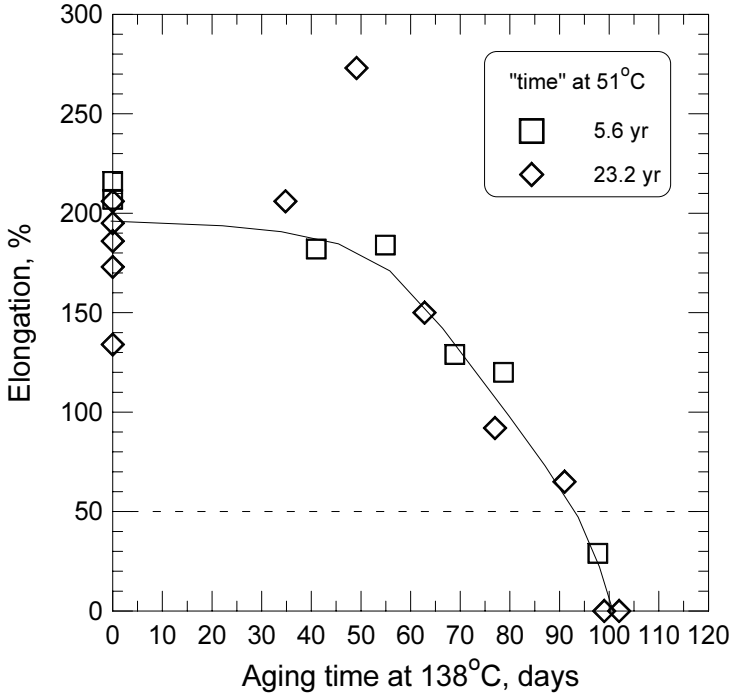

Figure XI-23. Elongation results versus aging time at 138°C for power plant aged EPR material that was preaged for the indicated times at an estimated 51°C aging temperature.

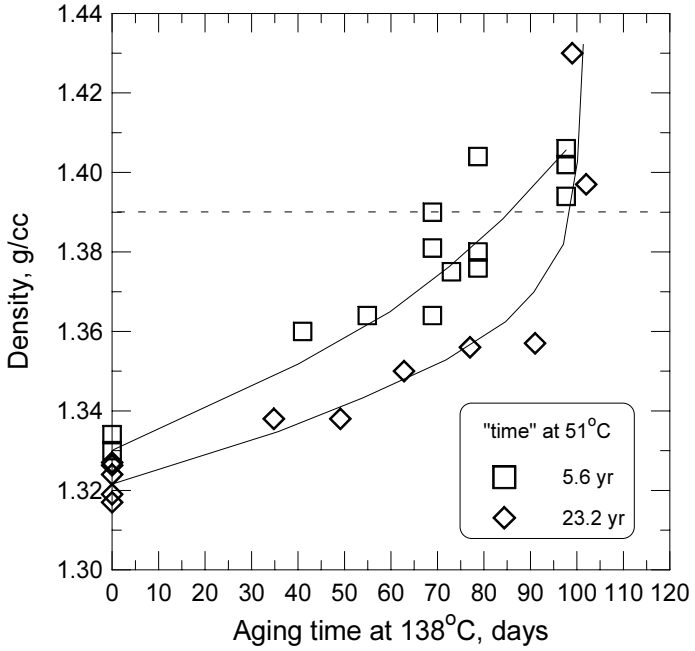

Figure XI-24. Density results versus aging time at 138°C for power plant aged EPR material that was preaged for the indicated times at an estimated 51°C aging temperature.

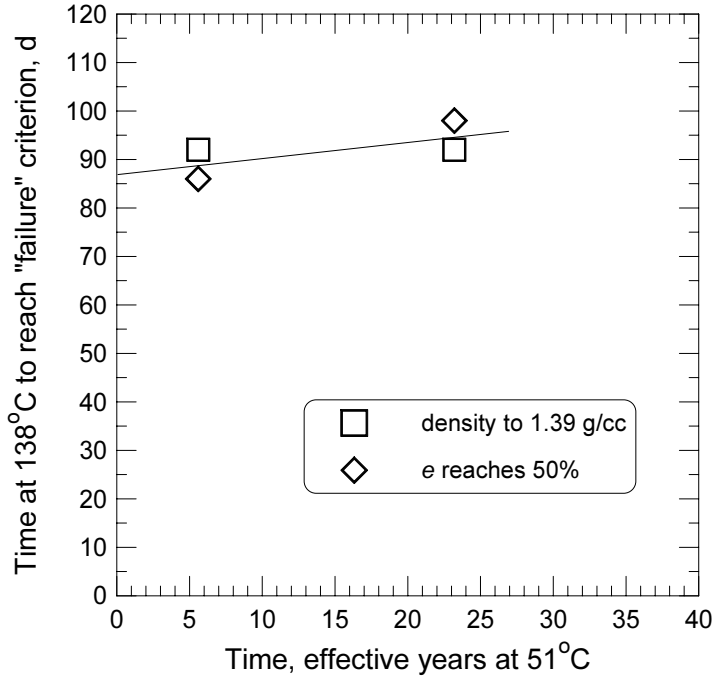

Figure XI-25. Wear-out plot for elongation and density end of life criteria versus EPR plant-aging time at an estimated temperature of 51°C.

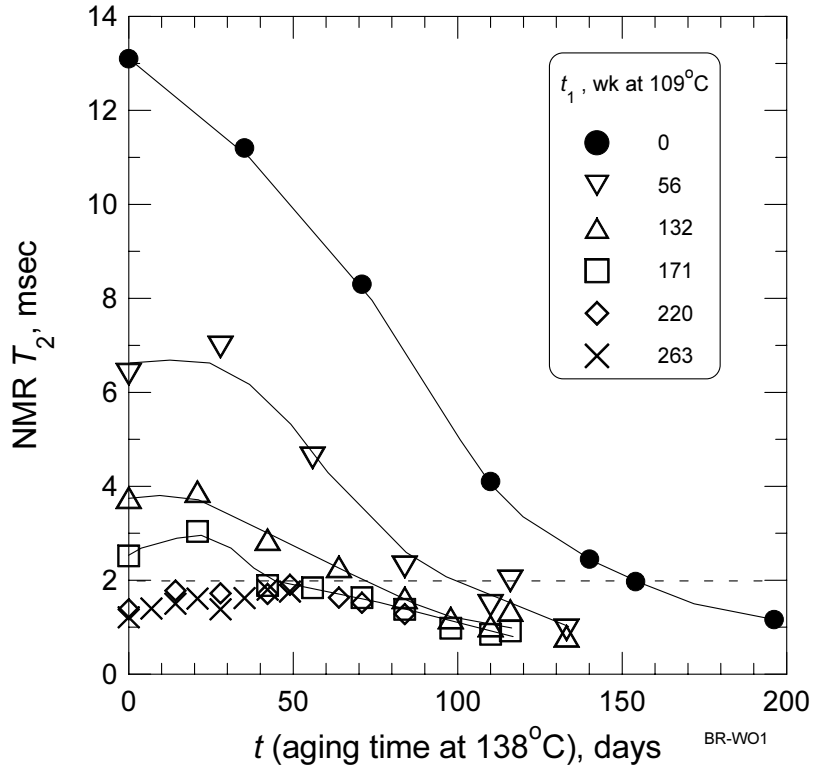

Figure XI-26. NMR T_2 results versus aging time at 138°C for XLPO-02B samples that were pre-aged at 109°C for the times indicated.

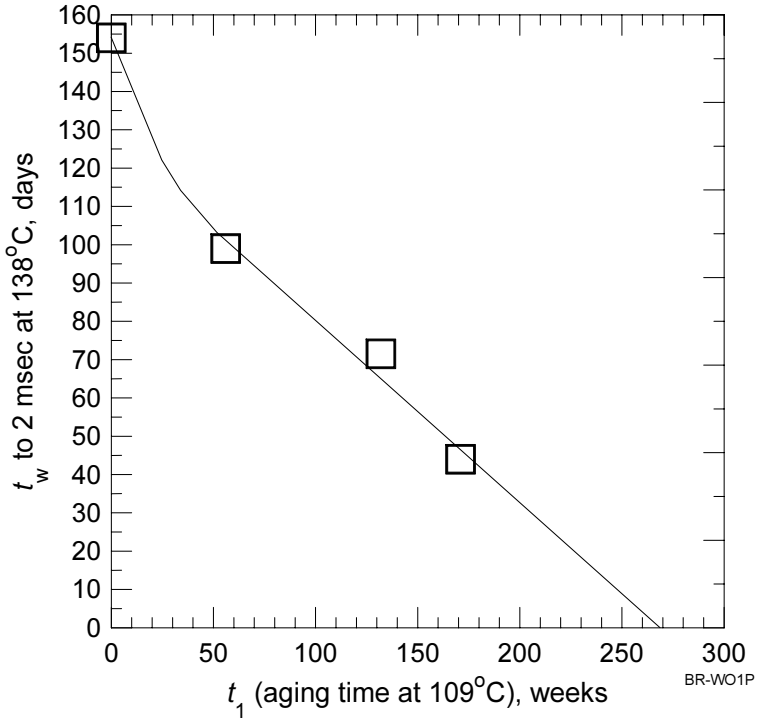

Figure XI-27. Wear-out times at 138°C to 2-msec NMR T_2 obtained from Fig. XI-26 plotted versus pre-aging time at 109°C.

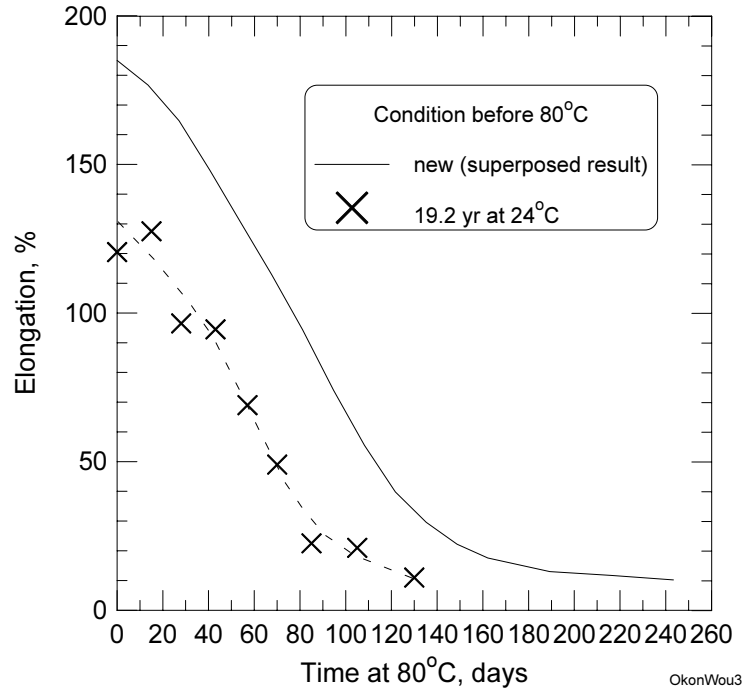

Figure XI-28. Elongation results versus aging time at 80°C for Neo-01 samples that were pre-aged at 24°C for 19.2 years.

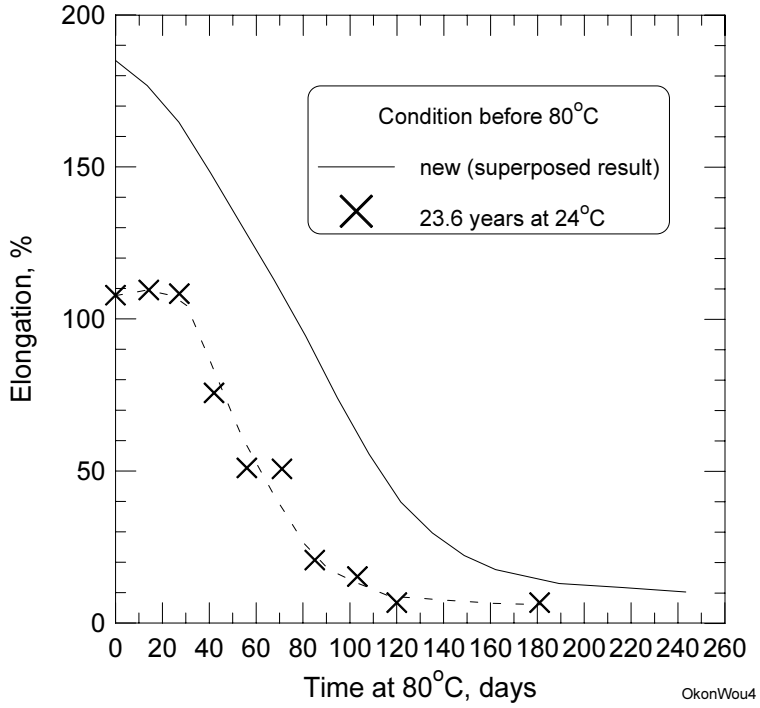

Figure XI-29. Elongation results versus aging time at 80°C for Neo-01 samples that were pre-aged at 24°C for 23.6 years.

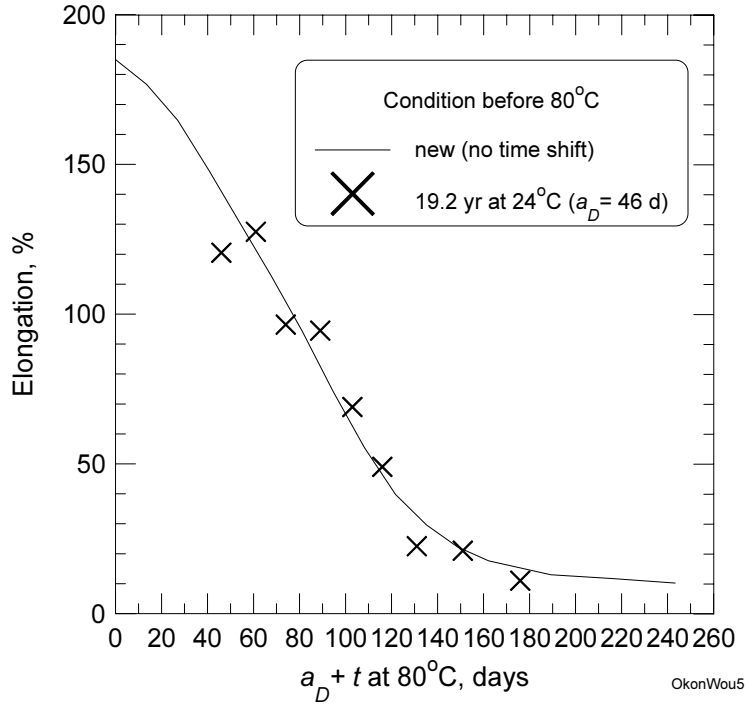

Figure XI-30. Time-degradation superposition of 80°C Wear-out results (19.2 years at 24°C pre-aging) with superposed 80°C curve from accelerated aging of new material.

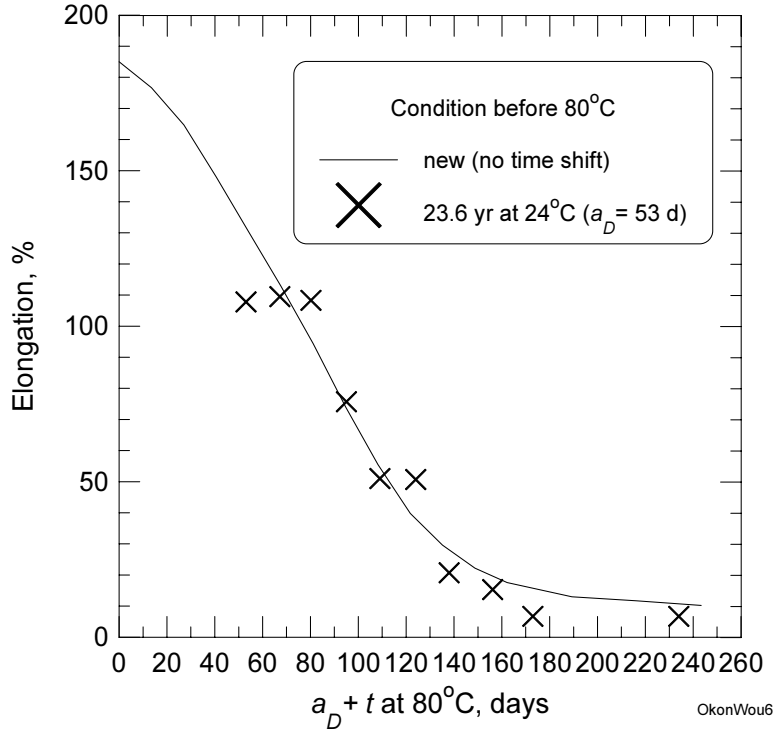

Figure XI-31. Time-degradation superposition of 80°C Wear-out results (23.6 years at 24°C pre-aging) with superposed 80°C curve from accelerated aging of new material.

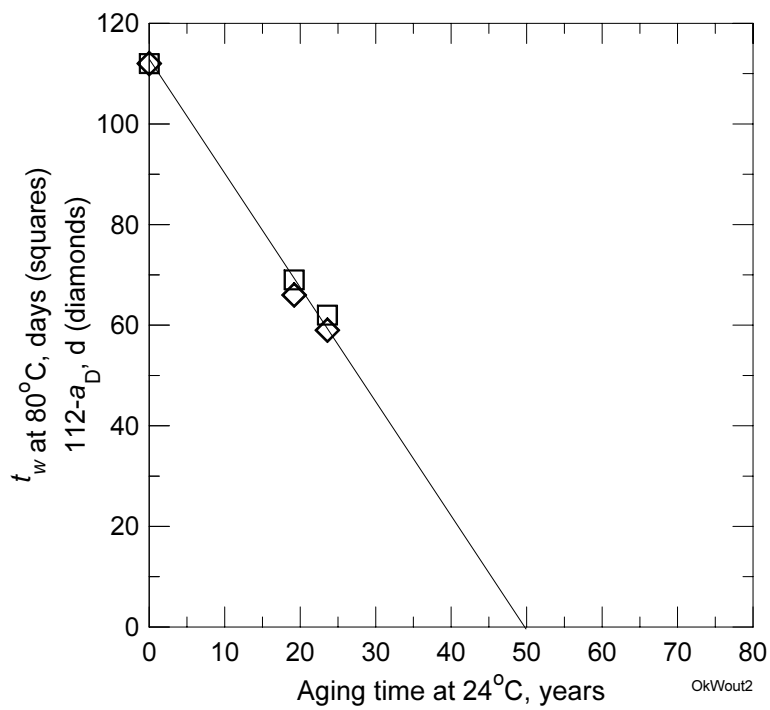

Figure XI-32. Wear-out times at 80°C to 50% elongation obtained from Figs. XI-28 through XI-31 plotted versus pre-aging time at 24°C.

XII. Summary and Conclusions

The NEPO cable-aging program concentrated on two important issues involving the development of better lifetime prediction methods as well as the development and testing of novel cable condition-monitoring (CM) techniques. To address improved life prediction methods, we first described in Section III of this report how the use of time-temperature superposition principles improves the testing of the Arrhenius model by utilizing all of the experimentally generated data instead of a few selected and processed data points. This allows one to quantitatively test the fundamental basis underlying accelerated aging protocols, that is the assumption that raising the temperature equally accelerates all of the reactions underlying degradation. Using rarely available long-term (up to 24 years) data on important nuclear power plant cable jacketing and insulation materials we showed that non-superposition can occur (EPR-04, XLPO-02B) violating the constant acceleration assumption. In addition the long-term results allowed us to show that curvature in Arrhenius plots for elongation are commonly observed if data are taken over a large enough temperature range (Neo-01, several hypalon materials). The long-term results also allowed us to test the significance of extrapolating through the crystalline melting point region of semi-crystalline materials where we found that some materials are unaffected by such an extrapolation (XLPO-04) while others can show important effects (XLPO-02B). Based on these results, we concluded that chloroprene based cable jackets may sustain significant degradation at 50°C aging temperatures whereas hypalon and CPE jackets should sustain much less damage under these conditions. For the EPR and XLPO cable insulations, simple Arrhenius extrapolations imply exceedingly long lifetimes. Even though there is significant concern about such extrapolations due to possible crystalline melting point effects and the possibility of downward curvature in the Arrhenius plots in the extrapolation region, the long-term data generated in the current study offers much confidence in the long-term viability of such materials.

In Section IV of the report, we bolstered such confidence by utilizing ultrasensitive oxygen consumption (UOC) measurements to probe the low temperature extrapolation region. The O_2 consumption results at higher temperatures overlapping mechanical property measurements showed that O_2 consumption measurements are usually well correlated with mechanical property (e.g., elongation) measurements as anticipated since the presence of oxygen during aging is usually found to dominate degradation. The advantage of O_2 consumption measurements is their sensitivity that allows the probing of lower temperatures. By utilizing such lower temperature data coupled with time-temperature superposition analyses, these capabilities allowed us to quantitatively test the Arrhenius extrapolation assumption. Such testing indicates that many materials show evidence of "downward" curvature (E_a values drop as the aging temperature is lowered) consistent with many literature results and with the results found in Section III for elongation measurements. The UOC approach also allows the probing of temperatures that cross through the crystalline melting point region of semi-crystalline materials such as XLPO and EPR cable insulations. Again the consumption results appear to be well-correlated with elongation results for the few cases where elongation results have been obtained below the main melting point of the material.

The evidence for correlations between elongation and UOC allows us to utilize the lower temperature E_a values obtained from O_2 consumption to more reliably extrapolate higher temperature mechanical property results. For an aging temperature of 50°C, the improved predictions allow us to conclude that the lifetime of hypalon jackets should be greater than 80 years whereas EPR and XLPO insulations have predicted lifetimes many times longer.

New results on combined environment aging (Section V) of neoprene and hypalon cable jacketing materials offer additional evidence in support of our time-temperature-dose rate (*t-T-DR*) superposition approach that had been used successfully in the past for such situations. The extrapolated predictions for these materials at a 50°C aging temperature indicate that dose rates below 0.1 Gy/h (10 rad/h) will normally not be important to the aging rates. Since most low voltage cables are exposed to lower levels than 0.1 Gy/h under typical nuclear power plant aging conditions, radiation effects are usually of little concern. Comparison for EPR-05 of two combined-environment aging conditions at a similar dose rate but differing temperatures (40°C versus 80°C) shows that inverse temperature effects are unimportant for this material. In addition, the robustness of this material in radiation environments underscores previous observations that nuclear power plant aging dose rates are typically too small to be of concern for EPR cable insulation materials.

As a prelude to discussing condition-monitoring (CM) techniques, we briefly described the implications of diffusion-limited oxidation (DLO) effects on the use of CM approaches in Section VI. We also described theoretical modeling that allows one to estimate the importance of DLO effects from measurements or estimates of the oxygen consumption rate and the oxygen permeability coefficient of the material under the aging condition of interest.

The first CM approach covered was modulus profiling (Section VII), a technique that can serve both as a CM approach and as a method for experimentally assessing the importance of DLO effects and other heterogeneously based artifacts. The results indicate that modulus profiling offers a very promising CM technique for nuclear power plant cable jacketing and insulation materials. It appears to be applicable to most materials that do not have important crystallinity including neoprene and hypalon jackets and EPR and silicone insulations. It shows sensitivity for these materials both in thermal-only and combined radiation plus thermal environments. In general modulus values increase with aging in both temperature-only and combined radiation-thermal environments. This implies that the overall crosslink density increases (crosslinking processes dominate scission processes) during the aging. For the neoprene and hypalon jacketing materials, the vast majority of the results both in thermal-only and combined radiation-thermal environments indicate that 50% absolute elongation is reached when modulus values get above ~35 MPa. For EPR insulations, modulus measurements are similar to other CM parameters in that they are relatively insensitive before the induction time but quite sensitive once the induction-time region is reached.

The second CM approach described involved NMR T_2 relaxation time measurements (Section VIII). For the current NMR T_2 studies, ~10 mg samples were used. However, a very significant advantage of the NMR approach is its capability for quickly and easily making measurements on extremely small samples. The 10 mg samples, that required less than 10 min per T_2 measurement on a fully automated NMR instrument, provided very high signal to noise ratios. We have shown in previous work that samples as small as 0.1 mg can easily be run, with samples in the μg region possible if desired. Most of the "essentially non-destructive" CM techniques examined to date require on the order of 10-20 mg. Since the NMR approach can be done on fractions of a mg, this represents an important step towards developing a true "non-destructive" CM technique. In addition, it should be noted that the NMR approach is applicable to at least some crosslinked polyolefin cable insulations. Because the mechanical properties of these semi-crystalline materials are dominated by their hard crystalline components, slight hardening of the amorphous regimes caused by aging has little effect on overall hardness, negating the applicability of such CM approaches as modulus profiling and indenter.

The next CM technique discussed involved gel and solvent uptake measurements (Section IX). These parameters are sensitive to the crosslink density of the material and therefore to the competition between scission and crosslinking that occurs during the aging of a crosslinked material. Since modulus and NMR relaxation times are also sensitive to changes in crosslink density, all three techniques tend to have similar applicability from a material point-of-view. In the case of gel and uptake, it appears that these approaches show promise for neoprene, hypalon and chlorinated polyethylene cable jackets both in thermal-only and combined radiation-thermal environments. These techniques also show promise for certain XLPO insulations. For EPR insulations and other XLPO insulations, these techniques are only sensitive in the "induction-time" region (the approximate point in time where the rapid changes in properties begin to occur), thereby offering little or no warning of impending end of life. Of the two approaches, uptake factor measurements look more promising for several reasons. For one thing, the changes in uptake factors tend to be greater than the changes in gel percentage mainly because additional crosslinks often have little effect on the already high initial gel percentage whereas new crosslinks can lead to substantial decreases in solvent weight pickup. In addition, it appears that a "universality" criterion may exist for hypalon cable jacketing (and perhaps neoprene cable jacketing) materials where the elongation reaches 50% absolute corresponds to the uptake factor reaching ~1.6. This "universality" criterion is similar to the 35 MPa criterion that appears to hold for the modulus of hypalon and neoprene materials. If true, such universality criteria might allow property condition estimates to be made on hypalon jacketing materials from other manufacturers in the absence of extensive laboratory testing results. It is also interesting to note that gel measurements can be easily and accurately made on very small samples (1 mg or less), implying that useful measurements could be made on very small pieces sliced from the outside of cable jackets.

The final CM approach covered looked at the applicability of density measurements (Section X). As found historically, density usually increased with aging in both thermal-only and combined radiation-thermal environments. For some materials the increases are

fairly small so that following density is not helpful. Even when the changes are significant, it is often found that the scatter in density is large enough to make its applicability as a CM approach more difficult than other available techniques. The scatter can come from variations in filler content along the cable as well as from variations in aging. When DLO effects are important, application of the density approach becomes very difficult. For materials with "induction-time" behavior, density tends to follow such behavior with small changes up to the induction-time region followed by large increases. Although this makes density useless as a CM technique for such materials, several advantages of density measurements make them appropriate for monitoring degradation of "induction-time" materials when applying the Wear-out approach.

The next section of the report (Section XI) focuses on the Wear-out approach, a new and useful method for estimating residual lifetimes of cable jacketing and insulation materials. It is shown that this method is especially useful for materials that show "induction-time" behavior since condition-monitoring techniques applied to such materials may give little warning of impending end of life. Through the use of the Wear-out approach, this non-predictability can be transformed into predictive results. When time-temperature superposition is valid over the temperature range from ambient to the Wear-out temperature, theory predicts a linear Wear-out plot. Wear-out experiments on two EPR insulation materials lead to fairly linear Wear-out predictive plots even though one of the materials does not show time-temperature superposition. Wear-out experiments on an EPR insulation obtained from a nuclear power plant environment estimated to be 51°C for up to 23 years indicated very long residual lifetime for this material. This prediction is consistent with the extrapolated results of accelerated aging experiments on five different EPR cable insulations.

Utilization of the above information by nuclear plant operators involves considering the above models, methods and approaches as part of a larger Toolbox of techniques and approaches available for determining the condition of cable materials. Each plant has a different aging environment containing different cable materials, different hot spots and different accessibility points for examining their cables. Techniques like modulus profiling and NMR profiling can be used to look for materials that age in unusual ways such as the inside anomalies found for Hyp-02 and Hyp-04 or the enhanced degradation due to copper-catalyzed oxidation found for EPR-01A. For plant locations where extracting larger pieces of jacket and/or insulation is possible, elongation measurements may be useful as a direct CM technique. When only smaller pieces or slices are available, other CM techniques are required. Roughly speaking, gram quantities are needed for elongation measurements, 50 mg for uptake, 5-10 mg for modulus profiling and 1 mg or less for NMR and percentage gel. When it is impossible to remove any material, the indenter approach may offer a totally non-destructive method. However, the indenter is most often applicable to cable jacketing materials since insulations are normally accessible only at terminations (places where small sacrificial specimens may be available for analyses). Often hot spots occur at terminations, thereby allowing access to insulation materials at higher-level aging conditions. The Wear-out approach is an ideal method to investigate the residual lifetimes of such materials. Similar to the result

found for the EPR insulation aged for 23 years at 51°C, Wear-out modeling of such extracted materials should be able to confirm very long lifetimes for many important insulation materials.

XIII. Acknowledgements

The current studies were part of the Nuclear Energy Plant Optimization (NEPO) program jointly funded by the DOE and by the Electric Power Research Institute (EPRI). The authors appreciate the many technical contributions made by Mathew Celina and the numerous helpful discussions with Gary Toman, the EPRI program manager. We also acknowledge the competent technical assistance provided by Mike Malone (tensile and modulus profiling), Lowell Jones (modulus profiling and density), Michelle Shedd (gel and uptake), Dora Derzon (O_2 consumption) and Brian Mather (NMR).

XIV. Published Papers Partially or Wholly Supported by the NEPO Program

Book Chapters and Invited Reviews

1. K. T. Gillen, E. R. Terrill and R. W. Winter, "Modulus Mapping of Rubbers Using Micro- and Nano-Indentation Techniques", Rubber Chemistry and Technology- Rubber Reviews. Invited Review, 74, 428 (2001).
2. R. A. Assink, M. Celina and K. T. Gillen, "Monitoring the Condition of Thermally Aged Polymers by NMR Relaxation Measurements", Polymer News, 28, 102 (2003).
3. K. T. Gillen, M. Celina and R. Bernstein, "Methods for Predicting Lifetimes and Remaining Lifetimes of Polymers", Service Life Prediction, Challenging the Status Quo. Eds., J. W. Martin, R. A. Ryntz and R. A Dickie, Chapter 4, pp. 67-78, 2005, Federation of Societies for Coating Technology.

Published Journal Articles

1. K. T. Gillen and M. Celina, "The Wear-out Approach for Predicting the Remaining Lifetime of Materials", Polym. Degrad. Stabil., 71, 15 (2001).
2. R. A. Assink, M. Celina, K. T. Gillen, R. L. Clough and T. M. Alam, "Morphology Changes During Radiation-Thermal Aging of an EPDM Copolymer and Polyethylene by Solid-State NMR Spectroscopy", Polym. Degrad. Stabil., 73, 355 (2001).
3. K. T. Gillen, M. Celina and R. Bernstein, "Residual Lifetime Estimates for Cable Materials from the Wear-out Approach", Transactions of the American Nuclear Society, 85, 389 (2001).
4. D. J. Harris, R. A. Assink and K. T. Gillen, ^{1}H T_2 NMR Monitoring of Crosslinked Polyolefin Aging", J. Appl. Poly. Sci., 90, 2578 (2003).
5. K. T. Gillen, R. A. Assink and R. Bernstein, "Condition Monitoring Approaches Applied to a Polychloroprene Cable Jacketing Material", Polym. Degrad. Stabil., 84, 419 (2004).
6. K. T. Gillen, M. Celina and R. Bernstein, "Review of the Ultrasensitive Oxygen Consumption Method Used for Making More Reliable Extrapolated Predictions of Polymer Lifetimes", ANTEC paper, 2004.
7. K. T. Gillen, R. Bernstein and D. K. Derzon, "Evidence of non-Arrhenius Behavior from Laboratory Aging and 24-year Field Aging of Chloroprene Rubber Materials, Polymer Degradation and Stability, 87, 57 (2005).
8. K. T. Gillen, R. Bernstein and M. Celina, "Non-Arrhenius Behavior for Oxidative Degradation of Chlorosulfonated Polyethylene Materials", Polymer Degradation and Stability, 87, 335(2005).
9. M. Celina and K. T. Gillen, "Oxygen Permeability Measurements on Elastomers at Temperatures up to 225°C", Macromolecules 38, 2754 (2005).

10. M. Celina, K. T. Gillen and R. A. Assink, "Accelerated aging and lifetime prediction: Review of non-Arrhenius behavior due to two competing processes", Polymer Degradation and Stability, 90, 395-404 (2005).
11. K. T. Gillen, R. A. Assink, R. Bernstein and M. Celina, "Condition-monitoring approaches applied to the degradation of chlorosulfonated polyethylene cable jacketing materials", Polymer Degradation and Stability, in press.
12. K. T. Gillen, R. Bernstein, R. L. Clough and M. Celina, "Lifetime Predictions for Semi-crystalline Cable Insulation Materials: I. Mechanical Property and Oxygen Consumption Measurements for EPR Materials, to be submitted.
13. K. T. Gillen, R. Bernstein, R. L. Clough and M. Celina, "Lifetime Predictions for Semi-crystalline Cable Insulation Materials: I. Mechanical Property and Oxygen Consumption Measurements for CLPO Materials, in preparation.
14. K. T. Gillen, M. Celina, R. Bernstein and M. Shedd, "The Wear-out Approach applied to Lifetime Predictions for EPR Cable Materials, in preparation.

Addendum- SCRAPS Excel file

An Excel file that contains much of the data used in this document is included on a cd containing this report. The file is labeled **SCRAPS80.xls** referring to the fact that this is the 80th update of this file that describes nuclear power plant cable aging data obtained over a more than 25 year period at Sandia National Laboratories. The acronym SCRAPS stands for Sandia's Cable Repository of Aged Polymer Samples.

Distribution

Unclassified Unlimited Release

Dr. Steven Boggs
Director, Electrical Insulation Research
University of Connecticut
Institute of Materials Science
Storrs Mansfield, CT 06269-0001

Dr. Kanapathi Anandakumaran
Sr. Research Engineer
Ontario Power Generation, Inc.
800 Kipling Ave
Toronto, Ontario M8Z 5S4
Canada

Dr. Tom Doyle
Veridian-PSR
1115 5th St SW
Charlottesville, VA 22902-6465

Mr. Jit P. Vora
U.S. Nuclear Regulatory Commission
One White Flint N (M/S T10E8)
11555 Rockville Pike
Rockville, MD 20852-2739

Professor Montgomery Shaw
University of Connecticut
97 N Eagleville Rd (Box U-136, Room 102)
Storrs Mansfield, CT 06269-9011

Mr. Robert Lofaro
Group Leader
Brookhaven National Laboratory
Nuclear Safety Library (M/S Bldg. 30)
Upton, NY 11973

Dr. David Bauer
Ford Motor Company
Research Laboratory
P.O. Box 2053
Dearborn, MI 48121

Dr. Jonathan Martin
NIST
100 Bureau Drive
MS 8616
Gaithersburg, MD 20899-8616

Professor William Meeker
Iowa State University
304C Snedecor Hall
Ames, IA 50011

Dr. James Pickett
GE Corporate Reaseach
Oe Research Circle
Bldg. K1, Room 5150
Niskayuna, NY 12309

Eric Skidmore
Principal Engineer
Westinghouse Savannah River Laboratory
Material NDE & Consultation Group
Aiken, SC

Dr. Paul Lieberman
Liberman Research Associates
19815 Mildred Avenue
Torrance, CA 90503-1121

Mr. John Dawson
AEA Technology
F 7 Culham
Abington
Oxon OX14 3ED
UK

Dr. Susan Burnay
White Hollow
High Street
E. Illsley
Newbury
Berks RG207LE
UK

Mr. Don J. Stonkus
DJS Associates
271 Lakeview Ave
Burlington, Ontario
Canada L7N1Y7

Dipl.Ing. Wolfgang Michel
FRAMATOME ANP NL
Frauenauracherstr. 85
D- 91050 Erlangen
Germany

Prof. G. C. Montanari
Dipartimento di Ingegneria Elettrica
University of Bologna
40136 Bologna
Italy

S. Giannoni
Underwriters Laboratory
Melville, NY 11747-3081

U.S. Nuclear Regulatory Commission
ATTN: Dr. Arthur Buslik, RES/DRAA/PRAB
Mail Stop: TWFN 10E50
11545 Rockville Pike
Rockville, MD 20852-2738

Dr. Ed Terrill
Akron Rubber Development Laboratory, Inc.
2887 Gilchrist Road
Akron, OH 44305

Dr. Abraham Pannikottu
Akron Rubber Development Laboratory, Inc.
2887 Gilchrist Road
Akron, OH 44305

Tim Eckert
EPRI- Plant Support Engineering
Engineering Support Center
1300 W. T. Harris Blvd.
Charlotte, NC 28262

Mark Kiesel
Caterpillar, Inc.
P.O. Box 4000
Mossville, Illinois 61552-4000

Christian E. Sabotta
Caterpillar, Inc.
P.O. Box 4000
Mossville, Illinois 61552-4000

2	MS-9018	Central Technical Files	8945-1
2	MS-0899	Technical Library	4536
1	MS-0161	Patent and Licensing Office	11500
1	MS-0887	Duane B. Dimos	1800
1	MS-0887	Richard J. Salzbrenner	1820
1	MS-0888	Roger. L. Clough	1821
1	MS-1411	Mathias C. Celina	1821
3	MS-1411	Roger A. Assink	1821
3	MS-0888	Robert Bernstein	1821
5	MS-1411	Kenneth T. Gillen	1821

SANDIA CABLE SAMPLE REPOSITORY

	PURPOSE
1.	Provide a summary of the radiation + thermal and thermal (only) aged samples and selected data taken on these samples that are available from the Sandia Polymer Laboratory
2.	By reviewing the "Experimental Conditions Summary Sheets" , other researchers can quickly identify the types of aged samples (natural and accelerated) that are stored at Sandia. On request, small pieces of these samples may be available for collaborative screening studies.
3.	Besides aging conditions, the data base will include such things as ultimate tensile elongation and tensile strength and density and
4.	The importance of diffusion-limited oxidation (DLO), if measured or estimated, will be included. This will allow other researchers to determine which samples might be adversely affected by anomalous DLO effects.
5.	Contact information: Ken Gillen Robert Bernstein Telephone: (505) 844-7494 Telephone: (505) 284-3690 ktgille@sandia.gov rbernst@sandia.gov
6.	LOCA test data is NOT contained in this file. See NUREG/CR-5772 and NUREG/CR-6202.

SANDIA CABLE SAMPLE REPOSITORY

Abbreviation	Description
Colors	
Blk	Black
Blu	Blue
G	Green
R	Red
W	White
Gases	
Air	Because of Albuquerque's elevation of ~5300', O_2 partial pressure = 13.2 cmHg
N_2	100% nitrogen
Modifiers	
FR	Fire (Flame) Retardant
Polymer Names	
CPE	Chlorinated Polyethylene
CSPE	Chlorosulfonated Polyethylene (Hypalon)
ETFE	Ethylene Tetrafluoroethylene (Tefzel)
EPR	Ethylene Propylene Rubber
Hyp	Hypalon (see CSPE), registered by du Pont
Ker	unknown, a Kerite proprietary formulation registered by Kerite
Neo	Chloroprene (often referred to as Neoprene- Registered by du Pont)
Sil	Silicone rubber- Poly dimethyl siloxane based elastomers
Tef	Tefzel (see ETFE), registered by General Electric
XLPE	Cross Linked Polyethylene
XLPO	Cross Linked Polyolefin

SANDIA CABLE SAMPLE REPOSITORY

Cable No.	Number used to designate a cable from which material(s) (insulations and/or jackets) were tested
Material	An arbitrary designation to identify a cable material received and tested at Sandia
Manufacturer and Trade Name	The name of the manufacturer that made the cable material and the manufacturer's Trade name for the product. NOTE: Some companies have since consolidated or changed names.
Outer Jacket	Abbreviation for the polymer material used to manufacture the outer jacket
Conductor Jacket	Abbreviation for the polymer material used to manufacture the conductor jacket
bonded?	Yes if jacket is bonded to insulation
Conductor Jacket Color(s)	The abbreviation for the color(s) of conductor jacket (i.e., a 3 conductor cable might include Blk, W, G conductor jackets).
Insulation	Abbreviation for the polymer material used to manufacture the insulation
Insulation Color(s)	The abbreviation for the color(s) of insulation (i.e., a 3 conductor cable might include Blk, W, G insulation).
Radiation Aging	"Yes," "Ongoing," or blank - "Yes": A significant volume of combined radiation and thermal test data are available from LICA aging "Ongoing": Tests are in progress.
Thermal (only) Aging	"Yes," "Ongoing," or blank - "Yes": A significant volume of thermal test data are available from oven aging "Ongoing": Tests are in progress.
Nom Thick (mm)	Nominal thickness (mm)
Initial Elongation, e_0 (%)	Measured elongation for unaged material using pneumatic grips and an attached extensometer
Initial modulus, MPa	Modulus measurement for unaged material in MPa measured using the Modulus Profiling Technique (ref- K. T. Gillen, et. al., Rubber Chem. Technol., Vol. 74, No. 3, pp428-450 (2001).
Initial Density (g/cc)	Measured density for unaged material using Archimedes approach
Uptake factor	Weight of sample gel plus weight of p-xylene dissolved in the gel after refluxing in p-xylene divided by the weight of sample gel
% gel	percentage of a sample that does not dissolve in refluxing p-xylene
NMR T2	Proton Nuclear magnetic resonance (NMR) spin-spin relaxation time for sample swollen in an appropriately chosen deuterated solvent- ref- R. A. Assink, et. al., Polymer, Vol. 43, pp. 1349-1355 (2002).
Model	"Arrhenius" - for thermal- only experiments, reasonable Arrhenius behavior is observed for a broad range of temperatures "t-T-DR" - time-Temperature-Dose Rate model (combined environments) appears to hold [ref- K. T. Gillen, et. al, Polym. Deg. Stabil., vol. 24, 137-168 (1989)]
Model (continued)	"Inverse-T" - inverse temperature behavior [refs.- Celina, et. al, Radiat. Phys. Chem., vol.48, 613-626 (1996), Polym. Degrad. Stabil., vol. 61, 231-244 (1998)] "Lazarus" - material can be annealed and mechanical properties recover significantly (same reference as Inverse T)

scraps 80.xls
Cable Info.

Cable No.	C-1
Manufacturer & Trade Name	General Electric Vulkene Supreme
Identifier on Cable Jacket	
Outer Jacket	
Conductor Jacket	
Conductor Jacket Color(s)	
bonded?	
Insulation	XLPE-01 (Crosslinked Polyethylene)
Insulation Colors	
Notes	#14 AWG, solid conductor with 30 mils of Black Vulkene Supreme insulation- 500 feet sent to Earl Minor (_____) in April, 1981. No unaged remaining
Cable No.	C-2
Manufacturer & Trade Name	Anaconda Flameguard FR/EP
Identifier on Cable Jacket	Anaconda-Y 3/C #12 AWG Flameguard FR-EP (UL) Type TC 600 V 90C
Outer Jacket	CPE-01 (Chlorinated polyethylene)
Conductor Jacket	
Conductor Jacket Color(s)	
bonded?	
Insulation	EPR-01 (Ethylene propylene rubber)
Insulation Colors	
Notes	No unaged left in storage
Cable No.	C-3
Manufacturer & Trade Name	Brandrex
Identifier on Cable Jacket	XLP/Cu Power & Control Cable 3/C #12 600 V Sun Res DB XHHW Type TC (UL)
Outer Jacket	Hyp-07 (Hypalon)
Conductor Jacket	
Conductor Jacket Color(s)	
bonded?	
Insulation	XLPO-02 (Crosslinked Polyolefin)
Insulation Colors	
Notes	used in NUREG/CR-5772 (cable type #1)- Reel #9 in storage (Reel #2 "identical")
	Reel #9 used for thermal aging started in 1993 (100C, 110C, 125C, 151C)
	Possible that Reel #2 was used for earlier thermal aging (120C, 140C, 150C, 160C) & reel to reel variation causes aging difference
Cable No.	C-4
Manufacturer & Trade Name	Eaton
Identifier on Cable Jacket	Dekoron Polyset Control Cable P/N 1X35 Aurora, OH Eaton 015800-1
Outer Jacket	

scraps 80.xls
Cable Info.

Conductor Jacket	
Conductor Jacket Color(s)	
bonded?	
Insulation	XLPO-03 (Crosslinked polyolefin)
Insulation Colors	Cream marked "one", "two" and "three"
Notes	No unaged left in storage
Cable No.	C-5
Manufacturer & Trade Name	Eaton
Identifier on Cable Jacket	Dekoron 2/C 16AWG 600 V Eaton Corp Dekoron Div Aurora OH Eaton 015601-1
Outer Jacket	Hyp-06 (Hypalon)
Conductor Jacket	
Conductor Jacket Color(s)	
bonded?	
Insulation	EPR-03 (Ethylene propylene rubber)
Insulation Colors	
Notes	Small remaining amount of cable in Bld 897
Cable No.	C-6
Manufacturer & Trade Name	Kerite
Identifier on Cable Jacket	Kerite 1977, 50 mil FR insulation, 60 mil FR jacket, 12 AWG, 1/C, 600V
Outer Jacket	Hyp-02 (Hypalon)
Conductor Jacket	
Conductor Jacket Color(s)	
bonded?	
Insulation	Ker-01 (proprietary)
Insulation Colors	
Notes	
Cable No.	C-7
Manufacturer & Trade Name	Rockbestos
Identifier on Cable Jacket	30 mil Firewall III Silicone Rubber Insulation, Fiberglass Braided Jacket, 16AWG, 1/C, 600V
Outer Jacket	
Conductor Jacket	
Conductor Jacket Color(s)	
bonded?	
Insulation	Sil-01 (silicone rubber)
Insulation Colors	
Notes	

scraps 80.xls
Cable Info.

Cable No.	C-8
Manufacturer & Trade Name	Rockbestos
Identifier on Cable Jacket	Copper Rockbestos (R) 600V Firewall (R) III XLPE NEOPRENE
Outer Jacket	Neo-02 (neoprene)
Conductor Jacket	
Conductor Jacket Color(s)	
bonded?	
Insulation	
Insulation Colors	
Notes	On spool- SO:92 36301, product code: CO6-0300d 31C #12 7/030S QT:536859C 1221 T:03202 B:00018 Reel #G 1160830 (02150 1989-9C-1221). Reel #4
Cable No.	C-9
Manufacturer & Trade Name	Samuel Moore
Identifier on Cable Jacket	US EPR 0815182-5 Samuel Moore Group Aurora, Ohio Dekoron 2/C 16 AWG 600V (UL)
Outer Jacket	Hyp-03 (Hypalon)
Conductor Jacket	
Conductor Jacket Color(s)	
bonded?	
Insulation	
Insulation Colors	
Notes	Same as used in US-French; Reel #15 in storage
Cable No.	C-10
Manufacturer & Trade Name	Anaconda
Identifier on Cable Jacket	Anaconda Flameguard 1 KV
Outer Jacket	Hyp-04 (Hypalon)
Conductor Jacket	
Conductor Jacket Color(s)	
bonded?	
Insulation	
Insulation Colors	
Notes	Reel #30 in storage
Cable No.	C-11
Manufacturer & Trade Name	Rockbestos
Identifier on Cable Jacket	12AWG 3/C Rockbestos 600V Firewall III XHHM NEC Type TC (UL) 1987-7C 1309 Copper Fr XLPE CSPE K-2 Colorcode
Outer Jacket	Hyp-05 (Hypalon)
Conductor Jacket	

scraps 80.xls
Cable Info.

Conductor Jacket Color(s)	
bonded?	
Insulation	
Insulation Colors	
Notes	Same as used in US-French+B7; Reels #1 and #17 in storage
Cable No.	C-12
Manufacturer & Trade Name	Anaconda
Identifier on Cable Jacket	Anaconda- M Durasheeth EP Type use for RHH or RHW VW-1 12AWG 600V (UL)
Outer Jacket	
Conductor Jacket	
Conductor Jacket Color(s)	
bonded?	
Insulation	EPR-04 (Ethylene propylene rubber)
Insulation Colors	
Notes	Reel #26 in storage
Cable No.	C-13
Manufacturer & Trade Name	ITT
Identifier on Cable Jacket	ITT Surprenant Div. EXANE II 3/C 12AWG 600V
Outer Jacket	
Conductor Jacket	
Conductor Jacket Color(s)	
bonded?	
Insulation	XLPO-04 (Crosslinked polyolefin)
Insulation Colors	
Notes	
Cable No.	C-14
Manufacturer & Trade Name	Anaconda Flameguard
Identifier on Cable Jacket	Anaconda Flameguard 1 KV
Outer Jacket	HYP-01A (Hypalon)
Conductor Jacket	Hypalon
Conductor Jacket Color(s)	black, white and red- latter two are painted on outside
bonded?	no
Insulation	EPR-01A (EPR)
Insulation Colors	black- #14 conductor size
Notes	Purchased in late 70's (~ 1 year after purchasing cable C-15)

scraps 80.xls
Cable Info.

Cable No.	C-15
Manufacturer & Trade Name	Anaconda Flameguard
Identifier on Cable Jacket	Anaconda Flameguard 1 KV
Outer Jacket	HYP-01B (Hypalon)
Conductor Jacket	Hypalon
Conductor Jacket Color(s)	all 3 are black-"red" and "white" stamped on 2 to distinguish colors
bonded?	no
Insulation	EPR-01B (EPR)
Insulation Colors	black- #12 conductor size
Notes	Purchased in late 70's
Cable No.	C-16
Manufacturer & Trade Name	Rockbestos Firewall III
Identifier on Cable Jacket	12 AWG 3/C Rockbestos Firewall III 600V XHHW NEC Type TC Hypalon Jacket
Outer Jacket	Hypalon
Conductor Jacket	
Conductor Jacket Color(s)	
bonded?	
Insulation	
Insulation Colors	XLPO-05 (XLPO insulations- red, black, and green)
Notes	used in NUREG/CR-5772 (cable #2) NUREG/CR-6202- #1 and #17 reels in storage
Cable No.	C-17
Manufacturer & Trade Name	Okonite 3 conductor
Identifier on Cable Jacket	NA
Outer Jacket	NEO-01 (Neoprene)
Conductor Jacket	
Conductor Jacket Color(s)	
bonded?	
Insulation	
Insulation Colors	
Notes	purchased in late 70's, On spool (hard to read)- Okonite , No. Bruswick, NJ 3/C 12-7X ?????????? 600V Order No. 02-??79 (1st ?= 8 or 9?, 2nd ?= 3 or 8
Cable No.	C-18
Manufacturer & Trade Name	Okonite
Identifier on Cable Jacket	The Okonite CO. PLT#7 1/C 12 AWG CU Okonite (EP)-CSPE (UL) RHH OR RHW OR USE VW-1 600V
Outer Jacket	N/A
Conductor Jacket	Hypalon

scraps 80.xls
Cable Info.

Conductor Jacket Color(s)	black
bonded?	yes- but can be separated
Insulation	EPR-05 (EPR)
Insulation Colors	black
Notes	
Cable No.	C-19
Manufacturer & Trade Name	BIW Multi Conductor Cable MFGD by BIW Cable Systems (Bostrad 7E)
Identifier on Cable Jacket	BIW Cable System (1987) 600V 1 SH Triple #10 AWG
Outer Jacket	HYP-08 (Hypalon)
Conductor Jacket	Hypalon
Conductor Jacket Color(s)	black
bonded?	yes
Insulation	EPR
Insulation Colors	pink, black and white
Notes	Received from Gary Toman (30 feet 10 AWG-shipped from Nutherm International)
Cable No.	C-20
Manufacturer & Trade Name	Anaconda Flameguard FR/EP
Identifier on Cable Jacket	Anaconda-Y 3/C 6 Flame Guard FR-EP 600V
Outer Jacket	CPE-02 (Chlorinated polyethylene)- black
Conductor Jacket	
Conductor Jacket Color(s)	
bonded?	
Insulation	EPR
Insulation Colors	red, white and black
Notes	50 feet ‘cable stock code AR505-8542/PO-90337 (3 conductor #6 Anaconda FR-EP with CPE jacket)- From Jeffery Lee Gebhardt

SANDIA CABLE SAMPLE REPOSITORY

Material	Cable No.	Manufacturer	Trade Name	Radiation Aging	Thermal (only) Aging	Nom Thick (mm)	Initial Elongation e_0 (%)	Initial TS, MPa	Initial Density (g/cc)	Initial Modulus (MPa)	Initial Uptake factor	Initial % gel	Initial NMR T2, msec	Model	Notes	
CPE-01	C-2	Anaconda	Flameguard FR-EP ("Y")	Yes		~1.9	240		1.376	90.0						
CPE-02	C-20	Anaconda	Flameguard FR-EP ("Y")		Ongoing	~1.8	310	14		90.0	N/A	0.0				
EPR-01A	C-14	Anaconda	Flameguard	Yes	Yes	0.9	336		1.325							
EPR-01B	C-15	Anaconda	Flameguard	Yes	No	1.1	346		1.325							
EPR-02	C-2	Anaconda	Flameguard FR-EP ("Y")	Yes	Yes	0.9	240		1.341							
EPR-03	C-5	Eaton	Dekoron Elastoset	Yes	Ongoing	0.8	400	11.5	1.288	62.0	4.4	72.0				
EPR-04	C-12	Anaconda	Durasheath	No	Yes	1.0	300	6.6	1.308	4.5	3.5	81.0				
EPR-05	C-18	Okonite	EPR	Yes	Ongoing	0.9	345	9	1.230	12.0						
ETFE-01		Teledyne	Thermatic	Yes		0.3	173		1.700						white	
ETFE-02		Teledyne			Yes	0.3	324			~500					red from Savannah River	
Hyp-01A	C-14	Anaconda	Flameguard	No	Yes	0.4	393	15	1.642	5.3						
Hyp-01B	C-15	Anaconda	Flameguard	Yes	No	0.4	340		1.607	5.0	4.9	54.0	10.9			
Hyp-02	C-6	Kerite	FR	Yes	Yes	~1.5	300	22	1.570	9.0						
Hyp-03	C-9	Samuel Moore	Dekoron	Yes	Yes	~1.2	381	20	1.461	14.0	3.7	78.2	13.0			
Hyp-04	C-10	Anaconda	Flameguard	Yes	Yes	~1.8	263	13	1.577	4.8	2.3	83.0	5.5			
Hyp-05	C-11	Rockbestos	Firewall III	Yes	Yes	~1.3	364	16	1.595	4.1	2.3	81.0	12.9			
Hyp-06	C-5	Eaton	Dekoron Elastoset	Yes	Yes	~1.4	316	20	1.467	18.0	3.5	78.0	9.4			
Hyp-07	C-3	Brandrex	??		Ongoing	~1.6	380	16	1.368	5.1	2.7	72.0				
Hyp-08	C-19	BIW	??		Ongoing	~1.7	257	13	1.475	8.7	2.5	72.0				
Ker-01	C-6	Kerite	FR	Yes	Yes	1.4	274		1.270	7.0	2.2	81.0				
Neo-01	C-17	Okonite	??	Yes	Yes	1.5	185		1.473							
Neo-02	C-8	Rockbestos	Firewall III	Yes	Yes	1.5	296		1.61+-.02	6.4	2.5	91.0	6.5			
Sil-01	C-7	Rockbestos	Firewall II	Yes		1.1	420		1.304	3.1	2.5	97.2				
XLPE-01	C-1	GE	Vulkene Supreme	Yes		0.8	345		1.152							
XLPO-02A	C-3	Brand-Rex	??	Yes	Yes	0.9	310		1.293						1987-1990	
XLPO-02B	C-3	Brand-Rex	??	No	Ongoing	0.9	347		1.293	140.0	8.0	57.0	13.5		1991 & after	
XLPO-03	C-4	Eaton	Dekoron Polyset	Yes		1.0	370		1.370							
XLPO-04	C-13	ITT Surprenant	Exane II (composite)	Yes	Yes	0.8	240		1.59/1.23							
XLPO-05	C-16	Rockbestos	Firewall III	Yes	Ongoing	0.9	300	14	1.362		5.0	72.0				

SANDIA CABLE SAMPLE REPOSITORY

	Column Descriptions for individual material tabs
Batch No.	Identification (letters and number) for a group of samples aged under identical environmental conditions T= Temperature alone. TR= Temperature plus Radiation.
Initial Date	Date the initial aging exposure started
Temperature (°C)	The average aging temperature
Average Dose Rate (Gy/h)	The average dose rate for radiation aging experiments
Gas	The gaseous environment surrounding samples during aging
Laboratory Notebook(s)	Reference to location of details on experiments
Diffusion- Limited Oxidation?	Diffusion-limited oxidation (DLO): Yes: DLO effects have been confirmed No: DLO effects do not exist for the conditions tested E: DLO effects expected based on models using estimates of O2 permeation & consumption NE: DLO effects are not expected based on models using estimates of O2 permeation & consumption
	U: Unknown- need profile data or reasonable estimates of O2 permeation & consumption
Data Columns	Data Column Definition
Batch No.	Identifying letters and number for a group of samples aged under identical environmental conditions T=Temperature alone. TR= Temperature plus Radiatiion
Sample No.	A group of samples (typically 2 to 6) aged for the same time interval
Aging Time	Aging time, as recorded in a lab notebook or on a sample envelope
Estimated Dose	Estimate dose, as recorded in a lab notebook or on a sample envelope
Average e/e_0	Average elongation for aged samples divided by average unaged elongation
Average TS/TS0	Average tensile strength (TS) for aged samples divided by average unaged tensile strength (TS0)
Average Density	Average density for aged samples
OIT	OIT results for aged samples
Modulus	Modulus measurement in MPa measured using the Modulus Profiling Technique (ref- K. T. Gillen, et. al., Rubber Chem. Technol., Vol. 74, No. 3, pp 428-450 (2001).
Outside surface modulus	Modulus Profiling result at the outside surface of the material for cases where the modulus varies across the sample cross-section (usually due to diffusion-limited oxidation effects)
% gel	percentage of a sample that does not dissolve in refluxing p-xylene
Uptake factor	Weight of sample gel plus weight of p-xylene dissolved in the gel after refluxing in p-xylene divided by the weight of sample gel
NMR T2	Proton Nuclear magnetic resonance (NMR) spin-spin relaxation time for sample swollen in an appropriately chosen deuterated solvent- ref- R. A. Assink, et. al., Polymer, Vol. 43, pp. 1349-1355 (2002).

SANDIA CABLE SAMPLE REPOSITORY

	A	B	C	D	E	F	G	H
1	Batch No.	Initial Date	Average Temp. (°C)	Average Dose Rate (Gy/h)	Gas	Laboratory Notebook	Diffusion -Limited Oxidation?	
2								
3					CPE-01 Anaconda Flameguard FR-EP 'Y'			
4	TR-1	06/17/82	70.0	128.0	air	CAQ-98		
5	TR-2	5/12/83	70.0	920.0	air	CAQ-115		
6	TR-3	1/27/83	70.0	960.0	air	CAQ-110		
7	TR-4	12/15/82	70.0	7100.0	air	CAQ-107,108		
8								
9					CPE-02 Anaconda Jacket			
10	T-1	4/12/02	95.0	0.0	Air	AG-II-1B		
11	T-2	9/25/02	99.0	0.0	Air	RB-IV-79C		
12	T-3	9/25/02	109.0	0.0	Air	RB-IV-79B		
13	T-4	9/25/02	124.0	0.0	Air	RB-IV-79A		
14	T-5	4/12/02	138.0	0.0	Air	AG-II-1A		
15	T-6	7/02/02	138.0	0.0	Air	AG-II-22		
16	T-7	6/03/03	138.0	0.0	Air	RB-VI-33		
17								
18					XLPE-01, GE Vulkene Supreme Insulation			
19	TR-1	06/03/1981	43.0	175.0	Air	LHJ-84		
20	TR-2	08/10/1981	43.5	8900.0	Air			
21	TR-3	06/16/1982	70.0	189.0	Air	KTG III-136		
22	TR-4	08/18/1982	70.0	1160.0	Air	CAQ-102		
23	TR-5	04/24/1981	70.0	640.0	Air	LHJ-80		
24	TR-6	01/05/1983	70.0	7000.0	Air	CAQ-103, 108		
25	TR-7	08/31/1981	80.0	187.0	Air	CAQ-51, 53		
26	TR-8	10/26/1981	80.0	666.0	Air	LHJ-92		
27	TR-9	09/14/1981	80.0	7750.0	Air	CAQE-57		
28	TR-10	06/09/1982	25.0	1200.0	Air	LHJ-118		
29	TR-11	07/16/1997	43.0	479.0	Air	Envelopes		
30								
31					XLPO-02, Brand Rex insulation			
32	TR-1	12/9/1991	25.0	16.8	Air	paper		
33	TR-2	12/9/1991	25.0	124.0	Air	paper		
34	TR-3	8/11/1987	60.0	317.0	Air	DS-II-5		
35	TR-4	11/2/1987	60.0	5240.0	Air	DS-II-19		
36	TR-5	8/11/1987	80.0	120.0	Air	DS-II-35		
37	TR-6	8/11/1987	80.0	323.0	Air	DS-II-10		
38	TR-7	10/26/1987	80.0	682.0	Air	DS-II-16-17		
39	TR-8	08/17/1987	100.0	700.0	Air	DS-II-15		
40	TR-9	08/24/1987	80.0	5350.0	Air	DS-II-25		
41	TR-10	01/18/1988	100.0	301.0	Air	DS-II-11		
42	TR-11	12/20/1988	110.0	25.4	Air	DS-II-31		
43	TR-12	12/20/1988	110.0	150.0	Air	DS-II-33		
44	TR-13	4/19/1989	115.0	92.4	Air	DS-III-75		
45	TR-14	02/22/1989	120.0	90.0	Air	DS-III- 73 (calc pg75)		
46	TR-15	1/18/1988	120.0	307.0	Air	DS-II-6		
47	TR-16	1/18/1988	120.0	664.0	Air	DS-II-14		
48	TR-17	2/29/1988	120.0	5030.0	Air	DS-II-29		
49	TR-18	10/31/1989	41.0	69.0	Air	Envelopes		
50	TR-19	10/31/1989	61.0	70.0	Air	Envelopes		

SANDIA CABLE SAMPLE REPOSITORY

	A	B	C	D	E	F	G	H
1	Batch No.	Initial Date	Average Temp. (°C)	Average Dose Rate (Gy/h)	Gas	Laboratory Notebook	Diffusion -Limited Oxidation?	
51								
52	T-1	6/9/1993	99.0	0.0	Air	Envelopes		
53	T-2	6/9/1993	109.0	0.0	Air	Envelopes		
54	T-3	4/1/1988	120.0	0.0	Air	DS-II-21-22		
55	T-4	6/9/1993	125.0	0.0	Air	Envelopes		
56	T-5	10/9/1989	140.0	0.0	Air	Envelopes		
57	T-6	10/9/1989	150.0	0.0	Air	Envelopes		
58	T-7		151.5	0.0	Air	Envelopes		
59	T-8	8/28/1989	160.0	0.0	Air	DS-IV- 9		
60								
61					HYP-01A- Anaconda Flameguard, Hypalon			
62	T-1	11/21/1978	100.4	0.0	Air	LB-II-111		
63	T-2	11/21/1978	120.0	0.0	Air	LB-II-111		
64	T-3	09/25/1978	130.0	0.0	Air	LB-II-102		
65	T-4	09/28/1978	139.5	0.0	Air	LB-II-102		
66	T-5	08/22/1978	149.5	0.0	Air	LB-II-98		
67								
68					HYP-01B- Anaconda Flameguard, Hypalon			
69	TR-1	04/26/1977	22	13.7	air	NRL B-16		
70	TR-1 RH	04/26/77	22	13.7	air + RH	NRL B-15		
71	TR-2	04/26/1977	22	90.6	air	NRL B-6		
72	TR-2 RH	04/26/77	22	90.6	air + RH	NRL B-2		
73	TR-3	04/26/1977	24	490	air	NRL A-19		
74	TR-3 RH	08/16/77	24	490	air + RH	NRL A-17		
75	TR-4	08/15/1977	30	2140	air	NRL A-5		
76	TR-4 RH	08/15/77	30	2140	air + RH	NRL A-4		
77	TR-5	05/03/1977	38	9550	air	NRL A-1		
78	TR-6	07/09/1980	35	3680	nitrogen	LHJ-60		
79	TR-7	09/06/1977	100	2140	air	NRL A-6		
80	TR-8 RH	12/12/1977	110	468	air + RH	NRL A-17		
81	TR-9	09/06/1977	120	2180	air	NRL A-7		
82	TR-10	09/12/1977	140	2120	air	NRL A-2		
83	TR-10 RH	09/12/1977	140	2120	air + RH	NRL A-4		
84								
85					HYP-02- Kerite outer jacket, Hypalon			
86	T-1	06/19/78	91	0	air	LB-II-86		
87	T-2	11/21/78	101	0	air	LB-II-110		
88	T-3	05/26/78	111	0	air	LB-II-86		
89	T-4	11/21/78	120.0	0.0	air	LB-II-110		
90	T-5	09/27/78	129.5	0.0	air	LB-II-101		
91	T-6	09/25/78	140.9	0.0	air	LB-II-101		
92	T-7	08/21/78	150.0	0.0	air	LB-II-97		
93	T-8	04/23/79	160.7	0.0	air	LHJ-7		
94								
95	TR-1	04/26/77	22.0	12.0	air	NRL B-16		
96	TR-1 RH	04/26/77	22.0	12.0	air + RH	NRL B-15		
97	TR-2	04/26/77	22.0	88.0	air	NRL B-6		
98	TR-2 RH	04/26/77	22.0	88.0	air + RH	NRL B-2		
99	TR-3	08/16/77	24.0	490.0	air	NRL A-19		
100	TR-3 RH	08/16/77	24.0	490.0	air + RH	NRL A-17		

SANDIA CABLE SAMPLE REPOSITORY

	A	B	C	D	E	F	G	H
1	Batch No.	Initial Date	Average Temp. (°C)	Average Dose Rate (Gy/h)	Gas	Laboratory Notebook	Diffusion -Limited Oxidation?	
101	TR-4	08/15/77	30.0	2100.0	air	NRL A-5		
102	TR-4 RH	08/15/77	30.0	2100.0	air + RH	NRL A-4		
103	TR-5 RH	05/03/77	38.0	9550.0	air + RH	NRL A-1		
104	TR-6	04/21/80	64.0	308.0	air	LHJ-44		
105	TR-7	11/13/78	73.0	1810.0	air	LB-II-116		
106	TR-8	12/22/78	78.0	368.0	air	LB-II-120		
107	TR-9	04/22/80	78.1	3750.0	air	LHJ-43		
108	TR-10	02/12/79	79.0	874.0	air	LB-II-127		
109	TR-11	04/21/80	82.0	188.0	air	LHJ-44		
110	TR-12	12/22/78	92.0	234.0	air	LB-II-120		
111	TR-13	04/21/80	96.0	92.0	air	LHJ-45		
112	TR-14	01/31/79	97.0	365.0	air	LB-II-128		
113	TR-15	07/16/79	97.1	830.0	air	LHJ-16		
114	TR-16	09/06/77	100.0	2140.0	air	NRL A-6		
115	TR-17	04/21/80	104.0	9790.0	air	LHJ-43		
116	TR-18 RH	12/12/77	110.0	470.0	air + RH	NRL A-17		
117	TR-19	01/31/79	118.0	880.0	air	LB-II-126		
118	TR-20	09/06/77	120.0	2180.0	air	NRL A-7		
119	TR-21	01/30/79	125.0	340.0	air	LB-II-128		
120	TR-22	03/12/79	132.0	1800.0	air	LB-II-143		
121	TR-23 RH	11/13/78	133.0	8900.0	air + RH	LB-II-116		
122	TR-24	01/29/79	137.0	880.0	air	LB-II-126		
123	TR-25	09/12/77	140.0	2120.0	air	NRL A-2		
124	TR-25 RH	09/12/77	140.0	2120.0	air + RH	NRL A-4		
125								
126					HYP-03- Samuel Moore jacket, Hypalon			
127	T-1	06/23/97	100.0	0.0	air	SMHY-ten.dat		
128	T-2	06/23/97	110.0	0.0	air	SMHY-ten.dat		
129	T-3	06/23/97	125.0	0.0	air	SMHY-ten.dat		
130								
131	TR-1	05/05/97	60.0	131.0	air	II-Bat60C.xls		
132	TR-2	05/05/97	80.0	51.0	air	I-Bat80C.xls		
133	TR-3	05/05/97	90.0	940.0	air	IV-Bat90C.xls		
134	TR-4	05/05/97	100.0	51.0	air	I-Cat100C.xls		
135								
136					HYP-04- Anaconda Flameguard jacket- Hypalon			
137	T-1	06/23/97	100.0	0.0	air	AnFl-ten.dat		
138	T-2	06/23/97	110.0	0.0	air	AnFl-ten.dat		
139	T-3	06/23/97	125.0	0.0	air	AnFl-ten.dat		
140								
141	TR-1	05/05/97	60.0	165.0	air	II-Bat60C.xls		
142	TR-2	05/05/97	80.0	59.0	air	I-Bat80C.xls		
143	TR-3	05/05/97	90.0	940.0	air	IV-Bat90C.xls		
144	TR-4	05/05/97	100.0	59.0	air	I-Cat100C.xls		
145								
146					HYP-05- Rockbestos jacket- Hypalon			
147	T-1	06/23/97	100.0	0.0	air	RBHY-ten.dat		
148	T-2	06/23/97	110.0	0.0	air	RBHY-ten.dat		
149	T-3	06/23/97	125.0	0.0	air	RBHY-ten.dat		
150								

SANDIA CABLE SAMPLE REPOSITORY

	A	B	C	D	E	F	G	H
1	Batch No.	Initial Date	Average Temp. (°C)	Average Dose Rate (Gy/h)	Gas	Laboratory Notebook	Diffusion -Limited Oxidation?	
151	TR-1	05/05/97	60.0	184.0	air	II-Bat60C.xls		
152	TR-2	05/05/97	80.0	62.0	air	I-Bat80C.xls		
153	TR-3	05/05/97	90.0	940.0	air	IV-Bat90C.xls		
154	TR-4	05/05/97	100.0	64.0	air	I-Cat100C.xls		
155								
156					HYP-06- Eaton Dekoron jacket- Hypalon			
157	T-1	06/23/97	100.0	0.0	air	Dek-ten.dat		
158	T-2	06/23/97	110.0	0.0	air	Dek-ten.dat		
159	T-3	06/23/97	125.0	0.0	air	Dek-ten.dat		
160								
161	TR-1	05/05/97	60.0	143.0	air	II-Bat60C.xls		
162	TR-2	05/05/97	80.0	55.0	air	I-Bat80C.xls		
163	TR-3	05/05/97	90.0	940.0	air	IV-Bat90C.xls		
164	TR-4	05/05/97	100.0	56.0	air	I-Cat100C.xls		
165								
166					HYP-07- Brandrex Hypalon Jacket			
167	T-1	4/16/01	99.0	0.0	air	RB-II-33C		
168	T-2	1/22/02	99.0	0.0	air	RB-III-25		
169	T-3	9/10/02	99.0	0.0	air	RB-IV-77		
170	T-4	4/16/01	109.0	0.0	air	RB-II-33B		
171	T-5	10/05/01	124.0	0.0	air	RB-II-83		
172	T-6	12/10/01	124.0	0.0	air	RB-III-17		
173	T-7	4/16/01	138.0	0.0	air	RB-II-33A		
174	T-8		125.0	0.0	air	GMM-envelopes		
175								
176					HYP-08- BIW-Hypalon Jacket			
177	T-1	6/07/01	80.0	0.0	air	RB-II-47		
178	T-2	4/16/01	99.0	0.0	air	RB-II-35C		
179	T-3	1/08/01	100.0	0.0	air	RB-II-93		
180	T-4	4/16/01	108.0	0.0	air	RB-II-35B		
181	T-5	9/07/01	124.0	0.0	air	RB-II-75		
182	T-6	4/16/01	138.0	0.0	air	RB-II-35A		
183	T-7							
184								
185					XLP-04- ITT Exane II Surprenant			
186	T-1	10/30/1979	90.6	0.0	air	LHJ-29		
187	T-2	10/26/1979	101.3	0.0	air	LHJ-29		
188	T-3	11/21/1978	110.6	0.0	air	LB-II-113		
189	T-4	11/20/1978	121.5	0.0	air	LB-II-107		
190	T-5	09/28/1978	130.2	0.0	air	LB-II-106		
191	T-6	09/27/1978	140.0	0.0	air	LB-II-104		
192	T-7	08/22/1978	151.2	0.0	air	LB-II-98		
193	T-8	11/27/1978	161.5	0.0	air	LB-II-107		
194	T-9	04/11/1979	170.3	0.0	air	LHJ-6		
195								
196	TR-1	04/26/1977	22.0	15.7	air	NRL B-16		
197	TR-1 RH	04/26/1977	22.0	15.7	air + RH	NRL B-15		
198	TR-2	04/26/1977	22.0	95.0	air	NRL B-6		
199	TR-2 RH	04/26/1977	22.0	95.0	air + RH	NRL B-2		
200	TR-3	08/16/77	24.0	515.0	air	NRL A-19		

SANDIA CABLE SAMPLE REPOSITORY

	A	B	C	D	E	F	G	H
1	Batch No.	Initial Date	Average Temp. (°C)	Average Dose Rate (Gy/h)	Gas	Laboratory Notebook	Diffusion -Limited Oxidation?	
201	TR-3 RH	08/16/1977	24.0	515.0	air + RH	NRL A-17		
202	TR-4	08/15/1977	30.0	2210.0	air	NRL A-5		
203	TR-4 RH	08/15/1977	30.0	2210.0	air + RH	NRL A-4		Note: RH= air flow bubbled
204	TR-5 RH	05/03/1977	38.0	12200.0	air + RH	NRL A-1		through water at room temperature.
205	TR-6	11/30/1979	66.0	820.0	air	LHJ-32		
206	TR-7	09/06/1977	100.0	2300.0	air	NRL A-6		
207	TR-8 RH	12/12/1977	110.0	500.0	air + RH	NRL A-17		
208	TR-9	09/06/1977	120.0	2300.0	air	NRL A-7		
209	TR-10 RH	12/12/1977	130.0	520.0	air + RH	NRL A-19		
210	TR-11	09/12/1977	140.0	2200.0	air	NRL A-2		
211	TR-11 RH	09/12/1977	140.0	2200.0	air + RH	NRL A-4		
212								
213					Ker-01 Kerite FR insulation			
214	T-1	02/26/1979	121.3	0.0	air	LB-II-133		
215	T-2	11/21/1978	130.4	0.0	air	LB-II-112		
216	T-3	09/25/1978	141.2	0.0	air	LB-II-105		
217	T-4	08/21/1978	150.0	0.0	air	LB-II-97		
218	T-5	11/27/1978	160.5	0.0	air	LB-II-112		
219								
220	TR-1	04/26/1977	22.0	12.0	air	NRL B-16		
221	TR-1 RH	04/26/1977	22.0	12.0	air + RH	NRL B-15		
222	TR-2	04/26/1977	22.0	88.0	air	NRL B-6		
223	TR-3 RH	04/26/1977	24.0	88.0	air + RH	NRL B-2		
224	TR-4	08/15/1977	30.0	2100.0	air	NRL A-5		
225	TR-5 RH	05/03/1977	38.0	9550.0	air + RH	NRL A-1		
226	TR-6	11/22/1988	100.0	264.0	air	DS-III-61		
227	TR-7	09/06/1977	100.0	2140.0	air	NRL A-6		
228	TR-8	11/22/1988	110.0	31.2	air	DS-III-63		
229	TR-9	04/19/1989	115.0	101.0	air	DS-III-67		
230	TR-10	02/22/1989	120.0	63.2	air	DS-III-69		
231	TR-11	05/31/1989	120.0	399.0	air	DS-III-71		
232	TR-12	09/06/1977	120.0	2180.0	air	NRL A-7		
233	TR-13	09/12/1977	140.0	2120.0	air	NRL A-2		
234	TR-13 RH	09/12/1977	140.0	2120.0	air + RH	NRL A-4		
235								
236					Neo-01 Okonite jacket			
237	T-0	01/01/79	24.0	0.0	air	envelopes		
238	T-1	04/11/79	70.1	0	air	LHJ-5		
239	T-2	04/11/79	80	0	air	LHJ-5		
240	T-3	06/19/78	90.6	0	air	LB-II-82		
241	T-4	05/23/78	101.0	0.0	air	LB-II-76		
242	T-5	05/26/78	111.2	0.0	air	LB-II-78		
243	T-6	06/02/78	120.9	0.0	air	LB-II-80		
244	T-7	06/09/78	131.3	0.0	air	LB-II-81		
245	T-8	08/06/78	140.6	0.0	air	LB-II-88		
246	T-9	10/17/79	160.5	0.0	air	LHJ-28		
247	Ox-1	10/5/81	110.3	0.0	80%Ox	LHJ-94		
248	Ox-2	12/14/81	130.0	0.0	80%Ox	LHJ-98 & LHJ-100		
249	Ox-3	10/30/81	90.0	0.0	80%Ox	LHJ-96		
250								

SANDIA CABLE SAMPLE REPOSITORY

	A	B	C	D	E	F	G	H
1	Batch No.	Initial Date	Average Temp. (°C)	Average Dose Rate (Gy/h)	Gas	Laboratory Notebook	Diffusion -Limited Oxidation?	
251	TR-1	04/26/77	22.0	14.8	air	NRL B-16		
252	TR-1 RH	04/26/77	22.0	14.8	air + RH	NRL B-15		
253	TR-2	04/26/77	22.0	84.0	air	NRL B-6		
254	TR-2 RH	04/26/77	22.0	84.0	air + RH	NRL B-2		Note: RH= air flow bubbled
255	TR-3	08/16/77	24.0	470.0	air	NRL A-19		through water at room temperature.
256	TR-3 RH	08/16/77	24.0	470.0	air + RH	NRL A-17		
257	TR-4	08/15/77	30.0	2010.0	air	NRL A-5		
258	TR-4 RH	08/15/77	30.0	2010.0	air + RH	NRL A-4		
259	TR-5 RH	05/03/77	38.0	9180.0	air + RH	NRL A-1		
260	TR-6	04/22/80	58.1	200.0	air	LHJ-46		
261	TR-7	07/07/78	62.2	904.0	air	LB-II-84		
262	TR-8	04/22/80	65.0	100.0	air	LHJ-46		
263	TR-9	05/01/81	66.0	32.3	air	LHJ-47		
264	TR-10	12/22/78	74.0	112.0	air	LB-II-119		
265	TR-11	06/19/78	75.7	908.0	air	LB-II-83		
266	TR-12	05/26/78	79.3	384.0	air	LB-II-77		
267	TR-13	11/13/78	83.0	1790.0	air	LB-II-115		
268	TR-14	05/05/80	87.4	9370.0	air	LHJ-47		
269	TR-15 RH	05/09/78	88.0	929.0	air + RH	LB-II-73		
270	TR-16	05/23/78	97.0	386.0	air	LB-II-75		
271	TR-17	09/06/1977	100.0	2050.0	air	NRL A-6		
272	TR-18	07/21/78	100.0	120.0	air	LB-II-85		
273	TR-19 RH	05/09/78	106.0	929.0	air + RH	LB-II-74		
274	TR-20	08/07/78	114.6	377.0	air	LB-II-91		
275	TR-21 RH	12/12/1977	110.0	470.0	air + RH	NRL A-17		
276	TR-22	11/07/78	120.0	8700.0	air	LB-II-115		
277	TR-23	09/06/1977	120.0	2090.0	air	NRL A-7		
278	TR-24	09/12/1977	140.0	2030.0	air	NRL A-2		
279	TR-24 RH	09/12/1977	140.0	2030.0	air + RH	NRL A-4		
280								
281					Neo-02 Rockbestos Firewall III Outer Jacket			
282	T-1	6/23/1997	80.0	0.0	air	Envelopes/Malone		
283	T-2	6/23/1997	95.0	0.0	air	Envelopes/Malone		
284	T-3	6/23/1997	110.0	0.0	air	Envelopes/Malone		
285	TR-1	5/5/1997	50.0	133.0	air	Envelopes/Malone		
286	TR-2	5/5/1997	60.0	45.0	air	Envelopes/Malone		
287	TR-3	5/5/1997	70.0	940.0	air	Envelopes/Malone		
288	TR-4	5/5/1997	80.0	42.0	air	Envelopes/Malone		
289								
290					EPR-01A Anaconda Flameguard			
291	T-1	12/12/78	100.9	0.0	air			
292	T-2	11/28/78	110.8	0.0	air	LB-II-108		
293	T-3	11/21/78	119.8	0.0	air	LB-II-108&135		
294	T-4	09/25/78	130.1	0.0	air	LB-II-105		
295	T-5	09/25/78	140.3	0.0	air	LB-II-104		
296	T-6	08/21/78	150.0	0.0	air	LB-II-98-99		
297	T-7	12/08/78	160.5	0.0	air	LB-II-118		
298	T-8	04/15/79	170.0	0.0	air	LHJ-6		
299								
300	TR-1	01/31/79	RT	870.0	air	LB-II-122		

SANDIA CABLE SAMPLE REPOSITORY

	A	B	C	D	E	F	G	H
1	Batch No.	Initial Date	Average Temp. (°C)	Average Dose Rate (Gy/h)	Gas	Laboratory Notebook	Diffusion -Limited Oxidation?	
301	TR-2	08/04/78	RT	980.0	air	LB-II-95		
302	TR-3	03/26/79	RT	1830.0	air	LB-II-146		
303	TR-4	04/09/79	RT	9070.0	air	LB-II-147		
304	TR-5	07/09/79	RT	870.0	Nitrogen	LHJ-15		
305	TR-6	07/18/79	117.0	370.0	air	LHJ-17		
306	TR-7	03/26/79	115.0	1890.0	air	LB-II-145		
307	TR-8	03/12/79	145.0	1835.0	air	LB-II-143		
308	TR-9	04/02/79	145.0	9200.0	air	LB-II-146		
309								
310					EPR-01B Anaconda Flameguard			
311	TR-1	04/26/77	22.0	15.7	air	NRL B-16		
312	TR-1 RH	04/26/77	22.0	15.7	air + RH	NRL B-15		
313	TR-2	04/26/77	22.0	80.0	air	NRL B-6		
314	TR-2 RH	04/26/77	22.0	80.0	air + RH	NRL B-2		Note: RH= air flow bubbled
315	TR-3	08/16/77	24.0	515.0	air	NRL A-19		through water at room temperature.
316	TR-3 RH	08/16/77	24.0	515.0	air + RH	NRL A-17		
317	TR-4	08/15/77	30.0	2210.0	air	NRL A-5		
318	TR-4 RH	08/15/77	30.0	2210.0	air + RH	NRL A-4		
319	TR-5 RH	05/03/77	38.0	11800.0	air + RH	NRL A-1		
320	TR-6	09/06/1977	100.0	2250.0	air	NRL A-6		
321	TR-7 RH	12/12/1977	110.0	495.0	air + RH	NRL A-17		
322	TR8	09/06/1977	120.0	2300.0	air	NRL A-7		
323	TR-9 RH	12/12/1977	130.0	515.0	air + RH	NRL A-19		
324	TR-10	09/12/1977	140.0	2310.0	air	NRL A-2		
325	TR-10 RH	09/12/1977	140.0	2030.0	air + RH	NRL A-4		
326								
327					XLPO-03 Dekoron Polyset CLPO insulation			
328	T-1	4/1/1988	120.0	0.0	air	DS-II-71-72		
329								
330	TR-1	10/31/1989	41.0	64.1	air	Envelopes		
331	TR-2	11/2/1987	60.0	5240.0	air	DS-II-59		
332	TR-3	5/15/1990	60.1	355.0	air	Envelopes		
333	TR-4	10/31/1989	61.0	68.7	air	Envelopes		
334	TR-5	8/11/1987	80.0	138.0	air	DS-II-75		
335	TR-6	8/11/1987	80.0	267.0	air	DS-II-50		
336	TR-7	10/26/1987	80.0	724.0	air	DS-II-56		
337	TR-8	8/24/1987	80.0	5350.0	air	DS-II-65		
338	TR-9	1/18/1988	100.0	238.0	air	DS-II-51		
339	TR-10	8/17/1987	100.0	742.0	air	DS-II-55		
340	TR-11	12/20/1988	110.0	28.8	air	DS-II-77		
341	TR-12	4/19/1989	115.6	97.8	air	DS-II-73		
342	TR-13	2/22/1989	120.0	88.6	air	DS-III-77		
343	TR-14	1/18/1988	120.0	252.0	air	DS-II-44		
344	TR-15	1/18/1988	120.0	705.0	air	DS-II-54		
345	TR-16	02/29/88	120.0	5030.0	air	DS-II-68-69		
346								
347					EPR-02 Anaconda Flameguard EPR insulation (Y)			
348	T-1A	4/1/1988	120.0	0.0	air	DS-I-21		
349	T-1B	5/6/1988	120.0	0.0	air	DS-I-21		
350	T-2	8/28/1989	140.0	0.0	air	DS-IV-1		

SANDIA CABLE SAMPLE REPOSITORY

	A	B	C	D	E	F	G	H
1	Batch No.	Initial Date	Average Temp. (°C)	Average Dose Rate (Gy/h)	Gas	Laboratory Notebook	Diffusion -Limited Oxidation?	
351	T-3	8/28/1989	150.0	0.0	air	DS-IV-7		
352	T-4	7/7/1989	160.0	0.0	air	DS-III-7		
353								
354	TR-1		41.0	58.6	air			
355	TR-2	8/11/1987	60.0	330.0	air	DS-I-5		
356	TR-3	1/18/1988	60.0	5140.0	air	DS-I-19		
357	TR-4		61.0	60.9	air			
358	TR-5	8/11/1987	80.0	133.0	air	DS-I-35		
359	TR-6	8/11/1987	80.0	314.0	air	DS-I-10		
360	TR-7	10/26/1987	80.0	790.0	air	DS-I-16-17		
361	TR-8	10/12/1987	80.0	5290.0	air	DS-I-25		
362	TR-9	5/31/1988	100.0	135.0	air	DS-I-34		
363	TR-10	5/31/1989	100.0	226.0	air	DS-III-53 Black		
364	TR-11	1/18/1988	100.0	313.0	air	DS-I-11		
365	TR-12	8/17/1987	100.0	810.0	air	DS-I-15		
366	TR-13	12/20/1988	110.0	26.9	air	DS-III-51 Black		
367	TR-14	4/19/1989	115.6	98.5	air	DS-I-8 Black		
368	TR-15	2/22/1989	120.0	71.5	air	DS-III-55 Black		
369	TR-16	8/9/1988	120.0	125.0	air	DS-I-33-32		
370	TR-17	1/18/1988	120.0	294.0	air	DS-I-6		
371	TR-18	5/31/1989	120.0	420.0	air	DS-III-57,79 Black		
372	TR-19	1/18/1988	120.0	773.0	air	DS-I-14		
373	TR-20	2/1/1988	120.0	5090.0	air	DS-I-29		
374								
375					EPR-03 Eaton Dekoron Elastoset EPR Insulation			
376	T-1	4/26/01	99.0	0.0	air	RB-II-45F		
377	T-2	4/26/01	109.0	0.0	air	RB-II-45D,RB-IV-67A		
378								
379								
380								
381	T-3	4/1/1988	120.0	0.0	air	(not long enough)		
382								
383	T-4	10/03/01	124.0	0.0	air	RB-II-81,RB-IV-67		
384								
385								
386								
387								
388	T-5	4/26/01	138.0	0.0	air	RB-II-45B		
389	T-6	7/7/1989	160.0	0.0	air	DS-III-11		
390								
391								
392	TR-1		23.0	210.0	air	Where are envelopes?		
393	TR-2	10/31/1989	40.0	58.0	air	Envelopes		
394	TR-3	5/11/1994	40.0	420.0	air	Envelopes		
395	TR-4	1/18/1988	60.0	5140.0	air	DS-I-59		
396	TR-5	8/11/1987	60.0	315.0	air	Envelopes		
397	TR-6	5/15/1990	60.0	355.0	air	Envelopes		
398	TR-7	10/31/1989	61.0	59.5	air	Envelopes		
399	TR-8	8/11/87	80.0	143.0	air	DS-I-75		
400	TR-9	8/11/87	80.0	314.0	air	DS-I-50		

SANDIA CABLE SAMPLE REPOSITORY

	A	B	C	D	E	F	G	H
1	Batch No.	Initial Date	Average Temp. (°C)	Average Dose Rate (Gy/h)	Gas	Laboratory Notebook	Diffusion -Limited Oxidation?	
401	TR-10	10/26/87	80.0	740.0	air	DS-I-56,57		
402	TR-11	10/12/87	80.0	5290.0	air	DS-I-65		
403	TR-12	5/31/89	100.0	226.0	air	DS-III-49		
404	TR-13	1/18/88	100.0	313.0	air	DS-I-51		
405	TR-14	8/17/87	100.0	761.0	air	DS-I-55		
406	TR-15	11/22/88	110.0	30.4	air	DS-I-79, 80		
407	TR-16	4/19/1989	110.0	106.0	air	Envelopes		
408	TR-17	4/19/89	115.6	104.0	air	DS-III-41		
409	TR-18	2/22/89	120.0	71.5	air	DS-III-47, 48		
410	TR-19	5/31/1989	120.0	228.0	air	Envelopes		
411	TR-20	1/18/88	120.0	294.0	air	DS-I-46		
412	TR-21	5/31/89	120.0	420.0	air	DS-III-45		
413	TR-22	1/18/88	120.0	725.0	air	DS-I-54		
414	TR-23	2/1/88	120.0	5090.0	air	DS-I-69		
415								
416					EPR-04 Anaconda Duraseath Insulation			
417	T-1	6/09/93	100.0	0.0	air	envelopes		
418	T-2	6/09/93	110.0	0.0	air	envelopes		
419	T-3	6/09/93	125.0	0.0	air	envelopes		
420	T-4	11/17/95	140.0	0.0	air	envelopes		
421								
422					EPR-05 Okonite EPR Insulation			
423	T-1	4/26/01	99.0	0.0	Air	RB-II-45E		
424	T-2	4/26/01	109.0	0.0	Air	RB-II-45C,RB-IV-75		
425	T-3	9/17/01	124.0	0.0	Air	RB-II-77		
426	T-4	4/26/01	138.0	0.0	Air	RB-II-45A,RB-II-73		
427								
428	TR-1	2/24/2003	40.0	430.0	Air	5C in LICA		
429	TR-2	2/24/2003	80.0	445.0	Air	5B in LICA		
430								
431					XLPO-05 Rockbestos Firewall III CLPO Insulation			
432	T-1		100.0	0.0	air	Not started		
433	T-2	6/11/01	109.0	0.0	air	RB-II-51B		
434	T-3	6/11/01	124.0	0.0	air	RB-II-51A		
435	T-4	6/26/01	138.0	0.0	air	RB-II-69,III-35		
436	T-5	7/03/01	151.0	0.0	air	RB-II-53		
437	T-6	4/25/01	151.0	0.0	air	RB-II-43		
438	T-7	6/19/03	150.0	0.0	air	RB-IV-47		
439	T-8	8/28/89	160.0	0.0	air	DS-IV-11		
440								
441								
442	TR-1		23.0	210.0	air	Malone		
443	TR-2		40.0	215.0	air	Envelopes		
444	TR-3		41.0	76.0	air	Envelopes		
445	TR-4		60.0	1850.0	air	Malone		
446	TR-5		60.1	360.0	air	Envelopes		
447	TR-6		61.0	80.0	air	Envelopes		
448	TR-7		80.0	353.0	air	Envelopes		
449	TR-8		80.0	3710.0	air	Envelopes		
450	TR-9		100.0	353.0	air	Envelopes		

SANDIA CABLE SAMPLE REPOSITORY

	A	B	C	D	E	F	G	H
1	Batch No.	Initial Date	Average Temp. (°C)	Average Dose Rate (Gy/h)	Gas	Laboratory Notebook	Diffusion -Limited Oxidation?	
451	TR-10		120.0	62.0	air	Envelopes		
452	TR-11		120.0	360.0	air	Envelopes		
453								
454					Sil-01 Rockbestos Firewall III Silicone Insulation			
455	T-1	11/1/1989	140.0	0.0	air	Envelopes		
456								
457	TR-1							
458	TR-2	10/31/1989	41.5	52.5	air	Envelopes		
459	TR-3	10/31/1989	60.7	54.4	air	Envelopes		
460	TR-4	5/2/1988	70.0	4600.0	air	DS-I-38		
461	TR-5	5/31/1988	100.0	114.0	air	DS-I-39		
462	TR-6	11/22/1988	100.0	176.0	air	DS-III-27		
463	TR-7	11/22/1988	110.0	26.6	air	DS-III-31,32		
464	TR-8	6/13/1989	115.0	112.0	air	DS-III-39		
465	TR-9	2/22/1989	120.0	77.3	air	DS-III-35		
466	TR-10	8/9/1988	120.0	118.0	air	DS-I-40		
467	TR-11	5/31/1989	120.0	176.0	air	DS-III-37		
468	TR-12	5/31/1989	120.0	397.0	air	DS-III-33,34		
469	TR-13	10/31/1989	130.0	50.2	air	Envelopes		
470								
471								
472					ETFE-02 Teledyne red tefzel insulation (from Savannah River)			
473	T-1	2/19/1979	202.0	0.0	Air	KTG LB-II, 130		
474								
475								
476					ETFE-01 Teledyne Thermatic white tefzel insulation			
477	TR-1	1/6/1983	70.0	5740.0	Air	CAQ-34,107		
478	TR-2	5/13/1983	70.0	840.0	Air	CAQ-115		
479	TR-3	6/16/1982	70.0	130.0	Air	CAQ-99		
480	TR-4	1/27/1983	70.0	40.0	Air	CAQ-111		
481	TR-5	6/15/1983	25.0	830.0	Air	envelopes		
482	TR-5	11/8/1983	70.0	8000.0	Vacuum	CAQ-125		

SANDIA CABLE SAMPLE REPOSITORY

	A	B	C	D	E	F	G	H	I
1	CPE-01 Anaconda Flameguard FR-EP 'Y'								
2	Sample No.	Aging Time (h)	Est. Dose (kGy)	Average e/e_0	Average $TS_{/TS0}$	Average density (g/cc)	Surface Modulus, MPa	Miscellaneous	
3	Batch TR-1, 06/17/82, 70 °C, 128 Gy/h, air, CAQ-98								
4	0	0	0	1.000		1.374	98.0		
5	1	666	85	1.000			79.0		
6	2	1170	150	0.770					
7	3	1604	205	0.600					
8	4	1990	255	0.550					
9	5	2610	334	0.260					
10	6	3350	428	0.210			160.0		
11	7	3620	463	0.200			130.0		
12	8	4820	617	0.170			85.0		
13									
14	Batch TR-2, 5/12/83, 70 °C, 920 Gy/h, air, CAQ-115								
15	1	95	87	0.720		1.374			
16	2	119	109	0.700		1.375			
17	3	168	155	0.570					
18	4	267	246	0.400		1.379	91.0		
19	5	360	331	0.200		1.379			
20	6	528	486	0.140		1.383	130.0		
21	7	600	552	0.100		1.383	163.0		
22	8	840	773	0.120		1.382	128.0		
23									
24	Batch TR-3, 1/27/83, 70 °C, 960 Gy/h, air, CAQ-110								
25	1	260	250	0.710					
26	2	355	341	0.590					
27	3	431	414	0.510					
28	4	527	506	0.400					
29	4	646	620	0.320					
30	5	864	829	0.120			167.0		
31		1031	990	0.120			380.0		
32									
33	Batch TR-4, 12/15/82, 70 °C, 7100 Gy/h, air, CAQ-107,108								
34	1	7	50	1.100			87.0		
35	2	13	90	0.990					
36	3	18	128	0.760					
37	4	25	177	0.700			91.0		
38	5	42	298	0.490			93.0		
39	6	49	348	0.490					
40	7	96	682	0.420			100.0		
41	8	128	910	0.200					
42	9	132	939	0.130			300.0		
43	10	144	1022	0.110					
44	11	168	1193	0.120			580.0		
45									
46									
47									
48									
49									
50									
51									
52									
53									
54	#REF!								
55	#REF!								
56	#REF!								
57	#REF!								
58	#REF!								
59	#REF!								
60	#REF!								
61	#REF!								
62	#REF!								
63	#REF!								

scraps 80.xls
CPE-02

Material- CPE-02- Anaconda Chlorinated Polyethylene Outer Jacket												
Sample No.	Aging Time (d)	Est. Dose (kGy)	Average e/e_0	Average $TS_{/TS0}$	Average density (g/cc)	Outside surface modulus, MPa	Uptake factor	% gel	NMR T2,msec	Miscellaneous		
Batch T-1, 4/12/02, 95 °C, 0 Gy/h, Air, AG-II-1B												
	0.0		1.000		1.374	100.0	N/A	0.0		completely soluble		
	9.8		0.901									
	80.8		0.755									
	205.8		0.878									
	605.0		0.661									
Batch T-2, 9/25/02, 99 °C, 0 Gy/h, Air, RB-IV-79C												
	198.0		0.782									
	404.0		0.684									
	616.0		0.745									
Batch T-3, 9/25/02, 109 °C, 0 Gy/h, Air, RB-IV-79B												
	82.0		0.818				3.94	41.4				
	132.0		0.729				4.03	47.2				
	202.1		0.679				4.06	48.4				
	314.0		0.507									
	397.3		0.497									
	484.0		0.377									
	576.0		0.288									
	617.0		0.382									
	617.0		0.214									
	761.1		0.256									
	923.2		0.097									
Batch T-4, 9/25/02, 124 °C, 0 Gy/h, Air, RB-IV-79A												
	0.0		1.000		1.374	100.0	N/A	0.0	13.920			
	30.0		0.730		1.379		3.88	46.4	12.080			
	61.2		0.565		1.381		4.00	43.6	9.400			
	107.0		0.546		1.381		3.73	51.4	10.750			
	152.0		0.081		1.381	100.0	3.17	59.0	5.750			
	161.2		0.240		1.379	130.0	3.25	59.6	6.800			
	222.2		0.117		1.377	205.0	2.54	74.0	3.960			
	246.0		0.039		1.375	580.0	2.18	78.8	2.890			
	281.0		0.049		1.372	520.0	2.36	79.7	2.720			
	314.0		0.034									
	355.1		0.000									
	363.0		0.000									
Batch T-5, 4/12/02, 138 °C, 0 Gy/h, Air, AG-II-1A												
	3.0		0.936				4.64	41.2				
	5.8		0.975									
	75.8		0.181				2.51	75.6				
	171.7		0.000									
Batch T-6, 7/02/02, 138 °C, 0 Gy/h, Air, AG-II-22												
	13.9		0.651				3.98	46.0				
	21.2		0.551									
	31.0		0.499				3.51	49.1				
	64.1		0.334				3.10	63.7				
	50.3		0.301									
	59.2		0.236									
	70.1		0.214									
Batch T-7, 6/03/03, 138 °C, 0 Gy/h, Air, RB-VI-33												
	41.7		0.355									
	71.0		0.120									
	92.9		0.022									
	103.8		0.049									
	121.8		0.000									
	142.0		0.000									

scraps 80.xls
EPR-01A

	A	B	C	D	E	F	G	H
1	**Material- EPR-01A- Anaconda Flameguard insulation**							
2	Sample No.	Aging Time (h)	Est. Dose (kGy)	Average e/e_0	Average $TS_{/TS0}$	NMR T2, msec	Miscellaneous	
3								
4								
5	Batch T-1, 12/12/78, 100.9 °C, 0 Gy/h, air,							
6	1	2062		0.930	1.080			
7	2	4366		0.820	0.992			
8	3	6718		0.720	0.944			
9	4	7390		0.760	0.988			
10	5	8206		0.710	1.020			
11	6	8880		0.730	0.980			
12	7	9580		0.560	0.790			
13	8	10322		0.560	0.820			
14	9	11330		0.600	0.830			
15	10	12340		0.460	0.500			
16	11	13420		0.250	0.266			
17	12	14188		0.006				
18								
19	Batch T-2, 11/28/78, 110.8 °C, 0 Gy/h, air, LB-II-108							
20	1	1030		0.870	1.065			
21	2	2157		0.850	1.052			
22	3	3360		0.740	0.940			
23	4	3691		0.740	0.870			
24	5	4099		0.710	0.830			
25	6	4435		0.630	0.810			
26	7	4770		0.580	0.710			
27	8	5706		0.410	0.540			
28	9	5441		0.140	0.250			
29	10	5780		0.020	0.250			
30								
31	Batch T-3, 11/21/78, 119.8 °C, 0 Gy/h, air, LB-II-108&135							
32	1	502		0.880	1.065			
33	2	1006		0.780	0.990			
34	3	1391		0.760	0.940			
35	4	1536		0.580	0.860			
36	5	1622		0.680	0.880			
37	6	1814		0.440	0.613			
38	7	2030		0.270	0.340			
39	8	2270		0.020	0.220			
40								
41	Batch T-4, 09/25/78, 130.1 °C, 0 Gy/h, air, LB-II-105							
42	1	238		0.920	1.040			
43	2	575		0.720	0.863			
44	3	719		0.700	0.766			
45	4	886		0.370	0.339			
46	5	908		0.240	0.258			
47	6	999		0.009	0.163			
48								
49	Batch T-5, 09/25/78, 140.3 °C, 0 Gy/h, air, LB-II-104							
50	1	102		0.900	0.976			
51	2	190		0.820	0.911			

scraps 80.xls
EPR-01A

	A	B	C	D	E	F	G	H
52	3	262		0.770	0.786			
53	4	334		0.650	0.718			
54	5	457		0.250	0.250			
55	6	503		0.015	0.194			
56								
57	Batch T-6, 08/21/78, 150 °C, 0 Gy/h, air, LB-II-98-99							
58	1	48		0.970	1.050			
59	2	120		0.820	0.806			
60	3	142		0.770	0.734			
61	4	175		0.720	0.472			
62	5	224		0.035	0.214			
63	6	312		0.020				
64								
65	Batch T-7, 12/08/78, 160.5 °C, 0 Gy/h, air, LB-II-118							
66	1	23		0.870	0.976			
67	2	71		0.750	0.645			
68	3	79		0.790	0.528			
69	4	90		0.870	0.516			
70	5	95		0.700	0.343			
71	6	115		0.110	0.266			
72	7	122		0.070	0.270			
73								
74	Batch T-8, 04/15/79, 170 °C, 0 Gy/h, air, LHJ-6							
75	1	16		0.930	0.944			
76	2	40		0.840	0.577			
77	3	48		0.850	0.444			
78	4	55		0.750	0.363			
79	5	64		0.098	0.246			
80	6	72		0.052	0.218			
81								
82								
83	Batch TR-1, 01/31/79, RT °C, 870 Gy/h, air, LB-II-122							
84	1	120		0.690				
85	2	334		0.590				
86	3	672		0.420				
87	4	945		0.320				
88								
89	Batch TR-2, 08/04/78, RT °C, 980 Gy/h, air, LB-II-95							
90	1	99		0.730				
91	2	240		0.600				
92	3	436		0.510				
93	4	647		0.410				
94								
95	Batch TR-3, 03/26/79, RT °C, 1830 Gy/h, air, LB-II-146							
96	1	48		0.760				
97	2	168		0.580				
98	3	336		0.420				
99	4	504		0.340				
100	5	671		0.280				
101	6	839		0.240				
102								
103	Batch TR-4, 04/09/79, RT °C, 9070 Gy/h, air, LB-II-147							
104	1	8		0.780				

scraps 80.xls
EPR-01A

	A	B	C	D	E	F	G	H
105	2	32		0.580				
106	3	56		0.450				
107	4	104		0.350				
108	5	166		0.290				
109	6	215		0.250				
110								
111	Batch TR-5, 07/09/79, RT °C, 870 Gy/h, Nitrogen, LHJ-15							
112	1	245		0.600				
113	2	533		0.480				
114	3	796		0.390				
115	4	1347		0.350				
116	5	1946		0.250				
117	6	2623		0.180				
118	7	3301		0.170				
119								
120	Batch TR-6, 07/18/79, 117 °C, 370 Gy/h, air, LHJ-17							
121	1	144		0.890				
122	2	287		0.730				
123	3	503		0.630				
124	4	672		0.430				
125	5	791		0.080				
126	6	891		0.030				
127	7	958		0.018				
128								
129	Batch TR-7, 03/26/79, 115 °C, 1890 Gy/h, air, LB-II-145							
130	1	48		0.790				
131	2	104		0.770				
132	3	168		0.660				
133	4	240		0.420				
134	5	335		0.050				
135	6	502		0.020				
136	7	670		0.010				
137								
138	Batch TR-8, 03/12/79, 145 °C, 1835 Gy/h, air, LB-II-143							
139	1	8		0.950				
140	2	24		0.910				
141	3	47		0.910				
142	4	79		0.620				
143	5	103		0.520				
144	6	167		0.026				
145								
146	Batch TR-9, 04/02/79, 145 °C, 9200 Gy/h, air, LB-II-146							
147	1	6		0.940				
148	2	24		0.670				
149	3	31		0.630				
150	4	47		0.370				
151	5	71		0.070				
152	6	95		0.035				

scraps 80.xls
EPR-01B

Material- EPR-01B- Anaconda Flameguard insulation									
Sample No.	Aging Time (h)	Est. Dose (kGy)	Average e/e_0	Average $TS_{/TS0}$		Miscellaneous			
Batch TR-1, 04/26/77, 22 °C, 15.7 Gy/h, air, NRL B-16									
0	0	0	1.000		1.325				
1	2592	52	1.060				0.000	1	1.3245
2	7392	146	0.780				135.000	0.695	1.329
3	17664	321	0.560				324.000	0.46	1.336
4	22704	400	0.430				530.000	0.26	1.3448
5	26928	456	0.430						
6	31392	507	0.410						
7	40128	597	0.330						
8	53136	710	0.270						
Batch TR-1 RH, 04/26/77, 22 °C, 15.7 Gy/h, air + RH, NRL B-15									
1	2592	45	1.140						
2	7392	124	0.900						
3	22704	342	0.550						
4	31392	440	0.380						
5	35472	482	0.380						
6	40128	530	0.310						
7	45048	575	0.250						
8	53136	643	0.230						
Batch TR-2, 04/26/77, 22 °C, 80 Gy/h, air, NRL B-6									
1	672	71	1.090						
2	2592	267	0.690						
3	5520	559	0.450						
4	11064	1080	0.300						
5	26928	2340	0.090						
Batch TR-2 RH, 04/26/77, 22 °C, 80 Gy/h, air + RH, NRL B-2									
1	672	71	1.010						
2	2592	267	0.790						
3	5520	559	0.440						
4	11064	1080	0.310						
5	17664	1640	0.140						
Batch TR-3, 08/16/77, 24 °C, 515 Gy/h, air, NRL A-19									
1	144	77	1.050						
2	336	180	0.870						
3	672	359	0.670						
4	1344	715	0.490						
5	2688	1413	0.280						
Batch TR-3 RH, 08/16/77, 24 °C, 515 Gy/h, air + RH, NRL A-17									
1	144	74	1.120						
2	336	172	0.870						
3	672	344	0.640						
4	1344	684	0.500						
5	2688	1353	0.300						

scraps 80.xls
EPR-01B

Batch TR-4, 08/15/77, 30 °C, 2210 Gy/h, air, NRL A-5									
1	48	105	0.960						
2	96	212	0.790						
3	240	531	0.580						
4	433	954	0.480						
5	671	1470	0.320						
Batch TR-4 RH, 08/15/77, 30 °C, 2210 Gy/h, air + RH, NRL A-4									
1	48	106	0.940						
2	96	214	0.740						
3	241	536	0.570						
4	434	965	0.440						
5	671	1493	0.310						
Batch TR-5 RH, 05/03/77, 38 °C, 11800 Gy/h, air + RH, NRL A-1									
1	8	95	0.980						
2	24	285	0.760						
3	48	567	0.610						
4	80	945	0.510						
5	144	1700	0.370						
Batch TR-6, 09/06/1977, 100 °C, 2250 Gy/h, air, NRL A-6									
1	32		1.080						
2	71		0.960						
3	214		0.660						
4	406		0.230						
5	549		0.060						
Batch TR-7 RH, 12/12/1977, 110 °C, 495 Gy/h, air + RH, NRL A-17									
1	222		1.120						
2	527		0.820						
3	840		0.490						
4	1174		0.060						
Batch TR8, 09/06/1977, 120 °C, 2300 Gy/h, air, NRL A-7									
1	32		1.090						
2	71		0.900						
3	214		0.530						
4	405		0.140						
5	549		0.056						
Batch TR-9 RH, 12/12/1977, 130 °C, 515 Gy/h, air + RH, NRL A-19									
1	168		0.960						
2	360		0.530						
3	528		0.000						
Batch TR-10, 09/12/1977, 140 °C, 2310 Gy/h, air, NRL A-2									
1	20		1.080						
2	31		1.020						
3	71		0.830						
4	142		0.530						
5	310		0.030						
Batch TR-10 RH, 09/12/1977, 140 °C, 2030 Gy/h, air + RH, NRL A-4									
1	22		1.070						
2	31		1.050						
3	71		0.830						
4	143		0.540						
5	310		0.060						

SANDIA CABLE SAMPLE REPOSITORY

Material- EPR-02- Anaconda Flameguard FR-EP insulation (Y)									
Sample No.	Aging Time (h)	Est. Dose (kGy)	Average e/e_0	Average $TS_{/TS0}$	Average density (g/cc)	OIT (___)	Indentor (____)	Miscellaneous	
Batch T-1A, 4/1/1988, 120 °C, 0 Gy/h, air, DS-I-21									
1	72	0	0.980						
2	168		0.920						
3	238		0.930						
4	337		0.990						
5	499		0.880						
6	744		0.910						
7	1003		0.910						
8	2012		0.900						
9	3360		0.027						
Batch T-1B, 5/6/1988, 120 °C, 0 Gy/h, air, DS-I-21								lots of scatter.	
1	2520		0.870					samples from same	
2	3020		0.570					batch as T-1A.	
3	3960		0.880					aging time much longer.	
4	4828		0.990						
5	5810		0.760						
Batch T-2, 8/28/1989, 140 °C, 0 Gy/h, air, DS-IV-1									
1	192		0.940						
2	336		0.620						
3	503		0.000						
Batch T-3, 8/28/1989, 150 °C, 0 Gy/h, air, DS-IV-7									
1	72		0.900						
2	192		0.920						
3	240		0.470						
4	336		0.029						
Batch T-4, 7/7/1989, 160 °C, 0 Gy/h, air, DS-III-7									
1	71		0.930						
2	239		0.004						
Batch TR-1, , 41 °C, 58.6 Gy/h, air,									
Batch TR-2, 8/11/1987, 60 °C, 330 Gy/h, air, DS-I-5									
1	337		0.580						
2	668		0.620						
3	1172		0.240						
4	1677		0.210						
5	2180		0.110						
6	2690		0.085						
7	3531		0.082						
8	3837		0.074						
Batch TR-3, 1/18/1988, 60 °C, 5140 Gy/h, air, DS-I-19									
1	22		0.720						

SANDIA CABLE SAMPLE REPOSITORY

Material- EPR-02- Anaconda Flameguard FR-EP insulation (Y)									
Sample No.	Aging Time (h)	Est. Dose (kGy)	Average e/e_0	Average $TS_{/TS0}$	Average density (g/cc)	OIT (___)	Indentor (____)	Miscellaneous	
2	40		0.620						
3	64		0.480						
4	88		0.380						
5	119		0.270						
6	143		0.140						
7	184		0.130						
8	256		0.092						
Batch TR-4, , 61 °C, 60.9 Gy/h, air,									
Batch TR-5, 8/11/1987, 80 °C, 133 Gy/h, air, DS-I-35									
1	837		0.750						
2	1676		0.560						
3	2180		0.480						
4	2858		0.370						
5	4027		0.200						
6	5540		0.092						
Batch TR-6, 8/11/1987, 80 °C, 314 Gy/h, air, DS-I-10									
1	337		0.710						
2	668		0.520						
3	1172		0.360						
4	1677		0.300						
5	2181		0.130						
6	2690		0.092						
7	3531		0.084						
8	3837		0.067						
Batch TR-7, 10/26/1987, 80 °C, 790 Gy/h, air, DS-I-16-17									
1	96		0.730						
2	216		0.550						
3	334		0.510						
4	509		0.340						
5	672		0.280						
6	840		0.082						
7	1012		0.072						
8	1345		0.059						
9	1679		0.045						
Batch TR-8, 10/12/1987, 80 °C, 5290 Gy/h, air, DS-I-25									
1	21		0.790						
2	40		0.630						
3	64		0.510						
4	87		0.400						
5	119		0.330						
6	143		0.260						
7	184		0.180						
8	256		0.079						

SANDIA CABLE SAMPLE REPOSITORY

Material- EPR-02- Anaconda Flameguard FR-EP insulation (Y)									
Sample No.	Aging Time (h)	Est. Dose (kGy)	Average e/e_0	Average $TS_{/TS0}$	Average density (g/cc)	OIT (___)	Indentor (____)	Miscellaneous	
Batch TR-9, 5/31/1988, 100 °C, 135 Gy/h, air, DS-I-34									
1	334		0.900						
2	671		0.840						
3	1174		0.740						
4	1679		0.670						
5	2374		0.500						
6	2927		0.310						
7	3358		0.230						
8	3861		0.180						
9	5344		0.075						
10	6022		0.046						
Batch TR-10, 5/31/1989, 100 °C, 226 Gy/h, air, DS-III-53 Black									
1	215		0.740						
2	479		0.810						
3	963		0.450						
4	1127		0.420						
5	1324		0.350						
6	1486		0.230						
7	1826		0.160						
8	2350		0.100						
Batch TR-11, 1/18/1988, 100 °C, 313 Gy/h, air, DS-I-11									
1	335		0.780						
2	671		0.640						
3	1174		0.390						
4	1678		0.250						
5	2182		0.130						
6	2686		0.100						
Batch TR-12, 8/17/1987, 100 °C, 810 Gy/h, air, DS-I-15									
1	95		0.720						
2	214		0.530						
3	334		0.460						
4	526		0.320						
5	670		0.300						
6	838		0.220						
7	1013		0.120						
8	1684		0.021						
Batch TR-13, 12/20/1988, 110 °C, 26.9 Gy/h, air, DS-III-51 Black									
1	672		0.850						
2	1349		0.850						
3	2017		0.700						
4	2688		0.680						
5	3744		0.360						
6	4369		0.380						
7	5548		0.210						
8	6551		0.160						

SANDIA CABLE SAMPLE REPOSITORY

Material- EPR-02- Anaconda Flameguard FR-EP insulation (Y)									
Sample No.	Aging Time (h)	Est. Dose (kGy)	Average e/e_0	Average $TS_{/TS0}$	Average density (g/cc)	OIT (___)	Indentor (____)	Miscellaneous	
Batch TR-14, 4/19/1989, 115.6 °C, 98.5 Gy/h, air, DS-I-8 Black									
1	480		0.860						
2	984		0.720						
3	1319		0.630						
4	1972		0.330						
5	2495		0.140						
6	2836		0.110						
7	3361		0.078						
Batch TR-15, 2/22/1989, 120 °C, 71.5 Gy/h, air, DS-III-55 Black									
1	167		0.990						
2	335		0.930						
3	480		0.850						
4	652		0.840						
5	988		0.780						
6	1654		0.490						
7	2159		0.360						
8	2661		0.240						
9	3195		0.220						
10	4177		0.095						
11	4845		0.130						
Batch TR-16, 8/9/1988, 120 °C, 125 Gy/h, air, DS-I-33-32									
11	193		0.930						
2	330		0.870						
3	509		0.870						
4	694		0.730						
5	837		0.760						
6	1247		0.240						
7	1678		0.150						
8	2014		0.061						
9	2731		0.050						
Batch TR-17, 1/18/1988, 120 °C, 294 Gy/h, air, DS-I-6									
1	168		0.790						
2	336		0.570						
3	504		0.190						
4	671		0.200						
5	911		0.092						
6	1174		0.076						
Batch TR-18, 5/31/1989, 120 °C, 420 Gy/h, air, DS-III-57,79 Black									
1	216		0.790						
2	360		0.690						
3	504		0.190						
4	700		0.180						
5	844		0.060						
6	1012		0.094						

SANDIA CABLE SAMPLE REPOSITORY

Material- EPR-02- Anaconda Flameguard FR-EP insulation (Y)									
Sample No.	Aging Time (h)	Est. Dose (kGy)	Average e/e_0	Average $TS_{/TS0}$	Average density (g/cc)	OIT (___)	Indentor (____)	Miscellaneous	
7	1176		0.060						
Batch TR-19, 1/18/1988, 120 °C, 773 Gy/h, air, DS-I-14									
1	71		0.850						
2	167		0.740						
3	336		0.480						
4	502		0.340						
5	671		0.210						
6	839		0.100						
7	1007		0.055						
8	1175		0.021						
Batch TR-20, 2/1/1988, 120 °C, 5090 Gy/h, air, DS-I-29									
1	21		0.850						
2	41		0.710						
3	64		0.500						
4	88		0.380						
5	119		0.250						
6	143		0.200						
7	184		0.140						
8	256		0.071						
9	328		0.085						

SANDIA CABLE SAMPLE REPOSITORY

Material- EPR-03- Eaton Dekoron Elastoset Insulation

Sample No.	Aging Time (h)	Est. Dose (kGy)	Average e/e_0	Average $TS_{/TS0}$	Average density (g/cc)	Outside surface modulus, MPa	Uptake factor	% gel	NMR T2,msec	Miscellaneous
Batch T-1, 4/26/01, 99 °C, 0 Gy/h, air, RB-II-45F										
1white	19454		0.916	1.000						
2white	23976		0.875	1.089						
3white	27192		1.035	1.121						
4white	30000		1.018	1.021						
Batch T-2, 4/26/01, 109 °C, 0 Gy/h, air, RB-II-45D,RB-IV-67A										
0white	0		1.000	1.000	1.285	62	4.413	71.7		
1white	1674		1.025	1.017						
2white	3359		1.015	1.061						
3white	4792		0.913	1.105						
4white	9719		0.975	1.092						
5white	19455		0.875	1.043						
6white	24015		0.738	1.147						
7white	27185		0.973	1.103						
8white	29998		0.948	1.041						
9white	32400		0.125							hardens slowly from ~1150 to 1500 d
0black	0		1.000	1.000	1.279					
1black	1674									
2black	3359									
3black	4792									
4black	9719									
5black	19455									
6black	24015									
7black	27185									
8black	29998									
9black	32400									
Batch T-3, 4/1/1988, 120 °C, 0 Gy/h, air, (not long enough)										
1	72		1.100							
2	168		1.090							
3	239		1.100							
4	337		1.110							

SANDIA CABLE SAMPLE REPOSITORY

Material- EPR-03- Eaton Dekoron Elastoset Insulation

Sample No.	Aging Time (h)	Est. Dose (kGy)	Average e/e_0	Average $TS_{/TS0}$	Average density (g/cc)	Outside surface modulus, MPa	Uptake factor	% gel	NMR T2,msec	Miscellaneous
5	502		1.060							
6	673		1.080							
7	1004		1.080							
8	2013		1.000							
9	2521		1.070							
10	3362		1.060							
11	4703		1.070							
12	6892		1.010							
Batch T-4, 10/03/01, 124 °C, 0 Gy/h, air, RB-II-81,RB-IV-67										
1white	1441		1.145	0.929	1.280					
2white	2784		0.976	0.072	1.291	45				
3white	4320		1.015	0.976	1.290					
4white	6693		1.008	0.963	1.295					
5white	7197		0.996	0.944	1.293	30				
6white	7747		0.975	0.937	1.295					
7white	8179		1.025	0.941	1.297					
8white	8706		1.010	0.960	1.296					
9white	9623		1.061	0.970	1.296	30				
10white	10199		0.650	0.736	1.295					
11a-whit	10457		0.745	0.828	1.248	30				
11b-whit	10457		0.250	0.494	1.228	~400				
12white	11129		0.000	0.330	1.295					
13a-whit	12066		0.000	0.230	1.358					
13b-whit	12072		0.000		1.387					
1black	1441		1.055	1.017	1.283					
2black	2784		0.990	1.036	1.283					
3black	4320		0.935	1.015	1.284					
4black	6693		1.063	1.009	1.284					
5black	7197		0.830	0.850	1.285					
6black	7747		0.975	1.007	1.288					
7black	8179		1.250	0.905	1.285					
8black	8706		0.965	0.992	1.287					

SANDIA CABLE SAMPLE REPOSITORY

Material- EPR-03- Eaton Dekoron Elastoset Insulation

Sample No.	Aging Time (h)	Est. Dose (kGy)	Average e/e_0	Average $TS_{/TS0}$	Average density (g/cc)	Outside surface modulus, MPa	Uptake factor	% gel	NMR T2,msec	Miscellaneous
9black	9623		1.070	1.038	1.289					
10black	10199		0.963	1.035	1.293					
11black	10457		0.433	0.647	1.288					
12a-blac	11129		0.000	0.457	1.413					
12b-blac	11136				1.551					
13a-blac	12066		0.125	0.167	1.386					
13a-blac	12066				1.387					
Batch T-5, 4/26/01, 138 °C, 0 Gy/h, air, RB-II-45B										
1white	168				1.288					
2white	334		1.093	1.170	1.289	85				
3white	503		1.079	1.080	1.290		4.20	72.6		
4white	672		0.926	1.060	1.291					
5white	954		0.898	0.910	1.292	85	4.35	72.5		
6white	1342		1.045	1.093	1.293					
7white	1673		1.033	1.107	1.293		4.69	73.4		
8white	2200		1.033	1.100	1.299	63	4.80	73.2		
9white	2680		0.510	0.707	1.300		4.14	73.6		
10a-whit	2832		0.035	0.457	1.432	85	5.03	71.8		
10b-whit	2832				1.341	670				
11a-whit	3000		0.025	0.514	1.463	100	3.97	68.8		
11b-whit	3000				1.390	2000				
11c-whit	2991				1.300					
1black										
2black										
3black										
4black										
5black										
6black										
7black										
8black										
9black										
10black										
11black										

SANDIA CABLE SAMPLE REPOSITORY

Material- EPR-03- Eaton Dekoron Elastoset Insulation

Sample No.	Aging Time (h)	Est. Dose (kGy)	Average e/e_0	Average $TS_{/TS0}$	Average density (g/cc)	Outside surface modulus, MPa	Uptake factor	% gel	NMR T2,msec	Miscellaneous
Batch T-6, 7/7/1989, 160 °C, 0 Gy/h, air, DS-III-11										
1white	72		1.110	1.110	1.287	70		70.4		
2white	168		1.100	1.130	1.292	70		69.8		
3white	336		1.060	1.150	1.293	70		69.8		
4white	572		0.610	0.990	1.305	90, 200		58.5		varies-soft vs. hard
5white	740		0.000	0.400	1.413	>1000		75.0		
1black	72		1.082	1.136	1.288			69.9		
2black	168		1.062	1.157	1.289			71.2		
3black	336		1.074	1.186	1.289			71.3		
4black	572		0.259	0.579	1.307			68.3		
5black	740		0.003		1.464			81.5		
Batch TR-1, , 23 °C, 210 Gy/h, air, Where are envelopes?										
Batch TR-2, 10/31/1989, 40 °C, 58 Gy/h, air, Envelopes										
1	504		1.000							
2	1007		0.900							
3	1512		0.860							
4	2016		0.700							
5	3044		0.540							
6	4036		0.430							
7	4703		0.360							
8	5036		0.360							
9	6379		0.200							
10	7057		0.180							
11	8568		0.059							
Batch TR-3, 5/11/1994, 40 °C, 420 Gy/h, air, Envelopes										
1	337		0.930							
2	672		0.760							
3	1029		0.580							
4	1512		0.350							

SANDIA CABLE SAMPLE REPOSITORY

Material- EPR-03- Eaton Dekoron Elastoset Insulation

Sample No.	Aging Time (h)	Est. Dose (kGy)	Average e/e_0	Average $TS_{/TS0}$	Average density (g/cc)	Outside surface modulus, MPa	Uptake factor	% gel	NMR T2,msec	Miscellaneous
5	2016		0.250							
6	2516		0.190							
7	3528		0.078							
Batch TR-4, 1/18/1988, 60 °C, 5140 Gy/h, air, DS-I-59										
1	22		0.830							
2	40		0.600							
3	64		0.510							
4	88		0.410							
5	119		0.130							
6	143		0.130							
7	184		0.096							
8	256		0.034							
Batch TR-5, 8/11/1987, 60 °C, 315 Gy/h, air, Envelopes										
1	337		0.700							
2	672		0.550							
3	1173		0.340							
4	1678		0.250							
5	2181		0.220							
6	2691		0.110							
7	3531		0.100							
8	3862		0.076							
Batch TR-6, 5/15/1990, 60 °C, 355 Gy/h, air , Envelopes										
1	168		0.950							
2	338		0.810							
3	504		0.720							
4	673		0.720							
5	840		0.590							
6	1178		0.450							
7	1680		0.310							
8	2353		0.180							
9	3193		0.000							

SANDIA CABLE SAMPLE REPOSITORY

Material- EPR-03- Eaton Dekoron Elastoset Insulation

Sample No.	Aging Time (h)	Est. Dose (kGy)	Average e/e_0	Average $TS_{/TS0}$	Average density (g/cc)	Outside surface modulus, MPa	Uptake factor	% gel	NMR T2,msec	Miscellaneous
Batch TR-7, 10/31/1989, 61 °C, 59.5 Gy/h, air, Envelopes										
1	1006		0.950							
2	2016		0.790							
3	3044		0.700							
4	4032		0.660							
5	5036		0.580							
6	6049		0.540							
7	7057		0.410							
8	8568		0.250							
Batch TR-8, 8/11/87, 80 °C, 143 Gy/h, air, DS-I-75										
1	836		0.790							
2	1676		0.660							
3	2180		0.620							
4	2858		0.470							
5	4027		0.280							
6	5540		0.074							
Batch TR-9, 8/11/87, 80 °C, 314 Gy/h, air, DS-I-50										
1	337		0.880							
2	668		0.780							
3	1173		0.560							
4	1677		0.390							
5	2181		0.250							
6	2690		0.160							
7	3531		0.100							
8	3837		0.072							
Batch TR-10, 10/26/87, 80 °C, 740 Gy/h, air, DS-I-56,57										
1	96		0.900							
2	215		0.710							
3	334		0.680							
4	508		0.460							

SANDIA CABLE SAMPLE REPOSITORY

Material- EPR-03- Eaton Dekoron Elastoset Insulation

Sample No.	Aging Time (h)	Est. Dose (kGy)	Average e/e_0	Average $TS_{/TS0}$	Average density (g/cc)	Outside surface modulus, MPa	Uptake factor	% gel	NMR T2,msec	Miscellaneous
5	671		0.320							
6	840		0.210							
7	1011		0.150							
8	1345		0.058							
9	1679		0.055							
Batch TR-11, 10/12/87, 80 °C, 5290 Gy/h, air, DS-I-65										
1	21		0.880							
2	40		0.750							
3	64		0.630							
4	87		0.550							
5	119		0.390							
6	143		0.330							
7	184		0.200							
8	256		0.110							
Batch TR-12, 5/31/89, 100 °C, 226 Gy/h, air , DS-III-49										
1	215		1.070							
2	479		0.940							
3	963		0.740							
4	1127		0.720							
5	1324		0.640							
6	1486		0.440							
7	1826		0.270							
8	2350		0.037							
Batch TR-13, 1/18/88, 100 °C, 313 Gy/h, air, DS-I-51										
1	335		0.920							
2	671		0.710							
3	1175		0.440							
4	1679		0.220							
5	2182		0.076							
6	2686		0.053							

SANDIA CABLE SAMPLE REPOSITORY

Material- EPR-03- Eaton Dekoron Elastoset Insulation

Sample No.	Aging Time (h)	Est. Dose (kGy)	Average e/e_0	Average $TS_{/TS0}$	Average density (g/cc)	Outside surface modulus, MPa	Uptake factor	% gel	NMR T2,msec	Miscellaneous
Batch TR-14, 8/17/87, 100 °C, 761 Gy/h, air, DS-I-55										
1	95		0.830							
2	214		0.660							
3	334		0.530							
4	525		0.410							
5	670		0.320							
6	838		0.260							
7	1013		0.160							
8	1684		0.042							
Batch TR-15, 11/22/88, 110 °C, 30.4 Gy/h, air, DS-I-79, 80										
1	665		1.100							
2	1338		1.090							
3	2013		1.040							
4	2682		1.010							
5	3353		0.960							
6	4362		0.850							
7	5034		0.890							can flooded
8	6213		0.740							
9	7216		0.620							
10	8465		0.550							
Batch TR-16, 4/19/1989, 110 °C, 106 Gy/h, air, Envelopes										
1	504		1.040							
2	1008		1.020							
3	1343		0.970							
4	1900		0.730							
5	2520		0.310							
6	2832		0.080							
Batch TR-17, 4/19/89, 115.6 °C, 104 Gy/h, air, DS-III-41										
1	480		1.040							
2	984		1.020							
3	1319		0.970							
4	1972		0.730							

SANDIA CABLE SAMPLE REPOSITORY

Material- EPR-03- Eaton Dekoron Elastoset Insulation

Sample No.	Aging Time (h)	Est. Dose (kGy)	Average e/e_0	Average $TS_{/TS0}$	Average density (g/cc)	Outside surface modulus, MPa	Uptake factor	% gel	NMR T2,msec	Miscellaneous
5	2495		0.310							
6	2836		0.130							
Batch TR-18, 2/22/89, 120 °C, 71.5 Gy/h, air, DS-III-47, 48										
1	167		1.080							
2	335		1.050							
3	480		1.010							
4	652		1.000							
5	988		1.020							
6	1654		0.870							
7	2157		0.530							
8	2661		0.400							
9	3195		0.720							scatter high
10	4177		0.130							scatter high
11	4845		0.170							scatter high
Batch TR-19, 5/31/1989, 120 °C, 228 Gy/h, air, Envelopes										
1	216		1.070							
2	504		0.940							
3	744		0.720							
4	960		0.740							
5	1488		0.440							
6	1828		0.280							
Batch TR-20, 1/18/88, 120 °C, 294 Gy/h, air, DS-I-46										
1	168		1.000							
2	336		0.900							
3	504		0.880							
4	671		0.380							
5	911		0.076							
6	1174		0.021							
Batch TR-21, 5/31/89, 120 °C, 420 Gy/h, air, DS-III-45										
1	192		1.060							
2	480		0.890							

SANDIA CABLE SAMPLE REPOSITORY

Material- EPR-03- Eaton Dekoron Elastoset Insulation

Sample No.	Aging Time (h)	Est. Dose (kGy)	Average e/e_0	Average $TS_{/TS0}$	Average density (g/cc)	Outside surface modulus, MPa	Uptake factor	% gel	NMR T2,msec	Miscellaneous
3	964		0.092							
4	1128		0.042							
Batch TR-22, 1/18/88, 120 °C, 725 Gy/h, air, DS-I-54										
1	71		1.000							
2	167		0.800							
3	335		0.700							
4	502		0.510							
5	671		0.340							
6	829		0.260							
7	1007		0.081							
8	1174		0.055							
Batch TR-23, 2/1/88, 120 °C, 5090 Gy/h, air, DS-I-69										
1	21		1.000							
2	41		0.890							
3	64		0.770							
4	88		0.610							
5	119		0.410							
6	143		0.220							
7	184		0.160							
8	256		0.089							
9	328		0.075							

SANDIA CABLE SAMPLE REPOSITORY

Material- EPR-04- Anaconda Durasheath Insulation														
Sample No.	Aging Time (h)	Est. Dose (kGy)	Average e/e_0	Average $TS_{/TS0}$	Average density (g/cc)	Outside surface modulus, MPa	Uptake factor	% gel	NMR T2,msec	Miscellaneous				
Batch T-1, 6/09/93, 100 °C, 0 Gy/h, air, envelopes														
1	2352		1.030	1.070	1.313									
2	4656		0.880	1.060	1.310	5.3								
3	9456		0.750	1.000	1.318									
4	11760		0.840	1.060	1.316	5.3								
5	18624		0.710	1.060	1.331									
6	25368		0.680	1.060	1.341	7.0								
7	34104		0.580	1.000	1.340	7.0								
8	42840		0.490	1.010	1.351									
9	52344		0.310	0.723	1.351	9.0								
10	56472		0.330	0.781	1.353	9.0								
11	58320		0.243	0.640	1.360	9.0				soft sample				
11	58320		0.017	0.686	1.594	70.0				hard sample				
11	58320		0.003		1.691	~2500				hard sample				
Batch T-2, 6/09/93, 110 °C, 0 Gy/h, air, envelopes														
1	1176		1.110	1.036	1.307	5.6	3.8	82.2						
2	2352		0.950	1.050	1.315									
3	3528		0.920	1.070	1.318		4.5	83.0						
4	5880		0.840	1.060	1.333	9.0	3.7	81.9						
5	8736		0.730	0.990	1.328		3.6	80.0						
6	11760		0.740	1.050	1.332	9.0	3.9	78.3						
7	15120		0.550	0.940	1.339	9.5	4.6	79.2						
8	18648		0.240	0.530	1.352	9.0	4.6	77.6		soft sample				
8	18648		0.240	0.530	1.448					medium sample				
8	18648		0.240	0.530	1.587					hard sample				
9	22176		dead		1.694	~1000	1.1	97.3						
9	22176		dead		1.690									
Batch T-3, 6/09/93, 125 °C, 0 Gy/h, air, envelopes														
1	336		1.030	1.085	1.313		4.0	83.6						
2	672		0.980	1.060	1.313			81.9						
3	1008		1.110	1.100	1.323	8.5	3.8	82.7						

SANDIA CABLE SAMPLE REPOSITORY

Material- EPR-04- Anaconda Durasheath Insulation

Sample No.	Aging Time (h)	Est. Dose (kGy)	Average e/e_0	Average $TS_{/TS0}$	Average density (g/cc)	Outside surface modulus, MPa	Uptake factor	% gel	NMR T2,msec	Miscellaneous				
4	1344		0.930	0.974	1.324			81.5						
5	1848		0.890	1.050	1.332		3.6	80.6						
6	2352		0.940	1.070	1.322	6.0	3.7	77.8						
7	3192		0.690	0.920	1.345			81.9						
8	3528		0.650	0.890	1.330	9.5	4.0	83.7						
9	4416		dead			40.0				soft sample				
9	4416		dead			190.0				medium sample				
9	4416		dead		1.580	~1100	1.7	96.0		hard sample				
10	4560		0.120	0.288	1.560		1.8	88.8						
Batch T-4, 11/17/95, 140 °C, 0 Gy/h, air, envelopes														
1	408		0.920	1.010	1.342	7.0								
2	672		0.730	0.870	1.340									
3	1056		0.030	0.240	1.363	7.0								
3	1056		0.030	0.240	1.421	40.0				softer sample				
3	1056		0.030	0.240	1.517	~3000				harder sample				
4	1152		dead			40.0				softer sample				
4	1152		dead		1.530	~2000				harder sample				
Batch , , °C, Gy/h, ,														

SANDIA CABLE SAMPLE REPOSITORY

Material- EPR-05- Okonite EPR Insulation													
Sample No.	Aging Time (h)	Est. Dose (kGy)	Average e/e_0	Average $TS_{/TS0}$	Average density (g/cc)	Outside surface modulus, MPa	Uptake factor	% gel	NMR T2,msec	Notes			
Batch T-1, 4/26/01, 99 °C, 0 Gy/h, Air, RB-II-45E													
1	11373		0.861										
2	11373		1.017										
3	17560		0.481										
4	17560		0.797										
5	21615		0.565										
6	21615		0.542										
7	24878		0.516										
8	24878		0.435										
9	27168		0.435										
10	30192		0.378										
Batch T-2, 4/26/01, 109 °C, 0 Gy/h, Air, RB-II-45C,RB-IV-75													
0	0		1.000		1.231	12			9.28				
1a	1674		0.994		1.248	15			6.89				
1b	1674		0.899		1.248								
2a	3359		0.951		1.248								
2b	3359		0.948		1.247				7.24				
3	4457		0.933		1.251				6.6				
3a	4792		0.951		1.252								
3b	4792		0.957		1.252				6.1				
4a	8727		0.414		1.258				6.02				
4b	8727		0.858		1.260								
5a	15951		0.270		1.269								
5b	15951		0.229		1.265				4.66				
6a	16268		0.238		1.269	14			4.59	soft			
6b	16268		0.191		1.325	~10000			2.910	hard			
6c	16268		0.064		1.310								
7a	19262		0.307		1.267								
7b	19262				1.270				4.79	soft			
8a	22096		0.000		1.524				2.31	medium			
8b	22096				1.555				0.407	hard			
9a	6024		0.936										

SANDIA CABLE SAMPLE REPOSITORY

Material- EPR-05- Okonite EPR Insulation													
Sample No.	Aging Time (h)	Est. Dose (kGy)	Average e/e_0	Average $TS_{/TS0}$	Average density (g/cc)	Outside surface modulus, MPa	Uptake factor	% gel	NMR T2,msec	Notes			
9b	6024		0.870										
10a	7894		0.841										
10b	7894		0.614										
11a	10901		0.348										
11b	10901		0.470										
12a	11974		0.241										
12b	11974		0.484										
12c	11974		0.290										
13	20477		0.368										
14	15144		0.496										
15	18624		0.301										
Batch T-3, 9/17/01, 124 °C, 0 Gy/h, Air, RB-II-77													
0	0		1.000		1.231	12							
1	2158		0.939		1.182	20							
2	3648		0.523		1.261								
3	4157		0.551		1.258								
4	4968		0.449		1.260	23							
5	5782		0.229		1.271								
6a	6000		0.116		1.267								
6b	6000		0.545		1.276	25							
7a	6312		0.299		1.267								
7b	6312		0.139		1.328								
8a	7320		0.377		1.269	35				soft			
8b	7320		0.116		1.374	~3000				hard			
9a	8088					25				soft			
9b	8088		0.000		1.322	~10000				hard			
10	8664		0.052		1.488								
Batch T-4, 4/26/01, 138 °C, 0 Gy/h, Air, RB-II-45A,RB-II-73													
0	0		1.000		1.231								

SANDIA CABLE SAMPLE REPOSITORY

Material- EPR-05- Okonite EPR Insulation													
Sample No.	Aging Time (h)	Est. Dose (kGy)	Average e/e_0	Average $TS_{/TS0}$	Average density (g/cc)	Outside surface modulus, MPa	Uptake factor	% gel	NMR T2,msec	Notes			
1	168		0.928		1.245	20							
2	334		0.890		1.248								
3	504		0.977		1.224								
4	672		0.977		1.249								
5	864		1.067		1.246								
6	953		0.990		1.263								
7	1082		0.875		1.256								
8	1337		0.910		1.267								
9	1342		0.328		1.277								
10	1579		0.316		1.259	22							
11	1430		0.762		1.275								
12a	1601		0.493		1.279								
12b	1601		0.562		1.262								
13	1673		0.786		1.269								
14	1762		0.235		1.334								
15	1913		0.316		1.267	25							
16	1985		0.577		1.278								
17a	2201		0.229		1.287	25				soft			
17b	2201		0.229		1.365	~3000				hard			
18a	2419		0.299		1.273	23				soft			
18b	2419		0.000		1.388	~10000				hard			
Batch TR-1, 2/24/2003, 40 °C, 430 Gy/h, Air, 5C in LICA													
	190	83	0.603		1.234								
	190	83	0.681		1.233								
	381	167	0.771										
	381	167	0.696										
	527	230	0.748		1.237								
	527	230	0.409		1.235								
	766	334	0.655		1.236								
	766	334	0.675		1.237								
	1054	459	0.699		1.237								

SANDIA CABLE SAMPLE REPOSITORY

Material- EPR-05- Okonite EPR Insulation													
Sample No.	Aging Time (h)	Est. Dose (kGy)	Average e/e_0	Average $TS_{/TS0}$	Average density (g/cc)	Outside surface modulus, MPa	Uptake factor	% gel	NMR T2,msec	Notes			
	1054	459	0.783		1.238								
	1510	657	0.707		1.236								
	1510	657	0.696		1.238								
	2013	873	0.681		1.239								
	2013	873	0.655		1.236								
	2446	1062	0.606		1.242								
	2446	1062	0.504		1.241								
	3355	1441	0.455		1.244								
	3355	1441	0.412		1.245								
	4603	1962	0.267		1.256								
	4603				1.257								
	5905	2490	0.174		1.271								
	5905				1.270								
	7056	2956	0.090		1.291								
	7056				1.290								
	8611		0.067		1.314								
	8611		0.035		1.315								
Batch TR-2, 2/24/2003, 80 °C, 445 Gy/h, Air , 5B in LICA													
	190	87	0.864										
	190	87	0.699										
	381	173	0.583										
	381	173	0.861										
	527	239	0.777										
	527	239	0.675										
	766	347	0.765										
	766	347	0.812										
	1054	477	0.823										
	1054	477	0.693										
	1510	682	0.733										
	1510	682	0.736										
	2014	907	0.501										
	2014	907	0.617										

SANDIA CABLE SAMPLE REPOSITORY

Material- EPR-05- Okonite EPR Insulation													
Sample No.	Aging Time (h)	Est. Dose (kGy)	Average e/e_0	Average $TS_{/TS0}$	Average density (g/cc)	Outside surface modulus, MPa	Uptake factor	% gel	NMR T2,msec	Notes			
	2446	1103	0.554										
	2446	1103	0.641										
	3355	1496	0.525										

SANDIA CABLE SAMPLE REPOSITORY

Material- ETFE-01- Teledyne Thermatic white insulation

Sample No.	Aging Time (h)	Est. Dose (kGy)	Average e/e_0	Average $TS_{/TS0}$	Average density (g/cc)	Outside surface modulus, MPa	Uptake factor	% gel	NMR T2,msec	Notes	
Batch TR-1, 1/6/1983, 70 °C, 5740 Gy/h, Air, CAQ-34,107											
1	2.0		0.84	0.99							
2	4.0		0.98	1.01							
3	5.5		0.94	0.97							
4	7.0		0.91	0.96							
5	16.5		0.75	0.82							
6	18.0		0.58	0.84							
7	21.5		0.50	0.78							
8	25.0		0.19	0.81							
9	54.0		dead	dead							
Batch TR-2, 5/13/1983, 70 °C, 840 Gy/h, Air, CAQ-115											
1	65.3		1.02	0.82							
2	95.0		0.89	0.75							
3	95.1		1.12	0.80							
4	101.5		0.77	0.78							
5	112.0		0.61	0.79							
6	118.0		0.54	0.78							
7	125.5		0.80	0.77							
8	142.0		0.66	0.78							
9	149.0		0.38	0.75							
10	168.0		0.17	0.71							
11	192.0		dead	dead							
Batch TR-3, 6/16/1982, 70 °C, 130 Gy/h, Air, CAQ-99											
1	120		1.03	0.97							
2	380		0.94	0.86							
3	506		1.00	0.94							
4	647		0.45	0.76							
5	691		0.35	0.74							
6	1127		dead	dead							
7	1630		dead	dead							

SANDIA CABLE SAMPLE REPOSITORY

Material- ETFE-01- Teledyne Thermatic white insulation

Sample No.	Aging Time (h)	Est. Dose (kGy)	Average e/e_0	Average $TS_{/TS0}$	Average density (g/cc)	Outside surface modulus, MPa	Uptake factor	% gel	NMR T2,msec	Notes	
Batch TR-4, 1/27/1983, 70 °C, 40 Gy/h, Air, CAQ-111											
1	600		1.03	0.95							
2	1464		0.98	0.85							
3	2880		dead	dead							
4	4340		dead	dead							
Batch TR-5, 6/15/1983, 25 °C, 830 Gy/h, Air, envelopes											
1	213		0.62	0.97							
2	237		0.32	0.72							
3	257		0.36	0.74							
Batch TR-5, 11/8/1983, 70 °C, 8000 Gy/h, Vacuum, CAQ-125											
1	20.8		0.85	0.93							
2	26.5		0.58	0.92							
3	40.4		0.58	0.95							
4	56.6		0.56	0.93							
5	72.0		0.41	0.95							
6	120.2		0.17	0.84							
7	122.8		0.17	0.90							
8	146.8		0.13	0.89							
9	170.8		0.10	0.88							

scraps 80.xls
ETFE-02

Material- ETFE-02- Teledyne red insulation (from Savannah River)											
Sample No.	Aging Time (h)	Est. Dose (kGy)	Average e/e_0	Average $TS_{/TS0}$	Average density (g/cc)	Outside surface modulus, MPa	Uptake factor	% gel	NMR T2,msec	Notes	
Batch T-1, 2/19/1979, 202 °C, 0 Gy/h, Air, KTG LB-II, 130											
1	0		1.00								
2	400		0.99			~500					
3	1024		1.01								
4	4176		0.66								
5	5930		0.59								
6	7202		0.35								
7	10060		0.27			~500					

SANDIA CABLE SAMPLE REPOSITORY

lameguard individual jacket (red & white paint on outside to distinguish 3 colors)												
Sample No.	Aging Time (h)	Est. Dose (kGy)	Average e/e_0	Average $TS_{/TS0}$	Average density (g/cc)	Outside surface modulus, MPa	Uptake factor	% gel	NMR T2,msec	Miscellaneous		
Batch T-1, 11/21/1978, 100.4 °C, 0 Gy/h, Air, LB-II-111										DLO unimportant		
1	0		1.000	1.000	1.642	8.14	4.92	54.2	10.90			
2	119		0.720				4.29	72.2				
3	287		0.654				4.00	30.7				
	287						7.06	45.9				
4	569		0.666	1.000	1.643	10.80	3.69	78.1	8.80			
5	1193		0.583	0.984	1.645	8.90	3.09	81.0	7.40			
6	2752		0.460	0.997	1.658	11.60	2.40	84.4	6.90			
7	4000		0.346	0.970	1.656	13.00	1.81	85.7	5.30			
8	5207		0.272	0.931	1.659	17.80	2.02	86.3	4.60			
9	7030		0.160	0.895	1.673	27.90	1.55	90.9	4.00			
	7030						1.61	90.1				
10	8180		0.018	1.410	1.746	288.00	1.75	94.0	1.80			
Batch T-2, 11/21/1978, 120 °C, 0 Gy/h, Air, LB-II-111										DLO unimportant		
1	143		0.641	0.955	1.640		3.38	73.9	8.44			
2	310		0.529	0.988	1.638	9.10	2.13	85.0	7.25			
3	694		0.324	0.934	1.647	13.40	1.99	83.9	5.48			
4	1006		0.181	0.885	1.659	27.10	1.51	89.8	4.11			
5	1318		0.087	0.920	1.682	67.40	1.32	91.6	3.32			
6	1586		0.051	1.160	1.720	116.00	1.36	93.0	3.10			

SANDIA CABLE SAMPLE REPOSITORY

lameguard individual jacket (red & white paint on outside to distinguish 3 colors)												
Sample No.	Aging Time (h)	Est. Dose (kGy)	Average e/e_0	Average $TS_{/TS0}$	Average density (g/cc)	Outside surface modulus, MPa	Uptake factor	% gel	NMR T2,msec	Miscellaneous		
Batch T-3, 09/25/1978, 130 °C, 0 Gy/h, Air, LB-II-102										DLO unimportant		
1	31		0.702	0.98			3.23	79.0	7.20			
2	99		0.659	0.96	1.644	10.20	3.41	76.3	7.70			
3	216		0.494	0.916	1.651	12.00	2.30	83.0	5.60			
4	335		0.356	0.91	1.658	15.10	2.14	84.4	5.00			
	335						2.75	77.7				
5	440		0.237	0.81	1.672	18.90	2.19	61.6	5.00			
	440						2.10	84.8				
6	605		0.102	0.84	1.693	55.40	1.52	90.6				
Batch T-4, 09/28/1978, 139.5 °C, 0 Gy/h, Air, LB-II-102										DLO unimportant		
1	16.5		0.725	0.954			3.00	80.7				
	16.5						6.23	74.8				
2	47.5		0.662	0.955	1.641	8.60	2.38	83.9	6.50			
3	112		0.481	0.882	1.649	16.10	2.00	85.5	6.30			
4	161		0.303	0.773	1.654	13.20	1.79	85.2	6.10			
5	214		0.204	0.780	1.660	24.50	1.68	87.4	4.60			
6	279		0.089	0.830	1.694	66.00	1.51	89.9	3.80			
7	281		0.125	0.817	1.697							
Batch T-5, 08/22/1978, 149.5 °C, 0 Gy/h, Air, LB-II-98										DLO unimportant		
1	15.8		0.804	0.970			3.28	77.6	6.74			
2	23.3		0.697	0.946		8.28	4.17	73.4				
3	40.1		0.590	0.880	1.641	8.50	2.63	81.4	6.15			
4	87.9		0.316	0.830	1.658	18.80	1.83	86.2				
5	160		0.071	0.860	1.713	112.00						
6	232		0.008	0.790	1.726		1.25	88.0	2.57			

scraps 80.xls
Hyp-01B

	A	B	C	D	E	F	G	H	I
1	Material-Hyp-01B- Anaconda Flameguard individual jacket (white print on black for 3 colors)								
2	Sample No.	Aging Time (h)	Est. Dose (kGy)	Average e/e_0	Average $TS_{/TS0}$	Outside surface modulus, MPa	Miscellaneous		
3	Batch TR-1, 04/26/1977, 22 °C, 13.7 Gy/h, air, NRL B-16								
4	1	2592		0.900					
5	2	7392		0.800					
6	3	17664		0.590					
7	4	22704		0.420					
8	5	26928		0.420					
9	6	31392		0.410					
10	7	40128		0.330					
11									
12	Batch TR-1 RH, 28241, 22 °C, 13.7 Gy/h, air + RH, NRL B-15								
13	1	2592		1.000					
14	2	7392		0.840					
15	3	22704		0.500					
16	4	26928		.45est					
17	5	31392		0.410					
18	6	35472		0.440					
19	7	40128		0.390					
20	8	45048		0.310					
21	9	53136		0.310					
22									
23	Batch TR-2, 04/26/1977, 22 °C, 90.6 Gy/h, air, NRL B-6								
24	1	672		0.960					
25	2	2592		0.700					
26	3	5520		0.510					
27	4	11064		0.310					
28	5	26928		0.090					
29									
30	Batch TR-2 RH, 28241, 22 °C, 90.6 Gy/h, air + RH, NRL B-2								
31	1	672		1.010					
32	2	2592		0.920					
33	3	5520		0.460					
34	4	11064		0.390					
35	5	17664		0.210					
36									
37	Batch TR-3, 04/26/1977, 24 °C, 490 Gy/h, air, NRL A-19								
38	1	144		0.990					
39	2	336		0.890					
40	3	672		0.650					
41	4	1344		0.440					
42	5	2688		0.220					
43									
44	Batch TR-3 RH, 28353, 24 °C, 490 Gy/h, air + RH, NRL A-17								
45	1	144		1.000					
46	2	336		0.880					
47	3	672		0.740					
48	4	1344		0.470					
49	5	2688		0.220					

scraps 80.xls
Hyp-01B

	A	B	C	D	E	F	G	H	I
50									
51	Batch TR-4, 08/15/1977, 30 °C, 2140 Gy/h, air, NRL A-5								
52	1	48		0.890					
53	2	96		0.820					
54	3	240		0.620					
55	4	433		0.390					
56	5	671		0.210					
57									
58	Batch TR-4 RH, 28352, 30 °C, 2140 Gy/h, air + RH, NRL A-4								
59	1	48		0.860					
60	2	96		0.820					
61	3	241		0.700					
62	4	434		0.390					
63	5	671		0.330					
64									
65	Batch TR-5, 05/03/1977, 38 °C, 9550 Gy/h, air, NRL A-1								
66	1	8		0.940					
67	2	24		0.830					
68	3	48		0.620					
69	4	80		0.400					
70	5	144		0.220					
71									
72	Batch TR-6, 07/09/1980, 35 °C, 3680 Gy/h, nitrogen, LHJ-60								
73	1	39		0.910					
74	2	111		0.660					
75	3	255		0.420					
76	4	303		0.320					
77	5	375		0.210					
78	6	543		0.140					
79	7	639		0.110					
80									
81	Batch TR-7, 09/06/1977, 100 °C, 2140 Gy/h, air, NRL A-6						DLO unimportant		
82	1	32		0.730		5.40	Unaged=4.7MPa		
83	2	71		0.760		7.60			
84	3	214		0.370		8.80			
85	4	406		0.190		37.20			
86	5	550		0.070		28.00			
87									
88	Batch TR-8 RH, 12/12/1977, 110 °C, 468 Gy/h, air + RH, NRL A-17								
89	1	78		0.700					
90	2	167		0.710					
91	3	360		0.450					
92	4	527		0.380					
93	5	671		0.221					
94									
95	Batch TR-9, 09/06/1977, 120 °C, 2180 Gy/h, air, NRL A-7								
96	1	32		0.730					
97	2	71		0.690					
98	3	214		0.180					
99	4	405		0.015					
100									

scraps 80.xls
Hyp-01B

	A	B	C	D	E	F	G	H	I
101	Batch TR-10, 09/12/1977, 140 °C, 2120 Gy/h, air, NRL A-2								
102	1	20		0.690					
103	2	31		0.680					
104	3	71		0.210					
105	4	142		0.014					
106									
107	Batch TR-10 RH, 09/12/1977, 140 °C, 2120 Gy/h, air + RH, NRL A-4								
108	1	22		0.850					
109	2	32		0.560					
110	3	72		0.260					
111	4	143		0.060					

SANDIA CABLE SAMPLE REPOSITORY

Sample No.	Aging Time (h)	Est. Dose (kGy)	Average e/e_0	Average $TS_{/TS0}$	Average density (g/cc)	Misc.
Batch T-1, 06/19/78, 91 °C, 0 Gy/h, air, LB-II-86						
1	0		1.000	1.000		
2	608		0.900	0.920		
3	1207		0.873	0.908		
4	1911		0.787	0.849		
5	5150		0.540	0.693		
6	8174		0.320	0.504		
7	10408		0.280	0.400		
8	12832		0.200	0.374		
9	15500		0.167	0.336		
10	17700		0.103	0.265		
11	21900		0.020			
Batch T-2, 11/21/78, 101 °C, 0 Gy/h, air, LB-II-110						
1	481		0.870			
2	737		0.817	0.882		
3	1896		0.423	0.567		
4	3208		0.310	0.418		
5	4600		0.263	0.350		
6	5752		0.187	0.320		
7	7024		0.060	0.268		
8	8133		0.017	0.252		
Batch T-3, 05/26/78, 111 °C, 0 Gy/h, air, LB-II-86						
1	95		0.933	0.933		
2	287		0.783	0.870		
3	720		0.523	0.485		
4	1140		0.433	0.421		
5	1408		0.363			
6	1810		0.383	0.390		
7	2313		0.220	0.353		
8	3345		0.086	0.253		
Batch T-4, 11/21/78, 120 °C, 0 Gy/h, air, LB-II-110						
1	7		0.963			
2	24		0.950			
3	49		0.904	0.838		
4	92		0.790	0.681		
5	143		0.653	0.546		
6	204		0.613	0.530		
7	383		0.488			
8	479		0.507	0.433		
9	743		0.354	0.398		
10	1006		0.167	0.322		
11	1318		0.050	0.284		
12	1656		0.017	0.235		

SANDIA CABLE SAMPLE REPOSITORY

Sample No.	Aging Time (h)	Est. Dose (kGy)	Average e/e_0	Average $TS_{/TS0}$	Average density (g/cc)	Misc.
Batch T-5, 09/27/78, 129.5 °C, 0 Gy/h, air, LB-II-101						
1	31		0.933	0.866		
2	99		0.633	0.520		
3	216		0.485	0.430		
4	335		0.350	0.415		
5	440		0.283	0.367		
6	606		0.140	0.310		
Batch T-6, 09/25/78, 140.9 °C, 0 Gy/h, air, LB-II-101						
1	17		0.917	0.958		
2	48		0.628	0.580		
3	112		0.479	0.493		
4	161		0.372	0.435		
5	214		0.262	0.403		
6	286		0.137	0.349		
Batch T-7, 08/21/78, 150 °C, 0 Gy/h, air, LB-II-97						
1	16		0.763	0.644		
2	23		0.735	0.597		
3	40		0.617	0.525		
4	88		0.320	0.429		
5	160		0.098	0.301		
6	232		0.023	0.315		
Batch T-8, 04/23/79, 160.7 °C, 0 Gy/h, air, LHJ-7						
1	4		0.853	0.739		
2	8		0.777			
3	16		0.640	0.597		
4	24		0.567			
5	40		0.455			
6	55		0.256	0.362		
7	80		0.150	0.311		
8	96		0.087	0.271		
Batch TR-1, 04/26/77, 22 °C, 12 Gy/h, air, NRL B-16						
1	2592	50	0.980			
2	7392	138	0.920			
3	17664	305	0.790			
4	22704	380	0.640			
5	26928	433	0.640			
6	31392	481	0.600			
7	40128	567	0.530			
8	53136	674	0.410			
Batch TR-1 RH, 04/26/77, 22 °C, 12 Gy/h, air + RH, NRL B-15						
1	2592	42	0.960			
2	7392	117	0.960			
3	22704	324	0.750			
4	26928	369	0.740			
5	31392	417	0.700			

SANDIA CABLE SAMPLE REPOSITORY

Sample No.	Aging Time (h)	Est. Dose (kGy)	Average e/e_0	Average $TS_{/TS0}$	Average density (g/cc)	Misc.
6	35472	458	0.620			
7	40128	503	0.610			
8	45048	546	0.550			
9	53136	610	0.530			
Batch TR-2, 04/26/77, 22 °C, 88 Gy/h, air, NRL B-6						
1	672	67	1.010			
2	2592	254	0.820			
3	5520	530	0.720			
4	11064	1025	0.500			
5	26928	2220	0.170			
Batch TR-2 RH, 04/26/77, 22 °C, 88 Gy/h, air + RH, NRL B-2						
1	672	67	0.980			
2	2592	254	0.840			
3	5520	530	0.750			
4	11064	1025	0.520			
5	17664	1560	0.340			
Batch TR-3, 08/16/77, 24 °C, 490 Gy/h, air, NRL A-19						
1	144	733	0.950			
2	336	171	0.970			
3	672	340	0.730			
4	1344	679	0.640			
5	2688	1342	0.290			
Batch TR-3 RH, 08/16/77, 24 °C, 490 Gy/h, air + RH, NRL A-17						
1	144	70	0.990			
2	336	164	0.940			
3	672	326	0.790			
4	1344	650	0.660			
5	2688	1285	0.330			
Batch TR-4, 08/15/77, 30 °C, 2100 Gy/h, air, NRL A-5						
1	48	100	0.920			
2	96	201	0.820			
3	240	504	0.710			
4	433	906	0.480			
5	671	1403	0.300			
Batch TR-4 RH, 08/15/77, 30 °C, 2100 Gy/h, air + RH, NRL A-4						
1	48	101	0.940			
2	96	203	0.760			
3	240	508	0.690			
4	433	916	0.490			
5	671	1417	0.340			
Batch TR-5 RH, 05/03/77, 38 °C, 9550 Gy/h, air + RH, NRL A-1						
1	8	90	0.960			
2	24	271	0.820			

SANDIA CABLE SAMPLE REPOSITORY

Sample No.	Aging Time (h)	Est. Dose (kGy)	Average e/e_0	Average $TS_{/TS0}$	Average density (g/cc)	Misc.
3	48	538	0.680			
4	80	897	0.510			
5	143	1620	0.320			
Batch TR-6, 04/21/80, 64 °C, 308 Gy/h, air, LHJ-44						
1	504		0.890			
2	1200		0.580			
3	1902		0.490			
4	2520		0.310			
5	3216		0.180			
6	3696		0.155			
7	4470		0.124			
Batch TR-7, 11/13/78, 73 °C, 1810 Gy/h, air, LB-II-116						
1	96		0.895			
2	263		0.717			
3	431		0.513			
4	551		0.435			
5	671		0.322			
Batch TR-8, 12/22/78, 78 °C, 368 Gy/h, air, LB-II-120						
1	263		0.870			
2	671		0.650			
3	1150		0.480			
4	1413		0.390			
5	1750		0.270			
6	1919		0.210			
Batch TR-9, 04/22/80, 78.1 °C, 3750 Gy/h, air, LHJ-43						
1	47		0.870			
2	145		0.620			
3	216		0.500			
4	311		0.290			
5	408		0.180			
6	507		0.150			
7	578		0.090			
Batch TR-10, 02/12/79, 79 °C, 874 Gy/h, air, LB-II-127						
1	167		0.910			
2	431		0.600			
3	553		0.500			
Batch TR-11, 04/21/80, 82 °C, 188 Gy/h, air, LHJ-44						
1	336		0.880			
2	865		0.710			
3	1270		0.570			
4	1902		0.380			
5	2520		0.260			
6	3216		0.140			
7	3696		0.100			

SANDIA CABLE SAMPLE REPOSITORY

Sample No.	Aging Time (h)	Est. Dose (kGy)	Average e/e_0	Average $TS_{/TS0}$	Average density (g/cc)	Misc.
Batch TR-12, 12/22/78, 92 °C, 234 Gy/h, air, LB-II-120						
1	263		0.870			
2	503		0.750			
3	933		0.510			
4	1150		0.400			
5	1751		0.200			
6	1920		0.160			
Batch TR-13, 04/21/80, 96 °C, 92 Gy/h, air, LHJ-45						
1	239		0.890			
2	671		0.710			
3	1200		0.450			
4	1515		0.340			
5	1901		0.250			
6	2520		0.170			
7	3216		0.090			
Batch TR-14, 01/31/79, 97 °C, 365 Gy/h, air, LB-II-128						
1	119		0.910			
2	333		0.740			
3	549		0.500			
4	790		0.310			
5	959		0.210			
Batch TR-15, 07/16/79, 97.1 °C, 830 Gy/h, air, LHJ-16						
1	96		0.910			
2	239		0.730			
3	360		0.540			
4	505		0.400			
5	670		0.250			
6	888		0.140			
7	939		0.130			
Batch TR-16, 09/06/77, 100 °C, 2140 Gy/h, air, NRL A-6						
1	31	71	0.977			
2	71	161	0.880			
3	214	486	0.380			
4	405	921	0.160			
5	549	1248	0.087			
Batch TR-17, 04/21/80, 104 °C, 9790 Gy/h, air, LHJ-43						
11	16		0.870			
2	40		0.630			
3	63		0.450			
4	89		0.330			
5	120		0.230			
6	146		0.170			
7	168		0.130			

SANDIA CABLE SAMPLE REPOSITORY

Sample No.	Aging Time (h)	Est. Dose (kGy)	Average e/e_0	Average $TS_{/TS0}$	Average density (g/cc)	Misc.
Batch TR-18 RH, 12/12/77, 110 °C, 470 Gy/h, air + RH, NRL A-17						
1	78		0.850			
2	167		0.670			
3	360		0.420			
4	527		0.280			
5	671		0.210			
Batch TR-19, 01/31/79, 118 °C, 880 Gy/h, air, LB-II-126						
1	26		1.020			
2	73		0.737			
3	145		0.487			
4	216		0.385			
5	338		0.241			
6	504		0.127			
7	673		0.070			
Batch TR-20, 09/06/77, 120 °C, 2180 Gy/h, air, NRL A-7						
1	32		0.860			
2	72		0.600			
3	214		20.000			
Batch TR-21, 01/30/79, 125 °C, 340 Gy/h, air, LB-II-128						
1	19		0.980			
2	67		0.710			
3	139		0.540			
4	210		0.440			
5	378		0.240			
6	569		0.080			
7	810		0.030			
Batch TR-22, 03/12/79, 132 °C, 1800 Gy/h, air, LB-II-143						
1	8		1.030			
2	24		0.860			
3	47		0.630			
4	103		0.400			
5	166		0.230			
6	238		0.110			
Batch TR-23 RH, 11/13/78, 133 °C, 8900 Gy/h, air + RH, LB-II-116						
1	8		0.950			
2	18		0.710			
3	25		0.590			
4	41		0.390			
5	55		0.310			
6	71		0.210			
Batch TR-24, 01/29/79, 137 °C, 880 Gy/h, air, LB-II-126						
1	7		1.000			
2	30		0.770			
3	55		0.590			

SANDIA CABLE SAMPLE REPOSITORY

Sample No.	Aging Time (h)	Est. Dose (kGy)	Average e/e_0	Average $TS_{/TS0}$	Average density (g/cc)	Misc.
4	96		0.470			
5	169		0.230			
6	216		0.150			
7	272		0.090			
Batch TR-25, 09/12/77, 140 °C, 2120 Gy/h, air, NRL A-2						
1	20		0.580			
2	31		0.540			
3	71		0.370			
4	142		0.130			
Batch TR-25 RH, 09/12/77, 140 °C, 2120 Gy/h, air + RH, NRL A-4						
1	22		0.630			
2	31		0.550			
3	71		0.400			
4	143		0.170			

SANDIA CABLE SAMPLE REPOSITORY

Sample No.	Aging Time (d)	Est. Dose (kGy)	Average e/e_0	Average $TS_{/TS0}$	Average density (g/cc)	Outside surface modulus, MPa	Uptake factor	% gel	NMR T2,msec	Miscellaneous	
Material Hyp-03 Samuel Moore Dekoron Jacket											
Batch T-1, 06/23/97, 100 °C, 0 Gy/h, air, SMHY-ten.dat										DLO unimportant	
1	0		1.000		1.461	14	3.65	78.20	12.99		
2	28		0.777		1.463		2.23	82.10	5.95		
3	59		0.738		1.460		2.17	82.70	5.96		
4	91		0.554		1.464	20	2.75	78.90	4.49		
5	128		0.583		1.468						
6	170		0.451		1.468		2.74	79.40			
7	210		0.383		1.475	22	1.89	84.80			
8	280		0.252		1.490		2.39	80.20	3.21		
9	302		0.197		1.494	37	1.63	88.80	3.33		
10	360		0.134		1.500	47	1.61	88.40	2.94		
11	421		0.076		1.508	88	1.40	90.70	1.91		
12	501		0.026		1.519	270	1.38	89.60	1.94		
Batch T-2, 06/23/97, 110 °C, 0 Gy/h, air, SMHY-ten.dat										DLO unimportant	
1	0		1.000		1.461	14	3.65	78.20	12.99		
2	14		0.787		1.473		3.32	82.36	12.7		
3	28		0.759		1.476		2.71	83.37	5.33		
4	49		0.606		1.492	30	3.38	82.47	5.49		
5	71		0.438		1.493		3.29	80.48	3.86		
6	102		0.325		1.493	31	2.33	80.70			
7	140		0.157		1.511	37	1.73	89.42	1.91		
8	171		0.071		1.523	68	1.62	90.97	1.88		
9	204		0.029		1.530	135	1.35	91.20	1.32		
10	234		0.000		1.548	200	1.25	89.22	1.277		
Batch T-3, 06/23/97, 125 °C, 0 Gy/h, air, SMHY-ten.dat										DLO unimportant	
1	0		1.000		1.461	14	3.65	78.20	12.99		
2	3		0.861		1.460		2.50	80.18			
3	8		0.727		1.473	18.3	2.71	82.15	8.78		
4	21		0.457		1.474		2.56	82.99			
5	14		0.651		1.463	17.6	2.59	76.57	6.02		
6	28		0.341		1.480	25	2.25	83.60	3.5		
7	40		0.184		1.505	42	1.62	90.54	2.21		
8	49		0.097		1.516	61	1.49	91.21	1.78		
9	63		0.070		1.509	86	1.54	89.63	2.36		
10	70		0.055		1.518	170	1.40	90.53	2.39		

SANDIA CABLE SAMPLE REPOSITORY

Sample No.	Aging Time (d)	Est. Dose (kGy)	Average e/e_0	Average $TS_{/TS0}$	Average density (g/cc)	Outside surface modulus, MPa	Uptake factor	% gel	NMR T2,msec	Miscellaneous	
Batch TR-1, 05/05/97, 60 °C, 131 Gy/h, air, II-Bat60C.xls										DLO unimportant	
1	0		1.000			14	3.65	78.20			
2	29		0.874				2.53	82.90			
3	57		0.656				2.11	85.90			
4	106		0.496			15	1.96	88.90			
5	151		0.398				1.75	90.50			
6	220		0.248				1.70	92.60			
7	260		0.129			43	1.53	93.10			
8	303		0.092			190	1.39	94.20			
9	371		0.018				1.26	93.70			
10	415		0.013			270	1.30	94.40			
11	515		0.010			200	1.20	93.70			
Batch TR-2, 05/05/97, 80 °C, 51 Gy/h, air, I-Bat80C.xls										DLO unimportant	
1	0		1.000			14					
2	29		0.835								
3	57		0.761								
4	106		0.554			16					
5	151		0.423								
6	200		0.343								
7	249		0.244			19.5					
8	303		0.238								
9	378		0.113			29.5					
10	464		0.060			45					
11	556		0.068			66					
Batch TR-3, 05/05/97, 90 °C, 940 Gy/h, air, IV-Bat90C.xls										DLO unimportant	
1	0		1.000			14	3.65	78.20			
2	3		0.796				2.33	83.34			
3	7		0.743				2.23	84.85			
4	14		0.438			17	1.84	88.10			
5	22		0.291			21	1.63	91.11			
6	29		0.157			28	1.65	92.49			
7	37		0.092			90	1.42	92.91			
8	45		0.047			76	1.34	92.64			
9	52		0.018			110					
Batch TR-4, 05/05/97, 100 °C, 51 Gy/h, air, I-Cat100C.xls										DLO unimportant	
1	0		1.000			14					
2	14		0.859								
3	29		0.774			22					
4	42		0.611								
5	63		0.420			25					
6	85		0.258								
7	113		0.157			32					
8	141		0.144			42					
9	161		0.066			68					

SANDIA CABLE SAMPLE REPOSITORY

Material Hyp-04 Anaconda Flameguard Jacket										
Sample No.	Aging Time (d)	Est. Dose (kGy)	Average e/e_0	Average $TS_{/TS0}$	Average density (g/cc)	Outside surface modulus, MPa	Uptake factor	% gel	NMR T2,msec	Miscellaneous
Batch T-1, 06/23/97, 100 °C, 0 Gy/h, air, AnFl-ten.dat										
1	0		1.000		1.578	4.8	2.334	83.30	5.53	
2	28		0.943		1.596		1.794	84.80	9.85	
3	59		0.779		1.5883		2.029	85.58	9.89	
4	91		0.665		1.596	7.6	2.147	83.70	7.43	
5	128		0.532		1.5966		2.491	80.76	7.68	
6	170		0.536		1.5969		2.101	83.80	6.46	
7	210		0.437		1.6103	12	1.959	86.63	5.6	
8	280		0.335		1.6173		2.467	79.40	7.05	
9	302		0.312		1.6184	10.2	1.667	88.14	5.32	
10	360		0.179		1.6315	11	1.686	89.30	5.81	
11	421		0.118		1.6749	40	1.531	91.81	3.84	
12	501		0.034			140	1.309	94.50	2.31	
Batch T-2, 06/23/97, 110 °C, 0 Gy/h, air, AnFl-ten.dat										
1	0		1.000		1.578	4.8	2.334	83.30	5.53	
2	14		0.867		1.6006		1.995	85.25	9.97	
3	28		0.768		1.6026		2.070	85.82	6.65	
4	49		0.593		1.615	6.6	2.425	82.99	7.33	
5	71		0.468		1.617		1.934	86.79	6.36	
6	102		0.319		1.635	7	1.908	86.94	4.36	
7	140		0.160		1.6534	27	1.607	91.44	3.62	
8	171		0.053		1.685	66	1.412	93.50	2.666	
9	204		0.030		1.6847	66	1.301	96.30	3.045	
10	234		0.000		1.705	360	1.248	96.34	1.54	
Batch T-3, 06/23/97, 125 °C, 0 Gy/h, air, AnFl-ten.dat										
1	0		1.000		1.578	4.8	2.334	83.30	5.53	
2	3		0.859		1.5883		2.055	84.23	9.62	
3	8		0.738		1.5981	4.4	2.167	85.19	6.6	
4	14		0.532		1.6076	5.8	2.190	84.78	5.3	
5	21		0.479		1.611	6	2.328	81.73	6.57	
6	28		0.365		1.6237	14	1.778	88.23	7.3	
7	40		0.156		1.6643	19	1.653	89.93	3.52	
8	49		0.099		1.661	28	1.448	91.50	3.76	
9	63		0.046			90	1.338	94.55		
10	70									
Batch TR-1, 05/05/97, 60 °C, 165 Gy/h, air, II-Bat60C.xls										
1	0		1.000			4.8	2.334	83.30		
2	29		0.904				2.217	83.90		
3	57		0.650				2.080	85.20		
4	106		0.544			6.4	1.920	87.00		
5	151		0.335				1.834	88.50		
6	220		0.200				1.600	91.60		
7	260		0.148			35	1.530	94.00		

SANDIA CABLE SAMPLE REPOSITORY

Material Hyp-04 Anaconda Flameguard Jacket										
Sample No.	Aging Time (d)	Est. Dose (kGy)	Average e/e_0	Average $TS_{/TS0}$	Average density (g/cc)	Outside surface modulus, MPa	Uptake factor	% gel	NMR T2,msec	Miscellaneous
8	303		0.148			45	1.575	94.10		
9	371		0.068				1.414	96.10		
10	415		0.034			280	1.424	96.00		
11	515		0.000			400	1.240	98.90		
Batch TR-2, 05/05/97, 80 °C, 59 Gy/h, air, I-Bat80C.xls										
1	0		1.000			4.8				
2	29		0.904							
3	57		0.806							
4	106		0.677			6.8				
5	151		0.548							
6	200		0.390							
7	249		0.331			17				
8	303		0.238							
9	378		0.125			19				
10	464		0.171			50				
11	556		0.076			125				
Batch TR-3, 05/05/97, 90 °C, 940 Gy/h, air, IV-Bat90C.xls										
1	0		1.000			4.8	2.334	83.30		
2	3		0.814			5.6	2.320	84.00		
3	7		0.703			13	2.313	83.50		
4	14		0.555			7.4	1.990	86.20		
5	22		0.357			12	1.820	88.60		
6	29		0.255			20	1.670	90.50		
7	37		0.186			30	1.610	92.10		
8	45		0.125			98	1.456	94.00		
9	52		0.080			103				
Batch TR-4, 05/05/97, 100 °C, 59 Gy/h, air, I-Cat100C.xls										
1	0		1.000			4.8				
2	14		0.868							
3	29		0.665			6.1				
4	42		0.568							
5	63		0.475			6.3				
6	85		0.370							
7	113		0.232			13				
8	141		0.103			27				
9	161		0.049			68				

SANDIA CABLE SAMPLE REPOSITORY

Sample No.	Aging Time (d)	Est. Dose (kGy)	Average e/e_0	Average $TS_{/TS0}$	Average density (g/cc)	Outside surface modulus, MPa	Uptake factor	% gel	NMR T2,msec	Miscellaneous	
Material	Hyp-05	Rockbestos	Firewall III								
Batch T-1, 06/23/97, 100 °C, 0 Gy/h, air, RBHY-ten.dat										DLO unimpiortant	
1	0		1		1.5951	4.05	2.27	81.4	12.87		
2	28		0.8956044		1.616		2.23	82.4	11.9		
3	59		0.8379121		1.6175	6.35			11.95		
4	91		0.7582418		1.6312		2.124	83.2	11.09		
5	128		0.5576923		1.637	7.5			10.42		
6	170		0.489011		1.6435				7.98		
7	210		0.4258242		1.6455	10	1.88	85.7	9.344		
8	280		0.3736264								
9	302		0.3461539		1.6552	13.2	1.894	86.3	8.48		
10	360		0.1923077		1.674		1.74	87	7.833		
11	421		0.1428571		1.6893	17.5	1.78	89.2	4.798		
12	501		0.08241758		1.707	45	1.417	93	4.09		
Batch T-2, 06/23/97, 110 °C, 0 Gy/h, air, RBHY-ten.dat										DLO unimportant	
1	0		1		1.5951	4.05	2.270	81.400	12.87		
2	14		0.8653846		1.634		1.930	85.900			
3	28		0.7802198		1.6444	7.2	1.830	87.400	8.6		
4	49		0.6071429		1.654	8.6	1.730	86.200	8.8		
5	71		0.5082418		1.6519	13	1.900	85.800	8.36		
6	102		0.3571429		1.6896	14.9	1.700	89.800	6.82		
7	140		0.2362637		1.694	25.6	1.610	90.600			
8	171		0.1401099		1.709	30.5	1.410	94.100	4.3		
9	204		0.04945055		1.7152	84.6	1.330	93.500	2.38		
10	234		0.01648352		1.759	620	1.160	94.300	1.55		
Batch T-3, 06/23/97, 125 °C, 0 Gy/h, air, RBHY-ten.dat										DLO minor	
1	0		1		1.5951	4.05	2.060	80.200	12.87		
2	3		0.9752747		1.6117		1.971	82.400	10.47		
3	8		0.8489011		1.628	5.4	1.894	82.900	10.01		
4	14		0.6483517		1.635	8	1.919	82.800			
5	21		0.543956		1.652	7.8	1.960	83.900	9.38		

SANDIA CABLE SAMPLE REPOSITORY

Sample No.	Aging Time (d)	Est. Dose (kGy)	Average e/e_0	Average $TS_{/TS0}$	Average density (g/cc)	Outside surface modulus, MPa	Uptake factor	% gel	NMR T2,msec	Miscellaneous	
6	28		0.4450549		1.6522	14.7	2.290	80.500			
7	49		0.1675824		1.698	26.1	1.672	88.500	4.67		
8	63		0.07967033		1.704	99	1.473	90.300	3.07		
9	70		0.01923077		1.71	312	1.333	88.200	2.53		
Batch TR-1, 05/05/97, 60 °C, 184 Gy/h, air, II-Bat60C.xls											
1	0		1			4.05	2.060	80.200			
2	29		1.03				2.320	81.800			
3	57		0.942				2.150	82.500			
4	106		0.7252747			6.5	1.830	85.600			
5	151		0.47				1.790	86.100			
6	220		0.209				1.530	86.900			
7	260		0.1428571			37	1.660	89.600			
8	303		0.09615385			78	1.420	90.800			
9	371		0.063				1.430	92.300			
10	415		0.03021978			430	1.324	91.500			
11	515		0.008241759			500					
Batch TR-2, 05/05/97, 80 °C, 62 Gy/h, air, I-Bat80C.xls											
1	0		1			4.05					
2	29		1.08								
3	57		0.938								
4	106		0.8571429			7					
5	151		0.696								
6	200		0.493								
7	249		0.3653846			10.5					
8	303		0.284								
9	378		0.1648352			23					
10	464		0.0989011			76					
11	556		0.04120879			460					
Batch TR-3, 05/05/97, 90 °C, 940 Gy/h, air, IV-Bat90C.xls											
1	0		1			4.05	2.060	80.200			
2	3		1.049451			4.9					
3	7		0.9587912			5	2.050	82.600			

SANDIA CABLE SAMPLE REPOSITORY

Sample No.	Aging Time (d)	Est. Dose (kGy)	Average e/e_0	Average $TS_{/TS0}$	Average density (g/cc)	Outside surface modulus, MPa	Uptake factor	% gel	NMR T2,msec	Miscellaneous	
4	14		0.728022			6.3	2.150	83.500			
5	22		0.5274726			8.8	1.740	87.000			
6	29		0.271978			12	1.790	88.400			
7	37		0.1868132			28	1.550	90.700			
8	45		0.1126374			35	1.540	91.600			
9	52		0.06593407			62					
Batch TR-4, 05/05/97, 100 °C, 64 Gy/h, air, I-Cat100C.xls											
1	0		1			4.05					
2	14		0.923								
3	29		0.7664835			6.9					
4	42		0.63								
5	63		0.4697802			8.4					
6	85		0.458								
7	113		0.2857143			14.5					
8	141		0.1236264			32					
9	161		0.1181319			40					

SANDIA CABLE SAMPLE REPOSITORY

Sample No.	Aging Time (d)	Est. Dose (kGy)	Average e/e_0	Average $TS_{/TS0}$	Average density (g/cc)	Outside surface modulus, MPa	Uptake factor	% gel	NMR T2,msec	Miscellaneous		
Material	Hyp-06	Eaton Dekoron Elastoset										
Batch T-1, 06/23/97, 100 °C, 0 Gy/h, air, Dek-ten.dat												
1	0		1.000		1.4666	18	3.490	77.700	9.44	DLO unimportant		
2	28		0.880		1.4647		2.180	82.900	6.03			
3	59		0.652		1.4781	9.6	2.040	83.500	5.61			
4	91		0.699		1.4791		2.450	82.100	3.84			
5	128		0.532		1.4766	9.6	2.190	83.600	4.01			
6	170		0.411		1.4953		2.330	81.900	3.23			
7	210		0.304		1.4979	16	1.890	87.200	2.2			
8	280		0.184		1.5016		1.670	88.200	2.15			
9	302		0.155		1.5063	45	1.630	89.000	2.03			
10	360		0.057		1.5153	100	1.490	90.000				
11	421		0.000		1.5408	400	1.330	88.200	2.09			
12	501		0.000						1.69			
Batch T-2, 06/23/97, 110 °C, 0 Gy/h, air, Dek-ten.dat												
1	0		1.000		1.4666	18	3.490	77.700	9.440	DLO unimportant		
2	14		0.804		1.4809		2.210	83.800				
3	28		0.718		1.4874	15	2.470	81.900	3.96			
4	49		0.541		1.4931	15	2.030	84.400	4.47			
5	71		0.342		1.4986	15	2.010	84.800	4.16			
6	102		0.209		1.5099	28	1.660	89.300	2.53			
7	140		0.066		1.5327	130	1.460	89.700	3.2			
8	171		0.003		1.5474	380	1.270	87.100	2.11			
9	204		0.000				1.220	89.200	1.88			
10	234		0.000						1.84			

SANDIA CABLE SAMPLE REPOSITORY

Sample No.	Aging Time (d)	Est. Dose (kGy)	Average e/e_0	Average $TS_{/TS0}$	Average density (g/cc)	Outside surface modulus, MPa	Uptake factor	% gel	NMR T2,msec	Miscellaneous		
Batch T-3, 06/23/97, 125 °C, 0 Gy/h, air, Dek-ten.dat										minor DLO		
1	0		1.000		1.4666	18	3.490	77.700	9.440			
2	3		0.870		1.4728		2.320	81.100	5.18			
3	8		0.706		1.482	16	2.370	79.600	6.14			
4	14		0.487		1.4894	22	2.330	82.800	5.57			
5	21		0.272		1.497	18.5	2.050	85.200	4.86			
6	28		0.231		1.5085	32	1.790	87.800	3.79			
7	40		0.032		1.522	270	1.370	88.000	1.11			
8	49		0.013		1.527	510	1.300	89.000	1.38			
9	63		0.000		1.544	1800	1.230	90.000	1.16			
10	70		0.000									
Batch TR-1, 05/05/97, 60 °C, 143 Gy/h, air, II-Bat60C.xls										DLO unimportant		
1	0		1.000			18	3.490	77.700				
2	29		0.986				2.414	81.600				
3	57		0.855				2.440	84.700				
4	106		0.585			14	1.870	89.300				
5	151		0.448				1.720	90.700				
6	220		0.211				1.515	92.100				
7	260		0.117			43	1.435	94.100				
8	303		0.079			52	1.385	94.200				
9	371		0.032				1.306	95.000				
10	415		0.047			125	1.233	93.900				
11	515		0.028			135	1.200	91.800				
Batch TR-2, 05/05/97, 80 °C, 55 Gy/h, air, I-Bat80C.xls										DLO unimportant		
1	0		1.000			18						
2	29		0.876									
3	57		0.832									
4	106		0.671			16.5						
5	151		0.507									
6	200		0.350									
7	249		0.304			17						
8	303		0.246									
9	378		0.152			31						
10	464		0.136			47						
11	556		0.041			72						

SANDIA CABLE SAMPLE REPOSITORY

Sample No.	Aging Time (d)	Est. Dose (kGy)	Average e/e_0	Average $TS_{/TS0}$	Average density (g/cc)	Outside surface modulus, MPa	Uptake factor	% gel	NMR T2,msec	Miscellaneous		
Batch TR-3, 05/05/97, 90 °C, 940 Gy/h, air, IV-Bat90C.xls										minor DLO		
1	0		1.000			18	3.490	77.700				
2	3		0.998				2.620	80.800				
3	7		0.880				2.190	83.100				
4	14		0.575				1.900	87.500				
5	22		0.392			17	1.752	90.000				
6	29		0.250			28	1.510	91.800				
7	37		0.161			50	1.524	92.900				
8	45		0.098			56	1.408	92.300				
9	52		0.038			80						
Batch TR-4, 05/05/97, 100 °C, 56 Gy/h, air, I-Cat100C.xls										DLO unimportant		
1	0		1.000			18						
2	14		0.842									
3	29		0.763			17						
4	42		0.633									
5	63		0.402			23						
6	85		0.254									
7	113		0.196			40						
8	141		0.076			60						
9	161		0.028			170						

scraps 80.xls
Hyp-07

	A	B	C	D	E	F	G	H	I	J	K
1	Material HYP-07-Brandrex Hypalon Jacket										
2	Sample No.	Aging Time (d)	Est. Dose (kGy)	Average e/e_0	Average $TS_{/TS0}$	Average density (g/cc)	Outside surface modulus, MPa	Uptake factor	% gel	NMR T2,msec	Miscellaneous
3	Batch T-1, 4/16/01, 99 °C, 0 Gy/h, air, RB-II-33C										DLO unimportant
4		0.0		1.000		1.376	5.2	2.690	71.6	16.45	inside of jacket has "channels" from
5		79.8		1.074		1.389	9.3				fill material- tensile failure often occurs
6		92.7		1.132							at these channels-could imply that inside
7		112.8		0.758		1.388					modulus determines tensile failure
8		143.0		0.716							
9		182.7		0.750							
10		217.7		0.584							
11		245.0		0.618		1.406	13				
12		357.0		0.737		1.416	18				
13		484.0		0.550		1.417					
14		602.0		0.529		1.420					
15		924.0		0.132		1.411	60				
16											
17	Batch T-2, 1/22/02, 99 °C, 0 Gy/h, air, RB-III-25										
18		203.2		0.726							
19		302.0		0.679							
20		405.0		0.703							
21		631.0		0.511			17				
22		730.0		0.305							
23		808.0		0.168							
24		876.0		0.089							
25		1007.0		0.005							
26											
27	Batch T-3, 9/10/02, 99 °C, 0 Gy/h, air, RB-IV-77										
28		301.0		0.634							
29		499.0		0.432							
30		651.0		0.147							
31		818.0		0.068							
32											
33	Batch T-4, 4/16/01, 109 °C, 0 Gy/h, air, RB-II-33B										DLO unimportant
34		38.7		0.879						9.31	
35		79.8		0.601				2.670	74.3	12.22	
36		84.7		0.511			18			14.99	
37		104.9		0.635				4.080	63.7	15.94	
38		132.9		0.555				3.970	67.9	7.2	
39		161.0		0.639			24.6	3.400	68.7		soft sample
40		161.0		0.079			182	1.376	91.2	0.92	hard sample
41		163.0		0.366			21	2.020	82.1		soft sample
42		163.0		0.039			270	1.314	92.1	0.87	hard sample
43		164.7		0.487						1.3	
44		171.0		0.458			24.5	2.140	80.8	11.64	soft sample
45		171.0		0.053			154	1.513	91.1		hard sample
46											
47											

scraps 80.xls
Hyp-07

	A	B	C	D	E	F	G	H	I	J	K
48											
49											
50	Batch T-5, 10/05/01, 124 °C, 0 Gy/h, air, RB-II-83										DLO minor
51		5.0		0.976							
52		10.2		0.829							
53		13.6		0.908							
54		18.9		0.718							
55		24.0		0.850							
56		30.9		0.803							
57		61.9		0.347							
58		73.2		0.247							
59		89.2		0.118							
60											
61	Batch T-6, 12/10/01, 124 °C, 0 Gy/h, air, RB-III-17										
62		25.0		0.755			10.6	2.420	76.0		
63		31.0		0.692			14	2.190	77.4		
64		38.0		0.637			14.9	2.350	77.6		
65		46.0		0.474			20	2.330	78.4		
66		56.0		0.053			77.8	1.580	87.4		
67		67.0		0.021			172	1.400	92.0		
68		73.0		0.000			450	1.460	92.5		
69											
70	Batch T-7, 4/16/01, 138 °C, 0 Gy/h, air, RB-II-33A										DLO minr
71		4.0		0.765			15.000	2.260	78.5		
72		8.9		0.582			20	2.070	77.3		
73		13.8		0.356			58	1.804	81.8		inside mod=33MPa
74		17.7		0.215			150	1.940	81.3		inside mod=28MPa
75		22.7		0.068			230	1.910	80.5		inside mod=150MPa
76		27.7		0.021				1.380	92.3		
77		28.7		0.000				1.250	96.3		
78											
79											
80	Batch T-8, , 125 °C, 0 Gy/h, air, GMM-envelopes										
81		3.0		0.797							
82		8.0		0.850							
83		14.0		0.668							
84		21.0		0.771							
85		28.0		0.616							
86		63.0		0.582							
87		75.0		0.571							soft sample
88		75.0		0.426							soft sample
89		75.0		0.050							hard sample
90		91.0		0.000							hard sample
91											

scraps 80.xls
Hyp-08

Material HYP-08-BIW Hypalon Jacket										
Sample No.	Aging Time (d)	Est. Dose (kGy)	Average e/e_0	Average $TS_{/TS0}$	Average density (g/cc)	Outside surface modulus, MPa	Uptake factor	% gel	NMR T2,msec	Miscellaneous
Batch T-1, 6/07/01, 80 °C, 0 Gy/h, air, RB-II-47										
	0.00		1.000		1.477	8.8	2.45	71.60	10.630	
	40.97		1.096							
	71.01		1.108							
	180.23		0.719							
	305.09		0.572							
	363.23		0.662							
	403.93		0.512							
	480.94		0.590							
	622.91		0.420							
	651.14		0.470							
	800.96		0.529							
	957.90		0.466							
	1245.00		0.342							
	1405.00		0.342							
Batch T-2, 4/16/01, 99 °C, 0 Gy/h, air, RB-II-35C										DLO unimportant
	20.96		0.948		1.481		2.51	72.20		
	41.92		0.836		1.477				9.290	
	62.95		0.781		1.472	7.8	2.10	74.80		
	92.70		0.552		1.471				10.570	
	100.70		0.521		1.488					
	106.70		0.738		1.484	9.6	2.02	75.60	8.540	
	121.70		0.540		1.489					
	150.00		0.567		1.492	9.5	1.92	76.40		
	195.70		0.350		1.519	15.0	1.65	79.60		
	217.70		0.229		1.517					
	224.00		0.058		1.514	28.0				
	228.00		0.214		1.511	31.0				
	129.90		0.461						7.820	
	164.80		0.374						6.870	
	209.00		0.183						5.790	
	224.00		0.068						6.740	
	249.70		0.039						6.130	
	278.00		0.000							
	300.70		0.000						7.260	

scraps 80.xls
Hyp-08

Batch T-3, 1/08/01, 100 °C, 0 Gy/h, air, RB-II-93										
	129.9		0.461							
	164.8		0.373							
	209		0.183							
	224.00		0.068				1.47	80.80		
	249.7		0.039							
	278		0.000							
	300.7		0.000							
Batch T-4, 4/16/01, 108 °C, 0 Gy/h, air, RB-II-35B										DLO unimportant
	14.66		0.719		1.491		2.20	75.50		
	23.9		0.754		1.497					
	34.7		0.626		1.476		3.11	68.90		
	45		0.451		1.508	20.0				
	51.7		0.634		1.497		1.87	77.10		
	63.00		0.462		1.508	18.0				
	72.90		0.358		1.508		1.64	80.80		
	79.70		0.241		1.519	24.0				
	84.70		0.175		1.516		1.46	81.00		
	91.00		0.198		1.514	57.0				
	100.70		0.078		1.504	150.0	1.50	81.20		
Batch T-5, 9/07/01, 124 °C, 0 Gy/h, air, RB-II-75										DLO minor
	6.04		1.014		1.485	7.6	2.15	73.30	12.21	
	6.95		0.812		1.477				10.51	
	9.90		0.738		1.482		2.03	75.50	9.93	
	12.28		0.602		1.479	8.5	2.04	75.30	9.11	
	16.90		0.291		1.487	14.0	1.79	76.80	9.18	
	18.06		0.272		1.486				8	
	19.15		0.237		1.479				7.73	
	20.00		0.225		1.494	20.0	1.70	79.50	7.83	
	24.80		0.113		1.489	55.0	1.74	79.20		
Batch T-6, 4/16/01, 138 °C, 0 Gy/h, air, RB-II-35A										
	4.03		0.455							
	8.87		0.000							
Batch T-7, , °C, Gy/h, ,										

SANDIA CABLE SAMPLE REPOSITORY

Material- Ker-01- Kerite FR Inner Insulation										
Sample No.	Aging Time (h)	Est. Dose (kGy)	Average e/e_0	Average $TS_{/TS0}$	Average density (g/cc)	Outside surface modulus, MPa	Uptake factor	% gel	NMR T2,msec	Miscellaneous
Batch T-1, 02/26/1979, 121.3 °C, 0 Gy/h, air, LB-II-133										
1	0		1.000	1.000	1.274	6.700				
2	136		0.830	1.007		7.000				
3	302		0.730	1.093	1.284					
4	638		0.780	1.220	1.291					
5	1141		0.710	1.273	1.297	10.200				
6	2488		0.490	1.367	1.305	13.000				
7	4918		0.360	1.440	1.325	16.500				
8	7440		0.230	1.640	1.338					
9	9936		0.120	1.380	1.349	26.500				
Batch T-2, 11/21/1978, 130.4 °C, 0 Gy/h, air, LB-II-112										
1	0		1.000	1.000	1.274	6.700				
2	191		0.890	1.080	1.285	9.500				
3	1586		0.470	1.300	1.308	11.500				
4	2590		0.340	1.347	1.322					
5	3073		0.270	1.573						
6	3429		0.210	1.433	1.328	17.500				
7	4195		0.190	1.600	1.345					
8	5011		0.134	1.380	1.356	26.000				
Batch T-3, 09/25/1978, 141.2 °C, 0 Gy/h, air, LB-II-105										
1	0		1.000	1.000	1.274	6.700				
2	335		0.790	1.193	1.303	9.800				
3	503		0.680	1.240	1.310					
4	720		0.530	1.140	1.321					
5	1007		0.440	1.240	1.329	12.500				
6	1703		0.190	1.427	1.344	17.500				
7	2340		0.110	1.227	1.369	22.500				
Batch T-4, 08/21/1978, 150 °C, 0 Gy/h, air, LB-II-97										

SANDIA CABLE SAMPLE REPOSITORY

Material- Ker-01- Kerite FR Inner Insulation										
Sample No.	Aging Time (h)	Est. Dose (kGy)	Average e/e_0	Average $TS_{/TS0}$	Average density (g/cc)	Outside surface modulus, MPa	Uptake factor	% gel	NMR T2,msec	Miscellaneous
1	0		1.000	1.000	1.274	6.700				
2	24		1.180	1.013	1.284	7.400				
3	88		0.960	1.073	1.296	11.000				
4	160		0.750	1.013	1.294					
5	264		0.730	1.113	1.309	12.000				
6	500		0.360	1.113	1.326	13.000				
7	770		0.240	1.233	1.344	16.500				
Batch T-5, 11/27/1978, 160.5 °C, 0 Gy/h, air, LB-II-112										
1	0		1.000	1.000		6.700				
2	30		1.020	0.960						
3	95		0.820	1.000		7.500				
4	214		0.500	1.160		12.500				
5	335		0.400	1.133		14.500				
6	406		0.290	1.147		18.000				
7	502		0.240	1.200		20.000				
8	575		0.190	1.227		26.000				
Batch TR-1 , 04/26/1977, 22 °C, 12 Gy/h, air , NRL B-16										
1	2592		0.910							
2	7392		0.730							
3	17664		0.720							
4	22704		0.730							
5	26928		0.650							
6	31392		0.460							
7	40128		0.780							
8	53136		0.590							
Batch TR-1 RH, 04/26/1977, 22 °C, 12 Gy/h, air + RH, NRL B-15										
1	2592		0.710							
2	7392		0.720							
3	22704		0.600							

SANDIA CABLE SAMPLE REPOSITORY

Material- Ker-01- Kerite FR Inner Insulation										
Sample No.	Aging Time (h)	Est. Dose (kGy)	Average e/e_0	Average $TS_{/TS0}$	Average density (g/cc)	Outside surface modulus, MPa	Uptake factor	% gel	NMR T2,msec	Miscellaneous
4	26928		0.680							
5	31392		0.620							
6	35472		0.660							
7	40128		0.790							
8	45048		0.680							
9	53136		0.610							
Batch TR-2, 04/26/1977, 22 °C, 88 Gy/h, air, NRL B-6										
1	672		0.660							
2	2592		0.940							
3	5520		0.710							
4	11064		0.680							
5	26928		0.370							
Batch TR-3 RH, 04/26/1977, 24 °C, 88 Gy/h, air + RH, NRL B-2										
1	672		0.870							
2	2592		0.710							
3	5520		0.580							
4	11064		0.550							
5	17664		0.460							
Batch TR-4, 08/15/1977, 30 °C, 2100 Gy/h, air, NRL A-5										
1	48		0.780							
2	96		0.740							
3	240		0.720							
4	433		0.650							
5	671		0.550							
Batch TR-5 RH, 05/03/1977, 38 °C, 9550 Gy/h, air + RH, NRL A-1										
1	8		0.710							
2	24		0.480							
3	48		0.640							
4	80		0.570							

SANDIA CABLE SAMPLE REPOSITORY

Material- Ker-01- Kerite FR Inner Insulation										
Sample No.	Aging Time (h)	Est. Dose (kGy)	Average e/e_0	Average $TS_{/TS0}$	Average density (g/cc)	Outside surface modulus, MPa	Uptake factor	% gel	NMR T2,msec	Miscellaneous
5	143		0.420							
Batch TR-6, 11/22/1988, 100 °C, 264 Gy/h, air, DS-III-61										
1	329	87	0.990							
2	665	175	0.830							
3	1001	263	0.640							
4	1337	350	0.530							
5	2156	561	0.500							
6	2680	694	0.450							
7	3351	861	0.420							
8	4024	1032	0.370							
9	4552	1165	0.340							
Batch TR-7, 09/06/1977, 100 °C, 2140 Gy/h, air, NRL A-6										
1	31		0.990							
2	71		1.080							
3	214		0.700							
4	405		0.550							
5	549		0.320							
Batch TR-8, 11/22/1988, 110 °C, 31.2 Gy/h, air, DS-III-63										
1	665	21	0.810							
2	1337	41	0.770							
3	2013	62	0.610							
4	2680	82	0.620							
5	3351	102	0.580							
6	4360	132	0.500							
7	5034	152	0.410							
8	6213	185	0.410							
9	7216	214	0.260							
Batch TR-9, 04/19/1989, 115 °C, 101 Gy/h, air, DS-III-67										
1	480	48	0.780							

SANDIA CABLE SAMPLE REPOSITORY

Material- Ker-01- Kerite FR Inner Insulation										
Sample No.	Aging Time (h)	Est. Dose (kGy)	Average e/e_0	Average $TS_{/TS0}$	Average density (g/cc)	Outside surface modulus, MPa	Uptake factor	% gel	NMR T2,msec	Miscellaneous
2	984	98	0.660							
3	1319	131	0.680							
4	1972	196	0.610							
5	2495	247	0.460							
6	2836	280	0.500							
7	3361	330	0.380							
Batch TR-10, 02/22/1989, 120 °C, 63.2 Gy/h, air, DS-III-69										
1	335	21	0.770							
2	652	41	0.800							
3	987	62	0.610							
4	1320	82	0.640							
5	2160	134	0.540							
6	2661	165	0.470							
7	3195	197	0.430							
8	4177	256	0.300							
9	4845	295	0.340							
Batch TR-11, 05/31/1989, 120 °C, 399 Gy/h, air, DS-III-71										
1	192	76	0.790							
2	480	191	0.720							
3	964	382	0.520							
4	1128	446	0.510							
5	1488	588	0.410							
6	1828	718	0.320							
Batch TR-12, 09/06/1977, 120 °C, 2180 Gy/h, air, NRL A-7										
1	32		1.130							
2	72		1.000							
3	214		0.610							
4	406		0.470							
5	550		0.310							

SANDIA CABLE SAMPLE REPOSITORY

Material- Ker-01- Kerite FR Inner Insulation										
Sample No.	Aging Time (h)	Est. Dose (kGy)	Average e/e_0	Average $TS_{/TS0}$	Average density (g/cc)	Outside surface modulus, MPa	Uptake factor	% gel	NMR T2,msec	Miscellaneous
Batch TR-13, 09/12/1977, 140 °C, 2120 Gy/h, air, NRL A-2										
1	22		1.060							
2	31		0.990							
3	71		0.710							
4	143		0.550							
5	310		0.430							
6	480		0.250							
Batch TR-13 RH, 09/12/1977, 140 °C, 2120 Gy/h, air + RH, NRL A-4										
1	20		0.790							
2	31		0.890							
3	71		0.860							
4	142		0.710							
5	310		0.370							
6	480		0.200							

SANDIA CABLE SAMPLE REPOSITORY

Material- Neo-01- Okonite jacket

Sample No.	Aging Time (h)	Est. Dose (kGy)	Average e/e_0	Average $TS_{/TS0}$	Density g/cc	Density-fabric g/cc	NMR T2, msec	Notes
Batch T-0, 01/01/79, 24 °C, 0 Gy/h, air, envelopes								
1	168000		0.654					
2	207000		0.584					
Batch T-1, 04/11/79, 70.1 °C, 0 Gy/h, air, LHJ-5								
1	0		1		1.473	1.480		fabric ground off for 2nd g/cc
2	1344		0.923			1.477		
3	3024		0.734		1.480	1.481		
4	5376		0.401		1.484	1.486		
5	6384		0.319		1.487	1.491		
6	7392		0.226		1.487	1.487		
7	8808		0.105		1.498	1.493		
Batch T-2, 04/11/79, 80 °C, 0 Gy/h, air, LHJ-5								
1	504		0.919					
2	1176		0.773					
3	2040		0.481					
4	2352		0.346					
5	2520		0.303					
6	3192		0.222					
7	3864		0.092					
8	4152		0.074					
Batch T-3, 06/19/78, 90.6 °C, 0 Gy/h, air, LB-II-82								
	238.08		0.94					
1	501.6		0.773					
2	669.6		0.643					
3	835.2		0.53					
4	1116		0.313					
5	1449.6		0.157					
6	1920		0.114					
Batch T-4, 05/23/78, 101 °C, 0 Gy/h, air, LB-II-76								

SANDIA CABLE SAMPLE REPOSITORY

Material- Neo-01- Okonite jacket

Sample No.	Aging Time (h)	Est. Dose (kGy)	Average e/e_0	Average $TS_{/TS0}$	Density g/cc	Density-fabric g/cc	NMR T2, msec	Notes
1	65.04		0.91					
2	160.08		0.786					
3	304.8		0.616					
4	400.8		0.43					
5	518.4		0.17					
6	844.8		0.076					
Batch T-5, 05/26/78, 111.2 °C, 0 Gy/h, air, LB-II-78								
1	28.56		0.99					
2	95.04		0.724					
3	124.56		0.616					
4	165.6		0.492					
5	238.08		0.195					
6	405.6		0.059					
7	499.2		0.054					
Batch T-6, 06/02/78, 120.9 °C, 0 Gy/h, air, LB-II-80								
1	23.04		0.897					
2	51.12		0.719					
3	65.04		0.646					
4	88.08		0.492					
5	139.44		0.135					
6	231.12		0.065					
Batch T-7, 06/09/78, 131.3 °C, 0 Gy/h, air, LB-II-81								
1	23.04		0.735					
2	48		0.438					
3	65.52		0.254					
4	89.04		0.089					
Batch T-8, 08/06/78, 140.6 °C, 0 Gy/h, air, LB-II-88								
1	7.2		0.94					
2	15.192		0.714					
3	22.392		0.56					

SANDIA CABLE SAMPLE REPOSITORY

Material- Neo-01- Okonite jacket

Sample No.	Aging Time (h)	Est. Dose (kGy)	Average e/e_0	Average $TS_{/TS0}$	Density g/cc	Density-fabric g/cc	NMR T2, msec	Notes
4	30.24		0.397					
5	38.496		0.211					
6	45.12		0.114					
Batch T-9, 10/17/79, 160.5 °C, 0 Gy/h, air, LHJ-28								
1	4.00		0.73					
2	8.70		0.32					
3	15.50		0.05					
Batch Ox-1, 10/5/81, 110.3 °C, 0 Gy/h, 80%Ox, LHJ-94								
1	7.50		1.01					
2	16.50		0.95					
3	24.00		1.04					
4	46.00		0.95					
5	71.00		0.75					
6	98.00		0.49					
7	170.00		0.16					
8	237.00		0.09					
Batch Ox-2, 12/14/81, 130 °C, 0 Gy/h, 80%Ox, LHJ-98 & LHJ-100								
1	5.00		0.94					
2	6.50		0.85					
3	18.50		0.41					
4	22.50		0.38					
5	24.50		0.31					
6	29.50		0.17					
7	48.00		0.07					
8	73.00		0.02					
Batch Ox-3, 10/30/81, 90 °C, 0 Gy/h, 80%Ox, LHJ-96								
1	92.00		0.92					
2	169.00		0.79					
3	237.00		0.75					
4	332.00		0.71					

SANDIA CABLE SAMPLE REPOSITORY

Material- Neo-01- Okonite jacket

Sample No.	Aging Time (h)	Est. Dose (kGy)	Average e/e_0	Average $TS_{/TS0}$	Density g/cc	Density-fabric g/cc	NMR T2, msec	Notes
5	503.00		0.48					
6	617.00		0.42					
7	837.00		0.14					
8	1001.00		0.14					
Batch TR-1, 04/26/77, 22 °C, 14.8 Gy/h, air, NRL B-16								
1	2592.00	47.50	0.96					
2	7392.00	132.00	0.79					
3	17664.00	292.00	0.45					
4	22704.00	364.00	0.29					
5	26928.00	415.00	0.24					
6	31392.00	461.00	0.17					
7	40128.00	543.00	0.21					
8	53136.00	646.00	0.20					
Batch TR-1 RH, 04/26/77, 22 °C, 14.8 Gy/h, air + RH, NRL B-15								
1	2592.00	40.50	0.98					
2	7392.00	112.00	0.83					
3	22704.00	310.00	0.43					
4	26928.00	351.00	0.44					
5	31392.00	400.00	0.30					
6	35472.00	439.00	0.31					
7	40128.00	482.00	0.16					
8	45048.00	523.00	0.20					
9	53136.00	584.00	0.18					
Batch TR-2, 04/26/77, 22 °C, 84 Gy/h, air, NRL B-6								
1	672.00	64.20	0.84					
2	2592.00	243.00	0.70					
3	5520.00	508.00	0.26					
4	11064.00	980.00	0.19					
5	26928.00	2120.00	0.01					
Batch TR-2 RH, 04/26/77, 22 °C, 84 Gy/h, air + RH, NRL B-2								

SANDIA CABLE SAMPLE REPOSITORY

Material- Neo-01- Okonite jacket

Sample No.	Aging Time (h)	Est. Dose (kGy)	Average e/e_0	Average $TS_{/TS0}$	Density g/cc	Density-fabric g/cc	NMR T2, msec	Notes
1	672.00	64.20	0.95					
2	2592.00	243.00	0.68					
3	5520.00	508.00	0.29					
4	11064.00	980.00	0.27					
5	17664.00	1490.00	0.03					
Batch TR-3, 08/16/77, 24 °C, 470 Gy/h, air, NRL A-19								
1	144.00	70.00	1.04					
2	336.00	164.00	1.00					
3	672.00	326.00	0.63					
4	1344.00	650.00	0.35					
5	2688.00	1285.00	0.05					
Batch TR-3 RH, 08/16/77, 24 °C, 470 Gy/h, air + RH, NRL A-17								
1	144.00	67.00	0.97					
2	336.00	157.00	0.92					
3	672.00	312.00	0.58					
4	1344.00	622.00	0.40					
5	2688.00	1230.00	0.14					
Batch TR-4, 08/15/77, 30 °C, 2010 Gy/h, air, NRL A-5								
1	48.00	95.00	0.93					
2	96.00	193.00	0.85					
3	240.00	483.00	0.51					
4	433.00	868.00	0.30					
5	671.00	1344.00	0.15					
Batch TR-4 RH, 08/15/77, 30 °C, 2010 Gy/h, air + RH, NRL A-4								
1	48.00	96.00	0.81					
2	96.00	194.00	0.65					
3	240.00	487.00	0.48					
4	433.00	877.00	0.24					
5	671.00	1357.00	0.12					

SANDIA CABLE SAMPLE REPOSITORY

Material- Neo-01- Okonite jacket													
Sample No.	Aging Time (h)	Est. Dose (kGy)	Average e/e_0	Average $TS_{/TS0}$	Density g/cc	Density-fabric g/cc	NMR T2, msec	Notes					
Batch TR-5 RH, 05/03/77, 38 °C, 9180 Gy/h, air + RH, NRL A-1													
1	8.00	89.00	0.89										
2	24.00	266.00	0.60										
3	48.00	531.00	0.37										
4	80.00	884.00	0.12										
5	143.00	1590.00	0.09										
Batch TR-6, 04/22/80, 58.1 °C, 200 Gy/h, air, LHJ-46													
1	337.00		0.87		1.482								
2	841.00		0.61		1.487								
3	1175.00		0.45		1.495								
4	1683.00		0.32		1.492								
5	2183.00		0.23		1.497								
6	2860.00		0.13		1.505								
7	3524.00		0.10										
Batch TR-7, 07/07/78, 62.2 °C, 904 Gy/h, air, LB-II-84													
1	115.00		0.91										
2	237.00		0.71										
3	402.00		0.42										
4	500.00		0.33										
5	666.00		0.21										
6	833.00		0.17										
Batch TR-8, 04/22/80, 65 °C, 100 Gy/h, air, LHJ-46													
1	337.00		0.87										
2	841.00		0.77										
3	1175.00		0.56										
4	1683.00		0.50										
5	2183.00		0.41										
6	2860.00		0.20										
7	3524.00		0.10										
Batch TR-9, 05/01/81, 66 °C, 32.3 Gy/h, air, LHJ-47													

SANDIA CABLE SAMPLE REPOSITORY

Material- Neo-01- Okonite jacket													
Sample No.	Aging Time (h)	Est. Dose (kGy)	Average e/e_0	Average $TS_{/TS0}$	Density g/cc	Density-fabric g/cc	NMR T2, msec	Notes					
1	510.00		0.87										
2	1468.00		0.84										
3	2352.00		0.68										
4	3024.00		0.53										
5	3694.00		0.30										
6	4373.00		0.20										
7	5978.00		0.10										
Batch TR-10, 12/22/78, 74 °C, 112 Gy/h, air, LB-II-119								note; 30% RH					
1	263.00		0.91										
2	671.00		0.70										
3	934.00		0.58										
4	1150.00		0.45										
5	1414.00		0.37										
6	1751.00		0.19										
Batch TR-11, 06/19/78, 75.7 °C, 908 Gy/h, air, LB-II-83													
1	69.00		1.02										
2	260.00		0.57										
3	406.00		0.30										
4	496.00		0.20										
5	666.00		0.16										
Batch TR-12, 05/26/78, 79.3 °C, 384 Gy/h, air, LB-II-77													
1	140.00		0.93										
2	284.00		0.72										
3	405.00		0.54										
4	500.00		0.47										
5	740.00		0.26										
6	955.00		0.17										
Batch TR-13, 11/13/78, 83 °C, 1790 Gy/h, air, LB-II-115													
1	48.00		0.90										

SANDIA CABLE SAMPLE REPOSITORY

Material- Neo-01- Okonite jacket

Sample No.	Aging Time (h)	Est. Dose (kGy)	Average e/e_0	Average $TS_{/TS0}$	Density g/cc	Density-fabric g/cc	NMR T2, msec	Notes					
2	96.00		0.72										
3	167.00		0.47										
4	199.00		0.38										
5	239.00		0.25										
6	335.00		0.15										
7	431.00		0.10										
Batch TR-14, 05/05/80, 87.4 °C, 9370 Gy/h, air, LHJ-47													
1	17.00		0.81										
2	31.00		0.54										
3	41.00		0.37										
4	55.00		0.26										
5	72.00		0.16										
6	102.00		0.10										
7	167.00		0.01										
Batch TR-15 RH, 05/09/78, 88 °C, 929 Gy/h, air + RH, LB-II-73													
1	76.50		0.88										
2	142.60		0.65										
3	237.00		0.38										
4	334.00		0.17										
5	404.00		0.14										
Batch TR-16, 05/23/78, 97 °C, 386 Gy/h, air, LB-II-75													
1	70.00		0.86										
2	168.00		0.60										
3	216.00		0.46										
4	240.00		0.43										
5	310.00		0.27										
6	406.00		0.16										
Batch TR-17, 09/06/1977, 100 °C, 2050 Gy/h, air, NRL A-6													
1	31.00		0.85										
2	71.00		0.61										

SANDIA CABLE SAMPLE REPOSITORY

Material- Neo-01- Okonite jacket

Sample No.	Aging Time (h)	Est. Dose (kGy)	Average e/e_0	Average $TS_{/TS0}$	Density g/cc	Density-fabric g/cc	NMR T2, msec	Notes
3	214.00		0.10					
Batch TR-18, 07/21/78, 100 °C, 120 Gy/h, air, LB-II-85								
1	89.50		0.97					
2	163.00		0.77					
3	235.00		0.58					
4	329.00		0.34					
5	403.00		0.26					
6	568.00		0.07					
Batch TR-19 RH, 05/09/78, 106 °C, 929 Gy/h, air + RH, LB-II-74								
1	28.70		0.80					
2	75.70		0.61					
3	113.00		0.34					
4	142.00		0.24					
5	167.00		0.15					
6	235.00		0.14					
Batch TR-20, 08/07/78, 114.6 °C, 377 Gy/h, air, LB-II-91								
1	43.00		0.82					
2	69.50		0.68					
3	91.50		0.47					
4	119.50		0.18					
5	164.00		0.10					
6	234.00		0.04					
Batch TR-21 RH, 12/12/1977, 110 °C, 470 Gy/h, air + RH, NRL A-17								
1	23.80		0.83					
2	47.50		0.42					
3	78.40		0.58					
4	102.40		0.23					
5	167.00		0.10					
Batch TR-22, 11/07/78, 120 °C, 8700 Gy/h, air, LB-II-115								

SANDIA CABLE SAMPLE REPOSITORY

Material- Neo-01- Okonite jacket

Sample No.	Aging Time (h)	Est. Dose (kGy)	Average e/e_0	Average $TS_{/TS0}$	Density g/cc	Density-fabric g/cc	NMR T2, msec	Notes					
1	5.75		0.89										
2	15.90		0.62										
3	21.60		0.40										
4	27.50		0.29										
5	39.80		0.19										
Batch TR-23, 09/06/1977, 120 °C, 2090 Gy/h, air, NRL A-7													
1	31.50		0.73										
2	71.30		0.14										
3	214.00		0.00										
Batch TR-24, 09/12/1977, 140 °C, 2030 Gy/h, air, NRL A-2													
1	7.50		0.73										
2	20.00		0.26										
3	31.00		0.15										
Batch TR-24 RH, 09/12/1977, 140 °C, 2030 Gy/h, air + RH, NRL A-4													
1	7.60		0.81										
2	22.10		0.28										
3	31.30		0.23										
4	47.60		0.10										
5	71.20		0.03										

SANDIA CABLE SAMPLE REPOSITORY

Material- Neo-02- Rockbestos Firewall III jacket														
Sample No.	Aging Time (d)	Est. Dose (kGy)	Average e/e_0	Average $TS_{/TS0}$	NMR T2,msec	Outside surface modulus	Uptake factor	% gel	Miscellaneous					
Note- scatter in density makes measurements impractical														
Batch T-1, 6/23/1997, 80 °C, 0 Gy/h, air, Envelopes/Malone									DLO unimportant					
1	0	0	1.000		6.46	7.4	2.63	90.90						
2	28		1.007		5.29	10.5	2.39	90.80						
3	59		0.970		5.81	14.0								
4	91		0.810		5.10	15.0	2.23	92.10						
5	121		0.700		4.91									
6	161		0.660		5.46		2.21	92.30						
7	206		0.440		3.82	16.0	2.01	92.80						
8	324		0.320		3.40	20.0	2.52	93.10						
9	415		0.200		2.29	32.0	1.99	93.10						
10	511		0.100			95.0								
11	652		0.040		1.32	61.0	1.48	90.80						
Batch T-2, 6/23/1997, 95 °C, 0 Gy/h, air, Envelopes/Malone									DLO unimportant					
1	8	0	0.970		4.37		2.14	93.40						
2	14		0.780		4.10									
3	21		0.780		3.70	13.0	2.17	92.70						
4	28		0.790		4.15		2.17	92.30						
5	63		0.400		3.92	23.0	2.08	92.20						
6	91		0.280		2.60	26.0	1.86	93.30						
7	112		0.140		2.46	38.0	1.67	94.00						
8	133		0.120		2.07	40.0	1.53	94.70						
9	171		0.007		1.12	60.0	1.40	92.80						
10	226		0.000		0.83		1.19	94.00						

SANDIA CABLE SAMPLE REPOSITORY

Material- Neo-02- Rockbestos Firewall III jacket														
Sample No.	Aging Time (d)	Est. Dose (kGy)	Average e/e_0	Average $TS_{/TS0}$	NMR T2,msec	Outside surface modulus	Uptake factor	% gel	Miscellaneous					
Batch T-3, 6/23/1997, 110 °C, 0 Gy/h, air, Envelopes/Malone									DLO unimportant					
1	3	0	0.930		5.51	11.0	2.66	92.40						
2	4		0.880		4.19									
3	8		0.750		5.28	11.0	2.60	92.60						
4	10		0.670		4.85	13.0	2.44	92.90						
5	14		0.520		3.25		2.23	94.20						
6	21		0.340		2.77	18.0	1.86	94.20						
7	28		0.230		2.57	20.0	1.71	94.50						
8	40		0.100		2.39	45.0	1.49	95.00						
9	49		0.060		1.27	120.0	1.39	95.40						
10	63		0.020		1.41	450.0	1.28	93.90						
Batch TR-1, 5/5/1997, 50 °C, 133 Gy/h, air, Envelopes/Malone									DLO unimportant					
1	0		1.000		5.90	7.5	2.38	90.80						
2	22		0.860		4.52	10.5	2.12	91.60						
3	42		0.710		4.03		2.10	91.61						
4	63		0.530		3.21	13.0	1.92	91.47						
5	85		0.430		2.93		1.68	92.81						
6	121		0.300		2.44	21.0	1.61	91.92						
7	161		0.150		2.15	27.0	1.46	91.41						
8	189		0.100		1.95	42.0	1.37	91.72						
9	220		0.050		1.37		1.31	90.90						
10	249		0.030		1.87	120.0	1.26	89.36						
11	282		0.017		1.27		1.22	92.50						
Batch TR-2, 5/5/1997, 60 °C, 45 Gy/h, air, Envelopes/Malone									DLO unimportant					
1	29		0.980		5.37	12.5	2.67	89.26						
2	57		0.770		5.60		2.29	88.46						
3	85		0.740		4.92	13.0	2.49	88.35						
4	121		0.570		3.80		2.01	91.95						
5	161		0.480		3.40	15.0	1.82	92.12						
6	200		0.330		2.57		1.72	93.07						
7	249		0.240		2.34	24.0	1.64	93.07						
8	291		0.100		1.96		1.78	93.44						
9	361		0.060		1.80	62.0	1.66	93.59						
10	429		0.044		1.92		1.52	92.53						
11	515		0.030		1.54	115.0	1.40	92.53						

SANDIA CABLE SAMPLE REPOSITORY

Material- Neo-02- Rockbestos Firewall III jacket														
Sample No.	Aging Time (d)	Est. Dose (kGy)	Average e/e_0	Average $TS_{/TS0}$	NMR T2,msec	Outside surface modulus	Uptake factor	% gel	Miscellaneous					
Batch TR-3, 5/5/1997, 70 °C, 940 Gy/h, air, Envelopes/Malone									DLO unimportant					
1	3		0.970		5.53	8.8	2.25	91.20						
2	7		0.740		4.28	11.0	2.21	91.20						
3	14		0.440		2.94	11.0	1.62	93.50						
4	22		0.220		1.96	21.0	1.46	94.20						
5	29		0.130		1.57	25.0	1.35	93.20						
6	37		0.057		1.53	33.0	1.35	91.80						
7	45		0.037		1.31		1.21	91.10						
8	52		0.040			45.0								
Batch TR-4, 5/5/1997, 80 °C, 42 Gy/h, air, Envelopes/Malone									DLO unimportant					
1	10		0.970		5.34		2.40	91.17						
2	22		0.890		5.55	11.0	2.34	91.31						
3	32		0.780		5.19		2.37	90.80						
4	42		0.640		5.34		2.33	90.30						
5	63		0.430		4.50	16.0	2.29	90.13						
6	85		0.350		3.77		2.01	91.58						
7	113		0.270		3.34	22.0	1.85	91.78						
8	151		0.180		2.53		1.72	92.19						
9	189		0.068		2.54	48.0	1.65	92.11						
10	220		0.064		2.47	76.0	1.57	91.19						
11	249		0.051		2.64	80.0	1.42	91.12						

SANDIA CABLE SAMPLE REPOSITORY

Material- Sil-01- Rockbestos Firewall II insulation										
Sample No.	Aging Time (h)	Est. Dose (kGy)	Average e/e_0	Average $TS_{/TS0}$	Average density (g/cc)	Outside surface modulus, MPa	Uptake factor	% gel	NMR T2,msec	Miscellaneous
Batch T-1, 11/1/1989, 140 °C, 0 Gy/h, air, Envelopes										
1	172	0	0.680							
2	340		0.750							
3	505		0.700							
4	673		0.550							
Batch TR-2, 10/31/1989, 41.5 °C, 52.5 Gy/h, air, Envelopes										
1	334		0.870							
2	507		0.870							
3	668		0.840							
4	1006		0.650							
5	1008		0.700							
6	1512		0.490							
7	2016		0.430							
8	2016		0.330							
9	2520		0.250							
10	3020		0.210							
11	3550		0.180							
12	4051		0.140							
Batch TR-3, 10/31/1989, 60.7 °C, 54.4 Gy/h, air, Envelopes										
1	334		0.910							
2	507		0.990							

SANDIA CABLE SAMPLE REPOSITORY

Material- Sil-01- Rockbestos Firewall II insulation										
Sample No.	Aging Time (h)	Est. Dose (kGy)	Average e/e_0	Average $TS_{/TS0}$	Average density (g/cc)	Outside surface modulus, MPa	Uptake factor	% gel	NMR T2,msec	Miscellaneous
3	668		0.790							
4	1006		0.730							
5	1512		0.670							
6	2012		0.500							
7	2521		0.370							
8	3020		0.310							
9	3527		0.270							
10	4032		0.190							
Batch TR-4, 5/2/1988, 70 °C, 4600 Gy/h, air, DS-I-38										
1	24		0.660							
2	48		0.280							
3	72		0.090							
4	96		0.040							
Batch TR-5, 5/31/1988, 100 °C, 114 Gy/h, air, DS-I-39										
1	166		0.880							
2	334		0.830							
3	505		0.490							
4	671		0.330							
5	836		0.270							
6	1173		0.210							
7	1679		0.140							
8	2374		0.080							
9	3358		0.030							
Batch TR-6, 11/22/1988, 100 °C, 176 Gy/h, air, DS-III-27										
1	166		0.670							
2	329		0.190							
3	497		0.130							
4	665		0.080							
5	1001		0.050							
Batch TR-7, 11/22/1988, 110 °C, 26.6 Gy/h, air, DS-III-31,32										

SANDIA CABLE SAMPLE REPOSITORY

Material- Sil-01- Rockbestos Firewall II insulation										
Sample No.	Aging Time (h)	Est. Dose (kGy)	Average e/e_0	Average $TS_{/TS0}$	Average density (g/cc)	Outside surface modulus, MPa	Uptake factor	% gel	NMR T2,msec	Miscellaneous
1	330		0.690							
2	665		0.450							
3	1001		0.380							
4	1337		0.310							
5	2013		0.240							
6	2680		0.180							
7	3351		0.140							
8	4360		0.110							
Batch TR-8, 6/13/1989, 115 °C, 112 Gy/h, air, DS-III-39										
1	168		0.830							
2	337		0.420							
3	510		0.360							
4	677		0.290							
5	841		0.230							
Batch TR-9, 2/22/1989, 120 °C, 77.3 Gy/h, air, DS-III-35										DLO unimportant
1	167		0.790			3.7	2.270	97.700		unaged=1.3104 g/cc
2	335		0.450		1.312	4.2	2.120	97.800		unaged=3.04 MPa
3	480		0.290							unaged= 2.525
4	652		0.230		1.310	5.000	2.220	97.900		unaged= 97.7%
5	988		0.150				2.180	97.700		
6	1321		0.120		1.313	7.800	1.920	98.100		
7	2159		0.050		1.317		1.820	98.500		
8	2661		0.080		1.321	12.300	1.650	98.500		
9	4173		dead		1.339		1.710	98.800		
Batch TR-10, 8/9/1988, 120 °C, 118 Gy/h, air, DS-I-40										
1	194		0.870							
2	330		0.460							
3	551		0.280							
4	695		0.310							
5	837		0.360							
6	1247		0.120							

SANDIA CABLE SAMPLE REPOSITORY

Material- Sil-01- Rockbestos Firewall II insulation										
Sample No.	Aging Time (h)	Est. Dose (kGy)	Average e/e_0	Average $TS_{/TS0}$	Average density (g/cc)	Outside surface modulus, MPa	Uptake factor	% gel	NMR T2,msec	Miscellaneous
7	1678		0.070							
8	2014		0.050							
Batch TR-11, 5/31/1989, 120 °C, 176 Gy/h, air, DS-III-37										
1	123		0.890							
2	215		0.750							
3	291		0.460							
4	479		0.140							
Batch TR-12, 5/31/1989, 120 °C, 397 Gy/h, air, DS-III-33,34										
1	120		0.520							
2	216		0.260							
3	292		0.190							
4	504		0.070							
5	1013		dead							
Batch TR-13, 10/31/1989, 130 °C, 50.2 Gy/h, air, Envelopes										
1	71		0.910							
2	164		0.700							
3	334		0.330							
4	407		0.330							
5	500		0.260							
6	668		0.210							

				Material- XLPE-01- GE Vulkene Supreme Insulation						
Sample No.	Aging Time (h)	Est. Dose (kGy)	Average e/e_0	Average TS/TS0	Average density (g/cc)	Outside surface modulus, MPa	Uptake factor	% gel	NMR T2,msec	Miscellaneous
Batch TR-1, 06/03/1981, 43 °C, 175 Gy/h, Air, LHJ-84										
1	497	87	0.960	0.978						
2	1338	234	0.750	0.893						
3	2518	436	0.520	0.822						
4	3640	621	0.290	0.809						
5	4870	823	0.120	0.813						
6	5322	897	0.126	0.800						
7	5753	971	0.040	0.804						
8	6493	1085	0.006	0.658						
Batch TR-2, 08/10/1981, 43.5 °C, 8900 Gy/h, Air,										
1	8	71	0.936	1.000						
2	16	142	0.791	0.973						
3	32	285	0.557	0.916						
4	48	427	0.614	0.920						
5	72	641	0.455	0.910						
6	96	854	0.310	0.907						
Batch TR-3, 06/16/1982, 70 °C, 189 Gy/h, Air, KTG III-136										
1	696		0.880							
2	1081		0.710							
3	1194		0.670							
4	1629		0.620							
5	2015		0.590							
6	2632		0.490							
7	3648		0.290							
8	4845		0.230							
Batch TR-4, 08/18/1982, 70 °C, 1160 Gy/h, Air, CAQ-102										
1	163	73	0.787	0.893						
2	308	357	0.632	0.893						
3	505	586	0.403	0.920						
Batch TR-5, 04/24/1981, 70 °C, 640 Gy/h, Air, LHJ-80										
1	169		0.860							
2	336		0.610							
3	504		0.560							
4	764		0.370							
5	1074		0.250							
6	1337		0.160							
7	1580		0.070							
8	1820		0.020							
Batch TR-6, 01/05/1983, 70 °C, 7000 Gy/h, Air, CAQ-103, 108										
1	58		0.860							
2	73		0.620							
3	97		0.540							
4	120		0.360							
5	287		0.040							
6	361		0.030							
7	432		0.020							
Batch TR-7, 08/31/1981, 80 °C, 187 Gy/h, Air, CAQ-51, 53										
1	100	19	0.864	0.898						
2	336	63	0.754	0.973						
3	510	96	0.629	0.924						
4	774	145	0.803	0.947						
5	1104	207	0.646	0.942						
6	1440	270	0.620	0.960						
7	360	68	0.826	0.956						
Batch TR-8, 10/26/1981, 80 °C, 666 Gy/h, Air, LHJ-92										
1	377	251	0.777	0.947						
2	550	367	0.649	0.947						
3	910	606	0.461	0.951						
Batch TR-9, 09/14/1981, 80 °C, 7750 Gy/h, Air, CAQE-57										
1	8	60	0.835	0.978						
2	16	124	0.809	0.889						
3	40	310	0.707	0.933						
4	48	372	0.490	0.884						
5	72	558	0.441	0.916						
6	88	682	0.371	0.916						
7	208	1612	0.156	0.876						
Batch TR-10, 06/09/1982, 25 °C, 1200 Gy/h, Air, LHJ-118										
1	150		0.830							
2	362		0.520							
3	650		0.250							
4	994		0.097							
5	1496		0.014							
Batch TR-11, 07/16/1997, 43 °C, 479 Gy/h, Air, Envelopes										
1	313		0.690							
2	720		0.670							
3	1056		0.410							
4	1372		0.310							
5	1680		0.200							
6	2016		0.130							
7	2351		0.080							
8	2712		0.030							
9	3143		0.030							
10	3412		0.000							
#REF!										

SANDIA CABLE SAMPLE REPOSITORY

Material- XLPO-02A, Brand Rex CLPO insulation										
Sample No.	Aging Time (h)	Est. Dose (kGy)	Average e/e_0	Average $TS_{/TS0}$	NMR T2, msec	% gel	Uptake factor	OIT, min	OITP, C	Modulus, MPa
NOTE- two "identical" cable reels (#2 and #9) purchased at same time (see Cable C-3 in Cable Info										
XLPO-02B- Reel #9 used for thermal aging started in 1993 (100C, 110C, 125C, 151C)										
Possible that Reel #2 was used for earlier thermal aging (120C, 140C, 150C, 160C) & reel to reel va										
Batch TR-1, 12/9/1991, 25 °C, 16.8 Gy/h, Air, paper										
1	1729.0	28.7	0.873	0.961						
2	3552.0	58.2	0.426	0.878						
3	5256.0	85.1	0.412	0.851						
4	7104.0	113.7	0.104	0.861						
5	9576.0	150.2	0.037	0.893						
6	15168.0	230.6								
Batch TR-2, 12/9/1991, 25 °C, 124 Gy/h, Air, paper										
1	576.0	71.1	0.805	0.884						
2	1008.0	124.1	0.036	0.918						
3	1536.0	188.6	0.000	0.931						
4	1728.0	211.9	0.024	0.904						
Batch TR-3, 8/11/1987, 60 °C, 317 Gy/h, Air, DS-II-5										
1	331.0	100.0	0.830	0.778						
2	337.0	106.0	0.800	0.923						
3	668.0	211.0	0.720	1.059						
4	840.0	254.0	0.610	0.966						
5	1172.0	368.0	0.520	1.059						
6	1677.0	525.0	0.340	0.943						
7	2180.0	681.0	0.310	1.044						
8	2690.0	836.0	0.110	1.026						
9	3530.0	1090.0	0.140	1.022						
10	3836.0	1180.0	0.077	0.982						
Batch TR-4, 11/2/1987, 60 °C, 5240 Gy/h, Air, DS-II-19										
1	21.0	110.0	0.740	0.910						
2	40.4	212.0	0.770	0.934						
3	64.3	337.0	0.560	0.912						
4	88.2	462.0	0.300	0.860						
5	118.7	622.0	0.130	0.847						

SANDIA CABLE SAMPLE REPOSITORY

Material- XLPO-02A, Brand Rex CLPO insulation										
Sample No.	Aging Time (h)	Est. Dose (kGy)	Average e/e_0	Average $TS_{/TS0}$	NMR T2, msec	% gel	Uptake factor	OIT, min	OITP, C	Modulus, MPa
6	142.5	747.0	0.042	0.841						
7	182.5	956.0	0.015	0.836						
8	256.0	1341.0	0.009	0.870						
Batch TR-5, 8/11/1987, 80 °C, 120 Gy/h, Air, DS-II-35										
1	836.0	128.0	0.790	1.007						
2	1676.0	255.0	0.530	0.976						
3	2180.0	330.0	0.430	1.172						
4	2858.0	431.0	0.320	1.129						
5	4027.0	602.0	0.100	1.035						
6	5540.0	819.0	0.035	1.118						
7	6888.0	1030.0	0.023	1.043						
9	8400.0	1262.0	0.055	1.543						
Batch TR-6, 8/11/1987, 80 °C, 323 Gy/h, Air, DS-II-10										
1	337.0	109.0	0.880	0.978						
2	668.0	217.0	0.640	1.022						
3	1172.0	380.0	0.440	1.079						
4	1677.0	541.0	0.300	1.060						
5	2180.0	702.0	0.140	1.053						
6	2689.0	862.0	0.130	1.126						
7	3530.0	1125.0	0.081	1.068						
8	3836.0	1217.0	0.063	1.041						
Batch TR-7, 10/26/1987, 80 °C, 682 Gy/h, Air, DS-II-16-17										
1	96.0	65.4	0.810	0.879						
2	215.0	146.0	0.650	0.930						
3	334.0	227.0	0.520	1.007						
4	508.0	345.0	0.300	1.002						
5	671.0	455.0	0.200	1.095						
6	839.0	569.0	0.260	1.039						
7	1011.0	684.0	0.051	1.028						
8	1343.0	907.0	0.025	1.021						
9	1678.0	1130.0	0.009	0.927						

SANDIA CABLE SAMPLE REPOSITORY

Material- XLPO-02A, Brand Rex CLPO insulation										
Sample No.	Aging Time (h)	Est. Dose (kGy)	Average e/e_0	Average $TS_{/TS0}$	NMR T2, msec	% gel	Uptake factor	OIT, min	OITP, C	Modulus, MPa
Batch TR-8, 08/17/1987, 100 °C, 700 Gy/h, Air, DS-II-15										
1	94.5	66.2	0.880	0.930						
2	214.0	150.0	0.780	1.016						
3	334.0	233.0	0.530	1.047						
4	525.0	366.0	0.330	1.048						
5	669.0	466.0	0.240	1.060						
6	837.0	582.0	0.150	0.969						
7	1012.0	701.0	0.098	0.988						
8	1683.0	1163.0	0.000	0.845						
Batch TR-9, 08/24/1987, 80 °C, 5350 Gy/h, Air, DS-II-25										
1	21.0	112.0	0.900	0.907						
2	40.0	214.0	0.740	0.950						
3	65.0	348.0	0.570	0.960						
4	87.7	469.0	0.500	1.018						
5	119.5	639.0	0.340	1.046						
6	144.0	770.0	0.230	1.037						
7	184.0	984.0	0.160	1.007						
8	256.0	1370.0	0.064	0.890						
Batch TR-10, 01/18/1988, 100 °C, 301 Gy/h, Air, DS-II-11										
1	335.0	101.0	0.760	0.929						
2	671.0	201.0	0.530	1.078						
3	1174.0	350.0	0.300	1.061						
4	1678.0	499.0	0.120	0.974						
5	2182.0	647.0	0.042	0.940						
6	2686.0	792.0	0.065	0.921						
7	3353.0	988.0	0.016	0.808						
Batch TR-11, 12/20/1988, 110 °C, 25.4 Gy/h, Air, DS-II-31										
1	1349.0	34.0	0.930	1.109						
2	2688.0	67.0	0.770	1.055						
3	3744.0	92.0	0.650	1.076						
4	4369.0	108.0	0.640	1.082						
5	5548.0	135.0	0.520	1.080						
6	6551.0	159.0	0.480	1.107						

Material- XLPO-02A, Brand Rex CLPO insulation										
Sample No.	Aging Time (h)	Est. Dose (kGy)	Average e/e_0	Average $TS_{/TS0}$	NMR T2, msec	% gel	Uptake factor	OIT, min	OITP, C	Modulus, MPa
7	7560.0	182.0	0.400	1.138						
8	9576.0	227.0								
Batch TR-12, 12/20/1988, 110 °C, 150 Gy/h, Air, DS-II-33										
1	504.0		0.905	1.039						
2	984.0		0.630	0.971						
3	1344.0		0.701	1.076						
4	1704.0		0.574	0.993						
5	2016.0		0.647	1.120						
6	2352.0		0.480	1.077						
Batch TR-13, 4/19/1989, 115 °C, 92.4 Gy/h, Air, DS-III-75										
1	480.0	44.0	0.820	0.980						
2	984.0	90.0	0.840	1.134						
3	1319.0	121.0	0.720	1.104						
4	1972.0	179.0	0.490	1.072						
5	2495.0	227.0	0.320	1.017						
6	2836.0	257.0	0.250	1.108						
7	3361.0	303.0	0.088	0.871						
Batch TR-14, 02/22/1989, 120 °C, 90 Gy/h, Air, DS-III- 73 (calc pg75)										
1	652.5	58.0	0.920	1.131						
2	1320.0	118.0	0.700	1.131						
3	1996.0	177.0	0.410	1.012						
4	2661.0	235.0	0.180	0.938						
5	3189.0	281.0	0.120	0.808						
6	4177.0	365.0	0.076	0.857						
7	4845.0	420.0	0.056	0.804						
8	5373.0		0.130	1.060						
9	5637.0		0.022	0.806						
Batch TR-15, 1/18/1988, 120 °C, 307 Gy/h, Air, DS-II-6										
1	335.0	103.0	0.830	1.014						
2	671.0	205.0	0.550	1.108						
3	1174.0	357.0	0.170	0.895						
4	1678.0	508.0	0.072	0.840						

SANDIA CABLE SAMPLE REPOSITORY

Material- XLPO-02A, Brand Rex CLPO insulation										
Sample No.	Aging Time (h)	Est. Dose (kGy)	Average e/e_0	Average $TS_{/TS0}$	NMR T2, msec	% gel	Uptake factor	OIT, min	OITP, C	Modulus, MPa
5	2181.0	660.0	0.027	0.745						
6	2690.0	809.0	0.012	0.718						
Batch TR-16, 1/18/1988, 120 °C, 664 Gy/h, Air, DS-II-14										
1	71.0	47.0	1.040	1.073						
2	167.0	111.0	0.880	1.085						
3	335.0	222.0	0.600	1.035						
4	502.0	332.0	0.340	1.029						
5	670.0	443.0	0.200	0.922						
6	838.0	553.0	0.140	0.845						
7	1007.0	663.0	0.062	0.763						
Batch TR-17, 2/29/1988, 120 °C, 5030 Gy/h, Air, DS-II-29										
1	21.0	106.0	0.950	1.036						
2	40.0	201.0	0.770	1.064						
3	64.0	322.0	0.620	1.012						
4	88.0	443.0	0.440	0.948						
5	119.6	602.0	0.280	0.892						
6	144.3	726.0	0.200	0.849						
7	184.5	928.0	0.110	0.749						
8	256.0	1288.0	0.066	0.709						
9	328.0	1647.0	0.047	0.563						
Batch TR-18, 10/31/1989, 41 °C, 69 Gy/h, Air, Envelopes										
1	1008.0	70.0	0.806	0.923						
2	1512.0		0.768	0.876						
3	2016.0	139.4	0.744	0.843						
4	2352.0		0.720	0.812						
5	3024.0	210.0	0.105	0.907						
6	3024.0		0.074	0.855						
7	4032.0		0.107	0.916						
8	4704.0		0.029	0.940						
9	5040.0		0.003	0.893						
10	6048.0		0.015	0.908						

SANDIA CABLE SAMPLE REPOSITORY

Material- XLPO-02A, Brand Rex CLPO insulation										
Sample No.	Aging Time (h)	Est. Dose (kGy)	Average e/e_0	Average $TS_{/TS0}$	NMR T2, msec	% gel	Uptake factor	OIT, min	OITP, C	Modulus, MPa
11	7056.0		0.000	0.921						
12	8568.0		0.000	0.882						
13	10248.0		0.000	2.860						
Batch TR-19, 10/31/1989, 61 °C, 70 Gy/h, Air, Envelopes										
1	1008.0	74.0	0.851	1.000						
2	2016.0	147.3	0.748	0.901						
3	3024.0	222.4	0.529	0.930						
4	3360.0	296.1	0.607	1.009						
5	5040.0	369.5	0.443	0.996						
6	6048.0	443.6	0.408	1.067						
7	7056.0		0.125	1.078						
8	8568.0		0.000	1.047						
Batch T-3, 4/1/1988, 120 °C, 0 Gy/h, Air, DS-II-21-22										
1	169.0	0.0	1.107	1.031						
2	337.0	0.0	0.929	0.941						
3	502.0	0.0	1.040	1.071						
4	1003.0	0.0	0.991	1.076						
5	2013.0	0.0	0.793	0.968						
6	2350.0	0.0	0.788	1.007						
7	3361.0	0.0	0.719	1.765						
8	3860.0	0.0	0.653	0.914						
9	4797.0	0.0	0.435	0.902						
10	5804.0	0.0	0.340	0.943						
Batch T-5, 10/9/1989, 140 °C, 0 Gy/h, Air, Envelopes										
1	336.0	0.0	0.720	1.104						
2	672.0	0.0	0.966	1.087						
3	1008.0	0.0	0.766	0.985						
4	1344.0	0.0	0.575	0.824						
5	1680.0	0.0	0.000	dead						
6	2016.0	0.0	0.000	dead						
Batch T-6, 10/9/1989, 150 °C, 0 Gy/h, Air, Envelopes										

SANDIA CABLE SAMPLE REPOSITORY

Material- XLPO-02A, Brand Rex CLPO insulation										
Sample No.	Aging Time (h)	Est. Dose (kGy)	Average e/e_0	Average $TS_{/TS0}$	NMR T2, msec	% gel	Uptake factor	OIT, min	OITP, C	Modulus, MPa
1	168.0	0.0	1.047	1.050						
2	336.0	0.0	1.013	1.074						
3	504.0	0.0	0.914	1.051						
4	672.0	0.0	0.729	0.974						
5	840.0	0.0	0.411	0.855						
6	1008.0	0.0	0.128	0.755						
7	1344.0	0.0	0.003	0.721						
Batch T-8, 8/28/1989, 160 °C, 0 Gy/h, Air, DS-IV- 9										
1	192.0	0.0	0.937	1.056						
2	336.0	0.0	0.808	0.908						
3	504.0	0.0	0.083	0.743						
4	673.0	0.0	0.000	dead						

scraps 80.xls
XLPO-02B

Material- XLPO-02B, Brand Rex CLPO insulation												
Sample No.	Aging Time (h)	Est. Dose (kGy)	Average e/e_0	Average $TS_{/TS0}$	NMR T2, msec	% gel	Uptake factor	OIT, min	OITP, C	Modulus, MPa	Average density (g/cc)	Miscellaneous
NOTE- two "identical" cable reels (#2 and #9) purchased at same time (see Cable C-3 in Cable Information Tab).												
XLPO-02B- Reel #9 used for thermal aging started in 1993 (99C, 109C, 125C, 151.5C)												
Possible that Reel #2 was used for earlier thermal aging (120C, 140C, 150C, 160C) & reel to reel variation causes aging difference												
Batch T-1, 6/9/1993, 99 °C, 0 Gy/h, Air, Envelopes												
1	7056.0		0.877		15.0	60.8	7.3					
2	11760.0		0.845		15.3	62.4	6.5					
3	28800.0		0.718		7.8	66.8	4.5					
4	42840.0		0.608		4.5	69.2	4.0					
5	52344.0		0.441		3.3	68.2	4.1					
6	56472.0		0.516			70.0	3.7					
7	60672.0		0.459									
Batch T-2, 6/9/1993, 109 °C, 0 Gy/h, Air, Envelopes												
1	4704.0		0.874		16.5							
2	7224.0		0.877			62.0	6.0					
3	9456.0		0.871		7.4	64.1	5.8					
4	15120.0		0.699		8.2	65.8	5.5					
5	22176.0		0.546			68.6	4.6					
6	28800.0		0.486		3.7	70.9	3.9					
7	36960.0		0.401		2.4	71.6	3.4					
8	44184.0		0.311		2.3	72.3	3.2					
9	52344.0		0.136		1.6	74.0	2.6					
10	56472.0		0.133		1.3	74.3	2.4					
11	60864.0		0.055									
Batch T-4, 6/9/1993, 125 °C, 0 Gy/h, Air, Envelopes												
1	0.0		1.000	1.000	13.7	57.2	8.1					
2	1848.0		0.926	1.204	12.8	62.4	7.1					
3	2352.0		0.959	1.226	13.7							
4	3192.0		0.919	1.177	16.9							
5	3864.0		0.906	1.216	13.4							
6	4560.0		0.851	1.179	12.5	64.6	6.0					
7	5400.0		0.828	1.113	10.1							
8	6072.0		0.761	1.129	10.8	66.4	5.7					
9	7056.0		0.568	0.955	10.2							
10	8016.0		0.433	0.922	7.7	67.7	5.0					
11	11784.0		0.130	0.832	4.1	72.4	2.9					
12	15168.0		0.009	0.750	2.9	73.9	2.7					
Batch T-7, , 151.5 °C, 0 Gy/h, Air, Envelopes												
	331.2		1.083573			66.3	6.126					
	664.8		1.054755			67.3	6.01					
	885.6		1.057637			68.2	5.8					
	1171.2		0.682997			70.5	5.28					
	1531.2		0.256484			73.7	3.55					
	1699.201		0.161383			74.7	3.15					
	1795.199		0.106628			75.5	2.73					
	1891.199		0.080692			75.5	2.84					
	2063.999		0.037464			76.5	2.38					

SANDIA CABLE SAMPLE REPOSITORY

Material- XLPO-03- Eaton Dekoron Polyset insulation										
Sample No.	Aging Time (h)	Est. Dose (kGy)	Average e/e_0	Average $TS_{/TS0}$	Average density (g/cc)	Outside surface modulus, MPa	Uptake factor	% gel	NMR T2,msec	Miscellaneous
Batch T-1, 4/1/1988, 120 °C, 0 Gy/h, air, DS-II-71-72										
1	168	0	1.060							
2	336		0.960							
3	504		0.940							
4	1008		0.880							
5	2016		0.900							
6	2352		0.880							
7	3360		0.800							
8	4368		0.770							
9	5880		0.790							
10	6048		0.650							
11	6888		0.720							
Batch TR-1, 10/31/1989, 41 °C, 64.1 Gy/h, air, Envelopes										
1	1007		0.920							
2	2016		0.860							
3	3044		0.810							
4	4056		0.690							
5	5036		0.700							
6	6049		0.690							
7	8568		0.520							
8	9578		0.410							
Batch TR-2, 11/2/1987, 60 °C, 5240 Gy/h, air, DS-II-59										
1	21		0.940							
2	40		0.850							
3	63		0.730							
4	88		0.630							
5	119		0.470							
6	143		0.360							
7	182		0.280							
8	256		0.180							

SANDIA CABLE SAMPLE REPOSITORY

Material- XLPO-03- Eaton Dekoron Polyset insulation										
Sample No.	Aging Time (h)	Est. Dose (kGy)	Average e/e_0	Average $TS_{/TS0}$	Average density (g/cc)	Outside surface modulus, MPa	Uptake factor	% gel	NMR T2,msec	Miscellaneous
Batch TR-3, 5/15/1990, 60.1 °C, 355 Gy/h, air, Envelopes										
1	172		0.950							
2	338		0.940							
3	510		0.800							
4	673		0.850							
5	840		0.720							
6	1178		0.700							
7	1680		0.550							
8	2353		0.350							
9	3193		0.190							
Batch TR-4, 10/31/1989, 61 °C, 68.7 Gy/h, air, Envelopes										
1	1006		0.900							
2	2016		0.840							
3	3044		0.790							
4	4056		0.710							
5	5036		0.650							
6	6049		0.680							
7	7057		0.570							
8	8568		0.490							
Batch TR-5, 8/11/1987, 80 °C, 138 Gy/h, air, DS-II-75										
1	836		0.810							
2	1676		0.710							
3	2180		0.670							
4	2858		0.570							
5	4027		0.420							
6	5540		0.260							
Batch TR-6, 8/11/1987, 80 °C, 267 Gy/h, air, DS-II-50										
1	337		0.830							
2	668		0.710							

SANDIA CABLE SAMPLE REPOSITORY

Material- XLPO-03- Eaton Dekoron Polyset insulation										
Sample No.	Aging Time (h)	Est. Dose (kGy)	Average e/e_0	Average $TS_{/TS0}$	Average density (g/cc)	Outside surface modulus, MPa	Uptake factor	% gel	NMR T2,msec	Miscellaneous
3	1172		0.500							
4	1677		0.380							
5	2180		0.290							
6	2689		0.170							
7	3530		0.096							
8	3836		0.100							
Batch TR-7, 10/26/1987, 80 °C, 724 Gy/h, air, DS-II-56										
1	96		0.840							
2	215		0.740							
3	334		0.650							
4	508		0.380							
5	671		0.380							
6	839		0.340							
7	1011		0.240							
8	1343		0.140							
9	1678		0.110							
Batch TR-8, 8/24/1987, 80 °C, 5350 Gy/h, air, DS-II-65										
1	21		0.820							
2	40		0.780							
3	65		0.750							
4	88		0.640							
5	120		0.520							
6	144		0.480							
7	184		0.420							
8	256		0.270							
Batch TR-9, 1/18/1988, 100 °C, 238 Gy/h, air, DS-II-51										
1	335		0.840							
2	671		0.650							
3	1174		0.530							
4	1678		0.360							

SANDIA CABLE SAMPLE REPOSITORY

Material- XLPO-03- Eaton Dekoron Polyset insulation										
Sample No.	Aging Time (h)	Est. Dose (kGy)	Average e/e_0	Average $TS_{/TS0}$	Average density (g/cc)	Outside surface modulus, MPa	Uptake factor	% gel	NMR T2,msec	Miscellaneous
5	2182		0.220							
6	2686		0.130							
7	3358		0.097							
Batch TR-10, 8/17/1987, 100 °C, 742 Gy/h, air, DS-II-55										
1	95		0.930							
2	214		0.830							
3	334		0.720							
4	525		0.560							
5	669		0.420							
6	837		0.370							
7	1012		0.270							
8	1683		0.051							
Batch TR-11, 12/20/1988, 110 °C, 28.8 Gy/h, air, DS-II-77										
1	1349		0.870							
2	2688		0.480							
3	3744		0.670							can flooded
4	4369		0.580							replaced can
5	5548		0.530							
6	6551		0.440							
7	7560		0.370							
Batch TR-12, 4/19/1989, 115.6 °C, 97.8 Gy/h, air, DS-II-73										
1	480		0.750							
2	984		0.700							
3	1319		0.620							
4	1972		0.570							
5	2495		0.350							
6	2836		0.390							
7	3361		0.300							
Batch TR-13, 2/22/1989, 120 °C, 88.6 Gy/h, air, DS-III-77										

SANDIA CABLE SAMPLE REPOSITORY

Material- XLPO-03- Eaton Dekoron Polyset insulation										
Sample No.	Aging Time (h)	Est. Dose (kGy)	Average e/e_0	Average $TS_{/TS0}$	Average density (g/cc)	Outside surface modulus, MPa	Uptake factor	% gel	NMR T2,msec	Miscellaneous
1	653		0.790							
2	1320		0.560							
3	1996		0.500							
4	2610		0.460							
5	3122		0.350							
6	4055		0.260							
7	4845		0.210							
8	5540		0.150							
9	5834		0.086							
Batch TR-14, 1/18/1988, 120 °C, 252 Gy/h, air, DS-II-44										
1	335		0.830							
2	671		0.630							
3	1174		0.380							
4	1678		0.210							
5	2181		0.080							
6	2690		0.082							
Batch TR-15, 1/18/1988, 120 °C, 705 Gy/h, air, DS-II-54										
1	71		0.910							
2	167		0.750							
3	335		0.550							
4	502		0.370							
5	670		0.250							
6	838		0.130							
7	1007		0.077							
Batch TR-16, 02/29/88, 120 °C, 5030 Gy/h, air, DS-II-68-69										
1	21		0.830							
2	40		0.720							
3	64		0.520							
4	88		0.550							
5	120		0.400							

SANDIA CABLE SAMPLE REPOSITORY

Material- XLPO-03- Eaton Dekoron Polyset insulation										
Sample No.	Aging Time (h)	Est. Dose (kGy)	Average e/e_0	Average $TS_{/TS0}$	Average density (g/cc)	Outside surface modulus, MPa	Uptake factor	% gel	NMR T2,msec	Miscellaneous
6	144		0.310							
7	185		0.190							
8	256		0.086							
9	288		0.064							
10	328		0.057							

SANDIA CABLE SAMPLE REPOSITORY

Material-XLPO-04- ITT Exane II Surprenant insulation									
Sample No.	Aging Time (h)	Est. Dose (kGy)	Average e/e_0	Average $TS_{/TS0}$	Outside surface modulus, MPa	Uptake factor	% gel	NMR T2,msec	Notes
No density measurements taken since insulation is dual layered (each with a different density)									
Batch T-1, 10/30/1979, 90.6 °C, 0 Gy/h, air, LHJ-29									
1	3335.0		0.895	1.090				1.69	NMR-green outside
2	8615.0		0.725	0.976				1.23	
3	16220.0		0.640	0.992				1.34	
4	20654.0		0.520	1.000					
5	25995.0		0.410	1.020				0.94	
6	31107.0							0.83	
Batch T-2, 10/26/1979, 101.3 °C, 0 Gy/h, air, LHJ-29									
1	1291.0		0.890	1.025				1.72	
2	3259.0		0.750	1.069				1.6	
3	8238.0		0.410	0.927				1.13	
4	16320.0		0.270	0.935				0.695	
5	20664.0		0.208	0.967				0.543	
6	25995.0		0.132	1.000				0.373	
7	29550.0		0.101	0.939				0.452	
8	31107.0							0.37	
Batch T-3, 11/21/1978, 110.6 °C, 0 Gy/h, air, LB-II-113									
1	574.0		0.910	1.000				1.73	
2	1656.0		0.697	0.902				1.52	
3	3264.0		0.506	0.955				1.33	
4	5784.0		0.335	0.894				0.574	
5	8140.0		0.198	0.906				0.935	
6	12004.0		0.133	0.990				0.338	
Batch T-4, 11/20/1978, 121.5 °C, 0 Gy/h, air, LB-II-107									
1	237.0		1.000	1.036				2.65	
2	669.0		0.686	0.980				2.04	
3	1270.0		0.471	0.914				1.54	
4	2256.0		0.302	0.833				0.992	
5	2950.0		0.233	0.820				0.732	
6	4390.0		0.127	0.833				0.579	
7	5902.0		0.037	0.837				0.473	

Material-XLPO-04- ITT Exane II Surprenant insulation									
Sample No.	Aging Time (h)	Est. Dose (kGy)	Average e/e_0	Average $TS_{/TS0}$	Outside surface modulus, MPa	Uptake factor	% gel	NMR T2,msec	Notes
Batch T-5, 09/28/1978, 130.2 °C, 0 Gy/h, air, LB-II-106									
1	96.0		0.876	0.963				2.13	
2	263.0		0.718	0.967				2.04	
3	479.0		0.450	0.865				1.63	
4	599.0		0.400	0.837				1.88	
5	862.0		0.355	0.849				1.4	
6	1367.0		0.271	0.820				1.29	
7	2304.0		0.122	0.820				0.584	
Batch T-6, 09/27/1978, 140 °C, 0 Gy/h, air, LB-II-104									
1	47.0		0.894	0.971				2.46	
2	119.0		0.694	0.910				2.05	
3	287.0		0.429	0.837				1.32	
4	456.0		0.361	0.837				1.17	
5	558.0		0.294	0.837				0.95	
6	840.0		0.184	0.820				0.598	
7	1020.0		0.113	0.784					
8	1356.0		0.020	0.878				0.507	
Batch T-7, 08/22/1978, 151.2 °C, 0 Gy/h, air, LB-II-98									
1	56.0		0.692	0.951				2.74	
2	79.5		0.655	0.951				2.46	
3	144.5		0.445	0.849				2.18	
4	216.5		0.343	0.837				2.06	
5	335.0		0.180	0.849				1.01	
6	505.0		0.078	0.845				0.614	
Batch T-8, 11/27/1978, 161.5 °C, 0 Gy/h, air, LB-II-107									
1	5.0		1.000	1.008				2.59	
2	29.5		0.695	0.980				2.64	
3	54.0		0.539	0.873				1.99	
4	101.0		0.387	0.824				1.66	
5	166.0		0.144	0.845					
6	190.0		0.077	0.861				0.57	
7	214.0		0.048	0.910				0.583	
Batch T-9, 04/11/1979, 170.3 °C, 0 Gy/h, air, LHJ-6									
1	7.5		0.800	0.943				3.6	
2	16.5		0.686	0.931				1.6	
3	31.3		0.518	0.882					
4	55.0		0.392	0.861				1.21	
5	79.0		0.216	0.861					
6	101.5		0.082	0.894				0.672	
7	120.0		0.060	0.906					

SANDIA CABLE SAMPLE REPOSITORY

Material-XLPO-04- ITT Exane II Surprenant insulation									
Sample No.	Aging Time (h)	Est. Dose (kGy)	Average e/e_0	Average $TS_{/TS0}$	Outside surface modulus, MPa	Uptake factor	% gel	NMR T2,msec	Notes
Batch TR-1, 04/26/1977, 22 °C, 15.7 Gy/h, air, NRL B-16									
1	2592.0	52	0.920	0.890					
2	7392.0	145	0.730	0.840					
3	12624.0	238	0.540	0.860					
4	17664.0	333	0.440	0.820					
5	22704.0	400	0.290	0.900					
6	26928.0	457	0.220	0.810					
7	31392.0	507	0.190	0.800					
8	40128.0	597	0.040	0.690					
9	53136.0	710	0.040	0.730					
Batch TR-1 RH, 04/26/1977, 22 °C, 15.7 Gy/h, air + RH, NRL B-15									Note: RH= air flow
1	2592.0	44	0.960	0.860					through water at ro
2	7392.0	124	0.850	0.840					
3	12624.0	202	0.670	0.840					
4	18552.0	286	0.390	0.810					
5	22704.0	342	0.300	0.870					
6	26928.0	389	0.470	0.820					e/eo strange value
7	31392.0	440	0.280	0.790					
8	35472.0	482	0.250	0.810					
Batch TR-2, 04/26/1977, 22 °C, 95 Gy/h, air, NRL B-6									
1	672.0	71	0.970	0.890					
2	2592.0	267	0.720	0.930					
3	5520.0	559	0.420	0.900					
4	11064.0	1080	0.060	0.640					
5	12624.0	1194	0.071	0.760					
Batch TR-2 RH, 04/26/1977, 22 °C, 95 Gy/h, air + RH, NRL B-2									
1	672.0	71	0.980	0.920					
2	2592.0	267	0.730	0.860					
3	5520.0	559	0.320	0.810					
4	11064.0	1080	0.020	0.520					
5	12624.0	1194	0.020	0.580					

SANDIA CABLE SAMPLE REPOSITORY

Material-XLPO-04- ITT Exane II Surprenant insulation									
Sample No.	Aging Time (h)	Est. Dose (kGy)	Average e/e_0	Average $TS_{/TS0}$	Outside surface modulus, MPa	Uptake factor	% gel	NMR T2,msec	Notes
Batch TR-3, 28353, 24 °C, 515 Gy/h, air, NRL A-19									
1	144.0	77	0.930	0.890					
2	336.0	180	0.830	0.910					
3	672.0	359	0.530	0.880					
4	1344.0	715	0.320	0.950					
5	2688.0	1413	0.120	1.030					
Batch TR-3 RH, 08/16/1977, 24 °C, 515 Gy/h, air + RH, NRL A-17									
1	144.0	74	0.920	0.920					
2	336.0	172	0.820	0.910					
3	672.0	344	0.590	0.930					
4	1344.0	684	0.300	0.960					
5	2688.0	1354	0.110	1.040					
Batch TR-4, 08/15/1977, 30 °C, 2210 Gy/h, air, NRL A-5									
1	47.7	105	0.820	0.900					
2	96.3	212	0.590	0.950					
3	240.5	531	0.340	1.100					
4	433.5	955	0.260	1.220					
5	671.0	1478	0.140	1.110					
Batch TR-4 RH, 08/15/1977, 30 °C, 2210 Gy/h, air + RH, NRL A-4									
1	47.7	106	0.800	0.970					
2	96.2	214	0.610	1.090					
3	240.5	536	0.320	1.130					
4	433.5	965	0.200	1.150					
5	671.0	1493	0.160	1.280					
Batch TR-5 RH, 05/03/1977, 38 °C, 12200 Gy/h, air + RH, NRL A-1									
1	8.0	98	0.830	0.890					
2	24.0	293	0.530	1.070					
3	47.8	584	0.340	1.110					
4	79.6	973	0.250	1.190					
5	143.5	1750	0.120	1.170					

SANDIA CABLE SAMPLE REPOSITORY

Material-XLPO-04- ITT Exane II Surprenant insulation									
Sample No.	Aging Time (h)	Est. Dose (kGy)	Average e/e_0	Average $TS_{/TS0}$	Outside surface modulus, MPa	Uptake factor	% gel	NMR T2,msec	Notes
Batch TR-6, 11/30/1979, 66 °C, 820 Gy/h, air, LHJ-32									
1	77.0	63	0.880	1.070					
2	292.0	239	0.610	1.130					
3	484.0	397	0.410	1.110					
4	844.0	692	0.250	1.180					
5	1172.0	961	0.160	1.350					
6	1610.0	1320	0.073	1.540					
Batch TR-7, 09/06/1977, 100 °C, 2300 Gy/h, air, NRL A-6									
1	31.5	71	1.030	1.030					
2	71.3	161	0.980	0.980					
3	213.8	486	0.620	1.080					
4	405.4	921	0.230	1.040					
5	549.0	1248	0.100	1.210					
Batch TR-8 RH, 12/12/1977, 110 °C, 500 Gy/h, air + RH, NRL A-17									
1	167.3	84	0.970	0.980					
2	359.6	180	0.780	0.950					
3	527.2	264	0.690	1.010					
4	840.0	420	0.190	0.830					
5	1174.0	587	0.040	0.930					
Batch TR-9, 09/06/1977, 120 °C, 2300 Gy/h, air, NRL A-7									
1	31.5	73	1.050	1.040					
2	71.5	165	0.880	0.980					
3	214.2	496	0.330	0.870					
4	406.0	941	0.020	59.000					
5	549.0	1275	0.000	0.000					
Batch TR-10 RH, 12/12/1977, 130 °C, 520 Gy/h, air + RH, NRL A-19									
1	168.0	87	0.850	0.980					
2	360.0	187	0.290	0.760					
3	528.0	275	0.090	0.800					
4	671.0	348	0.000	0.000					
Batch TR-11, 09/12/1977, 140 °C, 2200 Gy/h, air, NRL A-2									
1	20.0	47	1.000	0.990					
2	31.0	73	0.950	0.950					
3	70.7	166	0.760	0.920					
4	142.4	334	0.290	0.800					
5	309.9	727	0.000	0.000					
Batch TR-11 RH, 09/12/1977, 140 °C, 2200 Gy/h, air + RH, NRL A-4									
1	22.1	48	1.020	0.930					
2	31.3	68	0.980	0.930					
3	71.2	155	0.800	0.860					
4	142.7	311	0.370	0.770					
5	310.2	676	0.000	0.000					

SANDIA CABLE SAMPLE REPOSITORY

Material- XLPO-05- Rockbestos Firewall III Insulation										
Sample No.	Aging Time (h)	Est. Dose (kGy)	Average e/e_0	Average $TS_{/TS0}$	Average density (g/cc)	Outside surface modulus, MPa	Uptake factor	% gel	NMR T2,msec	Miscellaneous
Batch T-1, , 100 °C, 0 Gy/h, air, Not started										
Batch T-2, 6/11/01, 109 °C, 0 Gy/h, air, RB-II-51B										
1green	2517		0.803	1.022						
2g	4926		0.910	1.183						
3g	13798		0.667	1.061						
4g	16054		0.640	1.082						
5g	18168		0.680	1.120						
6g	22918		0.703	1.222						
1red	2517		0.983	1.071						
2r	4926		0.863	1.075						
3r	13798		0.397	1.001						
4r	16054		0.157	1.036						
5r	18168		0.697	1.075						
6r	22918		0.623	1.089						
1black	2517		0.887	1.054						
2b	4926		0.830	1.078						
3b	13798		0.643	0.970						
4b	16054		0.403	0.970						
5b	18168		0.707	1.089						
6b	22918		0.653	1.085						
Batch T-3, 6/11/01, 124 °C, 0 Gy/h, air, RB-II-51A										
0green	0		1.000	1.000					2.840	
0g-annea	0								6.210	
1green	1535		0.943	1.110					6.170	
2g	2592		0.797	1.019						
3g	3359		0.960	1.096					5.310	
4g	3885		0.787	1.043						
5g	8621		0.780	1.082					5.000	
6g	10275		0.657	1.001					4.710	
7g	11594		0.740	1.064					4.760	
8g	14378		0.600	1.005					3.880	
9g	18360		0.230	0.837					3.150	
10g	21720		0.000	0.640					0.919	
11green	26928		0.000	0.186						
1red	1535		0.947	1.113						
2r	2592		0.947	1.145						
3r	3359		1.143	1.208						
4r	3885		1.063	1.229						
5r	8621		0.730	1.040						
6r	10275		0.697	1.015						
7r	11594		0.833	0.903						
8r	14378		0.500	0.938						
9r	18360		0.293	0.865						
10r	21720		0.227	0.875						
11red	26928		0.133	0.833						
1black	1535		0.957	1.068						
2b	2592		0.820	1.026						
3b	3359		0.767	0.924						
4b	3885		0.893	1.075						

Material- XLPO-05- Rockbestos Firewall III Insulation										
Sample No.	Aging Time (h)	Est. Dose (kGy)	Average e/e_0	Average $TS_{/TS0}$	Average density (g/cc)	Outside surface modulus, MPa	Uptake factor	% gel	NMR T2,msec	Miscellaneous
5b	8621		0.763	1.029						
6b	10275		0.657	0.945						
7b	11594		0.743	0.980						
8b	14378		0.510	0.910						
9b	18360		0.407	0.868						
10b	21720		0.290	0.889						
11black	26928		0.240	0.823						
Batch T-4, 6/26/01, 138 °C, 0 Gy/h, air, RB-II-69,III-35										
1green	2399		0.847	1.072	1.358		4.840	73.200		
2g	2882		0.950	1.103	1.356		5.120	73.100		
3g	3195		0.477	0.876	1.360		4.830	73.500		
4g	3360		0.550	0.889	1.358		4.550	73.600		
5g	3846		0.283	0.842	1.411		4.430	74.200		
6g	4105		0.047	0.822	1.362		3.930	73.200		
7g	4345		0.000	0.720	1.364		3.720	74.700		
8g	4589		0.000	0.670	1.389		3.100	74.400		
9a-g	4849		0.000	0.649	1.434		3.090	83.800		
9b-g	4849		0.000	0.659						
10g	5088		0.000	0.710	1.386		2.710	70.600		
11a-g	5430		0.000	0.609	1.496		2.600	77.500		
11b-g	5430		0.000	0.629						
12g	5927		0.000	0.416	1.438		1.510	79.300		
13a-g	7104		0.000	0.426	1.504					
13b-g	7104		0.000	0.426	1.498					
1red	2399		0.903	1.051	1.363					
2r	2882		0.860	1.009	1.361					
3r	3195		0.543	0.884	1.363					
4r	3360		0.547	0.877	1.366					
5r	3846		0.420	0.822	1.366					
6r	4105		0.330	0.815	1.368					
7r	4345		0.343	0.784	1.369					
8r	4589		0.280	0.766	1.370					
9a-r	4849		0.273	0.777	1.369					
9b-r	4849		0.197	0.773						
10r	5088		0.197	0.735	1.372					
11a-r	5430		0.243	0.735	1.378					
11b-r	5430		0.207	0.739						
12r	5927		0.153	0.673	1.378					
13r	7104		0.097	0.628						
1black	2399		0.807	0.971	1.350					
2b	2882		0.797	0.957	1.349					
3b	3195		0.533	0.825	1.352					
4b	3360		0.547	0.818	1.350					
5b	3846		0.420	0.808	1.354					
6b	4105		0.380	0.795	1.355					
7b	4345		0.380	0.785	1.355					
8b-b	4589		0.397	0.771	1.355					
9a-b	4849		0.303	0.751	1.357					
9b-b	4849		0.300	0.764						
10b	5088		0.240	0.731	1.357					
11a-b	5430		0.293	0.778	1.360					
11b-b	5430		0.260	0.744						
12b	5927.167		0.303333	0.7440277	1.3571					
13b-g	7104		0.163	0.639						
Batch T-5, 7/03/01, 151 °C, 0 Gy/h, air, RB-II-53										
0green	0		1.000		1.362		5.038	72.000		
1green	329		1.070				4.670	72.200		
2g	571		0.954		1.360		3.720	73.000		

Material- XLPO-05- Rockbestos Firewall III Insulation										
Sample No.	Aging Time (h)	Est. Dose (kGy)	Average e/e_0	Average $TS_{/TS0}$	Average density (g/cc)	Outside surface modulus, MPa	Uptake factor	% gel	NMR T2,msec	Miscellaneous
3a-g	742		0.958		1.359		4.540	72.700		
3b-g	742		0.958		1.382		4.540	72.700		
4a-g	884		0.828		1.359		4.040	73.000		
4b-g	884		0.828		1.378		4.040	73.000		
5a-g	1051		0.547		1.367		5.360	72.400		
5b-g	1051		0.547		1.390		5.360	72.400		
6g	1316		0.051		1.395		4.000	73.000		
7g	1503		0.034		1.401		3.100	78.100		
8g	1528		0.055		1.401		2.610	78.000		
9green	1625		0.056		1.403		2.510	78.300		
Batch T-6, 4/25/01, 151 °C, 0 Gy/h, air, RB-II-43										
1green	139		1.077		1.359		4.700	72.000		
2g	329		1.070				4.670	72.200		
3g	502		0.814		1.358		4.240	73.100		
4g	672		1.005		1.364		4.600	72.900		
5g	1169		0.320		1.390		3.409	74.300		
6g	1456		0.090		1.397		2.970	75.400		
7g	1480		0.055		1.397		3.350	75.700		
Batch T-7, 6/19/03, 150 °C, 0 Gy/h, air, RB-IV-47										
1green	504		0.777	0.940						
2g	763		0.730	0.859						
3g	1122		0.917	1.007						
4g	1846		0.037	0.711						
5g	1867		0.000	0.805						
6g	2109		0.043	0.691						
7g	2466		0.000	0.616						
8g	3025		0.000	0.581						
9g	4003		0.000	0.384						
10g	4129		0.000	0.201						
11green	5201		0.000	0.121						
1red	504		0.863	0.990						
2r	763		0.730	1.030						
3r	1122		0.763	0.960						
4r	1846		0.150	0.770						
5r	1867		0.000	0.800						
6r	2109		0.180	0.720						
7r	2466		0.200	0.730						
8r	3025		0.110	0.650						
9r	4003		0.000	0.510						
10r	4129		0.000	0.410						
11red	5201		0.000	0.370						
1black	504		0.810	0.979						
2b	763		0.733	0.931						
3b	1122		0.707	0.933						
4b	1846		0.347	0.757						
5b	1867		0.417	0.799						
6b	2109		0.293	0.757						
7b	2466		0.263	0.729						
8b	3025		0.190	0.692						

Material- XLPO-05- Rockbestos Firewall III Insulation										
Sample No.	Aging Time (h)	Est. Dose (kGy)	Average e/e_0	Average $TS_{/TS0}$	Average density (g/cc)	Outside surface modulus, MPa	Uptake factor	% gel	NMR T2,msec	Miscellaneous
9b	4003		0.040	0.567						
10b	4129		0.000	0.531						
11black	5201		0.000	0.555						
Batch T-8, 8/28/89, 160 °C, 0 Gy/h, air, DS-IV-11										
1	168		0.950							
2	337		0.860							
3	504		0.720							
4	674		0.550							
Batch TR-1, , 23 °C, 210 Gy/h, air, Malone										
1	168		0.750							
2	336		0.850							
3	504		0.760							
4	672		0.620							
5	840		0.480							
6	1032		0.400							
7	1176		0.340							
8	1512		0.270							
9	2016		0.095							
10	2520		0.053							
Batch TR-2, , 40 °C, 215 Gy/h, air, Envelopes										
1	337		0.870							
2	672		0.730							
3	1029		0.310							
4	1177		0.370							
5	1512		0.190							
6	2016		0.110							
7	2517		0.100							
Batch TR-3, , 41 °C, 76 Gy/h, air, Envelopes										
1	1007		0.900							
2	2016		0.056							funny data?
3	3044		0.380							
4	3960		0.000							
Batch TR-4, , 60 °C, 1850 Gy/h, air, Malone										Times are approx.
1	24		0.890							
2	48		0.870							
3	72		0.820							
4	96		0.720							
5	120		0.770							
6	168		0.630							
7	216		0.600							
8	288		0.420							
9	336		0.310							
10	384		0.220							
11	480		0.120							
Batch TR-5, , 60.1 °C, 360 Gy/h, air, Envelopes										
1	173		0.950							
2	339		0.810							
3	510		0.550							
4	673		0.540							
5	840		0.440							
6	1010		0.049							
Batch TR-6, , 61 °C, 80 Gy/h, air, Envelopes										
1	1007		0.780							

Material- XLPO-05- Rockbestos Firewall III Insulation										
Sample No.	Aging Time (h)	Est. Dose (kGy)	Average e/e_0	Average $TS_{/TS0}$	Average density (g/cc)	Outside surface modulus, MPa	Uptake factor	% gel	NMR T2,msec	Miscellaneous
2	2016		0.630							
3	3044		0.690							
4	3960		0.510							
5	5036		0.240							
6	6049		0.036							
Batch TR-7, , 80 °C, 353 Gy/h, air, Envelopes										
1	172		0.900							
2	338		0.680							
3	509		0.760							
4	672		0.740							
5	840		0.620							
6	1177		0.370							
7	1680		0.000							
Batch TR-8, , 80 °C, 3710 Gy/h, air, Envelopes										
1	24		0.850							
2	48		0.800							
3	74		0.660							
4	98		0.630							
5	124		0.520							
6	168		0.400							
Batch TR-9, , 100 °C, 353 Gy/h, air, Envelopes										
1	168		0.960							
2	331		0.800							
3	504		0.790							
4	672		0.740							
5	835		0.580							
6	1009		0.630							
7	1340		0.530							
8	1681		0.360							
9	2011		0.310							
10	2516		0.260							
11	3163		0.000							
Batch TR-10, , 120 °C, 62 Gy/h, air, Envelopes										
1	509		0.920							
2	1010		0.780							
3	1513		0.860							
4	2017		0.760							
5	2688		0.580							
6	3529		0.150							
7	4537		0.000							
Batch TR-11, , 120 °C, 360 Gy/h, air, Envelopes										
1	173		0.910							
2	336		0.860							
3	504		0.820							
4	676		0.690							
5	845		0.700							
6	1008		0.600							
7	1445		0.360							
8	1851		0.440							
9	2352		0.170							
10	2855		0.000							